TRANSITION METAL-CATALYZED CYCLOADDITION REACTIONS FOR THE FORMATION OF EIGHT- AND SIX-MEMBERED RINGS

Nuria Llorente González

ADVERTIMENT. L'accés als continguts d'aquesta tesi doctoral i la seva utilització ha de respectar els drets de la persona autora. Pot ser utilitzada per a consulta o estudi personal, així com en activitats o materials d'investigació i docència en els termes establerts a l'art. 32 del Text Refós de la Llei de Propietat Intel·lectual (RDL 1/1996). Per altres utilitzacions es requereix l'autorització prèvia i expressa de la persona autora. En qualsevol cas, en la utilització dels seus continguts caldrà indicar de forma clara el nom i cognoms de la persona autora i el títol de la tesi doctoral. No s'autoritza la seva reproducció o altres formes d'explotació efectuades amb finalitats de lucre ni la seva comunicació pública des d'un lloc aliè al servei TDX. Tampoc s'autoritza la presentació del seu contingut en una finestra o marc aliè a TDX (framing). Aquesta reserva de drets afecta tant als continguts de la tesi com als seus resums i índexs.

ADVERTENCIA. El acceso a los contenidos de esta tesis doctoral y su utilización debe respetar los derechos de la persona autora. Puede ser utilizada para consulta o estudio personal, así como en actividades o materiales de investigación y docencia en los términos establecidos en el art. 32 del Texto Refundido de la Ley de Propiedad Intelectual (RDL 1/1996). Para otros usos se requiere la autorización previa y expresa de la persona autora. En cualquier caso, en la utilización de sus contenidos se deberá indicar de forma clara el nombre y apellidos de la persona autora y el título de la tesis doctoral. No se autoriza su reproducción u otras formas de explotación efectuadas con fines lucrativos ni su comunicación pública desde un sitio ajeno al servicio TDR. Tampoco se autoriza la presentación de su contenido en una ventana o marco ajeno a TDR (framing). Esta reserva de derechos afecta tanto al contenido de la tesis como a sus resúmenes e índices.

WARNING. Access to the contents of this doctoral thesis and its use must respect the rights of the author. It can be used for reference or private study, as well as research and learning activities or materials in the terms established by the 32nd article of the Spanish Consolidated Copyright Act (RDL 1/1996). Express and previous authorization of the author is required for any other uses. In any case, when using its content, full name of the author and title of the thesis must be clearly indicated. Reproduction or other forms of for profit use or public communication from outside TDX service is not allowed. Presentation of its content in a window or frame external to TDX (framing) is not authorized either. These rights affect both the content of the thesis and its abstracts and indexes.

UNIVERSITAT ROVIRA i VIRGILI

Transition Metal-Catalyzed Cycloaddition Reactions for the Formation of Eight- and Six-Membered Rings

Nuria Llorente González

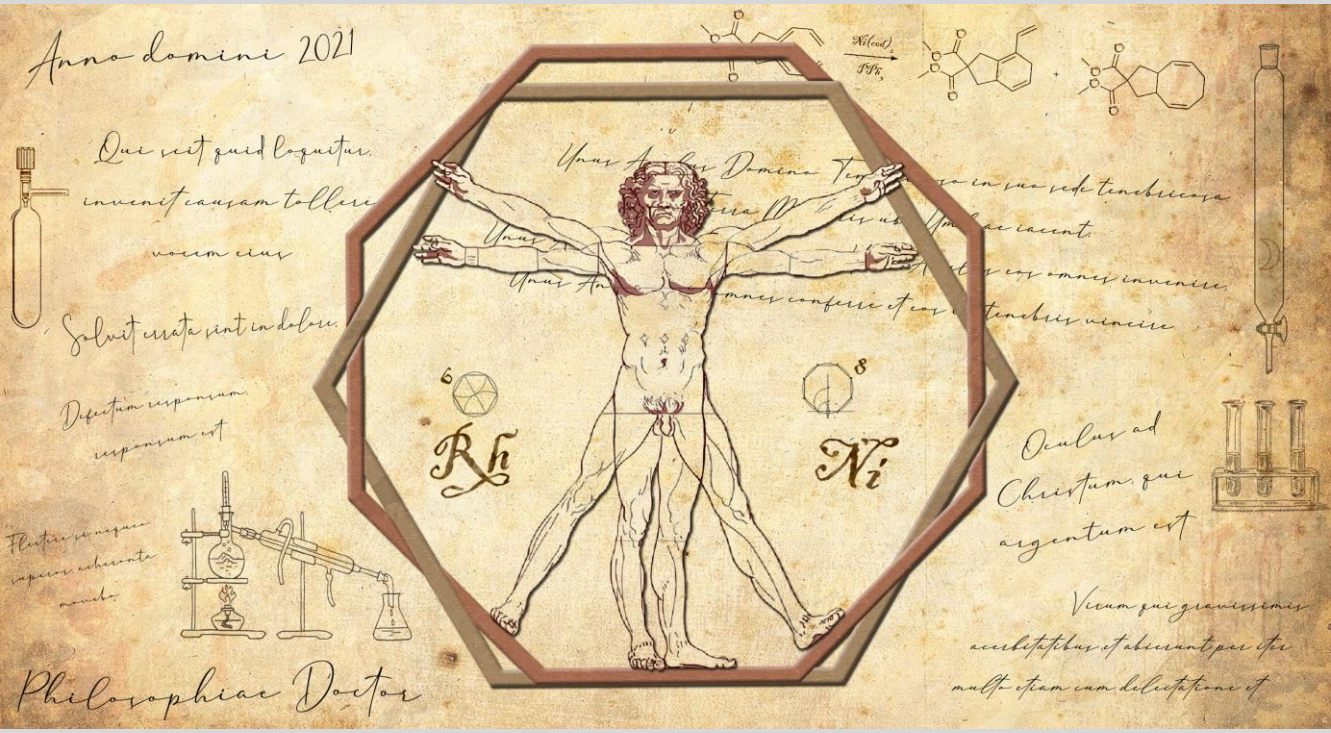

DOCTORAL THESIS
2021

UNIVERSITAT ROVIRA I VIRGILI
TRANSITION METAL-CATALYZED CYCLOADDITION REACTIONS FOR THE FORMATION
OF EIGHT- AND SIX-MEMBERED RINGS
Nuria Llorente González

UNIVERSITAT ROVIRA I VIRGILI
TRANSITION METAL-CATALYZED CYCLOADDITION REACTIONS FOR THE FORMATION
OF EIGHT- AND SIX-MEMBERED RINGS
Nuria Llorente González

Nuria Llorente González

Transition Metal-Catalyzed Cycloaddition Reactions for the Formation of Eight- and Six-Membered Rings

Doctoral Thesis

Supervised by Prof. Dr. Anton Vidal i Ferran

Institute of Chemical Research of Catalonia (ICIQ)

ICIQ
Institut Català d'Investigació Química

UNIVERSITAT ROVIRA i VIRGILI

Tarragona 2021

UNIVERSITAT ROVIRA I VIRGILI
TRANSITION METAL-CATALYZED CYCLOADDITION REACTIONS FOR THE FORMATION
OF EIGHT- AND SIX-MEMBERED RINGS
Nuria Llorente González

Prof. Dr. Anton Vidal i Ferran, former Group Leader of the Institute of Chemical Research of Catalonia (ICIQ) and Research Professor of the Catalan Institution for Research and Advance Studies (ICREA),

I STATE that the present Doctoral Thesis entitled "**Transition Metal-Catalyzed Cycloaddition Reactions for the Formation of Eight- and Six-Membered Rings**" that Nuria Llorente González presents to obtain the PhD degree in chemistry, has been carried out under my supervision, in the corresponding research group at the Institute of Chemical Research of Catalonia (ICIQ).

Barcelona, 1st March 2021

PhD Thesis Supervisor

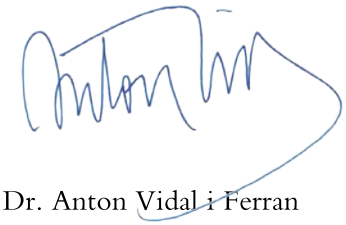

Prof. Dr. Anton Vidal i Ferran

UNIVERSITAT ROVIRA I VIRGILI
TRANSITION METAL-CATALYZED CYCLOADDITION REACTIONS FOR THE FORMATION
OF EIGHT- AND SIX-MEMBERED RINGS
Nuria Llorente González

ACKNOWLEDGEMENTS

En primer lugar, tengo que agradecer a mi supervisor, **Anton Vidal**, por aceptarme en su grupo hace 5 años y por darme la oportunidad de llevar a cabo mi tesis doctoral en el ICIQ. He aprendido mucho bajo su tutela, no solo de química, sino también importantes lecciones de vida que me acompañarán siempre en el futuro.

A lo largo de estos cinco años he tenido la oportunidad de compartir laboratorio con gente estupenda sin la cual las "medias jornadas" no habrían sido soportables. Gracias a Héctor, Jose Luís, Mónica, Rajesh, Laura, Bala, Joan, Lucas, Alicia, Ester, Alba, Andrés y Juanjo. He aprendido de todos y cada uno de ellos, y no solo química.

A mi abuela **Gloria**, gracias por recordarme a cada paso que deje de hacer tonterías y que me ponga a estudiar y a mis tíos **Ana** y **Javier**, gracias por estar siempre ahí. A los **Llorente** necesitaría una hoja entera para nombrarlos a todos. Gracias por darme siempre la alegría de volver.

Por último, pero no menos importante, gracias a mis padres, **Gloria** y **Secundino** por haber sido los patrocinadores oficiales en todos los pasos de mi vida, por empujarme siempre a dar lo mejor y por ser un apoyo constante en todas las decisiones, aunque muchas veces haya sido a regañadientes.

Tarragona, 24 de Enero de 2021

UNIVERSITAT ROVIRA I VIRGILI
TRANSITION METAL-CATALYZED CYCLOADDITION REACTIONS FOR THE FORMATION
OF EIGHT- AND SIX-MEMBERED RINGS
Nuria Llorente González

The research work developed in the present PhD thesis has been possible thanks to the ICIQ Foundation for the predoctoral fellowship (ICIQ 2016/01) and the financial support provided by the ICIQ Foundation and MINECO (CTQ2014-60256-P and CTQ201789814-P).

UNIVERSITAT ROVIRA i VIRGILI

UNIVERSITAT ROVIRA I VIRGILI
TRANSITION METAL-CATALYZED CYCLOADDITION REACTIONS FOR THE FORMATION
OF EIGHT- AND SIX-MEMBERED RINGS
Nuria Llorente González

A mi familia,

la de sangre y la que se elige.

UNIVERSITAT ROVIRA I VIRGILI
TRANSITION METAL-CATALYZED CYCLOADDITION REACTIONS FOR THE FORMATION
OF EIGHT- AND SIX-MEMBERED RINGS
Nuria Llorente González

"Nadie avisó de los baches y las caídas.

Aun así, un pie delante del otro,

un pie delante del otro,

desafiantes."

La Maravillosa Orquesta del Alcohol

"Flectere si nequeo superos,

Acheronta movebo"

Aeneis, Vergilius

UNIVERSITAT ROVIRA I VIRGILI
TRANSITION METAL-CATALYZED CYCLOADDITION REACTIONS FOR THE FORMATION
OF EIGHT- AND SIX-MEMBERED RINGS
Nuria Llorente González

LIST OF PUBLICATIONS

When this dissertation was submitted, the results described herein have so far resulted in the following publications:

- "Ni-Catalysed Intramolecular [4+4]-Cycloadditions of Bis-Dienes Towards Eight-Membered Fused Bicyclic Systems: A Combined Experimental and Computational Study" Llorente, N.; Fernández-Pérez, H.; Bauzá, A.; Frontera, A.; Vidal-Ferran, A, *Catal. Sci. Technol.* **2018**, *8*, 5251-5258. *D.O.I.* 10.1039/c8cy00684a

Other publications related to the topic covered in the present dissertation in a general way are presented below:

- "Efficient Modular Phosphorus-containing Ligands for Stereoselective Catalysis" (general overview on the research activities of the group) Llorente, N.; Fernández-Pérez, H.; Núñez-Rico, J. L.; Carreras, L.; Martínez-Carrión, A.; Iniesta, E.; Romero-Navarro, A.; Martínez-Bascuñana, A. Vidal-Ferran, A. *Pure Appl. Chem.* **2019**, *91*, 3-15. *D.O.I.* 10.1515/pac-2018-0805

UNIVERSITAT ROVIRA I VIRGILI
TRANSITION METAL-CATALYZED CYCLOADDITION REACTIONS FOR THE FORMATION
OF EIGHT- AND SIX-MEMBERED RINGS
Nuria Llorente González

TABLE OF CONTENTS

UNIVERSITAT ROVIRA I VIRGILI
TRANSITION METAL-CATALYZED CYCLOADDITION REACTIONS FOR THE FORMATION
OF EIGHT- AND SIX-MEMBERED RINGS
Nuria Llorente González

LIST OF ACRONYMS AND ABBREVIATIONS

The acronyms and abbreviations used in this manuscript have been used following the recommendations given by the American Chemical Society in the ACS guidelines for authors (accessed June 2020 (https://pubs.acs.org/doi/10.1021/bk-2006-STYG.ch010). Additional abbreviations and acronyms used in this manuscript are referenced in the list below:

[α]	specific rotation [expressed without units; the units, (deg·mL)/(g·dm), are understood]
Å	angstrom(s)
Ac	acetyl
acac	acetylacetonate
AcO	acetate
API	active pharmaceutical ingredient
aq.	aqueous
Ar	aryl, argon
atm	atmosphere(s)
BArF	tetrakis[3,5-bis(trifluoromethyl)phenylborate]
BINOL	1,1′-bi-2-naphthol
H8-BINOL	5,5',6,6',7,7',8,8'-octahydro-1,1'-bi-2-naphthol
br	broad (spectral)
Bu, ^{n}Bu	normal butyl
^{t}Bu	*tert*-butyl
°C	degrees, Celsius
ca.	*circa* (about)
calcd	calculated
cat.	catalyst
cm	centimeter(s)
cm^{-1}	wavenumber(s)

COD	1,5-cyclooctadiene
conv.	conversion
Cy	cyclohexyl (group), cyclohexane (solvent)
δ	chemical shift in ppm
d	doublet (spectral)
dad	diazadiene ligands or N^1,N^2-disubstituted ethane-1,2-diimine ligands
dppb	1,4-Bis(diphenylphosphino)butane
DCM	dichloromethane
DFT	density-functional theory
DIPA	diisopropylamine
DMA	dimethylacetamide
DMF	dimethylformamide
EDG	electron-donating groups
ee	enantiomeric excess
e.g.	exempli gratia (for example)
equiv.	equivalent(s)
er	enantiomeric ratio
ESI	electrospray ionization
et al.	*et alii* (and coworkers)
Et	ethyl
EWG	electron-withdrawing groups
FID	flame ionization detector
g	gram(s)
GC	gas chromatography
h	hour(s)
HMBC	heteronuclear multiple-bond correlation spectroscopy
HMPA	hexamethylphosphoramide
HPLC	high-performance liquid chromatography
HRMS	high resolution mass spectrometry

Hz	hertz
i.e.	*id est* (in other words)
IS	internal standard
IR	infrared
J	coupling constant (expressed in Hz)
L	liter(s)
L_n	undetermined number of ligand(s)
LDA	lithium diisopropylamide
μ	micro- (prefix)
m	multiplet (spectral); milli- (prefix)
M	molar (moles per liter)
M^+	parent molecular ion
Me	methyl
MHz	megahertz
min.	minute(s)
mM	millimolar (millimoles per liter)
mol	mole(s), molecular
mp	melting point
MS	mass spectrometry
MTBE	methyl *tert*-butyl ether
m/z	mass-to-charge ratio
n.d.	not detected
NMR	nuclear magnetic resonance
ORTEP	oak ridge thermal ellipsoid plot program
PFA	perfluoroalkoxy alkanes
Ph	phenyl
ppm	part(s) per million
^{i}Pr	isopropyl
q	quartet (spectral)

rac	racemic
ref	reference
s	singlet (spectral); second(s)
t	triplet (spectral); time
T	temperature
THF	tetrahydrofuran
TLC	thin layer chromatography
TMS	tetramethylsilyl; tetramethylsilane
TOF	time-of-flight; turnover frequency
TPP	tetra phenyl porphyrin
Ts	*p*-toluenesulfonyl (tosyl)
vol	volume
vs.	versus (opposed to)
XB	halogen bond

PROLOGUE

The present doctoral thesis has been divided in five sections: a general introduction and four chapters on the research activities of this thesis. Each chapter has been divided in the following parts: (1) introduction, (2) results and discussion, (3) conclusions and (4) experimental section. Compounds have been numbered independently in each chapter. References have been included as footnotes and numbered independently in each chapter.

The introduction has been divided in four parts. First, a general overview of the cycloaddition reactions and the relevance of eight-membered rings; second, a summary of the relevant examples on intramolecular [4+4] cycloadditions followed in third place by the intramolecular version of the same transformation. The fourth part covers a general overview of the [4+2+2] cycloaddition reactions.

Chapter I discloses our studies on Ni-catalyzed intramolecular [4+4] cycloadditions of bis-dienes towards eight-membered fused bicyclic systems. The computational studies about the favored reaction pathway were performed in collaboration with the group of Prof. Frontera (*Universitat de les Illes Balears*). This work has been published in *Catal. Sci. Technol.* **2018**, *8*, 5251-5258.

Chapter II presents our work on the development of an enantioselective version of Ni-catalyzed intramolecular [4+4] cycloadditions of bisdienes. An extensive screening of enantiopure ligands was performed by means of the High Throughput Experimentation (HTE) facilities at ICIQ.

Chapter III comprises our efforts in developing different approaches in the synthesis of eight-membered rings. The first part covers our attempts in Ni-catalyzed [(4+2)+2] cycloadditions. The second part reflects our preliminary studies on the intramolecular Fe-catalyzed [4+4] cycloaddition reactions.

Chapter IV includes the development of [XBPhosRh]/AgBArF-catalyzed intramolecular [4+2] cycloadditions of dienynes.

UNIVERSITAT ROVIRA I VIRGILI
TRANSITION METAL-CATALYZED CYCLOADDITION REACTIONS FOR THE FORMATION OF EIGHT- AND SIX-MEMBERED RINGS
Nuria Llorente González

INTRODUCTION

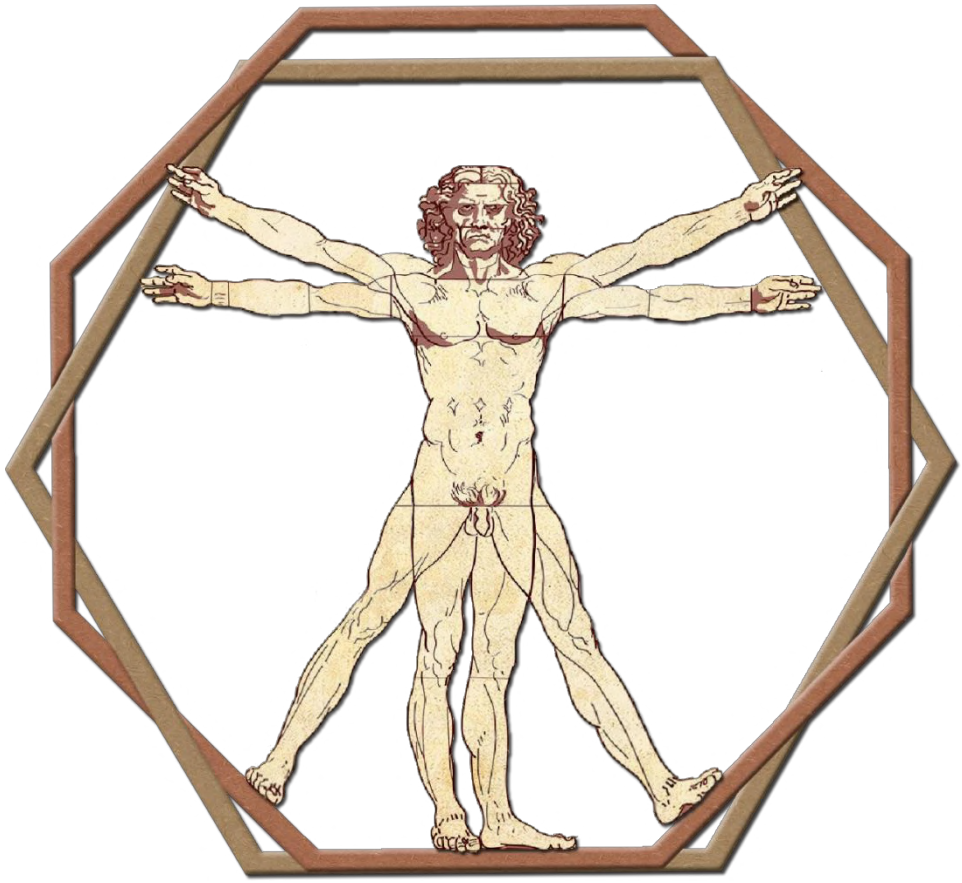

UNIVERSITAT ROVIRA I VIRGILI
TRANSITION METAL-CATALYZED CYCLOADDITION REACTIONS FOR THE FORMATION OF EIGHT- AND SIX-MEMBERED RINGS
Nuria Llorente González

Introduction

A cycloaddition is a cyclization reaction, in which a number of unsaturated molecules (or parts of the same molecule) combine with a net reduction of the bond multiplicity. These transformations have attracted much interest in organic synthesis because they facilitate the construction of difficult-to-form carbon frameworks in a single chemical process with good atom economy.[1] These reactions can be promoted by heat, light, catalysts, high pressure or sonication. However, most of them require the presence of functional groups in the substrate in order to activate the multiple bonds and make the transformation possible. One way to promote cycloadditions is the use of transition metal complexes as catalysts.

Transition-metal catalyzed cycloaddition reactions involve the complexation of an olefin, diene or acetylene unit to a metal center with a modification of the reactivity of such moieties.[2] This strategy has paved the way to new kinds of reactivity. Not only an enhancement on the reaction rate is observed in the presence of the metal catalyst, but also a change in the diastereoselectivity can be achieved in the presence of metal complexes as catalysts. Moreover, the formation of enantiopure (or enantioenriched) compounds can be accomplished by employing catalysts that combine an enantiopure ligand with a metal precursor.[3]

---

(1) For a comprehensive view on cycloaddition chemistry, see: (a) *Synthesis of Heterocycles via Cycloadditions I-II*, First ed.; Hassner, A., Ed.; Springer-Verlag: Heidelberg, 2008. (b) *Methods and Applications of Cycloaddition Reactions in Organic Syntheses*, First ed.; Nishiwaki, N., Ed.; John Wiley & Sons, Inc.: Hoboken, New Jersey, 2014. (c) *Modern Applications Of Cycloaddition Chemistry*, First ed.; Quadrelli, P., Ed.; Elsevier: Amsterdam, 2019, and references therein.

(2) For a general view on metal-catalyzed cycloadditions, see: (a) Lautens, M.; Klute, W.; Tam, W. *Chem. Rev.* **1996**, *96*, 49-92. (b) Saito, S. In *Modern Organonickel Chemistry*; Wiley-VCH Verlag GmbH & Co. KGaA: Weinheim, 2005; pp 171-204. For a general view on cycloadditions towards medium-sized rings, see (c) Yet, L. *Chem. Rev.* **2000**, *100*, 2963-3007. (d) Wender, P. A.; Croatt, M. P.; Deschamps, N. M. In *Comprehensive Organometallic Chemistry III*; Mingos, D. M. P.; Crabtree, R. H., Eds.; Elsevier: Oxford, 2007; pp 603-647. (e) Yu, Z.-X.; Wang, Y.; Wang, Y. *Chem.–Asian J.* **2010**, *5*, 1072-1088. (f) Inglesby, P. A.; Evans, P. A. In *Comprehensive Organic Synthesis II*; Second ed.; Knochel, P., Ed.; Elsevier B.V.: Amsterdam, 2014; pp 656-702. (g) Min, L.; Hu, Y.-J.; Fan, J.-H.; Zhang, W.; Li, C.-C. *Chem. Soc. Rev.* **2020**, *49*, 7015-7043, and references therein.

(3) For a comprehensive view, see (a) Marinetti, A.; Jullien, H.; Voituriez, A. *Chem. Soc. Rev.* **2012**, *41*, 4884-4908. (b) Buono, G.; Clavier, H.; Giordano, L.; Tenaglia, A. In *Stereoselective Multiple Bond-Forming Transformations in Organic Synthesis*; First ed.; Rodriguez, J.; Bonne, D., Eds.; John Wiley & Sons, Inc.: Chichester, 2015; pp 212-240, and references therein.

The Diels–Alder reaction is possibly the best-known and studied cycloaddition reaction, as it provides robust synthetic routes towards cyclic systems.[4] This transformation yields six-membered rings from a 1,3-diene and an alkene or alkyne unit in a highly regio- and stereoselective manner. In contrast, higher-order cycloadditions include a broad range of reactions that provide access to rings with seven or more members in an atom economical and often industrially practical manner. The term higher-order cycloaddition was originally coined by Houk and Woodward[5] following the prediction of the existence of the [6+4] cycloadditions according to the Woodward and Hoffmann rules.[6] In this work, the authors described pericyclic[7] cycloaddition reactions involving one or more extended π-systems relative to the Diels–Alder [4+2] cycloaddition. In the following years, however, this terminology was expanded to include non-pericyclic cycloaddition processes that produce rings with seven or more members.[8]

Although not as abundant as some of their smaller analogues, eight-membered carbocycles can be found often in natural products and are often incorporated into drugs (Scheme I.1).[9] Taxol, probably the best-known natural product of this category, is one of the most potent anticancer drugs in clinical use. Another appealing feature of eight-membered carbocycles is the general challenge of synthesizing them. Traditional ring-closure strategies are effective for small ring systems, but problematic for medium-sized rings (7 to 12- membered cycles), due to entropic and transannular costs that arise when bringing the two ends of a reactant together.[10] Interestingly, higher-order cycloadditions provide an elegant alternative to overcome these limitations.[11]

---

(4) Diels, O.; Alder, K. *Justus Liebigs Ann. Chem.* **1928**, *460*, 98–122.
(5) Houk, K. N.; Woodward, R. B. *J. Am. Chem. Soc.* **1970**, *92*, 4143–4145.
(6) (a) Woodward, R. B.; Hoffmann, R. *J. Am. Chem. Soc.* **1965**, *87*, 395–397. (b) Hoffmann, R.; Woodward, R. B. *J. Am. Chem. Soc.* **1965**, *87*, 2046–2048.
(7) The term pericyclic reaction indicates a chemical reaction in which a concerted reorganization of bonds takes place throughout a cyclic array of continuously bonded atoms (from Muller, P. *Pure Appl. Chem.* **1994**, *66*, 1077–1184).
(8) Rigby, J. H. *Acc. Chem. Res.* **1993**, *26*, 579–585.
(9) Hu, Y.-J.; Li, L.-X.; Han, J.-C.; Min, L.; Li, C.-C. *Chem. Rev.* **2020**, *120*, 5910–5953.
(10) (a) Illuminati, G.; Mandolini, L. *Acc. Chem. Res.* **1981**, *14*, 95–102. (b) Galli, C.; Mandolini, L. *Eur. J. Org. Chem.* **2000**, 3117–3125.
(11) For a comprehensive view, see (a) Kaupp, G. *Angew. Chem., Int. Ed. Engl.* **1992**, *31*, 422–424. (b) Sieburth, S. M.; Cunard, N. T. *Tetrahedron* **1996**, *52*, 6251–6282. (c) Mehta, G.; Singh, V. *Chem. Rev.* **1999**, *99*, 881–930.

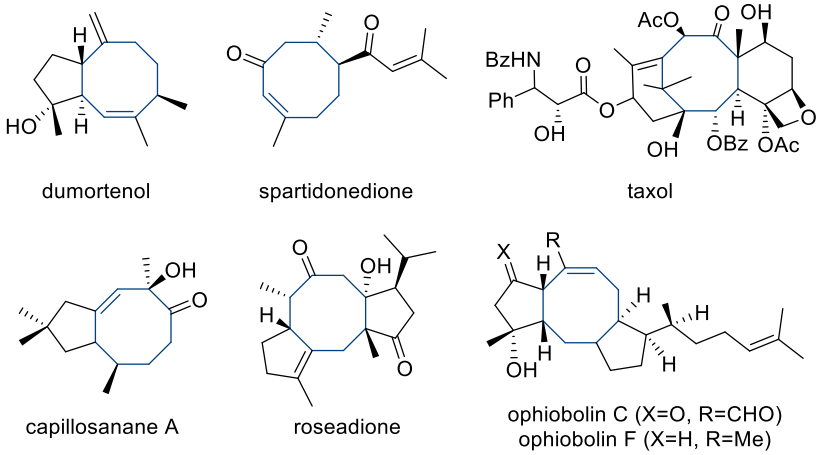

Scheme I.1 Representative natural products with eight-membered carbocyclic skeletons.

Cycloadditions towards eight-membered rings can take place in either an intramolecular or an intermolecular fashion, as well as in a combination of both.[2f] Cycloadditions can involve two, three or more components, however, the latter category does not fall within the scope of this thesis and will not be further discussed. Cycloadditions in general, and higher-order cycloadditions in particular, are traditionally named as [m+n], [m+n+o], indicating the number of atoms that participate in the reaction, and not the number of electrons involved.

[4+4] cycloadditions are, in general, less studied than the cycloadditions leading to smaller rings, such as the [4+2] cycloaddition reactions. These [4+4] cycloadditions leading to the formation of eight-membered rings are forbidden by the Woodward-Hoffman rules,[6] with the metal complex being a key component for promoting these reactions. In general, they involve the combination of two substituted or unsubstituted 1,3-diene moieties leading to the formation of a 1,5-cyclooctadiene derivative and they can take place in an inter- or intra-molecular fashion (Scheme I.2).

In the case of the [4+2+2] cycloadditions, there are two main classes of reactions that have been reported depending on the nature of the substrates. The first class ([4+(2+2)], Scheme I.2) involves the reaction of 1,3-dienes (the four-carbon component) with norbornadienes (both alkenyl groups in the norbornadiene motif as the two two-carbon components) and the second involves the reaction of 1,3-dienes with either two alkynes or an alkyne and an alkene as the two-carbon components ([4+2+2], Scheme I.2). Both classes of cycloadditions can occur in an inter- or intra-molecular fashion.

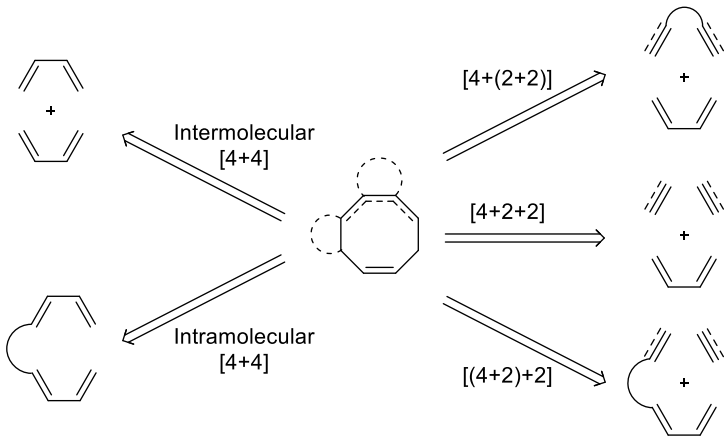

Scheme I.2. General scheme for the cycloadditions leading to eight-membered rings.

I.1. Intermolecular [4+4] Cycloadditions

The dimerization of butadiene to generate 1,5-cyclooctadiene (COD) is a well-established and industrially practiced procedure, using nickel complexes with phosphite ligands as catalysts and trialkylaluminium derivatives as activators.[12] This transformation has been known since the early 1950s, when Ziegler and Reed published that a nickel precursor in the presence of phosphine ligands catalyzed its dimerization and oligomerization reactions (Scheme I.3).[13]

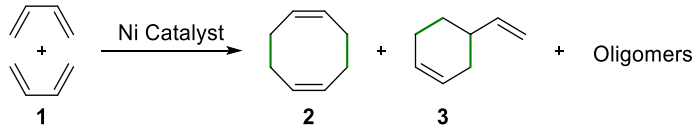

Scheme I.3. Dimerization of butadiene.

It was in the late 1960s, when Wilke and Heimbach optimized the conditions to obtain cyclooctadiene in a 95% yield by employing a bis(π-allyl) nickel complex and a phosphine ligand as catalyst.[14] Heimbach and coworkers further extended this seminal work with extensive mechanistic studies on all the possible oligomers obtained.[14c]

The first examples of the cyclodimerization of isoprene date back from the 70s and early 80s.[15] However, the regio- and stereo-selectivity of intermolecular nickel-catalyzed homodimerizations of substituted butadienes were first studied in 1985 by Waegell and coworkers.[16] They described that dienes with (trimethylsilyl)oxy and methoxycarbonyl groups underwent head-to-head

(12) Oenbrink, G.; Schiffer, T. In *Ullmann's Encyclopedia of Industrial Chemistry*; Wiley-VCH Verlag GmbH & Co. KGaA: Weinheim, 2009; Vol. 11, pp 37-40.
(13) (a) Reed, H. W. B. *J. Chem. Soc.* **1954**, 1931-1941. (b) Ziegler, K.; Holzkamp, E.; Breil, H.; Martin, H. *Angew. Chem.* **1955**, *67*, 426-426. (c) Ziegler, K.; Holzkamp, E.; Breil, H.; Martin, H. *Angew. Chem.* **1955**, *67*, 541-547.
(14) (a) Wilke, G.; Bogdanović, B.; Borner, P.; Breil, H.; Hardt, P.; Heimbach, P.; Herrmann, G.; Kaminsky, H.-J.; Keim, W.; Kröner, M.; Müller, H.; Müller, E. W.; Oberkirch, W.; Schneider, J.; Stedefeder, J.; Tanaka, K.; Weyer, K.; Wilke, G. *Angew. Chem., Int. Ed. Engl.* **1963**, *2*, 105-115. (b) Brenner, W.; Heimbach, P.; Hey, H.; Müller, E. W.; Wilke, G. *Liebigs Ann. Chem.* **1969**, *727*, 161-182. (c) Buchholz, H.; Heimbach, P.; Hey, H. J.; Selbeck, H.; Wiese, W. *Coord. Chem. Rev.* **1972**, *8*, 129-138.
(15) (a) Watanabe, S.; Suga, K.; Kikuchi, H. *Aust. J. Chem.* **1970**, *23*, 385-389. (b) Suga, K.; Watanabe, S.; Fujita, T.; Shimada, T. *J. Appl. Chem.* **1973**, *23*, 131-138. (c) Van Leeuwen, P. W. N. M.; Roobeek, C. F. *Tetrahedron* **1981**, *37*, 1973-1983.
(16) Tenaglia, A.; Brun, P.; Waegell, B. *J. Organomet. Chem.* **1985**, *285*, 343-357.

cycloadditions and the final products had the substituents in a *trans* relative orientation (Scheme I.4).

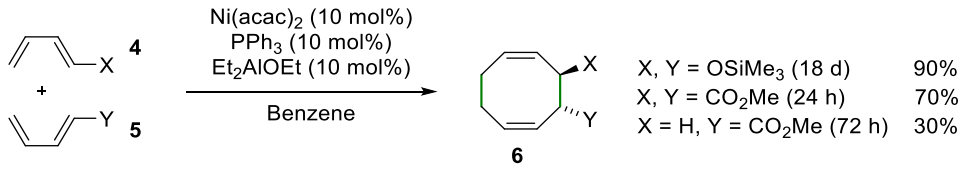

Scheme I.4. Ni-catalyzed homodimerization of substituted butadienes.

The *trans* stereoselectivity was rationalized by the reaction mechanism shown in Scheme I.5.[16] The intermediate complex with four *syn* substituents to the π-allyl ligands (**9**) proved to be the thermodynamically preferred complex. Nickel complex **9** underwent a number of *syn*-*anti* isomerization steps (Scheme I.5) in order to minimize the steric interactions between the X and Y groups. Formation of the corresponding metallacycle and subsequent reductive elimination led to the final *trans*-3,4-disubstituted (1*Z*,5*Z*)-cyclooctadiene.

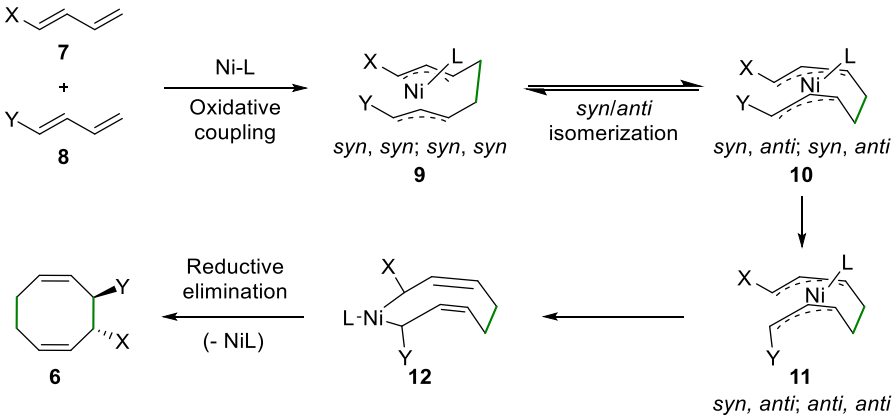

Scheme I.5. Reaction mechanism for the Ni-catalyzed homodimerization of substituted butadienes.

The organoaluminium reagent (*i.e.*, Et_2AlOEt, Scheme I.4) not only played a role as the reducing reagent for the Ni(II) species when $Ni(acac)_2$ was used as the metal precursor, but also as a Lewis acid, which was able to form a complex with the ester group and played a decisive role in the selectivity during the reductive elimination step from **12**. This effect, and the fact that the triphenylphosphine bound to the nickel center is a π-acceptor ligand, favored the reductive elimination step.

tom Dieck *et al.* described that iron-diazadiene (Fe-dad) complexes[17] were also able to catalyze the intermolecular [4+4] cycloaddition reaction of butadiene.[18] The substituents in the diazadiene ligand had a key effect on the control over the formation of cyclooctadiene *vs.* vinylcyclohexene derivatives **2** or **3**, respectively (Scheme I.6). In this case, the reaction was reductively activated by Grignard reagents or a 1,3-butadiene-magnesium adduct (*i.e.* $Mg{\cdot}C_4H_6{\cdot}2$ THF).

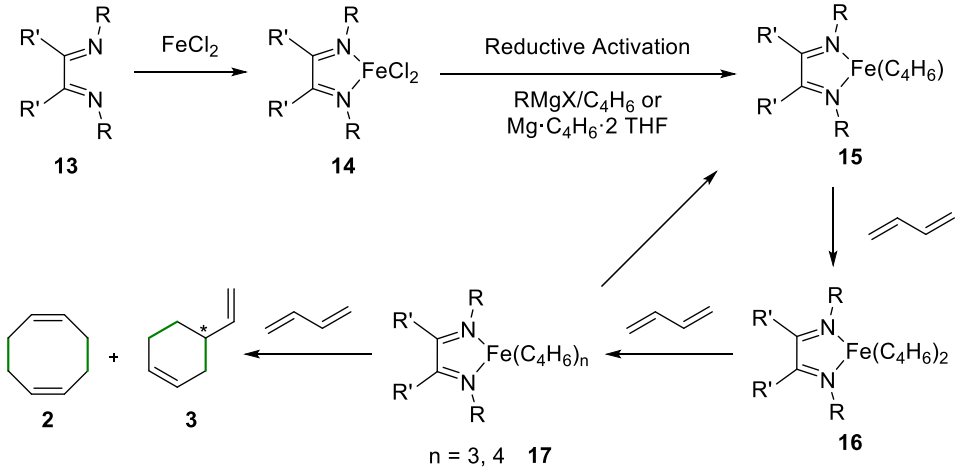

Scheme I.6. Fe-catalyzed dimerization of butadiene.

Up to 98% of **2** was formed when the diazadiene ligand incorporated 2,6-dimethylphenyl substituents at the nitrogen groups (structure **18a** in Figure I.1).[18] Alternatively, the use of ligand **18b** (Figure I.1), which contained a pyridyl substituent and a menthyl-imine group, led to the [4+2] cycloaddition product **3** as the major isomer (80% selectivity towards the [4+2] cycloaddition product and 20% selectivity towards the 8-membered cyclic compound **2**). Ligands **18c** and **18d**, which incorporated a bulkier substituent at the menthyl fragment, led to higher selectivities towards the [4+4] cycloaddition products (51% selectivity for **18c** and 67% for **18d**). It is interesting to note that ligands **18b–d** were enantiopure and that the [4+2] cycloaddition product **3** was obtained in an enantiomerically enriched form. In terms of optical purity, the ee's of the dimerization reaction towards **3** increased with the size of the R substituent (24% ee for **3** with ligand **18b**, 56% ee with **18c** and 62% ee with **18d**). It should also be noted that no oligomerization products of butadiene were detected with ligands **18b–d**.[18]

(17) dad = diazadiene ligands or N^1,N^2-disubstituted ethane-1,2-diimine ligands.
(18) tom Dieck, H.; Dietrich, J. *Angew. Chem., Int. Ed. Engl.* **1985**, *24*, 781-783.

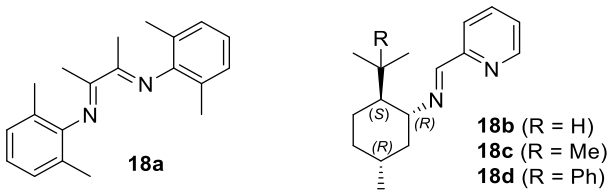

Figure I.1. Structure of the dad ligands.

Homodimerization of isoprene *via* [4+4] cycloaddition reaction was also achieved with iron complexes that contained other dad ligands, as those indicated in Scheme I.7. Homodimer **20** was preferentially formed when Fe(dad) complexes **21a** or **21b** were used as pre-catalysts.[19]

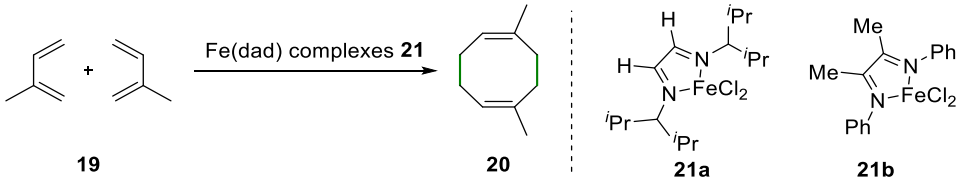

Scheme I.7. Fe-catalyzed homodimerization of isoprene.

The reaction between isoprene and *trans*-1,3-pentadiene in the presence of iron complex **21a**, which was activated with the 1,3-butadiene-magnesium adduct, provided compound **23** in 88% yield. None of the homodimerization compounds of the starting materials (*i.e.* dienes **19** or **22**) were detected. Most interestingly, tom Dieck and coworkers also developed an enantioselective version of this [4+4] cycloaddition reaction and reported that the use of menthyl-derived dad ligand **21c** provided compound **23** in excellent yield and 61% enantioselectivity in favor of (*S*)-**23** (Scheme I.8).[20]

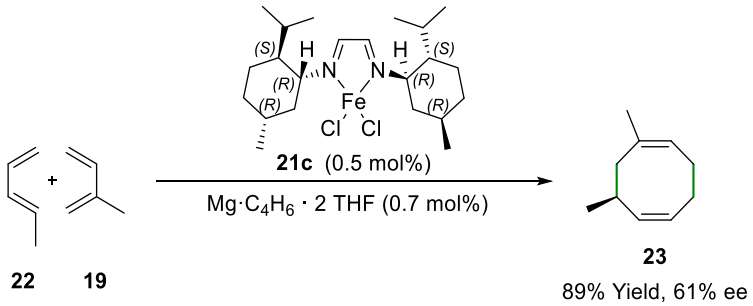

Scheme I.8. Enantioselective version of a Fe-catalyzed [4+4] cycloaddition reaction.

(19) Mallien, M.; Haupt, E. T. K.; tom Dieck, H. *Angew. Chem., Int. Ed. Engl.* **1988**, *27*, 1062-1064.

(20) Baldenius, K. U.; tom Dieck, H.; König, W. A.; Icheln, D.; Runge, T. *Angew. Chem., Int. Ed. Engl.* **1992**, *31*, 305-307.

In the past decade, the Fe-catalyzed dimerization of butadiene has re-emerged. First, Ritter *et al.* performed an extensive study on the mechanism of the transformation introduced by tom Dieck *et al.* in the 80s.[21] More precisely, their research on the structure and oxidation state of the active iron catalyst revealed that reversible dissociation of one of the alkenyl groups of the COD ligand throughout the catalytic cycle was crucial. This effect was facilitated by a high-spin Fe(I) center coupled antiferromagnetically to the diimine ligand radicals, along with partial metal–ligand antibonding orbital population. Their proposed mechanism is depicted in Scheme I.9, in which the Fe(I) complex **24** is the resting state of the catalyst. The reversible dissociation of one of the alkenyl groups of COD (accelerated by the Fe d–COD π-antibonding interaction) forms the steady-state intermediate **25**, followed by turnover-limiting butadiene association leading to **28**. Subsequent oxidative cyclization and reductive elimination of the resulting intermediate **29** regenerates the resting state of the catalyst **24**.

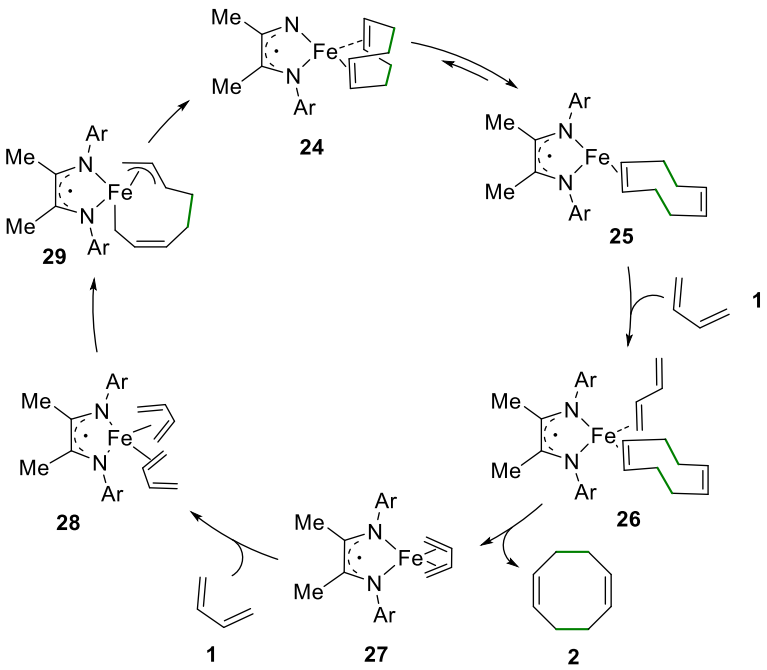

Scheme I.9. Mechanism proposed by Ritter *et al.*

(21) Lee, H.; Campbell, M. G.; Hernández Sánchez, R.; Börgel, J.; Raynaud, J.; Parker, S. E.; Ritter, T. *Organometallics* **2016**, *35*, 2923-2929.

In 2019, Chirik and coworkers further expanded these studies with the low-valent iron-catalyzed [4+4] cycloaddition of substituted 1,3-dienes with control of the chemo- and regio-selectivity.[22] The chemoselectivity of the transformation was demonstrated with the preparation of different dimethyl substituted COD isomers, depending on the Fe-catalyst used (Scheme I.10).

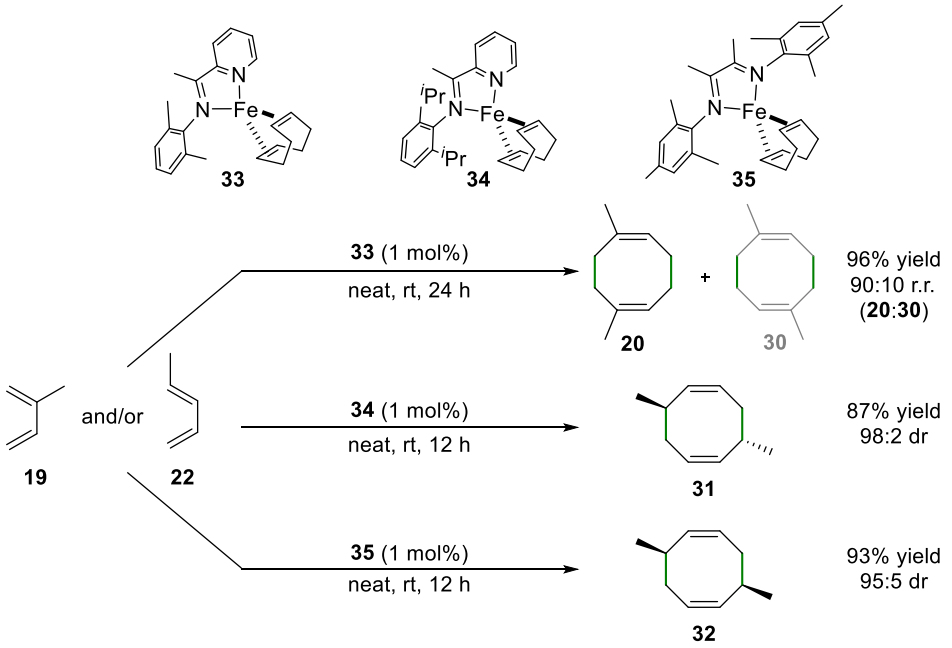

Scheme I.10. Scope for the regio- and diastereoselective iron-catalyzed [4+4] cycloaddition of substituted 1,3-dienes.

However, the most interesting conclusions extracted from their work are those related to the exhaustive analysis of the iron complexes involved. They determined that the catalytically active species involved an (imino)pyridine radical anion antiferromagnetically coupled with a high-spin iron(I) center (see complexes **33-35**, Scheme I.10). These results are in good agreement with the previous studies reported by Ritter *et al.* The proposed catalytic cycle (Scheme I.11), however, proceeds through coordination of two equivalents of isoprene (intermediate **37**) followed by an oxidative cyclization (intermediate **38**) and an allyl-isomerization/C–C bond-forming reductive elimination sequence (intermediates **39** and **41**, respectively), instead of the aforementioned reversible dissociation of COD leading to **40**.

(22) Kennedy, C. R.; Zhong, H.; Macaulay, R. L.; Chirik, P. J. *J. Am. Chem. Soc.* **2019**, *141*, 8557-8573.

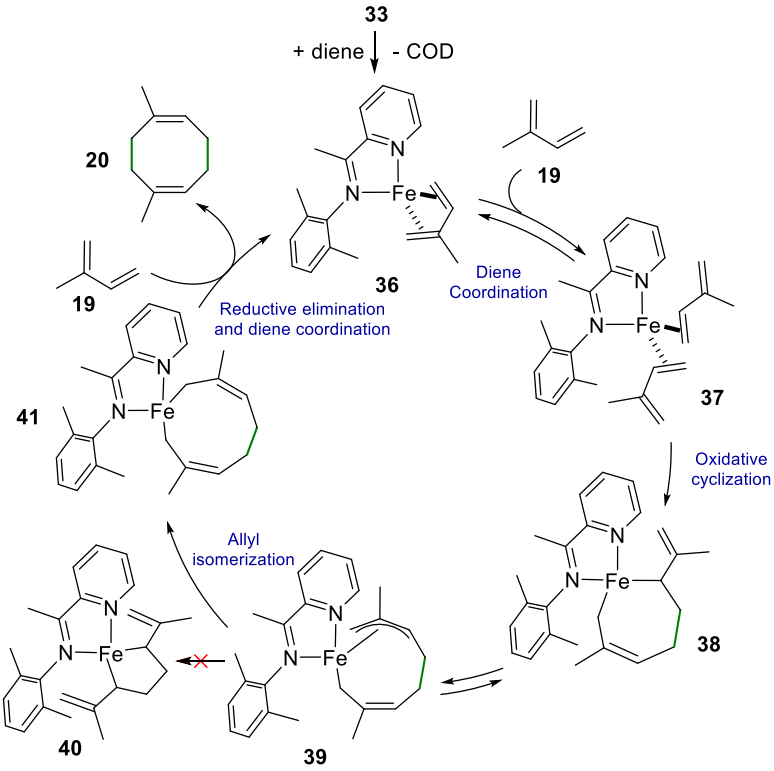

Scheme I.11. Proposed mechanism for the regio- and diastereo-selective iron-catalyzed [4+4] cycloaddition of substituted 1,3-dienes.

Intermediates **36** and **37** are proposed as the resting-states of the catalyst, which undergo a direct oxidative cyclization. A combination of the measurement of $^{13}C/^{12}C$ kinetic isotope effects (KIE) and computational studies have determined the oxidative cyclization process to be the rate determining step. The KIE measurements also enabled the identification of the irreversible and, therefore, regioselective-determining step, which was based on an oxidative cyclization process proceeding through [1,4] carbometalation from an iron bis-diene complex **37**.

The versatility and possible applications for these products was also described by Chirik's group in the past year.[23] An Fe(I)-catalyzed [4+4] cycloaddition of isoprene followed by a Pt(II)-catalyzed hydrogenation provided 1,4-dimethyl cyclooctanes (Scheme I.12), which can be mixed with a wide variety of blendstocks to create a high-performing jet fuel with enhanced properties.

(23) Rosenkoetter, K. E.; Kennedy, C. R.; Chirik, P. J.; Harvey, B. G. *Green Chem.* **2019**, *21*, 5616-5623.

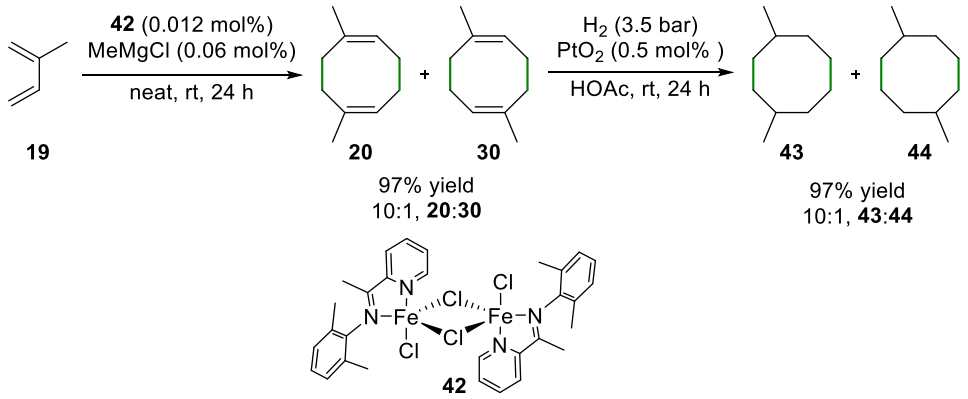

Scheme I.12. [4+4] cycloaddition of isoprene to produce jet fuel.

More recently, new advances in enantioselective intermolecular [4+4] cycloadditions have been reported. Cramer and coworkers described an Fe-dad complex, similar to those reported by tom Dieck,[20] which provided substituted cyclooctadienes with high enantioselectivity (up to a 95% ee).[24] A tailored enantiopure dad ligand was essential for the success of the transformation. The authors performed a detailed study on the effects in the enantioselectivity of the steric bulk of the side chains of the ligand in complex **47** (Scheme I.13a). These studies provided insights into the relationship between the structure of the catalyst and the regio- and enantio-selectivity. Regarding the scope of the reaction, dienes with unconjugated (hetero)aryl substituents were tolerated, leading to the corresponding eight-membered cyclic compounds in good yields (up to 95%) and high enantioselectivities (up to 90% ee). The best results were obtained for methyl substituted substrate **48** (R^2 = Me, Scheme I.13b) and the linear diene **45** with a protected terminal hydroxyl group (R^1 = CH_2-CH_2-OTIPS, Scheme I.13b). It is interesting to note that substrate **48**, containing an additional double bond (R^2 = CH_2-CH_2-CH=C(Me_2)), was selectively transformed into the desired product (84% yield, 95% ee). Moreover, furyl-substituted substrate **48** gave rise to the [4+4] cycloadduct in 79% yield and 90% ee without [4+2] cycloaddition products being observed.

(24) Braconi, E.; Götzinger, A. C.; Cramer, N. *J. Am. Chem. Soc.* **2020**, *142*, 19819-19824.

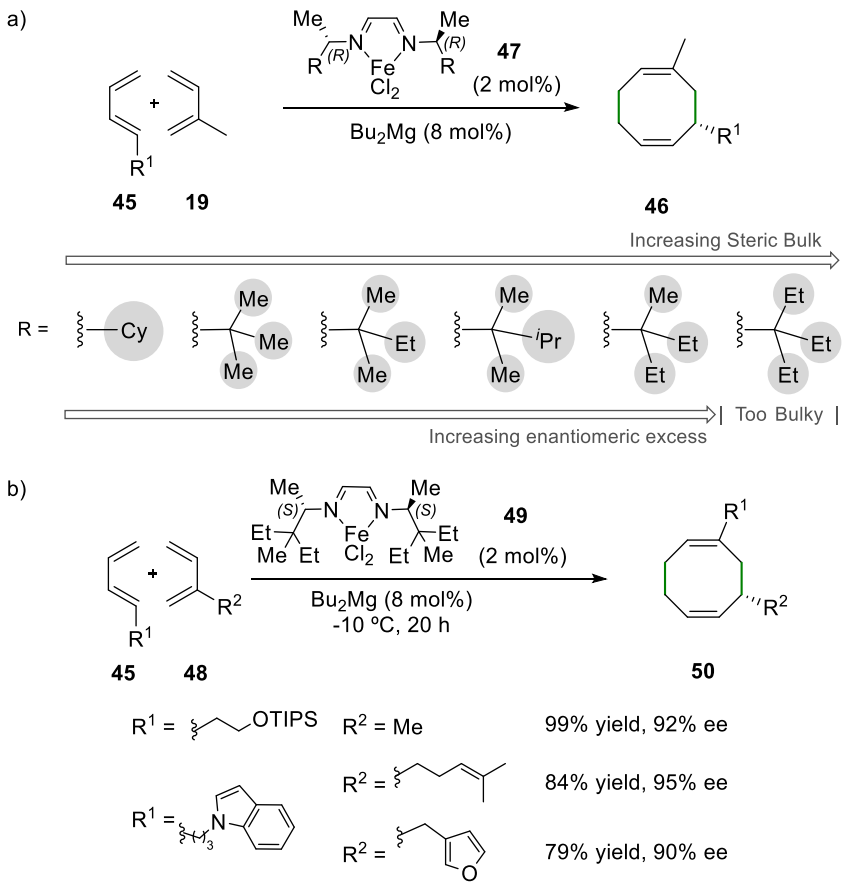

Scheme I.13. Enantioselective intermolecular Fe-catalyzed [4+4] cycloadditions.

In the last decade, two reports have demonstrated that cyclobutanones can also be used as butadiene analogues. The group of Martin described in 2015 a highly regioselective intermolecular [4+4] cycloaddition derived from a C–C cleavage of benzocyclobutenones and 1,3-dienes (Scheme I.14a).[25] Complexes based on $Ni(COD)_2$ and tris(4-(trifluoromethyl)phenyl)phosphine were found to be the most efficient in catalyzing the insertion of 1,3-dienes to give [4+4] adducts. In all cases, exclusive C1–C2 cleavage was observed. In their original work, the authors suggested that the mechanism consisted of a cyclometallation/β-carbon elimination sequence. However, a recent DFT study performed by Huang *et al.*[26] supports an oxidative addition-initiated pathway,

(25) Juliá-Hernández, F.; Ziadi, A.; Nishimura, A.; Martin, R. *Angew. Chem., Int. Ed.* **2015**, *54*, 9537-9541.
(26) Zou, H.; Wang, Z.-L.; Huang, G. *Chem. –Eur. J.* **2017**, *23*, 12593-12603.

followed by a migratory insertion into the Ni–C bond and a C–C reductive elimination process (Scheme I.14b).

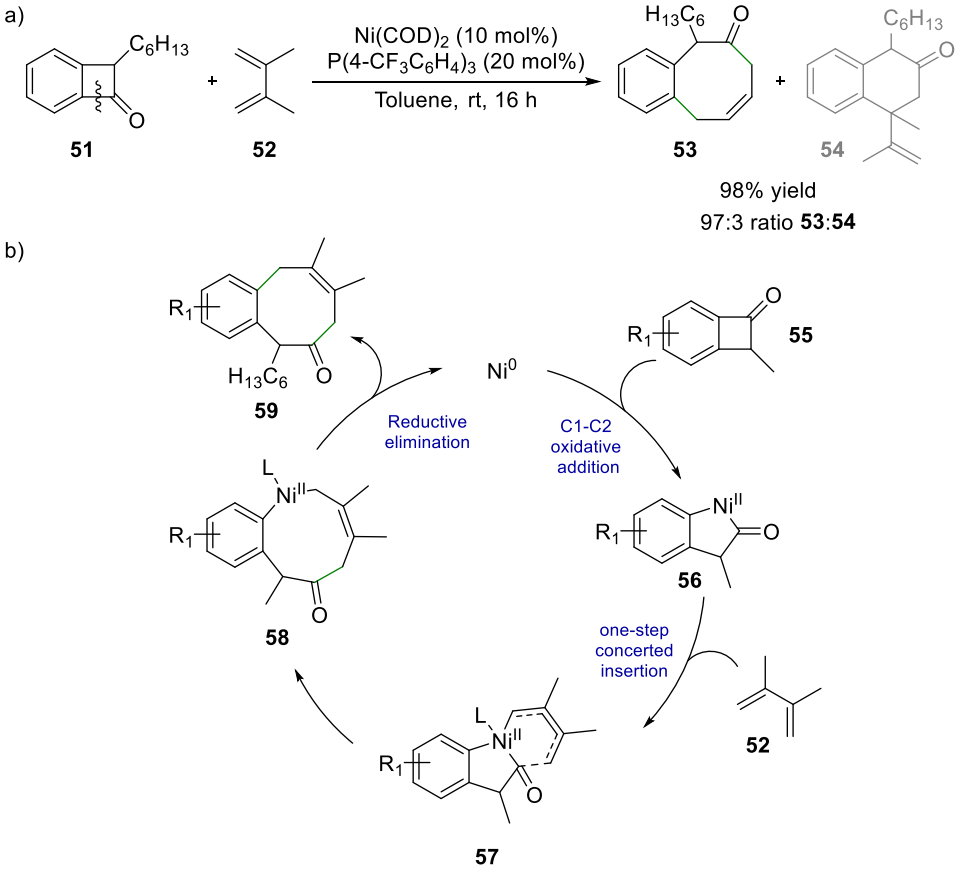

Scheme I.14. Nickel-catalyzed intermolecular cycloadditions of benzocyclobutenones with 1,3-dienes.

I.2. Intramolecular [4+4] Cycloadditions

To the best of our knowledge, Wender *et al.* developed the first intramolecular nickel-catalyzed [4+4] cycloaddition reaction in 1986.[27] When bisdiene **60**, which presents a $-CH_2-C(CO_2Et)_2-CH_2-$ motif connecting the two diene units, was treated in toluene at 60 °C in the presence of catalytic amounts of $Ni(COD)_2$ and a three-fold excess of PPh_3 with respect to the nickel precursor, a mixture of cyclization products was obtained (see Scheme I.15 for the structures).[28] The major compounds **61** and **62** arose from an intramolecular [4+4] cycloaddition reaction between the two 1,3–diene units (*i.e.* formation of bicyclic 5-8 fused ring systems) and were isolated in good yield as the *cis* and *trans* isomers, being the *cis* isomer **61** the most abundant product. The products derived from a [4+2] cycloaddition reaction (*i.e.* bicyclic 5-6 fused ring system **63**) and from a β-hydride elimination (*i.e.* compound **64**) were also observed.[29]

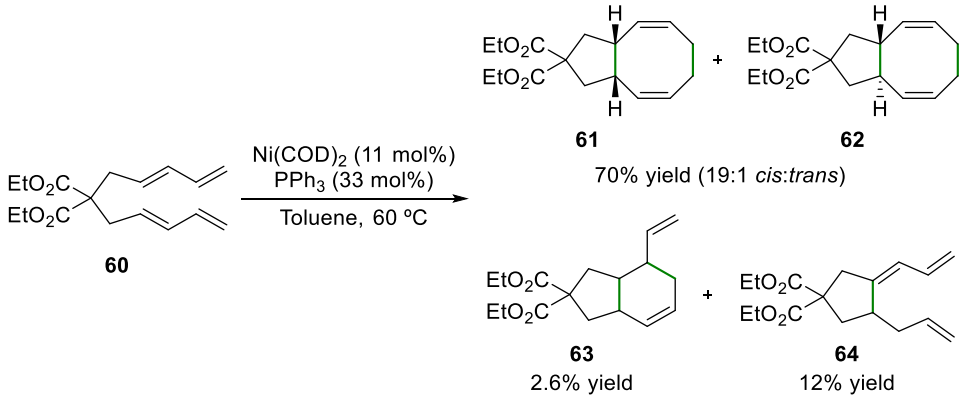

Scheme I.15. Ni-catalyzed intramolecular [4+4] cycloaddition of substrate **60**.

Wender *et al.* expanded the structural diversity of the 1,3-bisdiene unit by modifying the number of carbons connecting the two diene units, or by introducing diverse substituents at the connecting carbon chain and/or diene units.

As regards intramolecular [4+4] cycloaddition reactions between the two 1,3-diene units in systems presenting a substituted four-methylene group connecting

(27) Wender, P. A.; Ihle, N. C. *J. Am. Chem. Soc.* **1986**, *108*, 4678-4679.
(28) Whilst compound **61** is achiral, compounds **62** and **64** were obtained in racemic form and only one of the two possible enantiomers is depicted in the figure above. Compound **63** can be obtained as a mixture of 4 diastereomeric pairs of enantiomers and no details on the stereomeric composition of these compounds were provided by the authors.
(29) The mechanistic rationalization on the formation of all products will be discussed later.

the two diene units, the expected bicyclic 6-8 fused ring systems were obtained with yields ranging from 66 to 92% (see Scheme I.16).[27,30] In all cases studied, the reactions led to *trans*-fused products through an *exo* cycloaddition mode. The influence of the substituents was also studied by Wender *et al.* When one methylene carbon next to the diene unit had a substituent, the ratio between the two *trans*-isomers **66** Scheme I.16a) was as high as >70:1 between the α and β isomers (the isomers with the X substituents pointing up on the bicyclic systems in Scheme I.16 are described as β, whilst those with the X substituents pointing down on the ring system are described as α[31]). In contrast, lower ratios between the α and β isomers were observed when the carbons next to the diene units were methylene groups (ratio up to 1:2.2, see results for **68** in Scheme I.16).

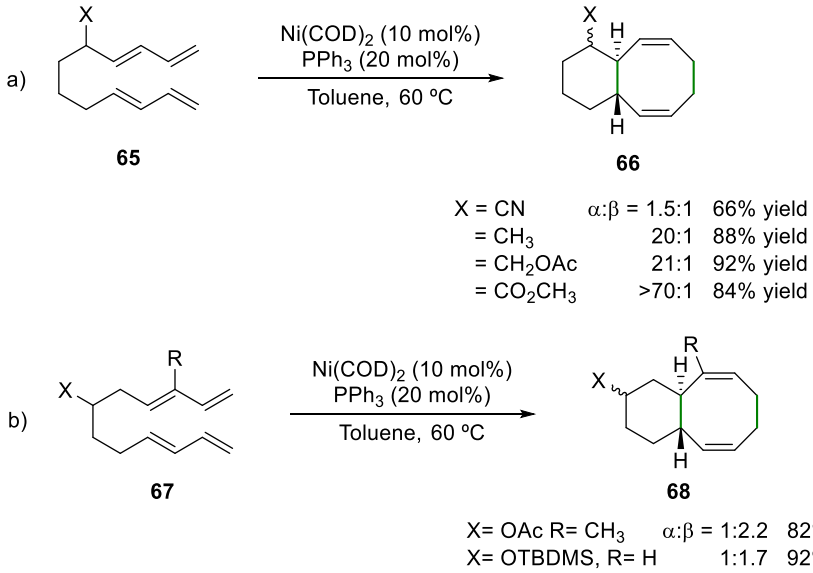

Scheme I.16. Intramolecular [4+4] cycloaddition reactions in systems with a substituted four-methylene group connecting the two diene units.

This synthetic methodology was then applied by Wender *et al.* to the synthesis of compounds having the taxane skeleton. Two different approaches, model A and model B, were studied and the corresponding starting materials, substitution patterns and final products are indicated in Scheme I.17.

(30) Wender, P. A.; Snapper, M. L. *Tetrahedron Lett.* **1987**, *28*, 2221-2224.

(31) The α and β stereodescriptors were originally devised for the nomenclature of stereoids and are only meaningful if there is an agreed absolute configuration and orientation of the structure so as to define the plane and how the molecule is represented. However, this nomenclature has been respected in this thesis, as it was used by Wender *et al.* in the original papers.

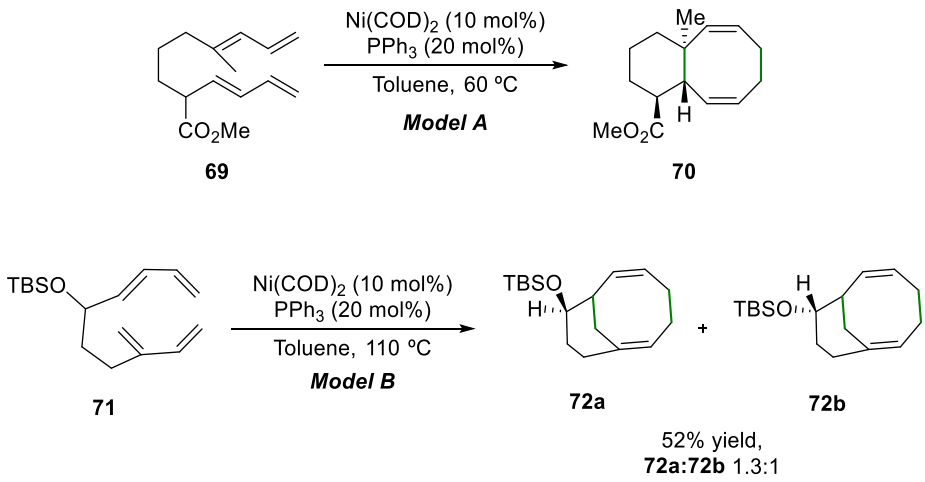

Scheme I.17. Approaches to the synthesis of the taxane skeleton.

Model A provided cycloadduct **70** in 92% yield and 97% diastereoselectivity in favor of the stereoisomer depicted in Scheme I.17 at 94% of conversion, whereas model B gave cycloadduct **72** in 52% yield (**72a**:**72b** ratio equal to 1.3:1) at 68% conversion.[32] In the case of model B, different ligands and ligand to metal ratios were explored. The best results were obtained with the reaction conditions indicated in Scheme I.18, which involved the use of P(O-*o*-BiPh)$_3$ as ligand[33] and a 3 to 1 ratio of ligand and nickel precursor.[34]

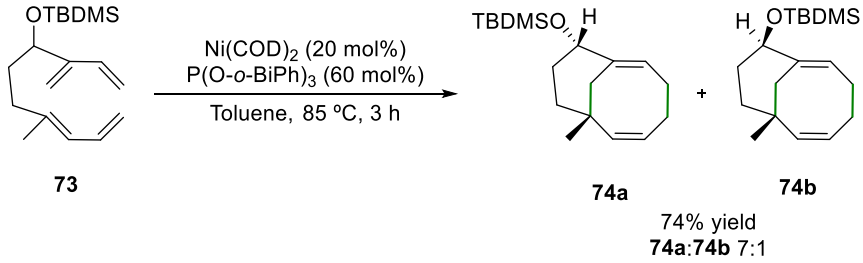

Scheme I.18. Synthesis of compounds containing the Taxane skeleton.

(32) Wender, P. A.; Ihle, N. C. *Tetrahedron Lett.* **1987**, *28*, 2451-2454.
(33) P(O-*o*-BiPh)$_3$ = tri([1,1'-biphenyl] 2-yl)phosphite. This ligand has a cone angle of 150° and a mid-range electron donating ability (estimated according to the χ value; χ = 29 for P(O-*o*-BiPh)$_3$; see ref. 34).
(34) Wender, P. A.; Tebbe, M. J. *Synthesis* **1991**, 1089-1094.

Wender *et al.* also applied this nickel catalyzed [4+4] intramolecular cycloaddition as the key step in the total synthesis of (+)-Asteriscanolide[35] and Ophiobolin F.[36] For the former compound, treatment of bisdiene **75** with $Ni(COD)_2$ and PPh_3 in toluene at 90 °C led to the formation of (+)-Asteriscanolide precursor **76** in 67% yield. As for the latter, treatment of bisdiene **77** with $Ni(COD)_2$ and PPh_3 in toluene, followed by desilylation, afforded bicyclic cyclooctadiene **78** in 60% yield (Scheme I.19). Further transformations yielded the core structure of Ophiobolin F. The same group further demonstrated the usefulness of this approach by reducing the steps on the total synthesis of (±)-sasolene oxide from **16** to **8**.[37]

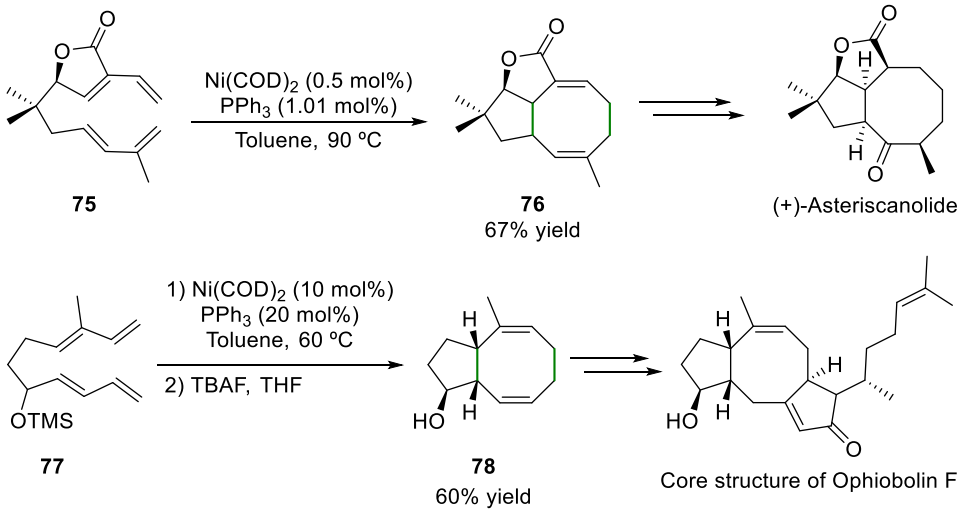

Scheme I.19. Intramolecular [4+4] cycloaddition reactions applied to the total synthesis of (+)-Asteriscanolide and Ophiobolin F.

In a more recent publication, Chung *et al.*[38] reported the first example of rhodium-catalyzed intramolecular [4+4] cycloaddition of bis(dienes). The reaction tolerates either carbon or heteroatoms in the chain connecting the diene moieties. The reaction is highly dependent on the reaction medium, temperature, catalyst and counterion of the silver derivative. For model substrate **79**, the optimized reaction conditions were found to involve the use of bis[μ-chloro(cyclooctadiene)rhodium] (5 mol%) and silver hexafluoroantimonate (10

(35) Wender, P. A.; Ihle, N. C.; Correia, C. R. D. *J. Am. Chem. Soc.* **1988**, *110*, 5904-5906.
(36) Wender, P. A.; Nuss, J.; Smith, D. B.; Suárez-Sobrino, A.; Vgberg, J.; Decosta, D.; Bordner, J. *J. Org. Chem.* **1997**, *62*, 4908-4909.
(37) Wender, P. A.; Croatt, M. P.; Witulski, B. *Tetrahedron* **2006**, *62*, 7505-7511.
(38) Park, J. W.; Park, J. E.; Park, J. H.; Hong, M. R.; Kim, S. M.; Chung, Y. K.; Kim, C. H. *Synlett* **2016**, *27*, 455-460.

mol%) in dichloroethane/ethyl acetate (2:1) as a solvent at 120 °C with a reaction time of 12 h (Scheme I.20). It is interesting to note that the efficiency of the reaction was reduced by the addition of a phosphine ligand such as PPh_3, dppe or PCy_3.

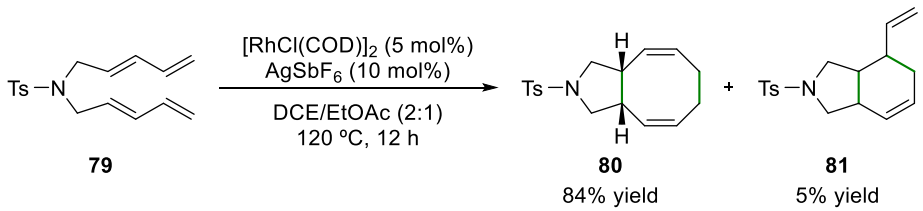

Scheme I.20. Rhodium-catalyzed intramolecular [4+4] cycloaddition of substrate **79**.

Minor modifications were needed depending on the substrate. For instance, the [4+4] cycloaddition of compound **82** benefited from the addition of 20 mol% of tris(4-fluorophenyl)phosphine (Scheme I.21).

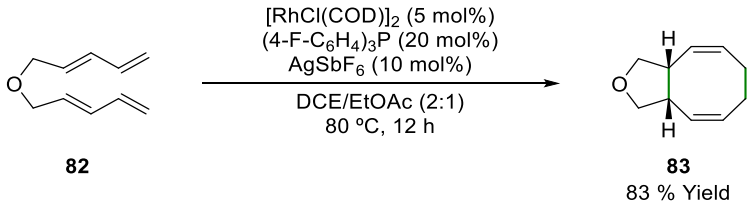

Scheme I.21. Rhodium-catalyzed intramolecular [4+4] cycloaddition of **82**.

Wender *et al.* have also described a photo-induced methodology for the cycloaddition of **60** and **82**, which after thermolysis yielded cycloadducts **61** and **83**, respectively.[39] Furthermore, thermally and photochemically induced CuOTf-catalyzed intramolecular cycloaddition reactions of **82** have also been reported, yielding mainly vinylcyclohexene derivatives.[40] This methodology falls beyond the scope of the present thesis and will not be discussed any further.

A different type of substrates for intramolecular [4+4] cycloadditions was introduced by Murakami and Ito in 1999.[41] They reported a palladium-catalyzed [4+4] cycloaddition reaction between vinyl allenes having a pendant phenyl or vinyl substituent (Scheme I.22a or 22b, respectively). The [4+2] cycloaddition competed with the [4+4] process, even to the point of being the major product for the vinyl substituted allene **87** (Scheme I.22b).

(39) Wender, P. A.; Correia, C. R. D. *J. Am. Chem. Soc.* **1987**, *109*, 2523-2525.
(40) Hertel, R.; Mattay, J.; Runsink, J. *J. Am. Chem. Soc.* **1991**, *113*, 657-665.
(41) Murakami, M.; Itami, K.; Ito, Y. *Synlett* **1999**, *1999*, 951-953.

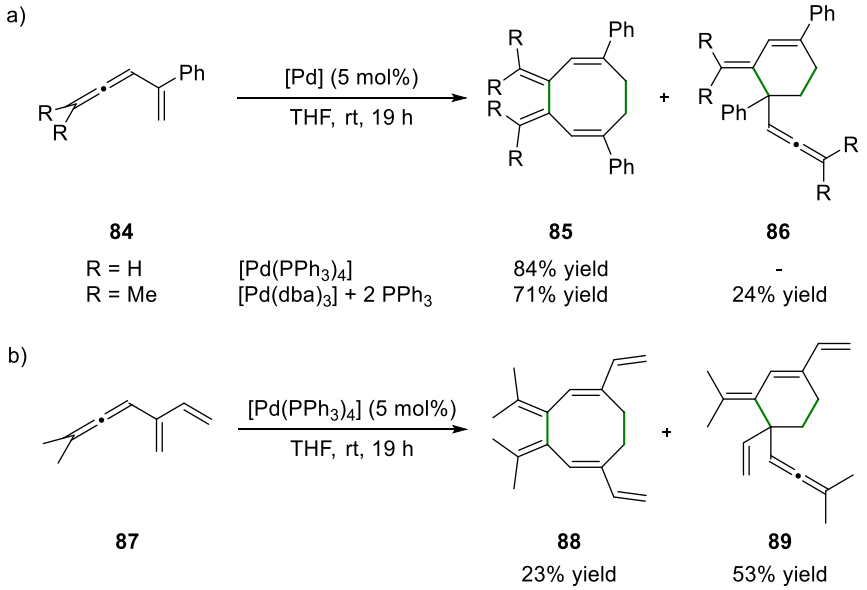

Scheme I.22. Eight-membered ring formation by palladium-catalyzed [4+4] cycloaddition of vinyl allenes.

Lee and coworkers further developed this transformation by expanding the scope to *in situ* formed vinyl allenes from α-bromovinyl arenes and propargyl bromides (Scheme I.23).[42] The formed [4+4] cycloadduct **93** further reacted with various dienophiles to give bicyclic 6-8 fused ring systems **94**. More importantly, this reaction was accomplished in one pot to efficiently yield the final product.

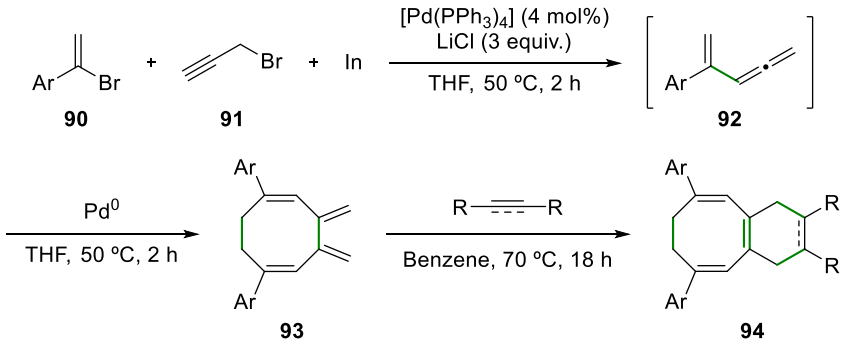

Scheme I.23. *In situ* formation of vinyl allenes and subsequent [4+4] cycloaddition.

In order to rationalize the outcome of the reaction, a tandem reaction pathway was suggested by Lee and coworkers. Their mechanistic rationalization complements the one originally proposed by Murakami and Ito.[41] Oxidative

(42) Lee, P. H.; Lee, K.; Kang, Y. *J. Am. Chem. Soc.* **2006**, *128*, 1139-1146.

addition of a Pd(0) catalyst to the vinyl bromide gives **95**. Then, transmetalation between **95** and the complex between indium and **91**, followed by reductive elimination, leads to the *in situ* formed vinyl allene **92**. Oxidative insertion of Pd(0) to this vinyl allene produces the five-membered palladacycle **96**, which subsequently reacts with another molecule of **92** at the internal double bond of the allene group to give a bis(σ-allyl)palladium intermediate **98**. Subsequent reductive elimination gives rise to the eight-membered carbocycle **93**.

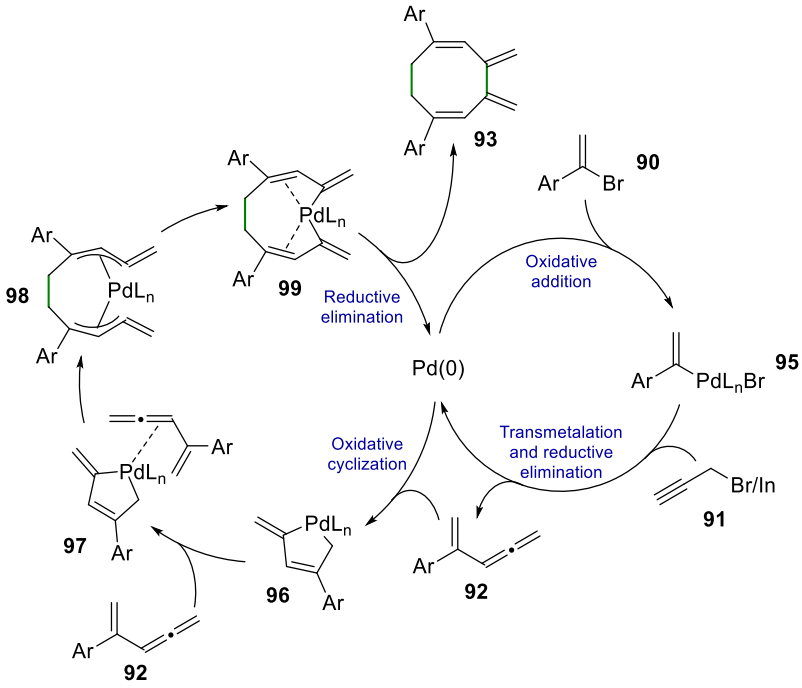

Scheme I.24. Mechanism proposed by Lee *et al.*

I.3. [4+2+2] Cycloadditions

In the early 70s, Carbonaro *et al.* first reported a cycloaddition reaction leading to an eight-membered ring with a different type of synthetic disconnection. In this case, the cycloaddition involved one conjugated diene in one molecule and an unconjugated diene motif in a second substrate. Thus, the Fe-catalyzed reaction between norbornadiene and 1,3-butadiene (Scheme I.25a) was the first [4+(2+2)][43] cycloaddition reported.[44] The same group described also a more selective catalytic system based on cobalt ($CoCl_2$/dppe/Et_2AlCl, in toluene at 75 °C for 5 h), which yielded the cycloadduct **101** in a 68% yield in a selective manner, without **102** being formed.[45] The first example of cobalt-catalyzed [4+(2+2)] cycloadditions of norbornadiene and substituted butadienes was reported by Lyons (Scheme I.25b), however, the yields were low and no stereoselectivity was reported.[46]

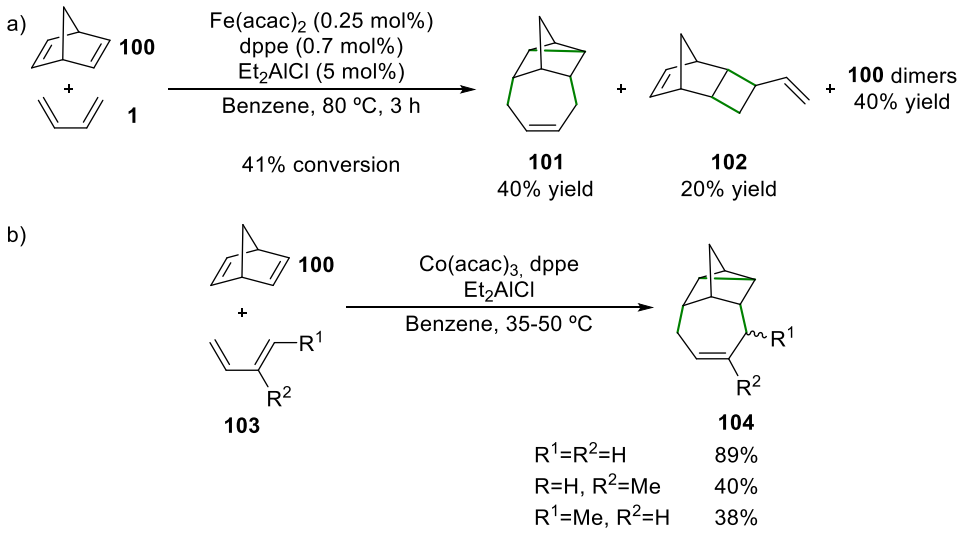

Scheme I.25. a) Seminal work by Carbonaro *et al.* and b) work reported by Lyons and coworkers.

(43) This nomenclature implies that the reaction is a two-component intermolecular reaction, where the first unit comes from one molecule and the last two from another.
(44) Greco, A.; Carbonaro, A.; Dall'Asta, G. *J. Org. Chem.* **1970**, *35*, 271-274.
(45) Carbonaro, A.; Cambisi, F.; Dall'Asta, G. *J. Org. Chem.* **1971**, *36*, 1443-1445.
(46) Lyons, J. E.; Myers, H. K.; Schneider, A. *Ann. N. Y. Acad. Sci.* **1980**, *333*, 273-285.

It was not until 1993, when Lautens and coworkers reported the first case of asymmetric induction for this transformation[47] employing a cobalt catalyst in the presence of an enantiopure phosphine ligand and Et_2AlCl as a reducing agent. Of the various enantiopure phosphines tested, (*R*)-Prophos gave the highest ee's, which were typically around 70% (see Scheme I.26).

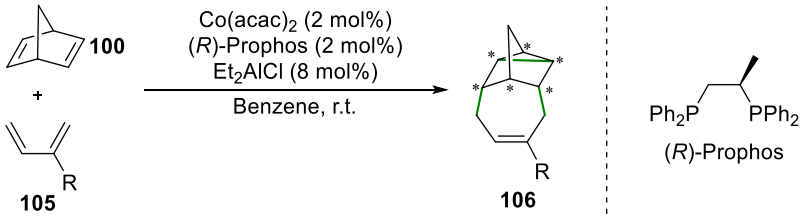

R= Me	66% yield	72% ee
$(CH_2)_8CH_3$	40% yield	74% ee
$CH_2CH_2CH{=}CMe_2$	49% yield	79% ee
$(CH_2)_3OTBS$	40% yield	73% ee
$(CH_2)_3OAc$	52% yield	73% ee
CH_2SiMe_3	49% yield	71% ee

Scheme I.26. Seminal enantioselective example of [4+(2+2)] cycloadditions.

The first intramolecular [4+2+2] cycloaddition was also reported by this group. Treatment of the polycyclic tetraene **107** with the cobalt-complex derived from $Co(acac)_2$, dppe and a Lewis acid furnished the polycyclic alkene **108** in modest yield as a single stereoisomer.[47b]

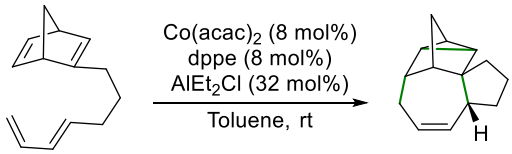

107 **108**
40% yield

Scheme I.27. Intramolecular [4+2+2] Cobalt-catalyzed cycloaddition.

In the late 90s, the group of Snyder expanded the scope of the achiral [4+(2+2)] cycloaddition to functionalized norbornadienes (Scheme I.28).[48] This approach also provided a more compelling synthetic utility of this process, since the cycloadducts could be transformed easily into useful bicyclo[5.3.0]decanes (Scheme I.28) by a Pt-catalyzed rearrangement and ring opening reaction.[48]

(47) (a) Lautens, M.; Tam, W.; Sood, C. *J. Org. Chem.* **1993**, *58*, 4513-4515. (b) Lautens, M.; Tam, W.; Lautens, J. C.; Edwards, L. G.; Crudden, C. M.; Smith, A. C. *J. Am. Chem. Soc.* **1995**, *117*, 6863-6879.

(48) Chen, Y.; Snyder, J. K. *J. Org. Chem.* **1998**, *63*, 2060-2061.

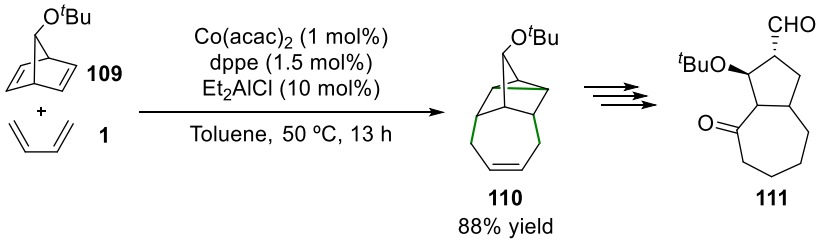

Scheme I.28. [4+(2+2)] Cycloaddition of functionalized norbornadiene and butadiene followed by derivatization.

The first [4+(2+2)] cycloaddition which did not involve a norbornadiene derivative was reported by Evans *et al.*[49] Rhodium was the metal of choice for this system consisting of butadiene and an heteroatom-tethered enyne derivative. Nitrogen, sulfur, and oxygen were tolerated as tethers, and the presence of a silver salt was critical to generate the cationic rhodium catalyst (Scheme I.29a). Interestingly, an example of an *in situ* generated enyne derivative was also reported, with good yield and selectivity (Scheme I.29b). In a subsequent work, the same group found that the use of a *N*-heterocyclic carbene (NHC) in combination with a rhodium precursor gave high diastereoselectivities for substituted enynes (Scheme I.29c).[50] This was the first example of a rhodium-NHC complex catalyzed three-component [m+n+o] cyclization to give eight-membered carbocycles with high diastereoselectivities.

(49) (a) Evans, P. A.; Robinson, J. E.; Baum, E. W.; Fazal, A. N. *J. Am. Chem. Soc.* **2002**, *124*, 8782-8783. For the diastereoselective version using a temporary silicon-tethered system, see (b) Evans, P. A.; Baum, E. W. *J. Am. Chem. Soc.* **2004**, *126*, 11150-11151.

(50) (a) Evans, P. A.; Baum, E. W.; Fazal, A. N.; Pink, M. *Chem. Commun.* **2005**, 63-65. For the computational study of the mechanism, see (b) Baik, M.-H.; Baum, E. W.; Burland, M. C.; Evans, P. A. *J. Am. Chem. Soc.* **2005**, *127*, 1602-1603.

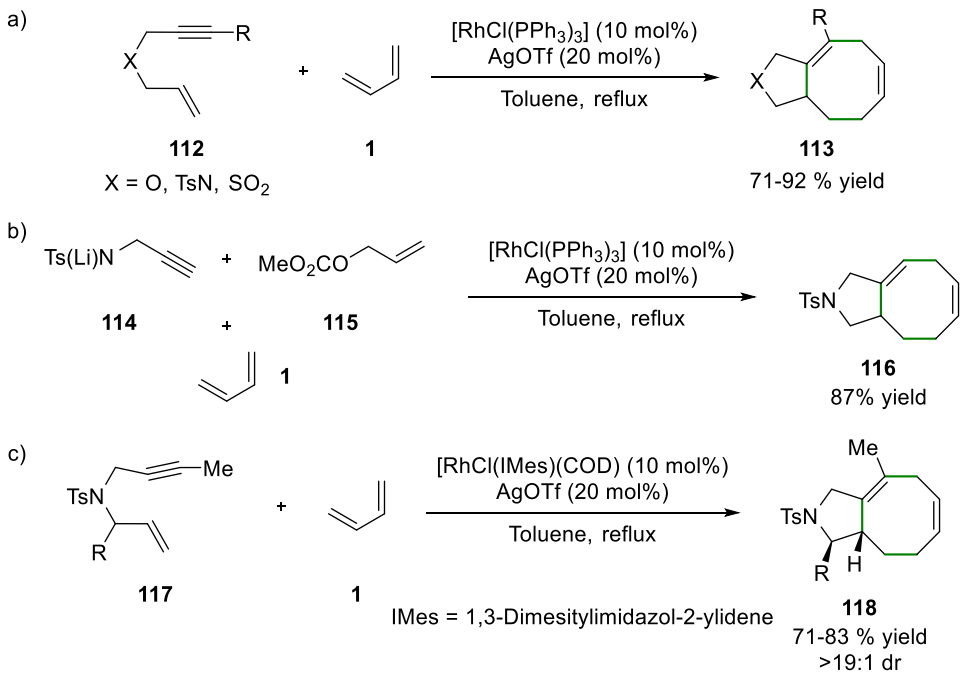

Scheme I.29. [4+(2+2)] cycloadditions reported by Evans *et al.*

After high-level DFT calculations and experimental evidences, a mechanism was proposed,[50b] in which, after coordination of **119** to the rhodium metal center from **121**, an intermolecular cyclization took place starting from the intermediate **122**. Surprisingly, this process was preferred over the 1,6-enyne cyclization typically described in a Pauson-Khand reaction mechanism which would lead to intermediate **125**. The coordination of an additional butadiene ligand formed the intermediate **124**, which after a reductive elimination and C–C bond formation across the ring gave the desired bicyclic product **120**. The high stereoselectivity could also be explained by this model. The two possible intermediates leading to their corresponding isomers were studied. If the carbocyclization proceeds through the typical Pauson-Khand mechanism, metallacycles **126** should furnish the bicyclooctadiene **120** as a mixture of diastereoisomers. Alternatively, the calculations predicted that, if the reaction would proceed through metallacycle **127**, it should be completely diastereoselective. Since the reaction took place with over a 19:1 diastereomeric ratio, the results support the theoretical predictions. Moreover, **127a** is energetically favored over **127b**, thus justifying the preferential formation of the major isomer. Later on, Chung and coworkers[51]

(51) Lee, S. I.; Park, S. Y.; Chung, Y. K. *Adv. Synth. Catal.* **2006**, *348*, 2531-2539.

expanded the scope of the [4+(2+2)] cyclizations to 2,3-substituted butadienes also employing rhodium-derived catalysts.

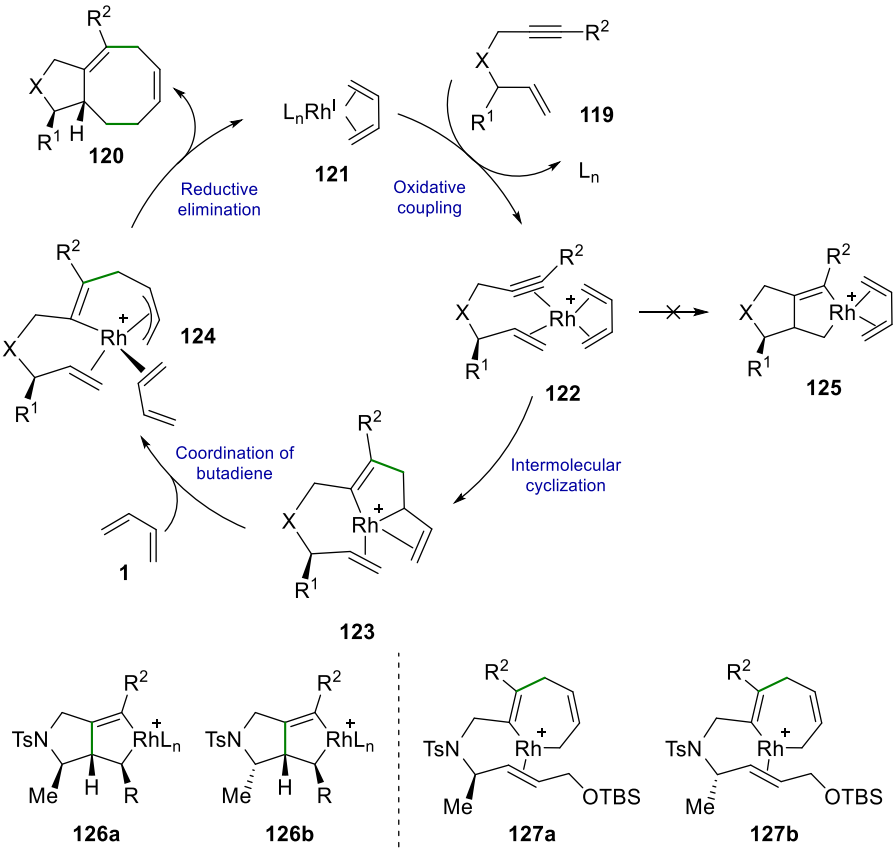

Scheme I.30. Mechanism proposed by Baik and Evans.

Saá and coworkers reported an approach towards eight-membered rings *via* a Ru-catalyzed [4+(2+2)] cycloaddition between diynes and 1,3-butadienes, which involved an unusual 8π-electrocyclization of a 1,3,5,7-tetraene (compound **136**, Scheme I.31b).[52] The reaction is really a tandem process with the Ru(II)-catalyzed formation of (*Z*)-tetraenes followed by a pure thermal conrotatory 8π-electrocyclization process taking place. This process required the addition of Et_4NCl to the reaction mixture to proceed (Scheme I.31a). The formation of the eight-membered ring is competing with the process leading to their six-membered analogues, which includes the formation of vinyl-(*Z*)-trienes **138** followed by a disrotatory 6π-electrocyclization process. The mechanism proposed by Saá is shown in Scheme I.31b.

(52) Varela, J. A.; Castedo, L.; Saá, C. *Org. Lett.* **2003**, *5*, 2841-2844.

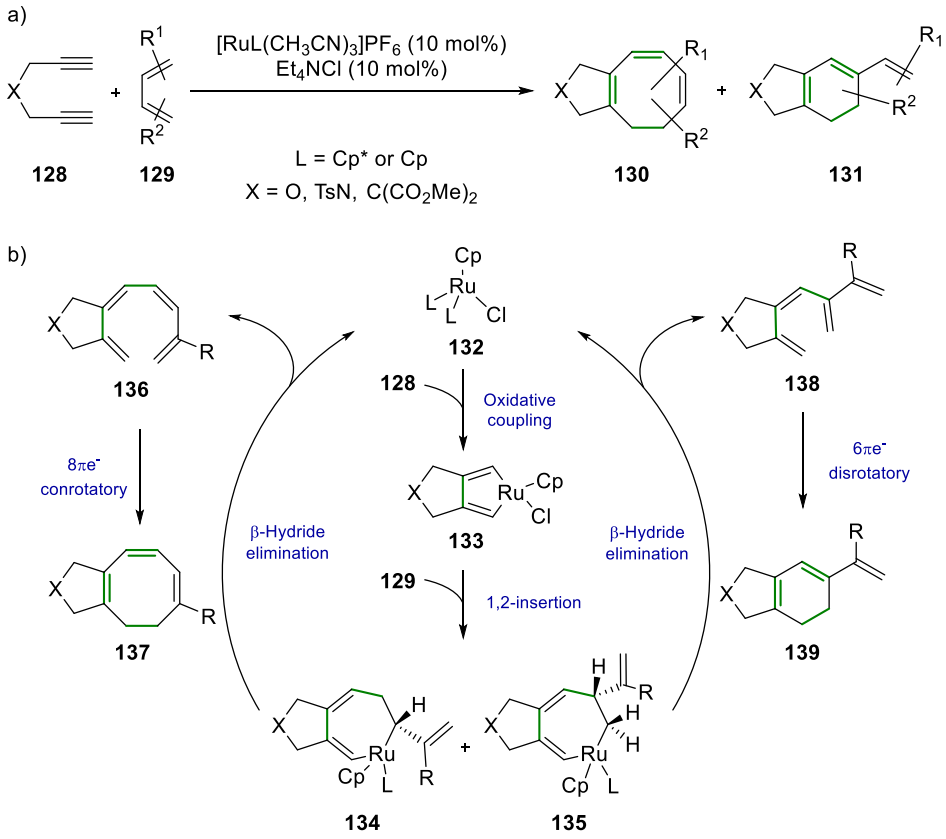

Scheme I.31. "Formal" ruthenium-catalyzed [4+(2+2)] cycloaddition.

In the first place, an oxidative coupling of the 1,6-diyne to the Ru catalyst yielded a ruthenium cyclic species (**133,** Scheme I.31b). Then, 1,2 insertion of the diene into the Ru–C bond gave rise to two seven-membered intermediates **134** and **135**. The ratio of these intermediates was determined by the substitution pattern in the butadiene component. Transition state **134** evolved through a reductive elimination to compound **136**, which finally yielded product **137** after an 8πe⁻ conrotatory electrocyclization process. Intermediate **135**, though, underwent a β-hydride elimination to give product **138**, which finally underwent a 6πe⁻ disrotatory electrocyclization process leading to vinylcyclohexadiene **139**. It was hypothesized that the role of Et_4NCl was to generate neutral complex **132** *in situ* from the cationic complex $[RuL(CH_3CN)_3]PF_6$ by exchange of the hexafluorophosphate counterion by the chlorido ligand.

To conclude with the published works involving butadiene substrates, Hilt *et al.*[53] reported a Co-based catalytic system, which mediated the coupling of two alkynes with a 1,3-diene to generate eight-membered ring systems in an unprecedented [4+2+2] fashion (Scheme I.32). The addition of iron powder to the mixture reduced the amount of side products and increased the yield of the eight-membered ring products. However, the actual role of the iron powder remains unclear. The electronic parameters responsible of the high selectivity and yield were also studied, and the authors concluded that excellent results were obtained when acceptor-substituted alkynes (terminal or internal) reacted with an electron-rich 1,3-diene, thereby generating ring systems with a high functional-group density. The products were formed regioselectively with the two substituents from the alkyne in a 1,2-relation.

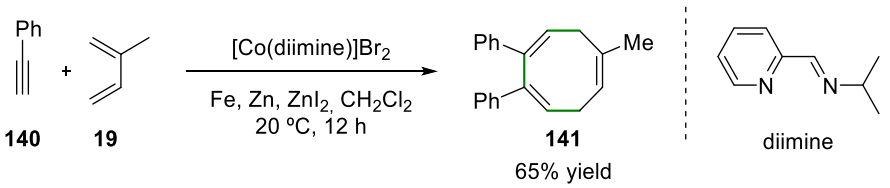

Scheme I.32. [4+2+2] Cycloaddition reported by Hilt *et al.*

Simultaneously to the work of Evans, the group of Gilbertson developed a new Rh-catalyzed [(4+2)+2] cycloaddition of dienynes and terminal alkynes (Scheme I.33a).[54] The authors observed that the cycloaddition reaction catalyzed by $[RhCl(nbd)]_2$ and $AgSbF_6$ in the presence of Me-DuPhos at 60 °C gave the final cycloadducts in good to excellent yields. The alkyne insertion was generally highly regioselective, with terminal dienes being the only exception (when R^1=H, a 1.6:1 ratio of **144**:**145** was obtained at most). Surprisingly, this reaction was discovered from the serendipitous isolation of the [(4+2)+2] cyclodimer of **142** during an investigation into intramolecular rhodium-catalyzed [4+2] cycloadditions. Compounds **146** and/or **147** can also be observed as major products in the absence of the external alkyne (Scheme I.33b). Moreover, for the [(4+2)+2] cycloadditions depicted in Scheme I.33a, the formation of the dimerization product was difficult to suppress, even in the presence of an excess of alkyne (5 equivalents). It is interesting to note that, even though an enantiopure ligand was used, no enantioselectivity was observed for acyclic

(53) Hilt, G.; Janikowski, J. *Angew. Chem., Int. Ed.* **2008**, *47*, 5243-5245.
(54) For the seminal work, see (a) Gilbertson, S. R.; DeBoef, B. *J. Am. Chem. Soc.* **2002**, *124*, 8784-8785. For optimization and expansion of the scope, see: (b) DeBoef, B.; Counts, W. R.; Gilbertson, S. R. *J. Org. Chem.* **2007**, *72*, 799-804. (c) Canlas, G. M. R.; Gilbertson, S. R. *Chem. Commun.* **2014**, *50*, 5007-5010.

substrates **142**. The substrate scope was expanded in subsequent studies,[54] with the most interesting example being the synthesis of tricyclic product **150** (Scheme I.33c), the core structure of asteriscanolide.[54]

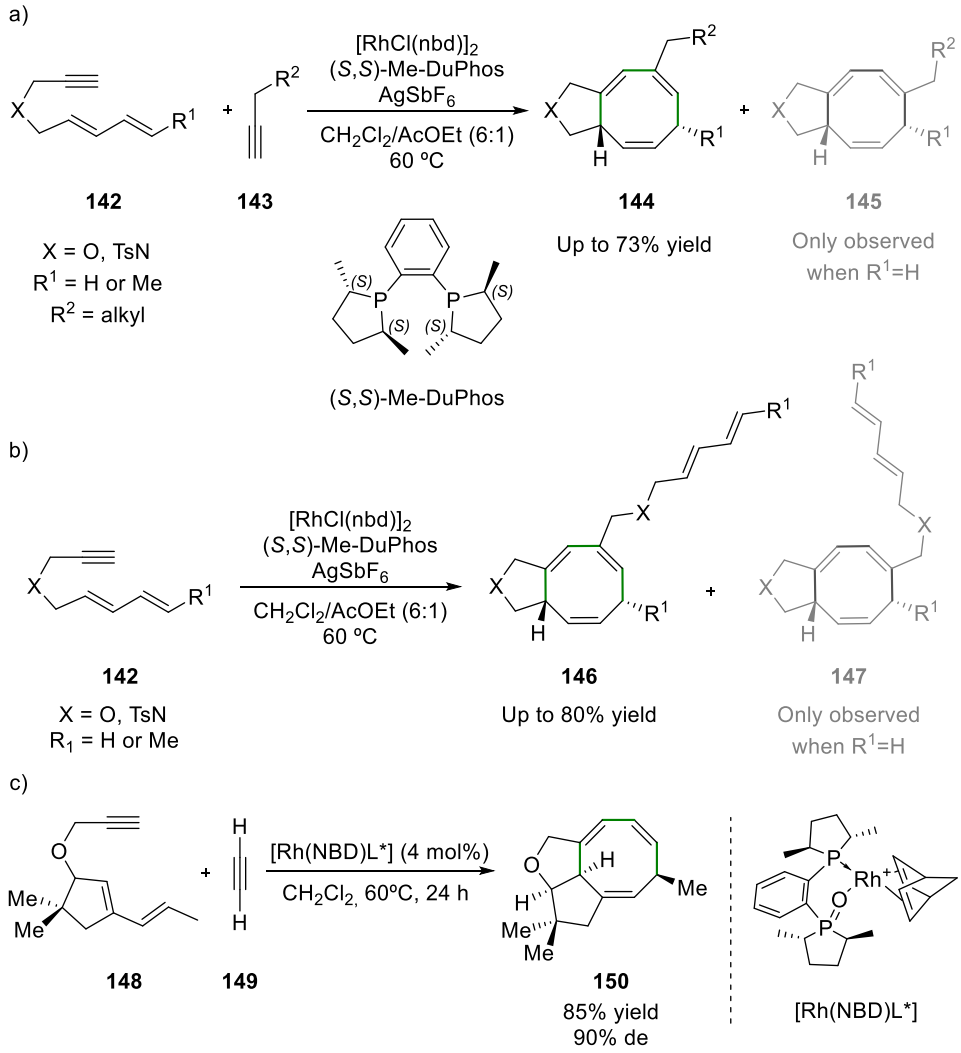

Scheme I.33. [(4+2)+2] cycloaddition of dienynes and terminal alkynes.

One important limitation of Evan's and Gilbertson's systems is the incompatibility with carbon-tethered containing dienynes. This drawback was overcome by Wender and coworkers in 2006.[55] The group reported a new [(4+2)+2] cycloaddition of dienenes and terminal alkynes catalyzed by $[RhCl(CO)_2]_2$ and $AgSbF_6$ in dichloroethane. In this system, carbon, nitrogen

(55) Wender, P. A.; Christy, J. P. *J. Am. Chem. Soc.* **2006**, *128*, 5354-5355.

and oxygen tethers can all be incorporated. The authors studied the effects of the substitution pattern of the starting materials in the regio- and diastereo-selectivity and determined that the regioselectivity of the alkyne insertion was influenced by both steric and electronic features of the alkyne. A particularly attractive feature with this approach was the ability to employ 1,1-disubstituted alkenes, which allowed the generation of quaternary stereogenic carbon centers (Scheme I.34).

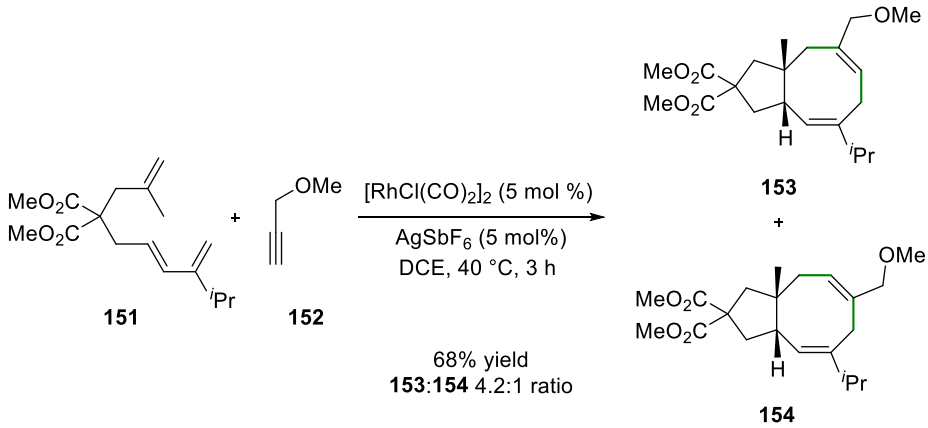

Scheme I.34. [(4+2)+2] cycloaddition of ene-dienes and terminal alkynes.

Remarkably, one example of intermolecular three-component [4+2+2] cycloaddition is also provided in Lee's study.[55] The reaction of three different unsaturated starting materials (norbornene, 2,3-dimethyl-1,3-butadiene, and methyl propargyl ether) with their reported catalytic system provided chemo-, regio-, and diastereo-selectively cycloadduct **156** (Scheme I.35).

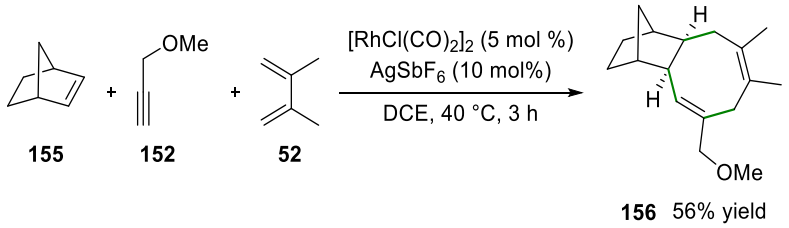

Scheme I.35. Intermolecular three-component [4+2+2] cycloaddition.

Even though most examples employ 1,3-dienes, cyclobutanones have proved to be excellent four-carbon synthons for cycloadditions. In 2006, Murakami and coworkers described the nickel-catalyzed [4+(2+2)] reaction of diynes with cyclobutanones for the construction of bicyclooctadienones (Scheme I.36).[56]

(56) (a) Murakami, M.; Ashida, S.; Matsuda, T. *J. Am. Chem. Soc.* **2006**, *128*, 2166-2167. (b) Ashida, S.; Murakami, M. *Bull. Chem. Soc. Jpn.* **2008**, *81*, 885-893.

These authors found that the *N*-heterocyclic carbene ligand IPr[57] improved the activity of the nickel catalyst compared to that for phosphine ligands, making the reaction occur at room temperature with excellent reaction yields for symmetrically substituted products **157**. The nickel–NHC catalyst also successfully converted unsymmetrical 1,6-enynes into the corresponding cycloadducts with excellent selectivity, notwithstanding the poor yields (43% yield for **157** R^1=H/Me). The phosphine ligand, however, yielded a mixture of regioisomers (**159**:**159'** ratio equal to 79:21), with the yield being higher (84% yield). The reaction is also sensitive to the nature of the diyne substituents. Terminal diynes suffered self-oligomerizations, which decreased the yield towards the desired product, and large substituents like Ph or ^{i}Pr prevented the reaction to take place, presumably due to steric reasons. Two interesting examples were substrates **160** and **163**, whose linkers were a CH_2 and CH_2-CH_2 groups, respectively. Both starting materials were converted into the desired bicyclic product with different ligands and reaction conditions for each substrate (Scheme I.36b), and with **163** being less reactive than **160**.

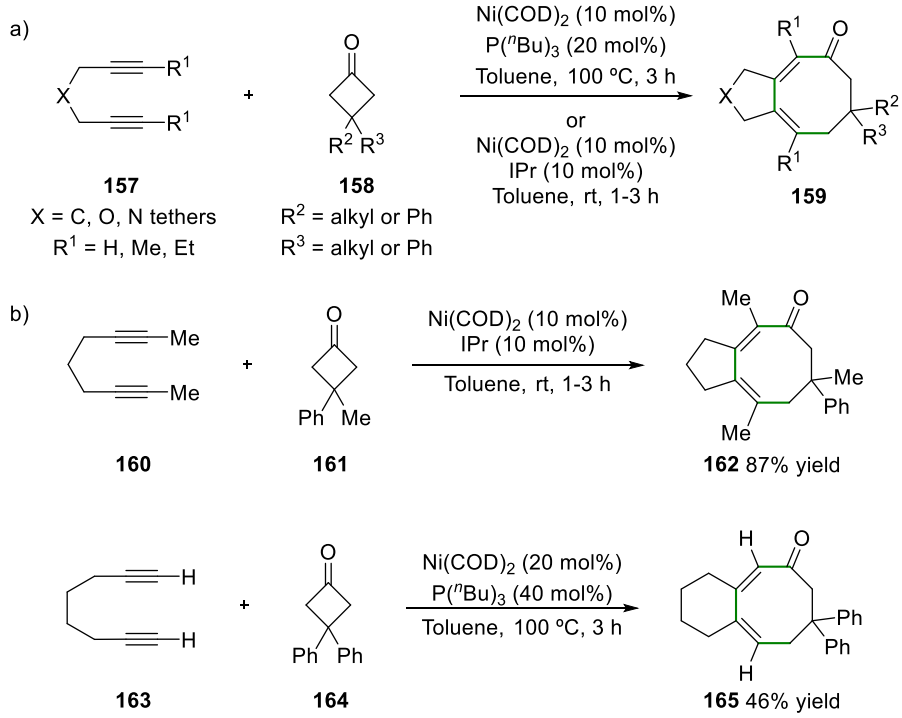

Scheme I.36. Ni-catalyzed [4+(2+2)] reaction of diynes with cyclobutanones.

(57) IPr = 1,3-Bis(2,6-diisopropylphenyl)imidazol-2-ylidene.

A mechanistic rationalization was also provided by Murakami and coworkers (Scheme I.37).[56b] The first step is the formation of the Ni(0)-diyne-cyclobutanone complex **166**, followed by intramolecular carbon–carbon bonding in the diyne *via* an oxidative cyclization leading to a five-membered ring intermediate **167**. The other possible five-membered cyclic intermediate (**167'**) resulted from an hetero-type oxidative cyclization of the carbonyl group and an alkyne moiety. Subsequent incorporation of the third unsaturated functionality into the Ni–C bond of either five-membered nickelacycles **167** or **167'** led to the formation of spirocyclic oxanickelacycloheptadiene **168**. The last step is a β-carbon elimination forming the 9-membered nickelacycle ring **169**, followed by catalyst regeneration and formation of the final product after reductive elimination. This proposed mechanism was later confirmed by computational studies[58] which also rationalized the higher reactivity of NHC ligands compared to that for phosphines. These studies revealed that a "dynamic electron density circuit" in the Ni–IPr system stabilizes the transition states during the reaction pathways.

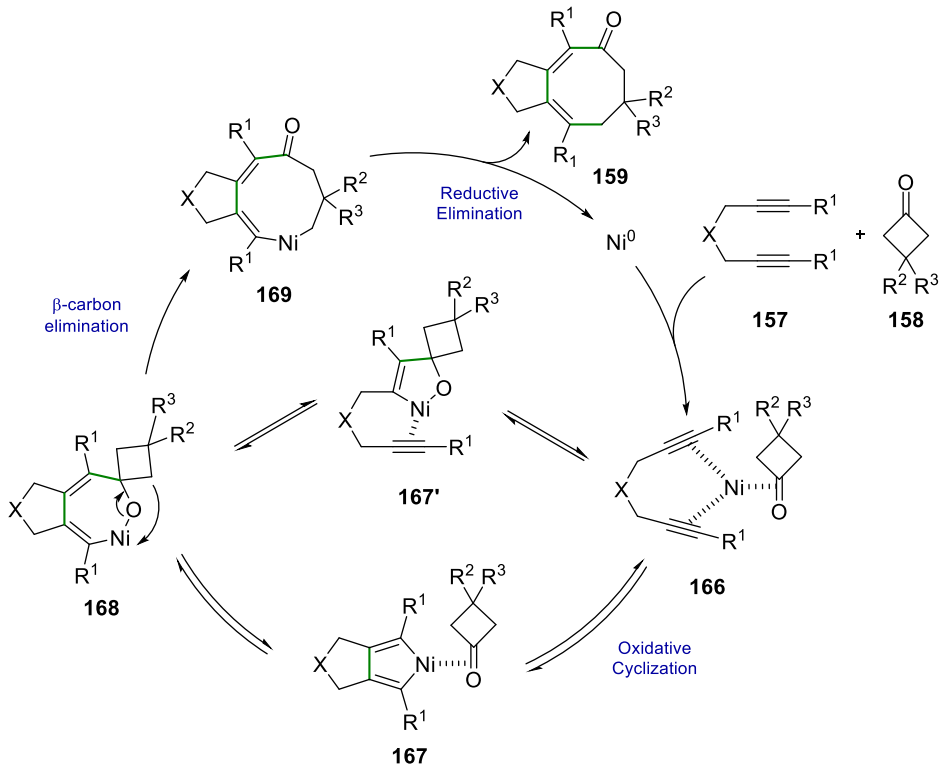

Scheme I.37. Proposed mechanism by Murakami *et al.*

(58) Tao, J.-Y.; Fang, D.-C.; Chass, G. A. *Phys. Chem. Chem. Phys.* **2012**, *14*, 6937-6945.

To the best of our knowledge, only one example of [4+2+2] cycloaddition of allenedienes and allenes for the construction of fused cyclooctanes has been reported (Scheme I.38).[59] This catalytic cycloaddition was successful with a diverse set of diene and allene components and provided unique bicyclic 5-8 *cis*-fused carbocycles. The use of phosphoramidite ligands enabled the synthesis of the corresponding [4+4] cycloadducts with high enantioselectivities, but the parallel formation of the [4+2] cycloaddition product could not be suppressed.

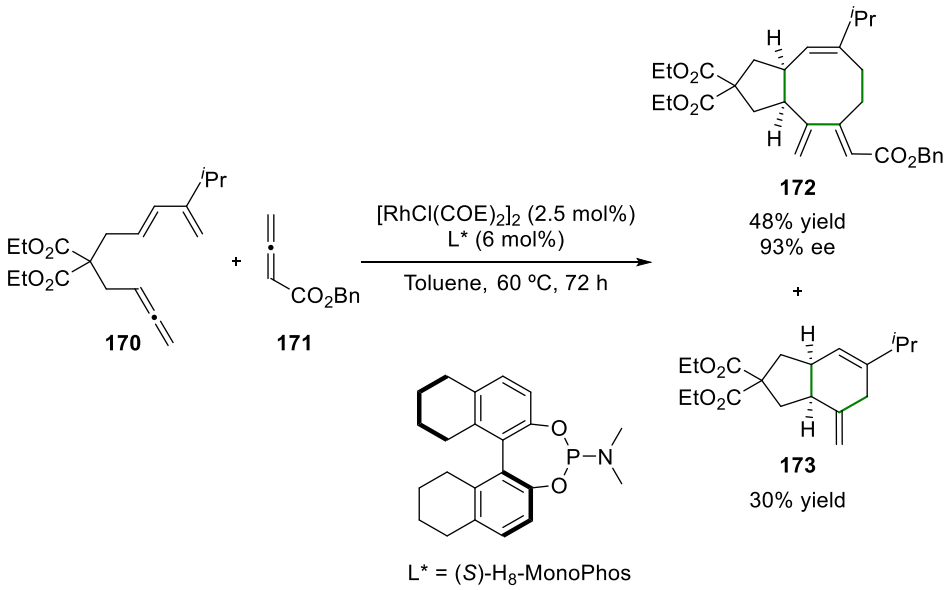

Scheme I.38. Enantioselective Rh-catalyzed [4+2+2] allenediene-allene cycloadditions.

(59) Lainhart, B. C.; Alexanian, E. J. *Org. Lett.* **2015**, *17*, 1284-1287.

UNIVERSITAT ROVIRA I VIRGILI
TRANSITION METAL-CATALYZED CYCLOADDITION REACTIONS FOR THE FORMATION OF EIGHT- AND SIX-MEMBERED RINGS
Nuria Llorente González

Objectives

As previously summarized in this section, cycloaddition reactions are an elegant and efficient atom-economical synthetic methodology towards the construction of medium-sized fused rings, which are key structural motifs in a significant number of natural products. To that end, several cycloaddition reactions yielding challenging eight-membered rings have been explored to date. Even though studies on intramolecular [4+4] cycloadditions of bis-dienes were pioneered by Wender in 1986, the study of this chemistry on prochiral bis-dienes containing heteroatoms as tethers remained scarcely explored at the beginning of the present PhD thesis, and no rationalization on the stereochemical outcome of the cycloadditions had been reported. More importantly, enantioselective versions of intramolecular [4+4] cycloadditions of bis-dienes to yield eight-membered carbocycles were, to the best of our knowledge, unexplored.

Moreover, our group has developed new catalytic systems based on the use of halogen bonding as a tool to construct the backbone of the catalyst. The new catalyst XBPhos-Rh was described by the group and used in the hydroboration of terminal alkynes with excellent regioselectivities towards the branched alkenylboronic acid derivatives. Being rhodium a privileged metal for cycloaddition reactions, studies on the use of XBPhos-Rh as catalyst in cycloaddition reactions remained also unexplored.

Therefore, the objectives of the present thesis are as follows:

1. Study of nickel(0)-based catalysts derived from achiral phosphine ligands for intramolecular [4+4] cycloaddition reactions on model bis-diene systems and further rationalization of the stereochemical outcome of the cycloaddition reactions.
2. Development of enantioselective catalytic systems for [4+4] cycloaddition reactions, based on the catalytic systems studied in the previous section. The aim of these studies encompassed the assessment of the activity and stereoselectivity of catalysts derived from structurally diverse enantiopure phosphorus ligands and nickel(0) precursors in intramolecular [4+4] cycloaddition reactions.
3. Evaluation of the catalytic activity of nickel and iron complexes derived from diverse ligand scaffolds for the synthesis of eight-membered rings through [4+2+2] and [4+4] cycloaddition reactions, respectively.
4. Assessment of the catalytic activity of halogen-bond-assembled diphosphine rhodium complexes in cycloaddition reactions.

UNIVERSITAT ROVIRA I VIRGILI
TRANSITION METAL-CATALYZED CYCLOADDITION REACTIONS FOR THE FORMATION OF EIGHT- AND SIX-MEMBERED RINGS
Nuria Llorente González

CHAPTER 1

Ni-Catalyzed Intramolecular [4+4] Cycloadditions of Bisdienes Towards Eight-Membered Fused Bicyclic Systems

A Combined Experimental and Computational Study

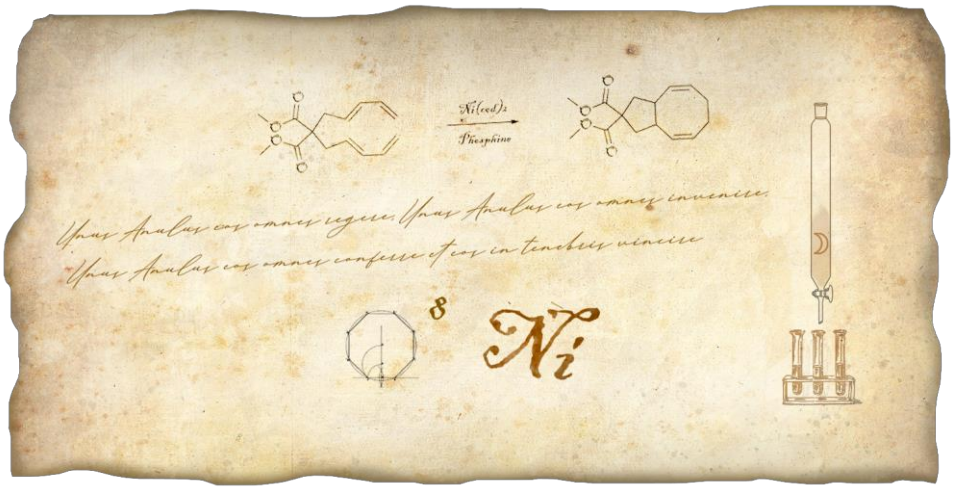

UNIVERSITAT ROVIRA I VIRGILI
TRANSITION METAL-CATALYZED CYCLOADDITION REACTIONS FOR THE FORMATION OF EIGHT- AND SIX-MEMBERED RINGS
Nuria Llorente González

Ni-Catalyzed Intramolecular [4+4] Cycloadditions of Bisdienes Towards Eight-Membered Fused Bicyclic Systems

A Combined Experimental and Computational Study

1.1 Introduction

Medium-sized cyclic compounds, and in particular eight-membered fused polycyclic systems, are key structural motifs in a significant number of natural products (Figure 1.1).[1] Among the different strategies for the preparation of such compounds,[2] metal-mediated intramolecular [4+4] cycloadditions are an elegant, efficient, and atom-economical synthetic methodology. Although metal-mediated [4+4] cycloadditions of two diene units have been known for some time,[3] it was Wender's research group[4] who pioneered the use of intramolecular nickel-catalyzed [4+4] cycloadditions for the highly diastereoselective synthesis of complex natural products (or advanced synthetic intermediates thereof). In Wender's studies, the configurations of the substituted carbons in the tether linking the two diene units were responsible for the high diastereoselectivities

(1) See, for example: (a) Blanchard, N.; Eustache, J. In *Metathesis in Natural Product Synthesis: Strategies, Substrates and Catalysts*; Cossy, J.; Arseniyadis, S.; Meyer, C., Eds.; Wiley-VCH Verlag GmbH & Co.: Weinheim, 2010; Vol. 1, pp 1-43. (b) Wang, Y.; Yu, Z.-X. *Acc. Chem. Res.* **2015**, *48*, 2288-2296.

(2) For general reviews, see: (a) Kaupp, G. *Angew. Chem., Int. Ed. Engl.* **1992**, *31*, 422-424. (b) Sieburth, S. M.; Cunard, N. T. *Tetrahedron* **1996**, *52*, 6251-6282. (c) Yu, Z.-X.; Wang, Y.; Wang, Y. *Chem.-Asian J.* **2010**, *5*, 1072-1088.

(3) (a) Reed, H. W. B. *J. Chem. Soc.* **1954**, 1931-1941. (b) Brenner, W.; Heimbach, P.; Hey, H.; Müller, E. W.; Wilke, G. *Liebigs Ann. Chem.* **1969**, *727*, 161-182. (c) van Leeuwen, P. W. N. M.; Roobeek, C. F. *Tetrahedron* **1981**, *37*, 1973-1983.(d) tom Dieck, H.; Dietrich, J. *Chem. Ber.* **1984**, *117*, 694-701. (e) tom Dieck, H.; Dietrich, J. *Angew. Chem., Int. Ed. Engl.* **1985**, *24*, 781-783. (f) Tenaglia, A.; Brun, P.; Waegell, B. *J. Organomet. Chem.* **1985**, *285*, 343-357. (g) Mallien, M.; Haupt, E. T. K.; tom Dieck, H. *Angew. Chem., Int. Ed. Engl.* **1988**, *27*, 1062-1064. (h) Baldenius, K. U.; tom Dieck, H.; König, W. A.; Icheln, D.; Runge, T. *Angew. Chem., Int. Ed. Engl.* **1992**, *31*, 305-307.

(4) (a) Wender, P. A.; Ihle, N. C. *J. Am. Chem. Soc.* **1986**, *108*, 4678-4679. (b) Wender, P. A.; Snapper, M. L. *Tetrahedron Lett.* **1987**, *28*, 2221-2224. (c) Wender, P. A.; Ihle, N. C. *Tetrahedron Lett.* **1987**, *28*, 2451-2454. (d) Wender, P. A.; Tebbe, M. J. *Synthesis* **1991**, 1089-1094. (e) Wender, P. A.; Nuss, J.; Smith, D. B.; Suárez-Sobrino, A.; Vgberg, J.; Decosta, D.; Bordner, J. *J. Org. Chem.* **1997**, *62*, 4908-4909.

UNIVERSITAT ROVIRA I VIRGILI
TRANSITION METAL CATALYZED CYCLOADDITION REACTIONS FOR THE FORMATION OF EIGHT- AND SIX-MEMBERED RINGS
Nuria Llorente González

observed.[4] The practicality of this approach was demonstrated by preparing (+)-asteriscanolide and (±)-salsolene oxide (Figure 1.1) using this chemistry as the key step.[5] More recently, Cheung and coworkers have used rhodium(I) complexes as catalysts in this type of cycloaddition for the efficient preparation of the corresponding cyclooctadiene derivatives,[6] though harsher reaction conditions than those reported by Wender are required.

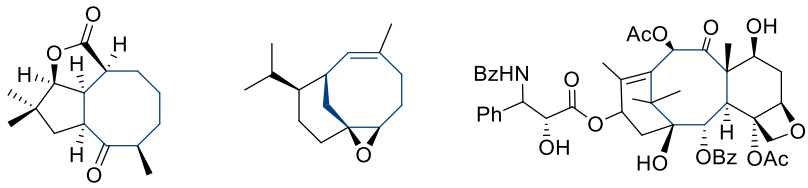

Figure 1.1. Representative examples of natural products incorporating an eight-membered carbocycle.

Whilst diastereoselective nickel-catalyzed intramolecular [4+4] cycloadditions of bisdienes have been reported, the study of this nickel chemistry on prochiral bisdienes containing heteroatoms in the tether between the two diene units remained scarcely explored.[4] Herein, we wish to report our findings on the development of nickel(0)-based achiral catalysts for intramolecular [4+4] cycloadditions of structurally diverse prochiral bisdiene substrates (Scheme.1.1). We also aim to disclose the effects of substituents and C=C double bond geometries on the outcome of the [4+4] cycloadditions. Computational studies have been performed to identify the relevant transition states of the stereo-determining step and their relative stabilities and consequently provide a rationalization of the stereochemical outcome of the reaction.

(5) (a) Wender, P. A.; Ihle, N. C.; Correia, C. R. D. *J. Am. Chem. Soc.* **1988**, *110*, 5904-5906. (b) Wender, P. A.; Croatt, M. P.; Witulski, B. *Tetrahedron* **2006**, *62*, 7505-7511.

(6) Park, J. W.; Park, J. E.; Park, J. H.; Hong, M. R.; Kim, S. M.; Chung, Y. K.; Kim, C. H. *Synlett* **2016**, *27*, 455-460.

1.2 Results and Discussion

1.2.1. Study of the [4+4] Cycloadditions

At the onset of our studies, we used oxygen-containing bisdiene **1a** as the model substrate, as its preparation was already reported.[7] The intramolecular [4+4] cycloaddition of **1a** was studied in the presence of catalytic amounts of [Ni(COD)$_2$] (COD = 1,5-cyclooctadiene) and a set of phosphorus monodentate ligands (**L1-L6**; see Table 1.1 for the structures), in order to test the influence of the ligand on both the reactivity and selectivity of the nickel catalyst.[8]

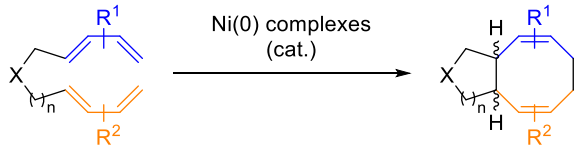

Scheme.1.1. Nickel-catalyzed intramolecular [4+4] cycloadditions studied.

When PPh_3 (**L1**) was used as the ligand, the *cis*-fused cyclooctadiene **2a** was obtained in good isolated yields (see entry 1 in Table 1.1). Under these reaction conditions, one of the possible [4+2] cycloaddition products (**3a**)[9] was identified in the crude mixture. We were then interested in studying how the electronic properties of the phosphorus ligands affected the outcome of the cycloaddition reactions. Interestingly, the electron-rich triarylphosphine **L2** provided compound **2a** in almost identical yield to triphenylphosphine and gave only minimal amounts of products **3a** (compare entry 2 with entry 1 in Table 1.1).

(7) Its reported preparation method involved using (*E*)-5-chloropenta-1,3-diene with small amounts of the *cis*-isomer (ratio *E*,*E*:*E*,*Z* isomers > 95:5). For the preparation of substrate **1a**, see also: (a) Hertel, R.; Mattay, J.; Runsink, J. *J. Am. Chem. Soc.* **1991**, *113*, 657-665. For the preparation of substrate **1b**, see also: (b) Takacs, J. M.; Lawson, E. C. *Organometallics* **1994**, *13*, 4787-4793. For the preparation of substrate **1c**, see also: (c) Takimoto, M.; Mori, M. *J. Am. Chem. Soc.* **2002**, *124*, 10008-10009.

(8) The reaction of substrate **1a** exclusively in the presence of Ni(COD)$_2$ (10.0 mol%) led to a complex mixture of unidentified products at 90% conversion.

(9) Given the small amounts of product, no attempts were made to elucidate the relative stereochemistry of the stereogenic carbons.

Table 1.1: Screening of ligands for the nickel-catalyzed intramolecular [4+4] cycloaddition of substrate **1a**.[a]

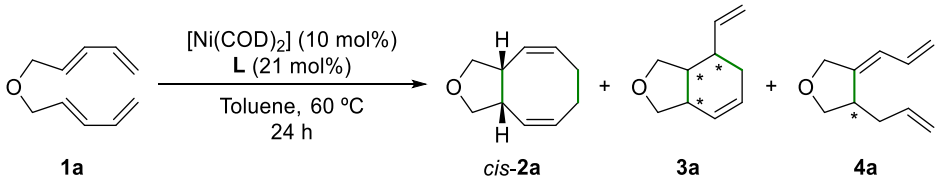

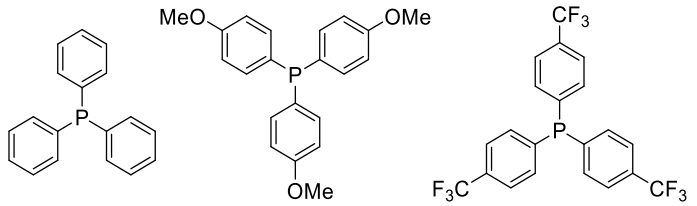

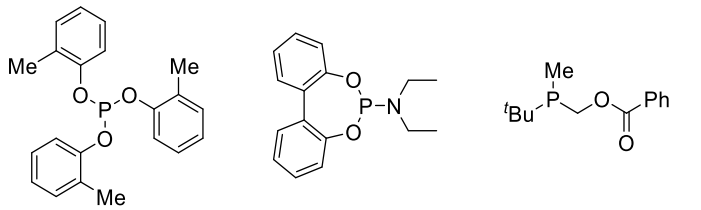

Entry	Ligand	Conv. (%)[b]	Yield *cis*-**2a** (%)[b]	Yield **3a** (%)[b]	Yield **4a** (%)[b]
1	**L1**	>99	58 (52)	6	-
2	**L2**	98	57 (56)	<1	2
3	**L3**	97	28	8	-
4	**L4**	74	42	-	-
5	**L5**	>99	56 (46)	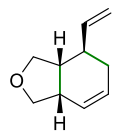 22 (16)	<1
6	**L6**	38	10	-	-

(a) The results are the average of at least two independent runs. (b) Calculated by ^{1}H NMR spectroscopy of the crude mixture using 1,3,5-trimethoxybenzene as internal standard. In parentheses: isolated yields after column chromatography on silica gel impregnated with $AgNO_3$ (10%).

On the contrary, the conversion of the reaction and selectivity towards product **2a** dropped when the reaction was conducted with ligand **L3**, which incorporates σ electron withdrawing groups (compare entry 3 with entries 1–2 in Table 1.1). Likewise, the use of monophosphite ligand **L4** did not significantly improve the previous results and led to decreased activity and yield for cyclooctadiene **2a** (see entry 4 in Table 1.1). As far as the phosphoramidite ligand **L5** is concerned, the corresponding nickel complex proved to be an active catalyst for the intramolecular [4+4] cycloaddition of substrate **1a**, with full conversion of **1a** obtained and the product **2a** isolated in a moderate yield (46%, see entry 5 in Table 1.1). It is interesting to note that **L5** allowed notable amounts of one of the possible [4+2] cycloadducts **3a** to be isolated and characterized. In particular, the [4+2] cycloaddition product **3a** using the phosphoramidite ligand **L5** corresponds to (3a*R*,4*R*,7a*S*)-4-vinyl-1,3,3a,4,5,7a-hexahydro-isobenzofuran (Table 1.1, entry 5), whose spectroscopic data are in good agreement with those previously reported in the literature.[7a,10] Finally, trialkylphosphine ligand **L6** was assessed in this initial screening. As shown in entry 6 (Table 1.1), low reactivity was observed towards the product **2a**.

The previous results demonstrate that changes in the electronic nature of the ligands led to significant differences in the yield and selectivity of the cycloaddition reactions. Interestingly, electron-rich triphenylphosphine **L2** was the most selective ligand for the nickel-catalyzed intramolecular [4+4] cycloaddition of bisdiene **1a** and was selected for further catalytic studies. Thus, with catalytic conditions in hand, we turned our attention to assessing the scope of the nickel-catalyzed intramolecular [4+4] cycloaddition over a set of structurally diverse prochiral bisdiene substrates. First, we focused our attention on bisdienes **1b–1f**,[7] substrates that lead to 10-substituted bicyclo[6.3.0] undeca-2,6-diene systems (see Table 1.2 for the structures). The results summarized in Table 1.2 indicate that the nickel-catalyzed cycloadditions to eight-membered fused bicyclic systems were successfully accomplished in almost all cases. Replacement of the oxa group in **1a** by a 1,3-dimethoxy-1,3-dioxopropan-2-yl (**1b**) or aza substituent (**1c**) was well tolerated and the corresponding [4+4] cycloadducts were isolated in satisfactory yields (see entries 1 and 2 in Table 1.2). Analysis of the NMR spectra of the eight-membered fused bicyclic systems derived from **1a–1c** revealed a *cis*-fusion between the five- and eight-membered rings. This type of ring fusion was in agreement with previous results in the

(10) See Figure 1.39 and Figure 1.40 in section 1.4.8 for details.

UNIVERSITAT ROVIRA I VIRGILI
TRANSITION METAL-CATALYZED CYCLOADDITION REACTIONS FOR THE FORMATION OF EIGHT- AND SIX-MEMBERED RINGS
Nuria Llorente González

literature,[4a] and was confirmed by X-ray analysis of a single crystal of compound **2c** (Figure 1.2).[11]

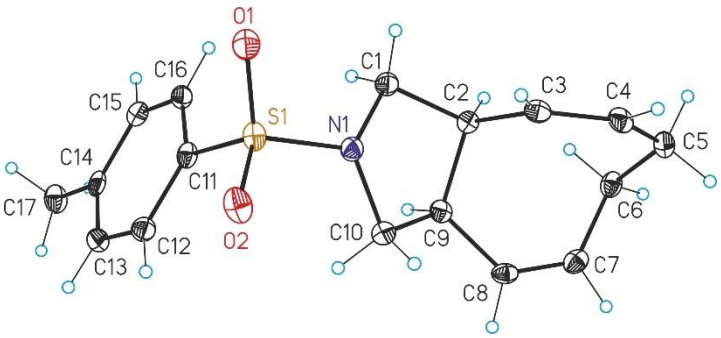

Figure 1.2. X-ray crystal structure of **2c** (ORTEP drawings showing thermal ellipsoids at 50% probability).

We also investigated the outcome of the reaction upon placing a methyl group at the 1-, 2- or 3-position of one of the diene units. Thus, intramolecular [4+4] cycloadditions of substrates **1d-1f** were examined. As shown in Table 1.2, the selectivities of the cycloadditions were heavily influenced by the substitution pattern of the diene. Introduction of a methyl group at the terminal position of the diene (substrate **1d**) was detrimental for the yield: compound **2d** was the only adduct that could be isolated in diastereomerically pure form, but in low yield (13%, see entry 3 in Table 1.2). The relative configuration of the three stereogenic carbons in **2d** was established by extensive ^{1}H-selective decoupling, 1D NOE and 2D NMR experiments.[12] Substitution of the diene at the 2-position (substrate **1e**) was detrimental, as the desired [4+4] cycloadduct could not be detected in the complex mixture of products that was obtained (see entry 4 in Table 1.2). Finally, substrate **1f** bearing a methyl group at the 3-position cyclized to the *cis*-fused bicyclic product **2f** in moderate yield (up to 35% isolated yield, see entry 5 in Table 1.2). The relative *cis*-configuration of the two stereogenic carbons in **2f** was established by extensive NMR experiments.[13]

(11) See the section 1.4.6 for details.
(12) See Figure 1.45 to Figure 1.47 in section 1.4.8 for further details.
(13) See Figure 1.48 to Figure 1.50 in section 1.4.8 for further details.

Table 1.2: Nickel-catalyzed intramolecular [4+4] cycloaddition towards bicyclo[6.3.0] ring systems.[a]

Entry	Substrate	Product	Conv.(%)[b]	Yield (%)[b]
1[c]	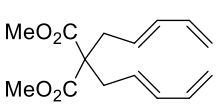 **1b**	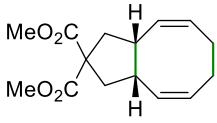 *cis*-**2b**	> 99	59 (56)
2[c]	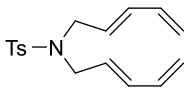 **1c**	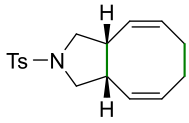 *cis*-**2c**	> 99	45 (40)
3	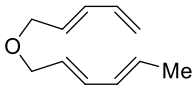 **1d**	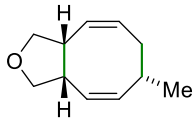 *cis*-**2d**	> 99	17 (13)
4	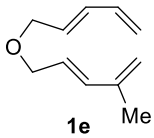 **1e**	Complex mixture of products	> 99	n.d.[d]
5	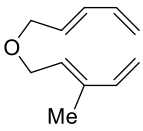 **1f**	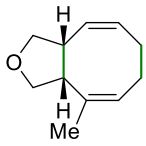 *cis*-**2f**	> 99	37 (35)

(a) The results are the average of at least two independent runs. Reactions performed in the presence of 10.0 mol% [Ni(COD)$_2$] and 21.0 mol% **L2** in toluene at 60 °C for 24 h. (b) Calculated by ^{1}H NMR spectroscopy of the crude mixture using 1,3,5-trimethoxybenzene as internal standard. In parentheses: isolated yields after column chromatography on silica gel impregnated with $AgNO_3$ (10%). (c) 31 mol% **L2** used as ligand. (d) Not determined.

Encouraged by these results, we extended the use of this [4+4] cycloaddition strategy to the preparation of 10-substituted bicyclo[6.4.0]dodeca-2,6-diene systems starting from the corresponding bisdienes **1g-1i** (see Table 1.3 for the structures). The required substrates were synthesized following well-established

UNIVERSITAT ROVIRA I VIRGILI
TRANSITION METAL-CATALYZED CYCLOADDITION REACTIONS FOR THE FORMATION OF EIGHT- AND SIX-MEMBERED RINGS
Nuria Llorente González

synthetic protocols,[14] though it should be noted that substrate **1i** could only be prepared as a mixture of isomers (*E*,*E*-**1i**:*E*,*Z*-**1i** ratio of 88:12), which were inseparable by standard column chromatography. Under our optimized reaction conditions, substrate **1g** gave [4+4] cycloadduct **2g** (up to 67% isolated yield, see entry 1 in Table 1.3). Spectroscopic data of the cycloaddition product pointed to the *trans*-eight-membered fused bicyclic system **2g**. This type of ring fusion was in agreement with previous results in the literature for comparable compounds,[4c] and was unambiguously confirmed by X-ray analysis (Figure 1.3).

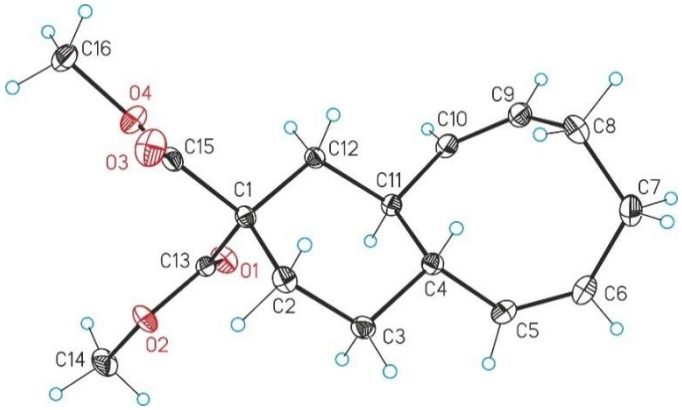

Figure 1.3. X-ray crystal structure of *trans*-**2g** (ORTEP drawings showing thermal ellipsoids at 50% probability).

The same trend was observed for the intramolecular [4+4] cycloaddition of substrates **1h** and **1i**, which contained oxa- and aza-substituted groups in the chain linking the two diene units. The eight-membered fused bicyclic systems were obtained in good isolated yields (61% and 67% for **1h** and **1i**, respectively; see entries 2 and 3 in Table 1.3). The [4+4] cycloadducts derived from **1i** were obtained as an inseparable mixture of two isomeric compounds in an 88:12 *trans*/*cis* ratio. It is interesting to note the close relationship between the *E*,*E*:*E*,*Z* isomer ratio of the starting material **1i** and the ratio of the isomeric [4+4] cycloadducts (*trans*-**2i** and *cis*-**2i**), thus suggesting a direct relationship between the geometry of the diene units and the structure of the final products.

(14) See section 1.4.3 for further details.

Table 1.3: Nickel-catalyzed intramolecular [4+4] cycloaddition towards bicyclo[6.4.0] ring systems.[a]

Entry	Substrate	Product	Conv.(%)[b]	Yield (%)[b]
1	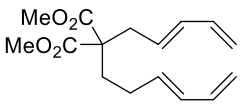 **1g**	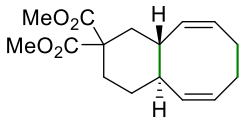 *trans*-**2g**	> 99	70 (67)
2	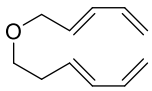 **1h**	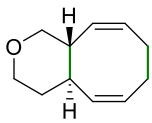 *trans*-**2h**	> 99	68 (61)
3	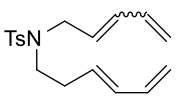 **1i** (*E*:*E*/*E*:*Z* ratio = 88:12)	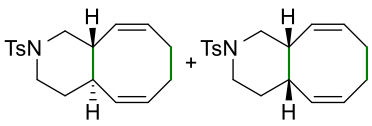 *trans*-**2i** + *cis*-**2i** (*trans*/*cis* ratio = 88:12)	> 99	79 (67)

(a) The results are the average of at least two independent runs. Reactions performed in the presence of 10 mol% [Ni(COD)$_2$] and 21 mol% **L2** in toluene at 60 °C for 24 h.

In order to fully understand the outcome of the cycloaddition reaction of **1i**, the separation of *E*,*E*-**1i** and *E*,*Z*-**1i** was attempted. The two isomers of **1i** could not be separated by standard column chromatography, but pure samples of *E*,*E*-**1i** and *E*,*Z*-**1i** could be obtained by semipreparative HPLC.[14] With *E*,*E*-**1i** and *E*,*Z*-**1i** in hand, we examined the Ni-catalyzed intramolecular [4+4] cycloadditions employing [Ni(COD)$_2$] and **L2** as catalyst. As shown in Scheme 1.2, each isomer of substrate **1i** exclusively led to one [4+4] cycloadduct. Whilst *E*,*E*-**1i** evolved under the reaction conditions to the *trans*-eight-membered fused bicyclic system **2i** in high isolated yield (78%), *E*,*Z*-**1i** led to the *cis*-fused analogue (55%). Structural assignments were made by analogy with the spectroscopic data of *trans*-fused product **2g** and by performing extensive NMR experiments on *cis*-**2i**. These results illustrate the importance of the geometry of the diene on the outcome of the cycloaddition, as *E*,*E*-**1i** and *E*,*Z*-**1i** lead to different diastereoisomeric cycloadducts (*i.e.*, *trans*-**2i** or *cis*-**2i**, respectively).

UNIVERSITAT ROVIRA I VIRGILI
TRANSITION METAL-CATALYZED CYCLOADDITION REACTIONS FOR THE FORMATION OF EIGHT- AND SIX-MEMBERED RINGS
Nuria Llorente González

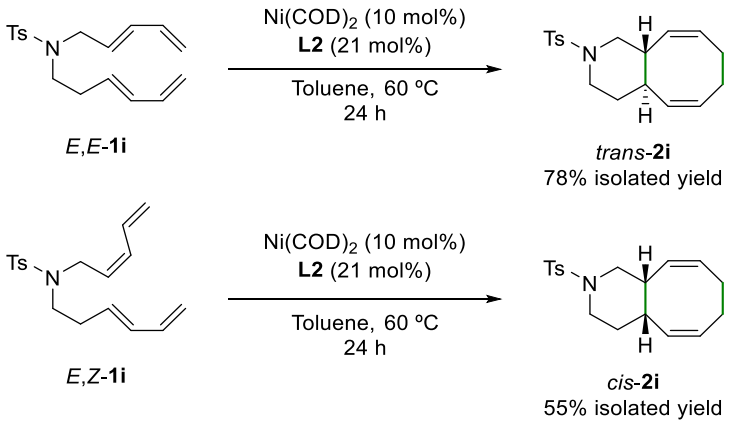

Scheme 1.2. Stereospecific nickel-catalyzed intramolecular [4+4] cycloaddition of **1i**.

1.2.2. Computational Studies

To shed light on the outcome of the [4+4] cycloaddition reactions, we performed a theoretical investigation (BP86-D3/def2-TZVP, see section 1.4.7) into the reactivity of substrates **1a**, *E,E*-**1h** and *E,Z*-**1h**. A tentative reaction pathway for the intramolecular nickel-catalyzed [4+4] cycloadditions of bisdienes is provided in Scheme 1.3. The accepted view for this transformation[3b,3c,3f,4a,4c,15] is that the nickel precursor reacts with the substrate to form bisdiene nickel complexes **5** that, after an oxidative cyclization of the two internal C=C bonds, lead to bis-allyl Ni(II) complexes **6**. Reductive elimination from these Ni(II)-complexes **6** leads to the cyclized product and nickel complexes which are capable of re-entering the catalytic cycle. We have focused our study on the first C–C bond formation, where the five- (for substrate **1a**) or six-membered ring (for compounds *E,E*-**1h** and *E,Z*-**1h**) is formed and the stereochemistry of the ring-fusion is defined. We have compared the energies of the transition states (TSs) for the paths leading to the *cis*- and *trans*-cycloadducts for the three substrates included in this computational study.

(15) Kimura, M.; Tamaru, Y. In *Modern Organonickel Chemistry*; Tamaru, Y., Ed.; Wiley-VCH Verlag GmbH & Co. KGaA: Weinheim: 2005; pp 137-170.

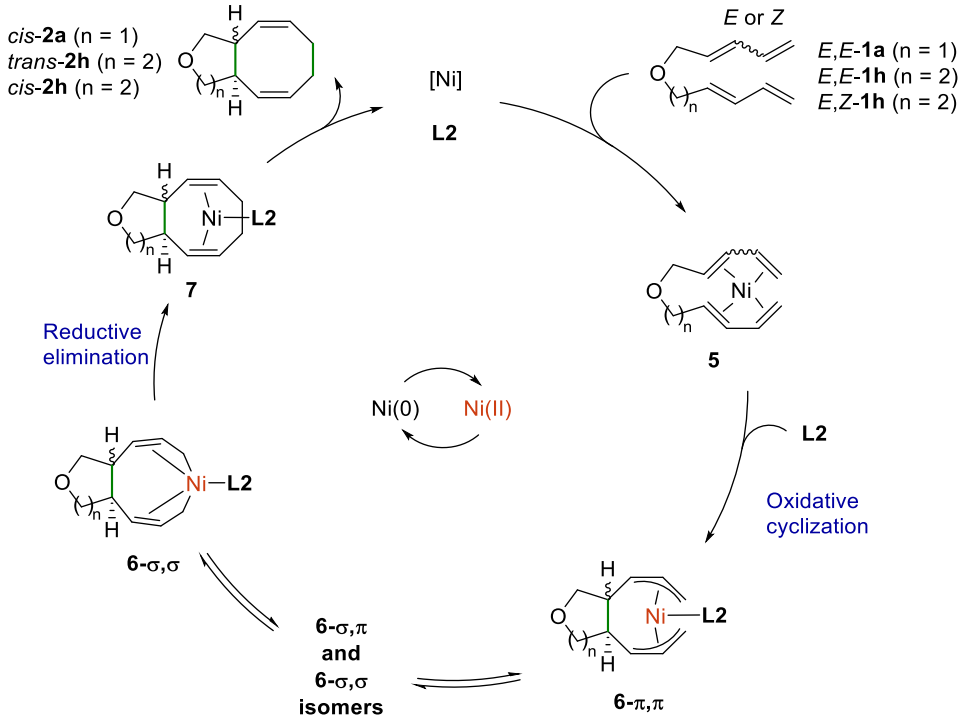

Scheme 1.3. Tentative reaction pathway rationale for nickel-catalyzed intramolecular [4+4] cycloadditions.

We first studied the reactivity of compound **1a** (see Figure 1.4). Experimentally, phosphine **L2** is used in the reaction. However, our computational studies did not incorporate **L2** in the coordination sphere of the Ni(0) center as, by coordinating to the four double bonds of the substrate, the nickel center had already accommodated eighteen electrons. We performed a conformational search on the starting complex [Ni(**1a**)] and found two possible binding modes (denoted as pre-**TS-1** and pre-**TS-2**) depending on the relative orientation of the diene units. Remarkably, pre-**TS-2** is considerably more stable than pre-**TS-1** and it has the adequate orientation to yield the *trans*-isomer. Both transition states on the potential hypersurface were located and the TS that yields the *cis*-isomer (denoted as **TS-1**) is lower in energy than the TS for the *trans*-isomer (**TS-2**; Figure 1.4), which is in good agreement with the experimental results.

The reaction barrier is 18.8 kcal/mol for **TS-1** and 26.3 kcal/mol for **TS-2**. The higher stability of **TS-1** (*i.e.* 7.5 kcal/mol) can be attributed to the closer proximity of the metal center to the C atoms that are forming the C–C bond in **TS-1** ($d_{Ni\cdots C}$ = 2.21 Å) than in **TS-2** ($d_{Ni\cdots C}$ = 2.85 Å). Consequently, the more

UNIVERSITAT ROVIRA I VIRGILI
TRANSITION METAL CATALYZED CYCLOADDITION REACTIONS FOR THE FORMATION OF EIGHT- AND SIX-MEMBERED RINGS
Nuria Llorente González

stable pre-**TS-2** *trans*-isomer needs to isomerize to the less stable pre-**TS-1** *cis*-isomer prior to the C–C bond formation. In the resulting intermediates (denoted as **I-1** and **I-2** in Figure 1.4) the Ni(II) center is able to incorporate the phosphine as an additional ligand, stabilizing the complexes. The reaction is highly exergonic in both cases.

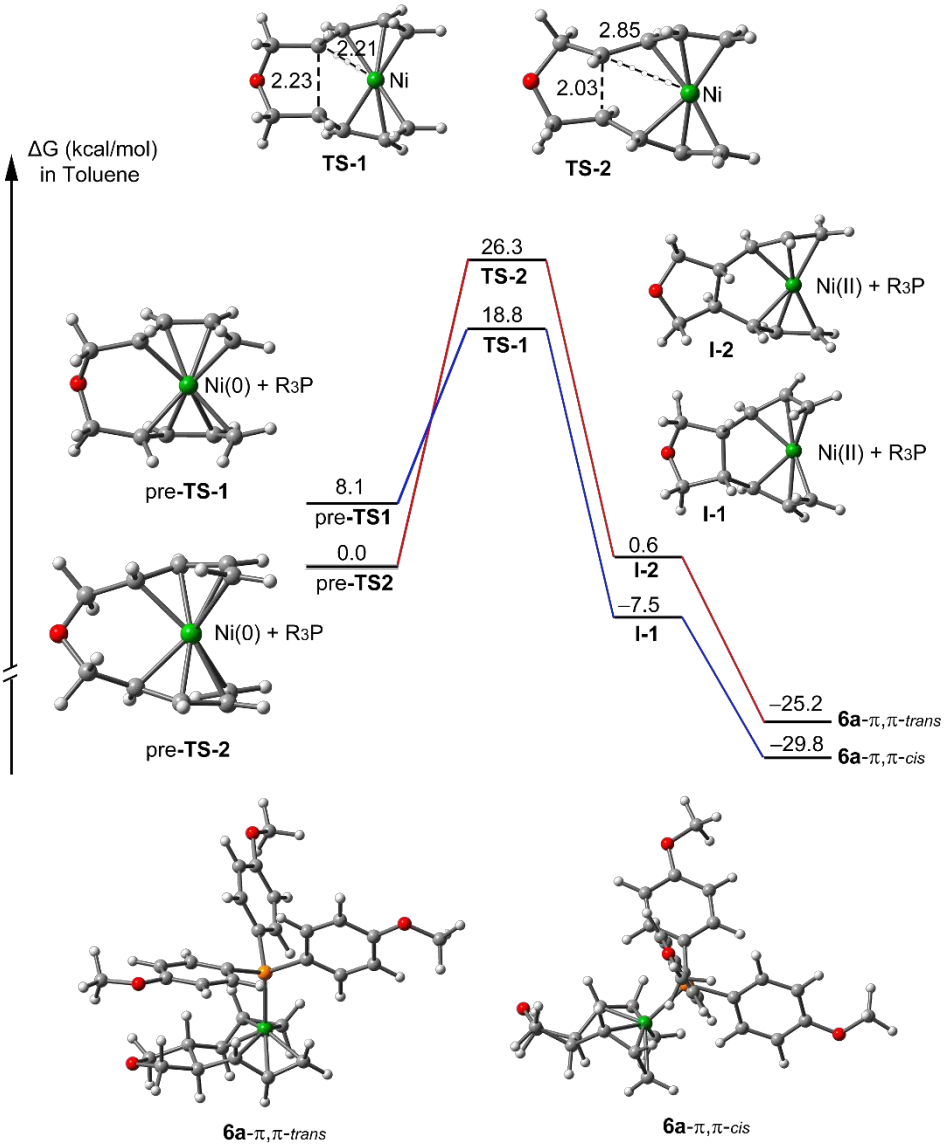

Figure 1.4. Optimized geometries at the BP86-D3/def2-TZVP level of theory for the pre-transition states (pre-TS), transition states (TS), intermediates (I) and products for the reaction of **1a** and their energetic profile (kcal/mol) in toluene (distances in Å).

We have also studied the reactivity of compound *E,E*-**1h** (see Figure 1.5). Experimentally, the cycloaddition of this substrate leads to *trans*-**2h** rather than *cis*-**2h** (in contrast with the outcome of the reaction in the case of substrates with one less carbon in the length of the spacer used to connect both π-systems, as for instance *E,E*-**1a**, which led to a *cis*-fusion between the five- and eight-membered rings).

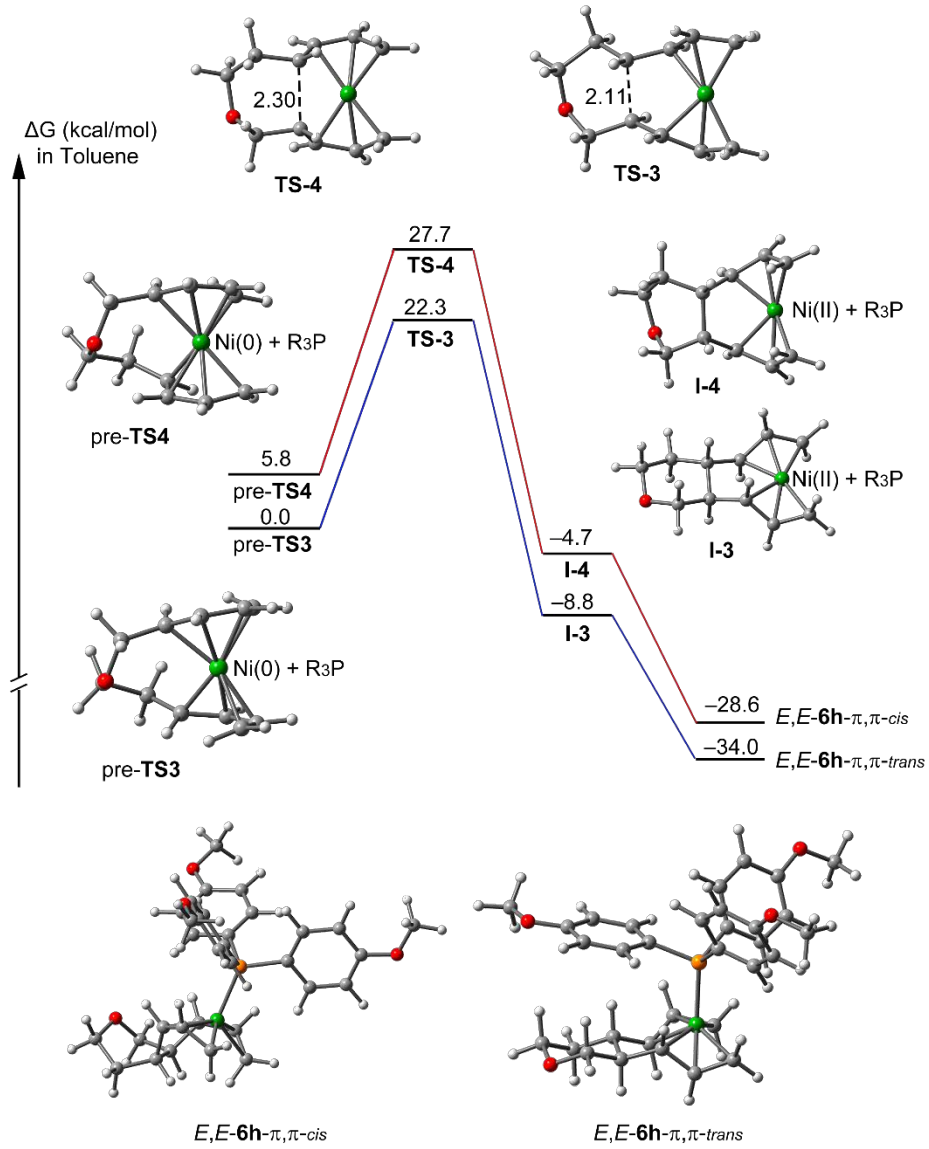

Figure 1.5. Optimized geometries at the BP86-D3/def2-TZVP level of theory for the pre-transition states (pre-TS), transition states (TS), intermediates (I) and products for the reaction of *E,E*-**1h** and its energetic profile (kcal/mol) in toluene (distances in Å).

Similarly to compound *E*,*E*-**1a**, we have also performed a conformational study of [Ni(*E*,*E*-**1h**)] and the *trans*-isomer is also the most stable (5.8 kcal/mol, denoted as pre-**TS-3** in Figure 1.5). We located both transition states on the potential hypersurface, and, as for the cycloadditions of **1a**, we considered that the phosphine does not participate in the process. Transition states for the cycloaddition reaction of *E*,*E*-**1h** with one uncoordinated terminal C=C bond of the substrate and ligand **L2** coordinated to the Ni(0) centre were located (see Figure 1.6 for details). In contrast with the computational results obtained for substrate *E*,*Z*-**1h**, the energies of the new TSs (**TS-3'**$_{cis}$ and **TS-4'**$_{trans}$, which lead to *cis*-**2h** and *trans*-**2h**, respectively) were higher in energy (*i.e.*, **TS-3'**$_{cis}$ = 27.3 kcal/mol and **TS-4'**$_{trans}$ = 27.9 kcal/mol) than those involving coordination of the substrate through the four C=C bonds (i.e., **TS-3** = 22.3 kcal/mol and **TS-4** = 27.7 kcal/mol).

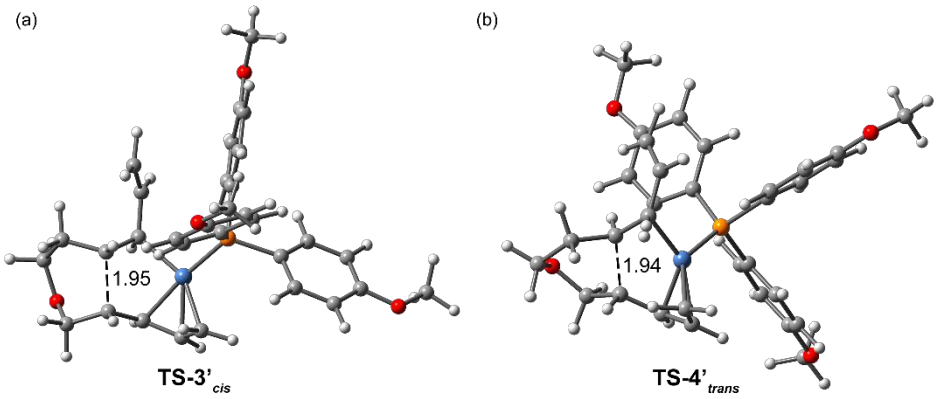

Figure 1.6. Optimized structures of **TS-3'**$_{cis}$ (a) and **TS-4'**$_{trans}$ (b) yielding compounds *E*,*E*-**6h**-π,π-*cis* and *E*,*E*-**6h**-π,π-*trans*, respectively, with the **L2** coordinated to the Ni metal center.

Gratifyingly, the TS that yields the *trans* isomer (**TS-3**) is lower in energy than the TS for the *cis* isomer (**TS-4**; see Figure 1.5), which is in good agreement with the experimental results. The reaction barrier is 22.3 kcal/mol for **TS-3** and 27.7 kcal/mol for **TS-4**. In this case, **TS-3** is more stable than **TS-4** because the former can adopt a perfect chair conformation in the formation of the six-membered ring (see Figure 1.7 for a detailed representation of the TSs). In contrast, the **TS-4** adopts a boat-like conformation in the C–C bond formation. The reaction is highly exergonic for both stereoisomers upon coordination of the phosphine.

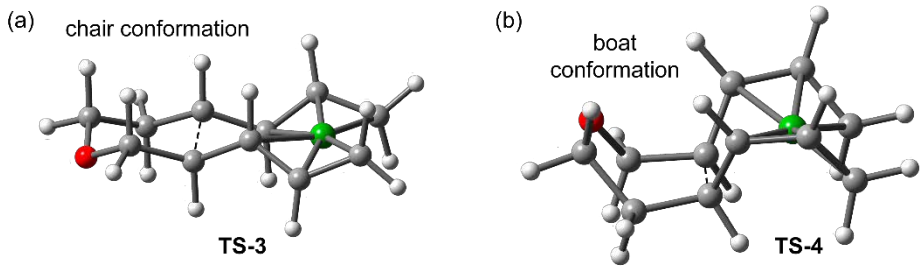

Figure 1.7. Optimized structures in chair (a) and boat (b) conformations of **TS-3** and **TS-4**, respectively.

In order to support the level of theory used herein, we have also computed the energies of the TSs for compounds **1a** and *E,E*-**1h** using MP2/def2-TZVP (in toluene) and we have observed the same trend. That is, the **TS-1** is lower than the **TS-2** for **1a** in 5.6 kcal/mol (7.5 kcal/mol using DFT) and the **TS-3** is lower than the **TS-4** for *E,E*-**1h** in 2.3 kcal/mol (5.4 kcal/mol using DFT).[16]

Finally, we studied the most favorable [4+4] cycloaddition reaction pathway for *E,Z*-**1h**, which has the same spacer as *E,E*-**1h** but has one (*Z*)-configured C=C double bond instead of two (*E*)-configured C=C bonds. Although the cycloaddition reaction of this substrate was not studied experimentally,[17] we carried out computational studies with *E,Z*-**1h** rather than *E,Z*-**1i** for the sake of consistency with the other bisdienes studied at the computational level. In this case, the conformational study of [Ni(*E,Z*-**1h**)] revealed that both isomers (pre-**TS-5** and pre-**TS-6**) were almost isoenergetic. Moreover, we could not locate any transition state with the four C=C bonds coordinated to the nickel center: the *Z*-configuration of the double bond in *E,Z*-**1h** hinders the coordination of its terminal double bond to the nickel center and facilitates the coordination of **L2**. Thus, we have located the corresponding transition states with **L2** and three C=C bonds coordinated to the nickel center on the potential hypersurface and, remarkably, the TS that leads to the *cis* isomer (**TS-5**) is slightly lower in energy than that for the *trans*-isomer (**TS-6**; see Figure 1.8). The reaction barrier is 20.6 kcal/mol for **TS-5** and 21.8 kcal/mol for **TS-6**. It should be noted that, whilst the computed results are in qualitative agreement with the experimental results, they do not quite match the relative magnitudes of the stereoselection (only one

(16) The calculations at the MP2 level have not been performed for *E,Z*-**1i** due to the size of the system incorporating ligand **L2** in its structure.
(17) Substrate *E,Z*-**1h** is contained as a minor impurity in the samples of substrate *E,E*-**1h** (< 5%, see reference 7). Accordingly, the [4+4] cycloadduct derived from *E,Z*-**1h** (*i.e. cis*-**2h**) was present in the corresponding amounts in the cycloaddition reaction mixture and could be separated by semipreparative HPLC (see section 1.4.5 for further details).

stereoisomer is experimentally observed from *E,Z*-**1h**, whilst the energy differences between **TS-5** and **TS-6** is *ca.* 1 kcal/mol). In spite of **TS-6** adopting a perfect chair conformation for the formation of the six-membered ring (see Figure 1.9 for a detailed representation of the transition states), **TS-5** presents an extra stabilization energy that comes from the interaction of a H atom of the uncoordinated double bond with a C=C bond of the aromatic ring (see dashed lines in Figure 1.8).

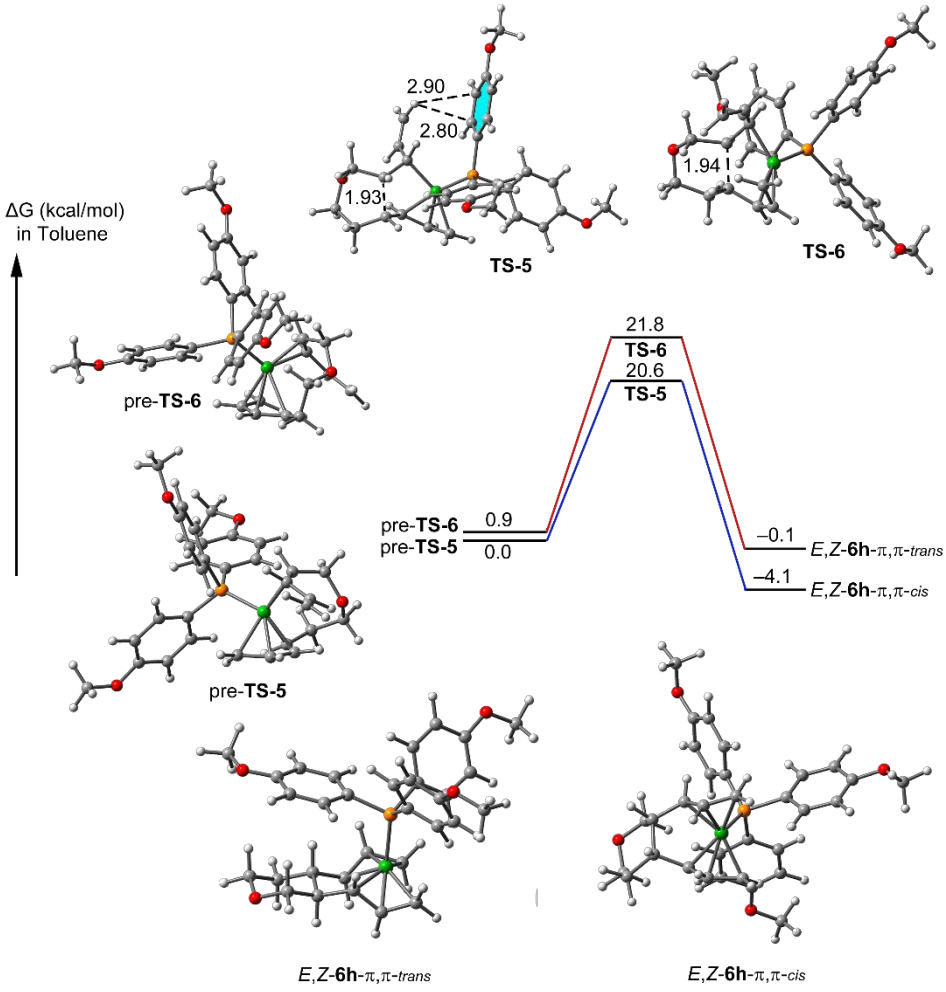

Figure 1.8. Optimized geometries at the BP86-D3/def2-TZVP level of theory for the pre-transition states (pre-TS), transition states (TS), intermediates (I) and products for the reaction of *E,Z*-**1h** and its energetic profile (kcal/mol) in toluene (distances in Å).

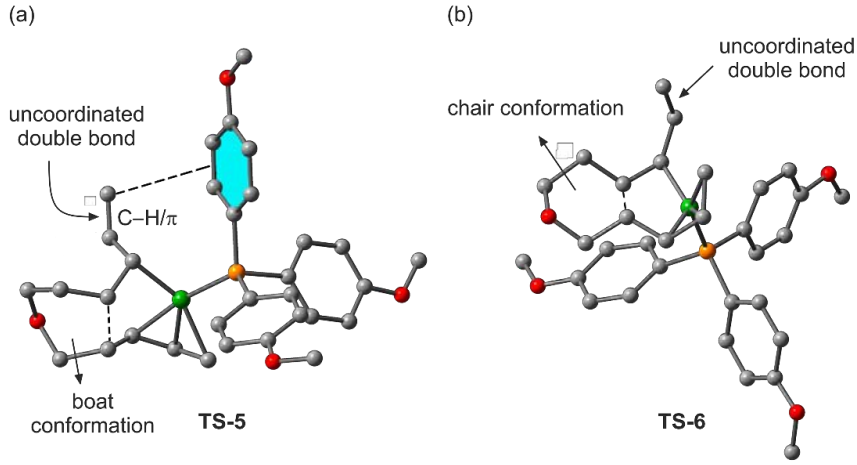

Figure 1.9. Optimized structures from in boat (a) and chair (b) conformations of **TS-5** and **TS-6**, respectively.

The non-coordinated double bond in **TS-6** is oriented totally different and does not establish any interaction with the phosphine. It should be noted that the reaction is exergonic for the *cis* isomer (-4.1 kcal/mol) and thermo-neutral for the *trans* isomer (-0.1 kcal/mol) (see Figure 1.8). These data therefore suggest that the ring fusion is thermodynamically rather than kinetically controlled. Consequently, the formation of *E,Z*-**6h**-π,π-*trans* is reversible and the selectivity can be explained by the energy difference between *cis* and *trans* isomers (-4.0 kcal/mol), which correlates with the selectivity observed experimentally.

1.3 Conclusions

In summary, nickel-catalyzed intramolecular [4+4] cycloadditions for the preparation of *cis*-eight-membered fused [6.3.0] bicyclic compounds and *trans*- or *cis*- eight-membered fused [6.4.0] bicyclic systems from structurally diverse bisdienes are reported. The catalytic intramolecular [4+4] cycloaddition reaction proceeds efficiently on a set of bisdienes linked by a three-atom chain to afford *cis*-configured eight-membered carbocycles fused to a five-membered ring. Analogously, the reported chemistry for bisdienes linked by a four-atom chain gives access to *trans*- or *cis*-configured eight-membered carbocycles fused to a six-membered ring. Computational studies on the stereo-determining step of the reaction have demonstrated that the stereochemical outcome of the reaction is dictated by the length of the chain linking the two diene units, and the geometry of the C=C double bonds in the diene units of the substrates. Research activities aimed at developing catalytic enantioselective versions of this transformation will be summarized in the following chapter of this thesis.

UNIVERSITAT ROVIRA I VIRGILI
TRANSITION METAL-CATALYZED CYCLOADDITION REACTIONS FOR THE FORMATION OF EIGHT- AND SIX-MEMBERED RINGS
Nuria Llorente González

1.4 Experimental Section

1.4.1. General Remarks

All syntheses were carried out on chemicals as purchased from commercial sources, unless otherwise stated. Air and moisture sensitive manipulations or reactions were run under inert atmosphere using anhydrous and deoxygenated solvents, either in a glove box or with standard Schlenk techniques. All solvents were dried by using a Solvent Purification System (SPS). Silica gel 60 (230-400 mesh) was used for column chromatography. Silica gel impregnated with silver nitrate was used to isolate the [4+4] and the [4+2] cycloaddition products **2** and **3**, respectively. It was prepared according to a procedure previously reported in the literature.[18] NMR spectra were recorded in $CDCl_3$ unless otherwise cited, on Bruker Avance 300 MHz, 400 MHz or 500 MHz Ultrashield spectrometers. ^1H NMR and $^{13}C\{^1H\}$ NMR chemical shifts are quoted in ppm relative to residual solvent peaks. $^{31}P\{^1H\}$ NMR chemical shifts are quoted in ppm relative to 85% phosphoric acid in water. High-resolution mass spectra (HRMS) were recorded by using either ESI or APCI ionization methods in positive mode. Conversion, and selectivity for the cycloaddition products were determined by ^1H NMR spectroscopy from the crude mixtures, using 1,3,5-trimethoxybenzene as internal standard. Melting points were measured in open capillaries and are uncorrected.

1.4.2. Experimental Procedure and Characterization Data for Ligand L6

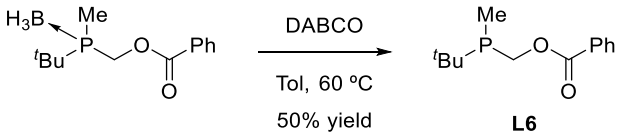

L6

The required amounts of phosphino-borane adduct[19] (233.0 mg, 0.925 mmol) and 1,4-diazabyciclo[2.2.2]octane (DABCO, 212.0 mg, 1.8 mmol) were loaded into a flame-dried Schlenk flask, to which dry toluene (5.0 mL) was added. The reaction mixture was heated at 60 °C and stirred during 24 h. After that, the toluene solvent was completely removed under high vacuum. Finally, the resulting residue was redissolved in diethyl ether (5.0 mL) and passed through a

(18) Li, T.-S.; Li, J.-T.; Li, H.-Z. *J. Chromatogr. A* **1995**, *715*, 372-375.
(19) The racemic sample of the corresponding starting phosphino-borane adduct has been previously prepared in our research group, see the following reference: Lao, J. R.; Benet-Buchholz, J.; Vidal-Ferran, A. *Organometallics* **2014**, *33*, 2960-2963.

short pad of silica (2.0 cm x 1.5 cm). Evaporation of the diethyl ether under high vacuum afforded the desired ligand **L6** as a colorless oil (0.109 g, 0.46 mmol, 50% yield, see Figure 1.12 to Figure 1.14). ^{1}H NMR (500 MHz, $CDCl_3$) δ 8.05 – 8.03 (m, 2H, H_{arom}), 7.57 – 7.54 (m, 1H, H_{arom}), 7.45 - 7.42 (m, 2H, H_{arom}), 4.69 (dd, $^{2}J_{H-H}$ = 13.1 Hz, $^{2}J_{H-P}$ = 5.6 Hz, 1H, C*H*H-PMe^{t}Bu), 4.55 (dd, $^{2}J_{H-H}$ = 13.1 Hz, $^{2}J_{H-P}$ = 4.0 Hz, 1H, CH*H*-PMe^{t}Bu), 1.13 (d, $^{3}J_{H-P}$ = 12.0 Hz, 9H, ^{t}Bu), 1.09 (d, $^{2}J_{H-P}$ = 3.4 Hz, 3H, Me) ppm. ^{13}C{^{1}H} NMR (125 MHz, $CDCl_3$) δ 166.8 (d, $^{3}J_{C-P}$ = 2.8 Hz, C=O), 133.1 (CH_{arom}), 130.2 (C_{arom}), 129.8 (CH_{arom}), 128.5 (CH_{arom}), 63.0 (d, $^{1}J_{C-P}$ = 20.4 Hz, CH_2–P), 27.5 (d, $^{2}J_{C-P}$ = 13.1 Hz, 3 x CH_3, ^{t}Bu), 4.2 (d, $^{1}J_{C-P}$ = 17.2 Hz, CH_3–P, Me) ppm. ^{31}P{^{1}H} NMR (202 MHz, $CDCl_3$) δ -13.2 (s, PMe^{t}Bu) ppm. HRMS (ESI^{+}) *m/z* calcd for $C_{13}H_{19}O_2PNa$ $[M+Na]^{+}$ 261.1015, found 261.1015.

1.4.3. Synthesis of Cycloaddition Substrates

- Synthesis of (*E*)-5-(((*E*)-penta-2,4-dien-1-yl)oxy)penta-1,3-diene (**1a**)

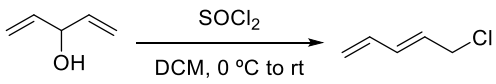

80% yield

Thionyl chloride (2.1 mL, 28.0 mmol) was added dropwise to a solution of 1,4-pentadiene-3-ol (2.3 mL, 23.3 mmol) in dichloromethane (DCM, 55.0 mL) at 0 °C. The reaction mixture was allowed to warm to room temperature and stirred for 2 h. The reaction was then quenched with water (15.0 mL) and the two phases were separated. The aqueous phase was extracted with DCM (2 x 15.0 mL). The combined organic phases were dried over magnesium sulfate and concentrated *in vacuo*. The desired 5-chloropenta-1,3-diene was isolated by distillation of the mixture (b.p. = 73 °C, p = 0.32 mbar) as a colorless oil (2.79 g, 76% yield, *E*:*Z* isomers = 95:5). ^{1}H NMR (400 MHz, $CDCl_3$) δ 6.48 – 6.23 (m, 4H), 5.96 – 5.74 (m, 2H), 5.31 (d, *J* = 15.4 Hz, 3H), 5.21 (d, *J* = 10.1 Hz, 2H), 4.14 (d, *J* = 7.2 Hz, 4H) ppm. ^{13}C{^{1}H} NMR (101 MHz, $CDCl_3$) δ 135.6 (CH=), 134.8 (CH=), 128.8 (CH=), 119.2 (CH_2=), 44.9 (CH_2) ppm. Spectroscopic data were in agreement with those previously reported in the literature.[20]

(20) González, A. Z.; Toste, F. D. *Org. Lett.* **2010**, *12*, 200-203.

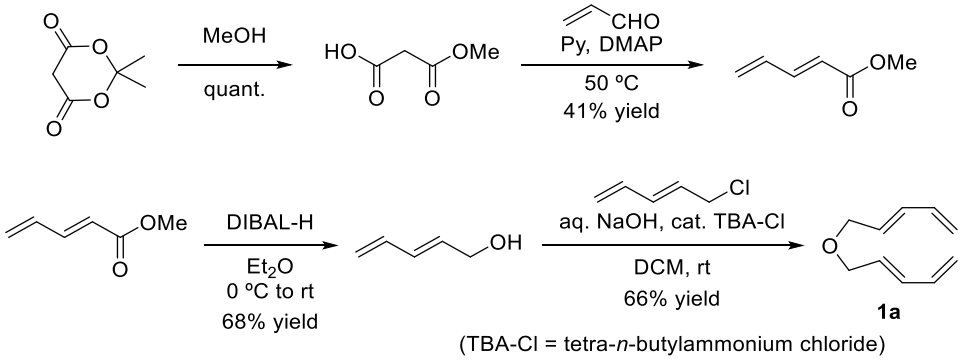

A mixture of Meldrum's acid (10.0 g, 69.4 mmol) and methanol (2.8 mL, 69.4 mmol) was heated at 80 °C for 20 h. Evaporation of acetone under reduced pressure gave 3-methoxy-3-oxopropanoic acid as a colorless oil (8.2 g, quantitative yield), which was directly used in the following step without further purification. ^{1}H NMR (400 MHz, $CDCl_3$) δ 9.82 (s, 1H), 3.73 (s, 3H), 3.42 (s, 2H) ppm. Spectroscopic data were in agreement with those previously reported in the literature.[21]

Acrolein (3.1 mL, 41.7 mmol) was added to a mixture of 3-methoxy-3-oxopropanoic acid (8.2 g, 62.4 mmol), anhydrous pyridine (12.0 mL), and 4-*N*,*N*-dimethylaminopyridine (406.0 mg, 3.3 mmol), and the reaction mixture was heated to 50 °C and allowed to stir at this temperature for 24 h. The reaction mixture was allowed to cool down to room temperature and partitioned with water (15.0 mL) and diethyl ether (30.0 mL). The aqueous phase was then extracted with diethyl ether (3 x 30.0 mL). The combined organic phases were washed with brine (1 x 30.0 mL), dried over magnesium sulfate and the solvents evaporated to dryness. The resulting residue was purified by distillation (b.p. = 56 °C, p = 0.27 mbar) to afford methyl (*E*)-penta-2,4-dienoate as a colorless liquid (1.92 g, 41% yield). ^{1}H NMR (500 MHz, $CDCl_3$) δ 7.27 (dd, J = 15.5, 11.0 Hz, 1H), 6.46 (dt, J = 17.1, 10.5 Hz, 1H), 5.92 (d, J = 15.4 Hz, 1H), 5.61 (d, J = 16.9 Hz, 1H), 5.50 (d, J = 10.0 Hz, 1H), 3.75 (s, 3H) ppm. ^{13}C{^{1}H} NMR (101 MHz, $CDCl_3$) δ 167.2 (C=O), 144.9 (CH=), 134.7 (CH=), 125.6 (CH=), 121.7 (CH_2=), 51.6 (CH_3) ppm. Spectroscopic data were in agreement with those previously reported in the literature.[22]

Diisobutylaluminum hydride (DIBAL-H, 1.0 M in hexane, 21.0 mL, 21.0 mmol) was added over 5 min to a solution of methyl (*E*)-penta-2,4-dienoate (1.2

(21) (a) For the synthetic method, see: Craig, D.; Grellepois, F. *Org. Lett.* **2005**, *7*, 463-465. (b) For the spectroscopic data, see: Niwayama, S.; Cho, H.; Lin, C. *Tetrahedron Lett.* **2008**, *49*, 4434-4436.
(22) Rodríguez, J.; Waegell, B. *Synthesis* **1988**, 534-535.

g, 10.5 mmol) in anhydrous diethyl ether (25.0 mL) at 0 °C. The mixture was stirred at this temperature for 20 min, and at room temperature for 4 h. The reaction was cooled to 0 °C and quenched carefully with 2M aqueous HCl solution until the pH of the mixture was 5-6. The aqueous phase was separated and extracted with diethyl ether (2 x 15.0 mL). The combined organic phases were washed with brine (1 x 25.0 mL), dried over magnesium sulfate and concentrated *in vacuo* to afford the desired (*E*)-penta-2,4-dien-1-ol (0.600 g, 68% yield) as a colorless oil which was immediately used in the following step without further purification. ^{1}H NMR (400 MHz, $CDCl_3$) δ 6.32 (ddt, J = 24.0, 14.9, 10.3 Hz, 2H), 5.86 (dt, J = 15.0, 5.7 Hz, 1H), 5.28 – 5.18 (m, 1H), 5.15 – 5.07 (m, 1H), 4.21 (m, 2H) ppm. Spectroscopic data were in agreement with those previously reported in the literature.[23]

A mixture of 5-chloropenta-1,3-diene (*E*:*Z* isomers in a 95:5 ratio; 4.0 g, 39.0 mmol), (*E*)-penta-2,4-dien-1-ol (2.1 g, 25.0 mmol), tetra-*n*-butylammonium chloride (368.0 mg, 1.3 mmol), and 50% aqueous NaOH (9.9 g, 250.0 mmol) in DCM (10.0 mL) was vigorously stirred at room temperature overnight. The reaction mixture was then poured into 15.0 mL of distilled water, the organic phases separated, and the aqueous phase extracted with pentane (5 x 40.0 mL). The combined organic phases were washed with brine (1 x 50.0 mL), dried over magnesium sulfate, and concentrated under reduced pressure. The resulting residue was purified by distillation (b.p. = 62 °C, p = 0.35 mbar) to yield the desired product **1a** as a colorless oil (2.49 g, 66% yield, *E*,*E*:*E*,*Z* isomers = 95:5, see Figure 1.15 and Figure 1.16). ^{1}H NMR (400 MHz, $CDCl_3$) δ 6.39 - 6.23 (m, 4H), 5.77 (dt, J = 15.0, 6.0 Hz, 2H), 5.21 (d, J = 17.6 Hz, 2H), 5.09 (d, J = 8.4 Hz, 2H), 4.02 (d, J = 6.0 Hz, 4H) ppm. ^{13}C{^{1}H} NMR (125 MHz, $CDCl_3$) δ 136.5 (CH=), 133.4 (CH=), 130.1 (CH=), 117.7 (CH_2=), 70.3 (CH_2) ppm. Spectroscopic data were in agreement with those previously reported in the literature.[7a]

(23) Llaveria, J.; Beltrán, A.; Díaz-Requejo, M. M.; Matheu, M. I.; Castillón, S.; Pérez, P. J. *Angew. Chem., Int. Ed.* **2010**, *49*, 7092-7095.

- Synthesis of dimethyl (*E*)-2-(penta-2,4-dien-1-yl)malonate (**1b**)

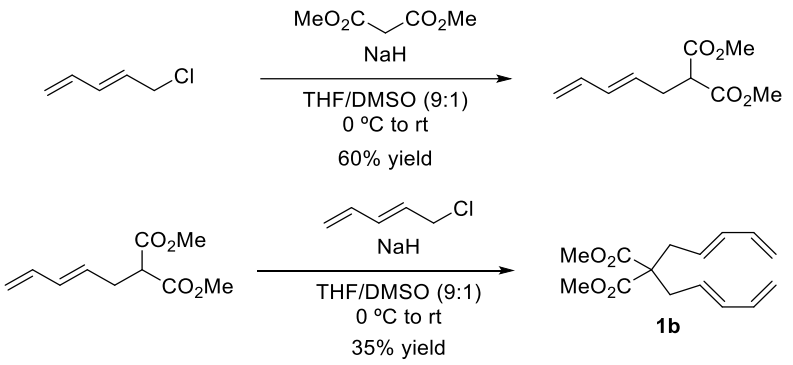

A solution of dimethyl malonate (4.5 mL, 39.4 mmol) in anhydrous tetrahydrofuran (THF, 2.5 mL) was added to a suspension of anhydrous NaH (0.538 g, 21.3 mmol) in anhydrous DMSO (6.0 mL) and THF (75.0 mL) at 0 °C. After 30 min at 0 °C, a solution of freshly prepared 5-chloropenta-1,3-diene (*E*:*Z* isomers in a 95:5 ratio; 1.6 g, 15.9 mmol) in anhydrous THF (4.0 mL) was added dropwise. The resulting mixture was allowed to warm to room temperature and stirred overnight. The reaction mixture was then quenched with distilled water (15.0 mL) and diluted with diethyl ether (25.0 mL). The two phases were separated, the aqueous phase was then extracted with diethyl ether (3 x 25.0 mL), and the resulting combined organic phases were washed with water (3 x 15.0 mL), dried over magnesium sulfate and concentrated *in vacuo*. Finally, the resulting residue was purified by distillation (b.p. = 78 °C, p = 0.12 mbar) to give the desired product dimethyl (*E*)-2-(penta-2,4-dien-1-yl)malonate as a colorless oil (1.880 g, 60% yield). ^{1}H NMR (500 MHz, $CDCl_3$) δ 6.25 – 6.11 (m, 1H), 6.10 – 5.97 (m, 1H), 5.60 – 5.48 (m, 1H), 5.05 (d, J = 16.9 Hz, 1H), 4.93 (d, J = 10.1 Hz, 1H), 3.64 (s, 6H), 3.37 (t, J = 7.5 Hz, 1H), 2.59 (t, J = 7.2 Hz, 2H) ppm. ^{13}C{^{1}H} NMR (125 MHz, $CDCl_3$) δ 169.2 (C=O), 136.5 (CH=), 133.8 (CH=), 129.4 (CH=), 116.6 (CH_2=), 52.5 (CH), 51.6 (CH_3), 32.4 (CH_2) ppm. Spectroscopic data were in agreement with those previously reported in the literature.[7b]

A solution of dimethyl (*E*)-2-(penta-2,4-dien-1-yl)malonate (842.0 mg, 4.2 mmol) in anhydrous THF (2.0 mL) was slowly syringed into a suspension of anhydrous NaH (134.0 mg, 5.3 mmol) in anhydrous DMSO (1.5 mL) and THF (19.5 mL) at 0 °C. After 30 min at 0 °C, a solution of 5-chloropenta-1,3-diene (*E*:*Z* isomers in a 95:5 ratio; 1.3 g, 8.5 mmol) in anhydrous THF (2.0 mL) was slowly added. The resulting mixture was allowed to warm to room temperature and stirred overnight, and then quenched with distilled water (10.0 mL). THF

was evaporated to dryness and the resulting residue was diluted with diethyl ether (15.0 mL). The two phases were separated, the aqueous phase was extracted with diethyl ether (2 x 15.0 mL), and the resulting combined organic phases were washed with water (3 x 15.0 mL), dried over magnesium sulfate and concentrated under reduced pressure. Purification by distillation (b.p. = 92 °C, p = 0.02 mbar) gave the desired substrate **1b** as a colorless oil (393.0 mg, 35% yield, *E,E*:*E,Z* isomers = 95:5, see Figure 1.17 and Figure 1.18). ^{1}H NMR (500 MHz, $CDCl_3$) δ 6.24 (dt, J = 17.0, 10.3 Hz, 2H), 6.05 (dd, J = 15.1, 10.5 Hz, 2H), 5.47 (dt, J = 15.2, 7.6 Hz, 2H), 5.09 (d, J = 17.0 Hz, 2H), 4.98 (d, J = 10.3 Hz, 2H), 3.67 (s, 6H), 2.62 (d, J = 7.7 Hz, 4H) ppm. ^{13}C{^{1}H} NMR (125 MHz, $CDCl_3$) δ 171.0 (C=O), 136.5 (CH=), 135.2 (CH=), 127.7 (CH=), 116.5 (CH_2), 58.0 (C_q), 52.4 (CH_3), 36.0 (CH_2) ppm. Spectroscopic data were in agreement with those previously reported in the literature.[7b]

- Synthesis of *N,N*-di((*E*)-penta-2,4-dien-1-yl)tosylamine (**1c**)

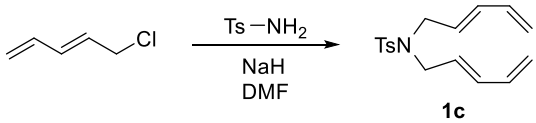

1c

75% yield

A solution of *p*-toluenesulfonamide (1.5 g, 8.8 mmol) in DMF (12.0 mL) was added to a cooled (0 °C) suspension of NaH (95%, 531.0 g, 21.0 mmol) in DMF (12.0 mL). The mixture was stirred at 0 °C for 30 min, after which a solution of previously prepared 5-chloropenta-1,3-diene (*E*:*Z* isomers in a 95:5 ratio; 2.6 g, 21.9 mmol) in DMF (6.0 mL) was added. The resulting mixture was stirred at room temperature for 2 h. The reaction was quenched by the addition of saturated aqueous solution of NH_4Cl (20.0 mL) at 0 °C, and extracted with ether (3 x 25.0 mL). The combined organic phases were dried over magnesium sulfate, filtered, and concentrated *in vacuo*. The residue was purified by silica gel column chromatography (hexane:EtOAc, 100:0→80:20) to afford the target substrate **1c** as a yellow oil (1.94 g, 75% yield, *E,E*:*E,Z* isomers = 95:5, see Figure 1.19 and Figure 1.20). ^{1}H NMR (400 MHz, $CDCl_3$) δ 7.69 (d, J = 8.3 Hz, 1H), 7.28 (d, J = 7.9 Hz, 2H), 6.24 (dt, J = 16.8, 10.3 Hz, 2H), 6.06 (dd, J = 15.2, 10.5 Hz, 2H), 5.48 - 5.41 (m, 2H), 5.15 (d, J = 16.8 Hz, 2H), 5.07 (d, J = 10.8 Hz, 2H), 3.81 (d, J = 6.7 Hz, 4H), 2.42 (s, 3H) ppm. ^{13}C{^{1}H} NMR (125 MHz, $CDCl_3$) δ 143.3 (C_{arom}), 137.5 (C_{arom}), 135.9 (CH=), 134.9 (CH=), 129.7 (CH_{arom}), 127.8 (CH=), 127.3 (CH_{arom}), 118.0 (CH_2=), 48.6 (CH_2), 21.6 (CH_3) ppm. Spectroscopic data were in agreement with those previously reported in the literature.[7c]

- Synthesis of (2*E*,4*E*)-1-(((*E*)-penta-2,4-dien-1-yl)oxy) hexa-2,4-diene (**1d**)

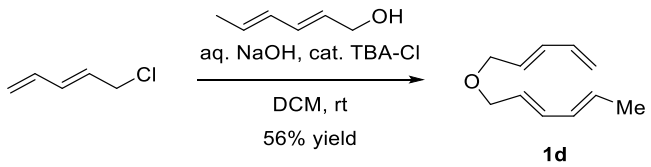

1d

A mixture of (2*E*,4*E*)-hexa-2,4-dien-1-ol (1.0 g, 9.9 mmol), previously prepared 5-chloropenta-1,3-diene (*E*:*Z* isomers in a 95:5 ratio; 1.6 g, 15.4 mmol), tetra-*n*-butylammonium chloride (0.146 g, 0.524 mmol), and 50% aqueous NaOH (3.9 g, 98.8 mmol) in dichloromethane (4.0 mL) was vigorously stirred at room temperature overnight. The reaction mixture was then poured into distilled water (14.0 mL). The phases were separated, and the aqueous phase was extracted with pentane (5 x 7.0 mL). The combined organic phases were washed with brine (2 x 7.0 mL), dried over magnesium sulfate, filtered and concentrated under reduced pressure. Finally, the resulting residue was purified by distillation (b.p. = 44 °C, p = 0.019 mbar) to afford the target substrate **1d** as a colorless liquid (0.904 g, 56% yield, *E*,*E*:*E*,*Z* isomers = 95:5, see Figure 1.21 and Figure 1.22). ^{1}H NMR (500 MHz, $CDCl_3$) δ 6.34 (dt, J = 16.8, 9.7 Hz, 1H), 6.27 – 6.17 (m, 2H), 6.05 (ddd, J = 15.0, 10.6, 1.2 Hz, 1H), 5.77 (dt, J = 15.2, 6.0 Hz, 1H), 5.70 (dq, J = 15.0, 6.8 Hz, 1H), 5.62 (dt, J = 15.1, 6.5 Hz, 1H), 5.20 (d, J = 16.8 Hz, 1H), 5.08 (d, J = 9.7 Hz, 1H), 3.99 (t, J = 6.5 Hz, 4H), 1.75 (d, J = 6.8 Hz, 3H) ppm. ^{13}C{^{1}H} NMR (125 MHz, $CDCl_3$) δ 136.5 (CH=), 133.4 (CH=), 133.2 (CH=), 130.9 (CH=), 130.3 (CH=), 130.1 (CH=), 126.7 (CH=), 117.5 (CH_2=), 70.6 (CH_2), 70.1 (CH_2), 18.2 (CH_3) ppm. Compound **1d** is too unstable to provide a good high-resolution mass spectrum under analysis conditions (using APCI as ionization source).

- Synthesis of (*E*)-2-methyl-5-(((*E*)-penta-2,4-dien-1-yl)oxy)penta-1,3-diene (**1e**)

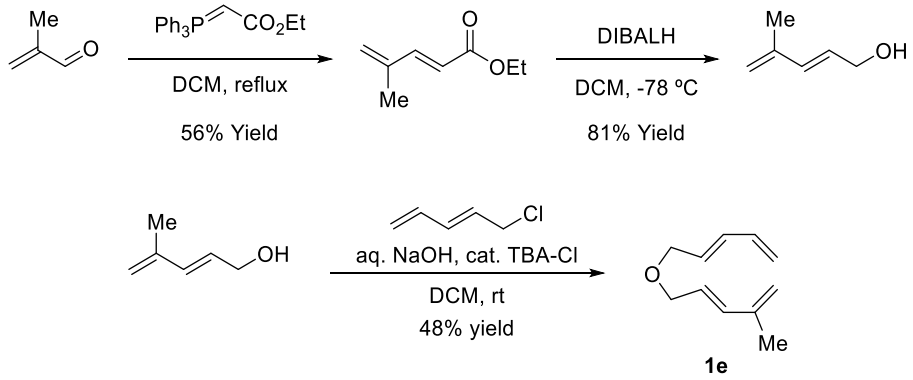

1e

A solution of 95% (carbethoxymethylene)-triphenylphosphorane (7.98 g, 21.8 mmol) and 90% methacrolein (2.0 mL, 21.8 mmol) in dichloromethane (80.0 mL) was added to a 250 mL round-bottom flask equipped with a stirring bar. The reaction mixture was stirred at reflux for 2 h, then cooled to 23 ºC and concentrated *in vacuo*. Pentane (250.0 mL) was added to the residue to precipitate triphenylphosphine oxide. The mixture was filtered through Celite® and the solvent evaporated to dryness. The filtration and evaporation steps were repeated until no white solid precipitated. Removal of the solvent yielded ethyl (*E*)-4-methylpenta-2,4-dienoate (1.7 g, 56% yield), which was directly used in the following step without further purification. ^{1}H NMR (400 MHz, $CDCl_3$) δ 7.35 (d, J = 15.8 Hz, 1H), 5.86 (d, J = 15.8 Hz, 1H), 5.34 (dt, J = 8.8, 1.6 Hz, 2H), 4.21 (q, J = 7.1 Hz, 2H), 1.88 (s, 3H), 1.39 – 1.10 (m, 3H) ppm. Spectroscopic data were in agreement with those previously reported in the literature.[24]

The previously obtained unsaturated ester (ethyl (*E*)-4-methylpenta-2,4-dienoate; 1.6 g, 11.4 mmol) was dissolved in dry DCM (14.0 mL) and cooled to -78 °C. To this solution, DIBAL-H (1.0 M in hexane, 28.5 mL, 28.5 mmol) was added dropwise. The reaction mixture was stirred at this temperature for 30 min. The reaction then was quenched with methanol (5.0 mL), saturated aqueous solution of the Rochelle salt (*i.e.*; potassium sodium tartrate) (120.0 mL) and diethyl ether (120.0 mL). The mixture was stirred vigorously a room temperature until there was sufficient separation of the two phases. The organic layer was separated, and the aqueous phase was extracted twice with DCM (2 x 20.0 mL).

(24) Marcus, A. P.; Lee, A. S.; Davis, R. L.; Tantillo, D. J.; Sarpong, R. *Angew. Chem., Int. Ed.* **2008**, *47*, 6379-6383.

The combined organic extracts were washed with water and brine, dried over magnesium sulfate and finally concentrated *in vacuo*. The mixture was distilled (b.p. = 77 °C, p = 6.8 mbar) to yield (*E*)-4-methylpenta-2,4-dien-1-ol pure (0.908 g, 81% yield). ^{1}H NMR (400 MHz, $CDCl_3$) δ 6.33 (dt, *J* = 15.7, 1.5 Hz, 1H), 5.86 – 5.74 (m, 1H), 5.01 – 4.95 (m, 2H), 4.24 – 4.17 (m, 2H), 1.85 (t, *J* = 1.1 Hz, 3H), 1.73 (s, 1H) ppm. ^{13}C{^{1}H} NMR (101 MHz, $CDCl_3$) δ 141.5 (C=), 134.2 (CH=), 128.5 (CH=), 116.9 (CH_2=), 63.7 (CH_2), 18.7 (CH_3) ppm. Spectroscopic data were in agreement with those previously reported in the literature.[25]

A mixture of (*E*)-4-methylpenta-2,4-dien-1-ol (450.0 mg, 4.6 mmol), previously prepared 5-chloropenta-1,3-diene (*E*:*Z* isomers in a 95:5 ratio; 863.0 mg, 7.1 mmol), tetra-*n*-butylammonium chloride (67.5 mg, 0.243 mmol), and 50% aqueous NaOH (1.8 g, 45.9 mmol) in DCM (2.0 mL) was vigorously stirred at room temperature overnight. The reaction mixture was then poured into distilled water (6.0 mL). The phases were separated and the aqueous phase was extracted with pentane (5 x 3.0 mL). The combined organic phases were washed with brine (2 x 3.0 mL), dried over magnesium sulfate, filtered and concentrated under reduced pressure. The target substrate **1e** was isolated by distillation of the crude (b.p. = 43 °C, p = 0.031 mbar) (0.360 g, 48 % yield, *E*,*E*:*E*,*Z* isomers = 95:5, see Figure 1.23 and Figure 1.24). ^{1}H NMR (500 MHz, $CDCl_3$) δ 6.39 - 6.22 (m, 3H), 5.81 - 5.70 (m, 2H), 5.20 (dd, *J* = 16,2, 1.5 Hz, 1H), 5.08 (dd, *J* = 9.9, 1.5 Hz, 1H), 4.97 (s, 2H), 4.04 (dd, *J* = 6.0, 1.3 Hz, 2H), 4.01 (dd, *J* = 5.9, 1.0 Hz, 2H), 1.85 (s, 3H) ppm. ^{13}C{^{1}H} NMR (125 MHz, $CDCl_3$) δ 141.5 (C=), 136.4 (CH=), 135.6 (CH=), 133.4 (CH=), 130.1 (CH=), 126.0 (CH=), 117.6 (CH_2=), 116.9 (CH_2=), 70.8 (CH_2), 70.3 (CH_2), 18.6 (CH_3) ppm. HRMS (APCI$^+$): *m*/*z* calcd for $C_{11}H_{17}O$ $[M+H]^+$ 165.1274, found 165.1274.

(25) (a) For the synthetic method, see: Zhou, J.-H.; Cai, S.-H.; Xu, Y.-H.; Loh, T.-P. *Org. Lett.* **2016**, *18*, 2355-2358. (b) For the spectroscopic data, see: Lai, M. T.; Li, D.; Oh, E.; Liu, H. W. *J. Am. Chem. Soc.* **1993**, *115*, 1619-1628.

- Synthesis of (*E*)-3-methyl-5-(((*E*)-penta-2,4-dien-1-yl)oxy)penta-1,3-diene (**1f**)

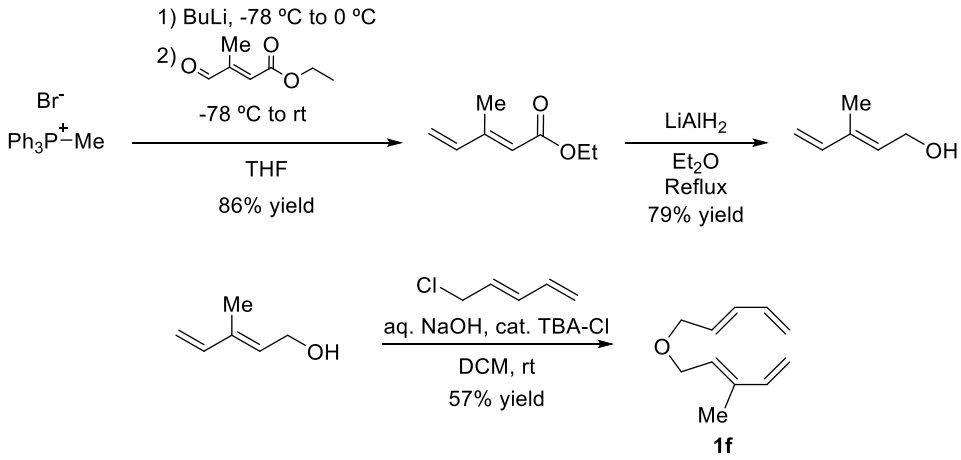

1f

A solution of *n*-butyllithium (2.5 M in hexane, 6.0 mL, 15.0 mmol) was added dropwise at -78 °C to a solution of methyltriphenylphosphonium bromide (5.3 g, 14.6 mmol) in dry THF (50.0 mL). The mixture was allowed to reach 0 °C and stirred for 1 h. After cooling to -78 °C, ethyl (*E*)-3-methyl-4-oxo-2-butenoate (2.0 g, 13.6 mmol) dissolved in dry THF (20.0 mL) was slowly added. The mixture was stirred for 24 h at room temperature. Water (30.0 mL) was added and the resulting mixture was extracted three times with diethyl ether (3 x 50.0 mL). The combined organic phases were dried with magnesium sulfate and the solvent was evaporated under reduced pressure. The residue was dissolved in pentane (50.0 mL), filtered through Celite® and then concentrated *in vacuo*. The filtration and concentration steps were repeated three times, until no white solid precipitated, to obtain ethyl (*E*)-3-methylpenta-2,4-dienoate (1.6 g, 86 % yield), which was used without any further purification. ^{1}H NMR (400 MHz, $CDCl_3$) δ 6.30 – 6.37 (ddd, J = 17.4, 10.6, 0.8 Hz, 1H), 5.74 – 5.71 (m, 1H), 5.54 (d, J = 17.4 Hz, 1H), 5.31 (d, J = 10.6 Hz, 1H), 4.11 (q, J = 7.2 Hz, 2 H), 2.20 (d, J = 1.3 Hz, 3H), 1.22 (t, J = 7.1 Hz, 3H) ppm. Spectroscopic data were in agreement with those previously reported in the literature.[26]

Ethyl (*E*)-3-methylpenta-2,4-dienoate (0.5 g, 3.6 mmol) was added to a suspension of $LiAlH_4$ (203.0 mg, 5.3 mmol) in dry diethyl ether (7.5 mL) under a N_2 atmosphere. The mixture was heated to reflux for 1 h and quenched by the careful addition of ice-cooled water. The residue formed was dissolved by addition of 10% H_2SO_4 (8.0 mL). The phases were separated and the aqueous

(26) Yildizhan, S.; Schulz, S. *Synlett* **2011**, 2831-2833.

phase was extracted with diethyl ether (3 x 10.0 mL). The combined organic phases were washed with a saturated solution of the Rochelle salt (1 x 10.0 mL), dried over magnesium sulfate, and the solvent was removed under reduced pressure. The residue of (*E*)-3-methylpenta-2,4-dien-1-ol was used in the next step without further purification (0.275 g, 79 % yield). ^{1}H NMR (400 MHz, $CDCl_3$) δ 6.45 – 6.33 (m, 1H), 5.73 – 5.63 (m, 1H), 5.22 (d, J = 16.9 Hz, 1H), 5.07 (d, J = 10.6 Hz, 1H), 4.29 (d, J = 6.8 Hz, 2H), 1.82 – 1.77 (m, 3H), 1.45 (br. s., 1H) ppm. Spectroscopic data were in agreement with those previously reported in the literature.[26]

A mixture of (*E*)-3-methylpenta-2,4-dien-1-ol (0.8 g, 8.1 mmol), previously prepared 5-chloropenta-1,3-diene (*E*:*Z* isomers in a 95:5 ratio; 1.5 g, 12.7 mmol), tetra-*n*-butylammonium chloride (120 mg, 0.43 mmol) and 50% aqueous NaOH (3.3 g, 81.5 mmol) in DCM (3.5 mL) was vigorously stirred at room temperature overnight. The reaction mixture was then poured into distilled water (10.0 mL). The phases were separated and the aqueous phase was extracted with pentane (5 x 5.0 mL). The combined organic phases were washed with brine (2 x 5.0 mL), dried over magnesium sulfate, filtered and concentrated *in vacuo*. The desired substrate **1f** was purified by distillation (b.p. = 34 °C, p = 0.04 mbar) (0.762 g, 57 % yield, *E*,*E*:*E*,*Z* isomers = 95:5, see Figure 1.25 and Figure 1.26). ^{1}H NMR (400 MHz, $CDCl_3$) δ 6.45 - 6.24 (m, 3H), 5.80 (dt, J = 15.0, 6.5 Hz, 1H), 5.65 (t, J = 6.4 Hz, 1H), 5.25 (d, J = 5.6 Hz, 1H), 5.20 (d, J = 5.7 Hz, 1H), 5.11 (d, J = 10.6 Hz, 1H), 5.06 (d, J = 10.7 Hz, 1H), 4.14 (d, J = 6.4 Hz, 2H), 4.04 (d, J = 6.5 Hz, 2H), 1.80 (s, 3H) ppm. ^{13}C{^{1}H} NMR (100 MHz, $CDCl_3$) δ 140.9 (CH=), 137.1 (C=), 136.4 (CH=), 133.4 (CH=), 130.2 (CH=), 128.4 (CH=), 117.7 (CH_2=), 113.0 (CH_2=), 70.4 (CH_2), 66.6 (CH_2), 12.2 (CH_3) ppm. HRMS (APCI$^+$): m/z calcd for $C_{11}H_{17}O$ $[M+H]^+$ 165,1274, found 165.1277.

- Synthesis of dimethyl 2-((*E*)-hexa-3,5-dien-1-yl)-2-((*E*)-penta-2,4-dien-1-yl)malonate (**1g**)

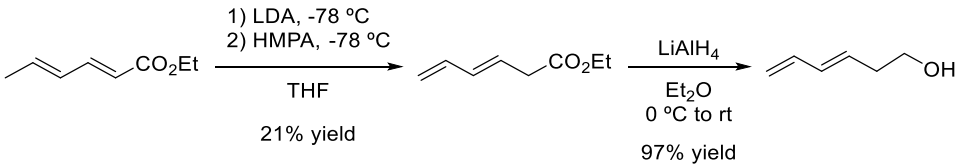

A flame-dried 500 mL Schlenk flask was loaded with dry THF (165.0 mL) and diisopropylamine (DIPA, 12.1 mL, 85.6 mmol) and cooled to -78 °C. A solution of *n*-butyllithium (2.5 M in hexane, 34.2 mL, 85.6 mmol) was then added dropwise and the reaction mixture was stirred at -78 °C for 1 h in order to form LDA *in situ*. Hexamethylphosphoramide (HMPA, 12.4 mL, 71.3 mmol) was then slowly added to the mixture. After 30 min stirring at -78 °C, a solution of ethyl sorbate (10.7 mL, 71.3 mmol) in THF (25.0 mL) was added dropwise, resulting in a red-orange solution. The reaction was stirred at -78 °C for 1 h and then ethanol (35.0 mL) was added. The reaction mixture was then quenched by pouring the mixture into a 1.0 L round-bottom flask containing water (140.0 mL) and glacial acetic acid (25.0 mL). After diluting with hexane (100.0 mL), the two phases were separated and the aqueous phase was extracted with hexane (3 x 125.0 mL). The combined organic phases were washed with saturated $NaHCO_3$ (2 x 75.0 mL), brine (2 x 75.0 mL) and dried over magnesium sulfate. The solvent was evaporated to dryness. The crude mixture containing the desired product and the starting material was purified by column chromatography on silica gel impregnated with $AgNO_3$ (10%)[18] (hexane:acetone 100:0→80:20) to yield ethyl (*E*)-hexa-3,5-dienoate (2.14 g, 21 % yield). ^1H NMR (300 MHz, $CDCl_3$) δ 6.32 (dt, J = 16.9, 10.4 Hz, 1H), 6.12 (dd, J = 15.2, 10.4 Hz, 1H), 5.77 (dt, J = 15.2, 7.2 Hz, 1H), 5.14 (d, J = 16.9 Hz, 1H), 5.04 (d, J = 10.1 Hz, 1H), 4.12 (q, J = 7.2 Hz, 2H), 3.09 (d, J = 7.2 Hz, 2H), 1.23 (t, J = 7.2 Hz, 3H) ppm. $^{13}C\{^1H\}$ NMR (75 MHz, $CDCl_3$) δ 171.1 (C=O), 136.1 (CH=), 133.9 (CH=), 135.4 (CH=), 116.5 (CH_2=), 60.4 (CH_2), 37.7 (CH_2), 13.8 (CH_3) ppm. Spectroscopic data were in agreement with those previously reported in the literature.[27]

$LiAlH_4$ (512.0 g, 13.5 mmol) was suspended in anhydrous diethyl ether (10.0 mL) in a flame-dried Schlenk flask and the suspension was cooled at 0 °C. Then, a solution of ethyl (*E*)-hexa-3,5-dienoate (1.35 g, 9.6 mmol) in anhydrous diethyl ether (3.0 mL) was slowly cannulated to the previous suspension. The reaction mixture was allowed to reach room temperature and stirred for 4.5 h. The

(27) Miller, C. A.; Batey, R. A. *Org. Lett.* **2004**, *6*, 699-702.

UNIVERSITAT ROVIRA I VIRGILI
TRANSITION METAL-CATALYZED CYCLOADDITION REACTIONS FOR THE FORMATION OF EIGHT- AND SIX-MEMBERED RINGS
Nuria Llorente González

reaction was cooled down to 0 °C again, diluted with diethyl ether (15.0 mL) and carefully quenched with a saturated aqueous solution of the Rochelle salt (25.0 mL). The biphasic mixture was vigorously stirred overnight. The two phases were then separated, and the aqueous phase was extracted with diethyl ether (2 x 50.0 mL). The combined organic phases were washed with brine (1 x 50.0 mL), dried over magnesium sulfate, filtered and concentrated *in vacuo* to provide the desired product (*E*)-hexa-3,5-dien-1-ol as a yellowish liquid (0.920 g, 97% crude yield), which was immediately used in the following step without further purification. ^{1}H NMR (300 MHz, $CDCl_3$) δ 6.41 (m, 1H), 6.12 (m, 1H), 5.67 (m, 1H), 5.12 (dt, J = 17.6, 0.5 Hz, 1H), 5.00 (dt, J = 9.6, 0.5 Hz, 1H), 3.66 (t, J = 6.6 Hz, 2H), 2.34 (qd, J = 6.6, 1.1 Hz, 2H), 1.93 (s, br, 1H) ppm. Spectroscopic data were in agreement with those previously reported in the literature.[28]

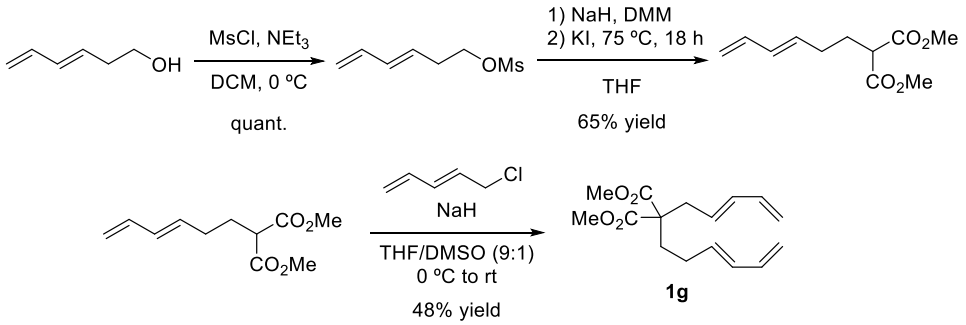

Methanesulfonyl chloride (0.6 mL, 7.4 mmol) was added to a solution of (*E*)-hexa-3,5-dien-1-ol (0.74 g, 7.09 mmol) and triethylamine (1.9 mL, 14.2 mmol) in DCM (22.0 mL) at 0 °C. The reaction mixture was stirred at 0 °C for 1 h, after which it was poured into a cooled 1.0 M HCl aqueous solution (15.0 mL). The aqueous phase was then extracted with DCM (3 x 25.0 mL). The combined organic phases were washed with brine (1 x 25.0 mL), dried over magnesium sulfate, filtered and the solvent evaporated to dryness to yield the crude mesylate compound as a yellowish oil in quantitative yield (1.249 g), which was immediately used in the following step without further purification. ^{1}H NMR (400 MHz, $CDCl_3$) δ 6.26 (m, 1H) 6.12 (m, 1H), 5.58 (dt, J = 14.7, J = 7.0 Hz, 1H), 5.10 (d, J = 16.7 Hz, 1H), 4.99 (d, J = 10.2 Hz, 1H), 4.19 (t, J = 6.7 Hz, 2H), 2.93 (s, 3H), 2.47 (q, J = 6.7 Hz, 2H) ppm. Spectroscopic data were in agreement with those previously reported in the literature.[29]

(28) DeBoef, B.; Counts, W. R.; Gilbertson, S. R. *J. Org. Chem.* **2007**, *72*, 799-804.
(29) Thanapipol, S.; Kündig, E. P. *Org. Biomol. Chem.* **2011**, *9*, 7564-7570.

A solution of dimethyl malonate (1.6 mL, 14.2 mmol) in anhydrous THF (18.5 mL) was added under inert atmosphere to a suspension of NaH (323.0 mg, 12.8 mmol) in anhydrous DMF (10.0 mL) previously placed in a 100 mL two-necked round-bottom flask. The mixture was stirred at room temperature for 15 min. After that, a solution of (*E*)-hexa-3,5-dien-1-yl methanesulfonate (1.2 g, 7.1 mmol) in anhydrous THF (17.0 mL) was slowly added followed by the addition of KI (235.0 g, 1.4 mmol) as solid. The resulting reaction mixture was heated at 75 °C and stirred overnight. After 18 h, the mixture was quenched with saturated aqueous NH_4Cl (25.0 mL) and extracted with diethyl ether (3 x 30.0 mL). The combined organic phases were dried over magnesium sulfate and concentrated *in vacuo*. Finally, the residue was purified by silica gel column chromatography (hexane:diethyl ether, 100:0→90:10) to yield (*E*)-2-(hexa-3,5-dien-1-yl)malonate as a colorless oil (0.9811 g, 65% yield). ^{1}H NMR (400 MHz, $CDCl_3$) δ 6.28 (td, J = 17.0, 10.3 Hz, 1H), 6.05 (dd, J = 15.2, 10.3 Hz, 1H), 5.62 (dt, J = 15.2, 7.6 Hz, 1H), 5.10 (d, J = 17.0 Hz, 1H), 4.98 (d, J = 10.3 Hz, 1H), 3.72 (s, 6H), 3.37 (t, J = 7.3 Hz, 1H), 2.12 (dd, J = 14.5, 7.12 Hz, 2H), 2.01 (dd, J = 14.5, 7.3 Hz, 2H) ppm. ^{13}C{^{1}H} NMR (101 MHz, $CDCl_3$) δ 169.8 (C=O), 136.9 (CH=), 132.7 (CH=), 132.5 (CH=), 115.8 (CH_2=), 52.6 (CH_3), 50.9 (CH), 30.2 (CH_2), 28.2 (CH_2) ppm. Spectroscopic data were in agreement with those previously reported in the literature.[29]

NaH (140.0 mg, 5.6 mmol) was added to a 50 mL bottom flask under inert atmosphere. Anhydrous THF (19.0 mL) and DMSO (2.0 mL) were syringed into the flask and the resulting suspension was cooled to 0 °C. Then, a solution of dimethyl (*E*)-2-(hexa-3,5-dien-1-yl)malonate (975.0 mg, 4.59 mmol) in anhydrous THF (2.5 mL) was slowly added. The resulting reaction mixture was allowed to reach room temperature and was stirred for 1 h. Then, the mixture was cooled down to 0 °C again and a solution of 5-chloropenta-1,3-diene (*E*:*Z* isomers in a 95:5 ratio; 0.69 g, 5.79 mmol) in anhydrous THF (2.0 mL) was added dropwise. The resulting mixture was allowed to reach room temperature and stirred overnight. Then, the mixture was quenched with distilled water (15.0 mL). The THF solvent was evaporated to dryness, the resulting residue was partitioned between diethyl ether (40.0 mL) and water (10.0 mL) and the two phases were separated. The organic phase was washed with distilled water (3 x 15.0 mL), dried over magnesium sulfate, filtered and concentrated *in vacuo*. Finally, the resulting residue was purified by silica gel column chromatography (hexane:diethyl ether, 90:10) to afford the desired compound **1g** as a yellow oil (0.620 g, 48% yield, *E,E*:*E,Z* isomers = 95:5, see Figure 1.27 and Figure 1.28). ^{1}H NMR (400 MHz, $CDCl_3$) δ 6.33 - 6.23 (m, 2H), 6.12 - 6.02 (m, 2H), 5.67

– 5.60 (m, 1H), 5.54 – 5.46 (m, 1H), 5.15 – 5.08 (m, 2H), 5.03 – 4.96 (m, 2H), 3.71 (s, 6H), 2.70 – 2.68 (m, 2H), 2.05 – 1.93 (m, 4H) ppm. $^{13}C\{^1H\}$ NMR (100 MHz, $CDCl_3$) δ 171.6 (C=O), 137.1 (CH=), 136.7 (CH=), 135.1 (CH=), 133.5 (CH=), 131.8 (CH=), 127.9 (CH=), 116.7 (CH_2=), 115.7 (CH_2=), 57.7 (C-$(CO_2Me)_2$), 52.6 (2 x CH_3, CO_2Me), 36.3 (CH_2), 32.2 (CH_2), 27.3 (CH_2) ppm. HRMS (ESI^+): *m/z* calcd for $C_{16}H_{22}O_4Na$ $[M+Na]^+$ 301.1410, found 301.1414.

- Synthesis of (*E*)-6-(((*E*)-penta-2,4-dien-1-yl)oxy)hexa-1,3-diene (**1h**)

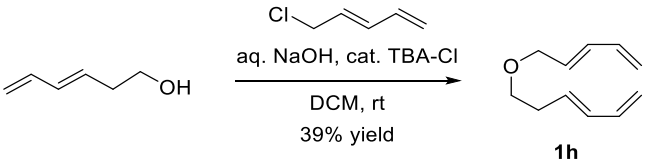

1h

A mixture of (*E*)-hexa-3,5-dien-1-ol (920.0 mg, 9.4 mmol), previously prepared 5-chloropenta-1,3-diene (*E*:*Z* isomers in a 95:5 ratio; 1.1 g, 11.2 mmol), tetra-*n*-butylammonium chloride (138.0 g, 0.497 mmol) and 50% aqueous NaOH (3.7 g, 93.7 mmol) in DCM (10.0 mL) was vigorously stirred at room temperature overnight. The reaction mixture was then poured into distilled water (20.0 mL). The phases were separated and the aqueous phase was extracted with pentane (5 x 15.0 mL). The combined organic phases were washed with brine (2 x 20.0 mL), dried over magnesium sulfate, filtered and concentrated under reduced pressure. The residue was purified by distillation (b.p. = 57 °C, p = 0.16 mbar) to afford the target substrate **1h** as a colorless liquid (0.600 g, 39% isolated yield, *E*,*E*:*E*,*Z* isomers = 95:5, see Figure 1.29 and Figure 1.30). ^1H NMR (400 MHz, $CDCl_3$) δ 6.39 – 6.21 (m, 3H), 6.16 – 6.08 (m, 1H), 5.81 – 5.68 (m, 2H), 5.23 – 5.08 (m, 3H), 5.00 – 4.97 (m, 1H), 4.03 – 4.01 (m, 2H), 3.48 (t, *J* = 6.8 Hz, 2H), 2.41 – 2.36 (m, 2H) ppm. $^{13}C\{^1H\}$ NMR (100 MHz, $CDCl_3$) δ 137.2 (CH=), 136.5 (CH=), 133.2 (CH=), 132.8 (CH=), 131.3 (CH=), 130.3 (CH=), 117.6 (CH_2=), 115.6 (CH_2=), 71.1 (CH_2), 89.8 (CH_2), 33.2 (CH_2) ppm. HRMS ($APCI^+$): *m/z* calcd for $C_{11}H_{17}O$ $[M+H]^+$ 165.1274, found 165.1279.

- Synthesis of *N*-((*E*)-hexa-3,5-dien-1-yl)-*N*-(penta-2,4-dien-1-yl) tosylamine (**1i**)

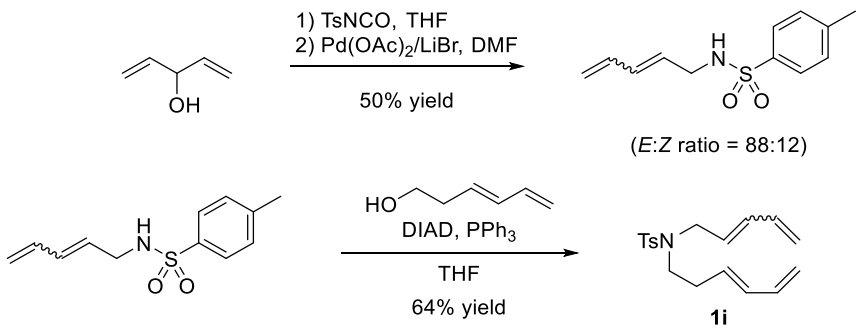

1,4-Pentadien-3-ol (1.0 g, 11.7 mmol) and 4-methylbenzenesulfonyl isocyanate (2.04 mL, 12.8 mmol) were placed into a flame-dried 100 mL Schlenk flask . Anhydrous THF (50.0 mL) was syringed into the flask and the resulting mixture was stirred at room temperature under inert atmosphere for 2 h. After that, the solvent was removed *in vacuo* and the resulting residue was dissolved in DMF (60.0 mL). Then, palladium acetate (131.0 mg, 0.583 mmol) and lithium bromide (4.1 g, 46.6 mmol) were added. The reaction mixture was heated at 90 °C and allowed to stir overnight at this temperature. Then, the reaction mixture was allowed to reach room temperature. Diethyl ether (600.0 mL) was added, and the organic phase was washed with distilled water (3 x 150.0 mL) and brine (3 x 150.0 mL), dried over magnesium sulfate, filtered and concentrated *in vacuo*. Finally, the resulting residue was purified by silica gel column chromatography (cyclohexane:EtOAc, 100:0→70:30) to yield the desired product 4-methyl-*N*-penta-2,4-dienyl-benzenesulfonamide as a white solid (1.38 g, 50% isolated yield, *E*:*Z* isomers = 88:12).[30] ^{1}H NMR (400 MHz, $CDCl_3$) δ 7.69 (d, *J* = 8.5Hz, 2H), 7.23 (d, *J* = 8.5Hz, 2H), 6.18 - 5.98 (m, 2H), 5.51-5.42 (m, 1H), 5.11- 4.99 (m, 2H), 4.57 (br, 1H), 3.55 (t, *J* = 6.3Hz, 2H), 2.35 (s, 3H) ppm. ^{13}C{^{1}H} NMR (101 MHz, $CDCl_3$) δ 143.7 (C_{arom}), 137.1 (C_{arom}), 132.9 (CH=), 130.7 (CH=), 129.9 (CH_{arom}), 127.3 (CH_{arom}), 125.5 (CH=), 120.2 (CH_2=), 44.9 (CH_2), 21.5 (CH_3) ppm. Spectroscopic data for the *E* isomer were in agreement with those previously reported in the literature.[30]

(30) The preparation of 4-methyl-*N*-penta-2,4-dienyl-benzenesulfonamide was performed using the experimental procedure reported in the following reference: Lei, A.; Lu, X. *Org. Lett.* **2000**, *2*, 2357-2360. The authors of the paper claimed that the reaction was regioselective affording exclusively the *E* isomer. In our hands, the target product was isolated as a mixture of *E*:*Z* isomers in a 88:12 ratio.

UNIVERSITAT ROVIRA I VIRGILI
TRANSITION METAL-CATALYZED CYCLOADDITION REACTIONS FOR THE FORMATION OF EIGHT- AND SIX-MEMBERED RINGS
Nuria Llorente González

A solution of diisopropyl azodicarboxylate (DIAD, 1.6 mL, 7.6 mmol) and triphenylphosphine (1.9 g, 7.6 mmol) in anhydrous THF (30.0 mL) was prepared at 0 °C in a flame-dried 50 mL Schlenk flask under argon atmosphere. After stirring for 1 h, a solution of 4-methyl-*N*-penta-2,4-dienyl-benzenesulfonamide (1.50 g, 6.3 mmol) and (*E*)-hexa-3,5-dien-1-ol (660 mg, 6.3 mmol) in anhydrous THF (10.0 mL) was added at 0 °C. The reaction mixture was slowly allowed to reach room temperature and stirred for 3 h. The solvent was then evaporated to dryness and the resulting mixture was purified by silica gel column chromatography (cyclohexane:EtOAc, 100:0→80:20) to yield the desired substrate **1i** as a colorless oil (1.29 g, 64% yield, *E*,*E*:*E*,*Z* isomers = 88:12, see Figure 1.31 and Figure 1.32).

The two *E*,*E*- and *E*,*Z*-isomers were isolated by semi-preparative HPLC using a Daicel Chiralpak® IA column (98:2 hexane/EtOH; 5 mL/min) on a 10 mg scale. Semi-preparative HPLC analysis, Daicel Chiralpak® IA column (25 cm x 0.46 cm), hexane/EtOH (95:5), 1 mL/min, 254 nm, t^R (*E*,*Z*-isomer) = 14.3 min, t^R (*E*,*E*-isomer) = 16.3 min.

E,*E*-**1i** (see Figure 1.33 and Figure 1.34): ^{1}H NMR (500 MHz, $CDCl_3$) δ 7.70 - 7.68 (m, 2H), 7.30 - 7.28 (m, 2H), 6.29 - 6.21 (m, 2H), 6.13 - 6.00 (m, 2H), 5.57 - 5.46 (m, 2H), 5.19 - 4.99 (m, 4H), 3.84 (d, J = 6.6 Hz, 2H), 3.19 - 3.16 (m, 2H), 2.42 (s, 3H), 2.33 - 2.28 (m, 2H) ppm. ^{13}C{^{1}H} NMR (125 MHz, $CDCl_3$) δ 143.3 (C_{arom}), 137.3 (C_{arom}), 136.9 (CH=), 135.9 (CH=), 134.6 (CH=), 133.4 (CH=), 130.8 (CH=), 129.8 (CH_{arom}), 128.4 (CH=), 127.3 (CH_{arom}), 118.2 (CH_2=), 116.1 (CH_2=), 49.9 (CH_2), 47.0 (CH_2), 32.0 (CH_2), 21.6 (CH_3) ppm. Spectroscopic data for the *E*,*E* isomer were in agreement with those previously reported in the literature.[6]

E,*Z*-**1i** (see Figure 1.35 and Figure 1.36): ^{1}H NMR (500 MHz, $CDCl_3$) δ 7.70 - 7.68 (m, 2H, H_{arom}), 7.30 - 7.28 (m, 2H, H_{arom}), 6.58 - 6.51 (m, 1H) 6.29 - 6.21 (m, 1H), 6.12 - 6.00 (m, 2H), 5.58 - 5.52 (m, 1H), 5.29 - 5.20 (m, 3H), 5.12 - 5.08 (m, 1H), 5.01 - 4.99 (m, 1H), 4.00 - 3.98 (m, 2H), 3.19 - 3.16 (m, 2H), 2.42 (s, 3H, Me), 2.34 - 2.29 (m, 2H) ppm. ^{13}C{^{1}H} NMR as DEPTQ135 (125 MHz, $CDCl_3$) δ 143.4 (C_{arom}), 137.2 (C_{arom}), 136.9 (CH=), 133.4 (CH=), 133.0 (CH=), 130.8 (CH=), 130.6 (CH=), 129.8 (CH_{arom}), 127.4 (CH_{arom}), 126.0 (CH=), 120.2 (CH_2=), 116.1 (CH_2=), 47.0 (CH_2), 44.9 (CH_2), 32.1 (CH_2), 21.6 (CH_3) ppm. HRMS (ESI$^+$): m/z calcd for $C_{18}H_{23}NO_2SNa$ $[M+Na]^+$ 340.1342, found 340.1350.

1.4.4. General Methodology for the Cycloaddition Reactions

A solution of the substrate (1.00 mmol) and ligand (0.21 mmol) in anhydrous and deoxygenated toluene was prepared under inert atmosphere. $Ni(COD)_2$ (0.10 mmol) was added dropwise from a stock solution in anhydrous toluene. The resulting mixture was carefully heated at 60 °C under argon atmosphere and stirred for 24 h. After that, the reaction mixture was allowed to reach room temperature and left stirring under air for 1 h. The mixture was filtered through a short pad of silica and further eluted with diethyl ether. The filtrate was concentrated *in vacuo* and the resulting crude mixture was analyzed by NMR spectroscopy. Purification of the desired product was carried out with column chromatography on silica gel impregnated with silver nitrate (10%) and mixtures of hexane:acetone (100:0→0:100) as the eluent.[18]

1.4.5. Characterization of [4+4] Cycloaddition Products

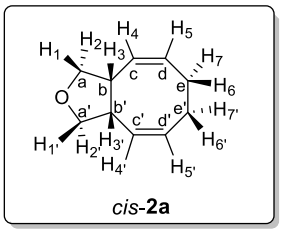

cis-**2a**

Product *cis*-**2a** was prepared following the general procedure starting from substrate **1a** (76.0 mg, 0.50 mmol), ligand **L2** (37.9 mg, 0.11 mmol), and $Ni(COD)_2$ (14.1 mg, 0.050 mmol). It was obtained as a colorless liquid (0.040 g, 56% yield, see Figure 1.37 and Figure 1.38). ^{1}H NMR (400 MHz, $CDCl_3$) δ 5.59 (m, 2H, $H_{5/5'}$), 5.40 (dd, $^3J_{4\text{-}5}$ = 11.1 Hz, $^3J_{4\text{-}3}$ = 2.3 Hz, 2H, $H_{4/4'}$), 4.02 (dd, $^2J_{1\text{-}2}$ = 8.0, $^3J_{1\text{-}3}$ = 6.9 Hz, 2H, $H_{1/1'}$), 3.60 (dd, $^2J_{2\text{-}1}$ = 8.0 Hz, $^3J_{2\text{-}3}$ = 6.1 Hz, 2H, $H_{2/2'}$), 3.31 (bs, 2H, $H_{3/3'}$), 2.74 – 2.41 (m, 2H, $H_{6/6'}$), 2.06 (m, 2H, $H_{7/7'}$) ppm. ^{13}C{^{1}H} NMR (101 MHz, $CDCl_3$) δ 129.5 ($C_{d/d'}$), 128.9 ($C_{c/c'}$), 73.9 ($C_{a/a'}$), 43.6 ($C_{b/b'}$), 27.9 ($C_{e/e'}$) ppm. Spectroscopic data were in agreement with those previously reported in the literature.[6]

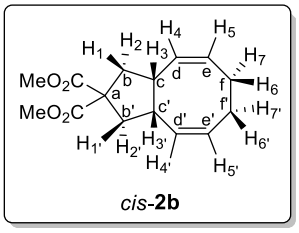

cis-**2b**

Product *cis*-**2b** was prepared following the general procedure starting from substrate **1b** (95.0 mg, 0.36 mmol), ligand **L2** (42.6 mg, 0.12 mmol), and $Ni(COD)_2$ (11.1 mg, 0.039 mmol). It was obtained as a colorless liquid (0.050 g, 56% yield, see Figure 1.41 and Figure 1.42). ^{1}H NMR (500 MHz, $CDCl_3$) δ 5.51 (dt, $^3J_{5\text{-}4}$ = 11.0 Hz, $^3J_{5\text{-}6/7}$ = 5.5 Hz, 2H, $H_{5/5'}$), 5.39 (dd, $^3J_{4\text{-}5}$ = 11.0 Hz, $^3J_{4\text{-}3}$ = 2.5 Hz, 2H, $H_{4/4'}$), 3.75 – 3.70 (m, 6H, H_{OMe}), 3.19 (bs,

2H, $H_{3/3'}$), 2.56 – 2.42 (m, 4H, $H_{6/6'}$ and $H_{1/1'}$), 2.15 (dd, $^2J_{2\text{-}1}$ = 13.6, $^3J_{2\text{-}3}$ = 7.5 Hz, 2H, $H_{2/2'}$), 2.03 – 1.96 (m, 2H, $H_{7/7'}$) ppm. $^{13}C\{^1H\}$ NMR (126 MHz, $CDCl_3$) δ 173.3 (s, C_7 or $C_{7'}$), 173.0 (s, C_e or $C_{e'}$), 131.6 ($C_{d/d'}$), 128.8 ($C_{e/e'}$), 57.8 (C_a), 52.9 (C_{OMe}), 52.9 (C_{OMe}), 43.3 ($C_{c/c'}$), 41.2 ($C_{b/b'}$), 28.1 ($C_{f/f'}$) ppm. Spectroscopic data were in agreement with those previously reported in the literature.[6]

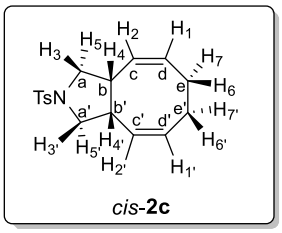

cis-**2c**

Product *cis*-**2c** was prepared following the general procedure starting from substrate **1c** (103.0 mg, 0.34 mmol), ligand **L2** (40.2 mg, 0.11 mmol), and $Ni(COD)_2$ (10.5 mg, 0.037 mmol). It was obtained as a white solid (0.041 g, 40% yield, see Figure 1.43 and Figure 1.44). ^1H NMR (500 MHz, $CDCl_3$) δ 7.73 (d, $^3J_{HTs\text{-}HTs}$ = 8.1 Hz, 2H, H_{Ts}), 7.32 (d, $^3J_{HTs\text{-}HTs}$ = 8.1 Hz, 2H, H_{Ts}), 5.49 (dt, $^3J_{H1\text{-}H2}$ = 11.3 Hz, $^3J_{H1\text{-}H6/7}$ = 5.6 Hz, 2H, $H_{1/1'}$), 5.09 (dd, $^3J_{H2\text{-}H1}$ = 11.3 Hz, $^3J_{H2\text{-}H4}$ = 2.3 Hz, 2H, $H_{2/2'}$), 3.49 (dd, $^2J_{H3\text{-}H5}$ = 9.5 Hz, $^3J_{H3\text{-}H4}$ = 6.8 Hz, 2H, $H_{3/3'}$), 3.19 (bs, 2H, H_4), 3.11 (dd, $^2J_{H5\text{-}H3}$ = 9.5 Hz, $^3J_{H5\text{-}H4}$ = 5.9 Hz, 2H, $H_{5/5'}$), 2.60 - 2.47 (m, 2H, $H_{6/6'}$), 2.43 (s, 3H, H_{Ts}), 2.05 - 1.97 (m, 2H, $H_{7/7'}$) ppm. $^{13}C\{^1H\}$ NMR (125 MHz, $CDCl_3$) δ 143.5 (C_{arom}, C_{Ts}), 134.3 (C_{arom}, C_{Ts}), 129.9 (CH_{arom}, C_{Ts}), 129.8 (CH=, C_d), 128.2 (CH=, C_c), 127.6 (CH_{arom}, C_{Ts}), 53.6 (CH_2, C_a), 42.6 (CH_2, C_b), 28.0 (CH_2, C_e), 21.7 (CH_3, C_{Ts}) ppm. Spectroscopic data were in agreement with those previously reported in the literature.[6]

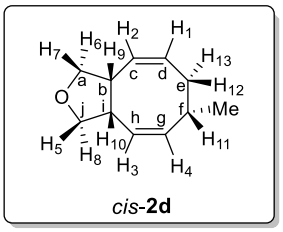

cis-**2d**

Product *cis*-**2d** was prepared following the general procedure starting from substrate **1d** (62.0 mg, 0.38 mmol), ligand **L2** (28.5 mg, 0.079 mmol), and $Ni(COD)_2$ (10.5 mg, 0.038 mmol). It was obtained as a colorless liquid (8.2 mg, 13% yield, see Figure 1.45 to Figure 1.47). ^1H NMR (800 MHz, $CDCl_3$) δ 5.61 - 5.56 (m, 1H, H_1), 5.36 (ddd, $^3J_{H2\text{-}H1}$ = 11.3 Hz, $^3J_{H2\text{-}H9}$ = 6.1 Hz, $^4J_{H2\text{-}H12}$ = 2.6 Hz, 1H, H_2), 5.33 (dd, $^3J_{H3\text{-}H4}$ = 10.7 Hz, $^3J_{H3\text{-}H10}$ = 2.5 Hz, 1H, H_3), 5.29 (ddd, $^3J_{H4\text{-}H3}$ = 10.7 Hz, $^3J_{H4\text{-}H11}$ = 7.3 Hz, $^4J_{H4\text{-}H10}$ = 2.5 Hz, 1H, H_4), 4.03 (dd, $^2J_{H5\text{-}H8}$ = $^3J_{H5\text{-}H10}$ = 7.9 Hz, 1H, H_5), 4.00 (dd, $^2J_{H6\text{-}H7}$ = 8.2 Hz, $^3J_{H6\text{-}H9}$ = 6.2 Hz, 1H, H_6), 3.69 (dd, $^2J_{H7\text{-}H6}$ = 8.3 Hz, $^3J_{H7\text{-}H9}$ = 4.0 Hz, 1H, H_7), 3.50 (dd, $^2J_{H8\text{-}H5}$ = 8.9 Hz, $^3J_{H8\text{-}H10}$ = 8.0 Hz, 1H, H_8), 3.36 (bs, 1H, H_9), 3.25 (ddddd, $^3J_{H10\text{-}H9}$ = $^3J_{H10\text{-}H8}$ = $^3J_{H10\text{-}H5}$ = 8.0 Hz, $^3J_{H10\text{-}H3}$ = 2.9 Hz, $^4J_{H10\text{-}H4}$ = 2.5 Hz, 1H, H_{10}), 3.02 - 2.97 (m, 1H, H_{11}), 2.60 - 2.55 (m, 1H, H_{12} or H_{13}), 1.82 - 1.80 (m, 1H, H_{12} or H_{13}), 1.04 (d, $^3J_{Me\text{-}H11}$ = 6.6 Hz, 3H,) ppm. $^{13}C\{^1H\}$ NMR (125 MHz, $CDCl_3$) δ 136.6 (CH=, C_g), 129.9 (CH=, C_c and C_d), 129.8 (CH=, C_c and

C_d), 126.3 (CH=, C_h), 75.0 (CH_2, C_a), 73.2 (CH_2, C_j), 44.4 (CH, C_i), 43.4 (CH, C_b), 37.5 (CH_2, C_e), 33.1 (CH, C_f), 22.0 (Me) ppm. HRMS (APCI$^+$): *m/z* calcd for $C_{11}H_{17}O$ $[M+H]^+$ 165.1274, found 165.1272.

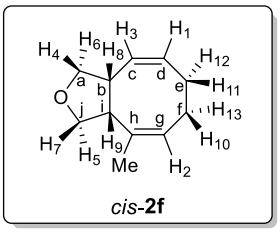

cis-**2f**

Product *cis*-**2f** was prepared following the general procedure starting from substrate **1f** (115.0 mg, 0.70 mmol), ligand **L2** (52.7 mg, 0.14 mmol), and $Ni(COD)_2$ (19.6 mg, 0.070 mmol). It was obtained as a colorless liquid (0.039 g, 35% yield, see Figure 1.48 to Figure 1.50). ^{1}H NMR (800 MHz, $CDCl_3$) δ 5.56 - 5.53 (m, 1H, H_1), 5.39 (tq, 1H, $^3J_{H2\text{-}H10} = {}^3J_{H2\text{-}H13} = 8.8$ Hz, $^4J_{H2\text{-}Me} = 1.3$ Hz, H_2), 5.36 (ddd, $^3J_{H3\text{-}H1} = 11.1$ Hz, $^3J_{H3\text{-}H8} = 6.9$ Hz, $^4J_{H3\text{-}H11} = 2.9$ Hz, H_3), 4.04 (dd, $^2J_{H4\text{-}H6} = 8.2$ Hz, $^3J_{H4\text{-}H8} = 5.8$ Hz, 1H, H_4), 4.03 (dd, $^2J_{H5\text{-}H7} = {}^3J_{H5\text{-}H9} = 7.8$ Hz, 1H, H_5), 3.73 (dd, $^2J_{H4\text{-}H6} = 8.2$ Hz, $^3J_{H6\text{-}H8} = 3.1$ Hz, 1H, H_6), 3.64 (dd, $^3J_{H7\text{-}H9} = 10.2$ Hz, $^2J_{H5\text{-}H7} = 7.9$ Hz, 1H, H_7), 3.53 (bs, 1H, H_8), 3.19 (ddd, $^3J_{H9\text{-}H7} = 10.2$ Hz, $^3J_{H9\text{-}H8} = 8.4$ Hz $^3J_{H9\text{-}H5} = 7.8$ Hz, 1H, H_9), 2.70 - 2.65 (m, 1H, H_{10}), 2.51 - 2.47 (m, 1H, H_{11} or H_{12}), 2.09 - 2.04 (m, 1H, H_{11} or H_{12}), 1.97 - 1.94 (m, 1H, H_{13}), 1.67 (s, 3H,) ppm. ^{13}C{^{1}H} NMR (100 MHz, $CDCl_3$) δ 134.9 (C=, C_h), 129.81 (CH=, C_e and C_d), 129.78 (CH=, C_e and C_d), 124.8 (CH=, C_g), 75.4 (CH_2, C_a), 70.8 (CH_2, C_j), 48.3 (CH, C_i), 42.1 (CH, C_b), 29.5 (CH_2, C_e), 26.4 (CH_2, C_f), 23.2 (Me) ppm. HRMS (APCI$^+$): *m/z* calcd for $C_{11}H_{17}O$ $[M+H]^+$ 165.1274, found 165.1272.

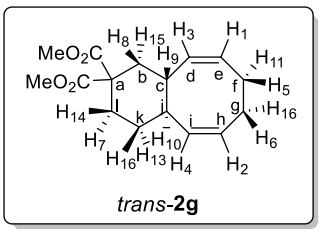

trans-**2g**

Product *trans*-**2g** was prepared following the general procedure starting from substrate **1g** (151.0 g, 0.514 mmol), ligand **L2** (38.8 mg, 0.11 mmol), and $Ni(COD)_2$ (14.4 mg, 0.05 mmol). It was obtained as a white solid (0.101 g, 67% yield, > 95% purity, see Figure 1.51 and Figure 1.52). m.p. = 85.6-87.9 °C. ^{1}H NMR (400 MHz, $CDCl_3$) δ 5.56 - 5.44 (m, 2H, H_1-H_2), 5.38 - 5.29 (m, 2H, H_3-H_4), 3.76 (s, 3H, Me), 3.70 (s, 3H, Me), 2.50 - 2.37 (m, 6H, H_5-H_{10}), 2.25 - 2.16 (m, 6H, H_{11}-H_{12}), 1.84 (dq, $^2J_{H13\text{-}H6} = 13.6$ Hz, $^3J_{H13\text{-}H7} = {}^3J_{H13\text{-}H14} = {}^3J_{H13\text{-}H10} = 3.4$ Hz, 1H, H_{13}), 1.71 (dt, $^2J_{H14\text{-}H7} = 13.6$ Hz, $^3J_{H14\text{-}H13} = {}^3J_{H14\text{-}H16} = 3.9$ Hz, 1H, H_{14}), 1.51 (dd, $^2J_{H15\text{-}H8} = 13.5$ Hz, $^3J_{H15\text{-}H9} = 11.8$ Hz, 1H, H_{15}), 1.26 - 1.16 (m, 1H, H_{16}) ppm. ^{13}C{^{1}H} NMR (100 MHz, $CDCl_3$) δ 172.8 (C=O), 171.6 (C=O), 133.8 (CH=, C_d or C_i), 133.4 (CH=, C_d or C_i), 127.4 (CH=, C_e or C_h), 127.1 (CH=, C_e or C_h), 55.3 (C_q, C_a), 52.8 (OMe), 52.7 (OMe), 42.7 (CH, C_j), 40.2 (CH, C_c), 38.9 (CH_2, C_b), 31.4 (CH_2, C_l), 30.6 (CH_2, C_k), 28.1 (CH_2, C_f or C_g), 27.8 (CH_2, C_f or C_g) ppm. HRMS (ESI$^+$): *m/z* calcd for $C_{16}H_{22}O_4Na$ $[M+Na]^+$ 301.1410, found 301.1417.

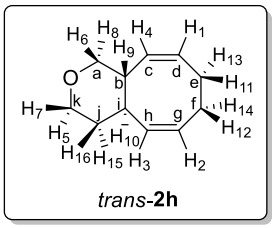

trans-**2h**

Product *trans*-**2h** was prepared following the general procedure starting from substrate **1h** (54.0 g, 0.310 mmol), ligand **L2** (23.4 mg, 0.065 mmol), and $Ni(COD)_2$ (8.7 mg, 0.031 mmol). It was obtained as colorless liquid (0.033 g, 61% yield, > 95% purity, see Figure 1.53 and Figure 1.54). ^1H NMR (400 MHz, $CDCl_3$) δ 5.63 – 5.56 (m, 1H, H_1), 5.55 – 5.48 (m, 1H, H_2), 5.38 – 5.33 (m, 1H, H_3), 5.21 – 5.17 (m, 1H, H_4), 4.01 – 3.93 (m, 2H, H_5-H_6), 3.44 – 3.37 (m, 1H, H_7), 3.06 (dd, $^2J_{H8\text{-}H6} = {}^3J_{H8\text{-}H9} = 10.8$ Hz, 1H, H_8), 2.70 – 2.62 (m, 1H, H_9), 2.60 – 2.50 (m, 3H, H_{10}, H_{11} or H_{13}, and H_{12} or H_{14}), 2.29 – 2.20 (m, 2H, H_{11} or H_{13}, and H_{12} or H_{14}), 1.75 – 1.70 (m, 1H, H_{15}), 1.51 – 1.40 (m, 1H, H_{16}) ppm. $^{13}C\{^1H\}$ NMR (100 MHz, $CDCl_3$) δ 133.4 (CH=, C_h), 129.6 (CH=, C_d), 128.7 (CH=, C_c), 127.4 (CH=, C_g), 72.9 (CH_2, C_a), 68.4 (CH_2, C_k), 43.2 (CH, C_b), 41.7 (CH, C_i), 33.8 (CH_2, C_j), 28.2 (CH_2, C_e or C_f), 27.9 (CH_2, C_e or C_f) ppm. HRMS (APCI$^+$): *m/z* calcd for $C_{11}H_{17}O$ $[M+H]^+$ 165.1274, found 165.1271.

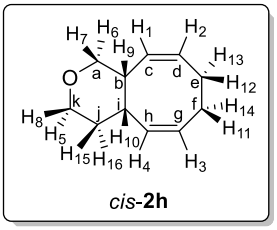

cis-**2h**

Samples of the product *trans*-**2h** (see Figure 1.55 and Figure 1.56) containing < 5% of product *cis*-**2h** (see Figure 1.57 and Figure 1.58) were separated by semi-preparative HPLC using a Daicel Chiralpak® IA column (hexane; 1 mL/min) on a 10 mg scale. Semi-preparative HPLC analysis, Daicel Chiralpak® IA column (25 cm x 0.46 cm), hexane, 1 mL/min, 210 nm, t_R(*cis*-isomer) = 13.5 min, t_R(*trans*-isomer) = 22.6 min. Characterization data for the product *cis*-**2h**: ^1H NMR (500 MHz, $CDCl_3$) δ 5.66 – 5.54 (m, 3H, H_1-H_3), 5.30 – 5.28 (m, 1H, H_4), 3.93 (dt, $^2J_{H5\text{-}H8} = 11.3$ Hz, $^2J_{H5\text{-}H15} = {}^3J_{H5\text{-}H16} = 4.0$ Hz, 1H, H_5), 3.67 (dd, $^2J_{H6\text{-}H7} = 11.3$ Hz, $^2J_{H6\text{-}H9} = 4.0$ Hz, 1H, H_6), 3.58 – 3.52 (m, 2H, H_7-H_8), 3.18 (bs, 1H, H_9), 2.86 – 2.75 (m, 2H, H_{10}-H_{11}), 2.56 – 2.53 (m, 1H, H_{12}), 2.14 – 1.98 (m, 2H, H_{13}-H_{14}), 1.64 – 1.46 (m, 2H, H_{15}-H_{16}) ppm. $^{13}C\{^1H\}$ NMR (125 MHz, $CDCl_3$) δ 133.7 (CH=, C_h), 128.62 (CH=, C_c), 128.60 (CH=, C_d), 127.8 (CH=, C_g), 70.7 (CH_2, C_a), 67.8 (CH_2, C_k), 39.7 (CH, C_i), 38.9 (CH, C_b), 30.1 (CH_2, C_j), 29.2 (CH_2, C_e), 26.8 (CH_2, C_f) ppm. HRMS (APCI$^+$): *m/z* calcd for $C_{11}H_{17}O$ $[M+H]^+$ 165.1274, found 165.1274.

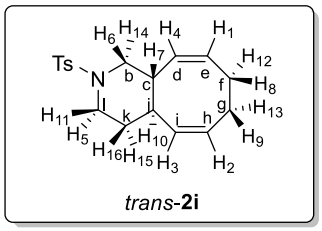

trans-**2i**

Product *trans*-**2i** was prepared following the general procedure starting from substrate *E,E*-**1i** (107.0 g, 0.34 mmol), ligand **L2** (25.5 mg, 0.071 mmol), and $Ni(COD)_2$ (9.5 mg, 0.034 mmol). It was obtained as a colorless liquid (0.084 g, 78% yield, see Figure 1.61 and Figure 1.62). ^1H NMR (500 MHz, $CDCl_3$) δ 7.66 – 7.64 (m, 2H, H_{arom}, H_{Ts}), 7.34 – 7.32 (m, 2H, H_{arom}, H_{Ts}), 5.60 – 5.55 (m, 1H, H_1), 5.53 – 5.48 (m, 1H, H_2), 5.33 – 5.29 (m, 1H, H_3), 5.25 – 5.22 (m, 1H, H_4), 3.88 – 3.82 (m, 2H, H_5-H_6), 2.72 – 2.65 (m, 1H, H_7), 2.47 – 2.37 (m, 5H, Me, H_8 or H_{12}, and H_9 or H_{13}), 2.27 – 2.17 (m, 4H, H_{10}, H_{11}, H_8 or H_{12}, and H_9 or H_{13}), 1.91 (dd, $^2J_{H14\text{-}H6} = {}^3J_{H14\text{-}H7} = 11.3$ Hz, 1H, H_{14}), 1.85 – 1.81 (m, 1H, H_{15}), 1.51 – 1.42 (m, 1H, H_{16}) ppm. $^{13}C\{^1H\}$ NMR (125 MHz, $CDCl_3$) δ 143.6 (C_{arom}), 133.5 (C_{arom}), 132.4 (CH=, C_h), 129.8 (CH_{arom}), 129.5 (CH=, C_d), 129.4 (CH=, C_c), 127.9 (CH=, C_g), 127.8 (CH_{arom}), 51.7 (CH_2, C_a), 46.7 (CH_2, C_k), 42.3 (CH, C_b), 41.8 (CH, C_i), 32.3 (CH_2, C_j), 27.9 (CH_2, C_e or C_f), 27.8 (CH_2, C_e or C_f), 21.7 (CH_3, Me) ppm. HRMS (ESI^+): *m/z* calcd for $C_{18}H_{24}NO_2S$ $[M+H]^+$ 318.1522, found 318.1519.

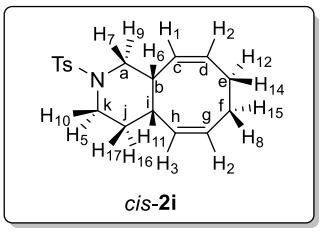

cis-**2i**

Product *cis*-**2i** was prepared following the general procedure starting from substrate *E,Z*-**1i** (15.0 mg, 0.0473 mmol), ligand **L2** (3.57 mg, 0.0099 mmol), and $Ni(COD)_2$ (1.33 mg, 0.0047 mmol). It was obtained as a colorless liquid (8.3 mg, 55% yield, see Figure 1.63 and Figure 1.64). ^1H NMR (400 MHz, $CDCl_3$) δ 7.64 (d, $^3J_{HTs\text{-}HTs} = 8.1$ Hz, 2H, H_{Ts}),, 7.32 (d, $^3J_{HTs\text{-}HTs} = 8.1$ Hz, 2H, H_{Ts}),, 5.64 – 5.59 (m, 2H, H_1-H_2), 5.59 – 5.49 (m, 1H, H_3), 5.23 – 5.14 (m, 1H, H_4), 3.52 – 3.47 (m, 1H, H_5), 3.31 – 3.25 (m, 2H, H_6-H_7), 2.76 – 2.66 (m, 1H, H_8), 2.66 – 2.53 (m, 4H, H_9-H_{12}), 2.43 (s, 3H, H_{Ts}), 2.14 – 1.97 (m, 2H, H_{13}-H_{14}), 1.67 – 1.58 (m, 2H, H_{15}-H_{16}) ppm. $^{13}C\{^1H\}$ NMR (100 MHz, $CDCl_3$) δ 143.5 (C_{arom}, C_{Ts}), 133.4 (C_{arom}, C_{Ts}), 132.1 (CH=, C_h), 129.8 (CH_{arom}, C_{Ts}), 128.9 (CH=, C_c), 128.3 (CH=, C_d), 128.2 (CH=, C_g), 127.8 (CH_{arom}, C_{Ts}), 49.7 (CH_2, C_a), 45.6 (CH_2, C_k), 39.6 (CH, C_i), 37.8 (CH, C_b), 29.1 (CH_2, C_e), 29.0 (CH_2, C_j), 26.9 (CH_2, C_f), 21.7 (CH_3, C_{Ts}) ppm. Spectroscopic data were in agreement with those previously reported in the literature.[6]

UNIVERSITAT ROVIRA I VIRGILI
TRANSITION METAL-CATALYZED CYCLOADDITION REACTIONS FOR THE FORMATION OF EIGHT- AND SIX-MEMBERED RINGS
Nuria Llorente González

1.4.6. Single Crystal X-Ray Structure Determinations

Crystal preparation: Crystals of products *cis*-**2c** and *trans*-**2g** were grown by slow diffusion in hexane/acetone (80:20, v/v). The crystals for these samples were selected using a Zeiss stereomicroscope using polarized light and prepared under inert conditions immersed in perfluoropolyether as protecting oil for manipulation.

Data collection: Crystal structure determination for product *trans*-**2g** was carried out using a Apex DUO Kappa 4-axis goniometer equipped with an APPEX 2 4K CCD area detector, a Microfocus Source E025 IμS using MoK$_\alpha$ radiation, Quazar MX multilayer Optics as monochromator and an Oxford Cryosystems low temperature device Cryostream 700 plus (T = -173 °C). Crystal structure determination for product *cis*-**2c** was carried out using a Rigaku diffractometer equipped with a Pilatus 200K area detector, a Rigaku MicroMax-007HF microfocus rotating anode with MoK$_\alpha$ radiation, Confocal Max Flux optics and an Oxford Cryosystems low temperature device Cryostream 700 plus (T = -173 °C). Full-sphere data collection was used with ω and φ scans. *Programs used:* Bruker Device: Data collection APEX-2,[31] data reduction Bruker Saint[32] V/.60A and absorption correction SADABS.[33] Rigaku device: Data collection and reduction with CrysAlisPro[34] and absorption correction with Scale3 Abspack scaling algorithm.[35]

Structure Solution and Refinement: Crystal structure solution was achieved using the computer program SHELXT.[36] Visualization was performed with the program SHELXle.[37] Missing atoms were subsequently located from difference Fourier synthesis and added to the atom list. Least-squares refinement on F^2 using

(31) Data collection with APEX II version v2013.4-1. Bruker (2007). Bruker AXS Inc., Madison, Wisconsin, USA.
(32) Data reduction with Bruker SAINT version V8.30c. Bruker (2007). Bruker AXS Inc., Madison, Wisconsin, USA.
(33) SADABS: V2012/1 Bruker (2001). Bruker AXS Inc., Madison, Wisconsin, USA. See the following reference: Blessing, R. H. *Acta Cryst.* **1995**, *A51*, 33-38.
(34) Data collection and reduction with CrysAlisPro 1.171.39.12b (Rigaku OD, 2015).
(35) Empirical absorption correction using spherical harmonics implemented in Scale3 Abspack scaling algorithm, CrysAlisPro 1.171.38.37f (Rigaku OD, 2015).
(36) For SHELXT; V2014/4 (Sheldrick 2014), see the following reference: Sheldrick, G. M. *Acta Cryst.* **2008**, *A64*, 112-122.
(37) For SHELXle, see the following reference: Hübschle, C. B.; Sheldrick, G. M.; Dittrich, B. *J. Appl. Cryst.* **2011**, *44*, 1281-1284.

all measured intensities was carried out using the program SHELXL 2015.[38] All non-hydrogen atoms were refined including anisotropic displacement parameters. CCDC 1834976 and 1834977 contains all the supplementary crystallographic data. These data can be obtained free of charge from The Cambridge Crystallographic Data Centre *via* www.ccdc.cam.ac.uk/data_request/cif.

- Crystal data and structure refinement for **2c**.

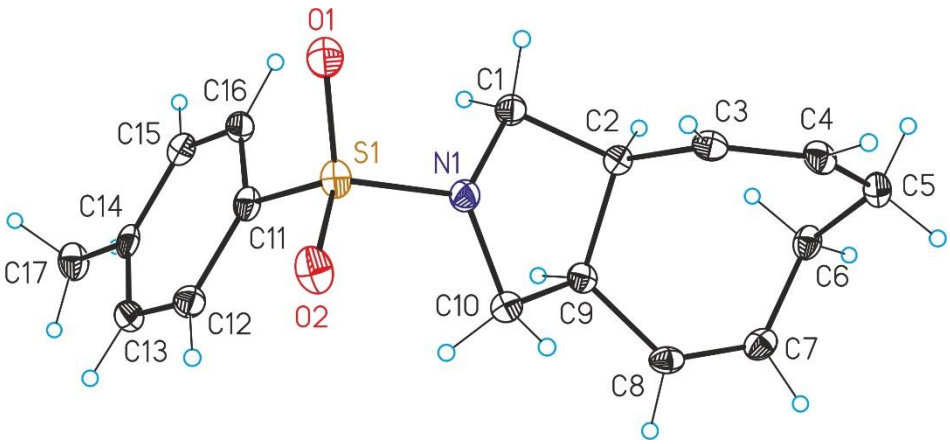

Figure 1.10. X-ray crystal structure of **2c** (ORTEP drawings showing thermal ellipsoids at 50% probability).

Empirical formula	$C_{17}H_{21}NO_2S$	
Formula weight	303,41	
Temperature	100(2) K	
Wavelength	0.71073 Å	
Crystal system	Triclinic	
Space group	P-1	
Unit cell dimensions	a = 7.4134(3)Å	α= 84.720(3)°
	b = 8.4142(3)Å	β = 88.990(3)°
	c = 12.1239(4)Å	γ = 84.549(3)°
Volume	749.62(5) $Å^3$	
Z	2	
Density (calculated)	1.344 Mg/m^3	
Absorption coefficient	0.220 mm^{-1}	
F(000)	324	
Crystal size	0.10 x 0.10 x 0.02 mm^3	
Theta range for data collection	2.442 to 27.916°	
Index ranges	-9<=h<=9,-9<=k<=10,-13<=l<=15	

(38) For SHELXL and SHELXL-2014/7 (Sheldrick 2014), see the following reference: Sheldrick, G. M. *Acta Cryst.* **2015**, *C71*, 3-8.

UNIVERSITAT ROVIRA I VIRGILI
TRANSITION METAL CATALYZED CYCLOADDITION REACTIONS FOR THE FORMATION OF EIGHT- AND SIX-MEMBERED RINGS
Nuria Llorente González

Reflections collected	9463
Independent reflections	3035[R(int) = 0.0318]
Completeness to theta =27.916°	84,70%
Absorption correction	Empirical
Max. and min. transmission	0.996 and 0.766
Refinement method	Full-matrix least-squares on F^2
Data / restraints / parameters	3035/ 0/ 191
Goodness-of-fit on F^2	1,033
Final R indices [I>2sigma(I)]	R1 = 0.0366, wR2 = 0.0852
R indices (all data)	R1 = 0.0477, wR2 = 0.0894
Largest diff. peak and hole	0.300 and -0.357 e.Å^{-3}

Bond lengths [Å]	
S1-O2	1.4348(13)
S1-O1	1.4366(13)
S1-N1	1.6206(14)
S1-C11	1.7696(16)
N1-C1	1.476(2)
N1-C10	1.487(2)
C1-C2	1.526(2)
C2-C3	1.514(2)
C2-C9	1.552(2)
C3-C4	1.329(2)
C4-C5	1.504(2)
C5-C6	1.535(2)
C6-C7	1.504(2)
C7-C8	1.327(2)
C8-C9	1.501(2)
C9-C10	1.539(2)
C11-C12	1.388(2)
C11-C16	1.392(2)
C12-C13	1.390(2)
C13-C14	1.391(2)
C14-C15	1.391(2)
C14-C17	1.508(2)
C15-C16	1.385(2)

Bond Angles [°]	
O2-S1-O1	120.58(7)
O2-S1-N1	106.71(7)
O1-S1-N1	105.90(7)
O2-S1-C11	107.66(8)
O1-S1-C11	107.31(7)
N1-S1-C11	108.16(7)
C1-N1-C10	110.21(13)
C1-N1-S1	118.88(11)
C10-N1-S1	121.39(11)
N1-C1-C2	102.30(12)
C3-C2-C1	110.96(13)
C3-C2-C9	114.43(13)
C1-C2-C9	100.55(12)
C4-C3-C2	129.15(15)
C3-C4-C5	130.21(15)
C4-C5-C6	116.05(14)
C7-C6-C5	111.32(14)
C8-C7-C6	127.63(16)
C7-C8-C9	127.68(16)
C8-C9-C10	112.98(13)
C8-C9-C2	118.46(13)
C10-C9-C2	103.34(13)
N1-C10-C9	103.77(13)
C12-C11-C16	120.46(15)
C12-C11-S1	119.68(13)
C16-C11-S1	119.86(13)
C11-C12-C13	119.07(16)
C12-C13-C14	121.30(16)
C15-C14-C13	118.56(15)
C15-C14-C17	120.89(15)
C13-C14-C17	120.55(15)
C16-C15-C14	121.00(16)
C15-C16-C11	119.53(15)

- Crystal data and structure refinement for *trans*-**2g**.

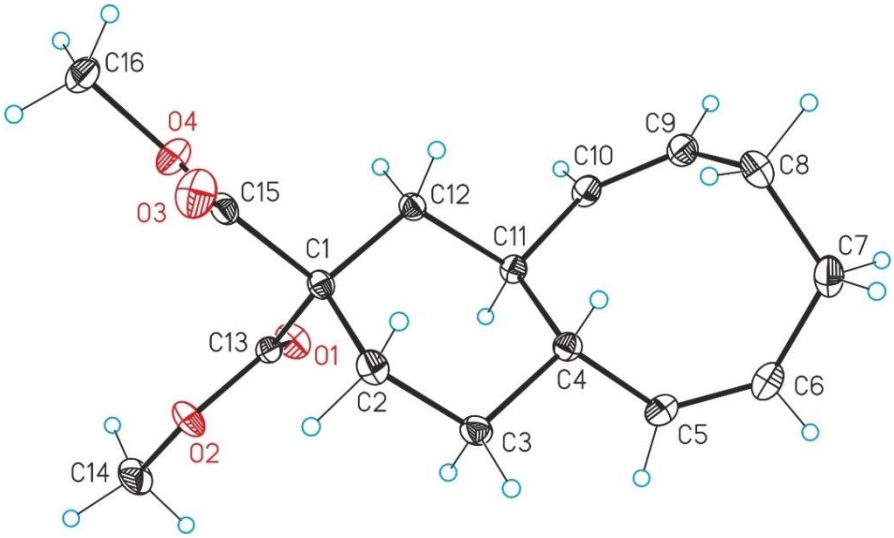

Figure 1.11. X-ray crystal structure of *trans*-**2g** (ORTEP drawings showing thermal ellipsoids at 50% probability).

Empirical formula	$C_{16}H_{22}O_4$	
Formula weight	278.33	
Temperature	100(2) K	
Wavelength	0.71073 Å	
Crystal system	Triclinic	
Space group	P-1	
Unit cell dimensions	a = 6.2605(4)Å	α= 67.7938(14)°.
	b = 9.8392(6)Å	β= 88.4599(15)°.
	c = 12.7844(7)Å	γ = 84.1325(16)°
Volume	725.21(8) $Å^3$	
Z	2	
Density (calculated)	1.275 Mg/m^3	
Absorption coefficient	0.090 mm^{-1}	
F(000)	300	
Crystal size	0.20 x 0.08 x 0.05 mm^3	
Theta range for data collection	1.721 to 33.109°	
Index ranges	-6<=h<=9,-14<=k<=14,-19<=l<=19	
Reflections collected	12624	
Independent reflections	5107[R(int) = 0.0209]	
Completeness to theta =33.109°	92.4%	
Absorption correction	Empirical	
Max. and min. transmission	0.995 and 0.919	
Refinement method	Full-matrix least-squares on F^2	
Data / restraints / parameters	5107/ 0/ 183	
Goodness-of-fit on F^2	1.025	
Final R indices [I>2sigma(I)]	R1 = 0.0364, wR2 = 0.0984	
R indices (all data)	R1 = 0.0416, wR2 = 0.1026	
Largest diff. peak and hole	0.429 and -0.223 $e.Å^{-3}$	

UNIVERSITAT ROVIRA I VIRGILI
TRANSITION METAL CATALYZED CYCLOADDITION REACTIONS FOR THE FORMATION OF EIGHT- AND SIX-MEMBERED RINGS
Nuria Llorente González

Bond lengths [Å]	
O1-C13	1.2024(9)
O2-C13	1.3430(9)
O2-C14	1.4460(9)
O3-C15	1.2043(9)
O4-C15	1.3419(9)
O4-C16	1.4444(10)
C1-C15	1.5273(10)
C1-C13	1.5324(10)
C1-C2	1.5381(10)
C1-C12	1.5456(10)
C2-C3	1.5265(11)
C3-C4	1.5322(10)
C4-C5	1.5072(10)
C4-C11	1.5430(10)
C5-C6	1.3345(11)
C6-C7	1.5063(12)
C7-C8	1.5406(12)
C8-C9	1.5052(12)
C9-C10	1.3377(11)
C10-C11	1.5114(10)
C11-C12	1.5442(10)

Bond Angles [°]	
C13-O2-C14	115.57(6)
C15-O4-C16	116.06(6)
C15-C1-C13	106.50(6)
C15-C1-C2	110.46(6)
C13-C1-C2	110.92(6)
C15-C1-C12	107.88(6)
C13-C1-C12	110.85(6)
C2-C1-C12	110.13(6)
C3-C2-C1	110.70(6)
C2-C3-C4	111.71(6)
C5-C4-C3	110.06(6)
C5-C4-C11	111.33(6)
C3-C4-C11	108.91(6)
C6-C5-C4	128.59(7)
C5-C6-C7	129.15(7)
C6-C7-C8	117.73(7)
C9-C8-C7	112.91(7)
C10-C9-C8	128.92(7)
C9-C10-C11	130.23(7)
C10-C11-C4	116.43(6)
C10-C11-C12	109.43(6)
C4-C11-C12	110.93(6)
C11-C12-C1	113.39(6)
O1-C13-O2	123.70(7)
O1-C13-C1	126.22(7)
O2-C13-C1	110.07(6)
O3-C15-O4	123.88(7)
O3-C15-C1	125.97(7)
O4-C15-C1	110.12(6)

1.4.7. Theoretical Methods

The energies of all complexes included in this study were computed at the BP86-D3/def2-TZVP level of theory. The calculations have been performed by using the program TURBOMOLE version 7.0.[98] For the calculations, the DFT-D functional with the latest available correction for dispersion (D3) was used.[99] TS structures were characterized by means of frequency analysis calculations at the BP86-D3/def2-TZVP level of theory. In order to reproduce solvent effects, the conductor-like screening model COSMO,[100] which is a variant of the dielectric continuum solvation models,[101] was used. We have used toluene as solvent. In order to give reliability to the results obtained using the BP86 method, single point calculations at the MP2/def2-TZVP level of theory using toluene as a solvent were performed.

For the cartesian coordinates of the atoms in the computed structures, see section 1.4.9.

(98) Ahlrichs, R.; Baer, M.; Haeser, M.; Horn, H.; Koelmel, C. *Chem. Phys. Lett.* **1989**, *162*, 165-169.
(99) Grimme, S.; Antony, J.; Ehrlich, S.; Krieg, H. *J. Chem. Phys.* **2010**, *132*, 154104/1-154104/19.
(100) Klamt, A.; Schüürmann, G. *J. Chem. Soc., Perkin Trans. 2* **1993**, 799-805.
(101) Klamt, A. *WIREs Comput. Mol. Sci.* **2011**, *1*, 699-709.

1.4.8. Copies of NMR Spectra

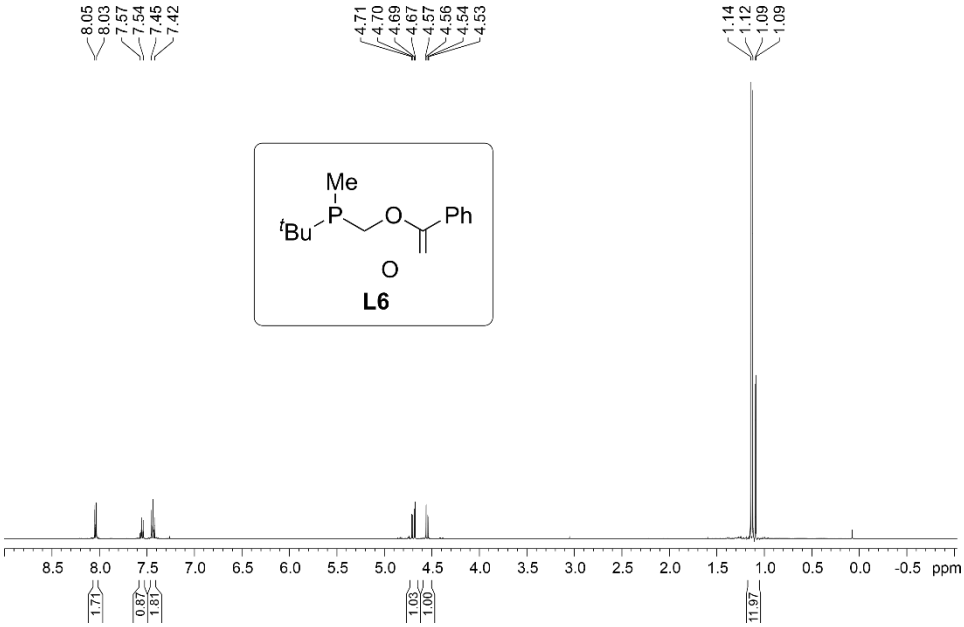

Figure 1.12. ^{1}H NMR spectrum of ligand **L6**.

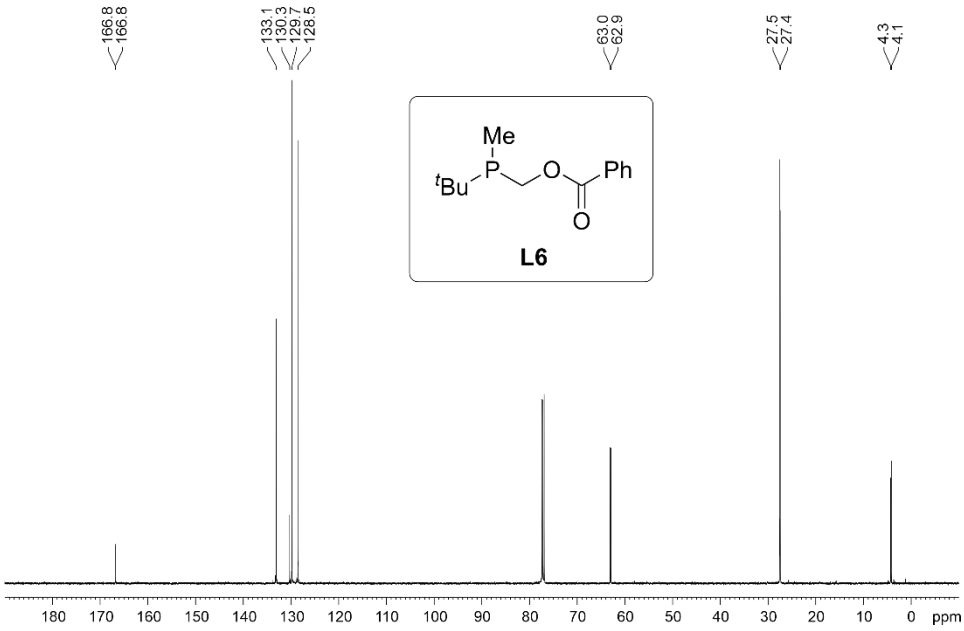

Figure 1.13. $^{13}C\{^{1}H\}$ NMR spectrum of ligand **L6**.

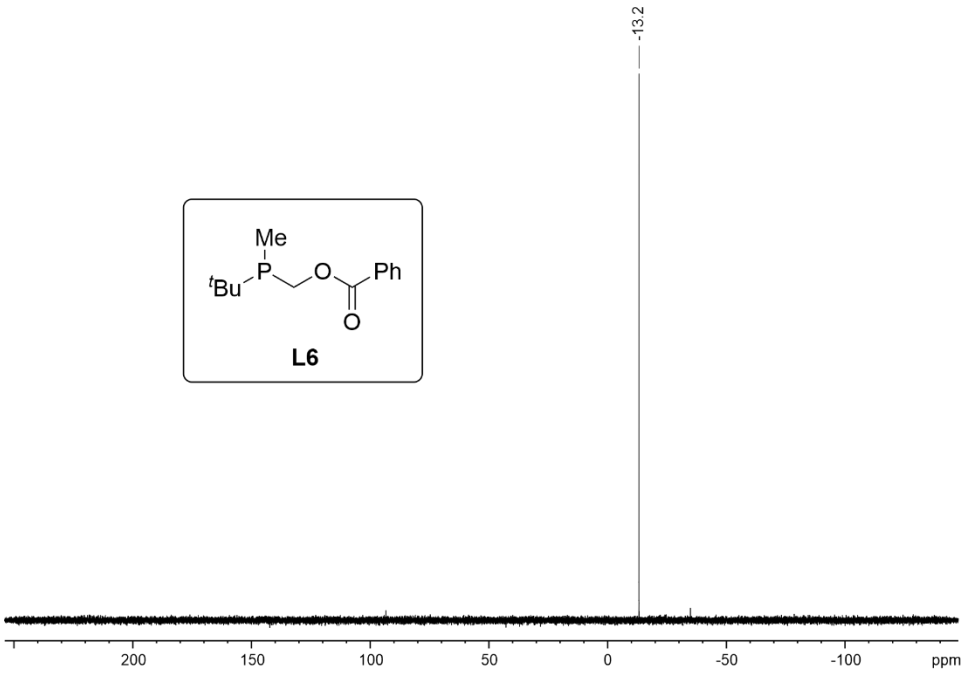

Figure 1.14. $^{31}P\{^{1}H\}$ NMR spectrum of ligand **L6**.

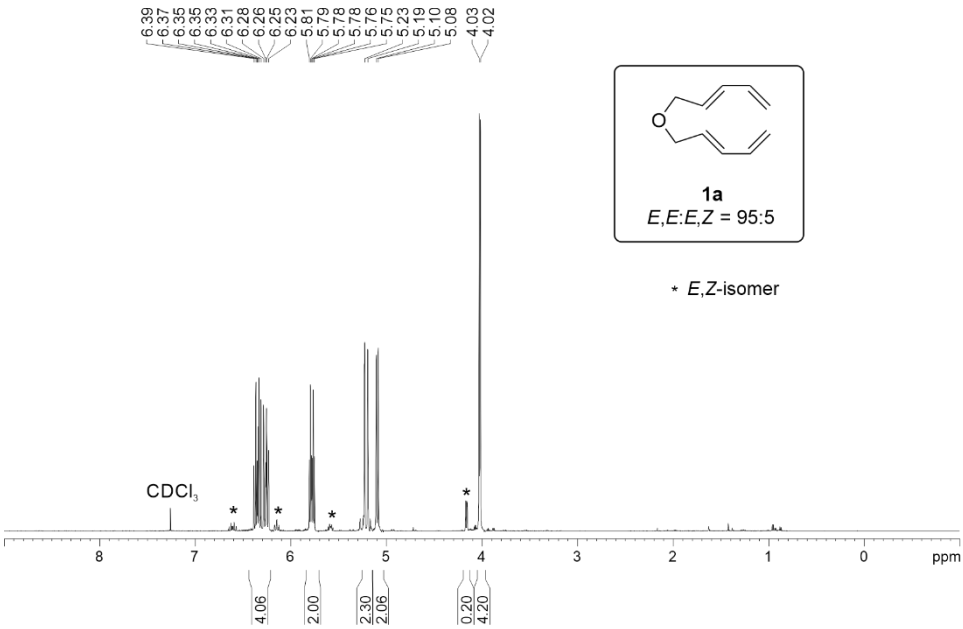

Figure 1.15. ^{1}H NMR spectrum of substrate **1a**.

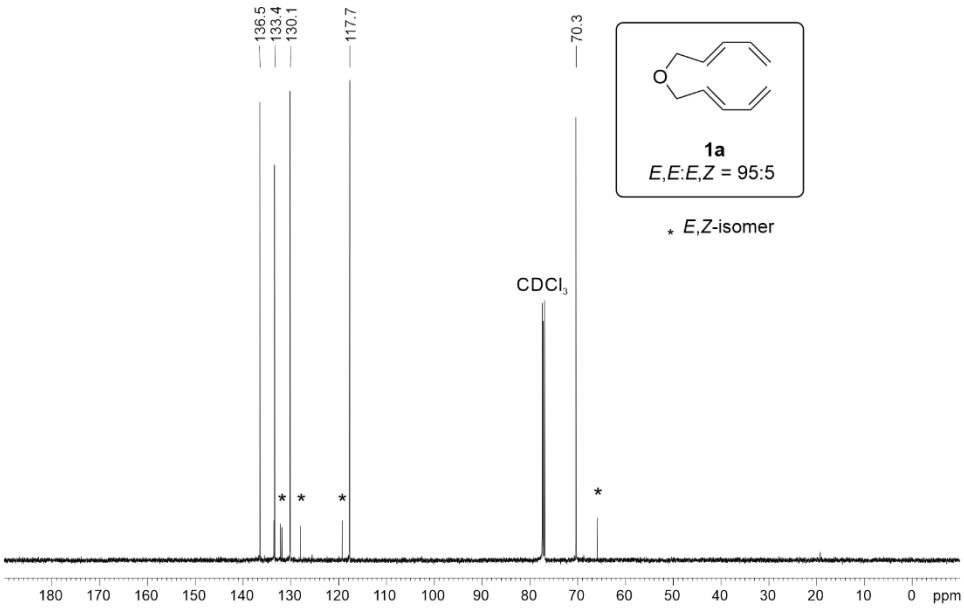

Figure 1.16. $^{13}C\{^{1}H\}$ NMR spectrum of substrate **1a**.

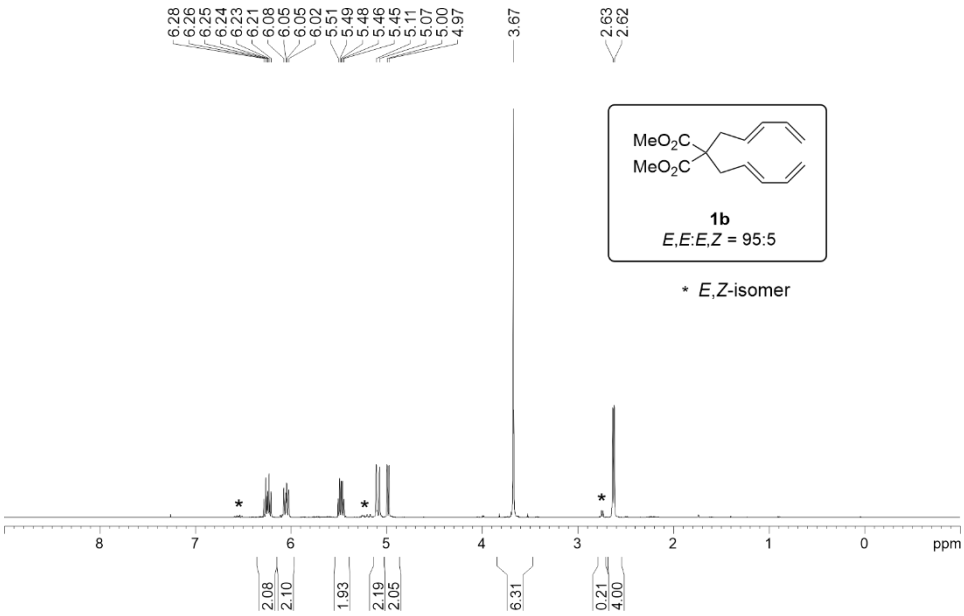

Figure 1.17. ^{1}H NMR spectrum of substrate **1b**.

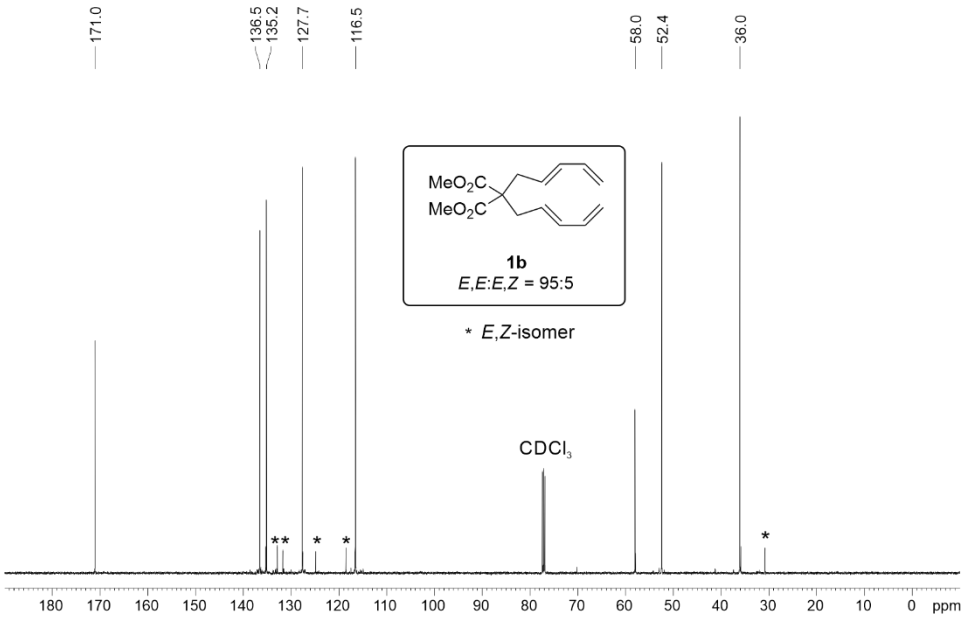

Figure 1.18. $^{13}C\{^{1}H\}$ NMR spectrum of substrate **1b**.

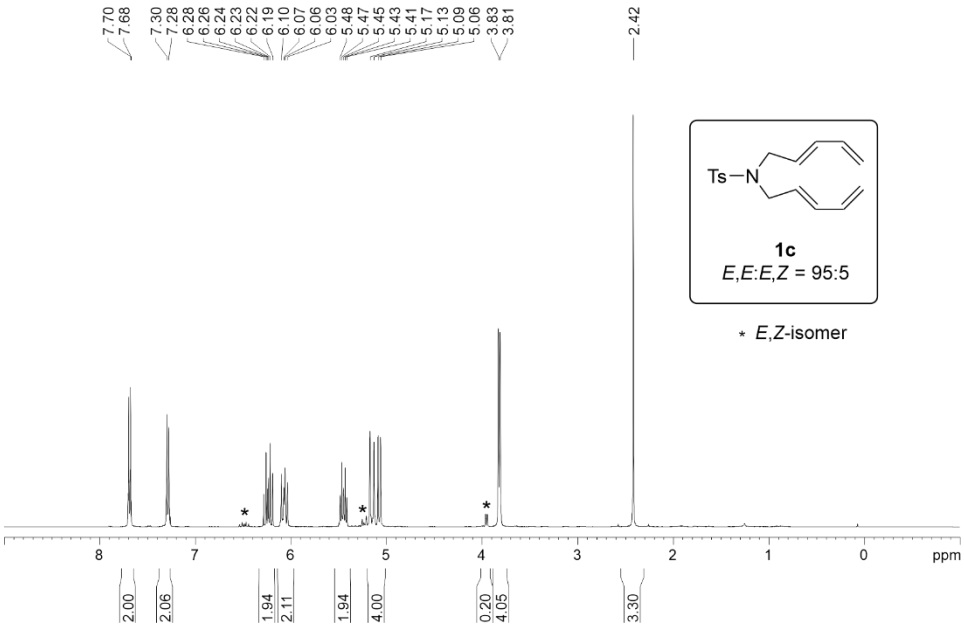

Figure 1.19. ^{1}H NMR spectrum of substrate **1c**.

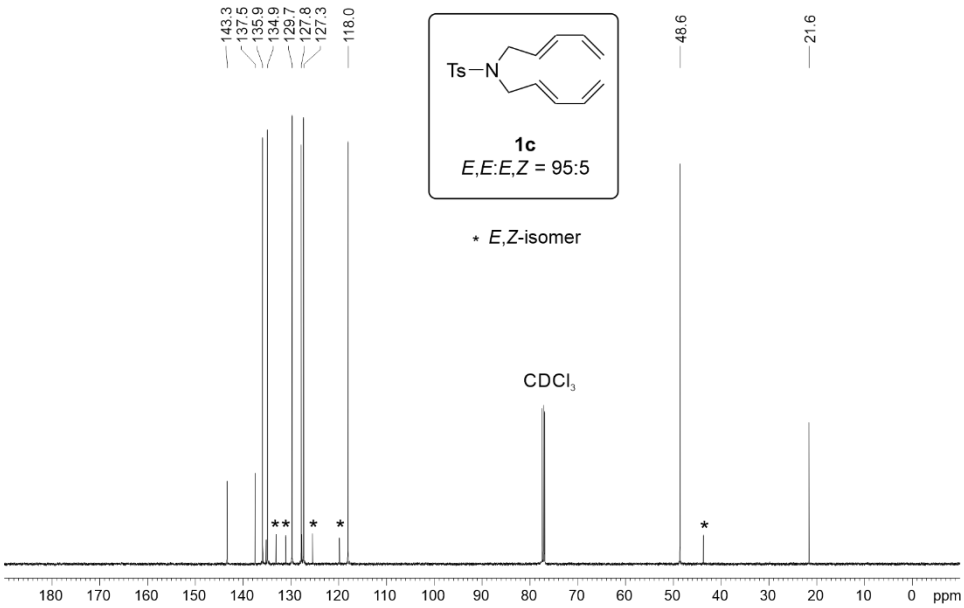

Figure 1.20. $^{13}C\{^{1}H\}$ NMR spectrum of substrate **1c**.

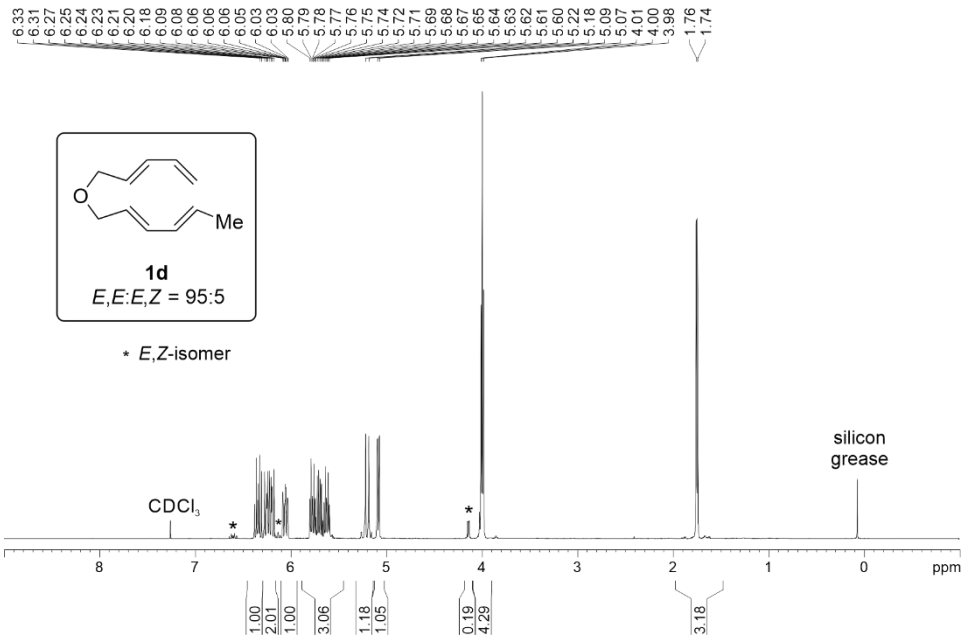

Figure 1.21. ^{1}H NMR spectrum of substrate **1d**.

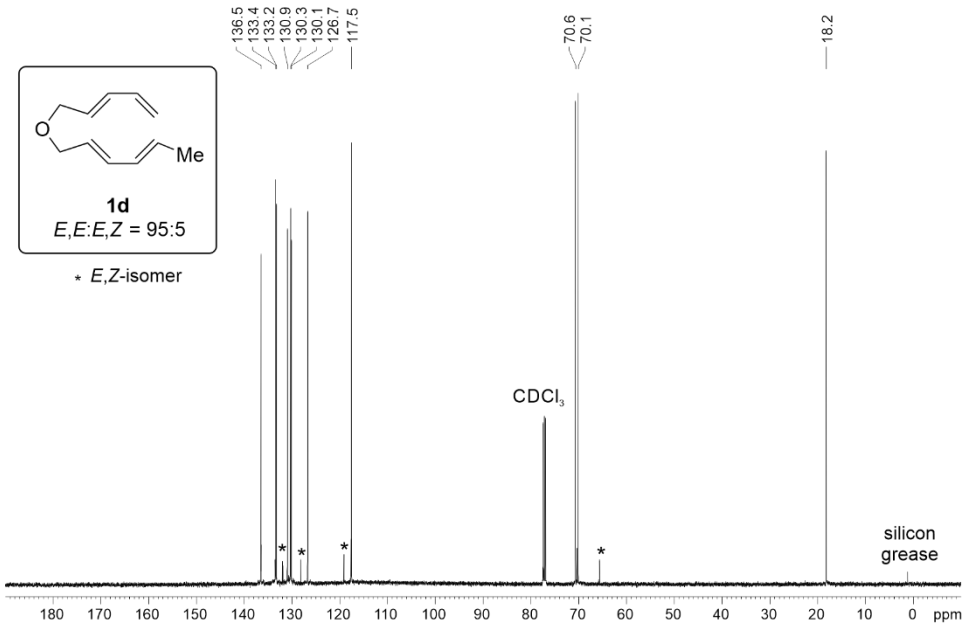

Figure 1.22. $^{13}C\{^{1}H\}$ NMR spectrum of substrate **1d**.

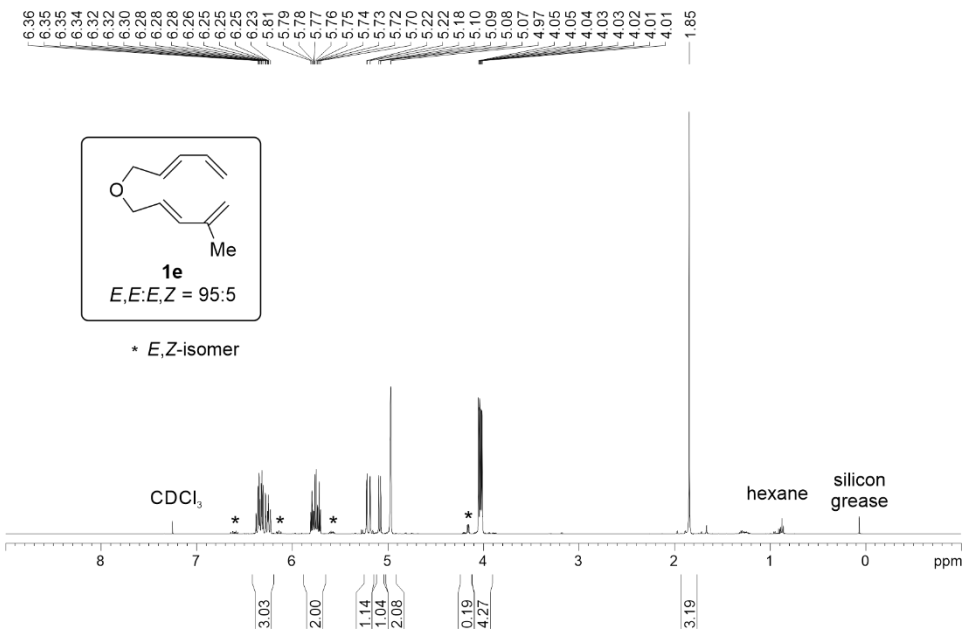

Figure 1.23. ^{1}H NMR spectrum of substrate **1e**.

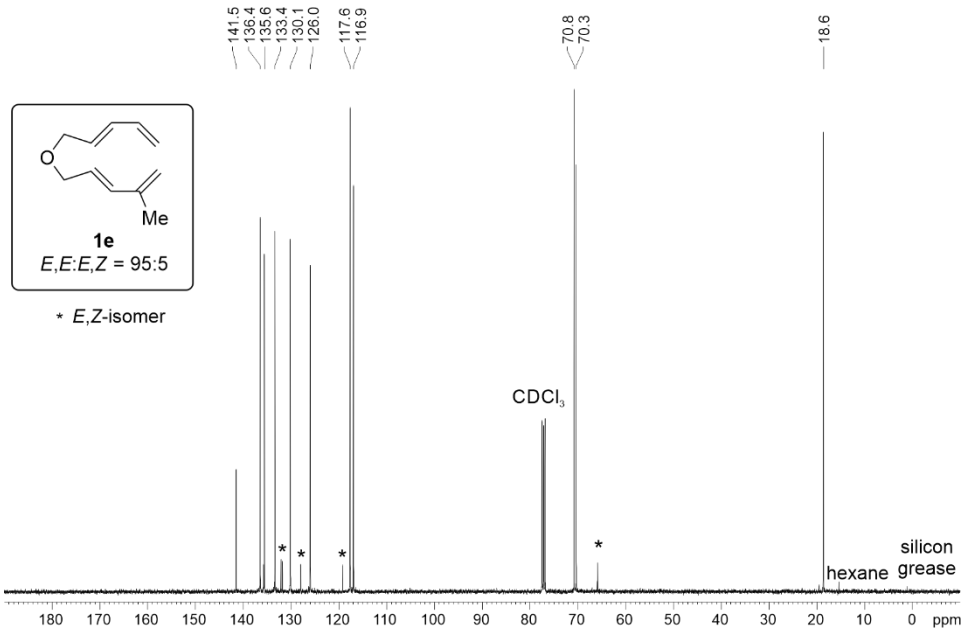

Figure 1.24. $^{13}C\{^{1}H\}$ NMR spectrum of substrate **1e**.

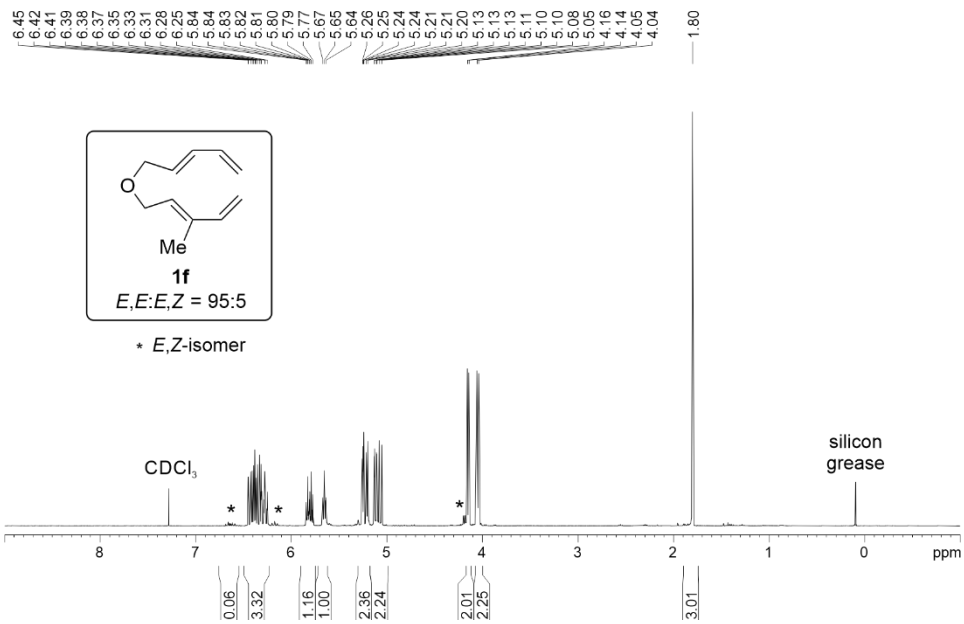

Figure 1.25. ^{1}H NMR spectrum of substrate **1f**.

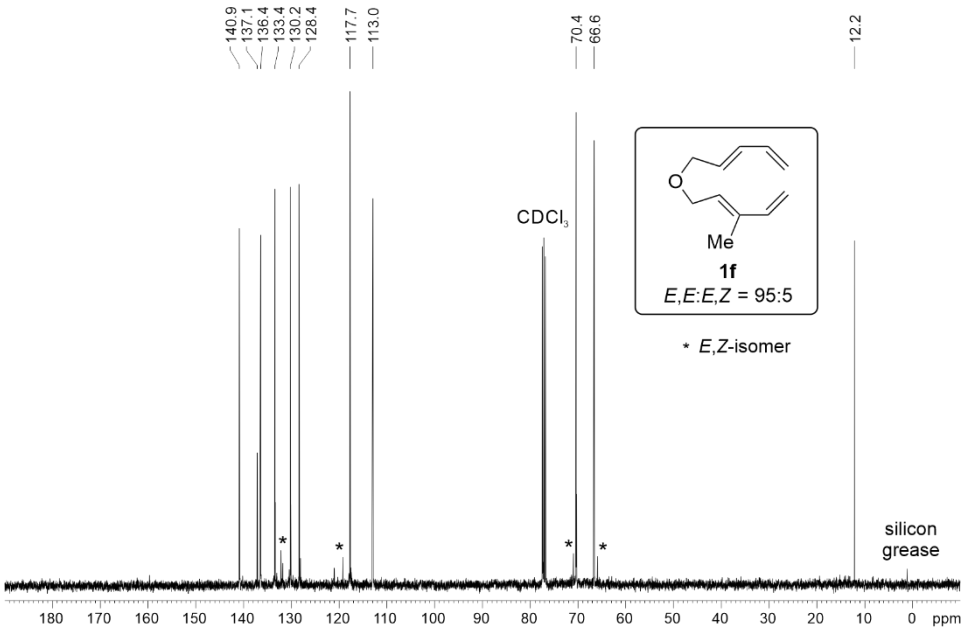

Figure 1.26. $^{13}C\{^{1}H\}$ NMR spectrum of substrate **1f**.

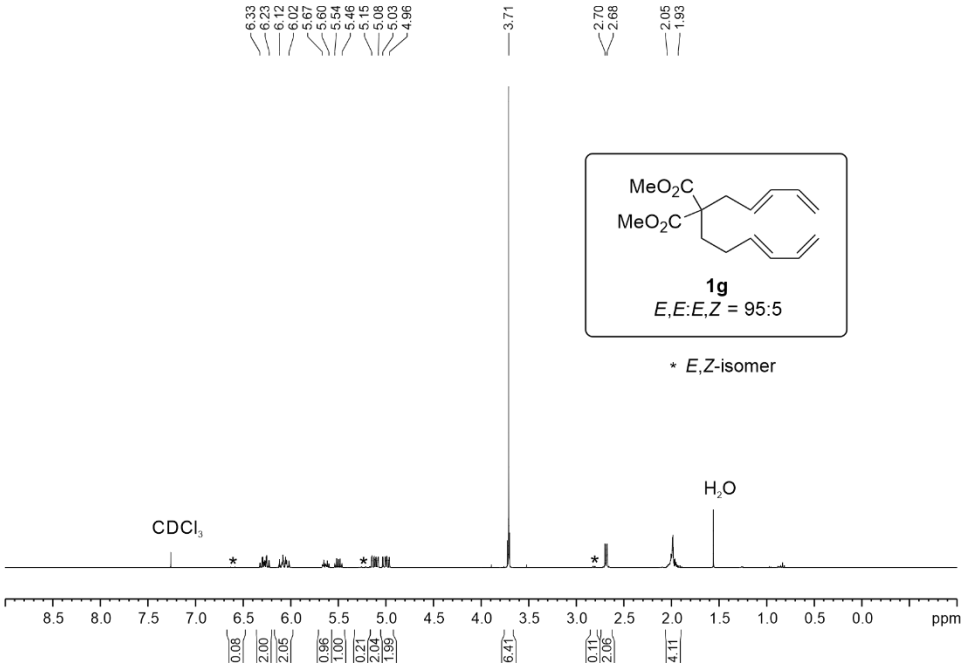

Figure 1.27. ^{1}H NMR spectrum of substrate **1g**.

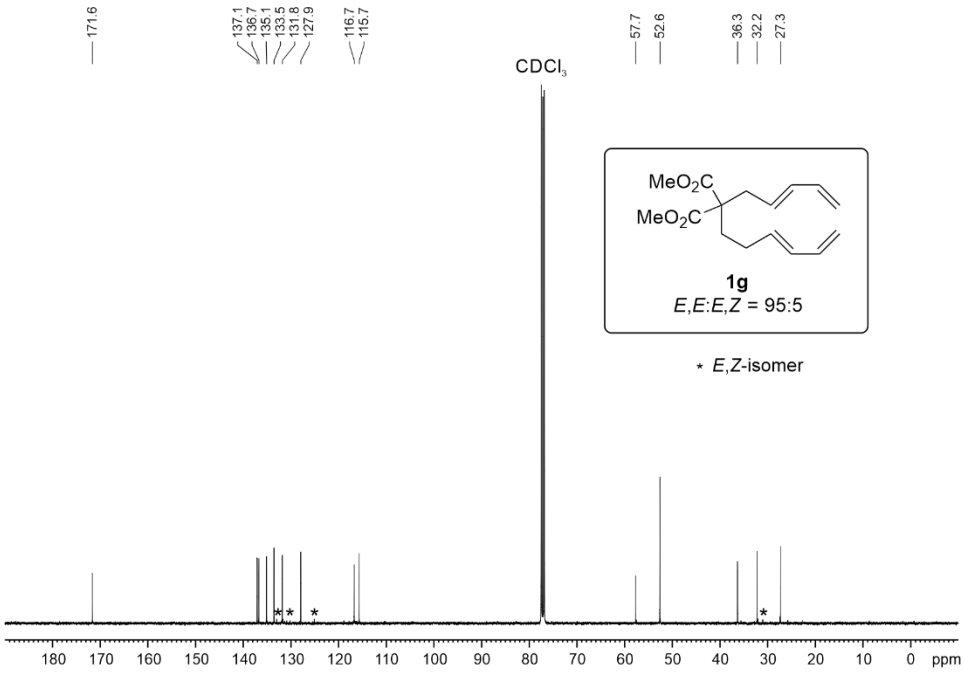

Figure 1.28. $^{13}C\{^{1}H\}$ NMR spectrum of substrate **1g**.

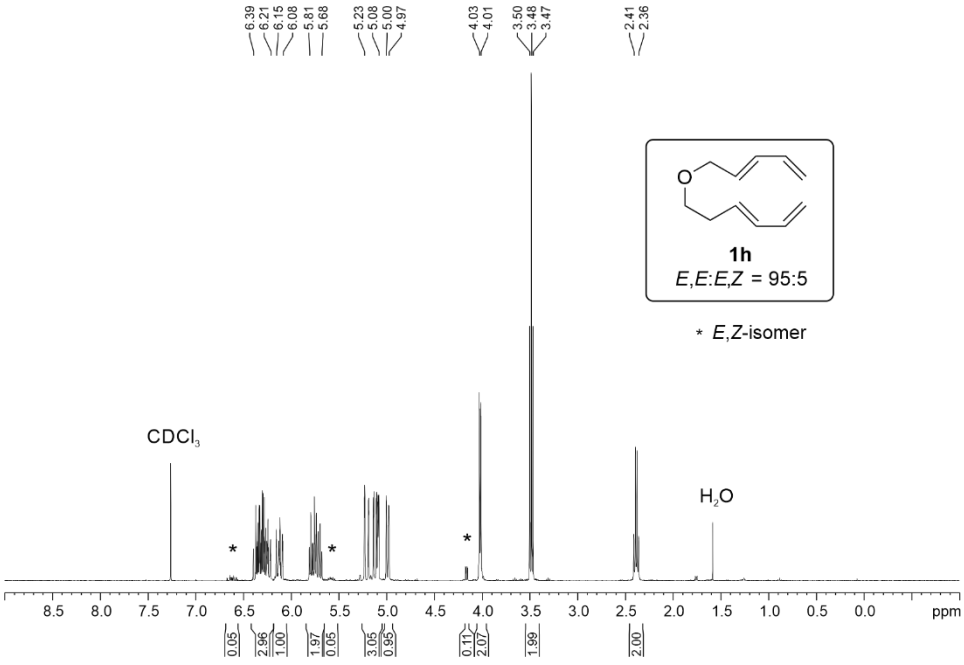

Figure 1.29. ^{1}H NMR spectrum of substrate **1h**.

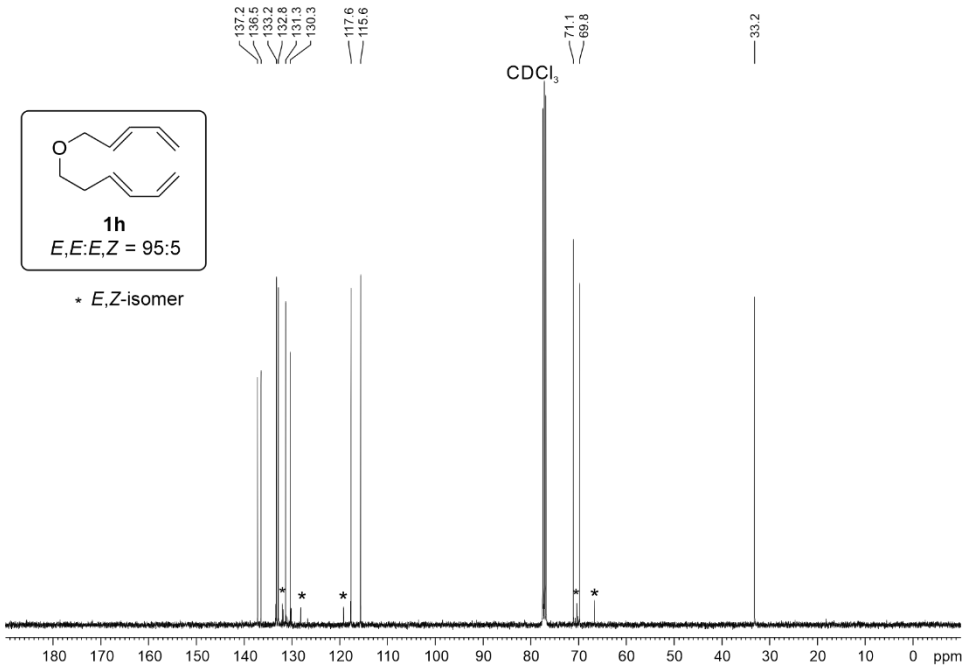

Figure 1.30. $^{13}C\{^{1}H\}$ NMR spectrum of substrate **1h**.

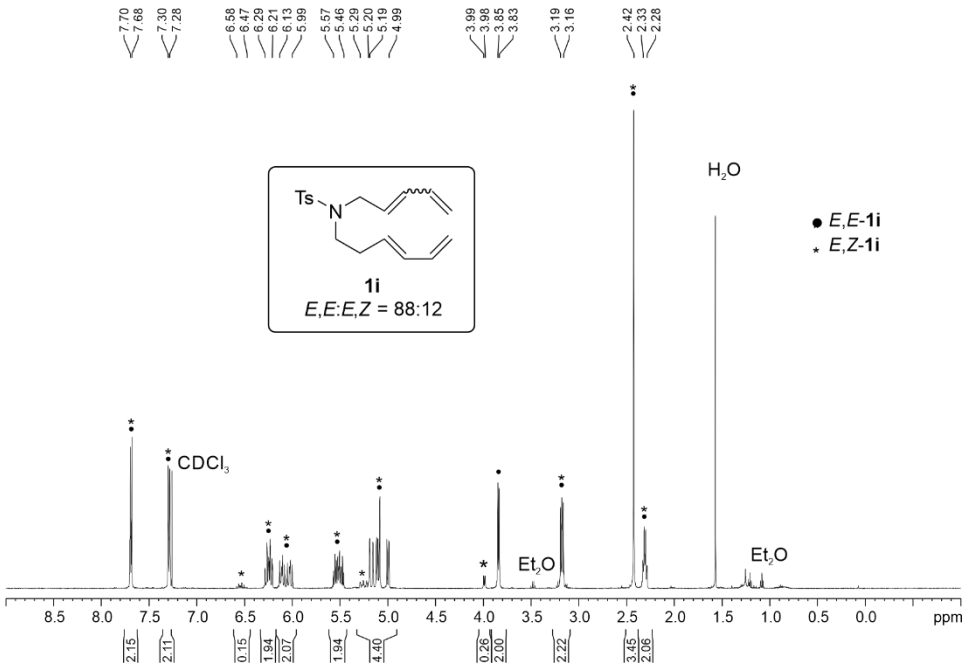

Figure 1.31. ^{1}H NMR spectrum of substrate **1i**.

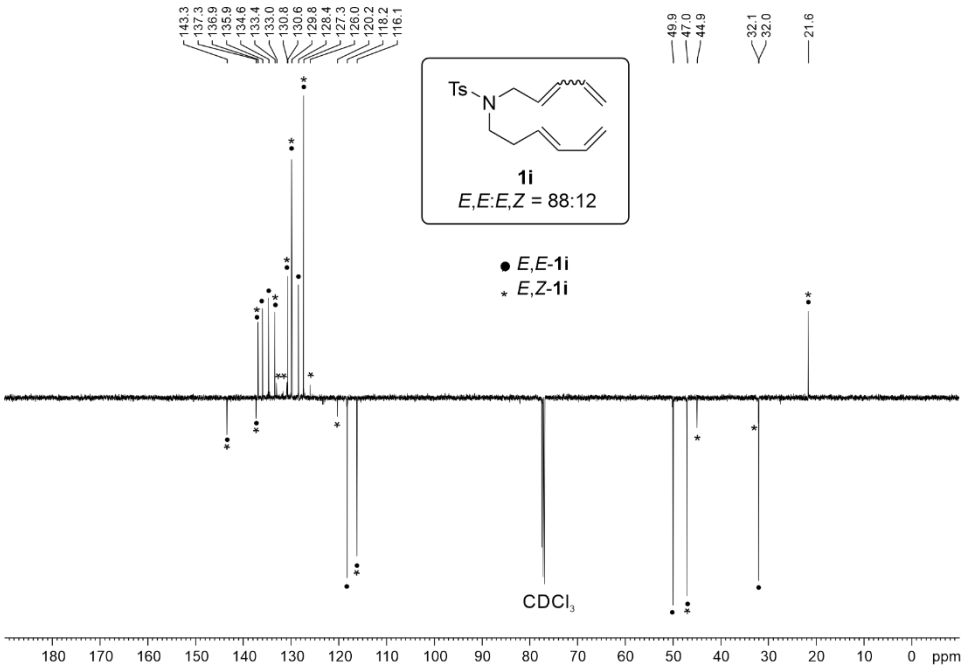

Figure 1.32. $^{13}C\{^{1}H\}$ NMR as DEPTQ135 spectrum of substrate **1i**.

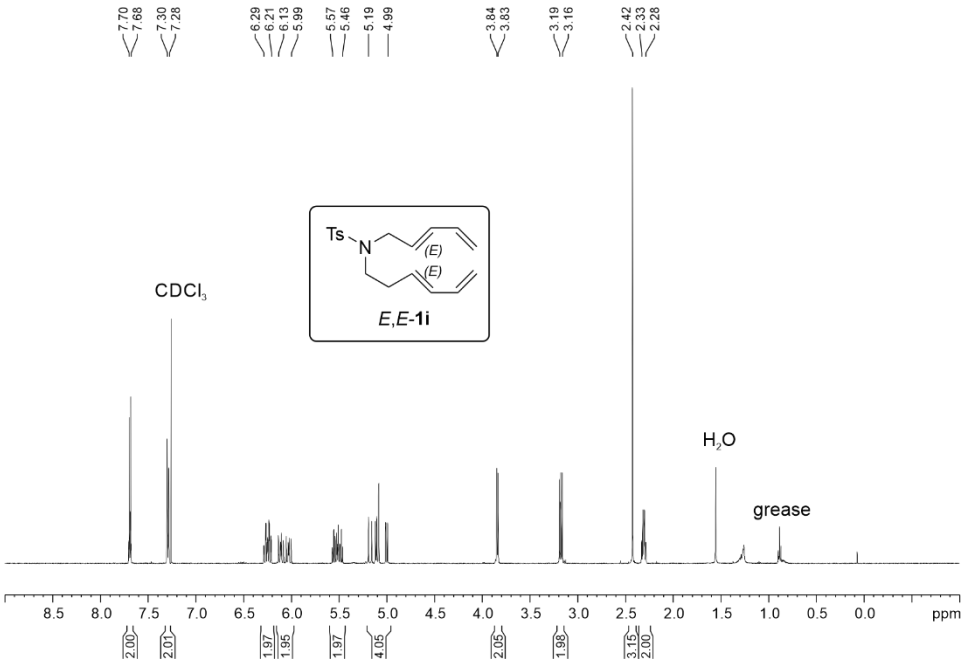

Figure 1.33. ^{1}H NMR spectrum of substrate *E,E*-**1i**.

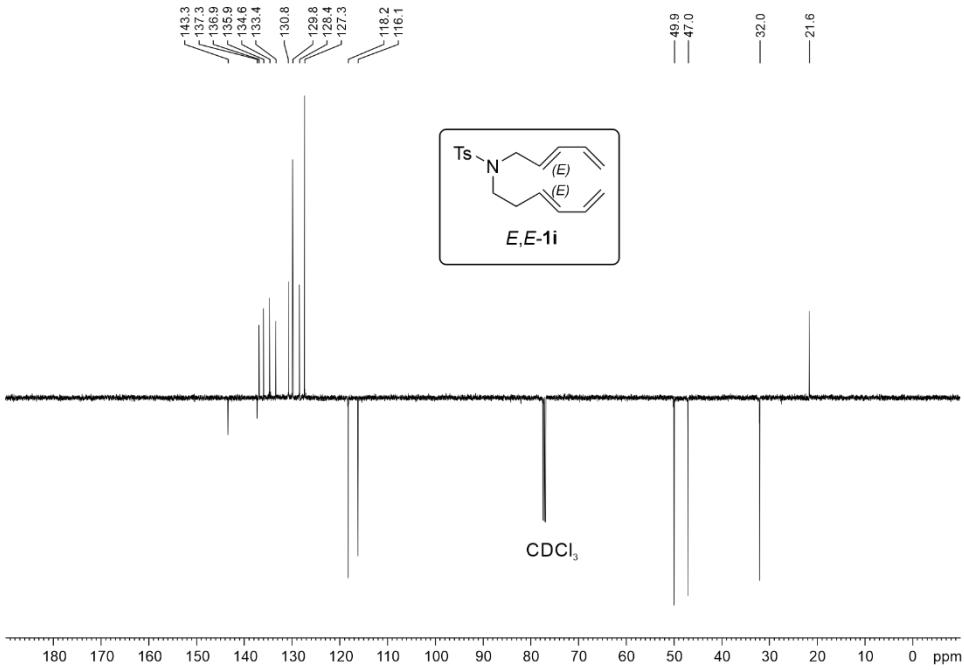

Figure 1.34. $^{13}C\{^{1}H\}$ NMR as DEPTQ135 spectrum of substrate *E,E*-**1i**.

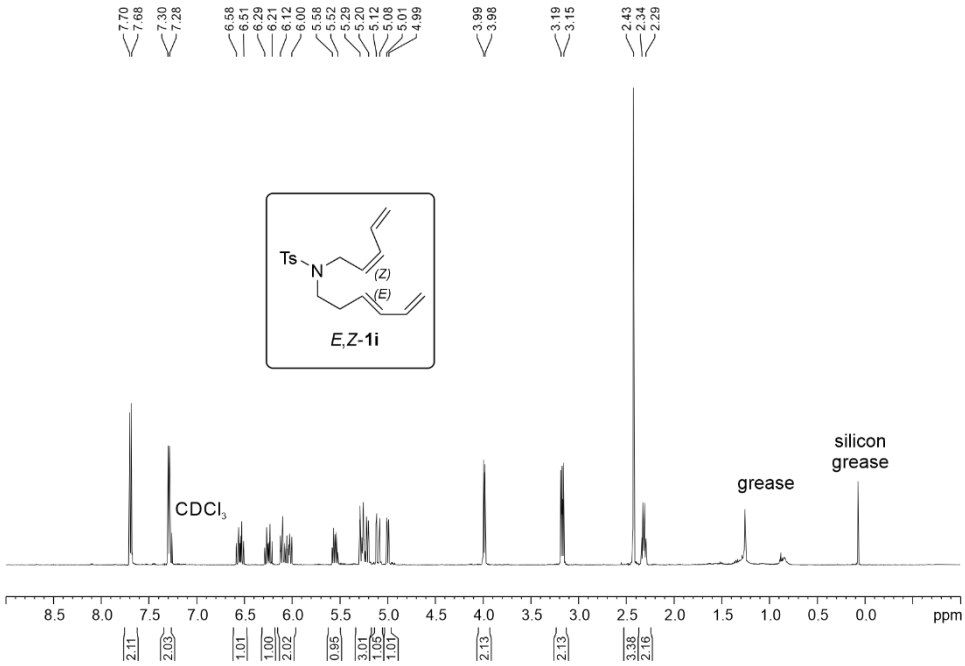

Figure 1.35. ^{1}H NMR spectrum of substrate *E,Z*-**1i**.

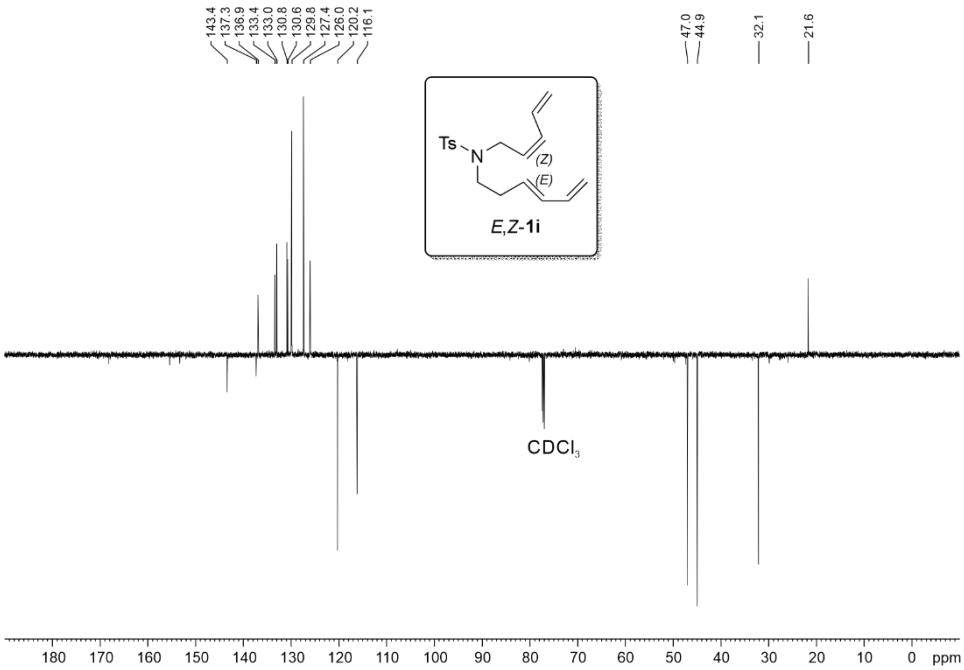

Figure 1.36. $^{13}C\{^{1}H\}$ NMR as DEPTQ135 spectrum of substrate *E,Z*-**1i**.

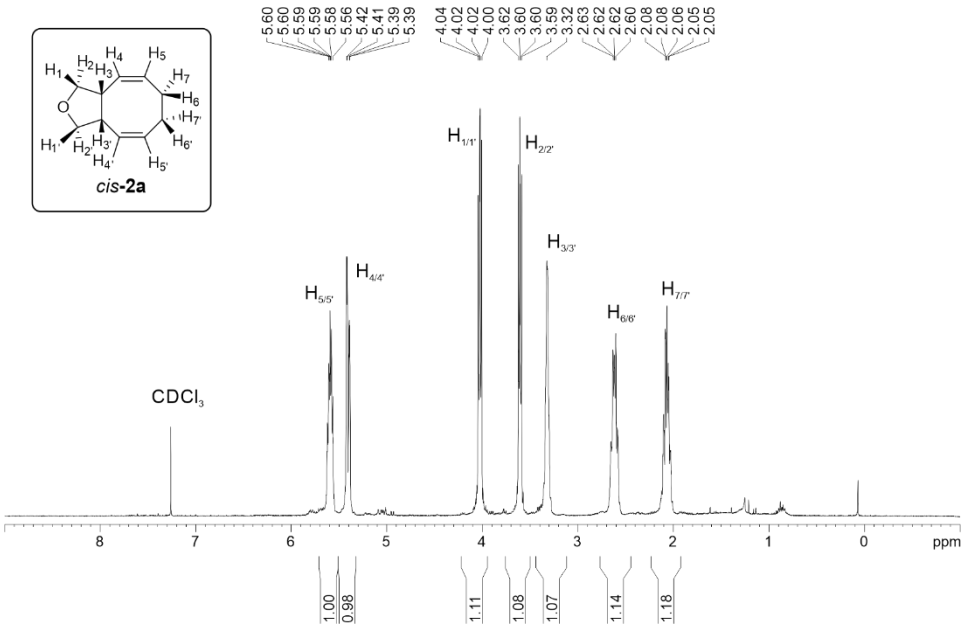

Figure 1.37. ^{1}H NMR spectrum of product *cis*-**2a**.

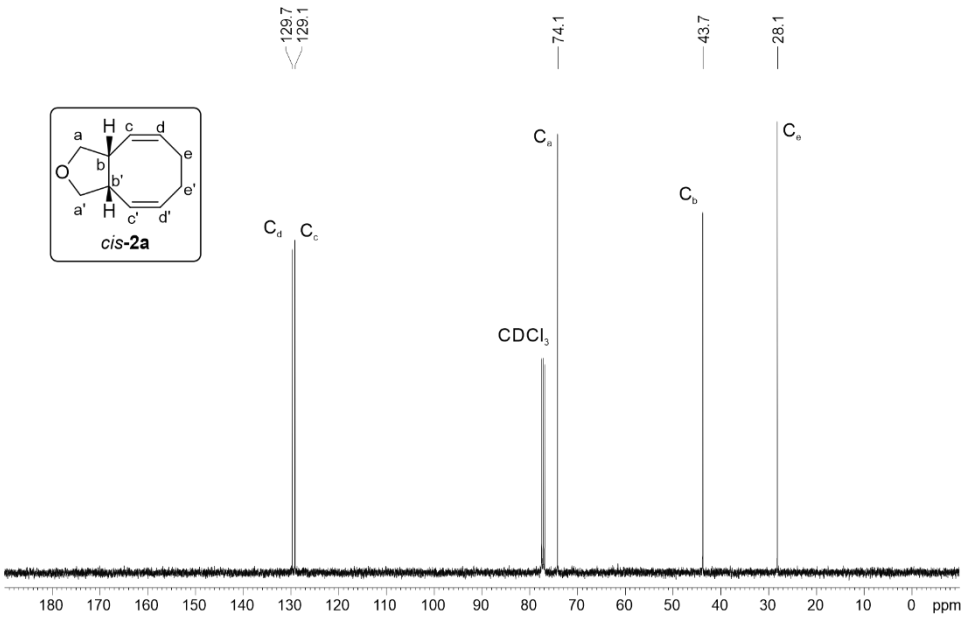

Figure 1.38. $^{13}C\{^{1}H\}$ NMR spectrum of product *cis*-**2a**.

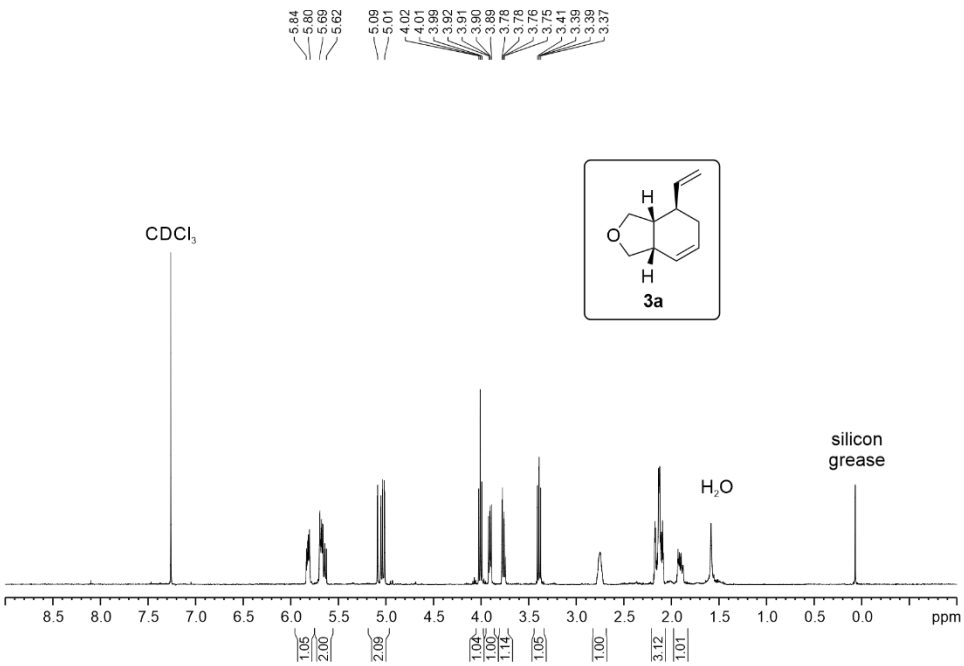

Figure 1.39. ^{1}H NMR spectrum of product **3a**.

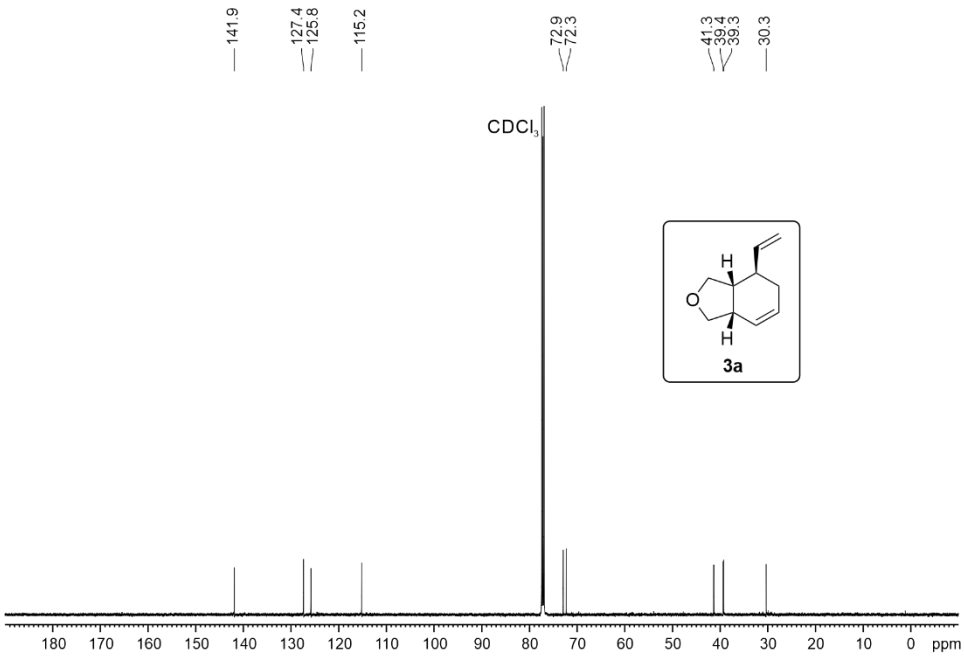

Figure 1.40. $^{13}C\{^{1}H\}$ NMR spectrum of product **3a**.

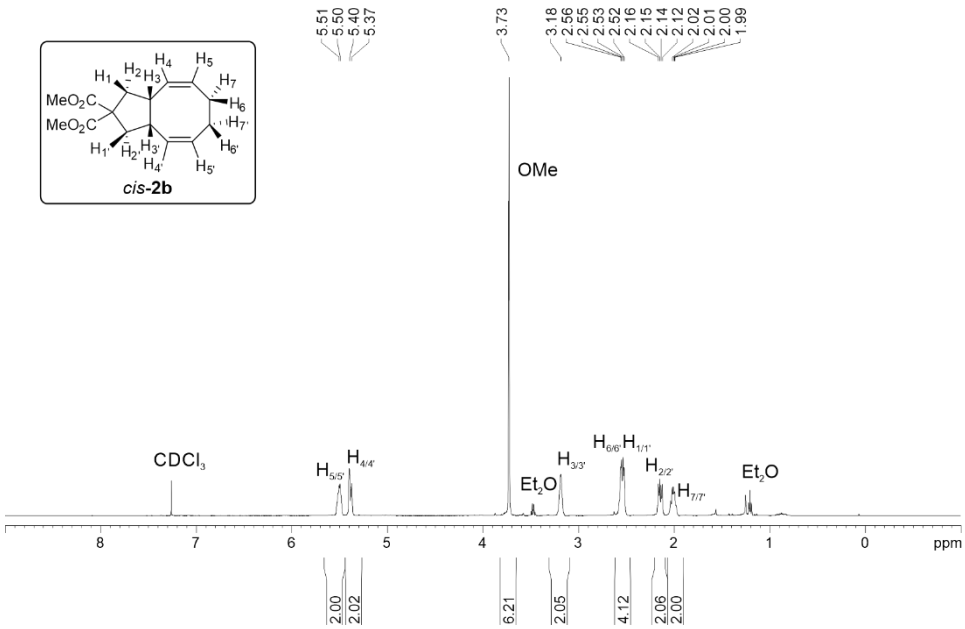

Figure 1.41. ^{1}H NMR spectrum of product *cis*-**2b**.

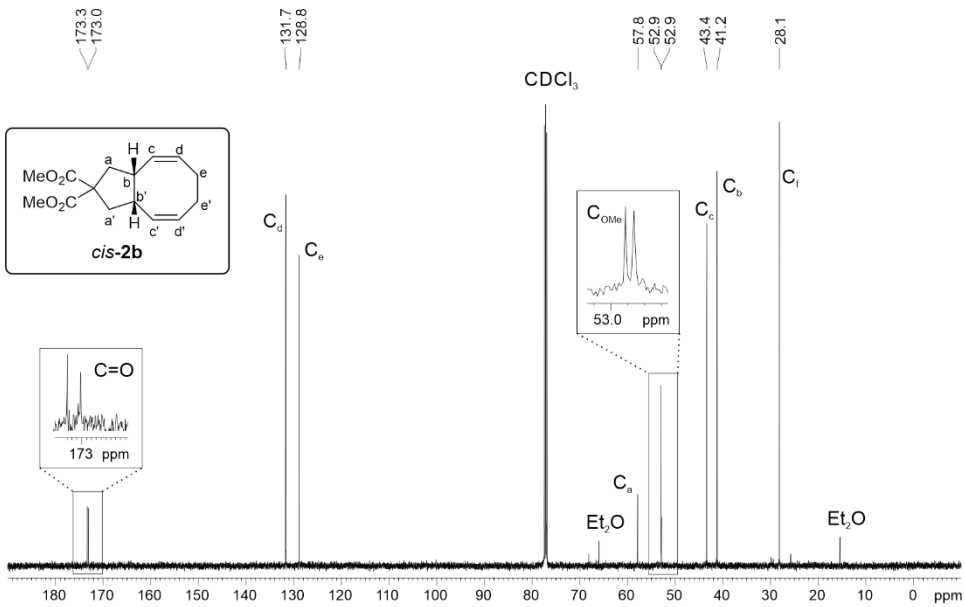

Figure 1.42. ^{13}C{^{1}H} NMR spectrum of product *cis*-**2b**.

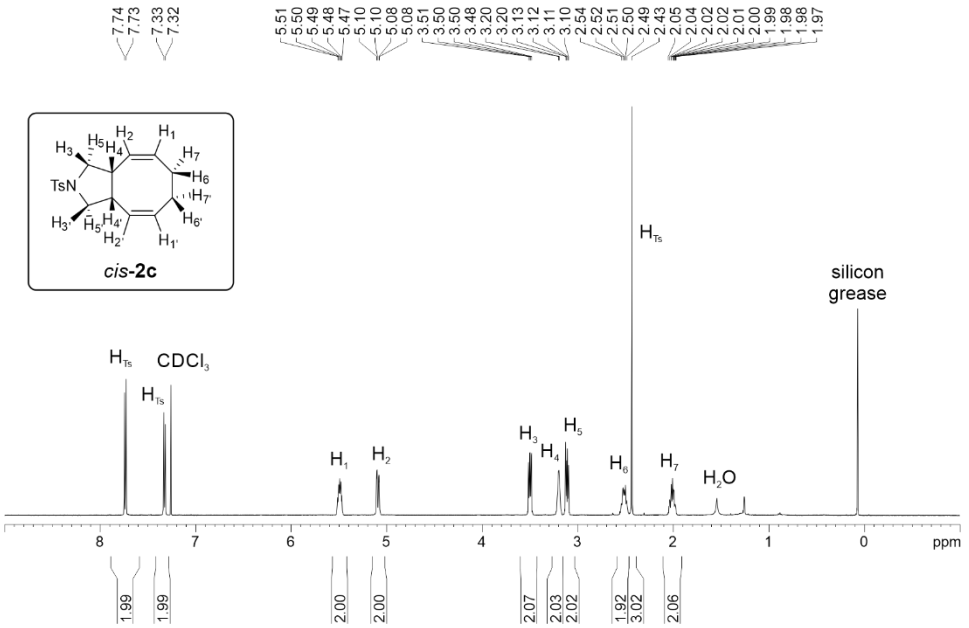

Figure 1.43. ^{1}H NMR spectrum of product *cis*-**2c**.

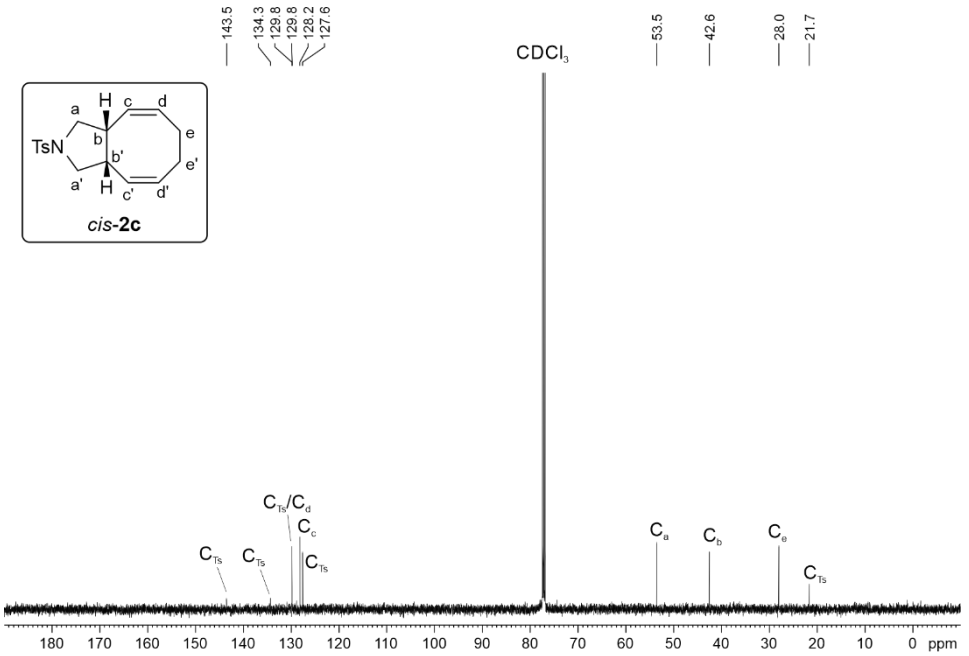

Figure 1.44. ^{13}C{^{1}H} NMR spectrum of product *cis*-**2c**.

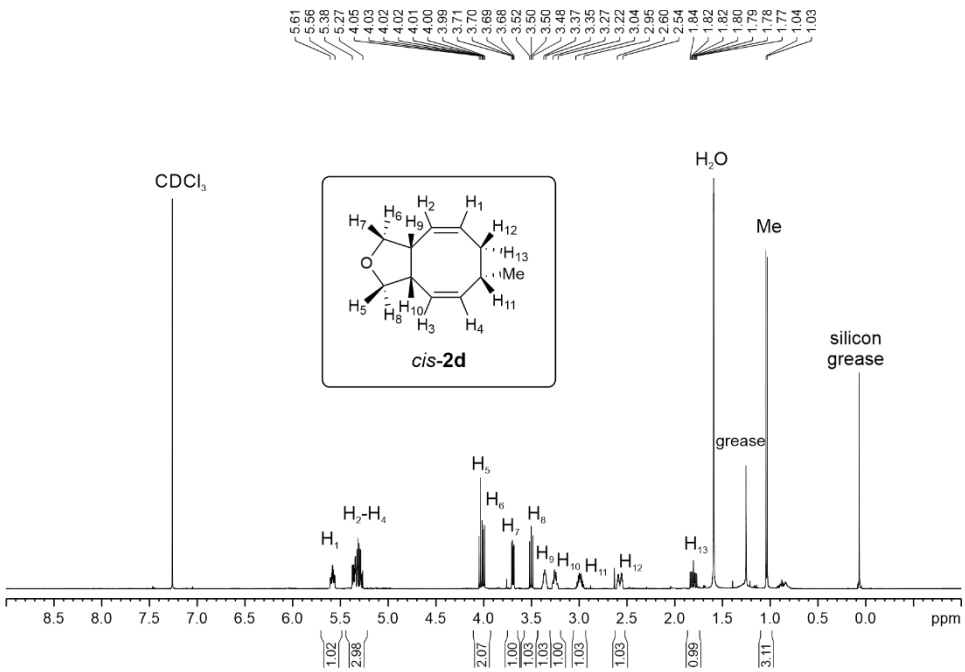

Figure 1.45. ^{1}H NMR spectrum of product *cis*-**2d**.

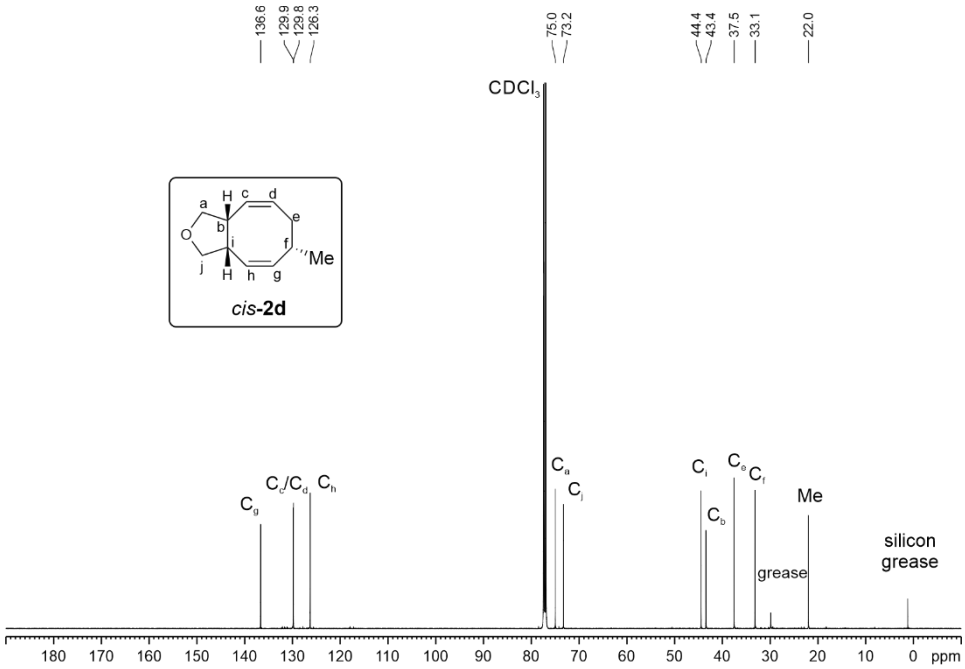

Figure 1.46. $^{13}C\{^{1}H\}$ NMR spectrum of product *cis*-**2d**.

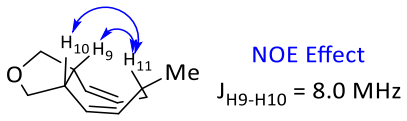

Figure 1.47. Stereochemical assignment of product *cis*-**2d**.

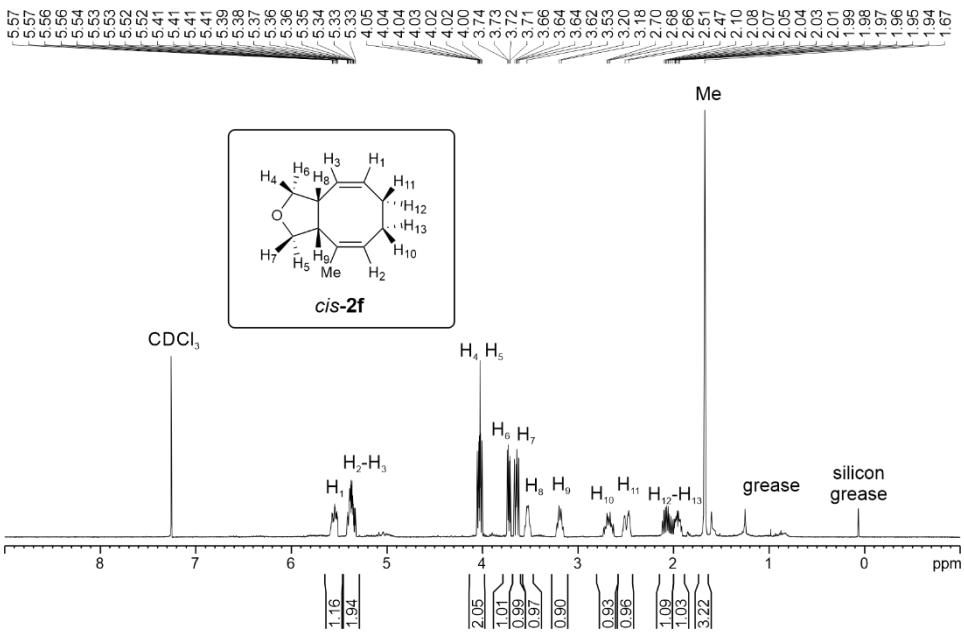

Figure 1.48. ^{1}H NMR spectrum of product *cis*-**2f**.

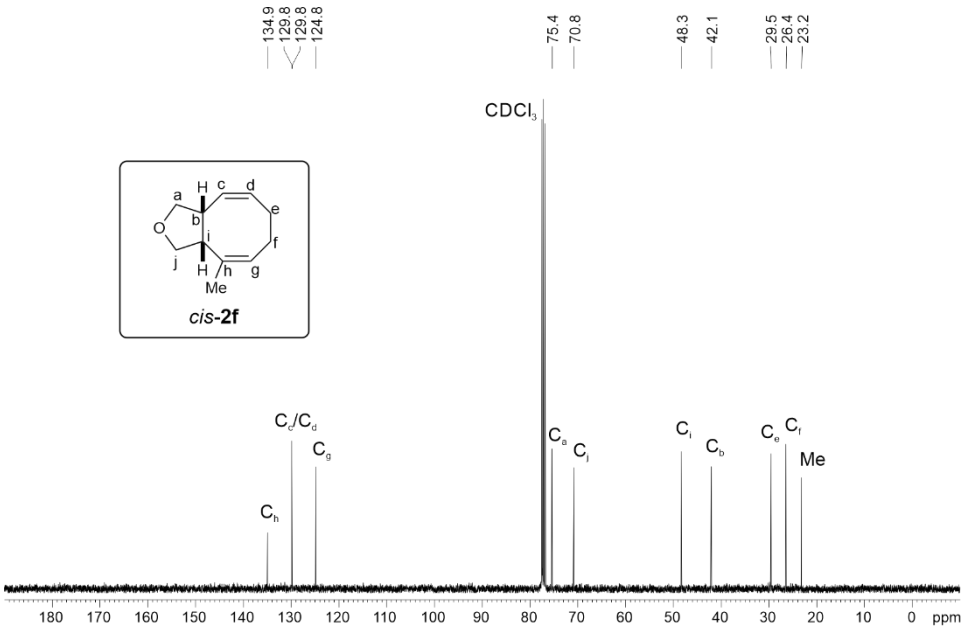

Figure 1.49. $^{13}C\{^{1}H\}$ NMR spectrum of product *cis*-**2f**.

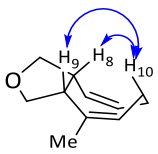

NOE Effect

J_{H8-H9} = 8.4 MHz

Figure 1.50. Stereochemical assignment of product *cis*-**2f**.

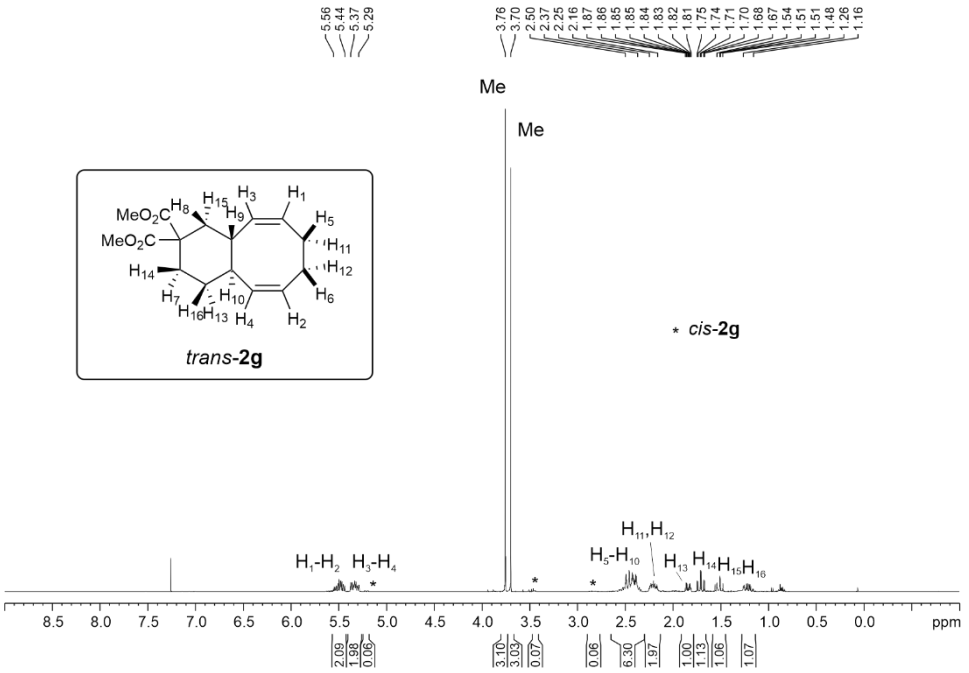

Figure 1.51. ^{1}H NMR spectrum of product *trans*-**2g**.

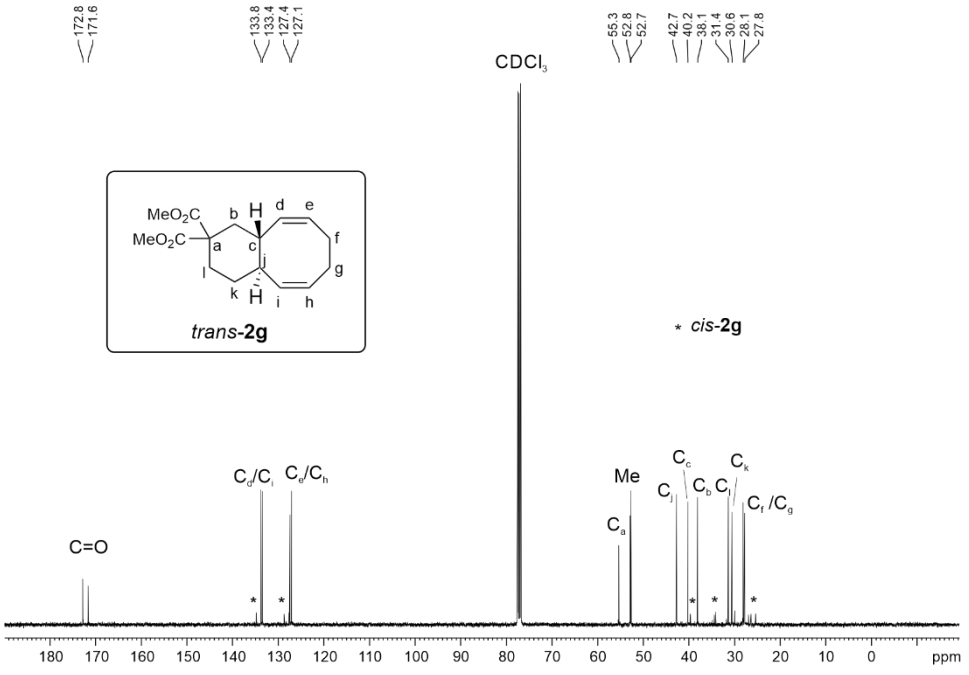

Figure 1.52. $^{13}C\{^{1}H\}$ NMR spectrum of product *trans*-**2g**.

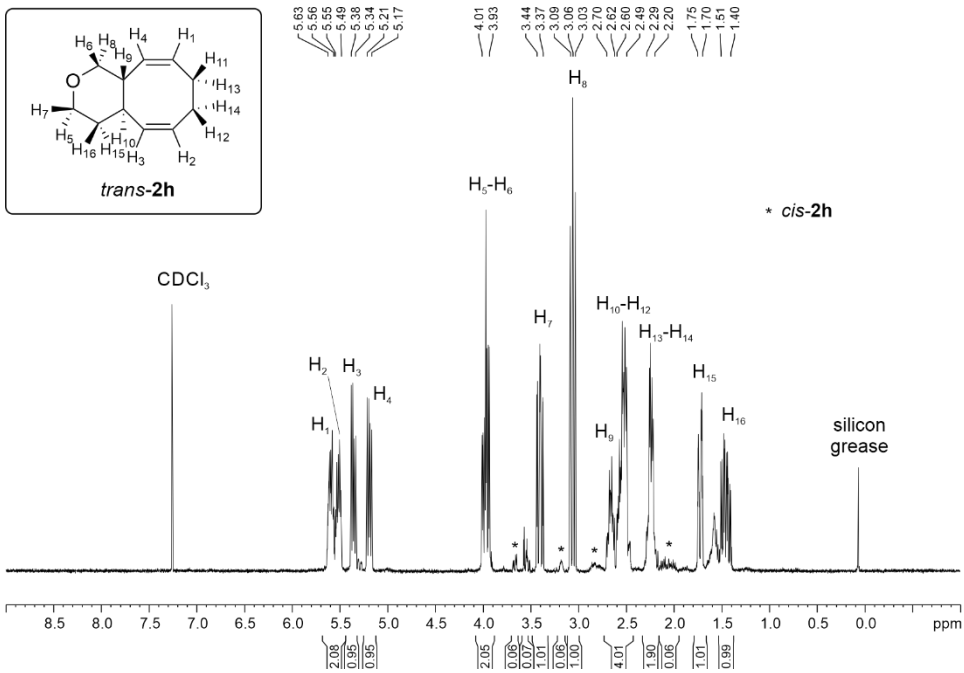

Figure 1.53. ^{1}H NMR spectrum of product *trans*-**2h**.

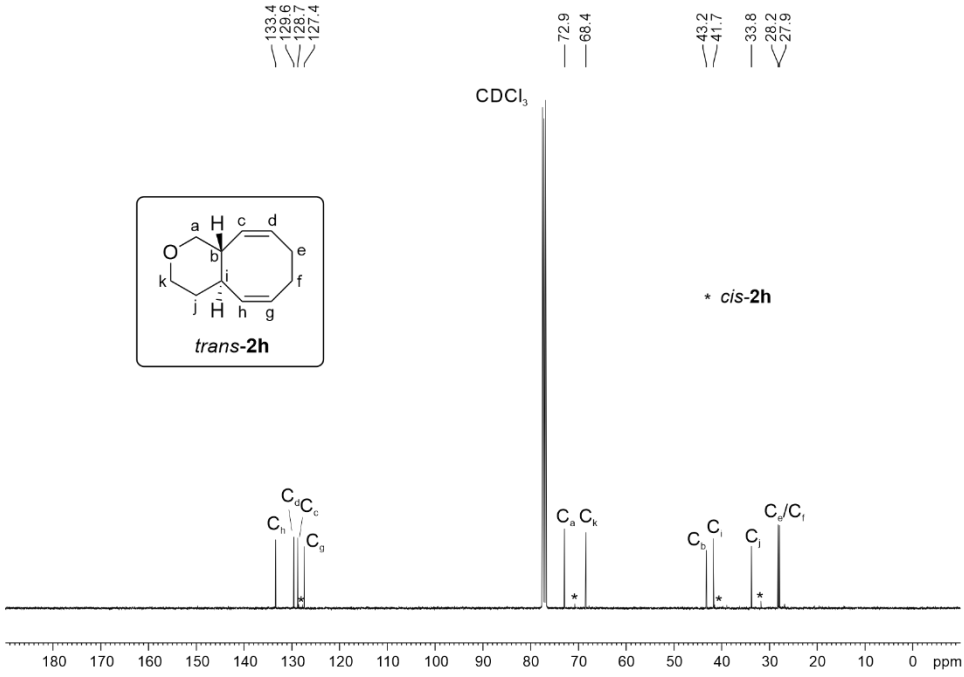

Figure 1.54. ^{13}C{^{1}H} NMR spectrum of product *trans*-**2h**.

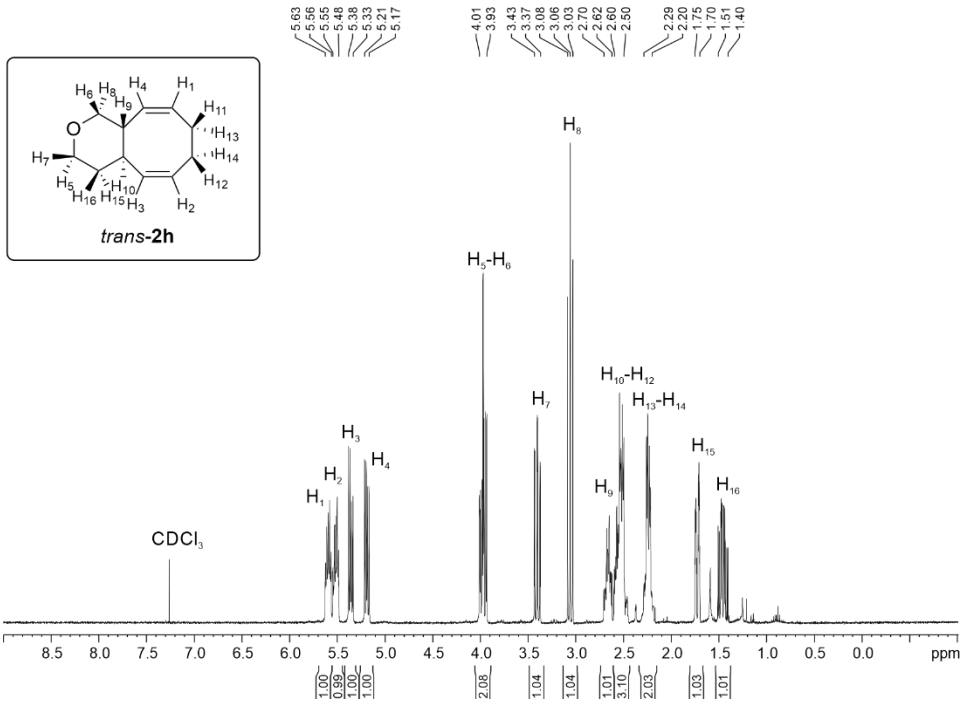

Figure 1.55. ^{1}H NMR spectrum of product *trans*-**2h**.

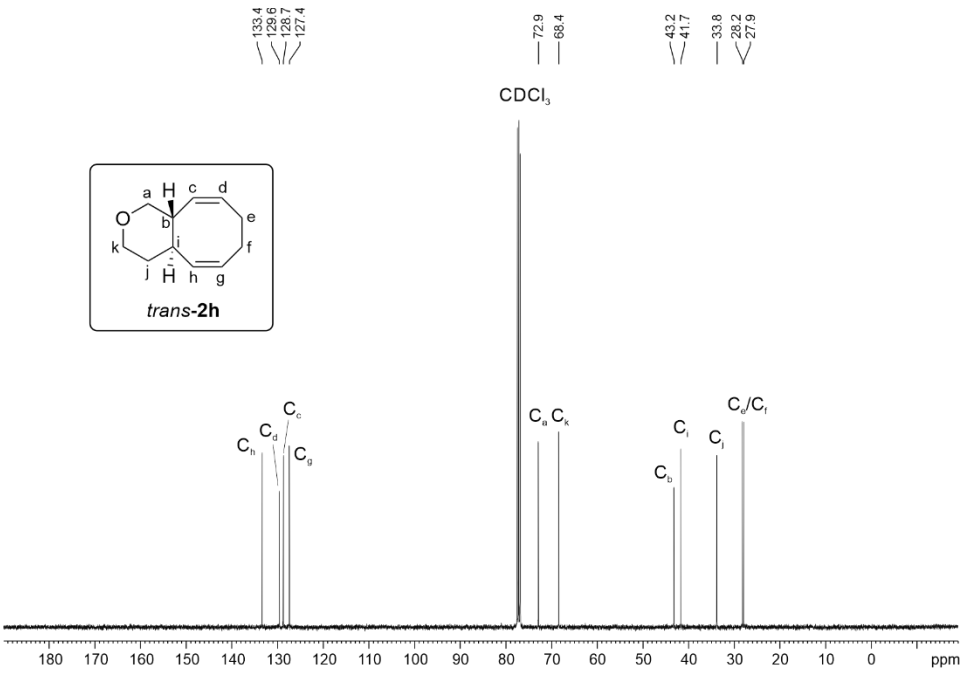

Figure 1.56. ^{13}C{^{1}H} NMR spectrum of product *trans*-**2h**.

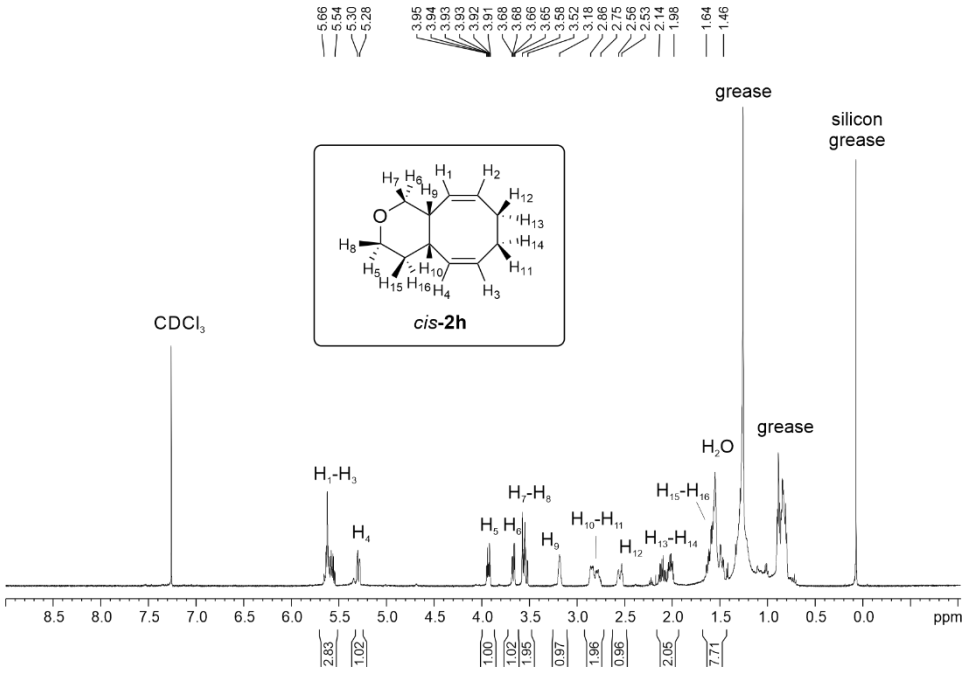

Figure 1.57. ^{1}H NMR spectrum of product *cis*-**2h**.

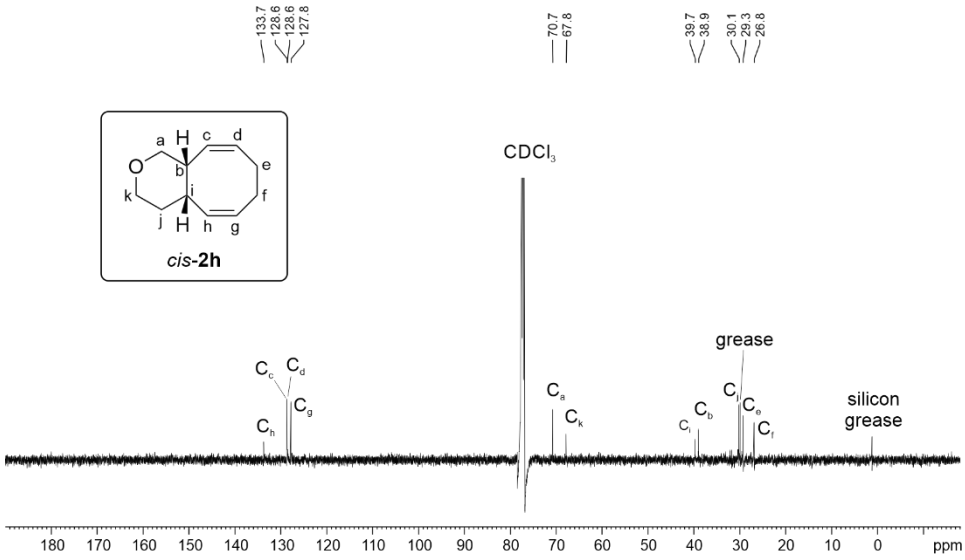

Figure 1.58. ^{13}C{^{1}H} NMR spectrum of product *cis*-**2h**.

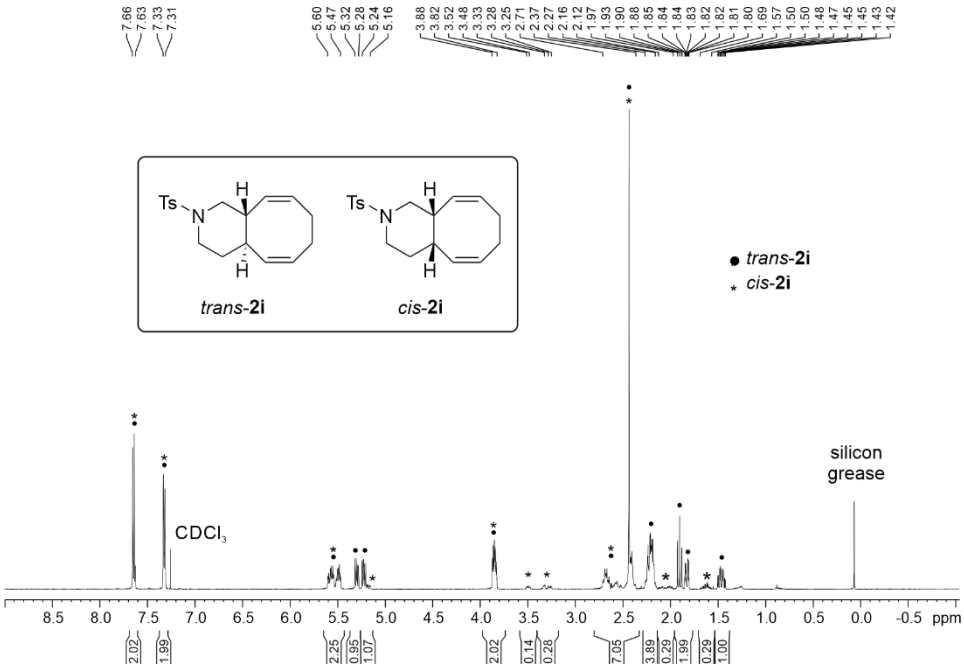

Figure 1.59. ^{1}H NMR spectrum of the mixture of products *trans*-**2i**:*cis*-**2i** (88:12).

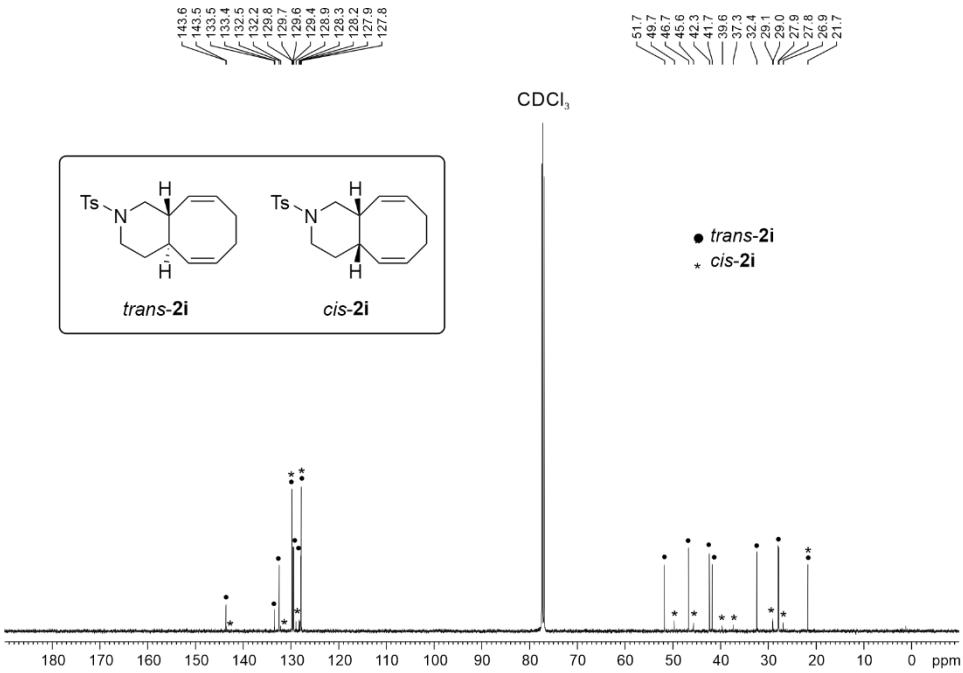

Figure 1.60. $^{13}C\{^{1}H\}$ NMR spectrum of the mixture of products *trans*-**2i**:*cis*-**2i** (88:12).

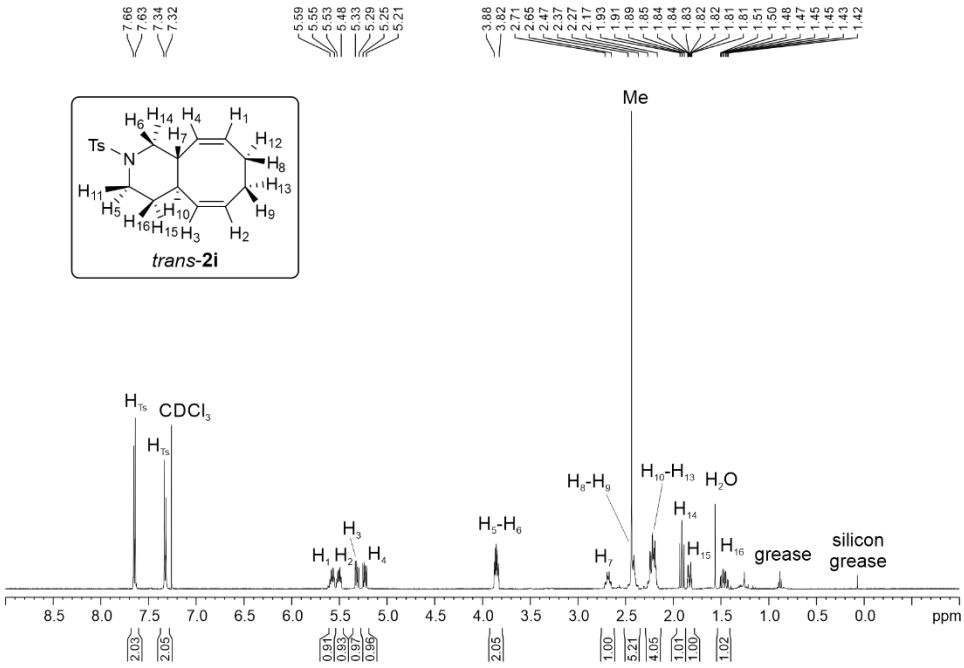

Figure 1.61. ^{1}H NMR spectrum of product *trans*-**2i**.

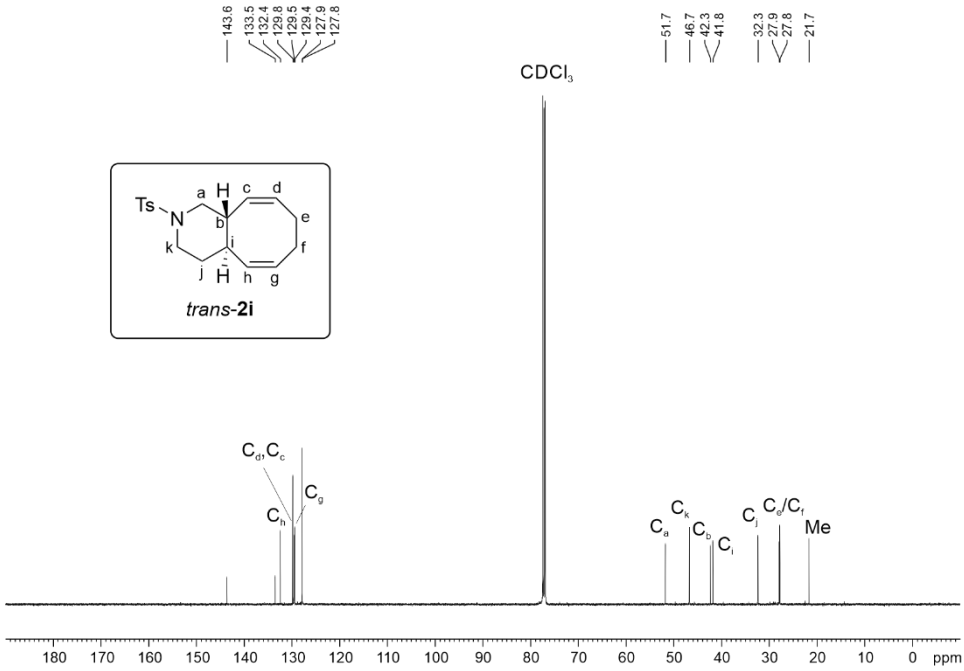

Figure 1.62. ^{13}C{^{1}H} NMR spectrum of product *trans*-**2i**.

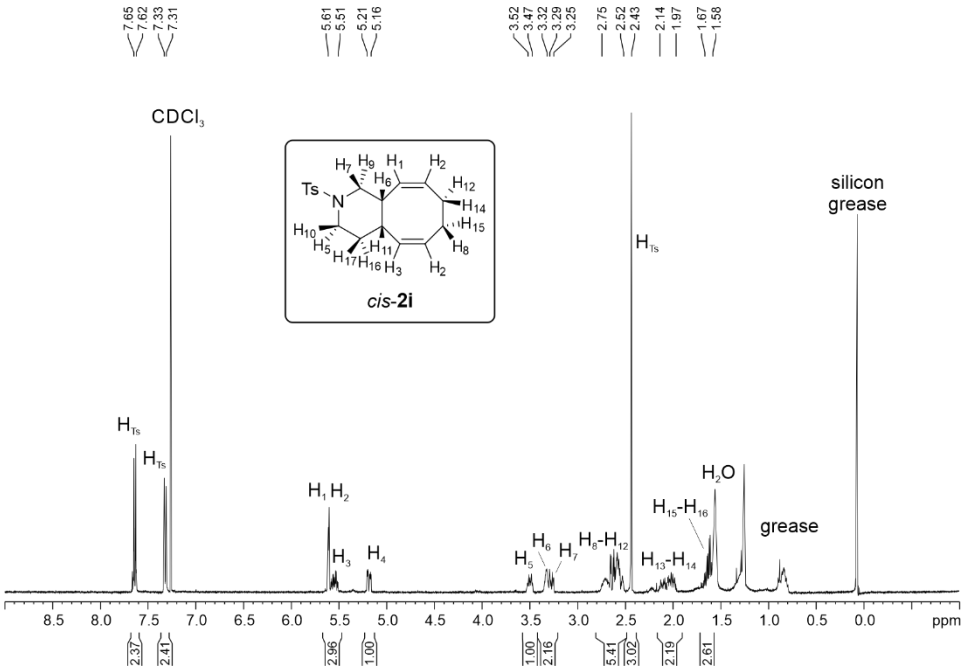

Figure 1.63. ^{1}H NMR spectrum of product *cis*-**2i**.

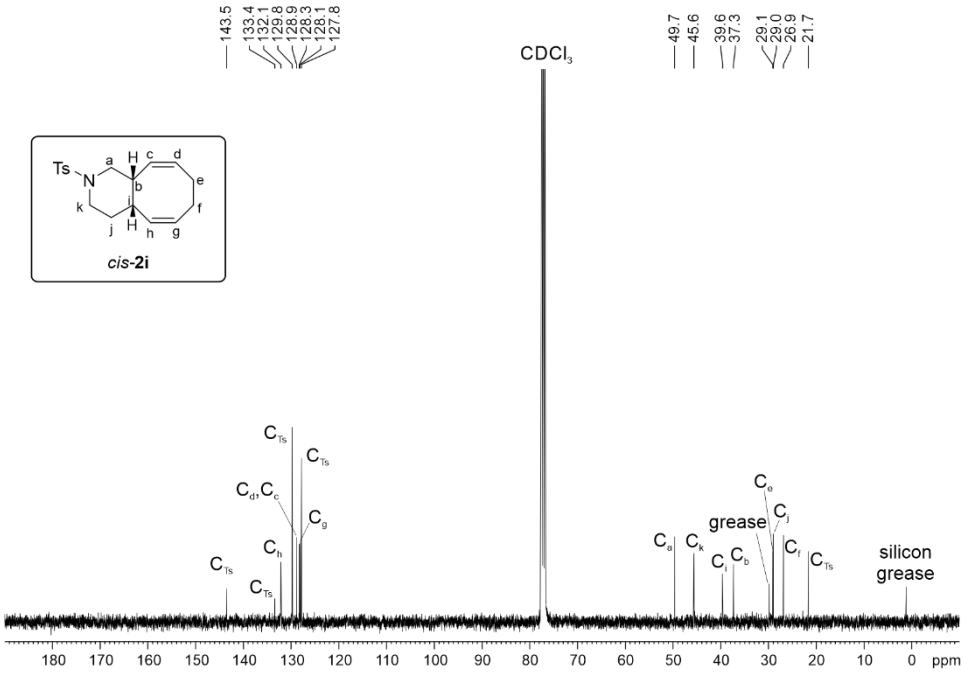

Figure 1.64. $^{13}C\{^{1}H\}$ NMR spectrum of product *cis*-**2i**.

1.4.9. Cartesian Coordinates

- Structures in Figure 1.4.

Pre-TS-1

C	1,9872057	1,4760146	0,5379472
C	1,4141443	1,7301033	-0,7650168
C	0,0065506	1,7094049	-0,8655952
C	-0,7433448	1,4556297	0,3462062
C	-2,2188732	1,1683204	0,2473772
C	-2,2040674	-1,1967225	0,2441351
C	-0,7250062	-1,4648071	0,3451154
C	0,0306992	-1,7104331	-0,8646343
C	1,4382123	-1,7123758	-0,7607369
C	2,0050907	-1,4490104	0,5432432
H	1,6171987	1,9995623	1,4229187
H	3,0535416	1,2524292	0,5784696
H	2,0300671	1,7636225	-1,6654787
H	-0,4897632	1,7196947	-1,8384309
H	-0,4575379	1,9850433	1,2602571
H	-2,6583526	1,1186247	1,2620540
H	-2,7254772	1,9810778	-0,3012625
H	-2,6459604	-1,1559291	1,2581445
H	-2,6988388	-2,0144135	-0,3079194
H	-0,4337408	-1,9888773	1,2605505
H	-0,4632016	-1,7285775	-1,8385766
H	2,0565859	-1,7393777	-1,6597547
H	3,0683932	-1,2117620	0,5856021
H	1,6401899	-1,9764111	1,4280592
O	-2,3597404	-0,0153289	-0,4851769
Ni	0,6760251	0,0044986	0,0325027

Pre-TS-2

C	-0,8189863	-0,9288637	-2,1248302
C	-0,1970981	-1,3971495	-0,8455265
C	0,8189863	0,9288637	-2,1248302
C	0,1970981	1,3971495	-0,8455265
C	0,9280911	1,7213211	0,3264197
C	0,1845339	1,8138445	1,5718391
C	-1,1972534	1,6524711	1,6433209
H	-1,8110037	-0,4872423	-1,9173460
H	-0,9585722	-1,7665372	-2,8282715
H	0,8145445	-1,8022937	-0,9685515
H	1,8110037	0,4872423	-1,9173460
H	0,9585722	1,7665372	-2,8282715
H	-0,8145445	1,8022937	-0,9685515
H	2,0188548	1,7450857	0,3437446
H	0,7651265	1,8643084	2,4956300
H	-1,6673246	1,5515174	2,6202027
H	-1,8665581	1,8649228	0,8108777
O	0,0000000	0,0000000	-2,8679940
Ni	0,0000000	0,0000000	0,6129757
C	-0,9280911	-1,7213211	0,3264197
H	-2,0188548	-1,7450857	0,3437446
C	-0,1845339	-1,8138445	1,5718391
H	-0,7651265	-1,8643084	2,4956300
C	1,1972534	-1,6524711	1,6433209
H	1,8665581	-1,8649228	0,8108777
H	1,6673246	-1,5515174	2,6202027

TS-1

C	2,0664144	1,5730274	0,5095193
C	1,3650031	1,9268352	-0,7019732
C	-0,0058124	1,6147165	-0,7960233
C	-0,7744054	1,1138552	0,3583661
C	-2,2817729	1,1221683	0,1981014
C	-2,2669844	-1,1516817	0,1983927
C	-0,7598677	-1,1236118	0,3590365
C	0,0154328	-1,615353	-0,7947369
C	1,3901805	-1,9094899	-0,6999573
C	2,0866569	-1,5453249	0,5113168
H	1,643861	1,8397552	1,4844504
H	3,1571371	1,5871346	0,488279
H	1,893205	2,2608692	-1,5978578
H	-0,5256341	1,7170363	-1,7509789
H	-0,4500088	1,4476362	1,3482059
H	-2,7646369	1,1644778	1,1946235
H	-2,6024537	1,9999327	-0,3845801
H	-2,7495347	-1,2001673	1,1948073
H	-2,3759864	-2,0336507	-0,384255
H	-0,4313915	-1,4525223	1,349144
H	-0,5027057	-1,725419	-1,7497417
H	1,9229456	-2,2375147	-1,5953689
H	3,1774692	-1,545362	0,4902938
H	1,6673023	-1,8162428	1,4864505
O	-2,7549707	-0,0179523	-0,5172194
Ni	1,0605776	0,0068479	-0,1982946

UNIVERSITAT ROVIRA I VIRGILI
TRANSITION METAL CATALYZED CYCLOADDITION REACTIONS FOR THE FORMATION OF EIGHT- AND SIX-MEMBERED RINGS
Nuria Llorente González

TS-2

C	-2,693039	-1,160541	0,284929
C	-1,329927	-0,976910	-0,286159
C	-2,693159	1,160549	-0,284935
C	-1,330080	0,977026	0,286325
C	-0,064539	1,402315	-0,337050
C	1,048547	1,842589	0,419407
C	2,357882	1,674083	-0,110626
H	-2,636914	-1,314561	1,365242
H	-3,230122	-1,999869	-0,155281
H	-1,295791	-0,940580	-1,368625
H	-2,636951	1,314670	-1,365270
H	-3,230601	1,999757	0,155348
H	-1,296011	0,940554	1,369001
H	-0,033086	1,450154	-1,421386
H	0,918061	2,014429	1,481511
H	3,205101	1,875741	0,524278
H	2,536945	1,788162	-1,170992
O	-3,490194	-0,000118	-0,000158
Ni	1,327488	-0,000030	-0,000004
C	-0,064471	-1,402129	0,337232
H	-0,033009	-1,450015	1,421502
C	1,048369	-1,842572	-0,419387
H	0,917656	-2,014386	-1,481334
C	2,357840	-1,674147	0,110457
H	2,537109	-1,787929	1,170705
H	3,204966	-1,875907	-0,524481

I-1

C	2,168442	1,648471	0,485197
C	1,285641	1,956868	-0,594004
C	0,026013	1,320076	-0,748662
C	-0,858863	0,785234	0,383064
C	-2,352318	1,115002	0,172485
C	-2,337154	-1,145890	0,174560
C	-0,848210	-0,795856	0,383844
C	0,042980	-1,319701	-0,748008
C	1,310748	-1,940123	-0,593606
C	2,189758	-1,619912	0,485301
H	1,791038	1,484084	1,499643
H	3,187620	2,033199	0,441593
H	1,692981	2,469907	-1,471778
H	-0,481513	1,450727	-1,708763
H	-0,505310	1,175498	1,347280
H	-2,861247	1,260958	1,146913
H	-2,522784	2,000353	-0,454778
H	-2,843751	-1,296651	1,149502
H	-2,496057	-2,034678	-0,450860
H	-0,488778	-1,180394	1,348157
H	-0,463157	-1,457110	-1,707932
H	1,724344	-2,448202	-1,471312
H	3,213800	-1,991460	0,441449
H	1,810577	-1,460396	1,499863
O	-2,903950	-0,019838	-0,504886
Ni	1,519150	0,009833	-0,504260

I-2

C	-2,537536	-1,159101	0,267832
C	-1,141921	-0,749862	-0,187657
C	-2,537691	1,158770	-0,267512
C	-1,142011	0,749699	0,187886
C	0,140623	1,332322	-0,382049
C	1,187591	1,885398	0,393403
C	2,539243	1,818029	-0,076200
H	-2,552529	-1,388874	1,350236
H	-2,957150	-2,016220	-0,279540
H	-1,092910	-0,813412	-1,289475
H	-2,552681	1,389117	-1,349781
H	-2,957562	2,015547	0,280221
H	-1,092827	0,813109	1,289693
H	0,192900	1,390617	-1,478689
H	1,003044	2,076100	1,458046
H	3,343023	2,115982	0,596485
H	2,755205	1,958715	-1,140883
O	-3,368612	-0,000308	-0,000161
Ni	1,608253	0,000070	-0,000081
C	0,140862	-1,332364	0,382038
H	0,193427	-1,390557	1,478686
C	1,187784	-1,885237	-0,393567
H	1,003092	-2,075976	-1,458181
C	2,539502	-1,817673	0,075807
H	2,755661	-1,958403	1,140450
H	3,343221	-2,115486	-0,597010
H	-0,431392	-1,452522	1,349144
H	-0,502706	-1,725419	-1,749742
H	1,922946	-2,237515	-1,595369
H	3,177469	-1,545362	0,490294
H	1,667302	-1,816243	1,486451
O	-2,754971	-0,017952	-0,517219
Ni	1,060578	0,006848	-0,198295

6a-π,π-*trans*

C	-2,706418	-2,173001	3,587131
C	-1,621816	-1,327916	2,927604
C	-3,648829	-0,121713	2,835072
C	-2,182816	0,087136	3,186031
C	-1,298830	1,126713	2,505001
C	-0,241310	1,741121	3,254252
C	0,830682	2,368406	2,585641
H	-2,586959	-2,206871	4,687325
H	-2,769705	-3,203089	3,206928
H	-1,664014	-1,502388	1,841786
H	-3,817471	-0,012877	1,748867
H	-4,337507	0,547867	3,372954
H	-2,117118	0,258497	4,278241
H	-1,687122	1,618952	1,609721
H	-0,166380	1,547285	4,329997
H	1,691545	2,710157	3,160317
H	0,669041	2,875810	1,632470
O	-3,939250	-1,492432	3,234643
Ni	0,553437	0,296924	2,115627
C	-0,174479	-1,262723	3,346194
H	0,004146	-0,901252	4,366468
C	0,950417	-1,616901	2,579333
H	0,857714	-2,275219	1,710945
C	2,151232	-0,871960	2,817869
H	2,352984	-0,498372	3,825687
H	3,042837	-1,072514	2,225052
P	0,437304	0,228946	-0,135332
C	-1,306307	0,310324	-0,696646
C	-1,952569	1,542797	-0,911838
C	-2,101021	-0,845501	-0,668516
C	-3,331467	1,614380	-1,081797
H	-1,368433	2,464273	-0,934236
C	-3,485178	-0,791289	-0,837085
H	-1,634867	-1,818290	-0,501036
C	-4,112205	0,449120	-1,033049
H	-3,830167	2,571190	-1,238472
H	-4,061692	-1,713313	-0,792707
C	1,099645	-1,216713	-1,067652
C	2,278988	-1,812013	-0,605155
C	0,555924	-1,687813	-2,278410
C	2,902081	-2,852302	-1,300148
H	2,735578	-1,440994	0,311449
C	1,158073	-2,724272	-2,979835
H	-0,351499	-1,236174	-2,680237
C	2,335580	-3,318859	-2,494757
H	3,818124	-3,285174	-0,902275
H	0,737847	-3,090527	-3,917031
C	1,272794	1,580657	-1,061191
C	2,358073	2,219237	-0,452407
C	0,954021	1,922683	-2,389295
C	3,111762	3,182773	-1,130214
H	2,613028	1,948630	0,574785
C	1,684707	2,884312	-3,072766
H	0,123490	1,426737	-2,894138
C	2,771185	3,522878	-2,446774
H	3,949416	3,658710	-0,623729
H	1,441671	3,157242	-4,100137
O	-5,460055	0,624680	-1,174188
O	2,845322	-4,332439	-3,256741
O	3,424925	4,452754	-3,205964
C	4,536916	5,129860	-2,618924
H	4,905144	5,818761	-3,387112
H	4,234708	5,705164	-1,727411
H	5,339598	4,425327	-2,344008
C	4,046869	-4,961599	-2,809259
H	3,911546	-5,434982	-1,822145
H	4,274162	-5,732584	-3,553500
H	4,883340	-4,244494	-2,758308
C	-6,297555	-0,523766	-1,020802
H	-7,325220	-0,156033	-1,114191
H	-6,105460	-1,272364	-1,807536
H	-6,162139	-0,989577	-0,030435

6a-π,π-*cis*

C	-0,453512	1,583294	3,253357
C	-1,127006	1,982637	2,082852
C	-2,385712	1,415177	1,735371
C	-3,440123	1,021535	2,785740
C	-4,904343	1,039692	2,266455
C	-4,699126	-0,938914	3,403676
C	-3,253799	-0,445985	3,254108
C	-2,525120	-1,202945	2,150669
C	-1,310212	-1,910058	2,267217
C	-0,296104	-1,509162	3,179887
H	-1,002472	1,277911	4,146197
H	0,570898	1,914191	3,421539
H	-0,604234	2,583925	1,333724
H	-2,776140	1,681302	0,748988
H	-3,357287	1,709123	3,642713
H	-5,535847	1,692595	2,898444
H	-4,989347	1,377817	1,223821
H	-5,128468	-0,633263	4,380407
H	-4,810565	-2,026271	3,288299
H	-2,696287	-0,505669	4,198391

UNIVERSITAT ROVIRA I VIRGILI
TRANSITION METAL-CATALYZED CYCLOADDITION REACTIONS FOR THE FORMATION OF EIGHT- AND SIX-MEMBERED RINGS
Nuria Llorente González

H	-3,164280	-1,455640	1,299441	C	-0,291248	5,854898	-3,395337
H	-1,057470	-2,620496	1,474313	H	-0,707333	6,520859	-4,159530
H	0,674353	-2,002079	3,113914	H	-0,555959	6,237364	-2,394861
H	-0,544765	-1,125606	4,170720	H	0,807433	5,827809	-3,494673
O	-5,395638	-0,310406	2,321326				
Ni	-0,862089	0,007787	1,862611				
P	0,372594	-0,086375	-0,021676				
C	0,078298	1,285046	-1,211227				
C	0,666167	2,533636	-0,953167				
C	-0,819580	1,196477	-2,290232				
C	0,383083	3,656877	-1,735252				
H	1,382838	2,633158	-0,135047				
C	-1,112062	2,304951	-3,076906				
H	-1,288550	0,242406	-2,532928				
C	-0,516384	3,546582	-2,804969				
H	0,870932	4,602259	-1,503686				
H	-1,800240	2,230089	-3,919728				
C	0,057305	-1,597421	-1,015458				
C	1,045240	-2,446922	-1,526343				
C	-1,291298	-1,971518	-1,197282				
C	0,714700	-3,619826	-2,214818				
H	2,098887	-2,205418	-1,381997				
C	-1,636470	-3,120619	-1,895044				
H	-2,074868	-1,346567	-0,763387				
C	-0,631600	-3,956480	-2,412068				
H	1,513546	-4,257632	-2,589617				
H	-2,679443	-3,404142	-2,039254				
C	2,200829	-0,025463	0,138193				
C	3,071234	0,176572	-0,942512				
C	2,753816	-0,159667	1,422658				
C	4,454999	0,224712	-0,761614				
H	2,662130	0,311479	-1,945557				
C	4,129184	-0,116780	1,621360				
H	2,073516	-0,279798	2,269185				
C	4,990148	0,071912	0,528354				
H	5,101552	0,385877	-1,622754				
H	4,563433	-0,217476	2,616543				
O	-0,871491	4,574692	-3,637489				
O	6,324818	0,102392	0,822578				
O	-1,069362	-5,070672	-3,074000				
C	7,243197	0,293654	-0,253855				
H	7,083662	1,263348	-0,755007				
H	8,240284	0,279684	0,199799				
H	7,168876	-0,517306	-0,997858				
C	-0,086571	-5,957453	-3,607517				
H	0,552351	-6,378682	-2,813019				
H	-0,645821	-6,766433	-4,090274				
H	0,547918	-5,454577	-4,356910				

- Structures in Figure 1.5

Pre-TS-3

C	1,983315	0,882799	-1,760831
C	2,210086	1,363211	-0,472156
C	1,124331	1,725924	0,429775
C	-0,202013	1,560214	-0,013237
C	-1,410814	1,565468	0,884623
C	-1,957225	-1,166211	-0,854755
C	-0,743984	-1,379720	0,014974
C	0,405271	-2,067545	-0,435742
C	1,601218	-2,061402	0,387149
C	1,625597	-1,438996	1,634832
H	1,101015	1,140231	-2,346518
H	2,816923	0,459011	-2,318910
H	3,218249	1,329119	-0,052977
H	1,358368	1,947133	1,473381
H	-0,428058	1,720314	-1,070196
H	-1,169305	1,038007	1,819387
H	-1,679220	2,598979	1,167887
H	-2,806825	-1,753114	-0,445703
H	-1,762275	-1,513592	-1,879336
H	-0,950224	-1,340826	1,090550
H	0,455273	-2,475211	-1,447929
H	2,528341	-2,423776	-0,061996
H	2,581992	-1,285814	2,133046
H	0,742760	-1,351289	2,268625
O	-2,372535	0,197258	-1,013790
Ni	0,926623	-0,181108	-0,083602
C	-2,653923	0,918794	0,186538
H	-3,202294	0,277969	0,902406
H	-3,340665	1,714171	-0,135495

Pre-TS-4

C	2,520413	1,288461	-0,674701
C	1,372783	1,479216	-1,460217
C	0,076620	1,594726	-0,843286
C	-0,128908	1,552697	0,558145
C	-1,479049	1,212921	1,156092
C	-1,859177	-1,371549	-0,758357
C	-0,554912	-1,504638	-0,016868
C	0,624676	-2,063324	-0,545663
C	1,834762	-1,839141	0,211739
C	1,801756	-1,158257	1,455703
H	2,649767	1,779035	0,291497
H	3,443963	0,967581	-1,158533
H	1,407946	1,333772	-2,541397
H	-0,778651	1,486261	-1,507631
H	0,582265	2,025390	1,240425
H	-1,320506	0,433755	1,920959
H	-1,887613	2,077055	1,712854
H	-2,646703	-1,942869	-0,225231
H	-1,772701	-1,774434	-1,777714
H	-0,669072	-1,475844	1,071432
H	0,670796	-2,486359	-1,550608
H	2,792287	-2,084526	-0,254931
H	2,752091	-0,874721	1,906159
H	0,976384	-1,276216	2,159973
O	-2,305192	-0,021538	-0,952811
Ni	0,987062	-0,073231	-0,165656
C	-2,618309	0,772959	0,196393
H	-3,401083	0,271122	0,799323
H	-3,071694	1,671695	-0,247090

TS-3

C	-2,415454	1,550555	-0,289471
C	-1,099595	1,033339	0,235258
C	-2,425762	-1,525713	0,259940
C	-1,101239	-1,019913	-0,262774
C	0,211411	-1,396855	0,341316
C	1,318462	-1,919483	-0,374894
C	2,653076	-1,746326	0,121420
H	-2,406156	1,553804	-1,390777
H	-2,654786	2,584627	0,033728
H	-1,067400	0,981544	1,339544
H	-2,428536	-1,495022	1,368261
H	-2,676020	-2,558992	-0,044213
H	-1,081064	-0,981402	-1,366475
H	0,239930	-1,406103	1,440266
H	1,175109	-2,157740	-1,436074
H	3,488102	-2,000489	-0,531198
H	2,858071	-1,858628	1,191981
O	-3,489842	-0,718193	-0,269786
Ni	1,638094	0,000942	0,001930
C	0,224382	1,402738	-0,355148
H	0,261554	1,412200	-1,453552
C	1,324246	1,922023	0,374213
H	1,169136	2,161814	1,433570
C	2,664415	1,744558	-0,104944
H	2,883405	1,854626	-1,172836
H	3,491896	1,995406	0,558390
C	-3,543467	0,622747	0,212285

H	-4,515817	1,002578	-0,131682
H	-3,548175	0,624912	1,322116

TS-4

C	2,451818	1,443315	0,407064
C	1,678338	1,819315	-0,751940
C	0,290749	1,566531	-0,740274
C	-0,399670	1,096583	0,471196
C	-1,898870	1,307869	0,520223
C	-1,922284	-1,379341	0,461864
C	-0,417387	-1,208507	0,502933
C	0,265641	-1,731538	-0,694986
C	1,644505	-2,015209	-0,706176
C	2,429858	-1,617146	0,438538
H	2,110961	1,728693	1,408583
H	3,537893	1,416256	0,307376
H	2,149827	2,134687	-1,685312
H	-0,286096	1,709683	-1,655153
H	0,061150	1,378266	1,422052
H	-2,283594	1,017787	1,507615
H	-2,087531	2,395501	0,439597
H	-2,394942	-1,050094	1,403282
H	-2,138355	-2,458026	0,362541
H	-0,010757	-1,500085	1,477412
H	-0,334021	-1,873466	-1,595260
H	2,106071	-2,365226	-1,632146
H	3,515923	-1,604761	0,333625
H	2,090323	-1,872299	1,448634
O	-2,528200	-0,781768	-0,682426
Ni	1,345124	-0,087209	-0,221994
C	-2,719985	0,634856	-0,579665
H	-3,792307	0,842020	-0,401240
H	-2,464180	1,053313	-1,565963

I-3

C	-2,067988	1,363144	-0,367847
C	-0,782300	0,703307	0,137053
C	-2,062316	-1,467184	0,297970
C	-0,782530	-0,805884	-0,217783
C	0,528586	-1,360275	0,317390
C	1,564387	-1,926210	-0,468718
C	2,916115	-1,891518	-0,001281
H	-2,076278	1,365881	-1,470140
H	-2,136491	2,410266	-0,031675
H	-0,760246	0,775241	1,241704
H	-2,074865	-1,441270	1,408653
H	-2,133188	-2,516711	-0,021202
H	-0,779947	-0,889882	-1,319278
H	0,594496	-1,434343	1,413386
H	1,372584	-2,101109	-1,534788
H	3,714431	-2,189530	-0,680399
H	3,132374	-2,050407	1,060739
O	-3,222753	-0,810913	-0,223439
Ni	2,005892	-0,057438	-0,035557
C	0,535823	1,250369	-0,393588
H	0,601373	1,323975	-1,489585
C	1,571736	1,812810	0,394041
H	1,378694	1,989659	1,459725
C	2,924937	1,770523	-0,070698
H	3,144185	1,930427	-1,131905
H	3,723339	2,063725	0,610517
C	-3,277110	0,570450	0,145092
H	-4,215580	0,952945	-0,279000
H	-3,337361	0,659952	1,250610

I-4

C	2,540725	1,572454	0,328005
C	1,573302	1,834160	-0,688731
C	0,307856	1,187605	-0,722826
C	-0,478393	0,695934	0,497702
C	-1,896597	1,293413	0,557187
C	-1,983504	-1,361010	0,323056
C	-0,533673	-0,883152	0,495866
C	0,330444	-1,437627	-0,645028
C	1,603544	-2,055729	-0,520099
C	2,536497	-1,689892	0,495488
H	2,249683	1,447911	1,375798
H	3,550236	1,959643	0,186612
H	1,910235	2,312791	-1,614755
H	-0,263109	1,280160	-1,650321
H	0,057512	1,022156	1,400448
H	-2,321792	1,098044	1,554102
H	-1,853202	2,387747	0,446208
H	-2,564246	-1,223818	1,256216
H	-2,009018	-2,431584	0,071677
H	-0,152652	-1,261393	1,457658
H	-0,215282	-1,614946	-1,575878
H	1,975053	-2,605308	-1,392070
H	3,555192	-2,071480	0,422390
H	2,207892	-1,468769	1,516470
O	-2,599470	-0,686991	-0,774093
Ni	1,822847	-0,107005	-0,542368
C	-2,818783	0,714902	-0,524999
H	-3,876710	0,874820	-0,242817
H	-2,654586	1,216961	-1,490895

E,E-**6h**-π,π-*trans*

C	-3,822738	1,895937	-2,269590
C	-2,592187	1,026980	-1,986266
C	-4,150482	-0,882199	-1,463982
C	-2,924582	-0,457674	-2,267026
C	-1,661015	-1,302553	-2,078376
C	-0,830356	-1,587461	-3,218378
C	0,490688	-2,044047	-3,053479
H	-4,070874	1,871907	-3,343780
H	-3,637100	2,945584	-1,989955
H	-2,347808	1,117801	-0,916674
H	-3,920416	-0,853979	-0,381381
H	-4,468287	-1,902133	-1,725300
H	-3,212345	-0,522719	-3,334827
H	-1,620061	-1,972771	-1,212918
H	-1,165190	-1,252698	-4,205907
H	1,144366	-2,114608	-3,922513
H	0,739783	-2,693899	-2,214491
O	-5,271106	-0,032845	-1,750026
Ni	0,037977	-0,144492	-2,136519
C	-1,334348	1,289234	-2,781348
H	-1,419689	1,101897	-3,859586
C	-0,125281	1,847662	-2,322537
H	-0,080432	2,374812	-1,363964
C	1,065215	1,477595	-3,020049
H	1,020494	1,292168	-4,096621
H	2,025114	1,829287	-2,645517
C	-5,001555	1,343008	-1,457300
H	-5,933555	1,879014	-1,685479
H	-4,788862	1,462057	-0,374303
P	0,643944	-0,229156	0,019268
C	-0,686437	0,537260	1,020606
C	-0,731546	1,924586	1,224339
C	-1,832125	-0,208159	1,366625
C	-1,871214	2,558123	1,730679
H	0,135649	2,537537	0,974028
C	-2,963502	0,402919	1,888581
H	-1,848584	-1,285691	1,199059
C	-3,000044	1,796438	2,060257
H	-1,863243	3,638776	1,861135
H	-3,848515	-0,177842	2,149762
C	2,162331	0,680931	0,515097
C	3,204248	0,752368	-0,415211
C	2,389245	1,179951	1,811567
C	4,439972	1,318459	-0,086585
H	3,040659	0,342659	-1,414125
C	3,605498	1,755448	2,151351
H	1,603535	1,110099	2,565817
C	4,641330	1,830912	1,202394
H	5,227542	1,354916	-0,837296
H	3,787159	2,146964	3,152880
C	0,993443	-1,822829	0,872922
C	1,816261	-2,734225	0,198475
C	0,606663	-2,133944	2,189748
C	2,228521	-3,930633	0,789996
H	2,167494	-2,488194	-0,804871
C	0,997815	-3,324722	2,789235
H	0,000871	-1,431500	2,762850
C	1,807261	-4,236837	2,092124
H	2,871074	-4,608242	0,230389
H	0,695856	-3,569080	3,808230
O	5,798184	2,414477	1,637672
O	2,131735	-5,379181	2,768764
O	-4,175526	2,303841	2,540491
C	2,964002	-6,332462	2,106738
H	3,093851	-7,157147	2,815995
H	2,489865	-6,712625	1,186488
H	3,950184	-5,904876	1,859140
C	-4,275891	3,720535	2,689268
H	-4,133900	4,237837	1,725492
H	-5,289951	3,910276	3,057478
H	-3,543963	4,103224	3,420441
C	6,886399	2,504542	0,717281
H	6,620257	3,110774	-0,165001
H	7,698657	2,996217	1,263751
H	7,219569	1,506410	0,386767

E,E-**6h**-π,π-*cis*

C	0,330024	1,817411	2,934012
C	-0,788948	2,014461	2,081554
C	-1,963789	1,234905	2,191493
C	-2,541528	0,647721	3,473260
C	-3,894264	1,282931	3,848201
C	-4,140835	-1,237400	2,928250
C	-2,683899	-0,889094	3,282537
C	-1,713039	-1,374554	2,189872
C	-0,396124	-1,842673	2,464310
C	0,366199	-1,243979	3,487944
H	0,209057	1,568933	3,989295
H	1,257047	2,338821	2,693924
H	-0,648538	2,601273	1,168562
H	-2,671282	1,301483	1,361038
H	-1,829466	0,837352	4,288991
H	-4,210721	0,887175	4,826332
H	-3,789250	2,371966	3,964973

UNIVERSITAT ROVIRA I VIRGILI
TRANSITION METAL CATALYZED CYCLOADDITION REACTIONS FOR THE FORMATION OF EIGHT- AND SIX-MEMBERED RINGS
Nuria Llorente González

H	-4,753079	-1,343798	3,846271	H	1,323519	6,624367	-1,363051
H	-4,195924	-2,189769	2,381141	H	2,701238	6,080522	-2,384203
H	-2,440478	-1,405525	4,228623	C	-2,551033	-4,498317	-4,323807
H	-2,190625	-1,773759	1,291196	H	-2,028188	-5,272629	-3,737233
H	0,076197	-2,535062	1,760986	H	-3,439485	-4,936076	-4,792240
H	1,415307	-1,509716	3,614609	H	-1,874499	-4,118078	-5,108015
H	-0,115245	-0,829899	4,376348	C	6,983796	-2,069621	-1,875735
O	-4,709337	-0,246891	2,069176	H	7,179860	-0,996828	-2,041355
Ni	-0,257636	0,082151	1,930481	H	7,931652	-2,587442	-1,691833
C	-4,963275	0,978223	2,778874	H	6,503449	-2,494917	-2,772842
H	-5,967605	0,934472	3,243409				
H	-4,984814	1,760054	2,006060				
P	0,634461	-0,046155	-0,136561				
C	-0,379730	-1,113551	-1,233480				
C	0,123543	-2,135676	-2,045028				
C	-1,777243	-0,922439	-1,200882				
C	-0,725698	-2,943165	-2,811317				
H	1,198137	-2,318107	-2,084874				
C	-2,631110	-1,701208	-1,968318				
H	-2,191542	-0,155155	-0,543940				
C	-2,109304	-2,722724	-2,781139				
H	-0,295886	-3,733794	-3,424176				
H	-3,710458	-1,549469	-1,942321				
C	2,338005	-0,685116	-0,392776				
C	3,082737	-0,460114	-1,558543				
C	2,928340	-1,436474	0,637750				
C	4,374296	-0,972096	-1,706689				
H	2,651393	0,133484	-2,366835				
C	4,207672	-1,962498	0,504442				
H	2,370840	-1,585220	1,563486				
C	4,940572	-1,733320	-0,671562				
H	4,926894	-0,770958	-2,623255				
H	4,669482	-2,544181	1,302899				
C	0,709386	1,541282	-1,056295				
C	1,509829	2,558830	-0,514358				
C	-0,032260	1,832646	-2,213745				
C	1,587222	3,823136	-1,101377				
H	2,092815	2,356119	0,386570				
C	0,026936	3,090802	-2,805927				
H	-0,662400	1,063720	-2,662154				
C	0,836846	4,095922	-2,256003				
H	2,224588	4,582306	-0,651221				
H	-0,546827	3,317187	-3,705378				
O	0,825299	5,297647	-2,912934				
O	-3,030975	-3,444550	-3,489853				
O	6,192490	-2,282987	-0,706489				
C	1,631363	6,350848	-2,386535				
H	1,475851	7,206828	-3,052588				

- Structures in Figure 1.8

Pre-TS-5

C	-4,2849744	-1,2273209	-3,4420658
C	-4,0823955	-0,8236379	-2,1709167
C	-2,9493721	-0,0358121	-1,7178132
C	-2,8583289	0,5876835	-0,4493757
C	-3,9925871	0,7327318	0,5588261
C	-3,0051841	-1,4047273	2,5674018
C	-2,2455890	-2,1520063	1,4989848
C	-2,8733377	-2,6615814	0,3600988
C	-2,1667371	-3,0328099	-0,8417705
C	-0,7784323	-2,9758077	-0,9565135
H	-3,5762576	-0,9821713	-4,2371682
H	-5,1644640	-1,8066386	-3,7226622
H	-4,8134472	-1,0962636	-1,4050061
H	-2,2881760	0,3399797	-2,5059256
H	-2,2094634	1,4728328	-0,4200621
H	-3,6100947	1,2295221	1,4687572
H	-4,7534547	1,4118398	0,1291039
H	-2,4190613	-0,5146473	2,8479534
H	-3,0728433	-1,9998449	3,4986160
H	-1,2424602	-2,4874038	1,7747811
H	-3,9537162	-2,5765652	0,2622942
H	-2,7754692	-3,1866723	-1,7361515
H	-0,3227441	-3,1133884	-1,9376150
H	-0,1149846	-3,1590870	-0,1108701
Ni	-1,6915406	-1,0857357	-0,3590093
P	0,2120276	-0,1125562	-0,0274390
C	0,6399031	0,9217678	-1,4825065
C	1,1298125	2,2297900	-1,4121713
C	0,4082238	0,3644303	-2,7565928
C	1,3941679	2,9698347	-2,5703379
H	1,3026075	2,6958629	-0,4413989
C	0,6858653	1,0769885	-3,9141707
H	-0,0147366	-0,6409098	-2,8195178
C	1,1793328	2,3910467	-3,8289048
H	1,7625421	3,9899657	-2,4767008
C	1,6792947	-1,1994546	0,1773840
C	1,7883859	-1,9386099	1,3722911
C	2,6400436	-1,4065836	-0,8155665
C	2,8191316	-2,8474742	1,5642278
H	1,0354469	-1,7866372	2,1674495
C	3,6843489	-2,3223783	-0,6388373
H	2,5863548	-0,8463172	-1,7501573
C	3,7766690	-3,0499201	0,5545976
H	2,9065068	-3,4173995	2,4897424
H	4,4155821	-2,4531816	-1,4347256
C	0,4496962	1,0145863	1,4035260
C	1,7203660	1,4132859	1,8438918
C	-0,6694400	1,4856555	2,1071802
C	1,8767988	2,2604646	2,9431234
H	2,6098763	1,0480904	1,3278354
C	-0,5353426	2,3292193	3,2026565
H	-1,6576822	1,1640090	1,7859882
C	0,7427465	2,7242864	3,6296640
H	2,8794810	2,5435179	3,2590433
H	-1,4058603	2,6888252	3,7520112
O	0,7767460	3,5467978	4,7193067
O	4,7495974	-3,9692534	0,8367649
C	2,0539587	3,9702767	5,1992863
H	2,5998455	4,5509215	4,4368657
H	1,8488375	4,6099954	6,0645362
H	2,6707838	3,1128337	5,5166343
C	5,7388665	-4,2187648	-0,1619519
H	6,4032687	-4,9805294	0,2606446
H	5,2866434	-4,6032059	-1,0916481
H	6,3229230	-3,3105803	-0,3890012
H	0,5103713	0,6471346	-4,9006660
O	1,4046847	3,0162514	-5,0231421
C	1,8755870	4,3640926	-4,9928650
H	1,9769408	4,6673058	-6,0407197
H	1,1574905	5,0312111	-4,4871216
H	2,8565652	4,4387632	-4,4941352
O	-4,6905931	-0,4634347	0,9123064
H	-5,1042311	-1,8773399	2,2647381
H	-4,8062542	-0,2805319	2,9867917
C	-4,4490664	-0,9946164	2,2178993

Pre-TS-6

C	-4,2503411	1,4647175	3,3312539
C	-2,9373363	1,7206117	3,5000383
C	-1,8477363	1,7790075	2,5246321
C	-1,8758554	1,7293117	1,1059124
C	-3,1101531	1,7670296	0,2112407
C	-3,9611805	-1,6610365	0,6209414
C	-3,0492557	-1,5155579	1,8056985
C	-1,8175731	-2,1083165	1,8607285
C	-0,7719637	-1,7559175	2,8092021
C	-0,9412001	-0,8028726	3,8127965
H	-4,6780271	1,2150205	2,3613526
H	-4,9210936	1,4896568	4,1910496

H	-2,6002350	1,9308459	4,5214068
H	-1,0705417	2,2960824	0,6222190
H	-3,6526001	2,7048393	0,4308427
H	-2,7713436	1,8192073	-0,8393624
H	-5,0145264	-1,7005220	0,9408032
H	-3,7445487	-2,5893267	0,0660691
H	-3,4079411	-0,8929115	2,6293590
H	-1,5351750	-2,8014776	1,0630550
H	0,1908227	-2,2544960	2,6860531
H	-0,0934917	-0,5442294	4,4478864
H	-1,9248256	-0,5570001	4,2134667
Ni	-1,0385574	0,0047303	1,8131278
P	0,4794423	-0,1375586	0,2578893
C	-0,2543609	-0,4830138	-1,3847554
C	-0,6413786	0,5545766	-2,2438736
C	-0,6835369	-1,7893400	-1,7004786
C	-1,4272080	0,3152912	-3,3759252
H	-0,3407803	1,5796023	-2,0225916
C	-1,4532890	-2,0446548	-2,8262927
H	-0,4212124	-2,6182960	-1,0416950
C	-1,8392456	-0,9906349	-3,6725526
H	-1,7115245	1,1527759	-4,0106141
C	1,8440663	-1,3626361	0,4150788
C	2,4490951	-1,4681629	1,6827486
C	2,3814618	-2,1146739	-0,6352354
C	3,5408646	-2,2983208	1,8945030
H	2,0540945	-0,8717714	2,5086110
C	3,4737741	-2,9662015	-0,4368501
H	1,9531879	-2,0389764	-1,6354794
C	4,0582465	-3,0622211	0,8342048
H	4,0115561	-2,3778463	2,8747479
H	3,8599689	-3,5394853	-1,2780771
C	1,4892520	1,3747694	-0,0196310
C	2,2900493	1,5482888	-1,1554571
C	1,5548144	2,3430412	0,9950428
C	3,1206334	2,6609107	-1,2956590
H	2,2714624	0,7996943	-1,9499131
C	2,3805258	3,4546805	0,8764500
H	0,9527974	2,2023401	1,8956799
C	3,1679001	3,6233042	-0,2734384
H	3,7289057	2,7636642	-2,1928504
H	2,4339762	4,2085278	1,6623630
O	3,9442011	4,7469940	-0,3016580
O	5,1249186	-3,8591449	1,1437012
C	4,7728724	4,9606511	-1,4453482
H	4,1742605	5,0510938	-2,3672794
H	5,2976673	5,9041587	-1,2596047
H	5,5107040	4,1300053	-1,3671976
C	5,6834070	-4,6590546	0,1016324
H	6,5063676	-5,2164343	0,5622857
H	4,9427914	-5,3694897	-0,3033426
H	6,0782326	-4,0363807	-0,7189035
H	-1,7825245	-3,0557177	-3,0679746
O	-2,6103077	-1,3429165	-4,7449900
C	-3,0616701	-0,3007174	-5,6107390
H	-3,6676372	-0,7934516	-6,3789470
H	-3,6825184	0,4325832	-5,0691192
H	-2,2167016	0,2206767	-6,0910209
H	-0,9511090	2,2451819	2,9488349
O	-4,0875828	0,7386525	0,3464142
C	-3,7740146	-0,4812009	-0,3357116
H	-2,7294521	-0,4688612	-0,6762521
H	-4,4318714	-0,5771400	-1,2199378

TS-5

C	-2,5840170	-0,2954209	-3,5100698
C	-2,9310517	-0,6252452	-2,2494055
C	-2,4932420	0,0630700	-1,0202410
C	-3,5922477	0,4472962	-0,0127364
C	-5,0012825	0,6462396	-0,5530498
C	-5,2316539	-1,0864598	1,6034313
C	-3,7532337	-0,9774956	1,2668600
C	-3,1256018	-2,1284601	0,5479737
C	-1,9921439	-2,8768567	0,9389485
C	-0,9531666	-2,3478421	1,7449549
H	-1,9448212	0,5645522	-3,7198162
H	-2,9220300	-0,8824824	-4,3653276
H	-3,6062931	-1,4731513	-2,1121892
H	-1,9348412	0,9746385	-1,2971100
H	-3,2843927	1,3059465	0,5974895
H	-5,6113250	1,2586516	0,1399286
H	-4,9699030	1,1660125	-1,5235526
H	-5,5283388	-0,1698186	2,1375678
H	-5,4235694	-1,9247568	2,2957666
H	-3,1702034	-0,6427419	2,1329202
H	-3,7278924	-2,5556889	-0,2559170
H	-1,7877358	-3,7909350	0,3706400
H	-0,0396941	-2,9321222	1,8547026
H	-1,1638541	-1,6614958	2,5716585
Ni	-1,3567402	-1,1730438	0,0912504
P	0,5074229	-0,1263683	0,0641202
C	0,9157150	0,7144282	-1,5089905
C	1,5450989	1,9595563	-1,6073080
C	0,6031985	0,0234441	-2,6944423
C	1,8773603	2,5048501	-2,8508698
H	1,7755487	2,5291741	-0,7064014

C	0,9453976	0,5430672	-3,9353954
H	0,0536441	-0,9181750	-2,6338562
C	1,5890478	1,7882780	-4,0226205
H	2,3565117	3,4813799	-2,8925663
C	2,0265045	-1,1166382	0,3797901
C	2,3171173	-1,5344956	1,6938084
C	2,8786270	-1,5343716	-0,6475278
C	3,4179635	-2,3331581	1,9668276
H	1,6747877	-1,2157110	2,5158190
C	3,9874039	-2,3488651	-0,3898515
H	2,6902212	-1,2190815	-1,6743383
C	4,2619836	-2,7526302	0,9229637
H	3,6490089	-2,6490693	2,9845888
H	4,6262541	-2,6514745	-1,2177149
C	0,6125996	1,1653919	1,3571717
C	1,8260177	1,7251181	1,7807547
C	-0,5749457	1,6148123	1,9599759
C	1,8631055	2,7178427	2,7626300
H	2,7645642	1,3706218	1,3512980
C	-0,5566476	2,6009366	2,9372526
H	-1,5216442	1,1658924	1,6543251
C	0,6648847	3,1638988	3,3434708
H	2,8234459	3,1274330	3,0707846
H	-1,4756861	2,9490331	3,4092462
O	0,5815140	4,1234618	4,3105278
O	5,3161418	-3,5399312	1,2941577
C	1,7954214	4,7231356	4,7675639
H	2,3217955	5,2427659	3,9495917
H	1,4979600	5,4521386	5,5289793
H	2,4691917	3,9763792	5,2200920
C	6,1924279	-4,0065572	0,2677532
H	6,9460262	-4,6187195	0,7753136
H	5,6554747	-4,6249482	-0,4710252
H	6,6898911	-3,1698301	-0,2506886
H	0,6951928	0,0148563	-4,8554281
O	1,8770600	2,2190386	-5,2873189
C	2,5033099	3,4937700	-5,4329734
H	2,6330495	3,6399353	-6,5109600
H	1,8719660	4,3027067	-5,0284319
H	3,4895617	3,5189248	-4,9395853
O	-5,6499634	-0,6061491	-0,8170526
C	-6,1180127	-1,2767225	0,3561413
H	-7,1502560	-0,9473014	0,5903185
H	-6,1656733	-2,3400350	0,0766497

TS-6

C	-3,2058824	2,6379265	3,1539815
C	-2,2438165	2,5113766	2,2152791
C	-1,9313855	1,4591003	1,2447667
C	-2,7834263	0,3039709	0,8434077
C	-4,3046348	0,4258278	0,9485914
C	-3,3234709	-2,2814652	0,5941628
C	-2,6203073	-1,4459482	1,6595082
C	-1,3404168	-1,9438009	2,1827285
C	-0,7909924	-1,3877682	3,3834855
C	-1,3169708	-0,1897723	3,9006667
H	-3,9661637	1,8830539	3,3460161
H	-3,2355341	3,5213604	3,7920107
H	-1,5358091	3,3466579	2,1452632
H	-2,5600831	0,0321635	-0,1924590
H	-4,6637251	0,2936605	1,9878542
H	-4,6043738	1,4303272	0,6167531
H	-3,3213697	-1,2427311	2,4791475
H	-0,8525860	-2,7987593	1,7082735
H	0,1474966	-1,7972486	3,7643932
H	-0,7668868	0,3503654	4,6702240
H	-2,3793366	0,0509296	3,8452368
Ni	-0,8050572	-0,0710684	1,8381569
P	0,6764844	-0,0465865	0,2964958
C	-0,1270072	-0,1626017	-1,3447451
C	-0,4925964	0,9806520	-2,0656257
C	-0,6414705	-1,4046488	-1,7708952
C	-1,3520636	0,9040484	-3,1681184
H	-0,1079343	1,9562122	-1,7645839
C	-1,4860881	-1,4982317	-2,8656028
H	-0,3782103	-2,3100320	-1,2204881
C	-1,8581051	-0,3386506	-3,5694040
H	-1,6182856	1,8170893	-3,6977034
C	1,9470340	-1,3673931	0,2681047
C	2,4066639	-1,8447110	1,5091145
C	2,5138762	-1,8967516	-0,8974202
C	3,4024176	-2,8087567	1,5848471
H	1,9665985	-1,4383557	2,4219358
C	3,5103507	-2,8757073	-0,8399676
H	2,1679450	-1,5530491	-1,8738377
C	3,9614217	-3,3338295	0,4070935
H	3,7633881	-3,1792569	2,5447148
H	3,9238853	-3,2706182	-1,7664608
C	1,6677536	1,4936294	0,1792100
C	2,6082321	1,7102528	-0,8354711
C	1,4844142	2,4917447	1,1500990
C	3,3477283	2,8927587	-0,8964455
H	2,7700686	0,9467146	-1,5986380
C	2,2129976	3,6747071	1,1049950
H	0,7531250	2,3158573	1,9430879
C	3,1492048	3,8839206	0,0795702

UNIVERSITAT ROVIRA I VIRGILI
TRANSITION METAL CATALYZED CYCLOADDITION REACTIONS FOR THE FORMATION OF EIGHT- AND SIX-MEMBERED RINGS
Nuria Llorente González

H	4,0705852	3,0313174	-1,6986027
H	2,0757988	4,4541040	1,8551006
O	3,8143545	5,0774780	0,1175324
O	4,9275910	-4,2839295	0,5838294
C	4,7846305	5,3366932	-0,8976260
H	4,3279955	5,3441158	-1,9015782
H	5,1886826	6,3304999	-0,6755354
H	5,6023120	4,5966517	-0,8740851
C	5,5322661	-4,8480154	-0,5803982
H	6,2673243	-5,5722030	-0,2124615
H	4,7905338	-5,3681801	-1,2096536
H	6,0460898	-4,0791758	-1,1816312
H	-1,8920106	-2,4571744	-3,1880549
O	-2,7106466	-0,5334199	-4,6201023
C	-3,1564586	0,6175833	-5,3369841
H	-3,8395705	0,2426910	-6,1071084
H	-3,6968326	1,3183336	-4,6785026
H	-2,3164002	1,1453038	-5,8195576
H	-1,4001858	1,8800963	0,3823938
H	-2,8030134	-2,1994281	-0,3709541
H	-3,3077108	-3,3457621	0,8851870
O	-4,9615200	-0,4882969	0,0707073
C	-4,7868178	-1,8553027	0,4451164
H	-5,3134161	-2,0452817	1,4046751
H	-5,2883771	-2,4400437	-0,3390207

E,Z-**6h**-π,π-*cis*

C	-4,0027740	-0,5465556	-3,5656868
C	-2,4587158	-0,6133502	-3,6190647
C	-2,6631775	-1,9405767	-1,4485293
C	-1,9052738	-1,8075327	-2,7800736
C	-0,4305170	-1,6029305	-2,4606130
C	0,4901950	-1,0018672	-3,4007327
C	1,7442153	-0,5177114	-3,0505724
H	-4,4159231	-1,3412520	-4,2078103
H	-4,3514357	0,4171169	-3,9686924
H	-2,3697320	-1,0905842	-0,8017436
H	-2,3736425	-2,8662105	-0,9303955
H	-2,0861497	-2,7461633	-3,3407605
H	-0,0198808	-2,3061891	-1,7282574
H	0,1350147	-0,7703881	-4,4102919
H	2,3359973	0,0359884	-3,7780118
H	2,2650469	-0,8423306	-2,1503095
O	-4,0819208	-1,9812335	-1,5966505
Ni	-0,1620553	0,3342308	-1,9538585
C	-1,7179014	0,6765859	-3,2768975
H	-1,2344120	1,1518266	-4,1390792
C	-1,7546588	1,4742847	-2,1086658
H	-2,4864440	1,3306342	-1,3105733
C	-0,6275605	2,3513111	-1,9370746
H	-0,1815995	2,8232227	-2,8179148
H	-0,5434124	2,9230905	-1,0117282
C	-4,5547944	-0,7555856	-2,1586558
H	-5,6517678	-0,8276296	-2,1733874
H	-4,2796367	0,0914278	-1,4968161
P	0,4351321	0,1473333	0,1469885
C	-0,6116585	1,1705668	1,2552701
C	-0,1032528	2,2417373	1,9988034
C	-2,0036689	0,9490942	1,2899034
C	-0,9393519	3,0657865	2,7600280
H	0,9667991	2,4499824	1,9871665
C	-2,8453475	1,7484868	2,0502246
H	-2,4348699	0,1292477	0,7133757
C	-2,3183453	2,8194881	2,7918249
H	-0,5021556	3,8902070	3,3205709
H	-3,9202596	1,5687815	2,0794213
C	2,1312530	0,7381291	0,5196850
C	2,7523560	1,6025228	-0,3875103
C	2,8169168	0,3943574	1,6997593
C	4,0230385	2,1274527	-0,1373935
H	2,2248365	1,8513837	-1,3119000
C	4,0819601	0,9031701	1,9602589
H	2,3518886	-0,2830188	2,4178254
C	4,6939901	1,7767774	1,0431146
H	4,4777967	2,7954801	-0,8670010
H	4,6237732	0,6389250	2,8690854
C	0,4360622	-1,5127162	0,9327990
C	1,3317029	-2,4687466	0,4297168
C	-0,4479838	-1,9125242	1,9489715
C	1,3530475	-3,7794762	0,9086933
H	2,0406724	-2,1875630	-0,3509763
C	-0,4458353	-3,2173398	2,4312032
H	-1,1450074	-1,1948574	2,3811125
C	0,4512287	-4,1635328	1,9131703
H	2,0676217	-4,4866837	0,4913506
H	-1,1323073	-3,5256317	3,2203739
O	5,9383750	2,2202648	1,3925143
O	0,3716474	-5,4183485	2,4508288
O	-3,2274475	3,5542069	3,4999566
C	1,2653909	-6,4142554	1,9529783
H	1,0315694	-7,3287565	2,5090638
H	1,1121069	-6,5929312	0,8752833
H	2,3185638	-6,1382875	2,1308033
C	-2,7412036	4,6594846	4,2624761
H	-2,2580066	5,4130245	3,6180832
H	-3,6221261	5,1015933	4,7405431

H	-2,0289313	4,3330208	5,0387915
C	6,6089608	3,1037040	0,4921728
H	6,0431570	4,0392730	0,3474988
H	7,5727085	3,3308538	0,9609291
H	6,7816951	2,6271245	-0,4872882
H	-2,1935758	-0,8184195	-4,6677040

E,Z-**6h**-π,π-trans

C	-3,8227377	1,8959365	-2,2695899
C	-2,5921868	1,0269804	-1,9862663
C	-4,1504817	-0,8821986	-1,4639817
C	-2,9245816	-0,4576736	-2,2670264
C	-1,6610146	-1,3025527	-2,0783755
C	-0,8303561	-1,5874614	-3,2183781
C	0,4906881	-2,0440469	-3,0534786
H	-4,0708743	1,8719072	-3,3437801
H	-3,6370999	2,9455839	-1,9899551
H	-2,3478080	1,1178010	-0,9166737
H	-3,9204160	-0,8539788	-0,3813814
H	-4,4682867	-1,9021334	-1,7253004
H	-3,2123451	-0,5227192	-3,3348271
H	-1,6200613	-1,9727713	-1,2129180
H	-1,1651904	-1,2526981	-4,2059073
H	1,1443659	-2,1146081	-3,9225130
H	0,7397830	-2,6938985	-2,2144914
O	-5,2711058	-0,0328453	-1,7500257
Ni	0,0379767	-0,1444922	-2,1365190
C	-1,3343478	1,2892338	-2,7813476
H	-1,4196889	1,1018970	-3,8595855
C	-0,1252805	1,8476619	-2,3225373
H	-0,0804319	2,3748122	-1,3659639
C	1,0652146	1,4775947	-3,0200487
H	1,0204942	1,2921683	-4,0966213
H	2,0251140	1,8292874	-2,6455173
C	-5,0015550	1,3430082	-1,4572996
H	-5,9335548	1,8790139	-1,6854785
H	-4,7888621	1,4620569	-0,3743031
P	0,6439437	-0,2291559	0,0192677
C	-0,6864369	0,5372597	1,0206063
C	-0,7315462	1,9245860	1,2243389
C	-1,8321254	-0,2081594	1,3666251
C	-1,8712142	2,5581229	1,7306793
H	0,1356491	2,5375371	0,9740281
C	-2,9635018	0,4029185	1,8885808
H	-1,8485839	-1,2856905	1,1990592
C	-3,0000441	1,7964378	2,0602574
H	-1,8632426	3,6387761	1,8611349
H	-3,8485145	-0,1778422	2,1497621
C	2,1623308	0,6809305	0,5150967
C	3,2042479	0,7523676	-0,4152106
C	2,3892449	1,1799510	1,8115666
C	4,4399719	1,3184592	-0,0865846
H	3,0406594	0,3426593	-1,4141254
C	3,6054982	1,7554479	2,1513514
H	1,6035348	1,1100991	2,5658168
C	4,6413303	1,8309117	1,2023935
H	5,2275415	1,3549155	-0,8372961
H	3,7871592	2,1469644	3,1528803
C	0,9934433	-1,8228285	0,8729222
C	1,8162605	-2,7342250	0,1984746
C	0,6066630	-2,1339436	2,1897480
C	2,2285205	-3,9306326	0,7899964
H	2,1674936	-2,4881939	-0,8048706
C	0,9978152	-3,3247223	2,7892346
H	0,0008708	-1,4314998	2,7628504
C	1,8072610	-4,2368372	2,0921242
H	2,8710738	-4,6082417	0,2303892
H	0,6958559	-3,5690804	3,8082303
O	5,7981836	2,4144767	1,6376716
O	2,1317346	-5,3791809	2,7687637
O	-4,1755264	2,3038412	2,5404908
C	2,9640022	-6,3324617	2,1067376
H	3,0938507	-7,1571467	2,8159952
H	2,4898651	-6,7126245	1,1864883
H	3,9501840	-5,9048759	1,8591396
C	-4,2758908	3,7205350	2,6892681
H	-4,1338999	4,2378373	1,7254915
H	-5,2899513	3,9102756	3,0574783
H	-3,5439634	4,1032243	3,4204405
C	6,8863993	2,5045423	0,7172812
H	6,6202565	3,1107735	-0,1650006
H	7,6986573	2,9962172	1,2637506
H	7,2195691	1,5064101	0,3867674

- Structures from Figure 1.6

TS-5'$_{cis}$ yielding compound *E,E*-**6h**-π,π-*cis*

C	-2,7873459	-0,2912903	-0,8497501
C	-3,3673336	0,0733747	0,3929658
C	-4,9525744	0,6687431	0,1891939
C	-5,3321375	-1,8084315	1,3768377
C	-3,8271785	-1,6005938	1,3664361
C	-3,0767056	-2,6167716	0,5711617
C	-1,8662766	-3,2656377	0,9071787
C	-0,8667645	-2,6711641	1,7145690
H	-3,0120304	0,6695047	1,1250951
H	-5,3112528	1,0551273	1,1566609
H	-4,8948413	1,5384362	-0,4894069
H	-5,8182781	-1,1142369	2,0890371
H	-5,5896777	-2,8346524	1,6889615
H	-3,4112111	-1,4172375	2,3650923
H	-3,6548434	-3,0736052	-0,2340858
H	-1,5875201	-4,1330449	0,2990214
H	0,0946728	-3,1769772	1,7975960
H	-1,1246214	-2,0264175	2,5614442
O	-5,8719225	-1,6677452	0,0600565
Ni	-1,4091044	-1,4817620	0,1131127
C	-5,9913980	-0,3094589	-0,3928096
H	-7,0077044	0,0621210	-0,1561428
H	-5,8940134	-0,3611342	-1,4852592
P	0,4289599	-0,4014269	-0,0295668
C	0,6142881	0,6686985	-1,5048260
C	1,2569049	1,9108821	-1,5170053
C	0,0963691	0,1690789	-2,7150620
C	1,4055297	2,6366397	-2,7030680
H	1,6421405	2,3381742	-0,5905658
C	0,2330100	0,8694179	-3,9031405
H	-0,4642537	-0,7683762	-2,7087219
C	0,9142156	2,1089124	-3,9066345
H	1,9018924	3,6051300	-2,6751268
C	1,9354791	-1,4353472	-0,1271650
C	2,4624911	-2,0308394	1,0460499
C	2,5413659	-1,7767268	-1,3464767
C	3,5520185	-2,8885594	0,9995221
H	2,0204716	-1,7868496	2,0129590
C	3,6342933	-2,6477514	-1,4110585
H	2,1682797	-1,3393748	-2,2730392
C	4,1452431	-3,2098789	-0,2340472
H	3,9661694	-3,3260517	1,9083901
H	4,0764247	-2,8714293	-2,3803202
C	0,7913701	0,6759641	1,4042875
C	2,0727084	1,1683335	1,6874981
C	-0,2605613	1,0208424	2,2699790
C	2,3048182	1,9958293	2,7884673
H	2,9129762	0,8883537	1,0499845
C	-0,0489025	1,8435523	3,3683308
H	-1,2557827	0,6179947	2,0735135
C	1,2377972	2,3414846	3,6337080
H	3,3140325	2,3557022	2,9812277
H	-0,8622729	2,1095412	4,0437680
O	1,3481121	3,1382883	4,7363538
O	5,2084796	-4,0669038	-0,1750549
C	2,6381437	3,6613021	5,0594198
H	3,0274247	4,3027125	4,2511555
H	2,4963863	4,2628409	5,9638067
H	3,3604357	2,8542653	5,2665647
C	5,8412939	-4,4275640	-1,4036094
H	6,6502571	-5,1142504	-1,1314594
H	5,1403083	-4,9399961	-2,0837741
H	6,2656093	-3,5462938	-1,9135848
H	-0,1526315	0,4868429	-4,8398896
O	1,0135321	2,7237841	-5,1230400
C	1,6525371	3,9996033	-5,1775540
H	1,6176780	4,3047792	-6,2291482
H	1,1199348	4,7447521	-4,5630953
H	2,7037770	3,9399291	-4,8491245
C	-2,4818876	0,8906710	-1,6789177
C	-2,2856883	2,1596580	-1,2694593
H	-2,2995215	2,4410112	-0,2142494
H	-2,4238025	0,7088483	-2,7560087
H	-2,0582083	2,9515453	-1,9831475
H	-3,3572599	-1,0071726	-1,4591857

TS-6'$_{trans}$ yielding compound *E,E*-**6h**-π,π-*trans*

C	-1,9870405	1,2446432	2,0992727
C	-2,9878024	0,4061112	1,3851006
C	-4,4149352	0,5478269	1,9173983
C	-3,8595016	-1,9237404	0,3331852
C	-2,9246933	-1,5285348	1,4745802
C	-1,6491284	-2,2603668	1,4901535
C	-0,8275022	-2,2315016	2,6594802
C	-1,1073561	-1,3065726	3,6874200
H	-2,9730233	0,5761407	0,3041889
H	-4,4245669	0,3929000	3,0083379

H	-4,7008793	1,5980557	1,7473271
H	-4,3268158	-2,8972352	0,5937340
H	-3,2907793	-2,0624934	-0,5981618
H	-3,4248532	-1,6042914	2,4485111
H	-1,3663126	-2,8902685	0,6429139
H	0,1140448	-2,7849330	2,6405247
H	-0,3648127	-1,1430565	4,4676302
H	-2,1337286	-1,0618867	3,9714821
O	-4,8770135	-0,9704926	0,0309006
Ni	-0,9630856	-0,4230007	1,7468586
C	-5,4242548	-0,4034360	1,2234619
H	-5,7516340	-1,2107990	1,9077885
H	-6,3232641	0,1416927	0,9069029
P	0,4318611	-0,0465963	0,1705569
C	-0,2543909	0,6998548	-1,3557246
C	0,2283280	1,8615750	-1,9648851
C	-1,4301448	0,1224323	-1,8732379
C	-0,4273896	2,4351379	-3,0601116
H	1,1167481	2,3534857	-1,5690704
C	-2,0902355	0,6715593	-2,9623703
H	-1,8402134	-0,7656460	-1,3900926
C	-1,5918314	1,8405499	-3,5646389
H	-0,0284500	3,3489067	-3,4969945
C	1,2744510	-1,5618366	-0,4426417
C	2,0386182	-2,2937586	0,4884934
C	1,1663560	-2,0612207	-1,7434593
C	2,6730244	-3,4738693	0,1296098
H	2,1436267	-1,9140535	1,5069746
C	1,7918909	-3,2571378	-2,1191601
H	0,5909776	-1,5130050	-2,4904629
C	2,5498913	-3,9691043	-1,1810606
H	3,2731157	-4,0361034	0,8458593
H	1,6839023	-3,6133996	-3,1422640
C	1,8703386	1,0015105	0,6114706
C	2,9995061	1,1156291	-0,2107358
C	1,8675009	1,6740259	1,8445156
C	4,0935220	1,8986023	0,1650870
H	3,0349101	0,5742761	-1,1581536
C	2,9472690	2,4569556	2,2340557
H	1,0032609	1,5482215	2,5001042
C	4,0662697	2,5790284	1,3937623
H	4,9572440	1,9628947	-0,4942750
H	2,9543147	2,9791255	3,1912653
O	5,0776240	3,3692534	1,8649622
O	3,2072729	-5,1423934	-1,4346591
C	6,2417423	3,5217233	1,0526340
H	5,9987792	3,9818332	0,0799009
H	6,9095530	4,1865075	1,6115897
H	6,7464279	2,5556897	0,8830904
C	3,1153782	-5,6838185	-2,7519487
H	3,7042458	-6,6074970	-2,7366736
H	2,0717264	-5,9203990	-3,0207006
H	3,5368113	-4,9944739	-3,5032987
H	-3,0066539	0,2284611	-3,3520849
O	-2,3179323	2,3172361	-4,6209806
C	-1,8713988	3,5209296	-5,2449535
H	-2,5883225	3,7238896	-6,0480598
H	-1,8675579	4,3657986	-4,5358884
H	-0,8629637	3,4030430	-5,6766364
C	-1,4995294	2,4953680	1,5124634
C	-1,7836431	3,0285123	0,3080055
H	-2,4499008	2,5457328	-0,4084767
H	-0,8211782	3,0570269	2,1633844
H	-1,3163160	3,9585484	-0,0139720
H	-2,1654713	1,3375631	3,1789282

UNIVERSITAT ROVIRA I VIRGILI
TRANSITION METAL-CATALYZED CYCLOADDITION REACTIONS FOR THE FORMATION OF EIGHT- AND SIX-MEMBERED RINGS
Nuria Llorente González

CHAPTER 2

Enantioselective Ni-Catalyzed Intramolecular [4+4] Cycloadditions of Bisdienes

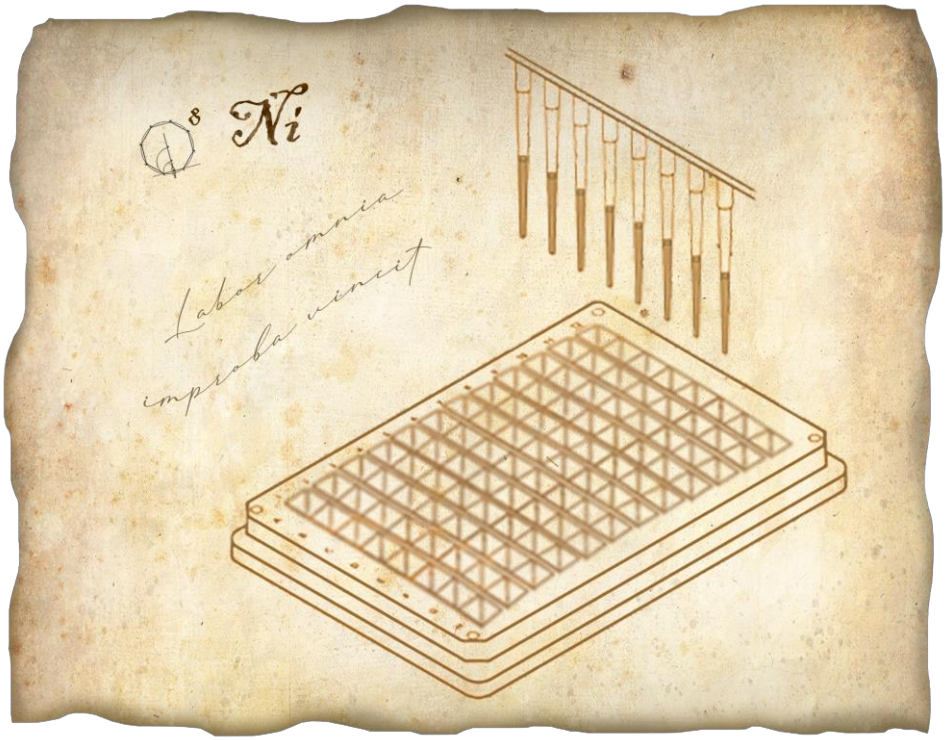

UNIVERSITAT ROVIRA I VIRGILI
TRANSITION METAL-CATALYZED CYCLOADDITION REACTIONS FOR THE FORMATION OF EIGHT- AND SIX-MEMBERED RINGS
Nuria Llorente González

Enantioselective Ni-Catalyzed Intramolecular [4+4] Cycloadditions of Bisdienes

2.1 Introduction

Although Nature frequently exhibits a high degree of symmetry in terms of general morphology at the molecular level, Nature is highly asymmetric. Enzymes, proteins, polysaccharides, nucleic acids, and many other basic components of plants and animals are chiral[1] and occur in enantiopure form. The demand for high optical purity in the pharmaceutical industry increased after the Thalidomide case.[2] Before then, drugs were usually prepared, tested and applied as racemic mixtures. Due to the observation of negative effects of one of the enantiomers of this drug ((*S*)-thalidomide had teratogenic properties), stricter regulations were introduced and, consequently, chiral drugs are now marketed and applied as single enantiomers in many cases, with strict requirements for high chemical and optical purity in active pharmaceutical ingredients.[3]

Following the results obtained for the achiral nickel-catalyzed [4+4] cycloaddition reactions (see Chapter 1), an approach towards an enantioselective cycloaddition process was envisioned. The computational studies previously discussed[4] showed that the stereochemical outcome of the reaction depends on the geometry of the C−C double bonds in the diene units of the substrates (Figure 2.1). This is due to the different coordination ability of the alkene units in the *E,Z*- or *E,E*-bisdiene substrates. In the case of the *E,E*-bisdiene substrate (Figure 2.1, left), the four C=C units are coordinated to the metal center in the oxidative cyclization of the two internal C=C bonds leading to the corresponding bis-allyl Ni(II) complexes. The Ni(0) center is thus coordinately saturated and there is no vacancy available to accommodate a ligand molecule capable of stereoselectively biasing the cyclization step. As regards the [4+4] cycloaddition of the *E,Z*-

(1) Chirality is the geometric property of a rigid object (or spatial arrangement of points or atoms) of being non-superposable on its mirror image; such an object has no rotation-reflection axes (S_{2n}; for instance, a mirror plane ($\sigma = S_1$) or a center of inversion ($i = S_2$). A superposable object on its mirror image is referred to as achiral (from Moss, G. P. *Pure Appl. Chem.* **1996**, *68*, 2193-2222.)
(2) (a) Kim, J. H.; Scialli, A. R. *Toxicol. Sci.* **2011**, *122*, 1-6. (b) Kim, J. H.; Scialli, A. R. *Toxicol. Sci.* **2012**, *125*, 613.
(3) Blaser, H.-U. *Rendiconti Lincei* **2013**, *24*, 213-216.
(4) For more information see section 1.2.2 in Chapter 1.

bisdiene substrates, computational studies could not locate any transition state with the four C=C bonds coordinated to the nickel center. In this case, the *Z*-configuration of the internal double bond hinders the coordination of the terminal one to the nickel center and allows for the coordination of one molecule of phosphine ligand (Figure 2.1, right). This observation paves the way to the design of enantioselective [4+4] cycloaddition processes: The use of an enantiopure phosphine ligand in the [4+4] cycloaddition reaction of *E*,*Z*-bisdiene substrates should in principle allow for biasing the reaction towards one of the two possible enantiomers of the bis-allyl Ni(II) complexes.

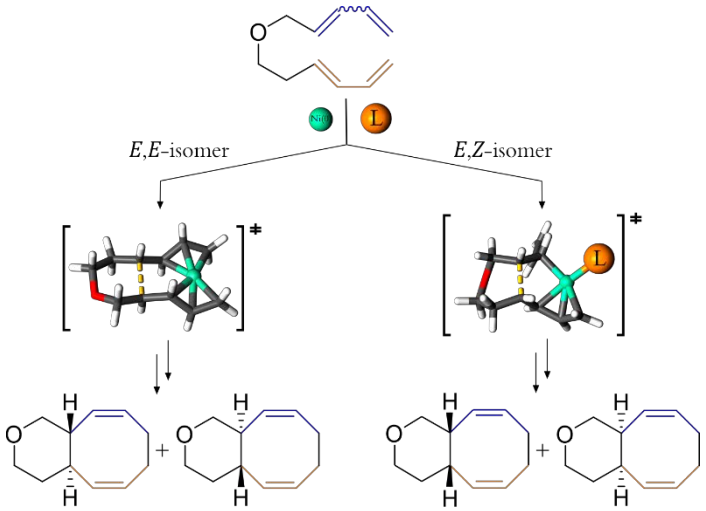

Figure 2.1. Transition states and possible stereoisomers resulting from the [4+4] cycloaddition of bisdiene substrates.

Thus, it was decided to explore this approach from *E*,*Z*-bisdiene substrates employing enantiopure P-based monodentate ligands. It should be noted that, to the best of our knowledge, no enantioselective catalytic intramolecular [4+4] cycloaddition methods have been reported up to now.[5] The results obtained in this study have been summarized in the following discussion.

(5) To the best of our knowledge, only two catalytic methods have been published for enantioselective intermolecular [4+4] cycloadditions and both are based on iron catalysts. These are as follows: (a) Baldenius, K. U.; tom Dieck, H.; König, W. A.; Icheln, D.; Runge, T. *Angew. Chem., Int. Ed. Engl.* **1992**, *31*, 305-307. (b) Braconi, E.; Götzinger, A. C.; Cramer, N. *J. Am. Chem. Soc.* **2020**, *142*, 19819-19824.

2.2 Results and Discussion

2.2.1. Retrosynthetic Pathway of Bisdiene 1

Our studies began with the synthesis of *E,Z*-bisdiene **1** as a model substrate to prove our hypothesis for developing enantioselective catalytic tools for intramolecular [4+4] cycloaddition reactions. With the know-how gained during the preparation of *E,Z*-configured bisdiene substrates,[6] several retrosynthetic pathways were considered, with the *a priori* optimal one being shown in Scheme 2.1.

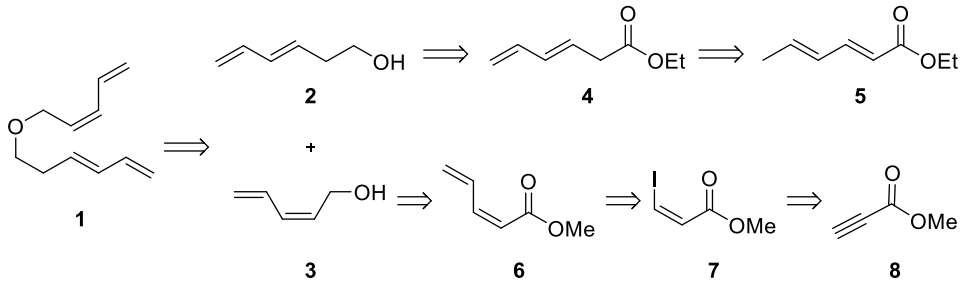

Scheme 2.1. Retrosynthetic pathway towards *E,Z*-configured bisdiene **1**.

The synthesis of compound **2** had been previously performed and optimized by the group (Scheme 2.2) for the synthesis of *E,E*-configured bisdiene substrates.[6]

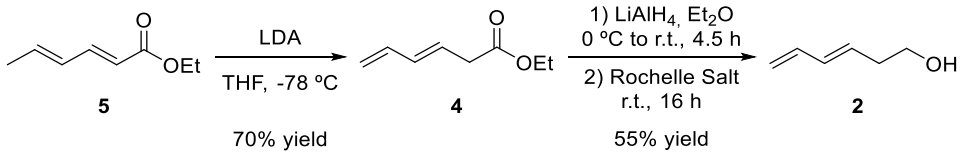

Scheme 2.2. Synthesis of alcohol **2**.

The selective synthesis of the *Z*-dienol **3** was achieved *via* a Stille coupling between *Z*-iodoacrylate **7** and commercially available tributyl(vinyl)stannane (Scheme 2.3).[7] Iodoacrylate substrate **7** was first commercially purchased but, due to stability issues, it was synthesized from methyl propiolate[8] before use (Scheme 2.3). Even though this synthetic path suffers from the low yields obtained in the

(6) For more information, see section 1.4.3 in Chapter 1.
(7) Method adapted from the synthesis of the *E*-configured compound, which is reported in: Lamande-Langle, S.; Abarbri, M.; Thibonnet, J.; Duchene, A. *J. Organomet. Chem.* **2009**, *694*, 2368-2374.
(8) Larsson, R.; Sterner, O.; Johansson, M. *Org Lett* **2009**, *11*, 657-660.

Stille coupling, it has proven to be the most selective towards the desired product, as the *Z*-configured product **6** was isolated without any trace of the undesired *E*-isomer. The reduction of methyl ester **6** to alcohol **3** was performed following the methodology previously optimized by the group for the equivalent *E*-dienol.[6]

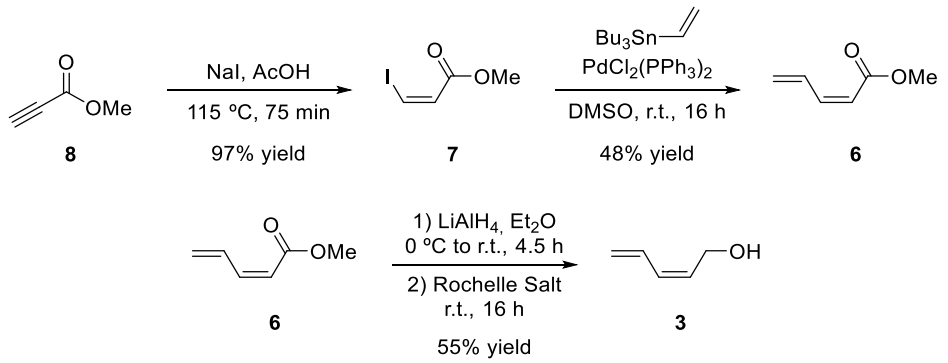

8 **7** **6** **6** **3**

Scheme 2.3. Synthesis of *Z*-alcohol **3** *via* Stille coupling and reduction of the ester.

The tosyl derivative **9** was then synthesized from the *Z*-dienol **3**.[9] However, the product was not stable and needed to be used in the following steps immediately after its preparation. After optimization of the reaction conditions, bisdiene **1** was obtained by warming up to 40 °C the reaction mixture between the *in situ* formed alcoholate of compound **2** and tosyl derivative **9** (Scheme 4).[10]

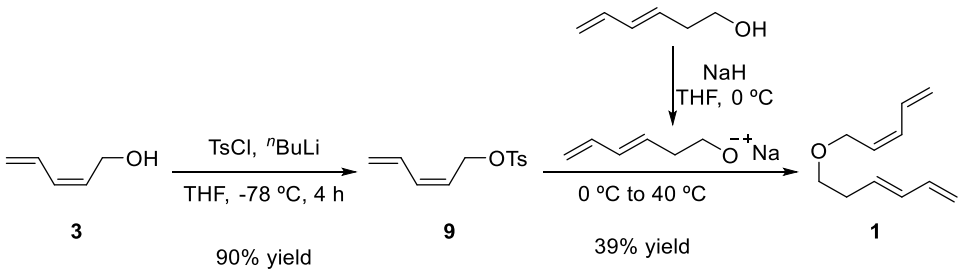

3 **9** **1**

90% yield 39% yield

Scheme 2.4. Synthesis of bisdiene **1**.

(9) In the literature, the tosyl derivative of the *E*-configured analogue was synthesized *in situ* and not isolated. For more information, see: Groves, A.; Martínez, J. I.; Smith, J. J.; Lam, H. W. *Chem.-Eur. J.* **2018**, *24*, 13432-13436.

(10) Synthetic methodology adapted from: Okamoto, R.; Tanaka, K. *Org. Lett.* **2013**, *15*, 2112-2115.

2.2.2. Enantioselective Intramolecular [4+4] Cycloadditions

Once the desired model substrate was obtained, an initial ligand screening was performed. Considering that monodentate phosphines and phosphoramidites were the best performing ligands for the non-enantioselective version of this transformation,[11] these were the first ligands tested (Table 2.1). Moreover, the optimal reaction conditions for non-enantioselective intramolecular [4+4] cycloadditions described in Chapter 1 were also maintained.

In all cases, conversion of the starting material was complete. In terms of selectivity, all ligands yielded the [4+4] intramolecular cycloaddition product **10** as a major product (Table 2.1). However, the yields were moderate for the MonoPhos-derived phosphoramidite ligands **L1**-**L6** and monodentate phosphines (*S*)-NMDP and (*R*)-MOP (see Table 1 for the structures of the ligands). These results corroborated, before further experiments for developing more efficient catalysts were made, that monodentate P-based ligands were active in this transformation. In terms of enantioselective induction, however, only ligand **L5** provided some level of enantioinduction, though it was low.

(11) For more information, see section 1.2.1 in Chapter 1.

UNIVERSITAT ROVIRA I VIRGILI
TRANSITION-METAL-CATALYZED CYCLOADDITION REACTIONS FOR THE FORMATION OF EIGHT- AND SIX-MEMBERED RINGS
Nuria Llorente González

Table 2.1: Initial screening of P-based ligands for the enantioselective [4+4] cycloaddition of compound **1**.

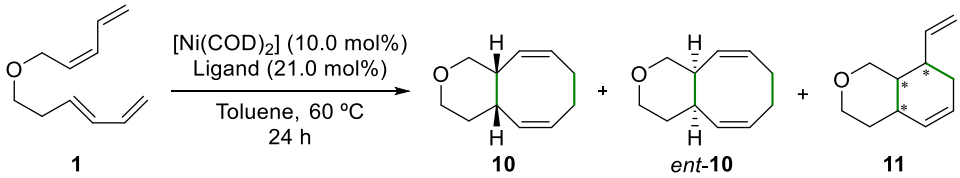

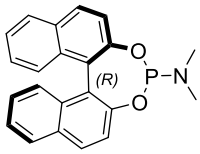

L1
(*R*)-MONOPHOS

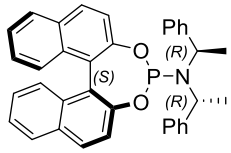

L2

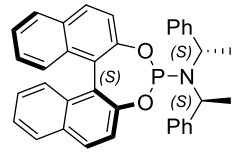

L3

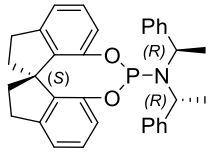

L4
(*S*)-SIPHOS-PE

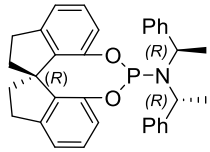

L5
(*R*)-SIPHOS-PE

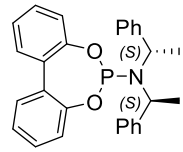

L6

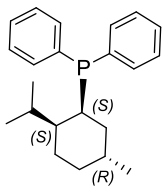

L7
(*S*)-NMDPP

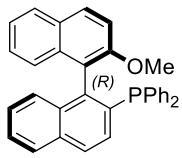

L8
(*R*)-MOP

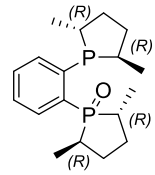

L9
(*R*,*R*)-Me-BozPhos

Entry	Ligand	Conv.[a] (%)	% yield[a,b] (10+*ent*-10)	% ee[c] (10/*ent*-10)	% yield of 11[a]
1	L1	>99	37	*rac*	n.d.[d]
2	L2	>99	34 (45)	*rac*	n.d.[d]
3	L3	>99	33	*rac*	n.d.[d]
4	L4	>99	35	*rac*	n.d.[d]
5	L5	>99	32 (39)	13	n.d.[d]
6	L6	>99	39 (46)	*rac*	n.d.[d]
7	L7	>99	24	*rac*	n.d.[d]
8	L8	>99	25	*rac*	n.d.[d]
9	L9	>99	5	-	n.d.[d]

(a) Calculated by ^{1}H NMR spectroscopy with 1,3,5-trimethoxybenzene as internal standard. (b) In brackets, isolated yield after column chromatography on SiO_2 impregnated with $AgNO_3$ (10%). (c) Determined by GC-MS on a chiral stationary phase (β-DexTM 120). (d) Not detected.

In order to assess the catalytic performance of nitrogen-based ligands and *N*-heterocyclic carbene ligands in this transformation, achiral carbene ligand (**L10**) and N-containing ligands **L11-13** were tested (Table 2.2). Surprisingly, **L10** led to full conversion of the starting material, but no traces of the desired [4+4] cycloadduct **10** were detected. Instead, several diastereoisomers of the undesired [4+2] cycloaddition product **11** were detected as major products. On the other hand, nitrogen-based ligands **L11-L13** did not mediate the formation of the desired [4+4] cycloaddition product or the [4+2] cycloaddition byproduct, with important amounts of the starting material being recovered.

Table 2.2: Initial screening of enantiopure nitrogen-based and *N*-heterocyclic carbene ligands for the enantioselective [4+4] cycloaddition of compound **1**.

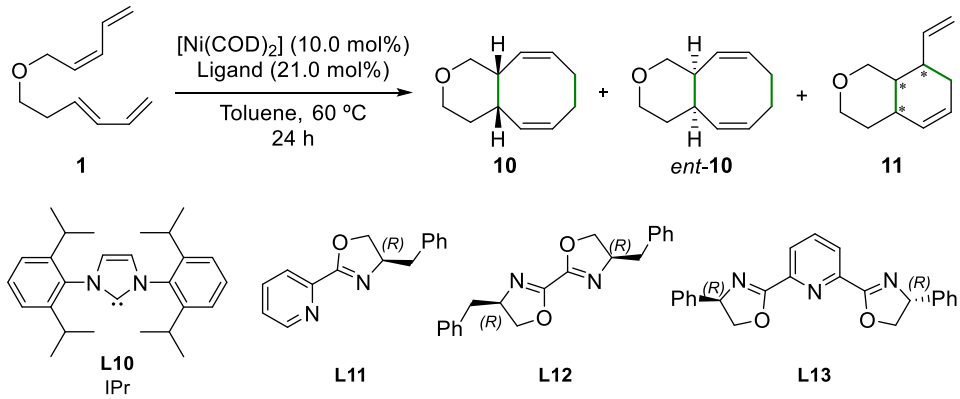

Entry	Ligand	Conv.[a] (%)	% yield[a] (10+*ent*-10)	% ee[b] (10/*ent*-10)	% yield of 11[a]
1	L10	>99	<1	-	83[c]
2	L11	51	<1	-	n.d.[d]
3	L12	14	<1	-	n.d.[d]
4	L13	22	<1	-	n.d.[d]

(a) Calculated by ^{1}H NMR spectroscopy with 1,3,5-trimethoxybenzene as internal standard. (b) Determined by GC-MS on a chiral stationary phase (β-DexTM 120). (c) Total yield of the mixture of diastereoisomers. (d) Not detected

Based on the results that have been summarized in this section, further studies aimed at discovering more efficient Ni-based catalytic systems by means of high throughput experimentation (HTE) techniques.

UNIVERSITAT ROVIRA I VIRGILI
TRANSITION METAL-CATALYZED CYCLOADDITION REACTIONS FOR THE FORMATION OF EIGHT- AND SIX-MEMBERED RINGS
Nuria Llorente González

2.2.3. HTE Screening for Intramolecular Enantioselective [4+4] Cycloadditions

Traditional drug development was based on the random screening of collections of chemically synthesized compounds or extracts, derived from natural sources or by modifications of chemicals with known physiological activities. This approach provided many important drugs, but in the mid-eighties the ratio of new to previously discovered compounds was starting to stagnate.[12] The main problem arose from the fact that the success rate depended directly on the number of samples tested. While the pharmaceutical industry was demanding more cost-effective and faster approaches in the drug discovery process, this scenario became more complicated: new methodologies in molecular biology, biochemistry, and genetics led to the identification and production of an ever-increasing number of enzymes, proteins, and receptors, thus increasing the number of good drug candidates available. In other words, the number of new molecules involved in biological processes was becoming vast for the so called "rational drug design".[13] Combinatorial chemistry technologies were then introduced based on the premise that the probability of finding a target molecule in a random screening process is proportional to the number of molecules subjected to said process.[14] In this new concept, the scientific reasoning was often replaced by the magic of large numbers: loads of hypothetical targets were exposed to large numbers of compounds representing variations on the chemical and/or biological conditions. In these high throughput screenings (HTS), the positive results obtained (also referred to as hits) facilitated the discovery and development of new biologically active targets, which, in turn, enlarged the libraries of compounds available for future HTS analyses.

These biological methodologies evolved into chemical high-throughput experimentation (HTE) platforms,[15] which were conceived as valuable tools to accelerate the discovery and implementation of efficient synthetic methodologies. In plain words, HTE is a system designed for running a large number of reactions

(12) (a) Drews, J. *Science* **2000**, *287*, 1960-1963. (b) Schreiber, S. L. *Science* **2000**, *287*, 1964-1969.
(13) Baxendale, I. R.; Hayward, J. J.; Ley, S. V.; Tranmer, G. K. *ChemMedChem* **2007**, *2*, 768-788.
(14) (a) *Combinatorial Chemistry: Synthesis, Analysis, Screening*, First ed.; Jung, G., Ed.; Wiley-VCH Verlag: Weinheim, 1999. (b) *Combinatorial Chemistry and Technologies: Methods and Applications*, Second ed.; Fassina, G.; Miertus, S., Eds.; CRC Press: Boca Raton, 2005.
(15) For a comprehensive view on HTE, see: (a) Shultz, C. S.; Krska, S. W. *Acc. Chem. Res.* **2007**, *40*, 1320-1326. (b) Schmink, J. R.; Bellomo, A.; Berritt, S. *Aldrichimica Acta* **2013**, *46*, 71-80. (c) Krska, S. W.; DiRocco, D. A.; Dreher, S. D.; Shevlin, M. *Acc. Chem. Res.* **2017**, *50*, 2976-2985. (d) Shevlin, M. *ACS Med. Chem. Lett.* **2017**, *8*, 601-607.

in parallel at the micromolar scale. These sets of reactions were rationally designed to answer specific chemical challenges or to achieve specific process chemistry goals.

HTE studies are challenging for several reasons. First, exploration of n variables creates an n-dimensional reaction space to be surveyed, requiring a thorough experimental work. Second, it requires a fast and reliable method for compiling and processing the experimental data obtained to avoid a bottleneck with the analytics. Third, the analysis and interpretation of n-dimensional data are nontrivial, and it is critical that results are presented in a clear way, so that scientists can use the information to solve specific problems. Finally, the variability in any experimental process is unavoidable. This means that multiple runs must be carried out for conclusions from the data to be made with confidence, and all studies must end with a scale-up in order to demonstrate their reproducibility at the laboratory scale. However, the advantages exceed those inconveniences, as the parallelization of experiments saves time and resources. In our case, 24 or 96 well plates were available at the ICIQ's HTE unit[16] (see Figure 2.2) with 100 µL vessels. The miniaturization implies a key factor: a broader screening can be achieved employing a small amount of substrate. Additionally, the extensive library of enantiopure ligands at our disposal at the ICIQ's HTE unit provided a unique opportunity to be explored in our transformation of interest.

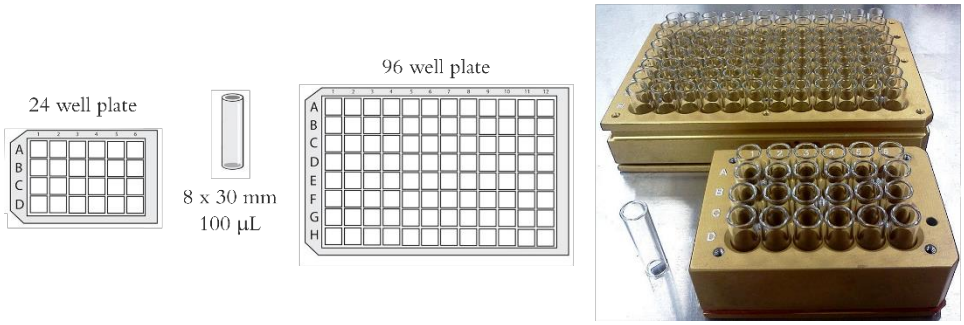

Figure 2.2. Typical 24 and 96 HTE well plates and 0.1 mL reaction vessels.

The process for adapting a reaction to the HTE system has a clear workflow that should be followed (see Figure 2.3). First of all, an analytical method that allows all the samples to be analyzed in a fast and reliable manner needs to be designed. In our case, the quantification of crude reaction mixtures had always

(16) CELLEX-ICIQ HTE Laboratory. http://www.iciq.org/research/research-support-area/cellex-iciq-hte-laboratory/

UNIVERSITAT ROVIRA I VIRGILI
TRANSITION METAL-CATALYZED CYCLOADDITION REACTIONS FOR THE FORMATION OF EIGHT- AND SIX-MEMBERED RINGS
Nuria Llorente González

been performed by ^{1}H NMR spectroscopy with 1,3,5-trimethoxybenzene as internal standard and the enantiomeric excesses were determined with a time-consuming GC method (see Table 2.1). These two techniques were not valid for an HTE screening, since they took long times and would lead to a bottleneck in the analytics. In order to have a fast and reliable analytical method, GC-MS and supercritical fluid chromatography (SFC) were chosen. We envisaged to use GC-MS for the quantification of the conversion and the yield with an internal standard (4,4′-dimethylbiphenyl), and samples with significant amounts of the target product would then be subjected to the determination of the ee with chiral SFC.

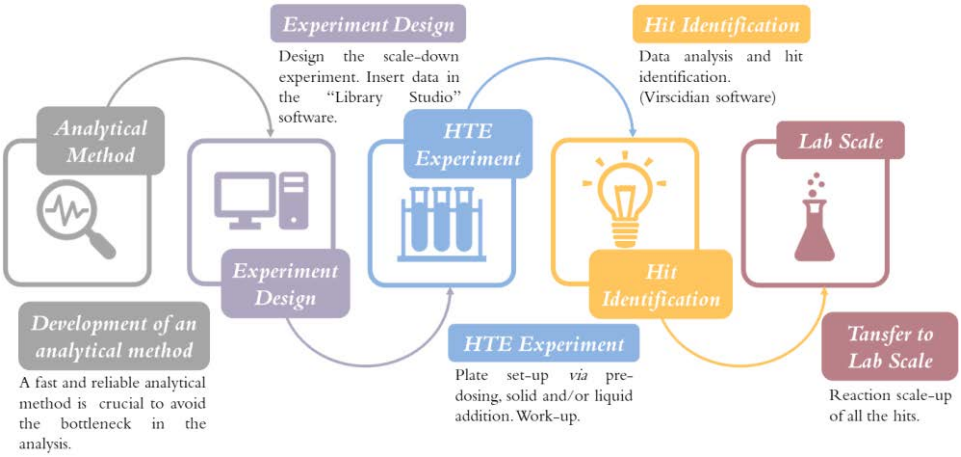

Figure 2.3. HTE workflow.

The HTE design is a process of balancing experimental goals with practical considerations. In our case, the goal was inducing enantioselectivity in the intramolecular [4+4] cycloaddition of compound **1** by using nickel-based catalytic systems incorporating enantiopure phosphorus ligands. As previously mentioned, a wide set of structurally diverse enantiopure phosphorus ligands was available at the ICIQ's HTE unit and, thus, an array of diverse phosphine, phosphine–phosphite, phosphoramidite and P,N-ligands was chosen for the screening (overall, 24 ligands). In addition, to ensure that all the practical considerations (dosing, addition, solvent evaporation, inert conditions of the vessels, etc.) were correct, a blank experiment with tris(4-methoxyphenyl)phosphine was included in the plate, as the performance of this achiral ligand had been thoroughly studied in Chapter 1. Then, all the data was

transferred to the Library Studio design software,[17] which supported the calculations and setup for each screening.

Once all the experimental considerations associated with working at the micromolar scale (concentration, solid dosing, addition in solution, etc) had been planned, the HTE experiment was set up inside the glove box, with the vessels in the plate being filled with all the required chemicals. The plate was sealed shut with a PFA mat and stirred in a regular magnetic plate for 24 h. The crudes were then filtered in parallel through a small silica gel pad and eluted with diethyl ether. The samples were analyzed by GC-MS and the results processed with the help of the Virscidian's Analytical Studio software.[18] The hits with over 20% yield towards product **10** (highlighted in yellow in the corresponding tables) were analyzed by SFC to determine the enantioselectivity obtained.

The results obtained from the HTE screening studies in a 24 well plate are shown in Table 2.3 to Table 2.5. The control experiment (in blue, entry 1, Table 2.3) showed that our experiments at the micromolar scale were well designed, and all the analyses were reliable, as the results were similar to the 60% yield obtained when working at the laboratory scale.[11]

The screening of phosphine ligands (**L8**, **L14-L21**, Table 2.3) showed that, even though most examples led to full conversion, the yields were, even in the best cases, low (entries 3, 5 and 7, Table 2.3). The poor performance of **L19** with the stereogenic phosphorus moiety was also disappointing (entry 6, Table 2.3). In all cases the [4+4] cycloadduct was racemic.

(17) LEA – Unchained Labs. http://www.unchainedlabs.com/lea/
(18) Virscidian – Customized analytical software solutions. http://www.virscidian.com/wp/wp-content/uploads/2014/01/Assay_and_Drug_Development_Technologies_Interview.pdf

Table 2.3: HTE ligand screening: Phosphine ligands.

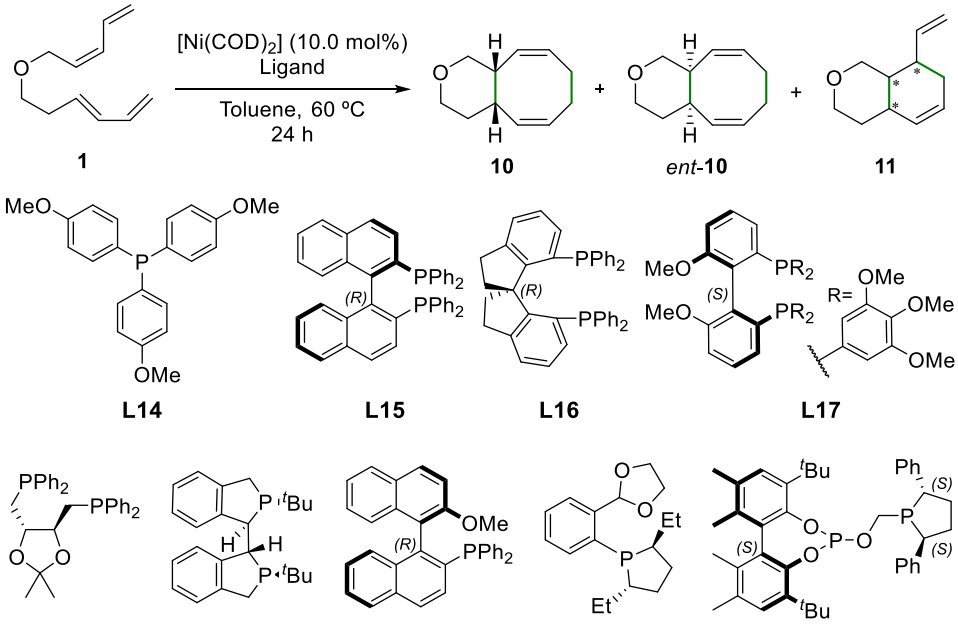

Entry	Ligand		$Ni(COD)_2$ (Equiv.)	Conv.[a] (%)	% yield[a] (10+*ent*-10)	% ee[b] (10/*ent*-10)
	L	Equiv.				
1[c]	**L14**	0.21	0.10	>99	53	-
2	**L15**	0.11	0.10	43	5	-
3	**L16**	0.11	0.10	97	20	*rac*
4	**L17**	0.11	0.10	65	6	-
5	**L18**	0.11	0.10	>99	26	*rac*
6	**L19**	0.11	0.10	50	5	-
7[d]	**L8**	0.21	0.10	90	25	*rac*
8	**L20**	0.21	0.10	>99	10	-
9	**L21**	0.11	0.10	80	30	*rac*

(a) Determined by GC-MS on an achiral stationary phase (HP-5) using 4,4′-dimethoxybiphenyl as internal standard. (b) Determined by SFC on a chiral stationary phase (Daicel Chiralpack® IG). (c) Control experiment. (d) Duplicate of the original screening (See Table 2.1).

The results of the phosphoramidite ligands, however, were much more encouraging (**L1**, **L22-L30**, Table 2.4). This screening showed that the MonoPhos family of ligands was promising for this transformation (entries 1-2 and 7-8, Table 2.4) in terms of yield and conversion. The most interesting result was obtained for **L27**, with full conversion, moderate yield and 31% ee, demonstrating that inducing enantioselectivity in the intramolecular [4+4] cycloaddition under study was possible.

Table 2.4: HTE ligand screening: Phosphoramidite ligands.

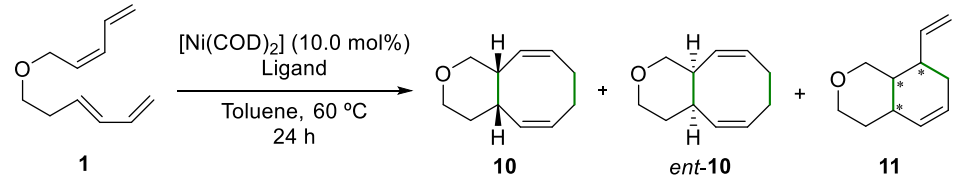

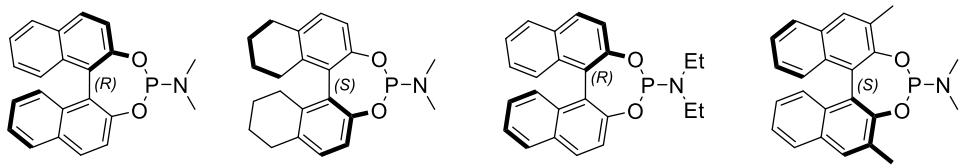

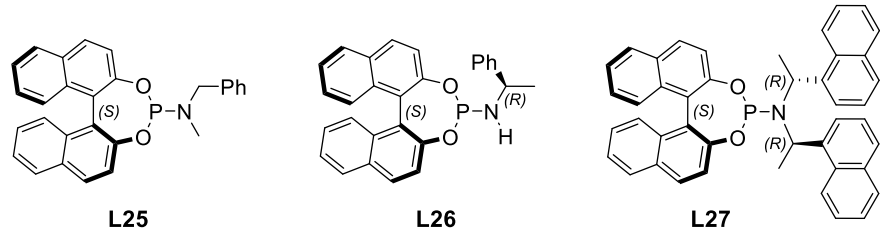

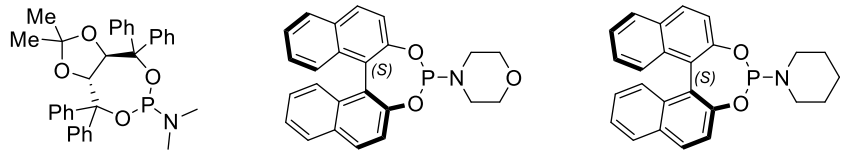

Entry	Ligand		$Ni(COD)_2$ (Equiv.)	Conv.[a] (%)	% yield[a] (10+*ent*-10)	% ee[b] (10/*ent*-10)
	L	Equiv.				
1[c,d]	L1	0.21	0.10	97	30	*rac*
2[d]	L22	0.21	0.10	80	27	*rac*
3	L23	0.21	0.10	67	6	-
4[d]	L24	0.21	0.10	>99	49	*rac*
5	L25	0.21	0.10	60	8	-
6	L26	0.21	0.10	29	1	-
7[d]	L27	0.21	0.10	>99	55	31
8[d]	L28	0.21	0.10	>99	20	*rac*
9	L29	0.21	0.10	62	2	-
10	L30	0.21	0.10	50	4	-

(a) Determined by GC-MS on an achiral stationary phase (HP-5) using 4,4′-dimethoxybiphenyl as internal standard. (b) Determined by SFC on a chiral stationary phase (Daicel Chiralpack® IG). (c) Duplicate of the original screening (See Table 2.1). (d) The results are the average of two independent runs.

The screening of the P,N-ligands (Table 2.5), only resulted in one hit for **L33**, but it was not a really promising result, since even though the conversion was complete, the yield was poor and the [4+4] cycloadduct was obtained as a racemic mixture (entry 5, Table 2.5).

Table 2.5: HTE ligand screening: P,N-Ligands.

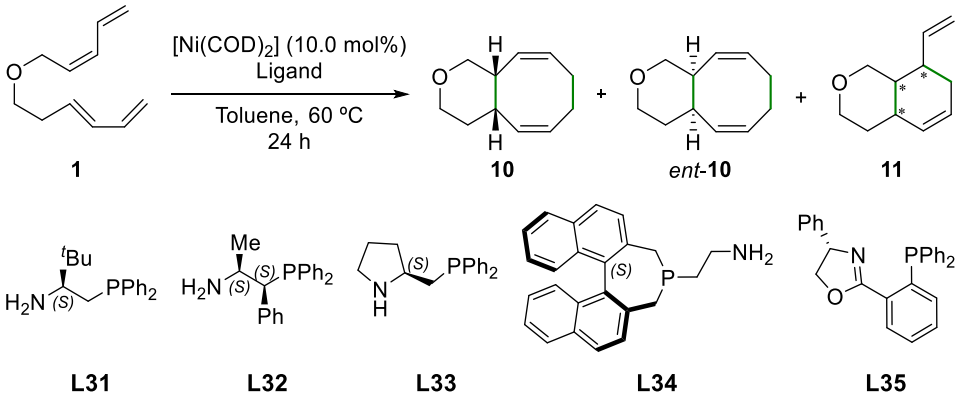

Entry	Ligand		$Ni(COD)_2$ (Equiv.)	Conv.[a] (%)	% yield[a] (10+*ent*-10)	% ee[b] (10/*ent*-10)
	L	Equiv.				
1	**L31**	0.11	0.10	46	3	-
2	**L32**	0.11	0.10	71	1	-
3	**L33**	0.11	0.10	>99	2	-
4	**L34**	0.11	0.10	>99	1	-
5	**L35**	0.11	0.10	>99	22	*rac*

(a) Determined by GC-MS on an achiral stationary phase (HP-5) using 4,4′-dimethoxybiphenyl as internal standard. (b) Determined by SFC on a chiral stationary phase (Daicel Chiralpack® IG). (c) Control experiment. (d) Duplicate of the original screening (See Table 2.1).

It should be highlighted at this point that phosphoramidite ligand **L27** provided the highest enantioselectivity in the study (99% conv., 55% yield, 31% ee; entry 7 in Table 2.4). These results highlight the importance of the steric hindrance at the amine moiety in the level of stereoinduction of the [4+4] cycloaddition of compound **1**. Once this promising hit was obtained, the last step of the HTE workflow was to scale it up in order to reproduce the results at the micromolar level in the HTE studies and under standard screening conditions in the laboratory. To our delight, the results with ligand **L27** were reproducible at the mmol scale (Scheme 2.5), which encouraged us to further expand the rational design of the ligand.

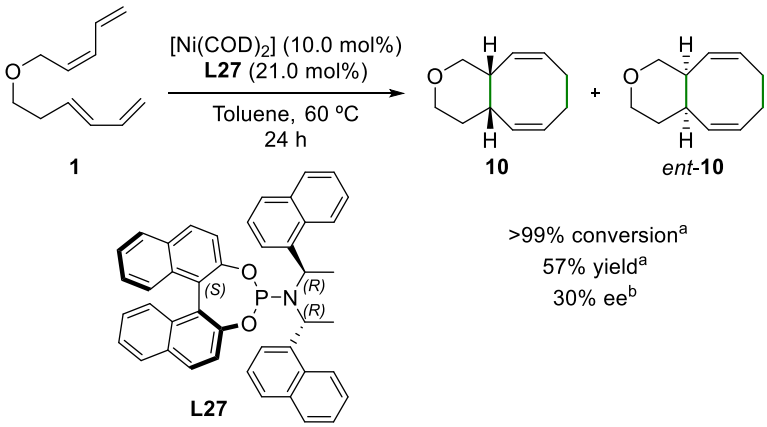

Scheme 2.5. Scale-up to the millimolar scale of the results for **L27** [(a) calculated by ^{1}H NMR spectroscopy with 1,3,5-trimethoxybenzene as internal standard; (b) determined by SFC on a chiral stationary phase (Daicel Chiralpack® IG).]

2.2.4. Further Development of the Results Obtained

In order to improve the results obtained, new phosphoramidite ligands were synthesized (Scheme 2.6). From the same enantiopure amine hydrochloride derivative, ligand **L36** was synthesized in order to test the matched-mismatched effects of the stereogenic elements contained in ligands **L27** and **L36** in the outcome of the reaction. In contrast, the structural variation introduced in **L37** aimed at studying the effects of an increase in the steric congestion around the P-centers by introducing phenyl substituents at the 3 and 3' positions of the [1,1'-biaryl]-2,2'-diol-derived phosphoramidite group.

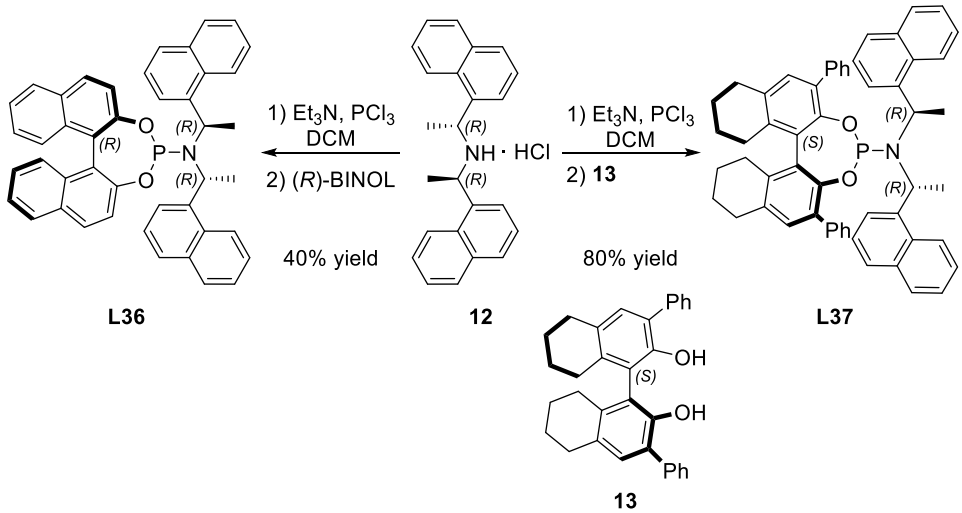

Scheme 2.6. Synthesis of **L36** and **L37**.

The results obtained with ligand **L36** (Scheme 2.7) clearly showed that there was a matched-mismatched effect in the stereogenic elements contained in ligands **L27** and **L36**, with the configuration of the stereogenic elements in **L27** being the matched combination. Whilst the yields of the cycloaddition are similar for **L27** and **L36**, the enantioselectivity of the matched ligand **L27** was higher than that with ligand **L36** (30% ee for **L27** compared to 12% ee for **L36**).

It is also interesting to note that an increase in the steric congestion around the P-center, due to the phenyl moieties and the extra rigidity provided by the H8-BINOL motif in ligand **L37**, was beneficial for the level of stereoinduction: a slight increase in the ee was observed for **L37** with respect to **L27** (38% ee for **L37** compared to 30% ee for **L27**; Scheme 7).

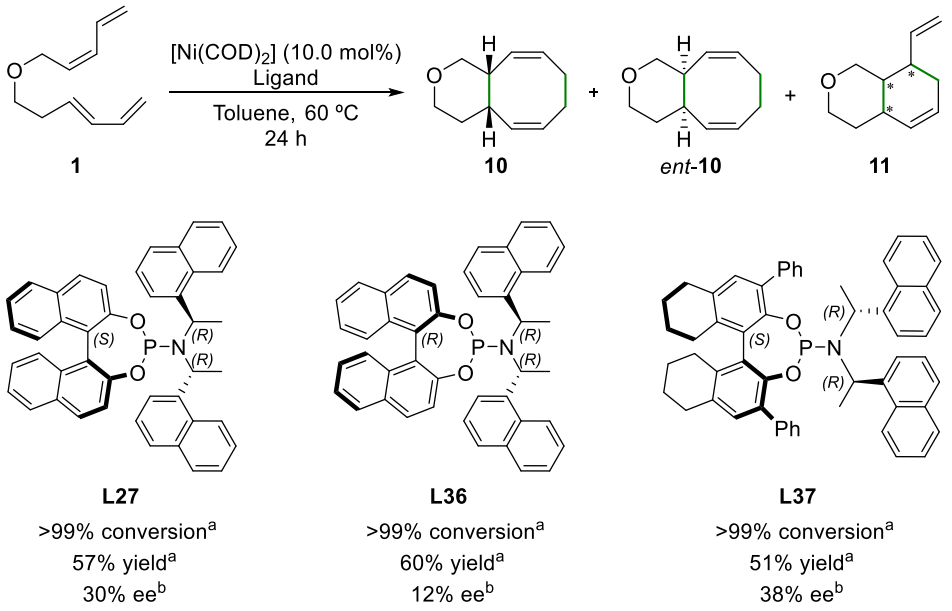

Scheme 2.7. Comparison of the results obtained with **L27**, **L36** and **L37** [(a) calculated by ^{1}H NMR spectroscopy with 1,3,5-trimethoxybenzene as internal standard; (b) Determined by SFC on a chiral stationary phase (Daicel Chiralpack® IG)].

It could be concluded then that steric congestion around the phosphorus moiety, in combination with the voluminous substituents in the amino motif, may justify the better results in terms of enantioselectivity with ligand **L37**, with minimal effects in the conversion and yield. Further modifications in the design of the ligands towards an enantioselective catalyst with higher levels of stereoinduction, should probably provide the highest possible level of steric hindrance around the P-center (for instance, by incorporating 9-anthryl substituents instead of 1-naphthyl groups).

2.3 Conclusions

An enantioselective version of the nickel-catalyzed intramolecular [4+4] cycloaddition of bisdiene substrates for the preparation of *cis*-eight-membered fused [6.4.0] bicyclic systems from (*E*,*Z*)-configured bisdiene **1** (*i.e.*, (*E*)-6-(((*Z*)-penta-2,4-dien-1-yl)oxy)hexa-1,3-diene) was developed. An initial evaluation of enantiopure ligands, followed by a thorough HTE screening study led to the discovery of phosphoramidite ligand **L27**, which was capable of catalyzing the intramolecular [4+4] cycloaddition reaction of substrate **1** in good yield (57% yield) and moderate levels of enantioselectivity (30% ee). Further ligand design, and incorporation of the required structural variations in **L27** for achieving higher levels of stereoinduction, led to the discovery of ligand **L37**, which provided a slightly higher enantioselectivity (38% ee) with the cycloaddition yields remaining similar to those with ligand **L27**. This is, to the best of our knowledge, the first example of a catalytic enantioselective intramolecular [4+4] cycloaddition reaction. As potential research activities for the future, it would be highly interesting to expand the research perspectives developed within this PhD thesis for this challenging chemistry.

UNIVERSITAT ROVIRA I VIRGILI
TRANSITION METAL-CATALYZED CYCLOADDITION REACTIONS FOR THE FORMATION OF EIGHT- AND SIX-MEMBERED RINGS
Nuria Llorente González

2.4 Experimental Section

2.4.1. General Remarks

All syntheses were carried out on chemicals as purchased from commercial sources, unless otherwise stated. Air and moisture sensitive manipulations or reactions were run under inert atmosphere using anhydrous and deoxygenated solvents, either in a glove box or with standard Schlenk techniques. All solvents were dried by using a Solvent Purification System (SPS). NMR spectra were recorded in $CDCl_3$ unless otherwise cited, on a Bruker Advance 300 MHz, 400 MHz or 500 MHz Ultrashield spectrometers. ^{1}H NMR and $^{13}C\{^{1}H\}$ NMR chemical shifts are quoted in ppm relative to residual solvent peaks. $^{31}P\{^{1}H\}$ NMR chemical shifts are quoted in ppm relative to 85% phosphoric acid in water. High-resolution mass spectra (HRMS) were recorded by using either ESI or APCI ionization method in positive mode. For the HTE screening, GC analyses were performed on an Agilent 7890B chromatograph equipped with a 5977A MS detector. The enantioselectivities were determined by chromatography on chiral stationary phases in an UltraPerformance Convergence Chromatography (UPC2) performed on Acquity UPC2 Waters instrument equipped with Photodiode Array Detector (PDA). Melting points were measured in open capillaries and are uncorrected. Specific optical rotation measurements were carried out on a Jasco P-1030 model polarimeter equipped with a PMT detector using the Sodium line at 589 nm.

2.4.2. Experimental Procedure and Characterization Data for the enantiopure ligands

- Synthesis of bis[(*R*)-(1-naphthyl)ethyl]amine hydrochloride **12**

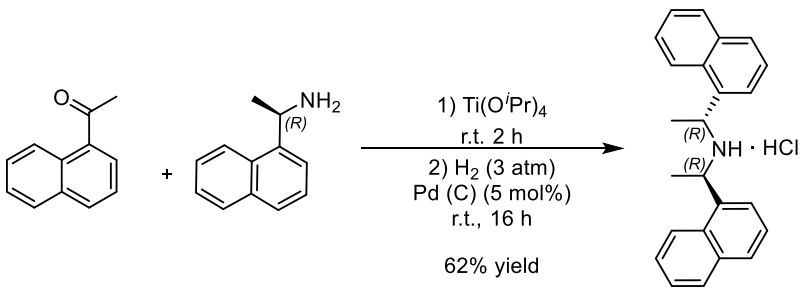

12

A mixture of methyl 1-naphthyl ketone (0.5 mL, 3.1 mmol), (*R*)-1-(naphthyl)ethylamine (0.5 mL, 3.1 mmol), and titanium(IV) isopropoxide (2.8 mL, 9.3 mol) was stirred at room temperature for 2 h. The mixture was then hydrogenated at 1 atm with 10 wt. % palladium on charcoal (180.0 mg, 2 mol %) under vigorous stirring at r.t. for 16 h. The reaction mixture was then filtered to remove the Pd(C), concentrated *in vacuo*, redissolved in DCM and washed with an aqueous solution of 2 M HCl to afford the crude amine hydrochloride. The organic phase was then concentrated *in vacuo* and the white solid obtained was washed with ethyl acetate to yield optically pure hydrochloride **12** (620.0 mg, 55% yield). ^{1}H NMR (400 MHz, $CDCl_3$) δ 10.98 (bs, 2H), 8.72 (bs, 2H), 7.84 (d, J = 8.0 Hz, 2H), 7.75 (bs, 2H), 7.63 (d, J = 8.2 Hz, 2H), 7.08 (t, J = 7.4 Hz, 2H), 6.58 (bs, 2H), 6.33 (bs, 2H), 4.98 (q, J = 6.7 Hz, 2H), 2.10 (d, J = 6.7 Hz, 6H) ppm. ^{13}C {^{1}H} NMR (101 MHz, $CDCl_3$) δ 133.7 (CH_{arom}), 132.9 (C_{arom}), 130.6 (CH_{arom}), 129.3 (CH_{arom}), 128.5 (CH_{arom}), 126.1 (CH_{arom}), 125.8 (CH_{arom}), 125.6 (C_{arom}), 120.7 (C_{arom}), 52.2 (CH), 22.0 (CH_3). All spectroscopic data were in agreement with those previously reported in the literature.[19]

- General methodology for the synthesis of the phosphoramidite ligands.

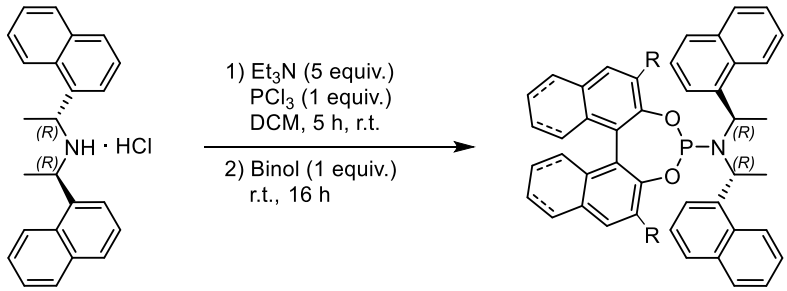

12

The hydrochloride of the amine **12** (1 equiv.) was added in one portion to a stirred mixture of Et_3N (5 equiv.) and PCl_3 (1 equiv.) at 0 °C in dichloromethane (0.5 M) under nitrogen atmosphere. The reaction mixture was stirred for 5 h at room temperature. The corresponding [1,1'-biaryl]-2,2'-diol derivative (1 equiv.) was added in one portion to the reaction mixture at 0 °C and the suspension was stirred at room temperature for 16 h. The reaction was quenched with water, the organic phase separated, dried over sodium sulfate, and purified

(19) Polet, D.; Alexakis, A.; Tissot-Croset, K.; Corminboeuf, C.; Ditrich, K. *Chem.-Eur. J.* **2006**, *12*, 3596-3609.

by flash chromatography on silica gel (pentane:DCM 100:0→50:50) affording the ligand as a white foam.[19]

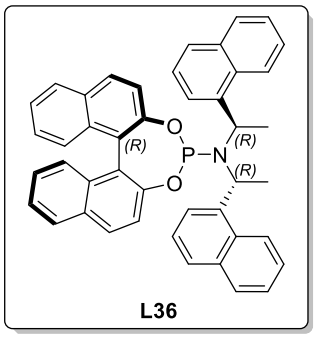

L36

Ligand **L36** was prepared following the general procedure starting from bis[(*R*)-(1-naphthyl)ethyl]amine hydrochloride (**12**, 0.300 g, 0.829 mmol) and (*S*)-BINOL (237.0 mg, 0.829 mmol). It was obtained as a white solid (212.0 mg, 40% yield, see Figure 2.6, Figure 2.7 and Figure 2.8).^{1}H NMR (400 MHz, $CDCl_3$) δ 8.03 (d, J = 8.8 Hz, 1H, H_{arom}), 7.93 (d, J = 8.3 Hz, 1H, H_{arom}), 7.75 – 7.59 (m, 8H, H_{arom}), 7.47 (d, J = 8.8 Hz, 1H, H_{arom}), 7.44 – 7.37 (m, 3H, H_{arom}), 7.36 – 7.26 (m, 5H, H_{arom}), 7.26 – 7.15 (m, 5H, H_{arom}), 7.04 (t, J = 7.7 Hz, 2H, C_{arom}), 5.46 (t, J = 7.2 Hz, 2H, CH), 1.69 (d, J = 7.2 Hz, 6H, 2xCH_3). ^{13}C {^{1}H} NMR (101 MHz, $CDCl_3$) δ 151.1 (C_{arom}), 151.0 (C_{arom}), 149.7 (C_{arom}), 139.2 (C_{arom}), 139.2 (C_{arom}), 133.4 (C_{arom}), 133.1 (C_{arom}), 132.9 (C_{arom}), 131.6 (C_{arom}), 130.9 (CH_{arom}), 130.6 (CH_{arom}), 130.5 (C_{arom}), 129.8 (CH_{arom}), 128.6 (CH_{arom}), 128.5 (CH_{arom}), 128.3 (CH_{arom}), 127.3 (CH_{arom}), 127.3 (CH_{arom}), 127.2 (CH_{arom}), 126.2 (CH_{arom}), 126.0 (CH_{arom}), 125.6 (C_{arom}), 125.1(CH_{arom}), 125.1 (CH_{arom}), 125.0 (CH_{arom}), 124.7 (CH_{arom}), 124.7 (CH_{arom}), 124.6 (CH_{arom}), 124.4 (C_{arom}), 123.3 (CH_{arom}), 123.2 (CH_{arom}), 122.5 (CH_{arom}), 122.5 (CH_{arom}), 122.2 (CH_{arom}), 121.7 (C_{arom}), 53.2 (CH), 53.1 (CH), 23.4 (CH_3), 23.3 (CH_3) ppm. ^{31}P{^{1}H} NMR (162 MHz, $CDCl_3$) δ 157.2 ppm. $[\alpha]^{24}_{D}$ = -218.0 (c = 7.5, $CHCl_3$) HRMS (ESI$^+$) *m/z* calcd for $C_{44}H_{34}NNaO_2P$ $[M+Na]^+$ 662.2225, found 662.2219.

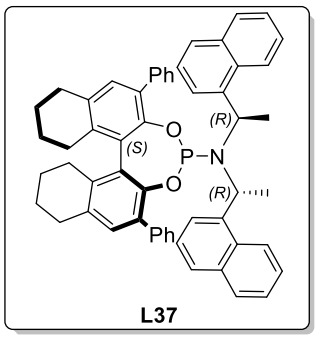

L37

Ligand **L37** was prepared following the general procedure starting from bis[(*R*)-(1-naphthyl)ethyl]amine hydrochloride (**12**, 300 mg, 0.829 mmol) and (*S*)-3,3'-diphenyl-5,5',6,6',7,7',8,8'- octahydro-[1,1'-binaphthalene]-2,2'-diol **13**[20] (237 mg, 0.829 mmol). It was obtained as white solid (212.0 mg, 40% yield, see Figure 2.9, Figure 2.10 and Figure 2.11). ^{1}H NMR (500 MHz, $CDCl_3$) δ 7.90 – 7.85 (m, 2H), 7.56 (d, J = 8.7 Hz, 4H), 7.48 (m, 3H), 7.40 – 7.29 (m, 7H), 7.16 (m, 3H), 7.12 – 7.01 (m, 3H), 6.70 (d, J = 7.3 Hz, 2H), 6.54 (s, 2H), 2.99 (t, J = 6.4 Hz, 2H),

(20) Erre, G.; Junge, K.; Enthaler, S.; Addis, D.; Michalik, D.; Spannenberg, A.; Beller, M. *Chem.–Asian J.* **2008**, *3*, 887-894.

2.91 – 2.75 (m, 4H), 2.73 – 2.64 (m, 1H), 2.57 – 2.48 (m, 1H), 2.36 (d, J = 16.2 Hz, 1H), 1.97 – 1.72 (m, 8H), 1.65 (dd, J = 8.5, 4.8 Hz, 1H), 1.13 (d, J = 7.1 Hz, 6H). $^{13}C\{^1H\}$ NMR (126 MHz, $CDCl_3$) δ 146.5 (C_{arom}), 146.4 (C_{arom}), 146.1 (C_{arom}), 138.9 (C_{arom}), 138.3 (C_{arom}), 137.6 (C_{arom}), 137.5 (C_{arom}), 137.5 (C_{arom}), 134.4 (C_{arom}), 133.5 (C_{arom}), 133.1 (C_{arom}), 132.5 (C_{arom}), 132.5 (C_{arom}), 131.6 (C_{arom}), 131.1 (CH_{arom}), 130.8 (CH_{arom}), 130.7 (C_{arom}), 130.7 (C_{arom}), 130.5 (CH_{arom}), 130.2 (CH_{arom}), 130.2 (CH_{arom}), 129.6 (C_{arom}), 129.6 (C_{arom}), 128.5 (CH_{arom}), 128.3 (CH_{arom}), 127.4 (CH_{arom}), 127.1 (CH_{arom}), 126.7 (CH_{arom}), 125.6 (CH_{arom}), 125.0 (CH_{arom}), 29.7 (CH_2), 28.4 (CH_2), 28.0 (CH_2), 23.5 (CH_2), 23.4 (CH_2), 23.3 (CH), 23.1 (CH_3) ppm. $^{31}P\{^1H\}$ NMR (202 MHz, $CDCl_3$) δ 145.1 ppm. $[\alpha]^{24}_D$ = 183.6 (c = 6.6, $CHCl_3$) HRMS (ESI$^+$) m/z calcd for $C_{57}H_{50}NO_2P$ $[M+H]^+$ 800.3652, found 800.3662.

2.4.3. Synthesis of (*E*)-6-(((*Z*)-penta-2,4-dien-1-yl)oxy)hexa-1,3-diene (1)

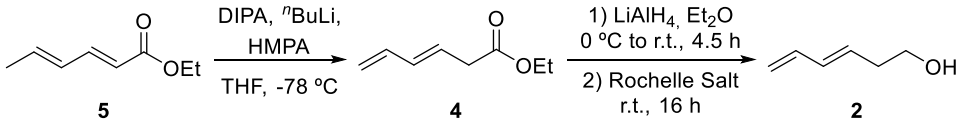

5 **4** **2**

70% yield 55% yield

A flame-dried 500 mL Schlenk flask was loaded with dry THF (300.0 mL) and diisopropylamine (DIPA, 22.6 mL, 160.0 mmol) and cooled to -78 °C. A solution of *n*-butyllithium (2.5 M in hexane, 64 mL, 160.0 mmol) was then added dropwise and the reaction mixture was stirred at -78 °C for 1 h in order to form LDA *in situ*. Hexamethylphosphoramide (HMPA, 23.2 mL, 133.0 mmol) was then slowly added to the mixture. After 30 min stirring at -78 °C, a solution of ethyl sorbate **5** (20.0 mL, 133.0 mmol) in THF (50.0 mL) was added dropwise, resulting in a red-orange solution. The reaction was stirred at -78 °C for 1 h and then ethanol (70.0 mL) was added. The reaction mixture was then quenched by pouring the mixture into a 1 L round-bottom flask containing water (260.0 mL) and glacial acetic acid (70.0 mL). After diluting with hexane (200.0 mL), the two phases were separated and the aqueous phase was extracted with hexane (3 x 300.0 mL). The combined organic phases were washed with saturated $NaHCO_3$ (2 x 150.0 mL), brine (2 x 150.0 mL) and dried over magnesium sulfate. The solvent was evaporated to dryness. The crude mixture was distilled to yield ethyl (*E*)-hexa-3,5-dienoate **4** (0.027 mBar, 36 °C) as a colorless oil (13.1 g, 70 % yield). ^1H NMR (300 MHz, $CDCl_3$) δ 6.32 (dt, J = 16.9, 10.4 Hz, 1H), 6.12 (dd, J = 15.2, 10.4 Hz, 1H), 5.77 (dt, J = 15.2, 7.2 Hz, 1H), 5.14 (d, J = 16.9

Hz, 1H), 5.04 (d, J = 10.1 Hz, 1H), 4.12 (q, J = 7.2 Hz, 2H), 3.09 (d, J = 7.2 Hz, 2H), 1.23 (t, J = 7.2 Hz, 3H). $^{13}C\{^1H\}$ NMR (75 MHz, $CDCl_3$) δ 171.1 (C=O), 136.1 (CH=), 133.9 (CH=), 135.4 (CH=), 116.5 (CH_2=), 60.4 (CH_2), 37.7 (CH_2), 13.8 (CH_3) ppm. Spectroscopic data were in agreement with those previously reported in the literature.[21]

$LiAlH_4$ (512.0 mg, 13.5 mmol) was suspended in anhydrous diethyl ether (10.0 mL) in a flame-dried Schlenk flask and the suspension was cooled at 0 °C. Then, a solution of **4** (1.3 g, 9.6 mmol) in anhydrous diethyl ether (3.0 mL) was slowly cannulated to the previous suspension. The reaction mixture was allowed to reach room temperature and stirred for 4.5 h. The reaction was cooled down to 0 °C again, diluted with diethyl ether (15.0 mL) and carefully quenched with a saturated aqueous solution of the Rochelle salt (25.0 mL). The biphasic mixture was vigorously stirred overnight. The two phases were then separated, and the aqueous phase was extracted with diethyl ether (2 x 50.0 mL). The combined organic phases were washed with brine (1 x 50.0 mL), dried over magnesium sulfate, filtered and concentrated *in vacuo* to provide the desired product (*E*)-hexa-3,5-dien-1-ol **2** as a yellowish liquid (0.92 g, 97% crude yield), which was immediately used in the following step without further purification. ^1H NMR (300 MHz, $CDCl_3$) δ 6.41 (m, 1H), 6.12 (m, 1H), 5.67 (m, 1H), 5.12 (dt, J = 17.6, 0.5 Hz, 1H), 5.00 (dt, J = 9.6, 0.5 Hz, 1H), 3.66 (t, J = 6.6 Hz, 2H), 2.34 (qd, J = 6.6, 1.1 Hz, 2H), 1.93 (s, br, 1H) ppm. Spectroscopic data were in agreement with those previously reported in the literature.[22]

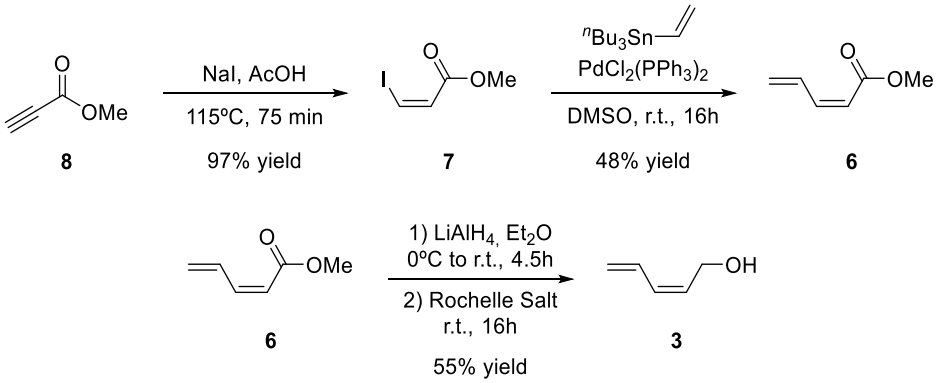

Methylpropiolate **8** (15.5 mL, 170.0 mmol) was added to a mixture of sodium iodide (40.7 g, 272.0 mmol) in acetic acid (60.0 mL). The mixture was heated at 115 °C and stirred for 90 min. The brown-red solution was then allowed to cool

(21) Miller, C. A.; Batey, R. A. *Org. Lett.* **2004**, *6*, 699-702.
(22) DeBoef, B.; Counts, W. R.; Gilbertson, S. R. *J. Org. Chem.* **2007**, *72*, 799-804.

to room temperature, after which it was poured into water (360.0 mL) and extracted with diethyl ether (3 x 300.0 mL). The combined organic phases were washed with saturated $NaHCO_3$ (5 x 180.0 mL), saturated $NaHSO_3$ (120.0 mL) and brine (180.0 mL). The resulting organic phase was dried over magnesium sulfate, filtered and concentrated *in vacuo* to provide the desired product methyl (*Z*)-3-iodoacrylate **7** (35.4 g, 98% yield), which was immediately used in the following step without further purification. ^{1}H NMR (500 MHz, $CDCl_3$) δ 7.44 (d, J = 8.9 Hz, 1H), 6.88 (d, J = 8.9 Hz, 1H), 3.74 (s, 3H) ppm. All spectroscopic data were in agreement with those previously reported in the literature.[8]

Dichlorobis(triphenylphosphine)palladium (169.0 mg, 0.236 mmol) was added to an anhydrous DMF solution (7 mL) of the previously synthesized **7** (1.0 g, 4.7 mmol) in a Schlenk flask under argon. The reaction mixture was stirred for 15 min and tributyl(vinyl)tin (1.6 mL, 5.7 mmol) was added. The resulting mixture was stirred for 12 h at room temperature and then treated with a 1 M solution of potassium fluoride (80 mL) and diethyl ether to eliminate the tributyltin iodide thus formed. The aqueous layer was extracted with diethyl ether (3 x 10.0 mL). The organic layer was washed with brine (2 x 10.0 mL) to remove the DMF and dried over magnesium sulfate. The crude was concentrated *in vacuo* and purified by column chromatography on silica gel (pentane:diethyl ether 100:0→90:10) to yield the desired methyl (*Z*)-penta-2,4-dienoate **6** (380 mg, 72 % yield, see Figure 2.12 and Figure 2.13) ^{1}H NMR (500 MHz, $CDCl_3$) δ 7.60 (ddd, $^3J_{H1\text{-}H4'}$ = 17.0 Hz, $^3J_{H1\text{-}H2}$ = 11.2 Hz, $^3J_{H1\text{-}H4}$ = 10.0 Hz, 1H, H_1), 6.57 (dd, $^3J_{H2\text{-}H1}$ = $^3J_{H2\text{-}H3}$ = 11.3 Hz, 1H, H_2), 5.70 (d, $^3J_{H3\text{-}H2}$ = 11.3 Hz, 1H, H_3), 5.57 – 5.49 (m, 2H, H_4 and $H_{4'}$), 3.72 (s, 6H, H_{Me}) ppm. ^{13}C{^{1}H} NMR (101 MHz, $CDCl_3$) δ 166.5 (C=O), 144.9 (CH=, C_a), 133.0 (CH=, C_b), 126.0 (CH=, C_c), 118.1 (CH=, C_d), 51.1 (CH_3, C_{Me}) ppm. HRMS (APCI$^+$): *m/z* calcd for $C_6H_9O_2$ $[M+H]^+$ 113.0597, found 113.0599.[7]

In a flame-dried Schlenk flask, $LiAlH_4$ (129.0 mg, 3.4 mmol) was suspended in anhydrous diethyl ether (2.0 mL) and the mixture cooled down to 0 °C. Then, a solution of methyl (*Z*)-penta-2,4-dienoate **6** (280.0 mg, 2.5 mmol) in anhydrous diethyl ether (1.0 mL) was slowly cannulated into the previous suspension. The reaction mixture was allowed to reach room temperature and stirred for 4.5 h. The reaction was cooled down to 0 °C again, diluted with diethyl ether (1.0 mL) and carefully quenched with a saturated aqueous solution of Rochelle salt (5.5 mL). The biphasic mixture was vigorously stirred overnight. The two phases were then separated and the aqueous phase was extracted with diethyl ether (2 x 5.0 mL). The combined organic phases were washed with brine (1 x 5.0 mL), dried over magnesium sulfate, filtered, and concentrated *in vacuo*

to provide the desired product (*Z*)-penta-2,4-dien-1-ol **3** as a yellowish liquid (0.118 g, 56% crude yield), which was immediately used for the following step without further purification.[23] ^{1}H NMR (500 MHz, $CDCl_3$) δ 6.63 (dddd, *J* = 16.8, 11.1, 10.1, 1.2 Hz, 1H), 6.10 (dd, *J* = 11.1, 10.6 Hz, 1H), 5.63 (dtd, *J* = 10.6, 6.9, 1.2 Hz, 1H), 5.27 (dd, *J* = 16.8, 1.9 Hz, 1H), 5.19 (dd, *J* = 10.1, 1.9 Hz, 1H), 4.33 (dd, *J* = 6.9, 5.5 Hz, 2H), 1.42 (t, *J* = 5.5 Hz, 1H) ppm. ^{13}C{^{1}H} NMR (126 MHz, $CDCl_3$) δ 131.6 (CH=), 131.5 (CH=), 130.2 (CH=), 119.5 (CH_2=), 58.9 (CH_2) ppm.

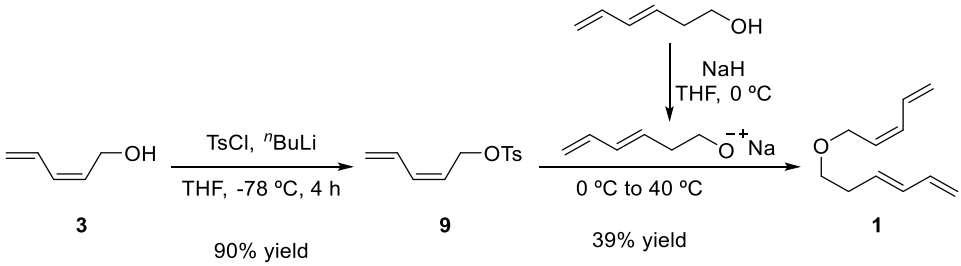

^{n}BuLi (2.5 M in hexanes, 0.5 mL, 1.2 mmol) was added dropwise to a solution of (*Z*)-penta-2,4-dien-1-ol **3** (100 mg, 1.2 mmol) in THF (1.2 mL) at -78 °C and the mixture was stirred for 15 min. A solution of *p*-toluenesulfonyl chloride (249.0 mg, 1.3 mmol) in THF (1.2 mL) was added dropwise and the mixture was stirred at -78 °C for 4 h. The reaction was then allowed to reach 0 °C, quenched with a saturated aqueous NH_4Cl solution and extracted with diethyl ether (3 × 20.0 mL). The combined organic layers were washed with brine (2 x 20.0 mL), dried over magnesium sulfate, filtered and concentrated *in vacuo*. (*Z*)-Penta-2,4-dien-1-yl tosylate **9** (265.0 mg, 93% crude yield) was used in the next step without further purification.[9] ^{1}H NMR (400 MHz, $CDCl_3$) δ 7.79 (d, *J* = 8.4 Hz, 2H), 7.34 (d, *J* = 8.4 Hz, 2H), 6.52 – 6.37 (m, 1H), 6.16 (dd, *J* = 11.1 Hz, 1H), 5.50 – 5.39 (m, 1H), 5.30 (dd, *J* = 16.7, 1.4 Hz, 1H), 5.24 (dd, *J* = 10.1, 1.4 Hz, 1H), 4.72 (d, *J* = 7.3 Hz, 2H), 2.45 (s, 3H). ^{13}C{^{1}H} NMR (101 MHz, $CDCl_3$) δ 144.9 (C_{arom}), 135.2 (CH=), 133.5 (C_{arom}), 130.6 (CH=), 130.0 (CH_{arom}), 128.1 (CH_{arom}), 122.3 (CH=), 121.6 (CH=), 65.9 (CH_2), 21.8 (CH_3) ppm.

To a stirred suspension of NaH (60% in paraffin oil, 1.3 g, 33.7 mmol) in THF (60.0 mL) at 0 °C, a THF (130.0 mL) solution of **2** (2.2 g, 22.5 mmol) was added. The mixture was stirred at 0 °C for 30 min and then a THF (130.0 mL) solution of (*Z*)-penta-2,4-dien-1-yl tosylate **9** (6.4 g, 27.0 mmol) was added. The

(23) Method adapted from the synthesis of (*E*)-penta-2,4-dien-1-ol reported in section 1.4.3, Chapter 1.

cold bath was removed and the resulting mixture was stirred at 40 °C overnight. The reaction was quenched by the addition of water (200.0 mL). The phases were separated and the aqueous phase was extracted with diethyl ether (3 x 500.0 mL). The combined organic phases were washed with brine (2 x 500.0 mL), dried over magnesium sulfate and concentrated. The residue was purified by column chromatography over silica gel (pentane:diethyl ether, 100:0→98:2→50:50), which furnished the product as a yellow oil. To ensure a further purification, the purest fraction was distilled (0.048 mbar, 43 °C) to afford the target substrate **1** as a colorless liquid (1.4 g, 39% yield, see Figure 2.14 and Figure 2.15) ^{1}H NMR (400 MHz, $CDCl_3$) δ 6.62 (ddd, $^3J_{H1\text{-}H7'}$ = 16.8 Hz, $^3J_{H1\text{-}H3}$ = $^3J_{H1\text{-}H7}$ = 10.6, 1H, H_1), 6.31 (ddd, $^3J_{H2\text{-}H8'}$ = 17.3 Hz, $^3J_{H2\text{-}H4}$ = $^3J_{H2\text{-}H8}$ = 10.3 Hz, 1H, H_2), 6.20 – 6.04 (m, 2H, H_3 and H_4), 5.71 (dt, $^3J_{H5\text{-}H4}$ = 14.4, $^3J_{H5\text{-}H11}$ = 6.9 Hz, 1H, H_5), 5.57 (dt, $^3J_{H6\text{-}H3}$ = 11.1, $^3J_{H6\text{-}H9}$ = 6.2 Hz, 1H, H_6), 5.30 – 4.94 (m, 4H, H_7 and H_8), 4.16 (dd, $^3J_{H9\text{-}H6}$ = 6.5, $^3J_{H9\text{-}H9}$ = 1.5 Hz, 2H, H_9), 3.49 (t, $^3J_{H10\text{-}H11}$ = 6.8 Hz, 2H, H_{10}), 2.38 (dt, $^3J_{H11\text{-}H5}$ = $^3J_{H11\text{-}H10}$ = 6.9 Hz, 2H, H_{11}) ppm. $^{13}C\{^1H\}$ NMR (101 MHz, $CDCl_3$) δ 137.1 (CH=, C_a), 132.7 (CH=, C_b), 131.9 (CH=, C_c), 131.7 (CH=, C_d), 131.2 (CH=, C_e), 128.0 (CH=, C_f), 119.1 (CH_2=, C_g), 115.5 (CH_2=, C_h), 69.7 (CH_2, C_i), 66.5 (CH_2, C_i), 33.1 (CH_2, C_k) ppm. HRMS (APCI$^+$): *m/z* calcd for $C_{11}H_{17}O$ $[M+H]^+$ 165.1274, found 165.1267.[10]

2.4.4. General Methodology for the Cycloaddition Reactions

- [4+4] Cycloadditions at the millimolar scale.

A solution of the substrate (1.00 mmol) and ligand (0.21 mmol) in anhydrous and deoxygenated toluene was prepared under inert atmosphere. $Ni(COD)_2$ (0.10 mmol) was added dropwise from a stock solution in anhydrous toluene. The resulting mixture was carefully heated at 60 °C under argon atmosphere and stirred for 24 h. After that, the reaction mixture was allowed to reach room temperature and left stirring under air for 1 h. The mixture was filtered through a short pad of silica and further eluted with diethyl ether. The filtrate was concentrated *in vacuo* and the resulting crude mixture was analyzed by NMR spectroscopy. Purification of the desired product was carried out with column chromatography on silica gel impregnated with silver nitrate (10%)[24] and mixtures of hexane:acetone (100:0→0:100) as the eluent.

(24) Li, T.-S.; Li, J.-T.; Li, H.-Z. *J. Chromatogr. A* **1995**, *715*, 372-375.

- [4+4] Cycloadditions at the micromolar scale (HTE Screening).

A 24 positions well plate was set up with the complementary number of 0.1 mL reaction vessels and magnetic stirring bars and dried in the oven at 120 °C overnight. Then, in a nitrogen-filled glove box, 0.2 μmol of each ligand were added from a stock solution in THF to their corresponding reaction vessel. The solvent was removed with a Genevac© centrifugal evaporator. The ligands were redissolved in anhydrous and deoxygenated toluene (0.1 M) and a stock solution (0.952 M) of the substrate in toluene (9.5 μmol) was added dropwise. $Ni(COD)_2$ (0.95 μmol) was then added dropwise from a stock solution in anhydrous toluene (0.048 M). The plate was sealed with a PFA mat under inert atmosphere, taken out of the glove box, carefully heated at 60 °C and stirred for 24 h. After that, the reaction mixture was allowed to reach room temperature and left stirring under air for 1 h. The mixtures were filtered in parallel through a short pad of silica and further eluted with diethyl ether (750 μL). A stock solution of 4,4′-dimethoxybiphenyl (500 μL, 5·mM) was added to the mixture. A 75 μL aliquote of each resulting solution was further diluted with ACN (425 μL) and this samples were analyzed by GC-MS with 4,4′-dimethoxybiphenyl as internal standard to determine the conversion and yield. Those samples with yields higher than 20% were analyzed by SFC to determine the enantiomeric excess. The results obtained are shown in Table 2.3 to Table 2.5 in the results and discussion section.

GC analysis conditions for the [4+4] cycloaddition products of **1** (Figure 2.4): Yield and conversion were determined by GC analysis with an HP-5 column (5% phenyl methyl siloxane; 30 m x 250 μm x 0.25 μm). Carrier gas: He; pressure: 13.4 psi. Injection volume: 2 μL; split ratio: 20:1; injector temperature: 280 °C. Flow rate: 1.5 mL/min; temperature program: 60 °C, 20 °C/min to 300 °C (4 min). Retention times: 4.8 min for starting material **1**; 5.9 min for the two enantiomers of **10**.

SFC analysis conditions for the [4+4] cycloaddition products of **1** (Figure 2.5): The enantiomeric excess was determined with a UltraPerformance Convergence Chromatography (UPC2) with a Daicel Chiralpack® IG column (Amylose tris(3-chloro-5-methylphenylcarbamate; 100 mm x 3 mm, 3 μm). Mobile phase: CO_2:ACN 90:10; 2 mL/min; 2000 psi. Detector: diode array; 210 nm. Retention times for **10** and *ent*-**10**: 2.70 min and 3.26 min.

2.4.5. Characterization of [4+4] Cycloaddition Product

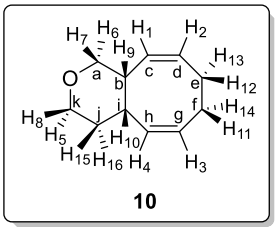

10

Characterization data for product **10** (Figure 2.16 and Figure 2.17): ^{1}H NMR (500 MHz, $CDCl_3$) δ 5.66 - 5.54 (m, 3H, H_1-H_3), 5.30 – 5.28 (m, 1H, H_4), 3.93 (dt, $^{2}J_{H5\text{-}H8}$ = 11.3 Hz, $^{2}J_{H5\text{-}H15}$ = $^{3}J_{H5\text{-}H16}$ = 4.0 Hz, 1H, H_5), 3.67 (dd, $^{2}J_{H6\text{-}H7}$ = 11.3 Hz, $^{2}J_{H6\text{-}H9}$ = 4.0 Hz, 1H, H_6), 3.58 - 3.52 (m, 2H, H_7-H_8), 3.18 (bs, 1H, H_9), 2.86 - 2.75 (m, 2H, H_{10}-H_{11}), 2.56 - 2.53 (m, 1H, H_{12}), 2.14 - 1.98 (m, 2H, H_{13}-H_{14}), 1.64 - 1.53 (m, 1H, H_{15}), 1.50 - 1.41 (m, 1H, H_{16}) ppm. ^{13}C{^{1}H} NMR (125 MHz, $CDCl_3$) δ 133.7 (CH=, C_h), 128.62 (CH=, C_c), 128.60 (CH=, C_d), 127.8 (CH=, C_g), 70.7 (CH_2, C_a), 67.8 (CH_2, C_k), 39.7 (CH, C_i), 38.9 (CH, C_b), 30.1 (CH_2, C_j), 29.2 (CH_2, C_e), 26.8 (CH_2, C_f) ppm. HRMS (APCI$^+$): *m/z* calcd for $C_{11}H_{17}O$ $[M+H]^+$ 165.1274, found 165.1274.

2.4.6. Selected Chromatograms of the HTE Screening

- Representative GC-MS chromatogram

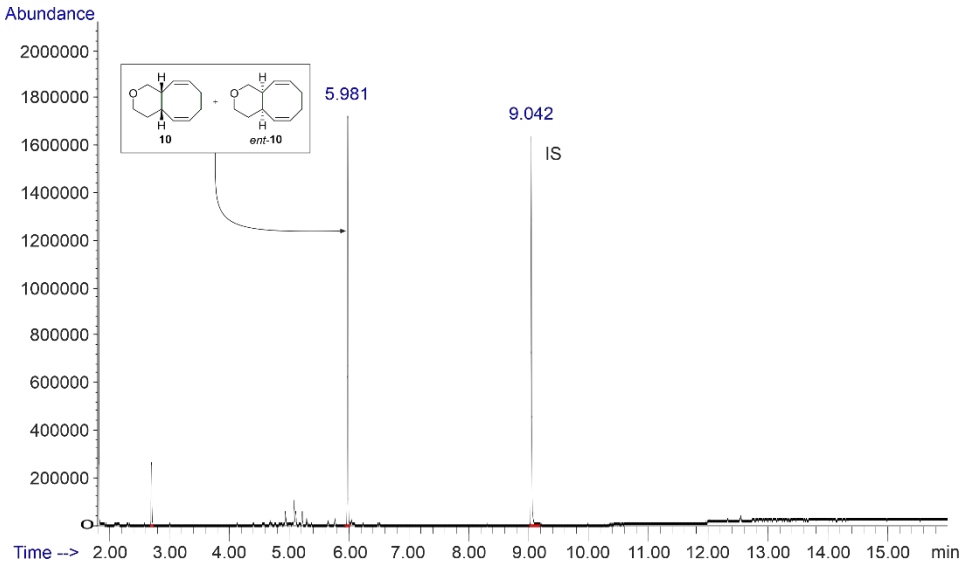

Figure 2.4. Reaction mixture GC-MS of the [4+4] cycloaddition of **1** at micromolar scale using **L14** as ligand. Peak 1: **10**, t^R = 5.981 min. Peak 2: internal standard; t^R = 9.042 min.

- Representative SFC chromatogram

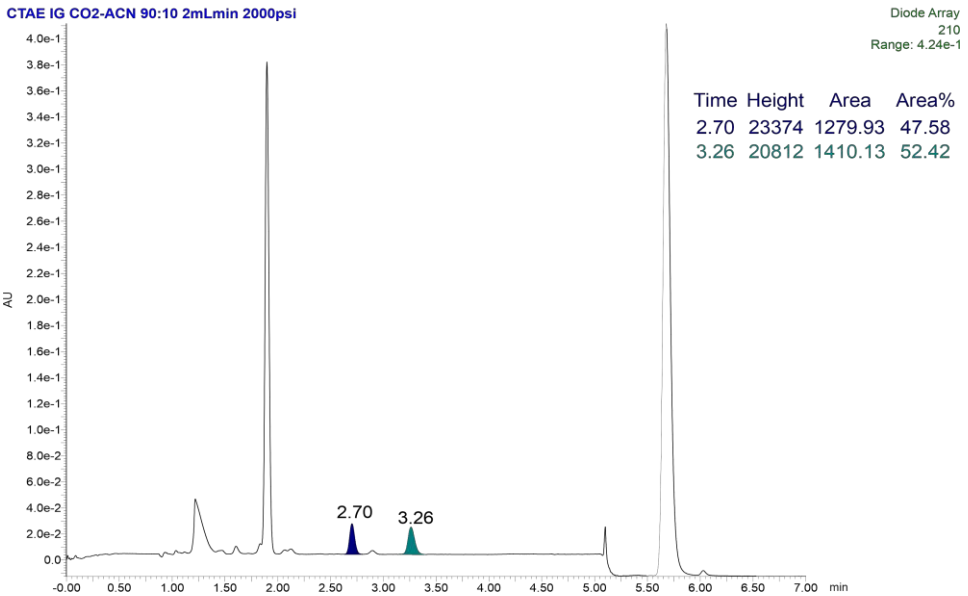

Figure 2.5. Reaction mixture SFC of the [4+4] cycloaddition of **1** at micromolar scale using **L14** as ligand; t^R of **10** and *ent*-**10** 2.70 min and 3.26 min.

2.4.7. Copies of NMR Spectra

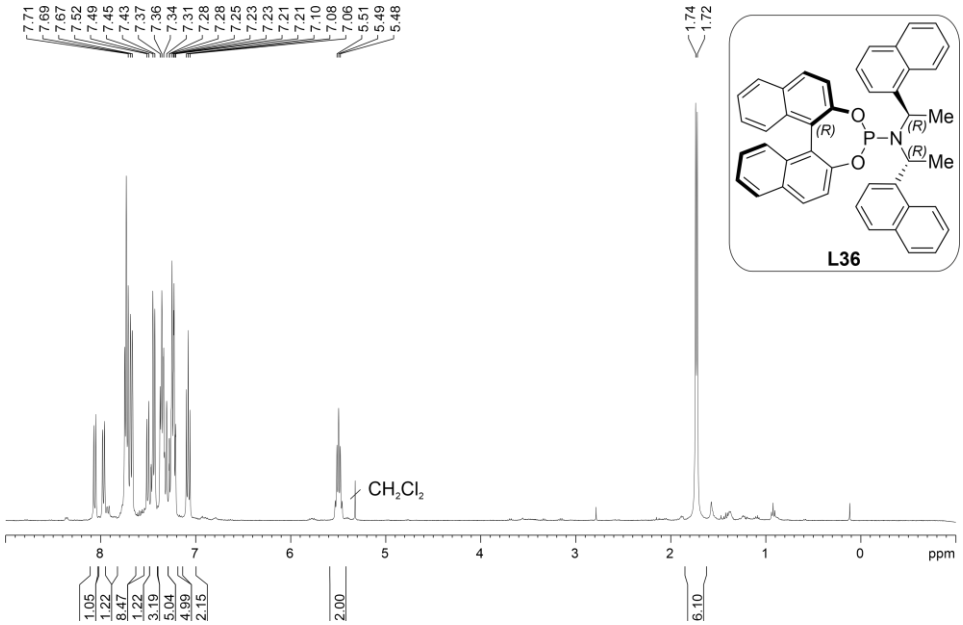

Figure 2.6. ^{1}H NMR spectrum of **L36**.

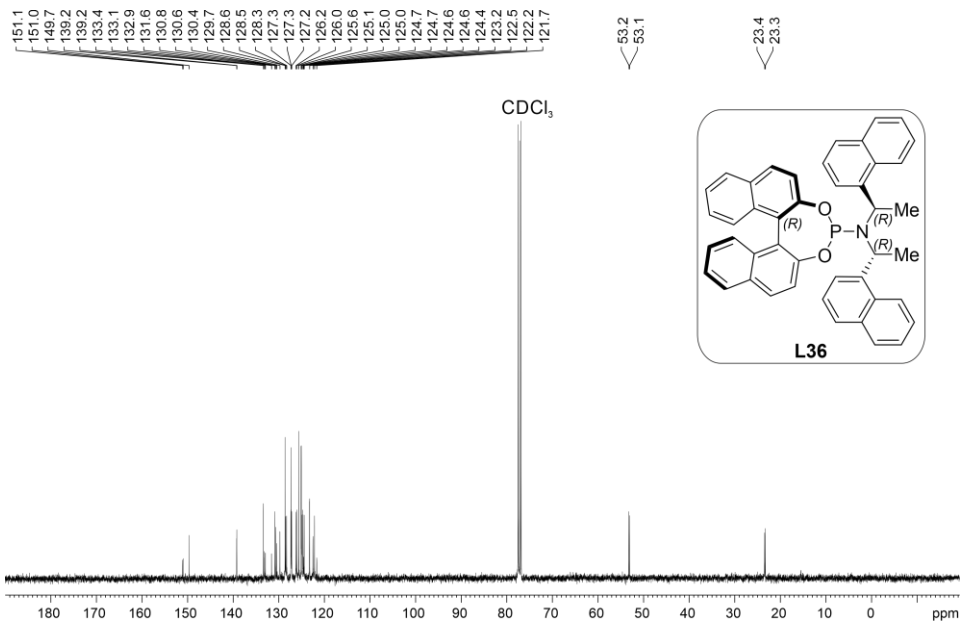

Figure 2.7. ^{13}C{^{1}H} NMR spectrum of **L36**

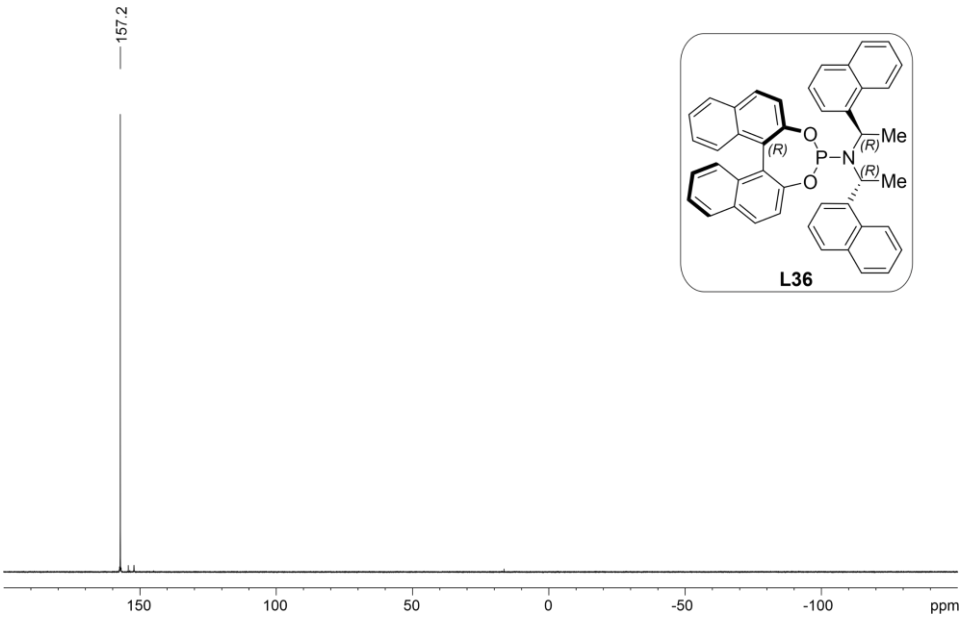

Figure 2.8. $^{31}P\{^{1}H\}$ NMR spectrum of **L36**.

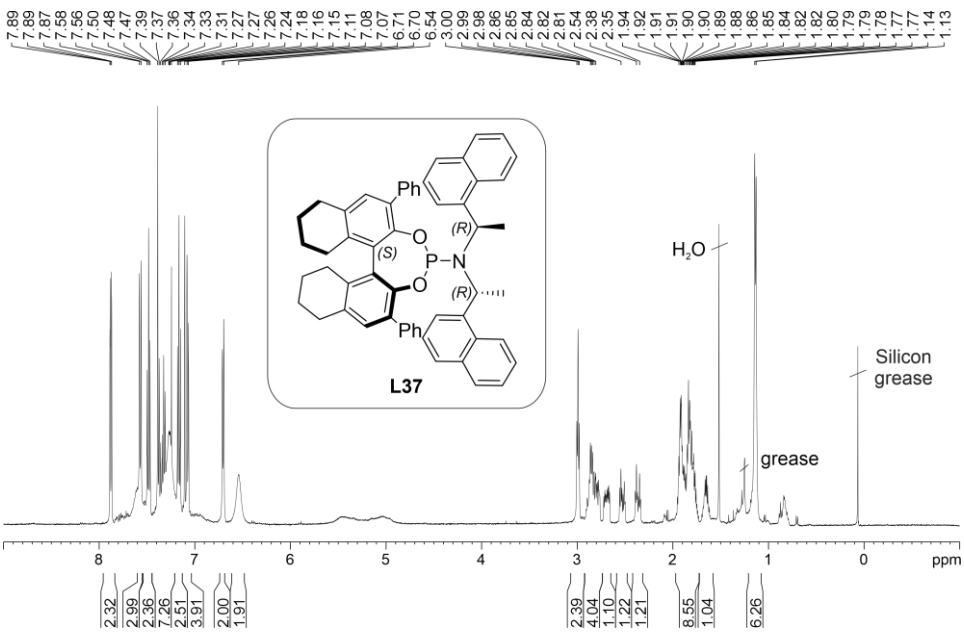

Figure 2.9. ^{1}H NMR spectrum of **L37**.

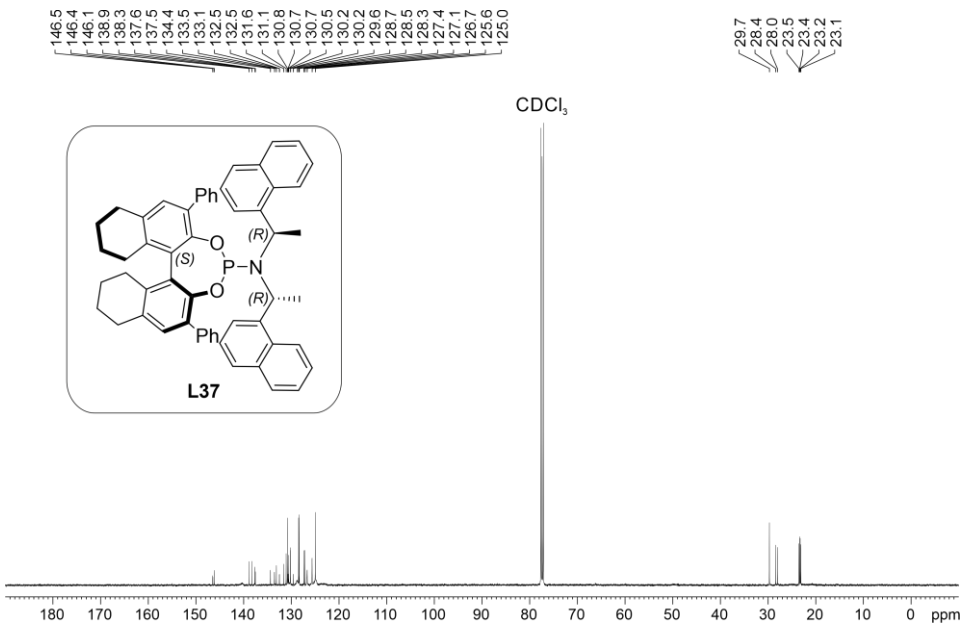

Figure 2.10. $^{13}C\{^{1}H\}$ NMR spectrum of **L37**.

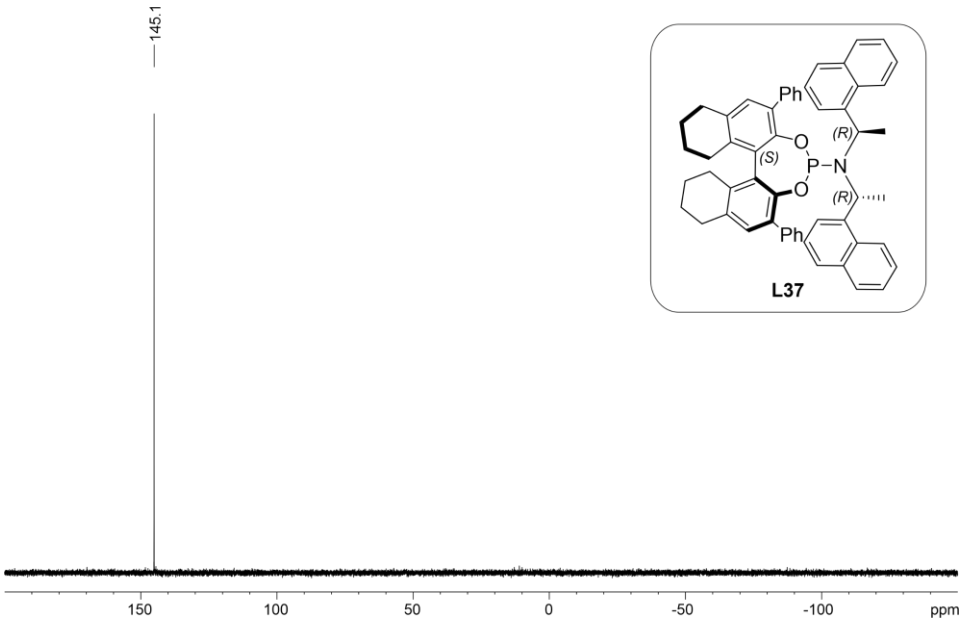

Figure 2.11. $^{31}P\{^{1}H\}$ NMR spectrum of **L37**.

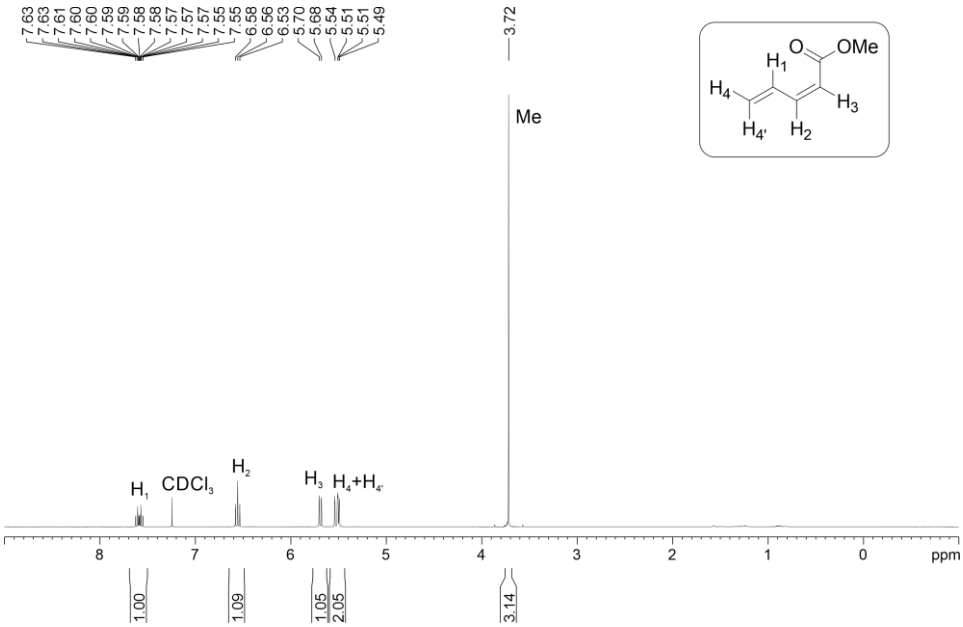

Figure 2.12. ^{1}H NMR spectrum of methyl (*Z*)-penta-2,4-dienoate.

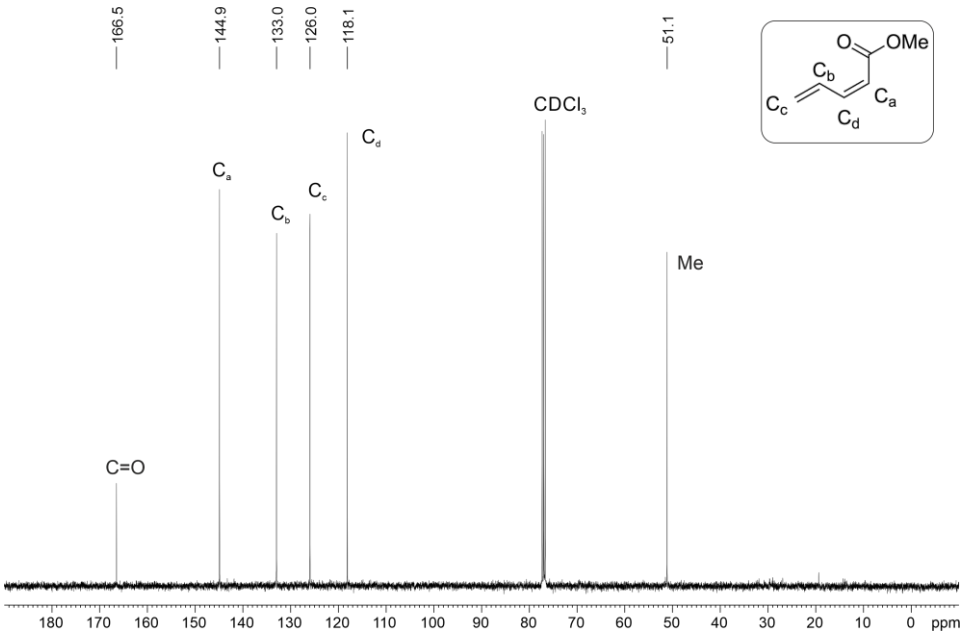

Figure 2.13. ^{13}C{^{1}H} NMR spectrum of methyl (*Z*)-penta-2,4-dienoate.

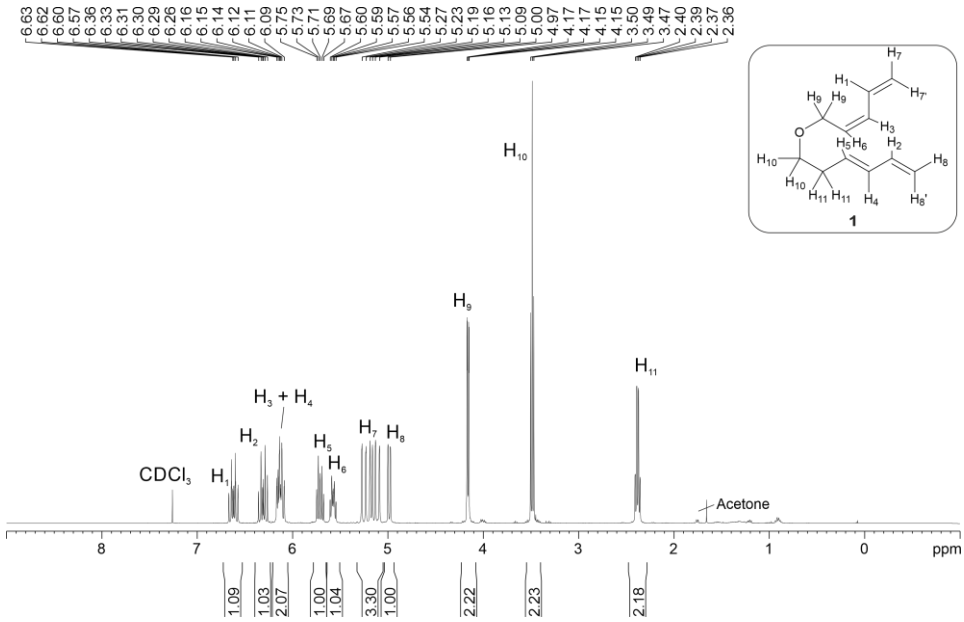

Figure 2.14. ^{1}H NMR spectrum of substrate **1**.

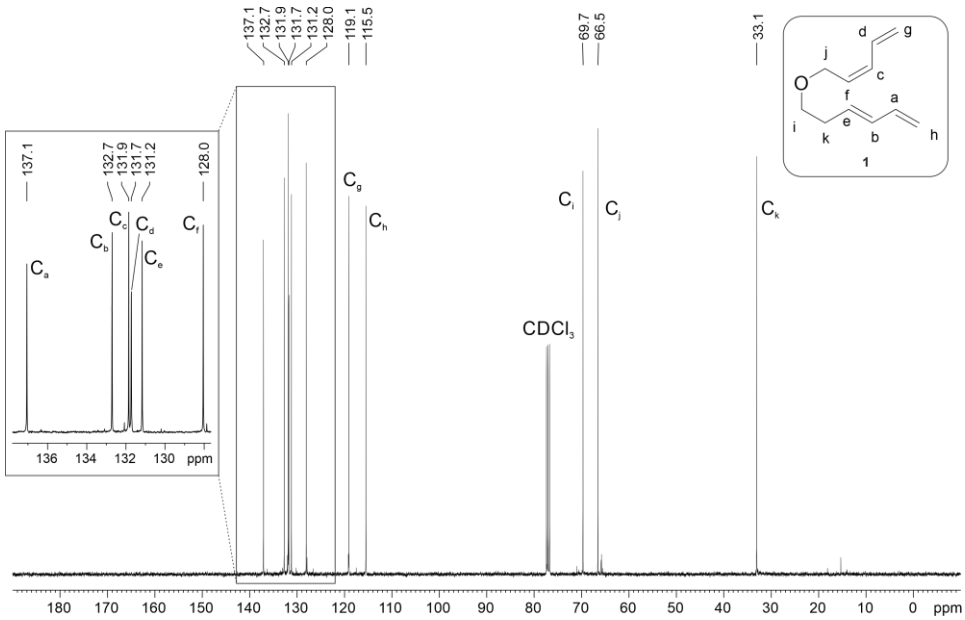

Figure 2.15. ^{13}C{^{1}H} NMR spectrum of substrate **1**.

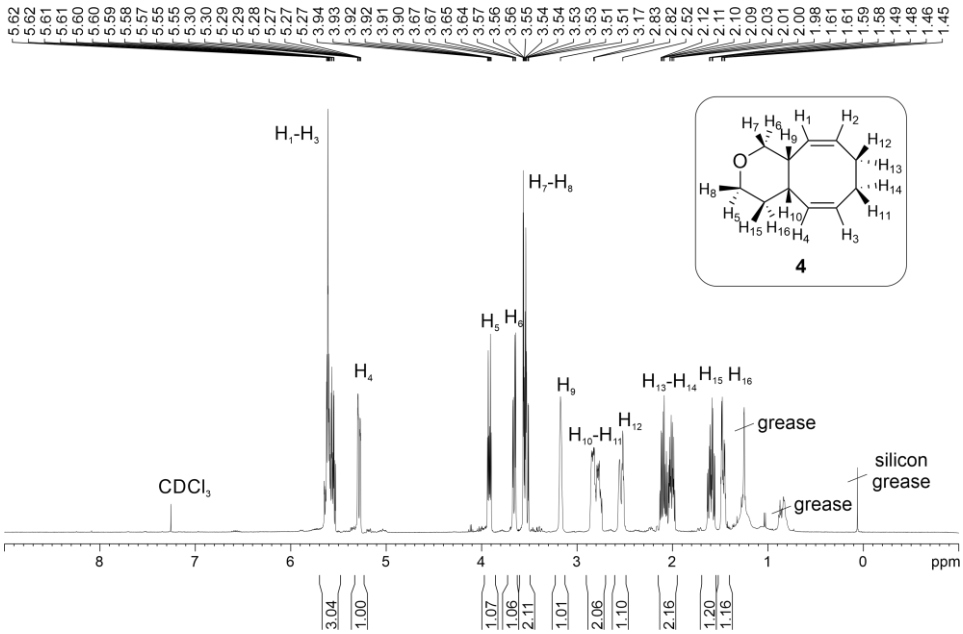

Figure 2.16. ^{1}H NMR spectrum of product **4**.

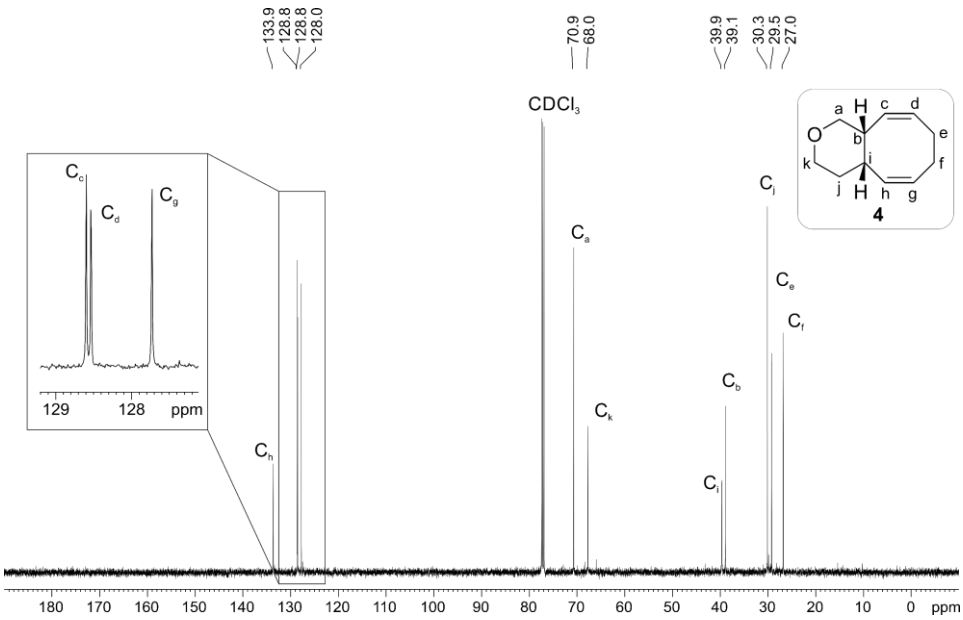

Figure 2.17. ^{13}C{^{1}H} NMR spectrum of product **4**.

CHAPTER 3

Alternative Approaches Towards the Synthesis of Eight-Membered Rings

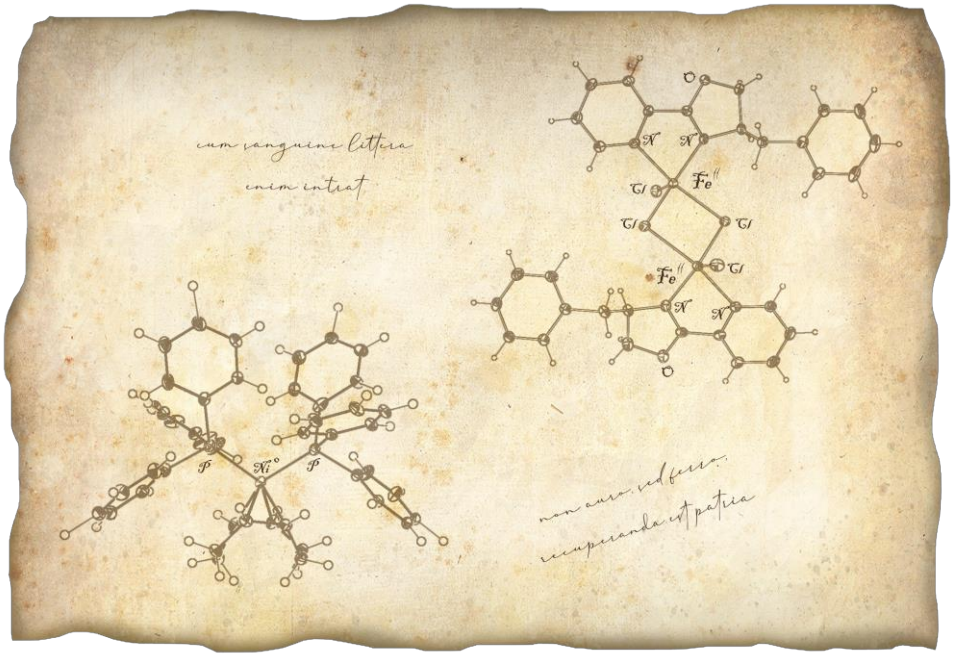

UNIVERSITAT ROVIRA I VIRGILI
TRANSITION METAL-CATALYZED CYCLOADDITION REACTIONS FOR THE FORMATION OF EIGHT- AND SIX-MEMBERED RINGS
Nuria Llorente González

Alternative Approaches Towards the Synthesis of Eight-Membered Rings

3.1. Attempts Towards Nickel-Catalyzed [(4+2)+2] Cycloadditions of 1,3-Dienes, Alkenes and Alkynes

3.1.1 Introduction

High order cycloadditions include a wide and versatile range of reactions that provide a very useful approach to the construction of medium-sized rings. Transition-metal catalyzed processes have proven to be practical approaches in this chemistry.[1] The synthesis of medium-sized rings with defined configurations is an important and challenging tool in organic synthesis, as seven- and eight-membered carbocyclic motifs are present in a wide range of natural products of biological importance.[2] Our group has recently reported efficient catalysts for the Ni-catalyzed intramolecular [4+4] cycloaddition of 1,3-bisdienes in the formation of eight-membered fused rings (Figure 3.1a).[3] However, [4+4] cycloadditions are not the only methodology available to obtain eight-membered carbocycles.

Amongst the different strategies available, [4+2+2] cycloadditions are straightforward transformations that yield eight-membered rings. Two main categories of [4+2+2] cycloadditions have been reported, depending on the nature of the substrates. In the first, the two unconjugated multiple bonds are in the same molecule ([4+(2+2)], Figure 3.1b) and, in the second, only one of the unsaturated C–C bonds is included in the same molecule than the diene fragment, while the other unsaturation is contained in a second molecule ([(4+2)+2], Figure 3.1c). The first type of [4+4+2] cycloadditions has been studied by the groups of

(1) For selected reviews see: (a) Lautens, M.; Klute, W.; Tam, W. *Chem. Rev.* **1996**, *96*, 49-92. (b) Yet, L. *Chem. Rev.* **2000**, *100*, 2963-3007. (c) Wender, P. A.; Croatt, M. P.; Deschamps, N. M. In *Comprehensive Organometallic Chemistry III*; Michael, D.; Mingos, P.; Crabtree, R. H., Eds.; Elsevier Ltd.: Oxford, 2007; Vol. 10, pp 603-647. (d) Inglesby, P. A.; Evans, P. A. *Chem. Soc. Rev.* **2010**, *39*, 2791-2805. (e) Inglesby, P. A.; Evans, P. A. In *Comprehensive Organic Synthesis II*; Second ed.; Knochel, P., Ed.; Elsevier B.V.: Amsterdam, 2014; pp 656-702.
(2) (a) Yu, Z.-X.; Wang, Y.; Wang, Y. *Chem.-Asian J.* **2010**, *5*, 1072-1088. (b) Buono, G.; Clavier, H.; Giordano, L.; Tenaglia, A. In *Stereoselective Multiple Bond-Forming Transformations in Organic Synthesis*; First ed.; Rodriguez, J.; Bonne, D., Eds.; John Wiley & Sons, Inc.: Chichester, 2015; pp 212-240.
(3) See Chapter 1.

Evans[4] or Chung[5] with Rh-complexes as catalysts and by Carbonaro,[6] Lautens[7] and more recently Hilt *et al.*[8] with earth-abundant metal complexes (iron and cobalt) (Figure 3.1b). The second category of cycloadditions, however, has been less studied, with the only examples having been reported by the groups of Wender[9] and Gilbertson[10] (Figure 3.1c).

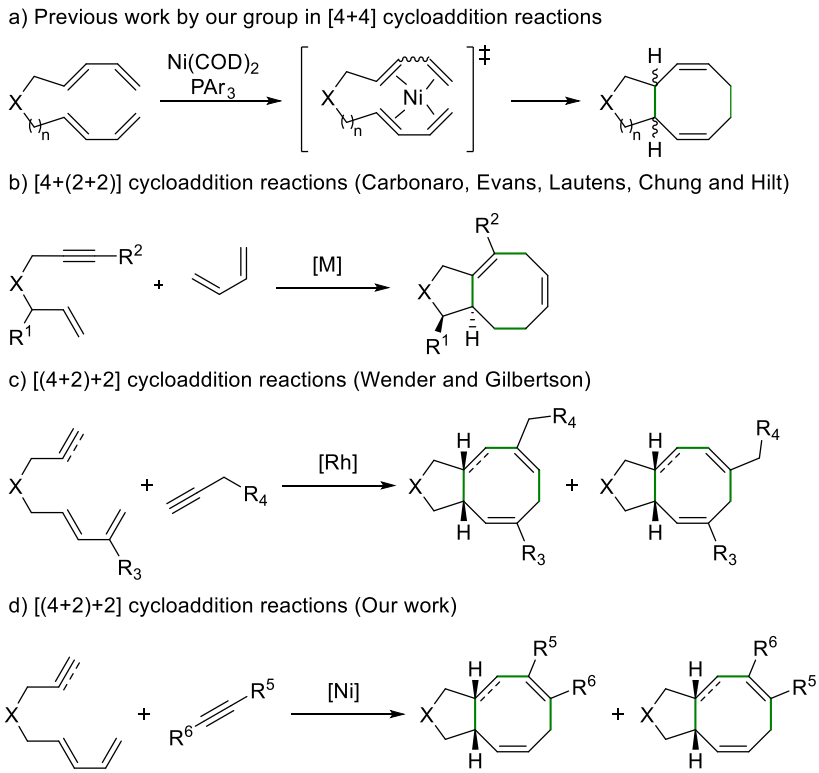

Figure 3.1. [4+2+2] Cycloaddition reactions.

(4) (a) Evans, P. A.; Robinson, J. E.; Baum, E. W.; Fazal, A. N. *J. Am. Chem. Soc.* **2002**, *124*, 8782-8783. (b) Evans, P. A.; Baum, E. W. *J. Am. Chem. Soc.* **2004**, *126*, 11150-11151. (c) Evans, P. A.; Baum, E. W.; Fazal, A. N.; Pink, M. *Chem. Commun.* **2005**, 63-65. (d) Baik, M.-H.; Baum, E. W.; Burland, M. C.; Evans, P. A. *J. Am. Chem. Soc.* **2005**, *127*, 1602-1603.

(5) Lee, S. I.; Park, S. Y.; Chung, Y. K. *Adv. Synth. Catal.* **2006**, *348*, 2531-2539.

(6) (a) Greco, A.; Carbonaro, A.; Dall'Asta, G. *J. Org. Chem.* **1970**, *35*, 271-274. (b) Carbonaro, A.; Cambisi, F.; Dall'Asta, G. *J. Org. Chem.* **1971**, *36*, 1443-1445.

(7) (a) Lautens, M.; Tam, W.; Sood, C. *J. Org. Chem.* **1993**, *58*, 4513-4515. (b) Lautens, M.; Tam, W.; Lautens, J. C.; Edwards, L. G.; Crudden, C. M.; Smith, A. C. *J. Am. Chem. Soc.* **1995**, *117*, 6863-6879.

(8) Hilt, G.; Janikowski, J. *Angew. Chem., Int. Ed.* **2008**, *47*, 5243-5245.

(9) Wender, P. A.; Christy, J. P. *J. Am. Chem. Soc.* **2006**, *128*, 5354-5355.

(10) (a) Gilbertson, S. R.; DeBoef, B. *J. Am. Chem. Soc.* **2002**, *124*, 8784-8785. (b) DeBoef, B.; Counts, W. R.; Gilbertson, S. R. *J. Org. Chem.* **2007**, *72*, 799-804. (c) Canlas, G. M. R.; Gilbertson, S. R. *Chem. Commun.* **2014**, *50*, 3007-5010.

With our background on the study of [4+4] cycloaddition reactions, we decided to tackle the challenge of using nickel complexes as catalysts for [(4+2)+2] cycloaddition reactions between a diene unit tethered to an alkene/alkyne motif in the presence of alkynes (Figure 3.1d).

3.1.2 Results and Discussion

At the onset of our studies, we planned to screen the reaction between substrate **1a** and a broad range of structurally diverse alkynes **2** under the experimental conditions previously studied in our group.[3] The results obtained in this initial screening are summarized in Table 3.1.

Table 3.1: Initial alkyne screening for diene-ene **1a**.[a]

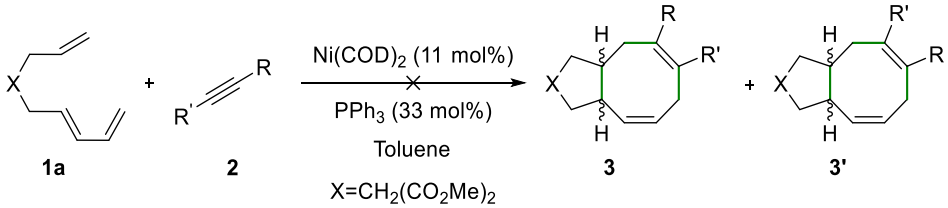

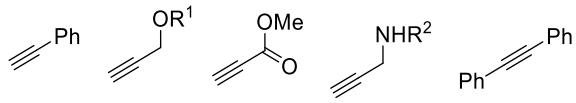

2a **2b** R^1=H, **2c** R^1=Ac, **2d** R^1=Ph, **2e**, **2f** R^2=H, **2g** R^2=Me, **2h**

Entry	Substrate 2	Conv. **1a** (%)[b]	Product 3
1[c]	**2a**	35	n.d.[d]
2	**2a**	42	n.d.
3	**2b**	64	n.d.
4	**2c**	18	n.d.
5	**2d**	33	n.d.
6	**2e**	37	n.d.
7	**2f**	23	n.d.
8	**2g**	22	n.d.
9	**2h**	36	n.d.
10[e]	**2h**	69	n.d.

(a) Conditions (unless otherwise noted): 1 equiv. of **1a**, 1.2 equiv. of **2**, 11.0 mol% [$Ni(COD)_2$] and 33.0 mol% PPh_3 (**L1**) in toluene at 60 °C for 24 h. (b) Calculated by ^1H NMR spectroscopy using 1,3,5-trimethoxybenzene as internal standard. (c) Reaction performed at 25 °C. (d) Not detected. (e) Reaction performed at 100 °C.

The reaction between commercially available aryl alkyne **2a** and model substrate **1a** resulted in a poor conversion with no cycloaddition product being detected (entries 1 and 2, Table 3.1). We then examined monosubstituted alkynes **2b–g** incorporating a potentially coordinating moiety (entries 3 to 8, Table 3.1). Again, the conversion of substrate **1a** was low and no cycloaddition products were detected. Nevertheless, trimers of **2** were detected as byproducts in the crude mixtures.[11] A brief review of the literature showed that monosubstituted acetylenes often undergo trimerization reactions in the presence of Ni catalysts.[12] Thus, disubstituted alkyne **2h** was finally tested but, to our dismay, the results did not improve and **2h** was partially recovered (entry 9, Table 3.1), even when the temperature was increased to 100 °C (entry 10, Table 3.1). Moreover, several alkenes were also tested in this reaction, but no cycloadduct was obtained.[13]

With these results in hand, we then moved to study the effects of the ligand on the reaction outcome between **1a** and a set of electronically diverse monoacetylenes **2d–e** and the disubstituted alkyne **2h** under standard reaction conditions. Three different ligands were tested: two triaryl phosphines (one with electron-withdrawing groups (**L2**) and the other with electron-donating groups (**L3**)) and a trialkyl phosphine (**L4**). The results obtained from this study are shown in Table 3.2. Unfortunately, the nickel catalysts derived from these ligands did not show any activity towards cycloaddition reactions (up to 58% conversion to unidentified products, see entry 2, Table 3.2).[13]

(11) The 1,3,5-substituted phenyl moieties resulting from the trimerization of substrates **2b–g** were detected by both ^{1}H NMR spectroscopy and GC-MS techniques.

(12) For comprehensive reviews, see for example: (a) Yamamoto, K.; Nagae, H.; Tsurugi, H.; Mashima, K. *Dalton Trans.* **2016**, *45*, 17072-17081. (b) Domínguez, G.; Pérez-Castells, J. *Chem. – Eur. J.* **2016**, *22*, 6720-6739, and references therein.

(13) For the synthetic routes of the substrates and further studies on the screening of reaction conditions, see the experimental section.

Table 3.2: Ligand screening for dienene **1a**.[a]

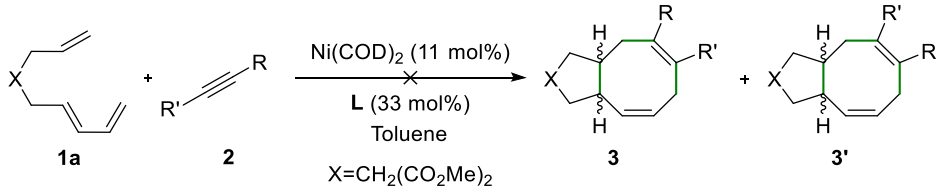

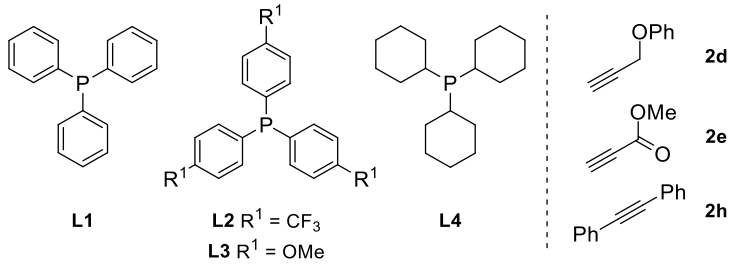

Entry	Substrate 2	Ligand	Conv. **1a** (%)[b]	Product 3
1	2d	L1	33	n.d.[c]
2		L2	58	n.d.
3		L3	46	n.d.
4		L4	41	n.d.
5	2e	L1	37	n.d.
6		L2	51	n.d.
7		L3	47	n.d.
8		L4	53	n.d.
9	2h	L1	36	n.d.
10		L2	43	n.d.
11		L3	39	n.d.
12		L4	45	n.d.

(a) Conditions (unless otherwise noted): 1 equiv. of **1a**, 1.2 equiv. of **2**, 11.0 mol% [$Ni(COD)_2$] and 33.0 mol% **L** in toluene at 60 °C for 24 h. (b) Calculated by ^1H NMR spectroscopy using 1,3,5-trimethoxybenzene as internal standard. (c) Not detected

We then centered our efforts in increasing the reactivity of the dienene unit. As poor results were obtained for substrate **1a**, the new substrate **1b** including an alkyne group instead of a double bond was synthesized.[13] This substrate was subjected to Ni-catalyzed cycloaddition reaction conditions using the same set of ligands than in Table 3.2. The corresponding results are summarized in Table 3.3.

Table 3.3: Ligand screening for dienyne **1b**.[a]

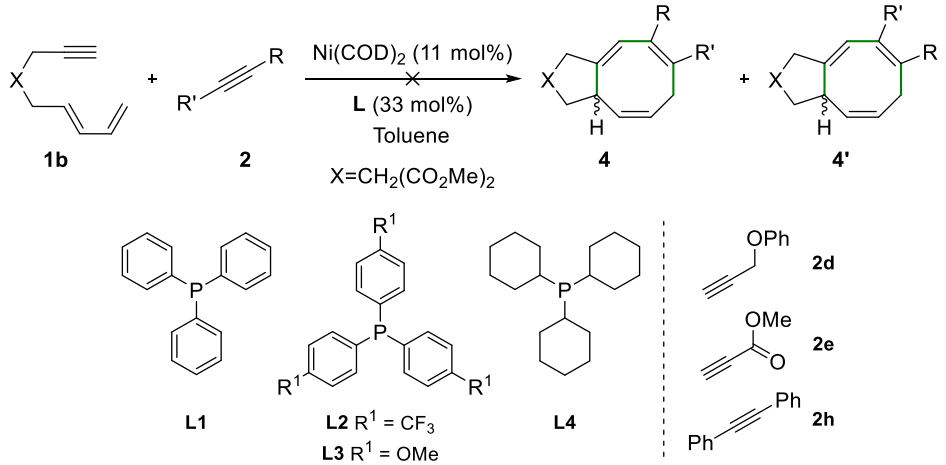

Entry	Substrate 2	Ligand	Conv. 1b (%)[b]	Product 4
1	2d	L1	>99%	n.d.
2		L2	>99%	n.d.
3		L3	>99%	n.d.
4		L4	>99%	n.d.
5	2e	L1	>99%	n.d.
6		L2	>99%	n.d.
7		L3	>99%	n.d.
8		L4	>99%	n.d.
9	2h	L1	>99%	n.d.
10		L2	>99%	n.d.
11		L3	>99%	n.d.
12		L4	>99%	n.d.
13[c]		L1	>99%	n.d.
14[d]		L1	58	n.d.

(a) Conditions (unless otherwise noted): **1** equiv. of **1b**, 1.2 equiv. of **2**, 11.0 mol% [$Ni(COD)_2$] and 33.0 mol% **L** in toluene at 60 °C for 24 h. (b) Calculated by ^1H NMR spectroscopy using 1,3,5-trimethoxybenzene as internal standard. (c) Reaction performed at 25 °C (d) Reaction performed at 0 °C.

As reflected in Table 3.3, the conversion of **1b** towards unidentifiable products was complete in all cases at 60 °C, and even at room temperature (see entry 13, Table 3.3). However, the reaction did not lead to the desired cycloaddition product. In an attempt to minimize the tendency of the substrate towards degradation, the temperature was decreased to 0 °C (see entry 14, Table 3.3). However, this strategy did not translate into the formation of the desired eight-membered product **4**.[13]

Taking into account that the terminal alkyne in substrate **1b** might play a significant role in the degradation reactions previously observed, we then decided to synthesize and examine the reactivity of substrate **1c**, which incorporates a methyl substituent at the terminal position of the alkyne group (Table 3.4).[13]

Table 3.4: Ligand screening for dienyne **1c**.[a]

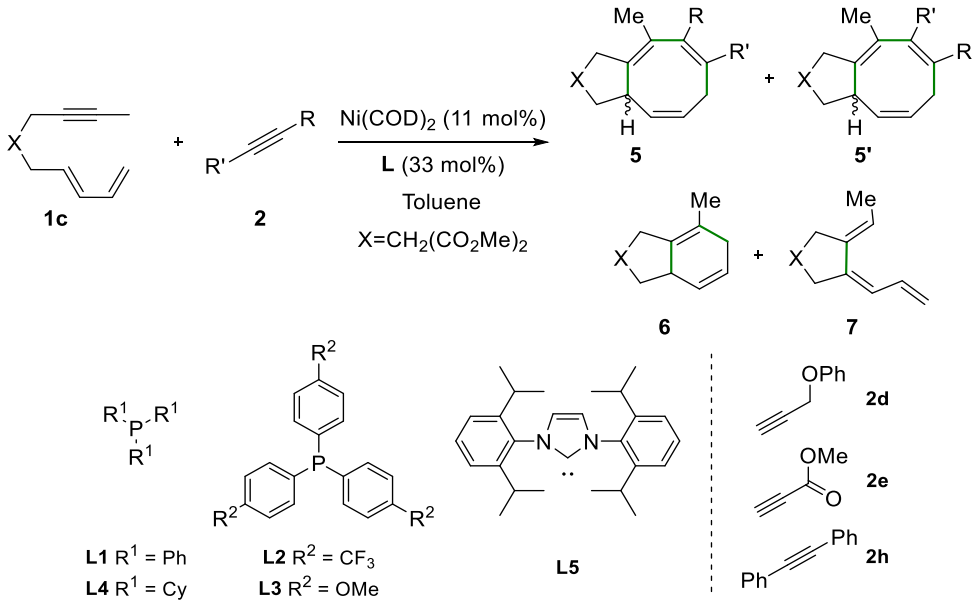

Entry	Substrate 2	Ligand	Conv. 1c (%)[b]	Prod. 5	Prod. 6	Prod. 7
1	2d	L1	>99%	n.d.	n.d.	77%
2		L2	>99%	n.d.	10%	10%
3		L3	>99%	n.d.	n.d.	44%
4		L4	>99%	n.d.	8%	18%
5[c]		L5	>99%	n.d.	37%	n.d.
6	2e	L1	>99%	n.d.	16%	n.d.
7		L2	>99%	n.d.	19%	n.d.
8		L3	>99%	n.d.	4%	12%
9		L4	>99%	n.d.	20%	3%
10[c]		L5	>99%	n.d.	49%	n.d.
11	2h	L1	>99%	n.d.	n.d.	n.d.
12		L2	>99%	n.d.	20%	n.d.
13		L3	>99%	n.d.	n.d.	n.d.
14		L4	>99%	n.d.	n.d.	n.d.
15[c]		L5	>99%	n.d.	55%	n.d.

(a) Conditions (unless otherwise noted): 1 equiv. of **1c**, 1.2 equiv. of **2**, 11.0 mol% [$Ni(COD)_2$] and 33.0 mol% **L** in toluene at 60 °C for 24 h. (b) Calculated by ^1H NMR spectroscopy using 1,2,4,5-tetramethylbenzene as internal standard. (c) The nickel catalyst was pre-formed by stirring a 0.2 M solution of $Ni(COD)_2$ and **L5** in a 1:1 ratio for 6 h (10 mol% of **L5**).

UNIVERSITAT ROVIRA I VIRGILI
TRANSITION METAL-CATALYZED CYCLOADDITION REACTIONS FOR THE FORMATION OF EIGHT- AND SIX-MEMBERED RINGS
Nuria Llorente González

Interestingly, even though our desired eight-membered ring product was not obtained, the results were different from the previous studies. The conversion of substrate **1c** was in all cases complete under these experimental conditions. However, the starting material partially evolved to the cycloaddition product **6** (derived from an intramolecular [4+2] cycloaddition process on **1c**) and monocyclic product **7**, with no traces of the desired cyclooctatriene compounds **5**. As reflected on Table 3.4, the ratio of products **6** and **7** greatly varied depending on the ligand and substrate **2** that were used. For instance, monocyclic product **7** was mostly obtained in a notable 77% yield using PPh_3 **L1** as ligand (see entry 1 in Table 3.4). On the other hand, the [4+2] cycloaddition product **6** was the only product obtained in moderate yields with ligand **L5** (see entry 15 in Table 3.4).

These results encouraged us to expand the screening of the reaction by using HTE[14] techniques with an array of structurally diverse ligands. For this purpose, the cycloaddition of substrates **1c** and **2d** under standard conditions [$Ni(COD)_2$] (11.0 mol%), toluene, 60 ºC, 24 h was examined. The results of assessing several bidentate phosphorus ligands (**L6 – L13**) in this chemistry are summarized in Table 3.5. Unfortunately, [4+4] cycloaddition products were not observed with the nickel catalysts derived from any of the ligands tested. As for cyclic products **6** and **7**, the highest yields were obtained with the alkyl-substituted narrow-bite-angle ligand **L6** (entry 2, Table 3.5).

(14) For more information about our efforts towards enantioselective intramolecular [4+4] cycloadditions and on HTE, see Chapter 2.

Table 3.5: HTE Screening: Bidentate phosphines.

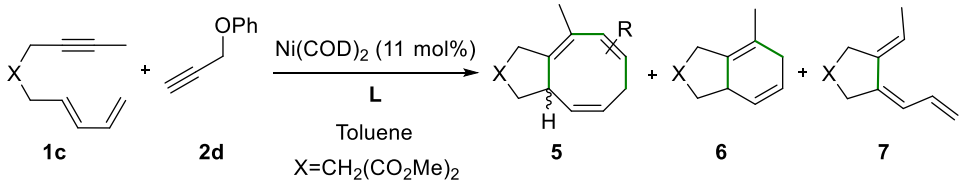

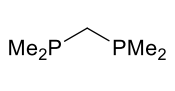

L6

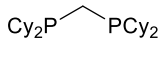

L7

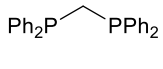

L8

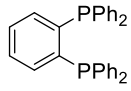

L9

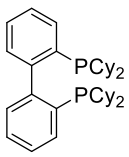

L10

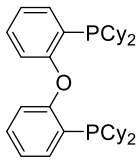

L11

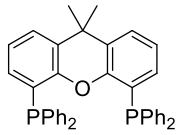

L12

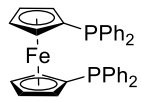

L13

Entry	Ligand		$Ni(COD)_2$ (Equiv.)	Conv. 1c (%)[a]	Yield (%)[a]		
	L	Equiv.			5	6	7
1	L6	0.16	0.11	50	n.d.	8	<1
2	L7	0.16	0.11	98	n.d.	32	35
3	L8	0.16	0.11	62	n.d.	<1	<1
4	L9	0.16	0.11	71	n.d.	<1	<1
5	L10	0.16	0.11	67	n.d.	<1	<1
6	L11	0.16	0.11	94	n.d.	16	21
7	L12	0.16	0.11	98	n.d.	<1	<1
8	L13	0.16	0.11	94	n.d.	10	15

(a) Determined by GC-MS on an achiral stationary phase (HP-5) using 4,4′-dimethoxybiphenyl as internal standard.

Monodentate phosphines (Table 3.6) also mediated the conversion of the starting material, with the desired cycloadduct **5** not being obtained with any of the ligands tested. The byproducts **6** and **7** were obtained in low to moderate yields with ligands **L15**, **L18** and **L19**. It is interesting to note that ligands **L18** and **L19**, which contained cyclohexyl-substituted phosphino groups, were more selective towards the [4+2] cycloaddition product (entries 2, 5 and 6, Table 3.6).

Table 3.6. HTE Screening: Monodentate phosphines.

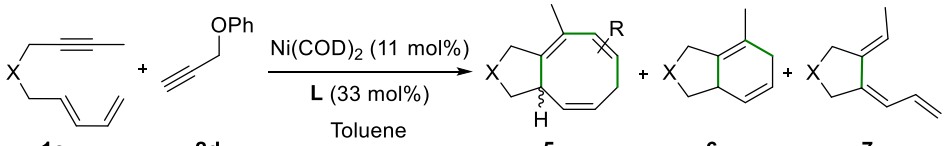

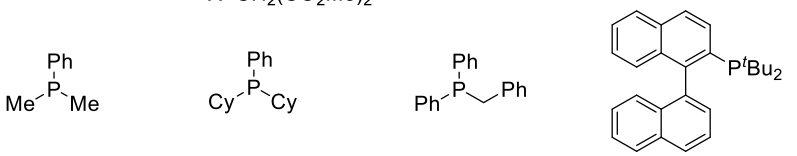

L14 L15 L16 L17

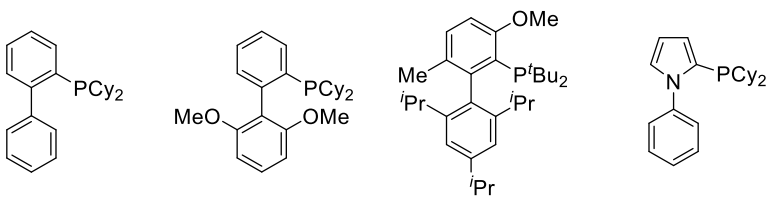

L18 L19 L20 L21

Entry	Ligand		$Ni(COD)_2$ (Equiv.)	Conv. 1c (%)[a]	Product yield (%)[a]		
	L	Equiv.			5	6	7
1	L14	0.33	0.11	74	n.d.	<1	<1
2	L15	0.33	0.11	98	n.d.	12	27
3	L16	0.33	0.11	98	n.d.	<1	<1
4	L17	0.33	0.11	81	n.d.	<1	<1
5	L18	0.33	0.11	97	n.d.	22	<1
6	L19	0.33	0.11	97	n.d.	12	<1
7	L20	0.33	0.11	98	n.d.	<1	<1
8	L21	0.33	0.11	98	n.d.	9	<1

(a) Determined by GC-MS on an achiral stationary phase (HP-5) using 4,4′-dimethoxybiphenyl as internal standard.

Finally, the activity of nickel catalysts derived from phosphinoamines and several other nitrogen-based ligands in this chemistry was also studied with the previously mentioned HTE methodology (Table 3.7). In all cases, important amounts of starting material evolved to unidentified products, without the target [(4+2)+2] cycloaddition product **5** being detected.

Table 3.7: HTE Screening: Phosphinoamines and other nitrogen-based ligands.

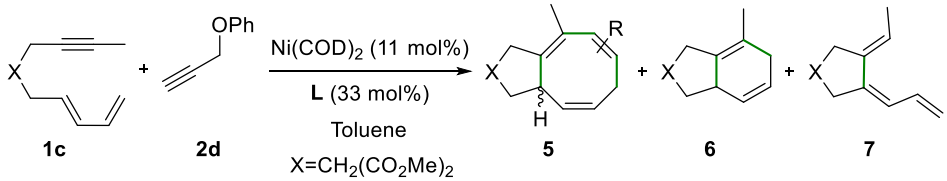

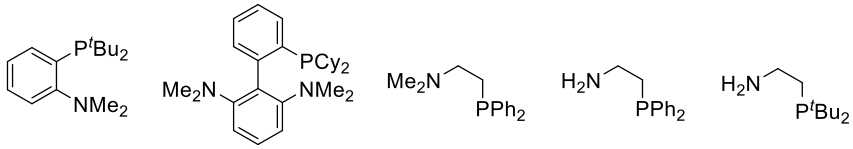

L22 L23 L24 L25 L26

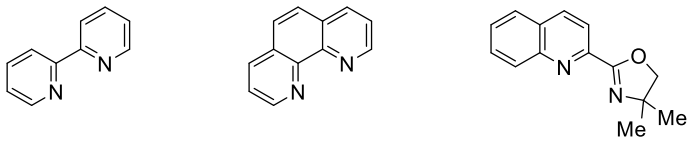

L27 L28 L29

Entry	Ligand		$Ni(COD)_2$ (Equiv.)	Conv. 1c (%)[a]	Product yield (%)[a]		
	L	Equiv.			5	6	7
1	L22	0.16	0.11	77	n.d.	<1	<1
2	L23	0.16	0.11	94	n.d.	<1	<1
3	L24	0.16	0.11	98	n.d.	<1	11
4	L25	0.16	0.11	74	n.d.	<1	<1
5	L26	0.16	0.11	71	n.d.	<1	<1
6	L27	0.16	0.11	98	n.d.	<1	<1
7	L28	0.16	0.11	71	n.d.	<1	<1
8	L29	0.16	0.11	75	n.d.	<1	<1

(a) Determined by GC-MS on an achiral stationary phase (HP-5) using 4,4′-dimethoxybiphenyl as internal standard.

In a last attempt to obtain the target [(4+2)+2] cycloadduct, and as the methyl substituent on the acetylene moiety seemed to us a suitable feature for the reactivity, substrate **2l**[13] was synthesized and tested in this chemistry (Table 3.8). As electron-rich aryl phosphines had proven to be the more active in this chemistry, only **L1** and **L3** were tested.

UNIVERSITAT ROVIRA I VIRGILI
TRANSITION METAL-CATALYZED CYCLOADDITION REACTIONS FOR THE FORMATION OF EIGHT- AND SIX-MEMBERED RINGS
Nuria Llorente González

Table 3.8: Ligand screening for dienyne **1c** and **2l**.[a]

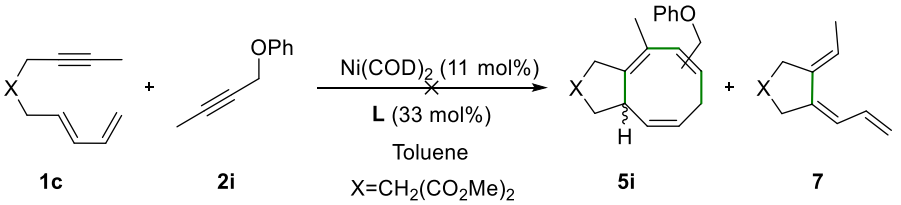

1c **2i** **5i** **7**

Entry	Substrate 2	Ligand	Conv. **1a** (%)[b]	Prod. **5i**	Prod. **7**
1	**2i**	**L1**	58%	n.d.	n.d.
2		**L3**	61%	n.d.	n.d.

(a) Conditions (unless otherwise noted): 1 equiv. of **1c**, 1.2 equiv. of **2i**, 11.0 mol% [$Ni(COD)_2$] and 33.0 mol% **L** in toluene at 60 °C for 24 h. (b) Calculated by ^1H NMR spectroscopy using 1,2,4,5-tetramethylbenzene as internal standard.

To our dismay, neither the desired product **5**, nor byproduct **6** were obtained with any of the ligands tested.

3.1.3 Conclusions

In conclusion, we have explored nickel-catalyzed [(4+2)+2] cycloaddition reactions between a diene unit tethered to an alkene/alkyne group (4+2 carbon component in the cycloaddition process) in the presence of alkynes to yield eight-membered rings. Unfortunately, none of the nickel catalysts derived from the studied ligands mediated the formation of the corresponding [4+4] cycloadducts. Under the assayed experimental conditions, substrates have been mainly transformed into unidentifiable products (probably oligomers/polymers of the starting materials). It is interesting to note that nickel catalysts derived from triphenylphosphine or ligands containing cyclohexyl-substituted phosphino groups led to the corresponding [4+2] cycloadducts and/or other cyclic byproducts.

3.2. Attempts Towards Fe-Catalyzed Intramolecular [4+4] Cycloadditions

3.2.1 Introduction

At the onset of this PhD thesis, the examples of Fe-catalyzed [4+4] cycloaddition reactions were scarce in the literature. Apart from the seminal work of tom Dieck *et al.*[15] on the dimerization of butadiene and isoprene (Figure 3.2a), only one report expanding the study of the mechanism of this process had been published by Ritter and coworkers.[16,17]

a) Fe-catalyzed dimerization of butadiene and isoprene (tom Dieck and Ritter)

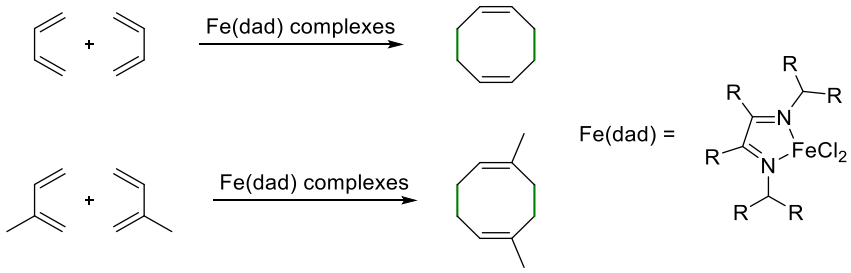

b) Enantioselective version of the Fe-catalyzed [4+4] cycloaddition reaction (tom Dieck)

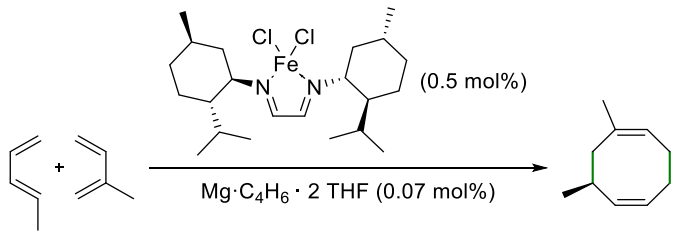

89% Yield, 61% ee

Figure 3.2. Precedents in Fe-catalyzed [4+4] cycloaddition reactions.

(15) (a) tom Dieck, H.; Dietrich, J. *Angew. Chem., Int. Ed. Engl.* **1985**, *24*, 781-783. (b) Mallien, M.; Haupt, E. T. K.; tom Dieck, H. *Angew. Chem., Int. Ed. Engl.* **1988**, *27*, 1062-1064.
(16) Lee, H.; Campbell, M. G.; Hernández Sánchez, R.; Borgel, J.; Raynaud, J.; Parker, S. E.; Ritter, T. *Organometallics* **2016**, *35*, 2923-2929.
(17) In the course of this PhD thesis, two more relevant studies on intermolecular Fe-catalyzed [4+4] cycloaddition reactions were published by Chirik *et al.* For more information, see: (a) Kennedy, C. R.; Zhong, H.; Macaulay, R. L.; Chirik, P. J. *J. Am. Chem. Soc.* **2019**, *141*, 8557-8573. (b) Rosenkoetter, K. E.; Kennedy, C. R.; Chirik, P. J.; Harvey, B. G. *Green Chem.* **2019**, *21*, 5616-5623.

UNIVERSITAT ROVIRA I VIRGILI
TRANSITION METAL-CATALYZED CYCLOADDITION REACTIONS FOR THE FORMATION OF EIGHT- AND SIX-MEMBERED RINGS
Nuria Llorente González

Moreover, only one example of the enantioselective version of this transformation had been published (Figure 3.2b).[18,19]

Considering our experience working with bisdiene substrates, we decided to attempt the development of a catalytic system for the Fe-catalyzed intramolecular [4+4] cycloaddition of bisdienes.

3.2.2 Results and Discussion

We started our studies by designing and synthesizing an Fe-catalyst derived from the enantiopure pyridine-oxazoline ligand **L30**. We reasoned that this ligand could be a good candidate for generating Fe-catalysts for [4+4] cycloadditions due to its similarities with the dad ligands previously reported in the literature.[15] Moreover, ligand **L30** was readily available from enantiopure amino alcohols from the chiral pool. To our delight, employing the method described by the group of tom Dieck for the synthesis of Fe(dad) complexes,[20] dimeric Fe(II) complex **C1** was obtained in high yield (up to 87% yield) by reacting $FeCl_2$ with a slight excess of the pyridine-oxazoline ligand **L30** (Scheme 3.1). Single crystals of the iron complex **C1** suitable for X-ray diffraction were grown and the structure of **C1** was unambiguously confirmed by X-ray diffraction analysis (Figure 3.3).

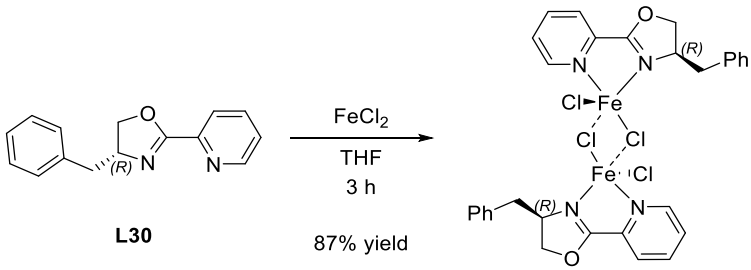

Scheme 3.1. Synthesis of complex **C1**.

It was clear from the literature that Fe-complexes in low oxidation states were needed for our desired transformation to proceed.[15-19] Thus, further studies aimed

(18) Baldenius, K. U.; tom Dieck, H.; König, W. A.; Icheln, D.; Runge, T. *Angew. Chem., Int. Ed. Engl.* **1992**, *31*, 305-307.
(19) A new study on the enantioselective Fe-catalyzed intermolecular [4+4] cycloaddition of 1,3-dienes was published last year by Cramer and *et al.*. For more information, see Braconi, E.; Götzinger, A. C.; Cramer, N. *J. Am. Chem. Soc.* **2020**, *142*, 19819-19824.
(20) tom Dieck, H.; Dietrich, J. *Chem. Ber.* **1984**, *117*, 694-701.

to transform iron(II) complex **C1** into low-valent analogues. Three reducing agents were tested, based on the methods reported in the literature.[16,21]

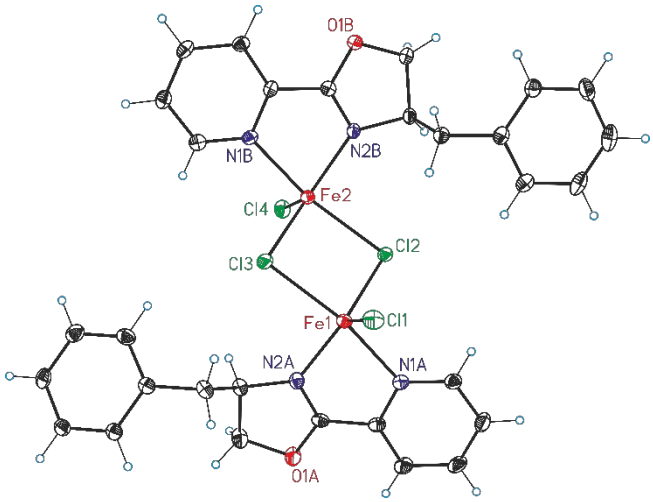

Figure 3.3. X-ray crystal structure of **C1** (ORTEP drawings showing thermal ellipsoids at 50% probability).

As reflected in Table 3.9, all our attempts in detecting the corresponding low oxidation state Fe-complexes derived from **C1** were unsuccessful. In every case, a complex mixture of species was observed, whose components could not be identified by spectroscopic analysis.

(21) (a) Bart, S. C.; Hawrelak, E. J.; Lobkovsky, E.; Chirik, P. J. *Organometallics* **2005**, *24*, 5518-5527. (b) Bouwkamp, M. W.; Bart, S. C.; Hawrelak, E. J.; Trovitch, R. J.; Lobkovsky, E.; Chirik, P. J. *Chem. Commun.* **2005**, 3406-3408.

Table 3.9. Reduction attempts of **C1**.

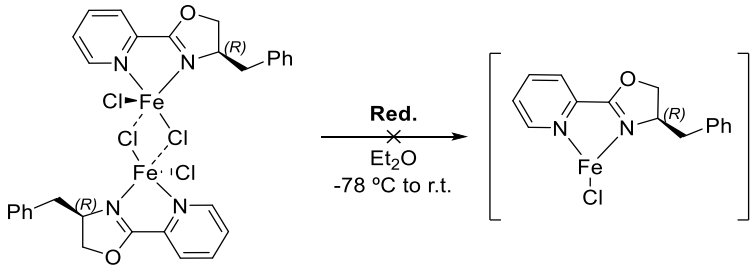

C1 **C2**

Entry	Reducing Agent	Product C2[a]
1	MeMgCl (2 equiv.)	n.d.[b]
2	$NaBHEt_3$ (2 equiv.)	n.d.
3	Mg-Anthracene (6 equiv.)	n.d.

(a) Analyzed with ^{1}H NMR spectroscopy or mass spectrometry. (b) not detected.

Previous studies on the *in situ* preparation and characterization of low-valent iron species relied on the use of the reducing agent (MeMgCl or $NaBHEt_3$) in the presence of a diene molecule.[16] Overall, the unsaturated molecule facilitated the isolation of the complexes $[Fe(diene)_x(ligand)]$ as crystalline solids. Moreover, in their seminal work, tom Dieck and coworkers did not isolate the low-valent iron complex, but synthesized it *in situ*. Thus, we decided to test the Fe-catalyzed intramolecular [4+4] cycloadditions of bisdiene **8** using complex **C1** in combination with the reducing agents previously tested (Table 3.10).

Table 3.10. Fe-Catalyzed intramolecular [4+4] cycloaddition of bisdiene **8**.

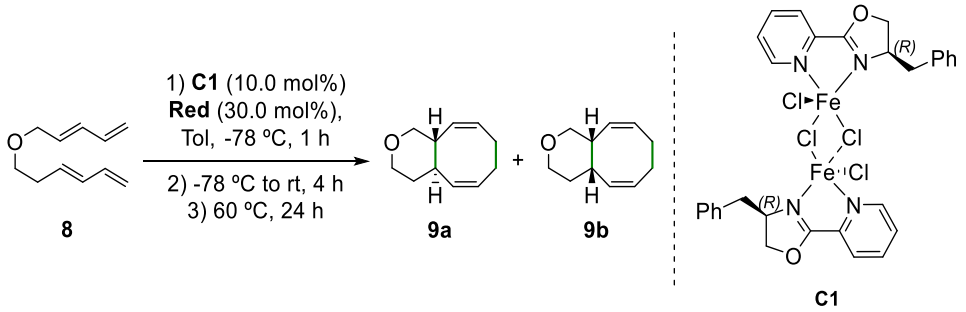

8 **9a** **9b** **C1**

Entry	Reducing Agent	Conv.[a] (%)
1	MeMgCl	<1
2	$NaBHEt_3$	<1
3	Mg-Anthracene	<1

(a) Determined by ^{1}H NMR spectroscopy.

As reflected in Table 3.10, no conversion of the starting material **8** was observed, with unreacted substrate being recovered in all cases. In light of the results obtained, we decided to prioritize other research activities.

3.2.3 Conclusions

A new Fe(II) dimeric complex derived from a pyridine-oxazoline ligand has been efficiently synthesized. The structure of this complex has been unequivocally determined by single crystal X-Ray crystallography. All attempts to isolate low-valent analogous complexes have failed. Attempts to generate *in situ* the low-valent analogous iron complexes as suitable catalysts for [4+4] cycloaddition reactions have also failed.

UNIVERSITAT ROVIRA I VIRGILI
TRANSITION METAL-CATALYZED CYCLOADDITION REACTIONS FOR THE FORMATION OF EIGHT- AND SIX-MEMBERED RINGS
Nuria Llorente González

3.3. Experimental Section

3.3.1 General Remarks

All syntheses were carried out on chemicals as purchased from commercial sources, unless otherwise stated. Air and moisture sensitive manipulations or reactions were run under inert atmosphere using anhydrous and deoxygenated solvents, either in a glove box or with standard Schlenk techniques. All solvents were dried by using a Solvent Purification System (SPS). Silica gel 60 (230–400 mesh) was used for column chromatography. NMR spectra were recorded in $CDCl_3$ unless otherwise cited, on a Bruker Avance 300 MHz, 400 MHz or 500 MHz Ultrashield spectrometers. ^1H NMR and $^{13}C\{^1H\}$ NMR spectroscopy chemical shifts are quoted in ppm relative to residual solvent peaks. High-resolution mass spectra (HRMS) were recorded by using either ESI or APCI ionization methods in positive mode. Conversion, and selectivity for the cycloaddition products were determined by ^1H NMR spectroscopy from the crude mixtures, using 1,3,5-trimethoxybenzene or 1,2,4,5-tetramethylbenzene as internal standard.

3.3.2 Synthesis of Cycloaddition Substrates[22]

- Synthesis of dimethyl (*E*)-2-allyl-2-(penta-2,4-dien-1-yl)malonate (**1a**)

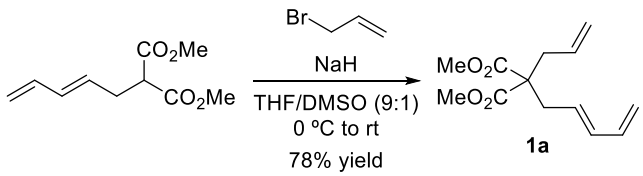

A solution of the previously prepared dimethyl (*E*)-2-(penta-2,4-dien-1-yl)malonate[23] (1.5 g, 7.57 mmol) in anhydrous THF (3.8 mL) was slowly added to a suspension of anhydrous NaH (0.229 mg, 9.08 mmol) in anhydrous DMSO (3.3 mL) and THF (32 mL) at 0 °C. After 30 min at 0 °C, a solution of allyl bromide (0.798 mL, 9.08 mmol) in anhydrous THF (3.8 mL) was slowly added. The resulting mixture was allowed to reach room temperature and stirred overnight. The reaction was then quenched with distilled water (9 mL) and the THF was removed *in vacuo*. The resulting aqueous mixture was diluted with

(22) For the synthesis of substrate **8**, see section 1.4.3, chapter 1.
(23) For the synthesis of dimethyl (*E*)-2-(penta-2,4-dien-1-yl)malonate, see section 1.4.3, chapter 1.

diethyl ether (55 mL), poured into a separatory funnel and the two phases (organic and aqueous) were separated. The aqueous phase was extracted with diethyl ether (2 x 15 mL) and the combined organic layers were washed with brine (2 x 15 mL) and dried over magnesium sulfate. The solvent was evaporated under reduced pressure. Purification by distillation (b.p. = 74 °C, p = 0.04 mbar) gave the desired substrate **1a** as a colorless oil (1.41 g, 78% yield; see Figure 3.6 and Figure 3.7).

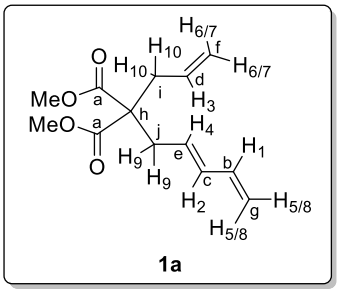

1a

^{1}H NMR (400 MHz, $CDCl_3$) δ 6.26 (dt, $^{3}J_{H1\text{-}H5}$ = 16.8 Hz, $^{3}J_{H1\text{-}H8}$ = $^{3}J_{H1\text{-}H2}$ = 10.4 Hz, 1H, H_1), 6.08 (dd, $^{3}J_{H2\text{-}H4}$ = 15.1 Hz, $^{3}J_{H2\text{-}H1}$ = 10.4 Hz, 1H, H_2), 5.62 (ddt, $^{3}J_{H3\text{-}H6/7}$ = 17.4 Hz, $^{3}J_{H3\text{-}H6/7}$ = 9.6 Hz, $^{3}J_{H3\text{-}H10}$ = 7.4 Hz, 1H, H_3), 5.49 (dt, $^{3}J_{H4\text{-}H2}$ = 15.1 Hz, $^{3}J_{H4\text{-}H9}$ = 7.6 Hz, 1H, H_4), 5.12 – 5.08 (m, 3H, H_5, H_6 and H_7), 5.01 (dd, $^{3}J_{H8\text{-}H1}$ = 10.1 Hz, $^{2}J_{H8\text{-}H5}$ = 1.5 Hz, 1H, H_8), 3.71 (s, 6 H, OMe), 2.66 (d, $^{3}J_{H9\text{-}H4}$ = 7.6 Hz, 2H, H_9), 2.63 (d, $^{3}J_{H10\text{-}H3}$ = 7.4 Hz, 2H, H_{10}) ppm. $^{13}C\{^{1}H\}$ NMR (101 MHz, $CDCl_3$) δ 171.3 (2C, C=O, C_a), 136.7 (CH=, C_b), 135.2 (CH=, C_c), 132.4 (CH=, C_d), 127.8 (CH=, C_e), 119.4 (CH_2=, C_f), 116.6 (CH_2=, C_g), 58.0 (C_{quat}, C_h), 52.5 (2C, CH_3, OMe), 37.2 (CH_2, C_i), 36.0 (CH_2, C_j) ppm. Spectroscopic data were in agreement with those previously reported in the literature.[9]

- Synthesis of dimethyl (*E*)-2-(penta-2,4-dien-1-yl)-2-(prop-2-yn-1-yl)malonate (**1b**)

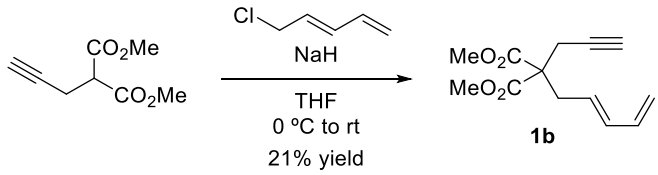

1b

Dimethyl propargylmalonate (0.894 mL, 5.58 mmol) was slowly added to a suspension of NaH (0.169 g, 6.7 mmol) in anhydrous THF (15 mL) under Ar atmosphere at 0 °C and the mixture was stirred at room temperature for 15 min. Then, 5-chloropenta-1,3-diene (0.808 g, 6.7 mmol, 1.2 equiv.) was added dropwise and the mixture was allowed to react at room temperature overnight. Most of the solvent was then removed under vacuum and water (7 mL) and diethyl ether (40 mL) were added into the resulting mixture. The aqueous layer was separated and extracted successively with diethyl ether (2 x 10 mL). The combined organic phases were washed with brine (2 x 10 mL) and dried over

magnesium sulfate. The solvent was removed *in vacuo* and the crude was purified by column chromatography (pentane:diethyl ether 100:0→50:50). The product obtained was distilled (b.p. = 87 °C, p = 0.068 mbar) to afford the target substrate **1b** as a colorless oil (272 mg, 21% yield; see Figure 3.8 and Figure 3.9).

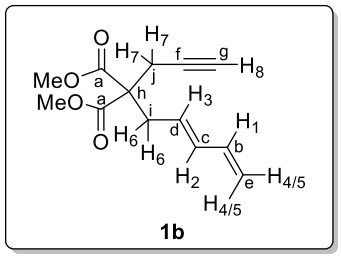

1b

^{1}H NMR (400 MHz, $CDCl_3$) δ 6.28 (dt, $^3J_{H1\text{-}H4}$ = 16.8 Hz, $^3J_{H1\text{-}H5}$ = $^3J_{H1\text{-}H2}$ = 10.2 Hz, 1H, H_1), 6.16 (dd, $^3J_{H2\text{-}H3}$ = 15.1 Hz, $^3J_{H2\text{-}H1}$ = 10.2 Hz, 1H, H_2), 5.48 (dt, $^3J_{H3\text{-}H2}$ = 15.1 Hz, $^3J_{H3\text{-}H6}$ = 7.7 Hz, 1H, H_3), 5.15 (dd, $^3J_{H4\text{-}H1}$ = 16.8 Hz, $^2J_{H4\text{-}H5}$ = 1.3 Hz, 2H, H_4), 5.04 (dd, $^3J_{H5\text{-}H1}$ = 10.2, $^2J_{H5\text{-}H4}$ = 1.3 Hz, 2H, H_5), 3.74 (s, 6 H, OMe), 2.84 (d, $^3J_{H6\text{-}H3}$ = 7.7 Hz, 2H, H_6), 2.79 (d, $^4J_{H7\text{-}H8}$ = 2.7 Hz, 2H, H_7), 2.03 (t, $^4J_{H8\text{-}H7}$ = 2.7 Hz, 1H, H_8) ppm. $^{13}C\{^1H\}$ (101 MHz, $CDCl_3$) δ 170.3 (2C, C=O, C_a), 136.6 (CH=, C_b), 135.8 (CH=, C_c), 127.1 (CH=, C_d), 117.0 (CH_2=, C_e), 78.9 (C≡, C_f), 71.7 (C≡, C_g), 57.2 (C_{quat}, C_h), 52.9 (2C, CH_3, OMe), 35.5 (CH_2, C_i), 23.0 (CH_2, C_j) ppm. Spectroscopic data were in agreement with those previously reported in the literature.[24]

- Synthesis of (2*E*,4*E*)-1-(((*E*)-penta-2,4-dien-1-yl)oxy)hexa-2,4-diene (**1c**)

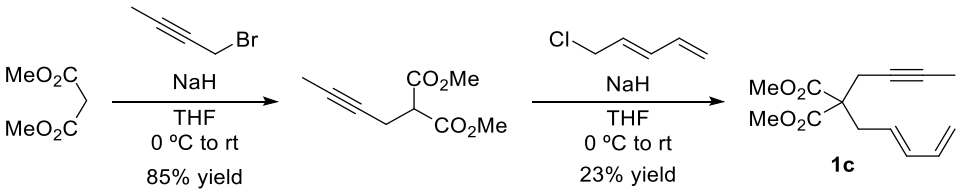

NaH (1.04 g, 60% dispersion in oil, 26.0 mmol) was added in portions to a solution of dimethylmalonate (7.37 mL, 64.5 mmol) and THF (20 mL) at 0 °C. 1-Bromo-2-butyne (2.08 mL, 23.6 mmol) was then slowly added and the solution was stirred for 30 min at this temperature, at which time a white precipitated was formed. The mixture was then warmed to room temperature and stirred for 5 h. Aqueous ammonium chloride (50 mL) was then added slowly and the resulting mixture was extracted with diethyl ether (3 x 100 mL). The organic fractions were washed with brine (3 x 100 mL), dried over magnesium sulfate and the solvent removed *in vacuo*. The crude product was then purified by column chromatography (pentane:diethyl ether 100:0→50:50). The purest

(24) López-Duran, R.; Martos-Redruejo, A.; Buñuel, E.; Pardo-Rodríguez, V.; Cárdenas, D. J. *Chem. Commun.* **2013**, *49*, 10691-10693.

fraction was then purified by distillation (b.p. = 48 °C, p = 0.018 mbar) to yield dimethyl 2-(but-2-yn-1-yl)malonate as a colorless oil (3.71 g, 85% yield). ^{1}H NMR (400 MHz, $CDCl_3$) δ 3.72 (s, 6 H), 3.51 (t, J = 7.7 Hz, 1H), 2.68 (dq, J = 7.7, 2.5 Hz, 2H), 1.70 (t, J = 2.5 Hz, 3H) ppm. ^{13}C{^{1}H} NMR (101 MHz, $CDCl_3$) δ 168.6 (C=O), 77.9 (C≡), 74.6 (C≡), 52.7 (OCH_3), 51.5 (CH), 18.9 (CH_2), 3.5 (CH_3) ppm. Spectroscopic data were in agreement with those previously reported in the literature.[25]

Dimethyl 2-(but-2-yn-1-yl)malonate (1.37 g, 7.44 mmol) was slowly added to a suspension of NaH (0.376 g, 14.9 mmol) in anhydrous THF (31 mL) under Ar atmosphere at 0 °C and the mixture was stirred at room temperature for 15 min. 5-chloropenta-1,3-diene (1.08 g, 22.3 mmol) was then added dropwise and the mixture was allowed to react at room temperature overnight. Most of the solvent was then removed under vacuum and water (15 mL) and diethyl ether (80 mL) were added into the resulting mixture. The aqueous layer was separated and extracted successively with diethyl ether (2 x 20 mL). The combined organic phases were washed with brine (2 x 20 mL) and dried over magnesium sulfate. The solvent was removed *in vacuo*. The crude was purified by column chromatography (pentane:diethyl ether 100:0⟶50:50) and the purest fraction was further purified by distillation (b.p. = 66 °C, p = 0.04 mbar) to yield the desired substrate **1c** as a colorless oil (432 mg, 23% yield; see Figure 3.10 and Figure 3.11).

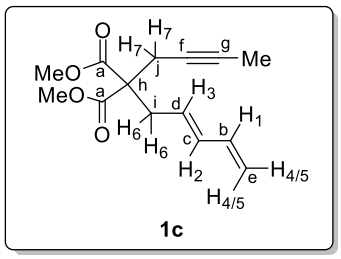

1c

^{1}H NMR (400 MHz, $CDCl_3$) δ 6.24 (dt, $^{3}J_{H1\text{-}H4}$ = 16.8 Hz, $^{3}J_{H1\text{-}H2}$ = $^{3}J_{H5\text{-}H1}$ = 10.5 Hz, 1H, H_1), 6.10 (dd, $^{3}J_{H3\text{-}H2}$ = 15.1 Hz, $^{3}J_{H2\text{-}H1}$ = 10.5 Hz, 1H, H_2), 5.46 (dt, $^{3}J_{H3\text{-}H2}$ = 15.1 Hz, $^{3}J_{H3\text{-}H6}$ = 7.7 Hz, 1H, H_3), 5.10 (dd, $^{3}J_{H4\text{-}H1}$ = 16.8 Hz, $^{2}J_{H4\text{-}H5}$ = 1.7 Hz, 1H, H_4), 4.98 (dd, $^{3}J_{H5\text{-}H1}$ = 10.5 Hz, $^{2}J_{H5\text{-}H4}$ = 1.7 Hz, 1H, H_5), 3.69 (s, 6 H, OMe), 2.77 (d, $^{3}J_{H6\text{-}H3}$ = 7.7 Hz, 2H, H_6), 2.69 (q, $^{5}J_{H7\text{-}Me}$ = 2.5 Hz, 2H, H_7), 1.73 (t, $^{5}J_{Me\text{-}H7}$ = 2.5 Hz, 3H, Me) ppm. ^{13}C NMR (101 MHz, $CDCl_3$) δ 170.5 (2C, C=O, C_a), 136.7 (CH=, C_b), 135.4 (CH=, C_c), 127.6 (CH=, C_d), 116.6 (CH_2=, C_e), 79.0 (C≡, C_f), 73.3 (C≡, C_g), 57.5 (C_{quat}, C_h), 52.7 (CH_3, OMe), 35.5 (CH_2, C_i), 23.3 (CH_2, C_j), 3.5 (CH_3, Me) ppm. Spectroscopic data were in agreement with those previously reported in the literature.[24]

(25) Trost, B. M.; Rudd, M. T. *J. Am. Chem. Soc.* **2005**, *127*, 4763-4776.

UNIVERSITAT ROVIRA I VIRGILI
TRANSITION METAL-CATALYZED CYCLOADDITION REACTIONS FOR THE FORMATION OF EIGHT- AND SIX-MEMBERED RINGS
Nuria Llorente González

- Synthesis of (but-2-yn-1-yloxy)benzene (**2l**)

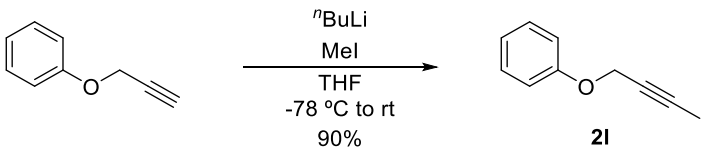

^{n}BuLi (2.5 M in hexanes, 4.54 mL, 11.3 mmol) was added to a solution of phenyl propargyl ether (1.00 mL, 7.6 mmol) in THF (160 mL) at -78 °C. After stirring for 2 h at this temperature, methyl iodine (1.41 mL, 22.7 mmol) was added dropwise and the mixture was then warmed to room temperature and stirred for 1 h. The resulting mixture was diluted with water (120 mL) and extracted with ether (3 x 80 mL). The combined organic layers were washed with brine (2 x 50 mL), dried over magnesium sulfate and concentrated *in vacuo*. The product was purified by silica gel chromatography (pentane:diethyl ether 100:0→80:20) to afford the product **2l** as a colorless oil (989 mg, 90% yield; see Figure 3.12 and Figure 3.13).

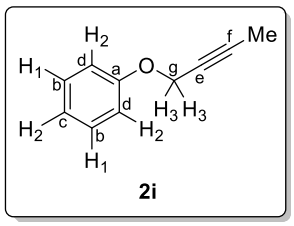

^{1}H NMR (400 MHz, $CDCl_3$) δ 7.33 – 7.29 (m, 2H, H_1), 6.99 – 6.97 (m, 3H, H_2), 4.66 (q, $^{4}J_{H3\text{-}HMe}$ = 2.3 Hz, 2H, H_3), 1.87 (t, $^{4}J_{HMe\text{-}H3}$ = 2.3 Hz, 3H, H_{Me}) ppm. $^{13}C\{^{1}H\}$ NMR (101 MHz, $CDCl_3$) δ 158.0 (C_{arom}, C_a), 129.5 (CH_{arom}, C_b), 121.3 (CH_{arom}, C_c), 115.0 (CH_{arom}, C_d), 83.8 (C≡, C_e), 74.2 (C≡, C_f), 56.5 (CH_2, C_g), 3.8 (CH_3, C_{Me}) ppm. Spectroscopic data were in agreement with those previously reported in the literature.[26]

3.3.3 Synthesis of Pyridine-Oxazoline Ligand (L30) and Complex C1

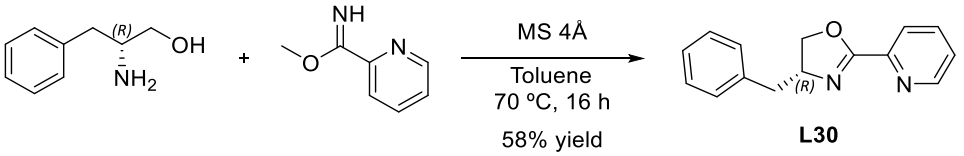

A mixture of methyl picolinimidate (0.509 g, 3.3 mmol), (*R*)-2-amino-3-phenylpropan-1-ol (0.473 g, 3.3 mmol) and 4 Å molecular sieves in anhydrous toluene (8 mL) was stirred in a sealed round bottom flask at 70 °C overnight. The solvent was then evaporated and the target product isolated after

(26) Wang, Y.; Jiang, M.; Liu, J.-T. *Chem. -Eur. J.* **2014**, *20*, 15315-15319.

silica gel column chromatography (cyclohexane:ethyl acetate 50:50, 0:100). The product was obtained as a yellowish oil (456 mg, 58% yield; see Figure 3.14 and Figure 3.15). ^{1}H NMR (500 MHz, $CDCl_3$) δ 8.70 (d, J = 4.8 Hz, 1H), 8.05 (d, J = 7.9 Hz, 1H), 7.81 – 7.74 (m, 1H), 7.39 (ddd, J = 7.5, 4.8, 1.0 Hz, 1H), 7.33 – 7.27 (m, 2H), 7.27 – 7.20 (m, 3H), 4.69 – 4.60 (m, 1H), 4.44 (t, J = 9.0 Hz, 1H), 4.26 – 4.19 (m, 1H), 3.29 (dd, J = 13.8, 5.1 Hz, 1H), 2.76 (dd, J = 13.8, 9.1 Hz, 1H) ppm. ^{13}C{^{1}H} NMR (126 MHz, $CDCl_3$) δ 163.3 (C_q), 149.9 (CH_{arom}), 146.9 (C_{arom}), 137.9 (C_{arom}), 136.7 (CH_{arom}), 129.3 (CH_{arom}), 128.7 (CH_{arom}), 126.7 (CH_{arom}), 125.7 (CH_{arom}), 124.1 (CH_{arom}), 72.6 (CH_2), 68.2 (CH), 41.8 (CH_2) ppm. Spectroscopic data were in agreement with those previously reported in the literature.[27]

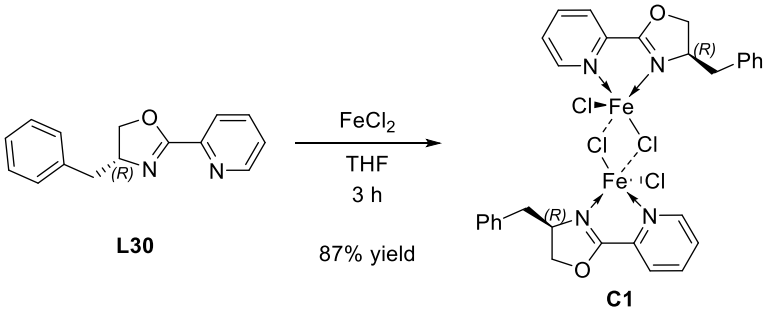

L30 **C1**

In the glove box, a mixture of **L30** (0.349 g, 1.46 mmol) and iron dichloride (0.169 mg, 1.32 mmol) in THF (6 mL) was stirred for 3 h at room temperature. The solvent was then evaporated and the resulting orange solid was washed with diethyl ether (2 x 5 mL) under inert atmosphere and dried under vacuum (423 mg, 87% yield; see Figure 3.16 and section 3.3.6). HRMS (ESI^{+}): m/z calcd for $C_{30}H_{28}ClFeN_4O_2$ [M–$ClFeCl_2$]$^{+}$ 567.1245, found 567.1243.

(27) Frauenlob, R.; McCormack, M. M.; Walsh, C. M.; Bergin, E. *Org. Biomol. Chem.* **2011**, *9*, 6934–6937.

3.3.4 General Methodology for the Cycloaddition Reactions

- Ni-catalyzed [(4+2)+2] cycloaddition reactions

$Ni(COD)_2$ (0.11 mmol) was added dropwise under inert atmosphere from a stock solution in anhydrous toluene to a solution of the substrate **1** (1.00 mmol) and ligand (0.33 mmol) in anhydrous and deoxygenated toluene. Substrate **2** (1.20 mmol) was then added dropwise. The resulting mixture was carefully heated at 60 °C under argon atmosphere and stirred for 24 h. After that, the reaction mixture was allowed to reach room temperature and left stirring under air for 1 h The mixture was filtered through a short pad of silica and further eluted with diethyl ether. The filtrate was concentrated *in vacuo* and the resulting crude mixture was analyzed by NMR spectroscopy.

- [(4+2)+2] Cycloadditions at the micromolar scale (HTE Screening).

A 24-well plate was set up with the corresponding number of 0.1 mL reaction vessels and magnetic stirring bars and dried in the oven at 120 °C overnight. Then, in a nitrogen-filled glove box, 0.2 μmol of each ligand were added from a stock solution in THF to the corresponding reaction vessel. The solvent was removed with a Genevac© centrifugal evaporator. The ligands were redissolved in anhydrous and deoxygenated toluene (0.1 M) and substrate **1c** (6.06 μmol) was added from a stock solution in toluene (0.606 M). $Ni(COD)_2$ (0.95 μmol) from a stock solution in toluene (0.033 M) and substrate **2d** (12.12 μmol) from a stock solution (1.21 M) in toluene were subsequently added. The plate was then sealed with a PFA mat under inert atmosphere, taken out of the glove box, carefully heated at 60 °C and stirred for 24 h. After that, the reaction mixture was allowed to reach room temperature and left stirring under air for 1 h. The mixtures were filtered in parallel through a short pad of silica and further eluted with diethyl ether (750 μL). A stock solution of 4,4′-dimethoxybiphenyl (500 μL, 5·mM) was added to the mixture. A 75 μL aliquot of each resulting solution was further diluted with ACN (425 μL) and these samples were analyzed by GC-MS with 4,4′-dimethoxybiphenyl as internal standard to determine the conversion and yield. The results obtained are shown in Table 3.5 to Table 3.7 in the results and discussion section.

GC analysis conditions for the [(4+2)+2] cycloaddition products of **1c** and **2d** (Figure 3.5): Yield and conversion were determined by GC analysis with an HP-5 column (5% phenyl methyl siloxane; 30 m x 250 μm x 0.25 μm). Carrier gas: He; pressure: 13.4 psi. Injection volume: 2 μL; split ratio: 20:1; injector temperature: 280 °C. Flow rate: 1.5 mL/min; temperature program: 60 °C, 20 °C/min to 300 °C (4 min). Retention times: 7.14 min for substrate **1c**; 7.90 min for byproduct **7**; 7.98 min for byproduct **6**.

- Fe-catalyzed [4+4] cycloaddition reactions

In a glove box under inert atmosphere, a solution of substrate **8** (0.202 mmol) and **C1** (0.05 mmol) in anhydrous and deoxygenated toluene (0,1 M) was prepared. Then, the solution was taken out of the glove box and cooled down to -78 °C and the reducing agent (0.30 mmol) was added dropwise. The reaction was stirred at -78 °C for 1 h, allowed then to slowly reach room temperature and, finally, stirred at 60 °C overnight. After that, the reaction mixture was cooled down to room temperature and left stirring under air for 1 h. The mixture was filtered through a short pad of silica and further eluted with diethyl ether. The filtrate was evaporated *in vacuo* and the resulting crude mixture was analyzed by ^{1}H NMR spectroscopy.

3.3.5 Characterization of the Cycloaddition Byproducts

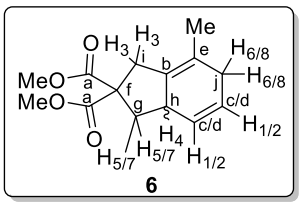

6

Product **6** was obtained following the general procedure for the Ni-catalyzed [(4+2)+2] cycloadditions starting from substrates **1c** (104.0 mg, 0.416 mmol) and **2e** (41.9 mg, 0.499 mmol), **L5** (17.8 mg, 0.0457 mmol) and Ni(COD)$_2$ (12.8 mg, 0.0457 mmol) after column chromatography on silica gel (pentane:diethyl ether 100:0⟶50:50) as colorless oil in a 47% yield (48.7 mg, 0.195 mmol) (See Figure 3.17 and Figure 3.18). ^{1}H NMR (400 MHz, $CDCl_3$) δ 5.80 – 5.68 (m, 2H, H_1 and H_2), 3.73 (s, 3H, OMe), 3.70 (s, 3H, OMe), 3.06 – 2.89 (m, 2H, H_3), 2.89 – 2.79 (m, 1H, H_4), 2.68 – 2.64 (m, 1H, H_5), 2.61 (dd, $^2J_{H6\text{-}H8}$ = 12.5 Hz, $^3J_{H6\text{-}H1/2}$ = 6.9 Hz, 1H, H_6), 2.53 – 2.38 (m, 1H, H_7), 1.74 (t, $^2J_{H6\text{-}H8}$ = 12.5 Hz, 1H, H_8), 1.63 (s, 3H, Me) ppm. ^{13}C{^{1}H} NMR (101 MHz, $CDCl_3$) δ 173.0 (C=O, C_a), 172.6 (C=O, C_a), 131.2 (C=, C_b), 126.8 (CH=, C_c), 125.7 (CH=, C_d), 122.7 (C=, C_e), 57.8 (C_{quat}, C_f), 52.9 (CH_3, OMe), 52.8 (CH_3, OMe), 40.1 (CH_2, C_g) 39.7 (CH, C_h), 36.1 (CH_2, C_i), 32.7 (CH_2, C_j), 18.9 (CH_3, Me) ppm. HRMS (ESI$^+$): *m/z* calcd for $C_{14}H_{18}O_4$ $[M+Na]^+$ 273.1097, found 273.1109.

UNIVERSITAT ROVIRA I VIRGILI
TRANSITION METAL-CATALYZED CYCLOADDITION REACTIONS FOR THE FORMATION OF EIGHT- AND SIX-MEMBERED RINGS
Nuria Llorente González

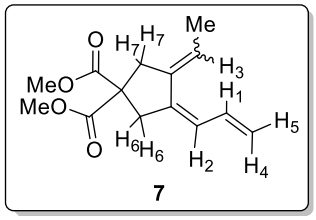

7

Product **7** was obtained following the general procedure for the Ni-catalyzed [(4+2)+2] cycloadditions starting from substrates **1c** (122.0 mg, 0.487 mmol) and **2d** (77.4 mg, 0.585 mmol), **L3** (57.8 mg, 0.161 mmol) and $Ni(COD)_2$ (15.0 mg, 0.0536 mmol) after two subsequent column chromatography purifications: the first one over SiO_2 (pentane:diethyl ether 100:0→50:50), and the purest fraction resulting from this separation was further purified by silica gel impregnated with silver nitrate (10%) (pentane:diethyl ether (100:0→50:50) to obtain product **7** as a colorless oil in a 4% yield (4.9 mg, 0.0196 mmol) (See Figure 3.19). ^{1}H NMR (400 MHz, $CDCl_3$) δ 6.48 (ddd, $^3J_{H1\text{-}H4}$ = 16.7 Hz, $^3J_{H1\text{-}H5}$ = $^3J_{H1\text{-}H2}$ = 10.6 Hz, 1H, H_1), 6.32 (d, $^3J_{H2\text{-}H1}$ = 10.6 Hz, 1H, H_2), 5.95 (q, $^3J_{H3\text{-}HMe}$ = 7.2 Hz, 1H, H_3), 5.20 (d, $^3J_{H4\text{-}H1}$ = 16.7 Hz, 1H, H_4), 5.09 (d, $^3J_{H5\text{-}H1}$ = 10.6 Hz, 1H, H_5), 3.74 (s, 6 H, H_{OMe}), 3.14 (s, 2H, H_6), 3.00 (s, 2H, H_7), 1.74 (d, $^3J_{HMe\text{-}H3}$ = 7.2 Hz, 3H, H_{Me}) ppm.

3.3.6 Single Crystal X-Ray Structure Determinations

Crystal preparation: Crystals of **C1** were grown by slow diffusion of pentane into solutions in dichloromethane. The measured crystals were prepared under inert conditions immersed in perfluoropolyether as protecting oil for manipulation.

Data collection: Crystal structure determination of **C1** was carried out using an Apex DUO Kappa 4-axis goniometer equipped with an APPEX 2 4K CCD area detector, a Microfocus Source E025 IuS using MoK_α radiation (0.71073 Å), Quazar MX multilayer Optics as monochromator and a Oxford Cryosystems low temperature device Cryostream 700 plus (T = -173 °C). Full-sphere data collection was used with ω and φ scans. *Programs used:* Data collection APEX-2,[28] data reduction Bruker Saint[29] V/.60A and absorption correction SADABS.[30]

Structure Solution and Refinement: The crystal structure solution was achieved using the computer program SHELXT.[31] Visualization was performed

(28) Data collection with APEX II v2014.9-0. Bruker (2014). Bruker AXS Inc., Madison, Wisconsin, USA.
(29) Data reduction with Bruker SAINT+ version V8.35A. Bruker (2013). Bruker AXS Inc., Madison, Wisconsin, USA.
(30) SADABS: V2012/1 Bruker (2001). Bruker AXS Inc., Madison, Wisconsin, USA. See the following reference: Blessing, R. H. *Acta Cryst.* **1995**, *A51*, 33-38.
(31) For SHELXT, see the following reference: Sheldrick, G. M. *Acta Cryst.* **2015**, *A71*, 3-8.

with the program SHELXle.[32] Missing atoms were subsequently located from difference Fourier synthesis and added to the atom list. Least-squares refinement on F^2 using all measured intensities was carried out using the program SHELXL 2015.[33] All non-hydrogen atoms were refined including anisotropic displacement parameters.

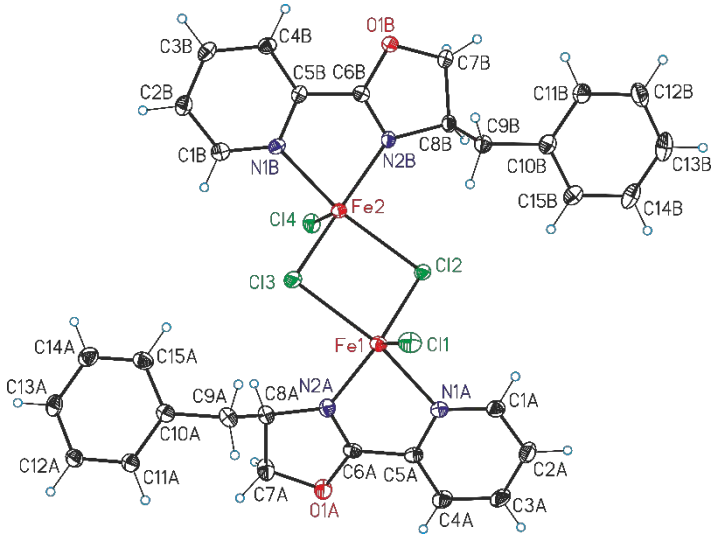

Figure 3.4. X-ray crystal structure of **C1** (ORTEP drawings showing thermal ellipsoids at 50% probability).

Empirical formula	$C_{30}H_{28}Cl_4Fe_2N_4O_2$	
Formula weight	730,06	
Temperature	100(2)K	
Wavelength	0.71073 Å	
Crystal system	triclinic	
Space group	P 1	
Unit cell dimensions	a = 8.9774(7)Å	α = 74.0643(19)°
	b = 9.1616(7)Å	β = 68.5924(19)°
	c = 11.6403(9)Å	γ = 62.1448(18)°
Volume	781.74(11) $Å^3$	
Z	1	
Density (calculated)	1.551 Mg/m^3	
Absorption coefficient	1.305 mm^{-1}	
F(000)	372	
Crystal size	0.200 x 0.100 x 0.100 mm^3	

(32) For SHELXle, see the following reference: Hübschle, C. B.; Sheldrick, G. M.; Dittrich, B. *J. Appl. Cryst.* **2011**, *44*, 1281-1284.
(33) For SHELXL, see the following reference: Sheldrick, G. M. *Acta Cryst.* **2015**, *C71*, 3-8.

Theta range for data collection	1.894 to 30.647°.
Index ranges	-9<=h<=12,-12<=k<=13,-11<=l<=16
Reflections collected	9874
Independent reflections	5732[R(int) = 0.0217]
Completeness to theta =30.647°	93,60%
Absorption correction	Multi-scan
Max. and min. transmission	0.74 and 0.63
Refinement method	Full-matrix least-squares on F^2
Data / restraints / parameters	5732/ 3/ 379
Goodness-of-fit on F^2	1,027
Final R indices [I>2sigma(I)]	R1 = 0.0379, wR2 = 0.1034
R indices (all data)	R1 = 0.0402, wR2 = 0.1066
Largest diff. peak and hole	1.203 and -0.831 e.Å^{-3}

Bond lengths [Å]	
O1-C13	1.2024(9)
O2-C13	1.3430(9)
O2-C14	1.4460(9)
O3-C15	1.2043(9)
O4-C15	1.3419(9)
O4-C16	1.4444(10)
C1-C15	1.5273(10)
C1-C13	1.5324(10)
C1-C2	1.5381(10)
C1-C12	1.5456(10)
C2-C3	1.5265(11)
C3-C4	1.5322(10)
C4-C5	1.5072(10)
C4-C11	1.5430(10)
C5-C6	1.3345(11)
C6-C7	1.5063(12)
C7-C8	1.5406(12)
C8-C9	1.5052(12)
C9-C10	1.3377(11)
C10-C11	1.5114(10)
C11-C12	1.5442(10)

Bond angles [°]	
N2A-Fe1-N1A	75.32(13)
N2A-Fe1-Cl1	123.02(10)
N1A-Fe1-Cl1	97.19(9)
N2A-Fe1-Cl2	125.44(10)
N1A-Fe1-Cl2	92.50(9)
Cl1-Fe1-Cl2	111.08(4)
N2A-Fe1-Cl3	88.86(9)
N1A-Fe1-Cl3	159.64(9)
Cl1-Fe1-Cl3	102.22(4)
Cl2-Fe1-Cl3	86.26(3)
N2B-Fe2-N1B	75.47(12)
N2B-Fe2-Cl4	119.71(10)
N1B-Fe2-Cl4	101.38(9)
N2B-Fe2-Cl3	130.51(10)
N1B-Fe2-Cl3	88.46(9)
Cl4-Fe2-Cl3	109.18(4)
N2B-Fe2-Cl2	90.53(9)
N1B-Fe2-Cl2	155.62(9)
Cl4-Fe2-Cl2	102.91(4)
Cl3-Fe2-Cl2	85.67(3)
Fe1-Cl2-Fe2	93.92(3)
Fe2-Cl3-Fe1	94.12(3)
N1A-C1A-C2A	122.6(4)
C3A-C2A-C1A	119.4(4)
C2A-C3A-C4A	118.8(4)
C5A-C4A-C3A	118.0(4)
N1A-C5A-C4A	123.6(4)
N1A-C5A-C6A	112.4(3)
C4A-C5A-C6A	124.0(3)
N2A-C6A-O1A	119.1(3)
N2A-C6A-C5A	121.2(3)
O1A-C6A-C5A	119.7(3)

O1A-C7A-C8A	104.8(3)
N2A-C8A-C9A	111.3(3)
N2A-C8A-C7A	102.6(3)
C9A-C8A-C7A	113.3(3)
C10A-C9A-C8A	110.0(3)
C15A-C10A-C11A	118.8(3)
C15A-C10A-C9A	120.2(3)
C11A-C10A-C9A	121.0(3)
C12A-C11A-C10A	120.4(3)
C13A-C12A-C11A	120.1(3)
C12A-C13A-C14A	119.6(4)
C15A-C14A-C13A	120.2(4)
C14A-C15A-C10A	121.0(4)
C1A-N1A-C5A	117.6(3)
C1A-N1A-Fe1	128.3(3)
C5A-N1A-Fe1	114.1(2)
C6A-N2A-C8A	107.5(3)
C6A-N2A-Fe1	116.9(3)
C8A-N2A-Fe1	135.5(3)
C6A-O1A-C7A	105.8(3)
N1B-C1B-C2B	122.2(4)
C3B-C2B-C1B	119.4(3)
C2B-C3B-C4B	119.0(4)
C5B-C4B-C3B	117.8(4)
N1B-C5B-C4B	124.1(3)
N1B-C5B-C6B	112.2(3)
C4B-C5B-C6B	123.6(3)
N2B-C6B-O1B	118.6(3)
N2B-C6B-C5B	121.5(3)
O1B-C6B-C5B	119.8(3)
O1B-C7B-C8B	103.8(3)
N2B-C8B-C9B	109.5(3)
N2B-C8B-C7B	101.4(3)
C9B-C8B-C7B	113.6(3)
C10B-C9B-C8B	111.8(3)
C15B-C10B-C11B	118.6(3)
C15B-C10B-C9B	119.7(3)
C11B-C10B-C9B	121.7(3)
C12B-C11B-C10B	120.4(4)
C11B-C12B-C13B	120.3(4)
C14B-C13B-C12B	119.5(4)
C13B-C14B-C15B	120.6(4)
C10B-C15B-C14B	120.5(4)
C1B-N1B-C5B	117.5(3)
C1B-N1B-Fe2	127.9(3)
C5B-N1B-Fe2	114.6(2)
C6B-N2B-C8B	106.7(3)
C6B-N2B-Fe2	115.7(2)
C8B-N2B-Fe2	137.3(2)
C6B-O1B-C7B	104.4(3)

3.3.7 Additional Tables with Results on Catalyst Screening Studies

Table 3.11: Screening with $Ni(acac)_2$ for substrates **1a**, **1b** and **1c**.[a]

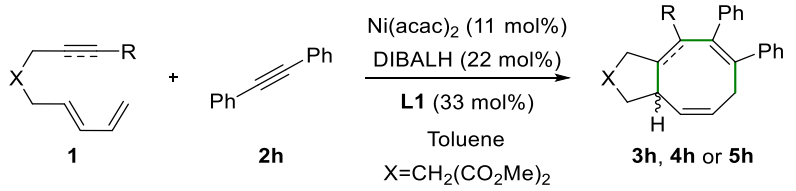

1 **2h** **3h**, **4h** or **5h**

Entry	Substrate **1**	Ligand	Conv. (%)[b]	Product
1	**1a**	**L1**	24	**3h**, n.d.[c]
2	**1b**	**L1**	>99	**4h**, n.d.
3	**1c**	**L1**	>99	**5h**, n.d.

(a) Conditions (unless otherwise noted): 1 equiv. of **1**, 1.2 equiv. of **2h**, 11.0 mol% $[Ni(COD)_2]$, 22.0 mol% of DIBALH and 33.0 mol% of PPh_3 (**L1**) in toluene at 60 °C for 24 h. (b) Calculated by ^1H NMR spectroscopy using 1,3,5-trimethoxybenzene and 1,2,4,5-tetramethylbenzene as internal standard. (c) Not detected.

Table 3.12: Alkene screening for dienene **1a**.[a]

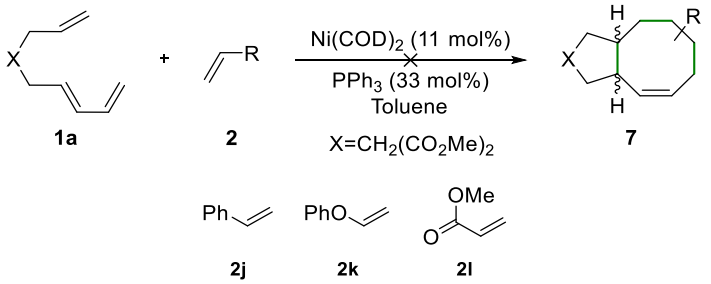

1a **2** **7**

2j **2k** **2l**

Entry	Substrate **2**	Conv. (%)[b]	Product **7**
1	**2j**	38	n.d.[c]
2	**2k**	36	n.d.
3	**2l**	41	n.d.

(a) Conditions (unless otherwise noted): 1 equiv. of **1a**, 1.2 equiv. of **2**, 11.0 mol% $[Ni(COD)_2]$ and 33.0 mol% PPh_3 (**L1**) in toluene at 60 °C for 24 h. (b) Calculated by ^1H NMR spectroscopy using 1,3,5-trimethoxybenzene as internal standard. (c) Not detected.

Table 3.13: Ligand screening for dienene **1a**.[a]

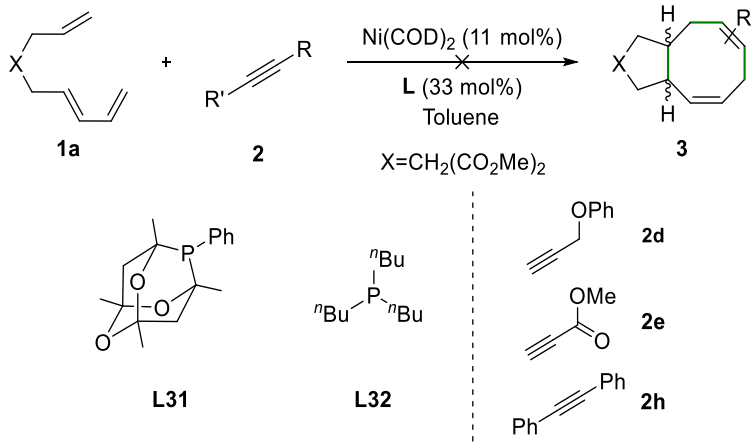

Entry	Substrate 2	Ligand	Conv. (%)[b]	Product 3
1	2d	L31	51	n.d.[c]
2		L32	34	n.d.
3	2e	L31	48	n.d.
4		L32	57	n.d.
5	2h	L31	46	n.d.
6		L32	33	n.d.

(a) Conditions (unless otherwise noted): 1 equiv. of **1a**, 1.2 equiv. of **2**, 11.0 mol% [Ni(COD)$_2$] and 33.0 mol% **L** in toluene at 60 °C for 24 h. (b) Calculated by ^{1}H NMR spectroscopy using 1,2,4,5-tetramethylbenzene as internal standard. (c) Not detected.

Table 3.14: Ligand screening for dienyne **1b**.[a]

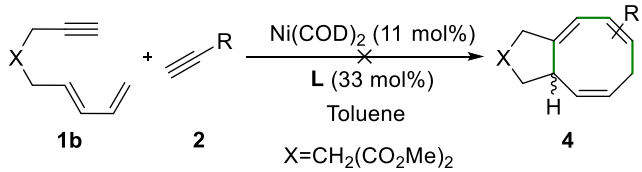

Entry	Substrate 2	Ligand	Conv. (%)[b]	Product 4
1[c]	2d	L31	>99	n.d.[c]
2		L32	>99	n.d.
3[c]	2e	L31	>99	n.d.
4		L32	>99	n.d.
5[c]	2h	L31	>99	n.d.
6		L32	>99	n.d.

(a) Conditions (unless otherwise noted): 1 equiv. of **1b**, 1.2 equiv. of **2**, 11.0 mol% [Ni(COD)$_2$] and 33.0 mol% **L** in toluene at 60 °C for 24 h. (b) Calculated by ^{1}H NMR spectroscopy using 1,2,4,5-tetramethylbenzene as internal standard. (c) Not detected.

Table 3.15: Ligand screening for dienyne **1c**.[a]

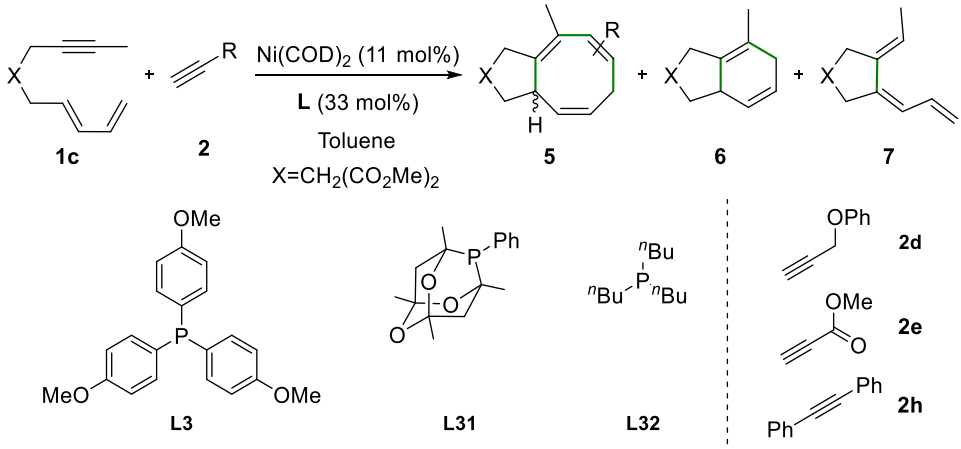

Entry	Substrate 2	Ligand	Conv. (%)[b]	Product 4	Product 6	Product 7
1	2d	L31	>99	n.d.	30%	n.d.[d]
2		L32	>99	n.d.	n.d.	42%
3		L3	>99	n.d.	n.d.	36%
4	2e	L31	>99	n.d.	31%	n.d.
5		L32	59	n.d.	n.d.	n.d.
6	2h	L31	>99	n.d.	12%	n.d.
7		L32	50	n.d.	n.d.	n.d.
8		–	>99	n.d.	n.d.	n.d.

(a) Conditions (unless otherwise noted): 1 equiv. of **1c**, 1.2 equiv. of **2**, 11.0 mol% [Ni(COD)$_2$] and 33.0 mol% **L** in toluene at 60 °C for 24 h. (b) Calculated by ^{1}H NMR spectroscopy using 1,2,4,5-tetramethylbenzene as internal standard. (c) 4 equiv. of **2d**. (d) Not detected.

3.3.8 Representative GC-MS Chromatogram of the HTE Screening

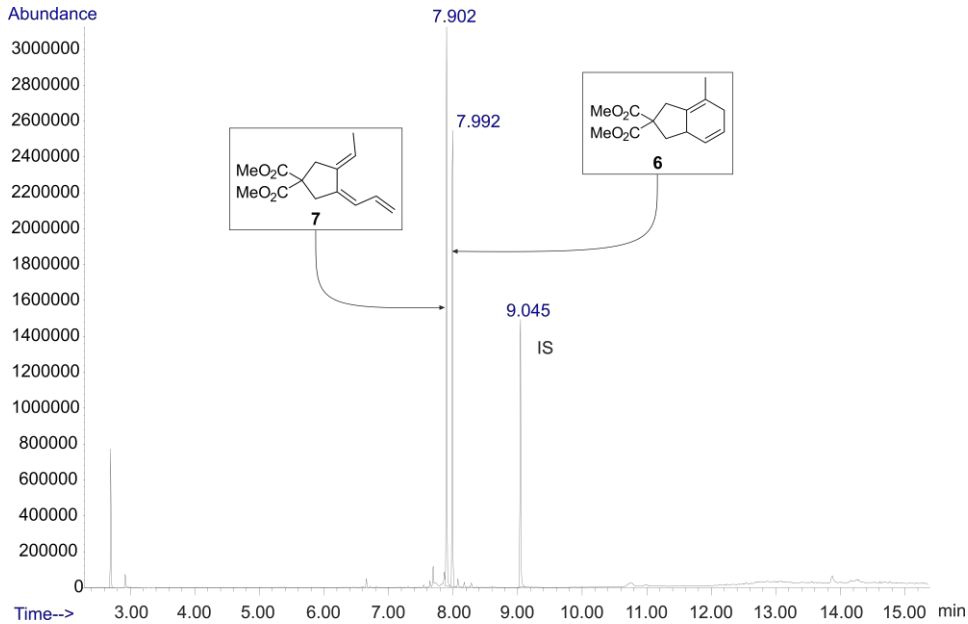

Figure 3.5. Reaction mixture GC-MS of the [(4+2)+2] cycloaddition of **1c** and **2d** at micromolar scale using **L7** as ligand. Peak 1: **7**, t^R = 7.902 min. Peak 1: **6**, t^R = 7.992 min. Peak 3: internal standard, t^R = 9.045 min.

3.3.9 Copies of NMR Spectra

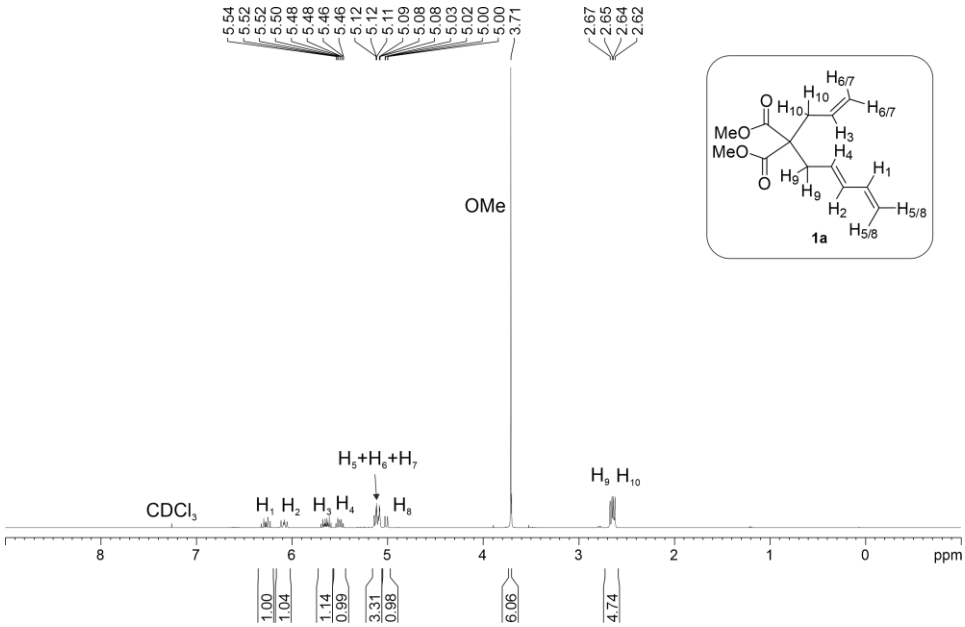

Figure 3.6. ^{1}H NMR spectrum of **1a**.

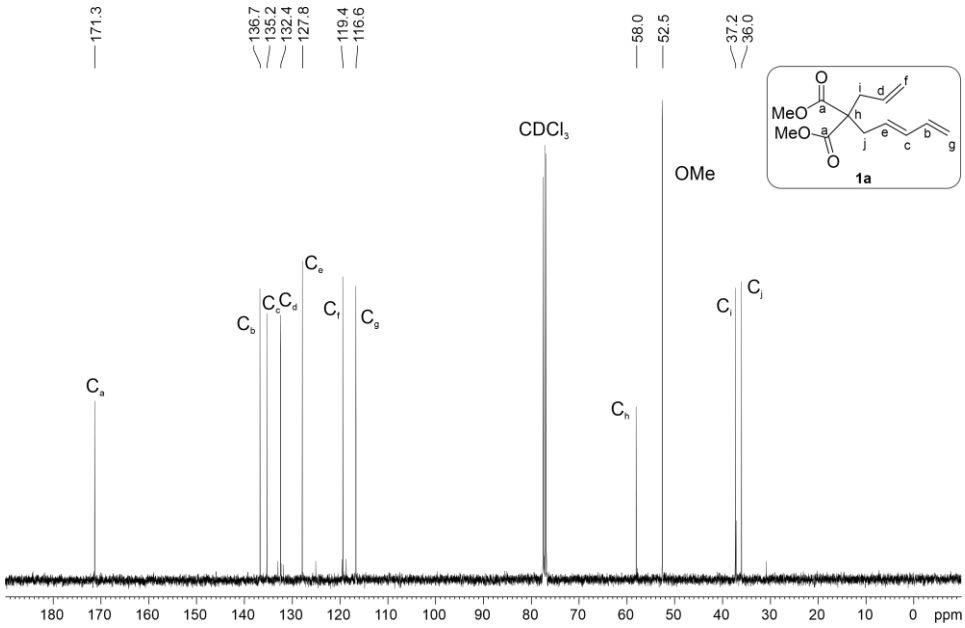

Figure 3.7. ^{13}C{^{1}H} NMR spectrum of **1a**.

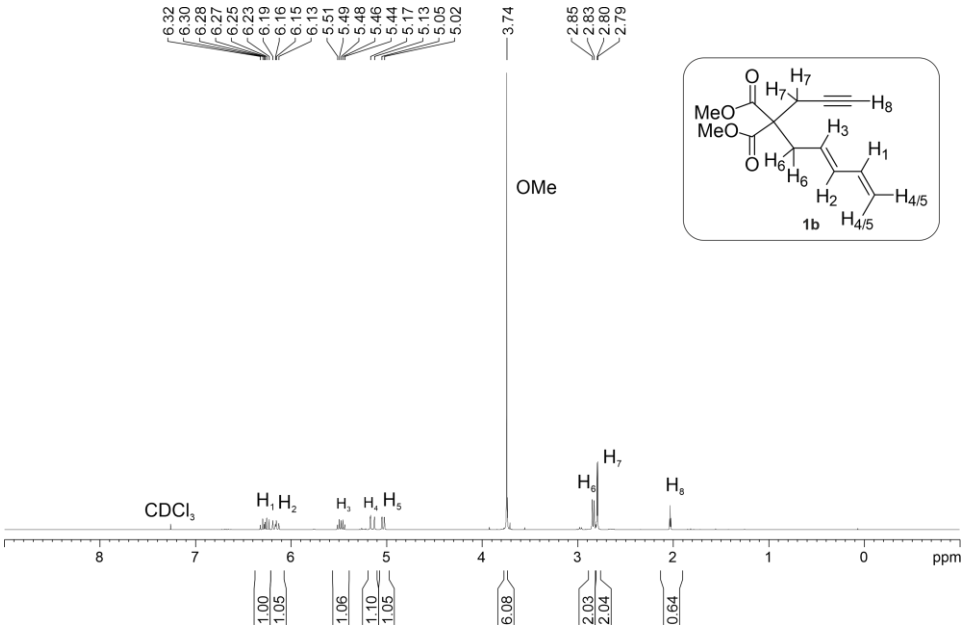

Figure 3.8. ^{1}H NMR spectrum of **1b**.

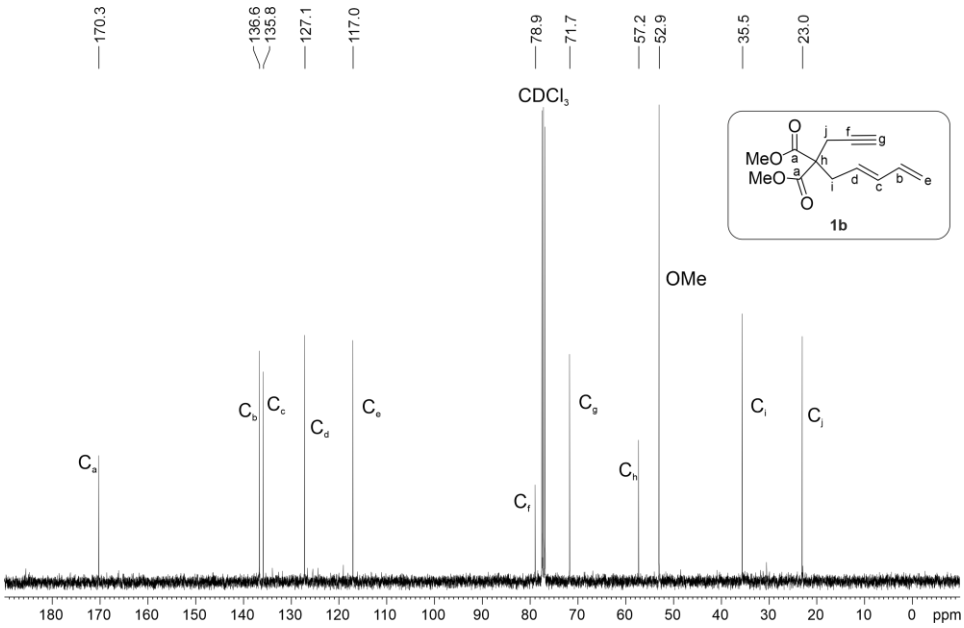

Figure 3.9. $^{13}C\{^{1}H\}$ NMR spectrum of **1b**.

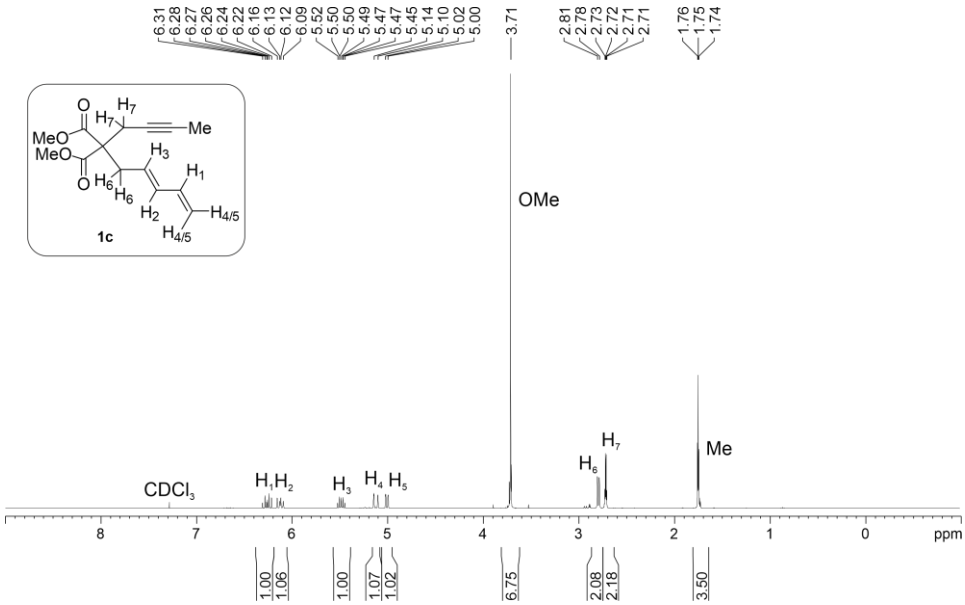

Figure 3.10. ^{1}H NMR spectrum of **1c**.

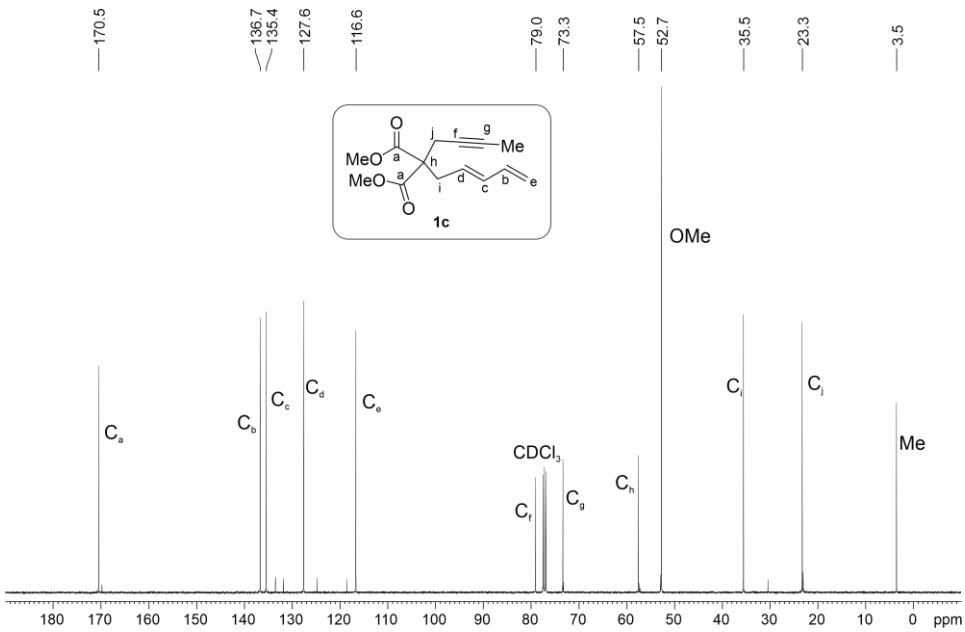

Figure 3.11. ^{13}C{^{1}H} NMR spectrum of **1c**.

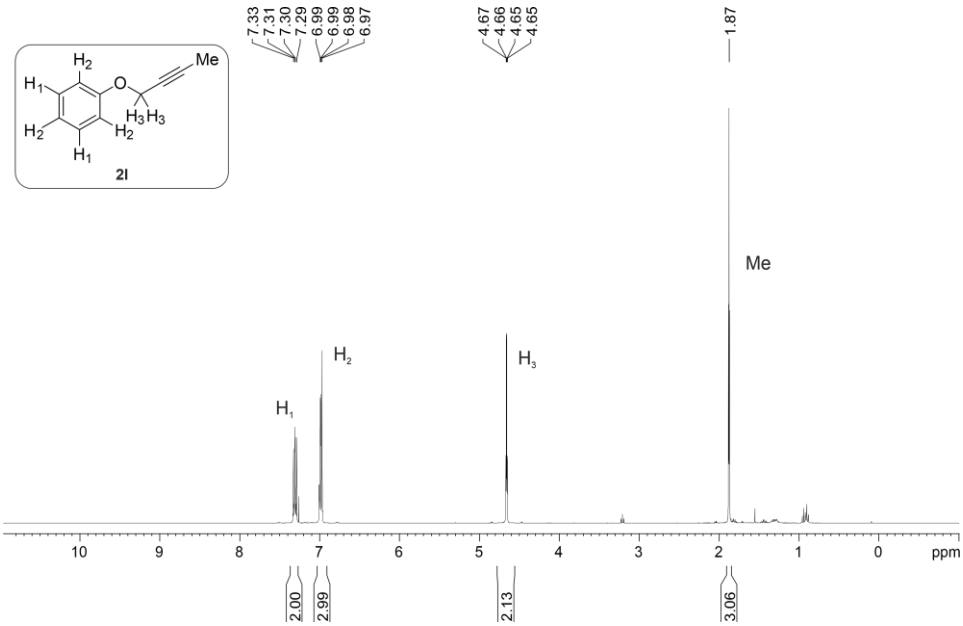

Figure 3.12. ^{1}H NMR spectrum of **2l**.

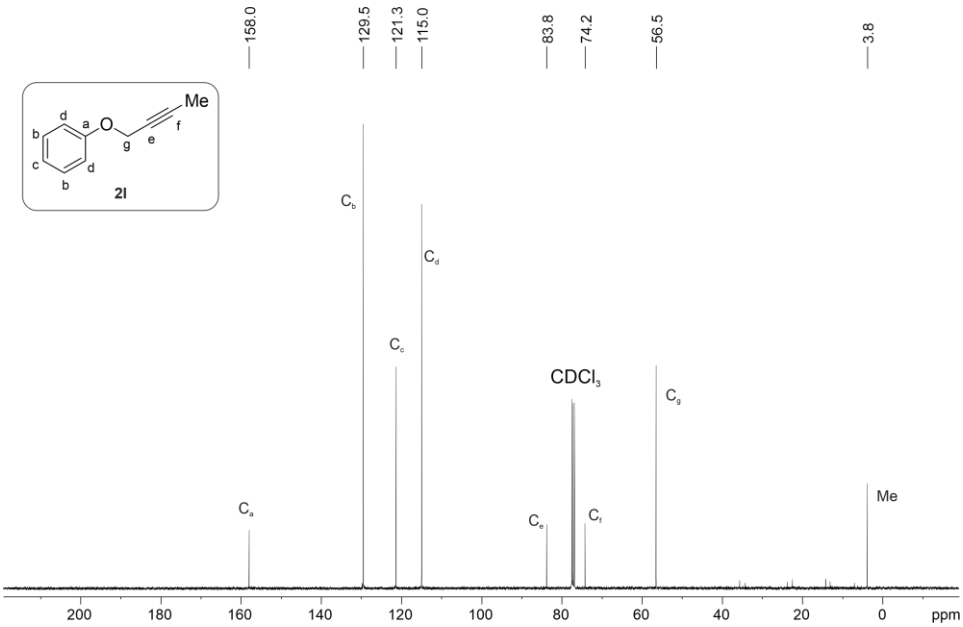

Figure 3.13. $^{13}C\{^{1}H\}$ NMR spectrum of **2l**.

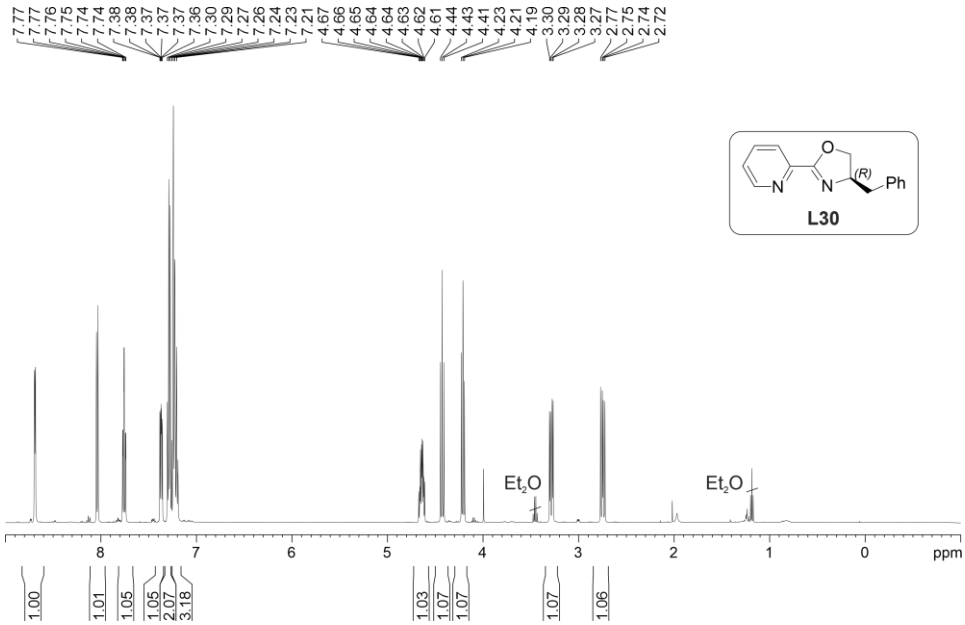

Figure 3.14. ^{1}H NMR spectrum of **L30**.

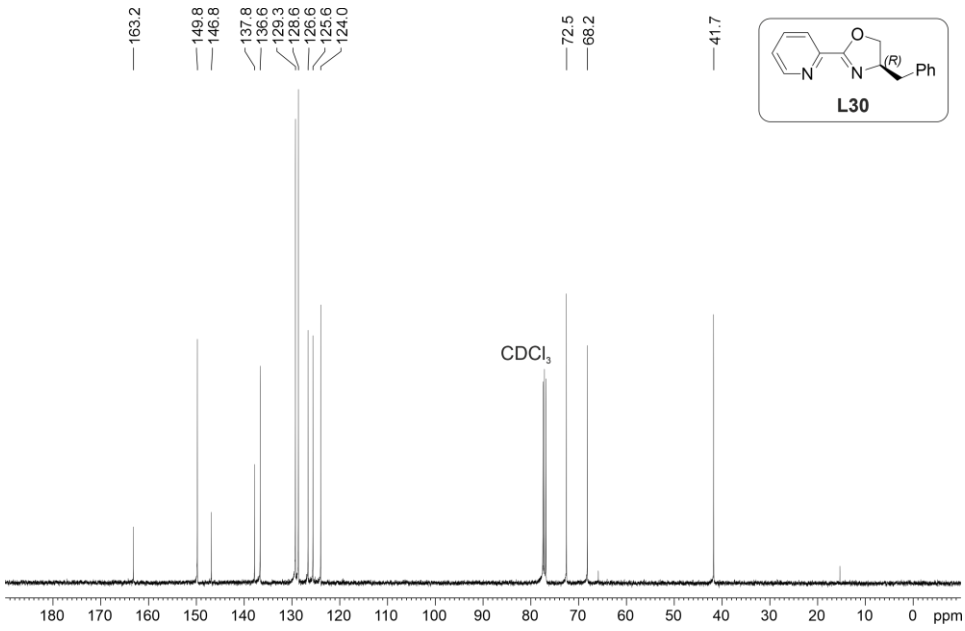

Figure 3.15. $^{13}C\{^{1}H\}$ NMR spectrum of **L30**.

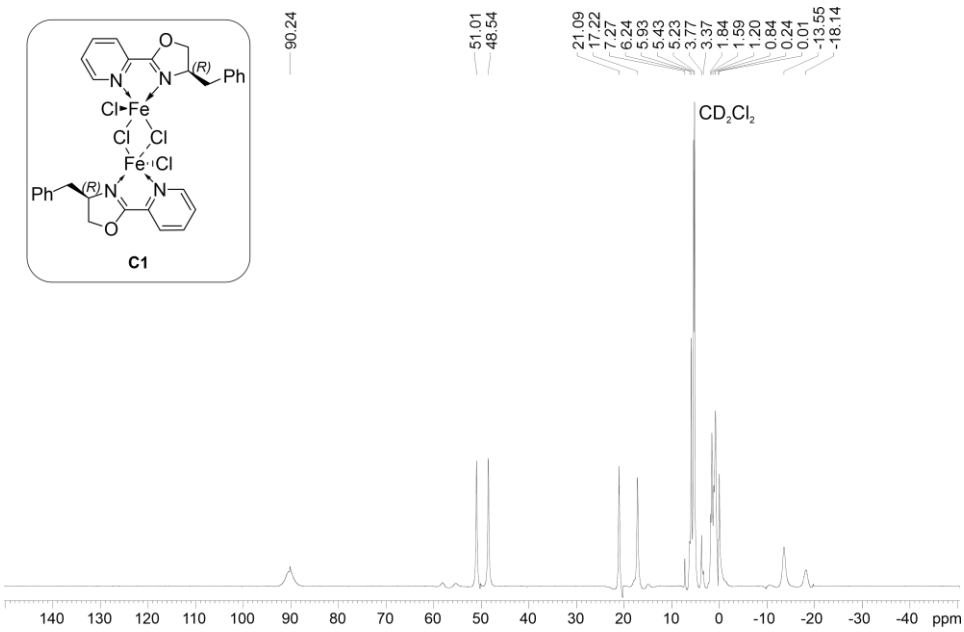

Figure 3.16. ^{1}H NMR spectrum of **C1**.

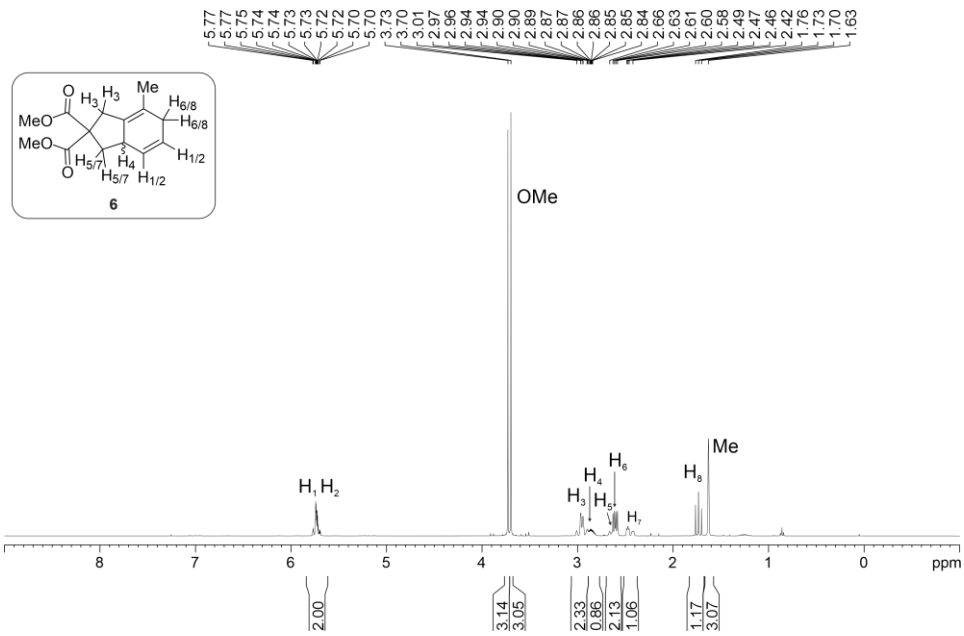

Figure 3.17. ^{1}H NMR spectrum of **6**.

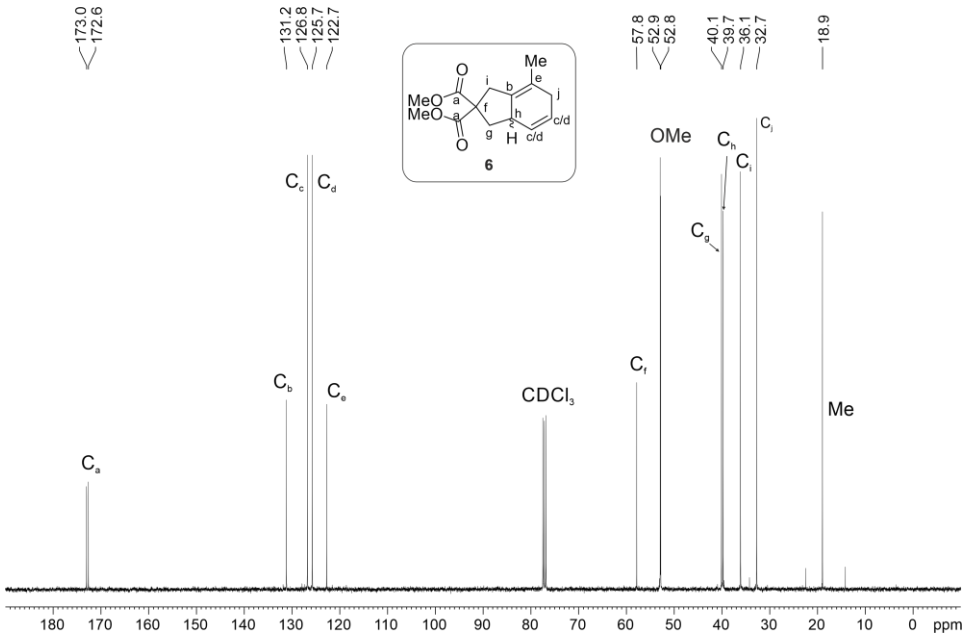

Figure 3.18. $^{13}C\{^1H\}$ NMR spectrum of **6**.

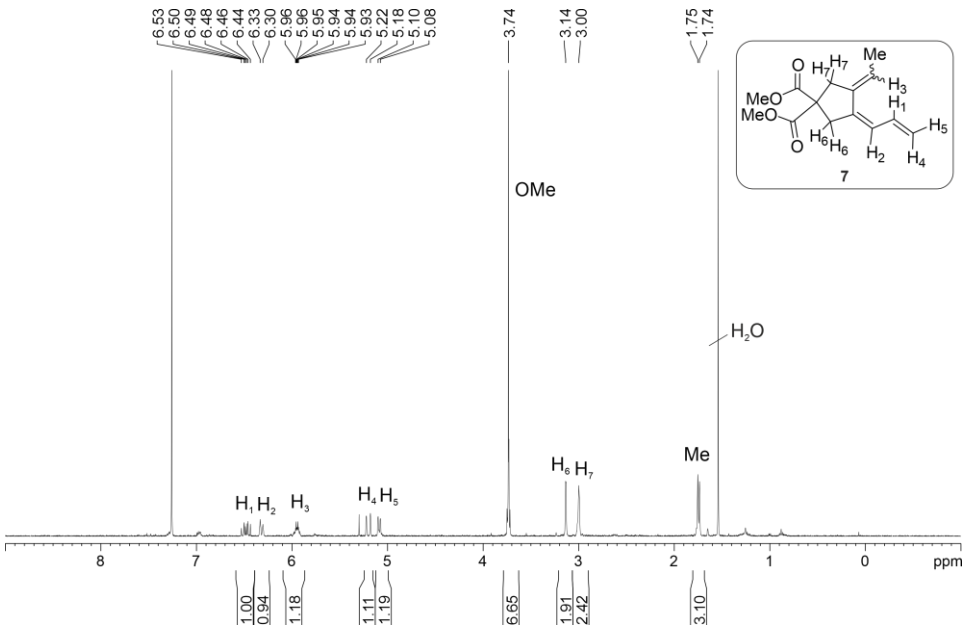

Figure 3.19. ^1H NMR spectrum of **7**.

CHAPTER 4

[XBPhos-Rh]-Catalyzed Intramolecular [4+2] Cycloadditions of Dienynes

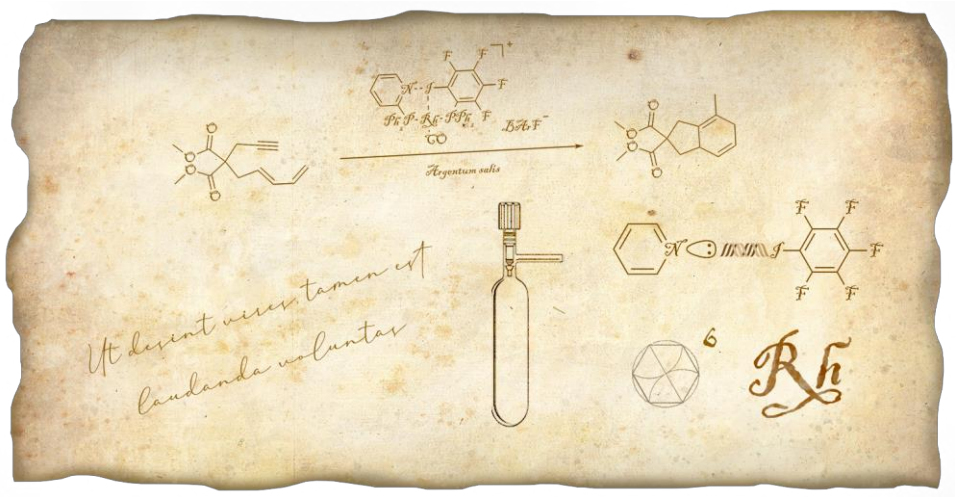

UNIVERSITAT ROVIRA I VIRGILI
TRANSITION METAL-CATALYZED CYCLOADDITION REACTIONS FOR THE FORMATION OF EIGHT- AND SIX-MEMBERED RINGS
Nuria Llorente González

UNIVERSITAT ROVIRA I VIRGILI
TRANSITION METAL-CATALYZED CYCLOADDITION REACTIONS FOR THE FORMATION OF EIGHT- AND SIX-MEMBERED RINGS
Nuria Llorente González

[XBPhos-Rh]-Catalyzed Intramolecular [4+2] Cycloadditions of Dienynes

4.1. Introduction

In the past decades, supramolecular catalysis, understood as the use of non-covalent interactions as a toolbox to be implemented in (stereoselective) catalysis, has undergone a major growth. One successful supramolecular strategy relies on the self-assembly of building blocks that contain both the complementary motifs required for the supramolecular assembly process and the binding groups necessary for the desired catalytic event. In this regard, hydrogen bonding[1] and metal-ligand interactions[2] have been historically the dominant interactions. However, in recent years, other non-covalent interactions[3] (in particular halogen bonding, referred to as XB in the discussion that follows) have gained more interest in this area of research.[4] Halogen bonding involves the interaction of the σ-hole, an electrophilic region with positive electrostatic potential of an halogen atom, and the lone pair of a nucleophile. The directionality[5a] and strength[5b] of the halogen bond, together with a greater tolerance to changes in the polarity of the solvent[5c] makes halogen bonding ideal for constructing the frameworks of supramolecular complexes and

(1) For a comprehensive view on the use of hydrogen bonding in catalysis, see: (a) Schreiner, P. R. *Chem. Soc. Rev.* **2003**, *32*, 289-296. (b) Doyle, A. G.; Jacobsen, E. N. *Chem. Rev.* **2007**, *107*, 5713-5743. (c) *Hydrogen Bonding in Organic Synthesis*, First ed.; Pihko, P. M., Ed.; Wiley-VCH Verlag GmbH & Co. KGaA: Weinheim, 2009. (d) Breit, B. In *Supramolecular Catalysis*; van Leeuwen, P. W. N. M., Ed.; Wiley-VCH Verlag GmbH & Co. KGaA: Weinheim, 2008; pp 29-55.(e) Nishikawa, Y. *Tetrahedron Lett.* **2018**, *59*, 216-223 and references cited therein.

(2) For a comprehensive view on the use of metal-ligand interactions in catalysis, see: (a) Alvarez, S.; Palacios, A. A.; Aullón, G. *Coord. Chem. Rev.* **1999**, *185-186*, 431-450. (b) Verhoeven, D. G. A.; Moret, M.-E. *Dalton Trans.* **2016**, *45*, 15762-15778. (c) Shimbayashi, T.; Fujita, K. *Catalysts* **2020**, *10*, 635-703.

(3) For an overview of the applications of non-covalent interactions, see: (a) Meyer, E. A.; Castellano, R. K.; Diederich, F. *Angew. Chem., Int. Ed.* **2003**, *42*, 1210-1250. (b) Carboni, S.; Gennari, C.; Pignataro, L.; Piarulli, U. *Dalton Trans.* **2011**, *40*, 4355-4373. (c) Vaquero, M.; Rovira, L.; Vidal-Ferran, A. *Chem. Commun.* **2016**, *52*, 11038-11051. (d) Yamada, S. *Chem. Rev.* **2018**, *118*, 11353-11432. (e) Vogel, L.; Wonner, P.; Huber, S. M. *Angew. Chem., Int. Ed.* **2019**, *58*, 1880-1891.

(4) For selected reviews on halogen bonding, see: (a) Gilday, L. C.; Robinson, S. W.; Barendt, T. A.; Langton, M. J.; Mullaney, B. R.; Beer, P. D. *Chem. Rev.* **2015**, *115*, 7118-7195. (b) Cavallo, G.; Metrangolo, P.; Milani, R.; Pilati, T.; Priimagi, A.; Resnati, G.; Terraneo, G. *Chem. Rev.* **2016**, *116*, 2478-2601. (c) Tepper, R.; Schubert, U. S. *Angew. Chem., Int. Ed.* **2018**, *57*, 6004-6016.

(5) (a) Huber, S. M.; Scanlon, J. D.; Jiménez-Izal, E.; Ugalde, J. M.; Infante, I. *Phys. Chem. Chem. Phys.* **2013**, *15*, 10350-10357. (b) Corradi, E.; Meille, S. V.; Messina, M. T.; Metrangolo, P.; Resnati, G. *Angew. Chem., Int. Ed.* **2000**, *39*, 1782-1786. (c) Ibrahim, M. A. A.; Hasb, A. A. M. *Theor. Chem. Acc.* **2019**, *138:2*, 1-12.

their application in catalysis. Though mainly restricted to organocatalysis,[6] the study of this interaction in combination with a metal center and its application to the field of transition-metal catalysis is emerging.[7]

In the past years, our group has contributed to the study of halogen bonding for the assembly of the backbone of catalysts. The versatility of phosphines, in combination with the template effect produced by the rhodium center, led to the efficient formation of pincer-type complexes. These studies resulted in the successful synthesis of the XBPhos-Rh complex (Scheme 4.1a), whose application in the hydroboration of terminal alkynes was demonstrated (Scheme 4.1b).[8]

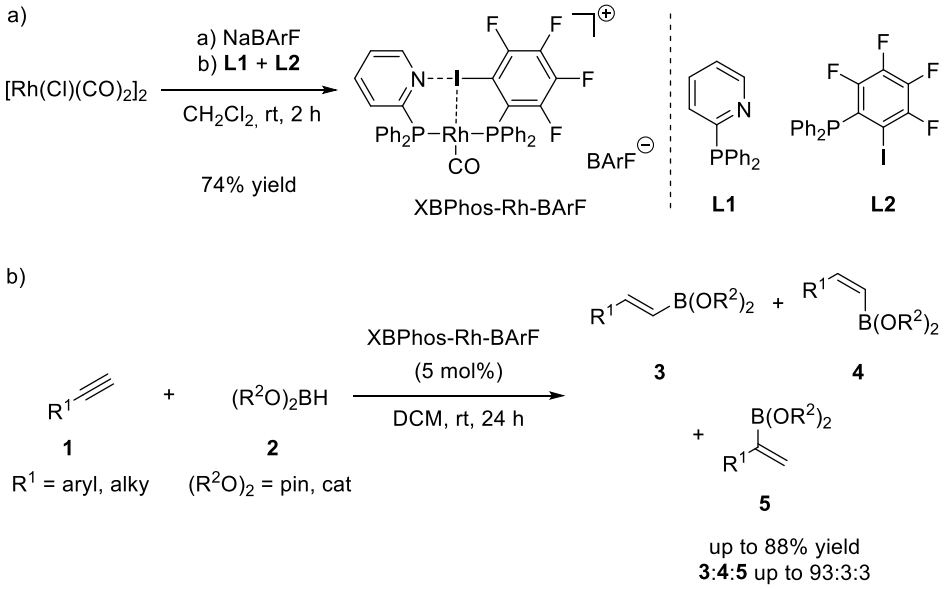

Scheme 4.1. (a) Synthesis of the halogen-bond assembled complex XBPhos-Rh-BArF and (b) its application in the hydroboration of terminal alkynes.

(6) Sutar, R. L.; Huber, S. M. *ACS Catal.* **2019**, *9*, 9622-9639.

(7) For selected examples on the influence of halogen bonding in the formation and reactivity of metal complexes, see: (a) Zordan, F.; Brammer, L.; Sherwood, P. *J. Am. Chem. Soc.* **2005**, *127*, 5979-5989. (b) Beweries, T.; Brammer, L.; Jasim, N. A.; McGrady, J. E.; Perutz, R. N.; Whitwood, A. C. *J. Am. Chem. Soc.* **2011**, *133*, 14338-14348. For selected examples of the use of XB in template effects exerted by metal centers in catalysis, see: (c) Lindsay, V. N. G.; Lin, W.; Charette, A. B. *J. Am. Chem. Soc.* **2009**, *131*, 16383-16385. (d) Lindsay, V. N. G.; Charette, A. B. *ACS Catal.* **2012**, *2*, 1221-1225.

(8) For the synthesis of XBPhos-Rh-BArF and its application in the hydroboration of terminal akynes, see (a) Carreras, L.; Serrano-Torné, M.; van Leeuwen, P. W. N. M.; Vidal-Ferran, A. *Chem. Sci.* **2018**, *9*, 3644-3648. For a study on the influence of the rhodium precursor and the geometry of the ligands in the formation of XBPhos-Rh and analogous complexes, see: (b) Carreras, L.; Benet-Buchholz, J.; Franconetti, A.; Frontera, A.; van Leeuwen, P. W. N. M.; Vidal-Ferran, A. *Chem. Commun.* **2019**, *55*, 2380-2383.

The Diels–Alder reaction has been one of the most widely used transformations in organic synthesis, due to its versatility for constructing substituted six-membered rings in a highly (stereo)selective fashion.[9] At first glance, metal-catalyzed [4+2] cycloadditions may seem less useful because a strictly thermal counterpart does exist, unlike for the [4+4] cycloadditions. However, purely thermal [4+2] cycloadditions often require high thermal levels, so historically various modifications have been studied for facilitating Diels–Alder reactions under mild conditions.[10] Metal-catalyzed [4+2] cycloadditions proceed at lower temperatures and are not subject to the often restrictive electronic requirements of the thermal Diels–Alder reaction. While Lewis acids remain the most effective catalysts in this chemistry,[9a] their applications are primarily limited to activated dienophiles. More specifically, the intramolecular [4+2] cycloaddition of unactivated trienes or dienynes under mild conditions has been successfully investigated with a broad array of transition metals, such as Ni,[11] Ir,[12] Au,[13] Pd[14] or Co.[15] However, Rh(I)-based complexes have demonstrated to be privileged catalysts for this type of cycloadditions.[16]

The first example of intramolecular [4+2] cycloaddition of dienynes was reported by Livinghouse *et al.* in the 90s.[17a] As Scheme 4.2a illustrates, the reaction occurs under mild reaction conditions in the presence of a Rh–phosphine complex to afford a variety of fused 5,6- and 6,6-bicyclic ring systems in good to

(9) For a comprehensive review on the Diels-Alder Reaction, see: (a) Kagan, H. B.; Riant, O. *Chem. Rev.* **1992**, *92*, 1007-1019. (b) Tietze, L. F.; Kettschau, G. *Top. Curr. Chem.* **1997**, *189*, 1-120. (c) Nicolaou, K. C.; Snyder, S. A.; Montagnon, T.; Vassilikogiannakis, G. *Angew. Chem., Int. Ed. Engl.* **2002**, *41*, 1668-1698. (d) Takao, K.; Munakata, R.; Tadano, K. *Chem. Rev.* **2005**, *105*, 4779-4807. (e) Jiang, X.; Wang, R. *Chem. Rev.* **2013**, *113*, 5515-5546. (f) Gregoritza, M.; Brandl, F. P. *Eur. J. Pharm. Biopharm.* **2015**, *97*, 438-453. and references therein.
(10) Pindur, U.; Lutz, G.; Otto, C. *Chem. Rev.* **1993**, *93*, 741-761.
(11) (a) Wender, P. A.; Jenkins, T. E. *J. Am. Chem. Soc.* **1989**, *111*, 6432-6434. (b) Wender, P. A.; Smith, T. E. *J. Org. Chem.* **1995**, *60*, 2962-2963. (c) Wender, P. A.; Smith, T. E. *J. Org. Chem.* **1996**, *61*, 824-825. (d) Wender, P. A.; Smith, T. E. *Tetrahedron* **1998**, *54*, 1255-1275.
(12) Shibata, T.; Takasaku, K.; Takesue, Y.; Hirata, N.; Takagi, K. *Synlett* **2002**, 1681-1682.
(13) (a) Kusama, H.; Karibe, Y.; Onizawa, Y.; Iwasawa, N. *Angew. Chem., Int. Ed.* **2010**, *49*, 4269-4272. (b) Kim, S.-M.; Park, J.-H.; Chung, Y.-K. *Chem. Commun.* **2011**, *47*, 6719-6721.
(14) Kumar, K.; Jolly, R. S. *Tetrahedron Lett.* **1998**, *39*, 3047-3048.
(15) (a) Park, K. H.; Choi, S. Y.; Kim, S. Y.; Chung, Y. K. *Synlett* **2006**, 527-532. (b) Biletskyi, B.; Tenaglia, A.; Clavier, H. *Tetrahedron Lett.* **2018**, *59*, 103-107.
(16) For selected reviews, see: (a) Ojima, I.; Vu, A. T.; Bonafoux, D. In *Science of Synthesis, Category 1*; Lautens, M., Ed.; Georg Thieme Verlag: Stuttgart, 2002; Vol. 1, pp 531-616. (b) Marinetti, A.; Jullien, H.; Voituriez, A. *Chem. Soc. Rev.* **2012**, *41*, 4884-4908.
(17) (a) Jolly, R. S.; Luedtke, G.; Sheehan, D.; Livinghouse, T. *J. Am. Chem. Soc.* **1990**, *112*, 4965-4966. (b) McKinstry, L.; Livinghouse, T. *Tetrahedron* **1994**, *50*, 6145-6154.

excellent yields. The intramolecular [4+2] cycloaddition takes place with terminal and internal alkynes and, more importantly, with unactivated alkenes. In addition, rhodium(I)-catalyzed [4+2] cycloadditions were found to proceed with excellent diastereoselectivity, providing cycloadducts exclusively as single diastereomers. The enantioselective version of this reaction was subsequently reported by the same group,[17b] who disclosed rhodium-DIOP complexes as suitable catalysts for this transformation (Scheme 4.2b). The best enantiomeric excess (79% yield, 87% ee) was attained by using a rhodium-DIOP complex generated *in situ* from $[RhCl(COE)]_2$[18] and DIOP ligand **L1**, while the highest yield was obtained with **L2** (99% yield, 42% ee). The same group also published a study on the effects of the counterion on the rate, chemo-, diastereo- and enantio-selectivity, reaching the conclusion that cationic species with the hexafluoroantimonate counterion were more reactive than the triflate analogs and were less affected by the olefin substitution pattern.[19]

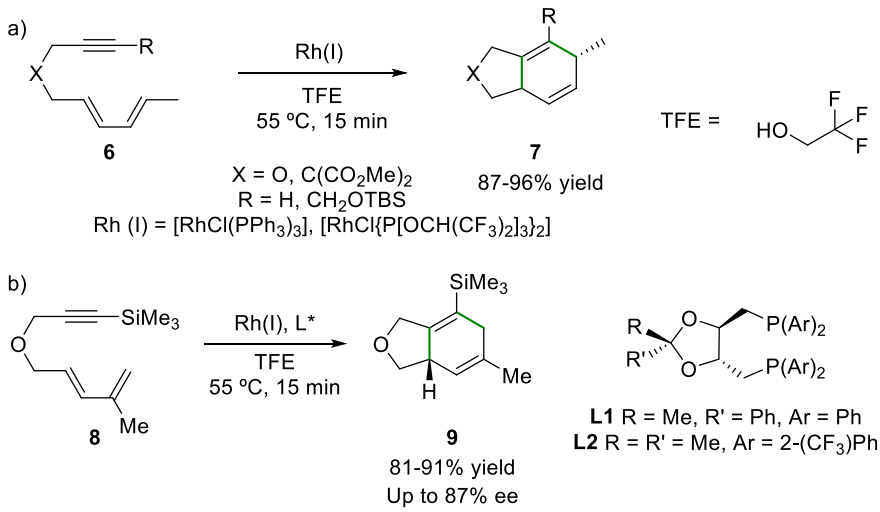

Scheme 4.2. [4+2] cycloadditions on dienynes reported by Livinghouse *et al.*

These reactions were further developed by Gilbertson and coworkers.[20] With the *in situ* formation of $[Rh(CH_2Cl_2)_2(DiPhos)]SbF_6$[21] as the active catalyst by hydrogenation of $[Rh(NBD)(DiPhos)]SbF_6$ in DCM, the authors managed to reduce the temperature to 25 °C, even though the yields were lower (65-80%).[20a] An enantioselective version was also described using (*S,S*)-Me,Me-DuPhos as the

(18) COE = Cyclooctene
(19) O'Mahony, D. J. R.; Belanger, D. B.; Livinghouse, T. *Synlett* **1998**, 443-445.
(20) (a) Gilbertson, S. R.; Hoge, G. S. *Tetrahedron Lett.* **1998**, *39*, 2075-2078. (b) Gilbertson, S. R.; Hoge, G. S.; Genov, D. G. *J. Org. Chem.* **1998**, *63*, 10077-10080.
(21) DiPhos = 1,2-Bis(diphenylphosphino)ethane.

UNIVERSITAT ROVIRA I VIRGILI
TRANSITION METAL-CATALYZED CYCLOADDITION REACTIONS FOR THE FORMATION OF EIGHT- AND SIX-MEMBERED RINGS
Nuria Llorente González

enantiopure ligand, based on the same principle of activating the complex by hydrogenation before the addition of the substrate.[20b] This method afforded the corresponding bicyclic products in good yields (78–85%) and enantioselectivities (81–95% ee).

The group of Zhang published in 2000 [4+2] cycloadditions on the broadest array of substrates to date (Scheme 4.3).[22] The reaction conditions were mild, at 25 °C, with low reaction times and low catalyst loadings (TON = 1000 for [4+2] cycloaddition reactions at 25 °C). The authors also described excellent isolated yields with no detectable amounts of byproducts. The active catalytic species [Rh(dppb)]SbF_6 was generated *in situ* from [Rh(Cl)(dppb)]$_2$ and $AgSbF_6$. The catalysts demonstrated good tolerance towards oxygen and nitrogen substituents in the substrate, as well as a variety of terminal substituents in the acetylene moiety.

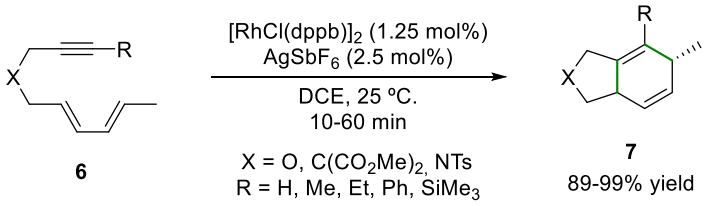

Scheme 4.3. Intramolecular [4+2] cycloadditions reported by Zhang *et al.*

Subsequent studies from Tam and coworkers[23] described the use of cationic rhodium(I) catalysts in intramolecular [4+2] cycloadditions of substrates containing alkynyl halides in good yields and stereoselectivities (70–87% yield for single stereoisomers; Scheme 4.4a). The halide group was well tolerated, as no oxidative addition to the metal center was observed. The halogen-containing cycloadducts could be transformed into a variety of products that were difficult or impossible to obtain *via* direct cycloaddition.

Saito and Hanzawa described the [4+2] cycloaddition of sorbates and propiolates (Scheme 4.4b).[24] It is interesting to note that, in the case of sorbates, the authors were not able to isolate the corresponding product in pure form, but as a mixture of the [4+2] cycloadduct and the aromatized product. To overcome this obstacle, the authors performed an oxidative work-up and reported the yield of the aromatized product. This problem was not encountered in the [4+2] cycloadditions

(22) Wang, B.; Cao, P.; Zhang, X. *Tetrahedron Lett.* **2000**, *41*, 8041-8044.
(23) Yoo, W.-J.; Allen, A.; Villeneuve, K.; Tam, W. *Org. Lett.* **2005**, *7*, 5853-5856.
(24) (a) Saito, A.; Ono, T.; Hanzawa, Y. *J. Org. Chem.* **2006**, *71*, 6437-6443. (b) Saito, A.; Ono, T.; Takahashi, A.; Taguchi, T.; Hanzawa, Y. *Tetrahedron Lett.* **2006**, *47*, 891-895.

of the propiolates, which rendered the final cycloadducts with excellent yields, even quantitative in some cases. In 2019, Shu, Shen *et al.* reported another interesting example of [4+2] cycloadditions yielding cyclic vinyl azides.[25] These products were otherwise difficult to access due to the instability of the azide group in the presence of a neighboring unsaturated double bond, which accentuated its reactivity. Cycloaddition of these substrates benefitted from the mild conditions provided by a Rh(I) catalytic system. The scope included alkyl, halogen and aryl substituents in the acetylene moiety as well as nitrogen and oxygen substituents (Scheme 4.4c). It is also interesting to mention that, in 2004, Shinokubo and Oshima[26] described a micellar catalyst in water derived from [RhCl(NBD)]-SDS (SDS or sodium dodecyl sulfate acting as a surfactant), which provided cationic rhodium species that acted as a highly active catalyst for the [4+2] cycloaddition of 1,3-dien-8-ynes.

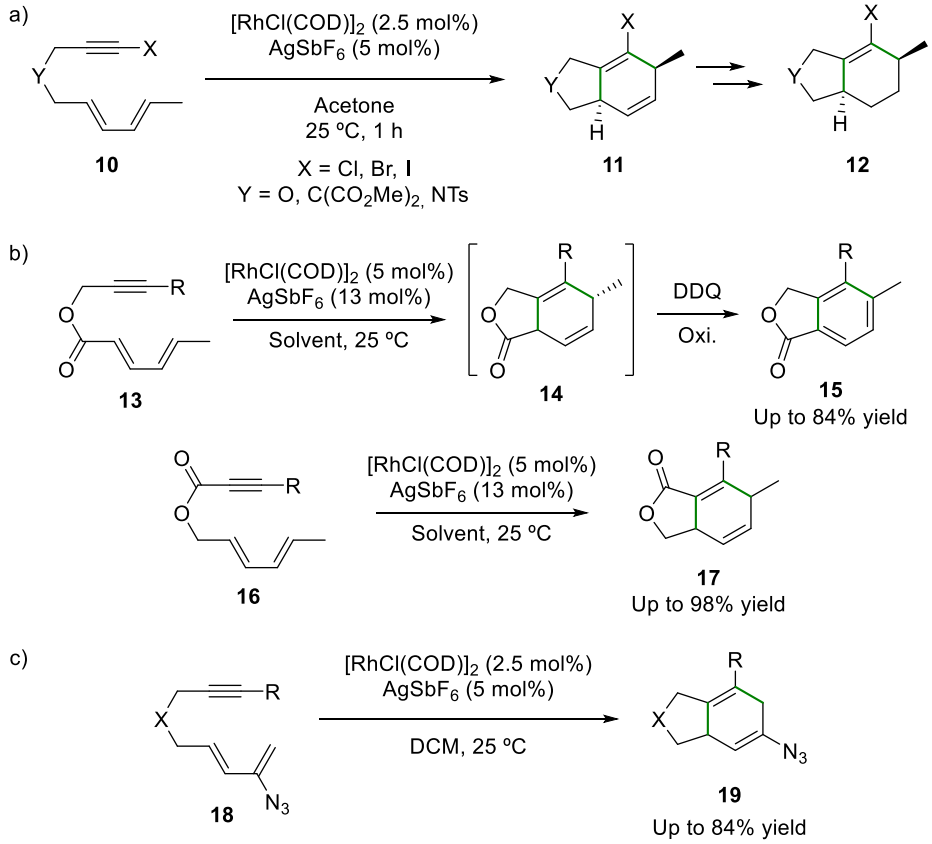

Scheme 4.4. Selected [4+2] cycloadditions.

(25) Shen, M.-H.; Liang, X.-C.; Li, C.; Wu, H.; Qu, H.-Y.; Wang, F.-M.; Xu, H.-D. *Tetrahedron Lett.* **2019**, *60*, 1025-1028.
(26) Motoda, D.; Kinoshita, H.; Shinokubo, H.; Oshima, K. *Angew. Chem., Int. Ed.* **2004**, *43*, 1860-1862.

UNIVERSITAT ROVIRA I VIRGILI
TRANSITION METAL-CATALYZED CYCLOADDITION REACTIONS FOR THE FORMATION OF EIGHT- AND SIX-MEMBERED RINGS
Nuria Llorente González

Enantioselective versions of this transformation have been developed by the groups of Mikami[27] and Hayashi,[28] who discovered rhodium catalysts incorporating enantiopure diene ligands. Mikami[27] envisioned a catalyst based on a proper combination of diene and a bidentate phosphine, both in enantiomerically pure form. Remarkably, combinations of Et-DuPhos with enantiopure bicyclic dienes (Diene*, see Scheme 4.5a) provided very efficient catalysts. The enantiopure diene was prepared from (−)-carvone. The authors demonstrated that the relative stereochemistry of the two enantiopure components from the catalysts had an important effect on the stereochemical outcome of the cycloadditions. This observation was in agreement with a simultaneous coordination of the diene and diphosphine to the metal center during the catalytic cycle. The authors postulated that the diene was coordinated to the rhodium center as a monodentate ligand in the key cyclization step. This concept was further developed by Hayashi, Shintani and coworkers,[28] who described a rhodium–diene catalyst much more active than its rhodium–diphosphine counterpart for the intramolecular [4+2] cycloaddition of alkyne-tethered 1,3-dienes. The authors developed a highly active and enantioselective asymmetric variant by employing an enantiopure diene ligand. Dienynes **1** with X = C-, N- or O-based groups were converted into fused bicyclic derivatives with high enantioselectivities (83–99% ee, Scheme 4.5b). The catalyst loading could be decreased to 0.5 mol%, even at 0 °C, for the O-containing bicyclic substrate **1** (X = O, R = Ph) without any decrease in the yield and the enantiomeric excess.

(27) Aikawa, K.; Akutagawa, S.; Mikami, K. *J. Am. Chem. Soc.* **2006**, *128*, 12648-12649.
(28) Shintani, R.; Sannohe, Y.; Tsuji, T.; Hayashi, T. *Angew. Chem., Int. Ed.* **2007**, *46*, 7277-7280.

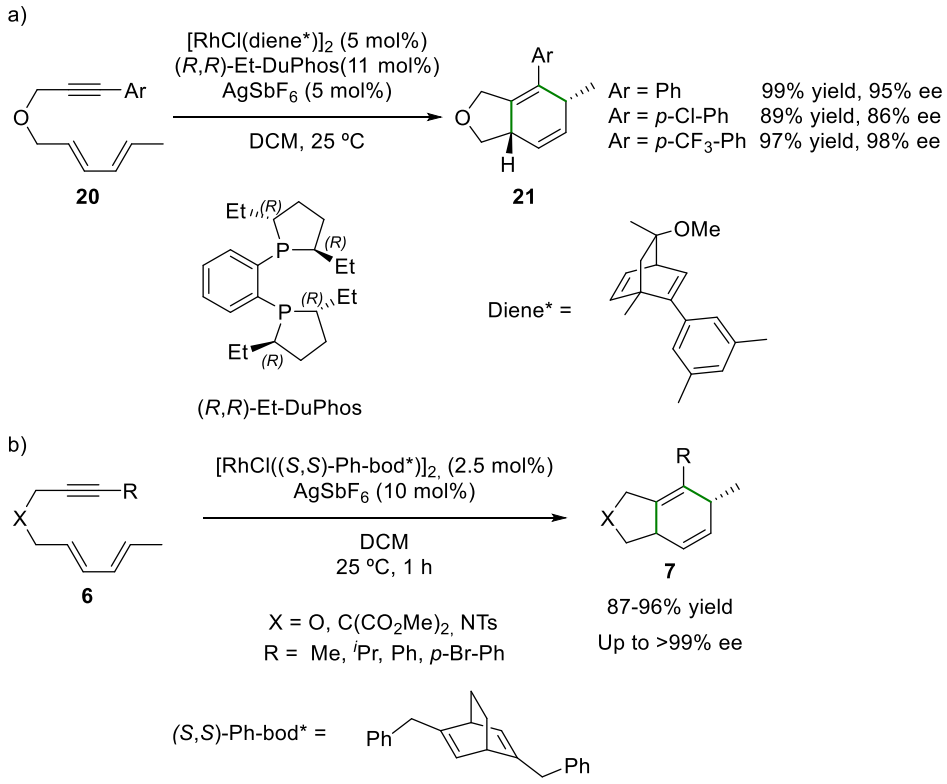

Scheme 4.5. Enantioselective [4+2] cycloadditions reported by (a) Mikami *et al.* and (b) Hayashi *et al.*

N-heterocyclic carbenes (NHC) have also proven to be useful ligands for the rhodium-catalyzed intramolecular [4+2] cycloadditions of dienynes. In 2006, Chung *et al.*[29] reported a catalytic system that was especially active for intramolecular [4+2] cycloaddition reactions (Scheme 4.6a). The cycloadducts were obtained as single diastereoisomers in 91-99% yields after short reaction times. The catalytic system tolerated oxygen and nitrogen substituents in the substrate. Moreover, substituents in the alkyne and in the diene units were also tolerated with little effect on the outcome of the reaction. Wender and coworkers published an example of a similar catalytic system (Scheme 4.6b).[30] The [4+2] cycloaddition of the O-containing dienyne **24** was accomplished in nearly quantitative yield. The catalytic activity of this new Rh(I)-NHC complex was comparable to that reported for the Rh(I)-NHC complex reported by Chung and coworkers.

(29) Lee, S. I.; Park, S. Y.; Park, J. H.; Jung, I. G.; Choi, S. Y.; Chung, Y. K.; Lee, B. Y. *J. Org. Chem.* **2006**, *71*, 91-96.
(30) Gómez, F. J.; Kamber, N. E.; Deschamps, N. M.; Cole, A. P.; Wender, P. A.; Waymouth, R. M. *Organometallics* **2007**, *26*, 4541-4545.

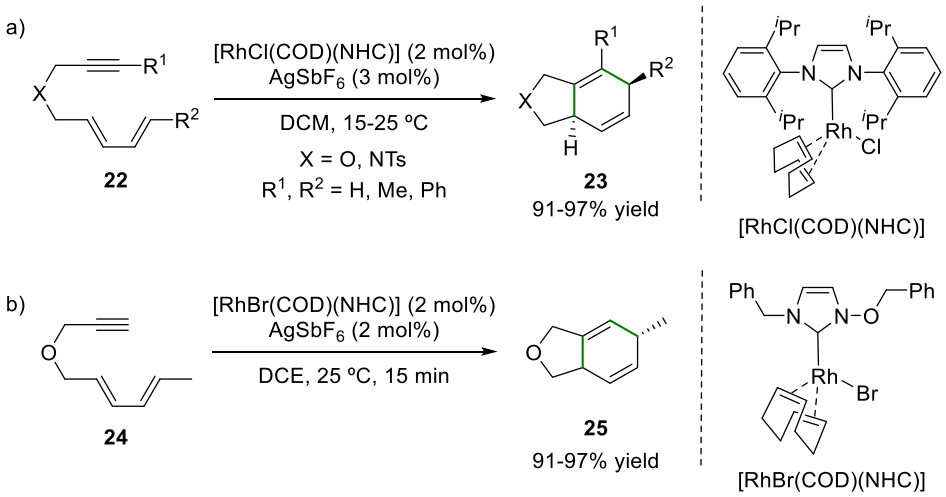

Scheme 4.6. Rh-catalyzed [4+2] cycloadditions of dienynes with NHC-derived catalysts.

As it has been summarized in this section, the utility of Rh(I) complexes as catalysts for intramolecular [4+2] cycloadditions is well established in the literature. In the past years, our group has developed new catalytic systems based on the use of halogen bonding as a tool to construct the backbone of the catalyst. The efficacy of XBPhos-Rh as catalyst was demonstrated in the hydroboration of terminal alkynes with excellent regioselectivities towards the branched alkenylboronic acid derivatives.[8a] To further expand the reactivity of XBPhos-Rh as catalyst, we initiated studies of its catalytic activity in intramolecular [4+2] cycloaddition reactions of dienynes.

4.2. Results and Discussion

With the aim of expanding the structural diversity of our library of complexes with halogen bonds as structural motif for the supramolecular assembly process, we developed a new complex **C1** incorporating an imine moiety as halogen bond acceptor. Following the same synthetic methodology reported for XBPhos-Rh-BArF[8a], we obtained the corresponding rhodium complex derived from an halogen-bonded diphosphine in a 78% yield (Scheme 4.7). Even though no single crystals suitable for X-ray analysis were obtained, NMR and MS spectroscopic data were in agreement with the proposed structure. Interestingly, $^{31}P\{^{1}H\}$ NMR spectroscopy showed a phosphorus-phosphorus coupling constant through two bonds of 277 Hz, which was only in agreement with a *trans*-coordination of the halogen-bonded diphosphine to the metal center.[31]

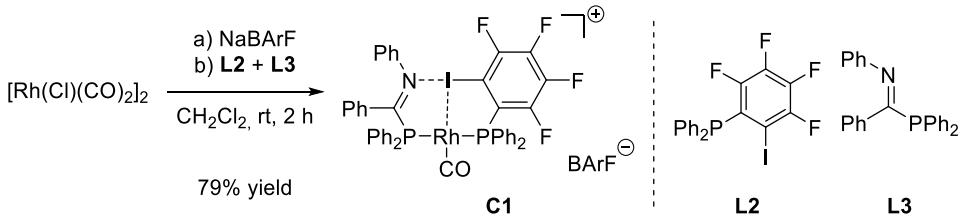

Scheme 4.7. Synthesis of complex **C1**.

With our potential rhodium catalysts in hand (*i.e.*, XBPhos-Rh-BArF and **C1**), we chose dienyne **26a** as a model substrate for our studies, since it had been previously identified as a good candidate to undergo [4+2] cycloadditions. In an initial experiment, the reaction of the model dienyne **26a** with 2.5 mol% of Rh(I) precursors typically used for cycloaddition reactions (*i.e.*, $[RhCl(CO)_2]_2$ or $[RhCl(COD)]_2$) was studied in the presence of 20 mol% of $AgSbF_6$ in DCM at room temperature. In the absence of a phosphorus ligand, the conversion was complete but the desired cycloadduct **27a** was obtained in 63% and 24% yield for $[RhCl(COD)]_2$ and $[RhCl(CO)_2]_2$, respectively (entries 1 and 2, Table 4.1), with small amounts of the aromatized product **28a** being obtained in both cases. Interestingly, the combination of $AgSbF_6$ with Rh complexes **C1** and XBPhos-Rh-BArF, which contain halogen-bond-assembled diphosphine ligands, provided **27a** with perfect selectivity and similar yields (entries 3 and 4, Table 4.1).

(31) For more information, see 4.4.4 and Figure 4.24-4.27.

Table 4.1: Screening of rhodium-catalysts for the [4+2] cycloadditions of substrate **26a**.

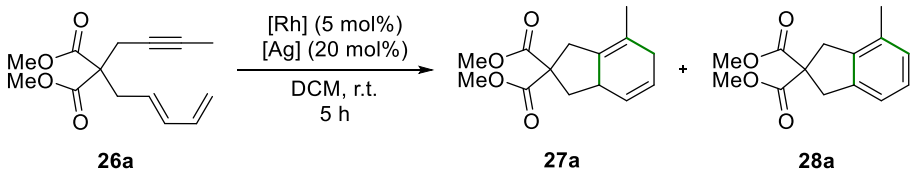

26a **27a** **28a**

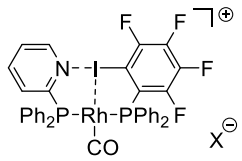

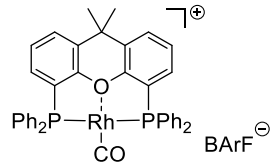

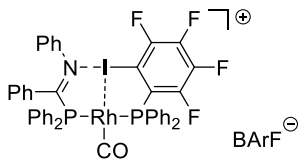

C1

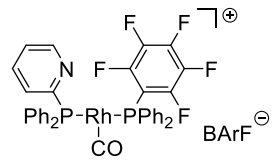

C2

Entry	Rh catalyst	Ag salt		Conv.[a] (%)	Yield[a] (%)	
			mol%		**27a**	**28a**
1[b]	$[RhCl(COD)]_2$	$AgSbF_6$	20	>99	63	7
2[b]	$[RhCl(CO)_2]_2$	$AgSbF_6$	20	>99	24	8
3	**C1**	$AgSbF_6$	20	>99	68	<1
4	XBPhos-Rh-BArF	$AgSbF_6$	20	>99	67	<1
5	**C1**	AgBArF	20	>99	69	<1
6	XBPhos-Rh-BArF	AgBArF	20	>99	87	<1
7	XBPhos-Rh-SbF_6	$AgSbF_6$	20	>99	63	<1
8	**C2**	AgBArF	20	63	28	<1
9	[Rh(CO)(XantPhos)]BArF	AgBArF	20	70	38	<1
10	$[RhCl(PPh_3)_3]$	$AgSbF_6$	20	71	39	<1

(a) Determined by ^1H NMR spectroscopy using 1,3,5-trimethoxybenzene as internal standard. (b) 2.5 mol% of Rh catalyst.

The effect of counterions in the outcome of transformations involving cationic Rh(I) complexes is well studied in the literature.[32] In order to avoid the presence of two different counteranions in the mixture, AgBArF was used in our catalyst screening studies. To our delight, even though for **C1** the results were similar to the ones obtained with $AgSbF_6$ (compare entries 3 and 5, Table 4.1),

(32) For a review on the effects of the counterions in [4+2] cycloadditions, see for example: Macchioni, A. *Chem. Rev.* **2005**, *105*, 2039-2073.

the combination of XBPhos-Rh-BArF with AgBArF salt resulted in the formation of cycloadduct **27a** in a higher yield and perfect selectivity (entry 6, Table 4.1).

To determine whether the improvement in the yield was specifically an effect of the BArF anion or not, the cycloaddition of **26a** with XBPhos-Rh-SbF_6 in the presence of $AgSBF_6$ was also performed (entry 7, Table 4.1). In this case, the conversion was complete, but the yield remained moderate, which clearly indicates that the BArF anion was indeed beneficial for the activity and selectivity of the rhodium-catalyst in this chemistry.

It is interesting to note that complex **C2**, in which halogen bonding between the two phosphines is not taking place, led to the poorest results of the study in terms of yield (entry 8, Table 4.1). To aid comparison, the complex [Rh(CO)(XantPhos)]BArF (as a model catalyst with a pincer-type ligand and no XB-backbone), and Wilkinson catalyst (*i.e.*, $[RhCl(PPh_3)_3]$) were included in this study (entries 9 and 10 respectively, Table 4.1). In both cases, the yield of the cycloadduct was low.

Several experiments were also performed to determine the amount of silver salt needed. Its presence in the media was crucial for the reaction to proceed, since in its absence no cycloaddition product was observed (entry 1, Table 4.2). However, in the absence of XBPhos-Rh, the silver salt alone did not suffice for the reaction to proceed (entry 2, Table 4.2). Reducing the amounts of silver also provided worse results, as the yields were moderate when 10 mol% and 5 mol% of AgBArF were used (compare a 87% yield with a 20 mol% of AgBArF with 68% and 57% yield for 10 mol% and 5 mol% respectively; entries 3 – 5, Table 4.2).

Table 4.2: Effects of AgBArF in the outcome of the reaction.

Entry	Rh catalyst[a]	Ag salt		Conv.[b] (%)	Yield[b] (%)	
			mol%		**27a**	**28a**
1	XBPhos-Rh-BArF	none	-	17	<1	<1
2	none	AgBArF	20	4	<1	<1
3	XBPhos-Rh-BArF	AgBArF	20	>99	87	<1
4	XBPhos-Rh-BArF	AgBArF	10	95	68	<1
5	XBPhos-Rh-BArF	AgBArF	5	80	57	<1

(a) 5.0 mol%. (b) Determined by ^1H NMR spectroscopy using 1,3,5-trimethoxybenzene as internal standard.

UNIVERSITAT ROVIRA I VIRGILI
TRANSITION METAL-CATALYZED CYCLOADDITION REACTIONS FOR THE FORMATION OF EIGHT- AND SIX-MEMBERED RINGS
Nuria Llorente González

In conclusion, the combination of a 5 mol% of XBPhos-Rh-BArF and a 20 mol% AgBArF represented the highest performing catalytic conditions (entry 6, Table 4.1) for the [4+2] cycloaddition of dienyne model substrate **26a**.

With the optimal conditions in hand, we then moved to expand the structural diversity of the substrates (Table 4.3). Triene substrate **26b** did not lead to the desired [4+2] cycloadduct (<1%, Table 4.3). The dienyne **26c** with an unsubstituted terminal acetylene group led to the desired [4+2] cycloadduct, though in low yield (14%, Table 4.3). Further investigations focused on dienynes with the acetylene group being in an internal position. The purely hydrocarbonated dienyne **26d** and its N- and O-containing analogues were transformed into the corresponding [4+2] cycloadducts under the catalytic effects of XBPhos-Rh and AgBArF. Good yields were obtained for the purely hydrocarbonated dienyne **26d** (88 % isolated yield for **27d**, Table 4.3).

In contrast, the isolated yields of the O-containing substrates (**26g** and **26h**, Table 4.3) decreased dramatically (34% and 22% yield for 27g and 27h, respectively, Table 4.3). It should be noted that the aromatized cycloadducts were present in both crude mixtures in minor amounts (<5%). Nitrogen-containing dienynes 26e and 26f, however, led to the cyclized products in 54% and 97% yield, respectively (Table 4.3). Substitution in the diene moiety was detrimental to the reactivity, as the desired product was not obtained for 26i (Table 4.3). Unfortunately, with our catalytic system, the substrate evolved to polymeric material rather than to the desired cycloadduct. In an attempt to reduce this effect, the reaction was performed with lower amounts of AgBArF to prevent polymerization (see footnotes e-f in Table 4.3), without any change in the outcome of the reaction being observed. We also performed the cycloaddition reaction of substrate 26i in the presence of tert-butylcatechol (a well-known polymerization inhibitor33), but no changes in the outcome of the reaction were observed (footnote g, Table 4.3). Our initial attempts to obtain 6/6-fused heterocycles via [4+2] cycloadditions have been, so far, unsuccessful. Substrate 26j (Table 4.3) did not yield the desired product with our reaction conditions.

(33) Gogotov, A. F. *Pet. Chem.* **2017**, *57*, 891-896.

Table 4.3: XBPhos-Rh-BArF/AgBArF-catalyzed [4+2] cycloaddition for an array of structurally diverse substrates.

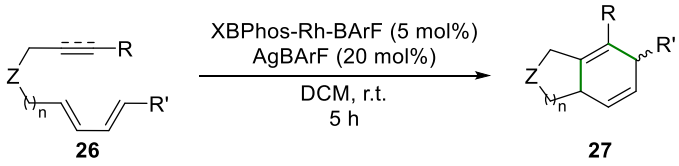

Substrate	Conv.[a]	Product	Yield[a,b]	Substrate	Conv.[a]	Product	Yield[a,b]
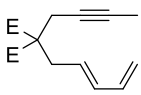 **26a**[c]	>99%	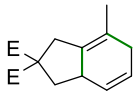 **27a**[c]	87% (90%)	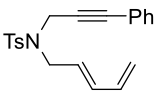 **26f**	>99%	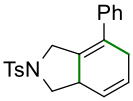 **27f**	97% (71%)
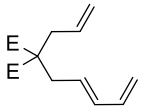 **26b**[c]	23%	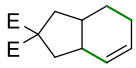 **27b**[c]	<1%	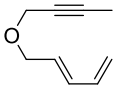 **26g**	>99%	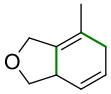 **27g**	28% (34%)
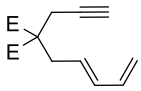 **26c**[c]	64% 39%[d]	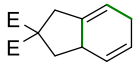 **27c**[c]	14% 14%	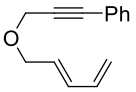 **26h**	>99%	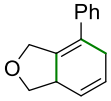 **27h**	24% (22%)
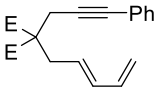 **26d**[c]	>99%	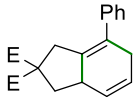 **27d**[c]	82% (88%)	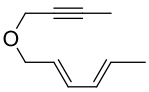 **26i**	>99% >99%[e] >99%[f] >99%[g]	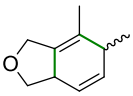 **27i**	<1% <1% <1% <1%
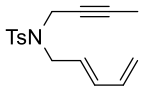 **26e**	>99%	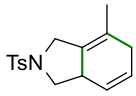 **27e**	54% (60%)	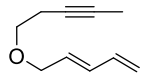 **26j**	44% 62%[h]	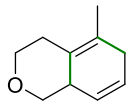 **27j**	<1% <1%

(a) Determined by ^{1}H NMR spectroscopy using 1,3,5-trimethoxybenzene as internal standard. (b) In brackets isolated yields after column chromatography on silica gel. (c) E= CO_2Me (d) Reaction run in the absence of AgBArF (e) 5 mol% AgBArF (f) 10 mol% AgBArF (g) 0.65 mol% of *tert*-butylcatechol. (h) Reaction run for 16 h.

Cycloaddition products were characterized with standard spectroscopic techniques. Moreover, crystals suitable for X-ray diffraction analysis were grown for **27d**, **27e** and **27f** and their structures were univocally confirmed with this technique (Figure 4.1).

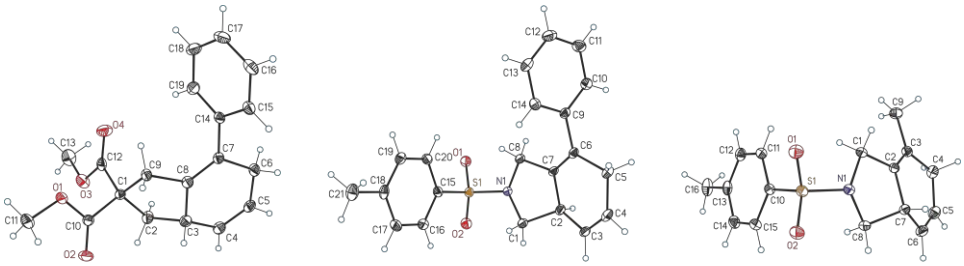

Figure 4.1. Single-crystal X-Ray structures of **27d**, **27e** and **27f**.

At this point of our studies, the role of the silver salt was unclear. It has always been suggested in the literature for this chemistry that silver is required as a halide scavenger to generate *in situ* cationic Rh(I) species from the neutral rhodium complexes generally used as precursors (for instance $[RhCl(CO)_2]_2$ or $[RhCl(COD)]_2$). Thus, it is normally proposed in the literature that silver does not intervene in the catalytic cycle. Moreover, it is commonly accepted in the literature that rhodium-catalyzed [4+2] cycloadditions follow the reaction pathway indicated in Scheme 4.8.[28]

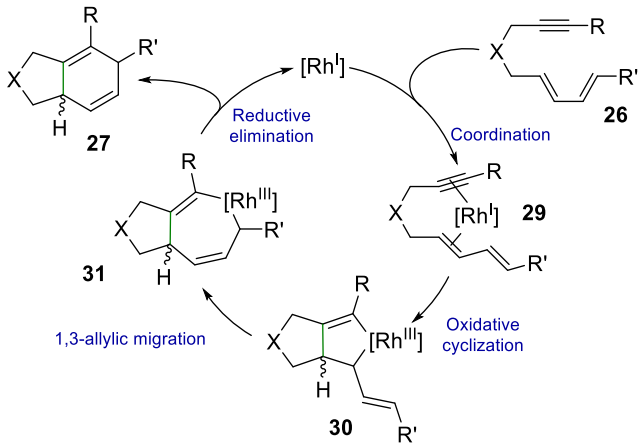

Scheme 4.8. Typically proposed reaction pathway for [4+2] cycloadditions of dienynes catalyzed by rhodium-complexes.

According to the literature, the reaction starts by coordination of the dienyne **26** to the cationic Rh(I) center of the catalyst. Subsequent oxidative cyclization leads to the five-membered rhodacycle **30**, which evolves to the seven-membered rhodacycle **31** by a 1,3-allylic migration process. Subsequent reductive elimination yields the [4+2] cycloadduct **27** and regenerates the cationic rhodium(I) complex, which reenters the catalytic cycle.

As for the cycloaddition reactions studied in the present thesis, neither XBPhos-Rh-BArF alone nor AgBArF on its own,[34] were capable of catalyzing the [4+2] cycloadditions of dienynes **26** (see entries 1 and 2, in Table 4.2). The combined use of rhodium and silver species were required for the reaction to proceed. A review of the literature showed us that rhodium/silver cooperative catalysis is not uncommon in carbocyclizations.[35] In these cases, the silver cation interacts with the substrate prior to the cyclization process. Moreover, several studies report the cooperative effect of Lewis acids in rhodium catalysis, suggesting that the activation effects from silver may be due to its Lewis acidic character.[36] In order to test the effect of silver on substrate **26a**, complexation studies were performed by ^{1}H NMR spectroscopy. The ^{1}H NMR spectra of dienyne **26a** and a 1:1 molar mixture of **26a** and AgBArF are shown in Figure 4.2.

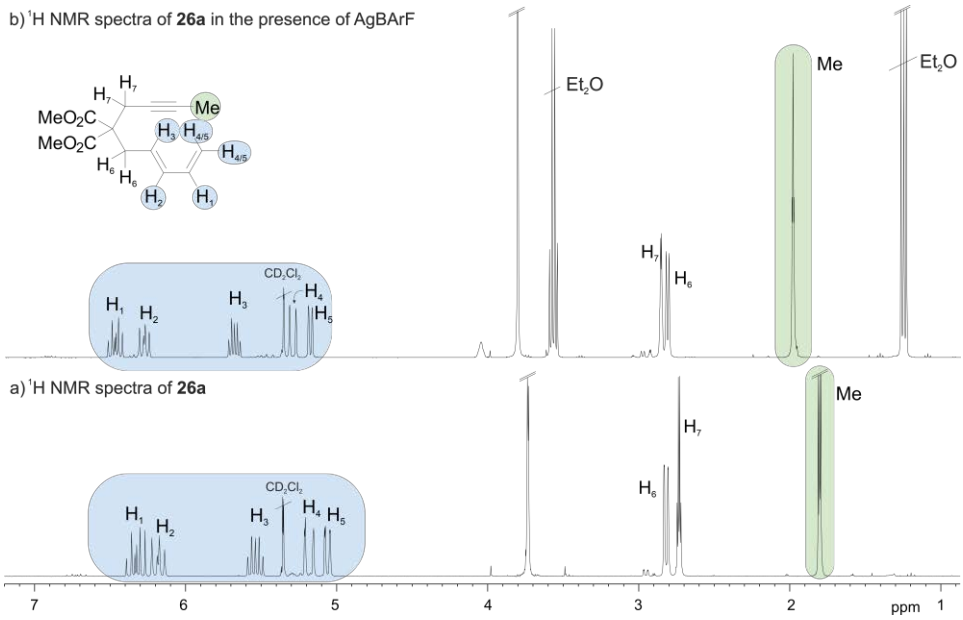

Figure 4.2. Stacked plot of the ^{1}H NMR spectra of (a) **26a** and that of (b) a 1:1 mixture of **26a** and AgBArF in CD_2Cl_2 at 25 °C.

(34) Silver salts are known to promote cycloaddition reactions. For more information, see: Szpilman, A. M.; Carreira, E. M. In *Silver in Organic Chemistry*; Harmata, M., Ed.; John Wiley & Sons, Inc.: Hoboken, 2010; pp 43-82.

(35) (a) Yao, L.; Yu, X.; Mo, C.; Wu, J. *Org. Biomol. Chem.* **2012**, *10*, 9447-9451. (b) Liu, H.; Liu, G.; Qiu, G.; Pu, S.; Wu, J. *Tetrahedron* **2013**, *69*, 1476-1480. (c) Yang, S.; Rui, K.-H.; Tang, X.-Y.; Xu, Q.; Shi, M. *J. Am. Chem. Soc.* **2017**, *139*, 5957-5964.

(36) (a) Wang, C.; Xi, Z. *Chem. Soc. Rev.* **2007**, *36*, 1395-1406. (b) Yasukawa, T.; Kobayashi, S. *Chem. Lett.* **2017**, *46*, 98-100. (c) Zheng, W.-F.; Xu, Q.-J.; Kang, Q. *Organometallics* **2017**, *36*, 2323-2330.

As expected,[37] changes in the chemical shift of the signals corresponding to the protons on the diene unit and the groups bonded to the C≡C triple bond were observed. All the signals shifted downfield, which was in good agreement with the coordination of substrate **26a** to the silver cation through the diene and alkyne groups. This effect was most noticeable for the signal of the methyl group attached to the alkyne group, which shifted from 1.80 ppm to 1.99 ppm (see signals shadowed in green, Figure 4.2).

After these studies, we hypothesized that the role of silver could probably be to facilitate the cycloaddition process by pre-organizing the substrate towards oxidative cyclization. A tentative rationalization of the reaction pathway leading to the [4+2] cycloadducts *via* a cooperative Rh/Ag cooperative process is depicted in Scheme 4.9.

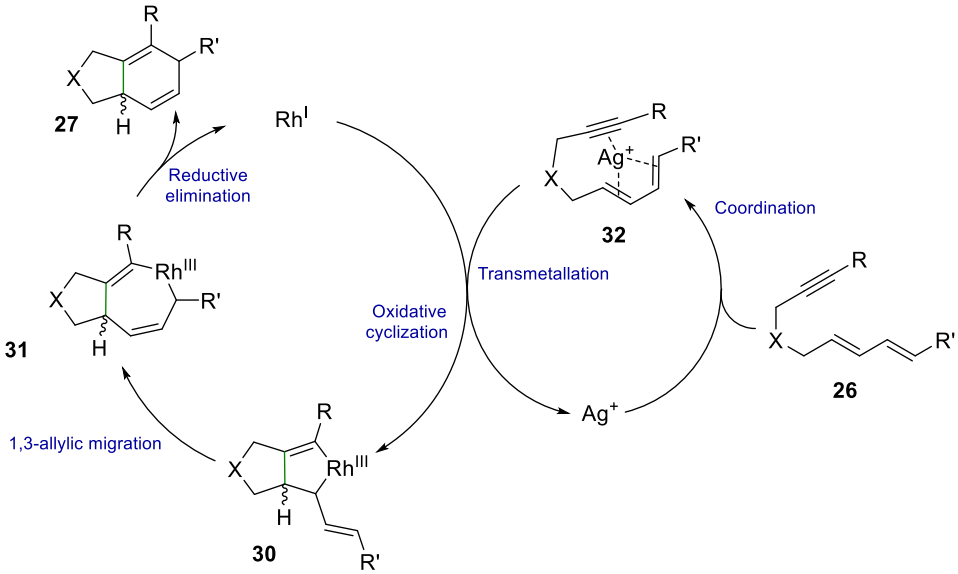

Scheme 4.9. Tentative rationalization of the reaction pathway for intramolecular [4+2] cycloadditions of dienynes

We hypothesized that prior to the commonly accepted catalytic cycle for rhodium-mediated [4+2] cycloadditions (see Scheme 4.8), the dienyne **26** would form a 1:1 complex with AgBArF, yielding intermediate **32**. Transmetallation followed by oxidative cyclization would afford intermediate **30**. Whether

(37) The affinity of silver towards unsaturated bonds has been well studied. For selected examples, see: (a) Winstein, S.; Lucas, H. J. *J. Am. Chem. Soc.* **1938**, *60*, 836-847. (b) Trueblood, K. N.; Lucas, H. J. *J. Am. Chem. Soc.* **1952**, *74*, 1338-1339. (c) Dias, H. V. R.; Wu, J. *Eur. J. Inorg. Chem.* **2008**, 509-522 and references therein.

oxidative cyclization takes place between the alkyne group and the internal C=C bond of **26** as indicated in Scheme 4.9, or between other combinations of unsaturated C-C bonds from the substrate, needs to be studied in detail. The potential effects of silver on the oxidative cyclization process need also to be investigated. A 1,3-allylic migration process followed by a reductive elimination step from intermediate **31** would afford the final cycloaddition product **32**. This preliminary hypothesis on a plausible reaction pathway towards [4+2] cycloadducts would also provide a rationalization to the lack of reactivity of substrates **26c** and **26i**. Whilst **26c**, which contains an unsubstituted terminal alkyne, would react with silver BArF to yield an unreactive silver-alkynyl complex, dienyne **26i**, which incorporates substituents at the diene motif, has a lower affinity towards coordination to the silver center.[38]

4.3. Conclusions

We have demonstrated the versatility and efficacy of XBPhos-Rh-BArF combined with silver BArF as catalyst for intramolecular [4+2] cycloadditions of dienynes. This cycloaddition reaction proceeded efficiently on a set of structurally diverse dienynes to afford six-membered carbocycles fused to a five-membered ring. The products were isolated as 1,4-unconjugated cyclohexenes, without aromatization taking place. The halogen-bonded complex **C1** has been prepared and used in this chemistry, albeit with less efficiency compared to that of XBPhos-Rh-BArF. A tentative rationalization of the reaction pathway involving a Rh/Ag cooperative process has also been provided. Coordination of the dienyne to silver has been demonstrated, which led us to preliminary hypothesize that the intramolecular [4+2] cyclizations may be proceeding *via* a silver complexation, transmetallation, oxidative cyclization, 1,3-allyl migration and reductive elimination sequence as a probable reaction pathway towards the final cycloadducts.

(38) For more information on the formation on the stability of Ag(I) complexes of olefins and acetylenes, see: Pettit, L. D.; Barnes, D. S. In *π-Complexes of Transition Metals*; Springer: Berlin, Heidelberg, 1972; pp 85-139 and references therein.

4.4. Experimental Section

4.4.1 General Remarks

All syntheses were carried out on chemicals as purchased from commercial sources, unless otherwise stated. Air and moisture sensitive manipulations or reactions were run under inert atmosphere using anhydrous and deoxygenated solvents, either in a glove box or with standard Schlenk techniques. All solvents were dried by using a Solvent Purification System (SPS). Silica gel 60 (230–400 mesh) was used for column chromatography. NMR spectra were recorded in $CDCl_3$ unless otherwise cited, on a Bruker Avance 300 MHz, 400 MHz or 500 MHz Ultrashield spectrometers. ^1H NMR and $^{13}C\{^1H\}$ NMR chemical shifts are quoted in ppm relative to residual solvent peaks. High-resolution mass spectra (HRMS) were recorded by using either ESI or APCI ionization method in positive mode. Conversion and selectivity for the cycloaddition products were determined by ^1H NMR spectroscopy from the crude mixtures, using 1,3,5-trimethoxybenzene as internal standard. Melting points were measured in open capillaries and are uncorrected. For the synthesis and characterization of substrates **26a**, **26b** and **26c**, see Chapter 3. AgBArF[39] and XBPhos-Rh-BArF[8a] were synthesized following the methodologies reported in the literature. Complexes [Rh(CO)(XantPhos)]BArF and Complex **C2** were prepared by Dr. L. Carreras and A. Martínez-Bascuñana.

4.4.2 Synthesis of Cycloaddition Substrates

- Synthesis of dimethyl (*E*)-2-(penta-2,4-dien-1-yl)-2-(3-phenylprop-2-yn-1-yl)malonate (**26d**)

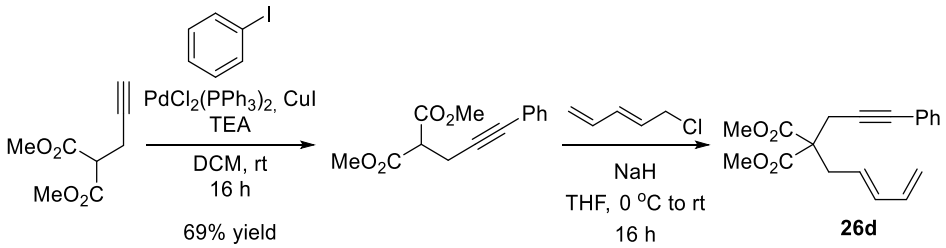

Copper (I) iodide (0.043 g, 0.219 mmol), bis(triphenylphosphine)palladium(II) dichloride (0.157 g, 0.219 mmol) and

(39) Hayashi, Y.; Rohde, J. J.; Corey, E. J. *J. Am. Chem. Soc.* **1996**, *118*, 5502-5503.

iodobenzene (1 mL, 8.76 mmol) were added to a solution of dimethyl 2-(prop-2-yn-1-yl)malonate (1.4 mL, 8.76 mmol) in DCM (17 mL) and triethylamine (TEA, 4.6 mL). The reaction mixture was stirred at room temperature for 16 h. The reaction was then quenched with saturated ammonium chloride (30 mL). The aqueous layer was extracted with diethyl ether (3 x 30 mL). The combined organic layers were successively washed with aqueous hydrochloric acid (0.2 M, 20 mL), a saturated solution of sodium bicarbonate (20 mL), and water (2 x 30 mL). The resulting organic layers were dried over magnesium sulfate, filtered and concentrated under reduced pressure. The resulting product was purified by column chromatography on silica gel (pentane:diethyl ether, 80:20) to afford dimethyl 2-(3-phenylprop-2-yn-1-yl)malonate as a yellowish oil (1.59 g, 69% yield). ^{1}H NMR (500 MHz, $CDCl_3$) δ 7.40 – 7.34 (m, 2H), 7.30 – 7.26 (m, 3H), 3.79 (s, 6H), 3.70 (t, J = 7.7 Hz, 1H), 3.02 (d, J = 7.7 Hz, 2H) ppm. ^{13}C {^{1}H} NMR (126 MHz, $CDCl_3$) δ 168.6 (C=O), 131.8 (CH_{arom}), 128.3 (CH_{arom}), 128.2 (C_{arom}), 123.3 (C_{arom}), 85.3 (C≡), 82.7 (C≡), 52.9 (CH_3), 51.3 (CH), 19.7 (CH_2) ppm. Spectroscopic data were in agreement with those previously reported in the literature.[40]

Dimethyl 2-(3-phenylprop-2-yn-1-yl)malonate (1.0 g, 3.86 mmol) was slowly added to a suspension of sodium hydride (0.185 g, 4.63 mmol) in anhydrous THF (15 mL) under Ar atmosphere at 0 °C. The mixture was stirred at room temperature for 15 min. After this time, 5-chloropenta-1,3-diene[41] (0.559 g, 4.63 mmol) was added dropwise and the mixture was allowed to react at room temperature for 16 h. Most of the solvent was then removed *in vacuo* and water (7 mL) and diethyl ether (40 mL) were added into the resulting mixture. The aqueous layer was separated and extracted successively with diethyl ether (2 x 10 mL). The combined organic phases were washed with brine (2 x 10 mL) and dried over anhydrous magnesium sulfate. The solvent was removed *in vacuo* and the desired product was purified by column chromatography (pentane:diethyl ether, 100:00→90:10) to yield the product as a yellowish oil (521 mg, 44% yield).

(40) Schiller, R.; Pour, M.; Fakova, H.; Kunes, J.; Cisarova, I. *J. Org. Chem.* **2004**, *69*, 6761-6765.
(41) For the synthesis of 5-chloropenta-1,3-diene, see the experimental section in Chapter 1.

UNIVERSITAT ROVIRA I VIRGILI
TRANSITION METAL-CATALYZED CYCLOADDITION REACTIONS FOR THE FORMATION OF EIGHT- AND SIX-MEMBERED RINGS
Nuria Llorente González

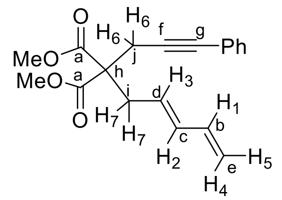

26d

^{1}H NMR (500 MHz, $CDCl_3$) δ 7.35 – 7.31 (m, 2H, H_{Ph}), 7.25 – 7.20 (m, 3H, H_{Ph}), 6.25 (ddd, $^{3}J_{H1-H4}$ = 16.7 Hz, $^{3}J_{H1-H2}$ = 10.3 Hz, $^{2}J_{H1-H5}$ = 10.1 Hz, 1H, H_1), 6.14 (dd, $^{3}J_{H2-H3}$ = 15.0 Hz, $^{3}J_{H2-H1}$ = 10.3 Hz, 1H, H_2), 5.50 (dt, $^{3}J_{H3-H2}$ = 15.0, $^{3}J_{H3-H7}$ = 7.6 Hz, 1H, H_3), 5.11 (dd, $^{3}J_{H1-H4}$ = 16.7 Hz, $^{2}J_{H4-H5}$ = 1.4 Hz, 1H, H_4), 5.00 (dd, $^{2}J_{H1-H5}$ = 10.1, $^{2}J_{H5-H4}$ = 1.4 Hz, 1H, H_5), 3.72 (s, 6H, H_{OMe}), 2.97 (s, 2H, H_6), 2.86 (dd, $^{3}J_{H7-H3}$ = 7.6 Hz, $^{2}J_{H7-H7}$ = 0.8 Hz, 2H, H_7) ppm. ^{13}C {^{1}H} NMR (126 MHz, $CDCl_3$) δ 170.4 (C=O, C_a), 136.7 (s, CH=, C_b), 135.8 (s, CH=, C_c), 131.8 (CH_{arom}, C_{Ph}), 128.4 (CH=, C_{Ph}), 128.2 (CH_{arom}, C_{Ph}), 127.4 (s, CH=, C_d), 123.3 (C_{arom}, C_{Ph}), 117.0 (CH_2=, C_e), 84.4 (C≡, C_f), 83.9 (C≡, C_g), 57.7 (C_q, C_h), 52.9 (CH_3, OMe), 35.86 (CH_2, C_i), 23.99 (s, CH_2, C_j) ppm. Spectroscopic data were in agreement with those previously reported in the literature.[40]

- Synthesis of (*E*)-*N*-(but-2-yn-1-yl)-*N*-(penta-2,4-dien-1-yl)-*p*-toluenesulfonamide (**26e**)

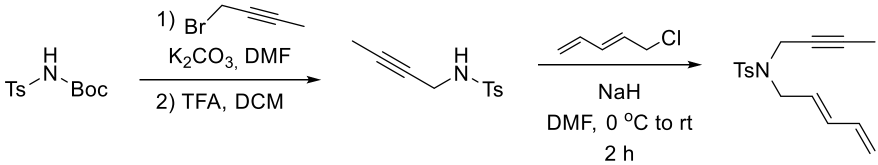

66% yield 84% yield **26e**

N-(*tert*-Butoxycarbonyl)-*p*-toluenesulfonamide (2 g, 7.37 mmol) was added to a suspension of potassium carbonate (1.63 g, 11.8 mmol) in DMF (7 mL). The suspension was stirred for 1 h at room temperature. 3-Bromo-1-propyne (0.655 mL, 7.37 mmol) was added dropwise and the resulting mixture was stirred for an additional 2 h at the same temperature. The solution was diluted with diethyl ether (9 mL) and washed with water (2 x 10 mL). The aqueous layer was extracted with diethyl ether (3 x 20 mL). The combined organic layers were washed with brine (15 mL), dried over anhydrous magnesium sulfate, filtered and concentrated under reduced pressure. The resulting crude product was dissolved in DCM (2.5 mL) and trifluoro acetic acid (2.5 mL) was added. The resulting mixture was stirred overnight at room temperature. After removal of the solvent, the residue was purified by silica gel chromatography (pentane:EtOAc, 80:20) to yield *N*-(but-2-yn-1-yl)-*p*-toluenesulfonamide as a white solid (1.09 g, 66% yield). ^{1}H NMR (400 MHz, $CDCl_3$) δ 7.77 (d, *J* = 8.3 Hz, 2H), 7.31 (d, *J* = 8.3 Hz, 2H), 4.49 (t, *J* = 5.8 Hz, 1H), 3.76 (dq, *J* = 5.8, 2.5 Hz, 3H), 2.43 (s, 5H), 1.60 (t, *J* = 2.5 Hz, 4H) ppm. ^{13}C {^{1}H} NMR (101 MHz, $CDCl_3$) δ 143.7 (C_{arom}), 136.9

(C_{arom}), 129.7 (CH_{arom}), 127.6 (CH_{arom}), 81.2 (C≡), 73.3 (C≡), 33.6 (CH_2), 21.7 (CH_3), 3.4 (CH_3) ppm. Spectroscopic data were in agreement with those previously reported in the literature.[42]

A solution of *N*-(but-2-yn-1-yl)-4-methylbenzenesulfonamide (0.5 g, 2.24 mmol) in DMF (3.0 mL) was added to a cooled (0 °C) suspension of sodium hydride (60% in mineral oil, 0.134 g, 3.36 mmol) in DMF (3.0 mL). The mixture was stirred at 0 °C for 30 min, after which a solution of freshly prepared 5-chloropenta-1,3-diene[41] (0.405 g, 3.36 mmol) in DMF (1.0 mL) was added. The resulting mixture was stirred at room temperature for 2 h. The reaction was quenched by the addition of a saturated aqueous solution of ammonium chloride (5.0 mL) at 0 °C and extracted with diethyl ether (3 x 5.0 mL). The combined organic phases were dried over magnesium sulfate and concentrated *in vacuo*. The residue was purified by silica gel column chromatography (pentane: diethyl ether, 90:10) to yield **26e** pure as a white solid (542 mg, 84% yield).

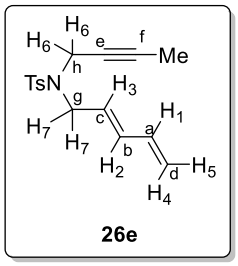

26e

^{1}H NMR (500 MHz, $CDCl_3$) δ 7.73 (d, $^3J_{HTs\text{-}HTs}$ = 8.3 Hz, 2H, H_{Ts}), 7.29 (d, $^3J_{HTs\text{-}HTs}$ = 8.3 Hz, 2H, H_{Ts}), 6.30 (ddd, $^3J_{H1\text{-}H4}$ = 16.7 Hz, $^3J_{H1\text{-}H2}$ = 10.5 Hz, $^3J_{H1\text{-}H5}$ = 10.0 Hz, 1H, H_1), 6.20 (dd, $^3J_{H2\text{-}H3}$ = 14.8 Hz, $^3J_{H2\text{-}H1}$ = 10.5 Hz, 1H, H_2), 5.58 (dt, $^3J_{H3\text{-}H2}$ = 14.8 Hz, $^3J_{H3\text{-}H7}$ = 7.0 Hz, 1H, H_3), 5.20 (d, $^3J_{H4\text{-}H1}$ = 16.7 Hz, 1H, H_4), 5.10 (d, $^3J_{H5\text{-}H1}$ = 10.0 Hz, 1H, H_5), 4.00 (q, $^5J_{Me\text{-}H6}$ = 2.3 Hz, 2H, H_6), 3.82 (d, $^3J_{H7\text{-}H3}$ = 7.0 Hz, 2H), 2.42 (s, 3H), 1.55 (t, $^5J_{Me\text{-}H6}$ = 2.3 Hz, 3H) ppm. ^{13}C {^{1}H} NMR (126 MHz, $CDCl_3$) δ 143.6 (C_{arom}, C_{Ts}), 136.6 (C_{arom}, C_{Ts}), 136.2 (CH=, C_a), 135.6 (CH=, C_b), 129.6 (2C, CH_{arom}, C_{Ts}), 128.3 (2C, CH_{arom}, C_{Ts}), 127.7 (CH=, C_c), 118.5 (CH_2=, C_d), 82.0 (C≡, C_e), 72.0 (C≡, C_f), 48.4 (CH_2, C_g), 36.8 (CH_2, C_h), 21.62 (CH_3, C_{Ts}), 3.37 (CH_3, Me) ppm. Spectroscopic data were in agreement with those previously reported in the literature.[47]

(42) Schroder, F.; Tugny, C.; Salanouve, E.; Clavier, H.; Giordano, L.; Moraleda, D.; Gimbert, Y.; Mouries-Mansuy, V.; Goddard, J.-P.; Fensterbank, L. *Organometallics* **2014**, *33*, 4051-4056.

- Synthesis of (*E*)-*N*-(penta-2,4-dien-1-yl)-*N*-(3-phenylprop-2-yn-1-yl)-*p*-toluenesulfonamide (**26f**)

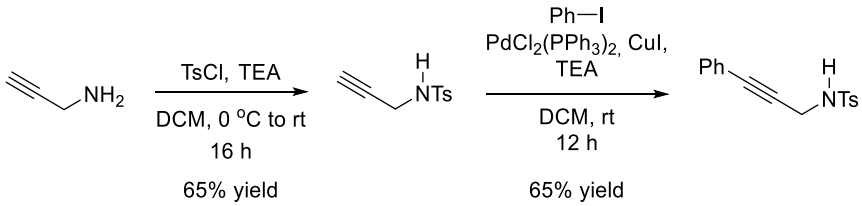

Prop-2-yn-1-amine (1.3 mL, 20 mmol) was dissolved in anhydrous DCM (50 mL) and cooled to 0 °C, followed by the addition of TEA (7.0 mL, 50 mmol) and tosyl chloride (3.827 g, 20.07 mmol). The mixture was allowed to warm to room temperature and stirred for 16 h, before being diluted with diethyl ether (200 mL). The mixture was washed with hydrochloric acid (1M, 150 mL), saturated aqueous sodium bicarbonate (50 mL), dried over magnesium sulfate and concentrated *in vacuo*. The crude mixture was dissolved in DCM and allowed to stand at 5 °C for 2 h. The precipitate obtained was washed with pentane and the solvent was then evaporated to dryness to obtain *N*-(prop-2-yn-1-yl)-*p*-toluenesulfonamide as a white solid (2.1 g, 65% yield). ^{1}H NMR (300 MHz, $CDCl_3$) δ 7.77 (d, J = 8.2 Hz, 2H), 7.31 (d, J = 8.2 Hz, 2H), 4.84 (t, J = 5.9 Hz, 1H), 3.82 (dd, J = 5.9, 2.5 Hz, 2H), 2.43 (s, 3H) ppm. ^{13}C {^{1}H} NMR (75 MHz, $CDCl_3$) δ 144.0 (C_{arom}), 136.6 (C_{arom}), 129.8 (CH_{arom}), 127.5 (CH_{arom}), 78.1 (C≡), 73.1 (C≡), 33.0 (CH_2), 21.7 (CH_3) ppm. Spectroscopic data were in agreement with those previously reported in the literature.[43]

Copper (I) iodide (0.034 g, 0.173 mmol), bis(triphenylphosphine)palladium(II) dichloride (0.163 g, 0.173 mmol) and iodobenzene (0.788 mL, 6.9 mmol) were added to a solution of *N*-(prop-2-yn-1-yl)-*p*-toluenesulfonamide (1.5 g, 6.9 mmol) in DCM (15 mL) and TEA (3.6 mL). The reaction mixture was stirred at room temperature for 16 h. The reaction was then quenched with saturated ammonium chloride (30 mL). The aqueous layer was extracted with diethyl ether (3 x 30 mL). The combined organic layers were washed with aqueous hydrochloric acid (0.2 M, 20 mL), a saturated solution of sodium bicarbonate (20 mL), and water (2 x 30 mL). The organic layers were dried over magnesium sulfate and concentrated under reduced pressure. The resulting product was purified by silica gel column chromatography (pentane:diethyl ether, 80:20) to afford *N*-(3-phenylprop-2-yn-1-yl)-*p*-

(43) Dimirjian, C. A.; Castineira Reis, M.; Balmond, E. I.; Turman, N. C.; Rodriguez, E. P.; Di Maso, M. J.; Fettinger, J. C.; Tantillo, D. J.; Shaw, J. T. *Org. Lett.* **2019**, *21*, 7209-7212.

toluenesulfonamide compound as a pale yellow solid (1.25 g, 65% yield). ^{1}H NMR (300 MHz, $CDCl_3$) δ 7.88 (d, J = 8.4 Hz, 2H), 7.40 - 7.26 (m, 5H), 7.25 - 7.16 (m, 2H), 4.68 (t, J = 6.3 Hz, 1H), 4.15 (d, J = 6.3 Hz, 2H), 2.43 (s, 3H) ppm. ^{13}C {^{1}H} NMR (75 MHz, $CDCl_3$) δ 143.8 (C_{arom}), 136.9 (C_{arom}), 131.6 (CH_{arom}), 129.7 (CH_{arom}), 128.7 (C_{arom}), 128.6 (CH_{arom}), 128.2 (CH_{arom}), 127.5 (CH_{arom}), 95.2 (C≡), 83.2 (C≡), 33.8 (CH_2), 21.5 (CH_3) ppm. Spectroscopic data were in agreement with those previously reported in the literature.[43]

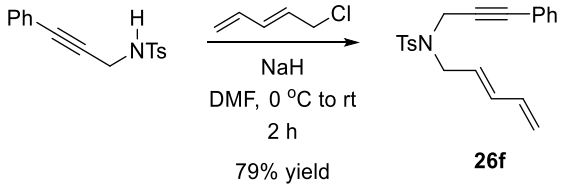

A solution of *N*-(3-phenylprop-2-yn-1-yl)-*p*-toluenesulfonamide (0.5 g, 1.75 mmol) in DMF (2.5 mL) was added to a cooled suspension (0 °C) of sodium hydride (60% in mineral oil, 105 mg, 2.63 mmol) in DMF (2.5 mL). The mixture was stirred at 0 °C for 30 min, after which a solution of previously prepared 5-chloropenta-1,3-diene[41] (0.317 g, 2.63 mmol) in DMF (0.5 mL) was added. The resulting mixture was stirred at room temperature for 2 h. The reaction was quenched by the addition of a saturated aqueous solution of ammonium chloride (5.0 mL) at 0 °C and extracted with ether (3 x 5.0 mL). The combined organic phases were dried over magnesium sulfate and concentrated *in vacuo*. The residue was purified by silica gel column chromatography (pentane: diethyl ether, 90:10) to yield **26f** as a pale yellow solid (486 mg, 79% yield).

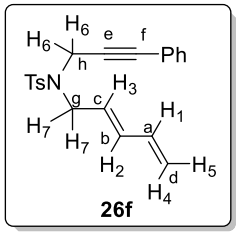

^{1}H NMR (400 MHz, $CDCl_3$) δ 7.74 (d, $^3J_{HTs-HTs}$ = 8.3 Hz, 2H, H_{Ts}), 7.26 - 7.16 (m, 5H, 3H_{Ph}, 2H_{Ts}), 7.07 - 7.00 (m, 2H, H_{Ph}), 6.31 (ddd, $^3J_{H1-H4}$ = 16.0 Hz, $^3J_{H1-H2}$ = 10.3 Hz, $^3J_{H1-H5}$ = 9.7 Hz, 1H, H_1), 6.23 (dd, $^3J_{H2-H3}$ = 14.2 Hz, $^3J_{H1-H2}$ = 10.3 Hz, 1H, H_2), 5.61 (dt, $^3J_{H3-H2}$ = 14.2 Hz, $^3J_{H3-H7}$ = 6.9 Hz, 1H, H_3), 5.19 (dd, $^3J_{H1-H4}$ = 16.0 Hz, $^2J_{H4-H5}$ = 1.0 Hz, 1H, H_4), 5.10 (dd, $^3J_{H5-H1}$ = 9.7 Hz, $^2J_{H5-H4}$ = 1.0 Hz, 1H, H_5), 4.26 (s, 2H, H_6), 3.89 (d, $^3J_{H3-H7}$ = 6.9 Hz, 2H, H_7), 2.30 (s, 3H, H_{Ts}) ppm. ^{13}C {^{1}H} NMR (101 MHz, $CDCl_3$) δ 143.6 (C_{arom}, C_{Ts}), 136.1 (C_{arom}, C_{Ts}), 136.0 (CH=, C_a), 135.7 (CH=, C_b), 131.6 (2C, CH_{arom}, C_{Ph}), 129.7 (2C, CH_{arom}, C_{Ts}), 128.5 (C_{arom}, C_{Ph}), 128.3 (2C, CH_{arom}, C_{Ph}), 128.0 (2C, CH_{arom}, C_{Ts}), 127.2 (CH=, C_c), 122.4 (C_{arom}, C_{Ph}), 118.5 (CH_2=, C_d), 85.9 (C≡, C_e), 81.8 (C≡, C_f), 48.5 (CH_2,

C_g), 37.0 (CH_2, C_h), 21.5 (CH_3, C_{Ts}) ppm. Spectroscopic data were in agreement with those previously reported in the literature.[44]

- Synthesis of (*E*)-5-(but-2-yn-1-yloxy)penta-1,3-diene (**26g**)

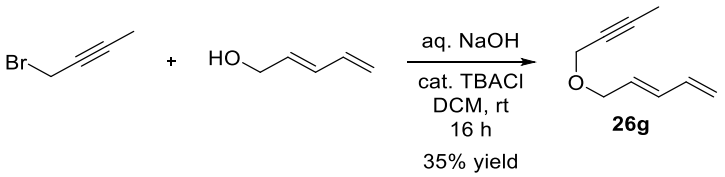

A mixture of (*E*)-penta-2,4-dien-1-ol[45] (0.743 g, 8.83 mmol), 1-bromo-2-butyne (1.21 mL, 13.8 mmol), tetrabutylammonium chloride (0.13 g, 0.468 mmol), 50% aqueous NaOH (3.53 g, 88.3 mmol) and DCM (5.0 mL) was vigorously stirred at room temperature overnight. The reaction mixture was then poured into 14 mL of distilled water. The phases were separated and the aqueous phase was extracted with pentane (5 x 7 mL). The combined organic phases were washed with brine (2 x 7 mL), dried over magnesium sulfate and concentrated *in vacuo*. The desired product was purified by distillation (b.p. = 66 °C, p = 6.4 mbar) to afford the target product **26g** pure as a colorless oil (425 mg, 35% yield).

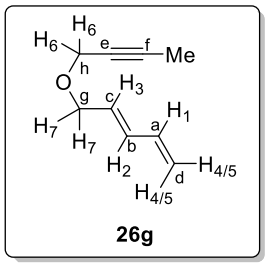

H NMR (400 MHz, $CDCl_3$) δ 6.39 - 6.21 (m, 2H, H_1 and H_2), 5.76 (dt, $^3J_{H3\text{-}H2}$ = 14.6 Hz, $^3J_{H3\text{-}H7}$ = 6.2 Hz, 1H, H_3), 5.21 (dd, $^3J_{H4\text{-}H1}$ = 15.6, $^2J_{H4\text{-}H5}$ = 1.3 Hz, 1H, H_4), 5.10 (dd, $^3J_{H5\text{-}H1}$ = 9.2 Hz, $^2J_{H5\text{-}H4}$ = 1.3 Hz, 1H, H_5), 4.10 (q, $^5J_{H6\text{-}Me}$ = 2.3 Hz, 2H, H_6), 4.08 (d, $^3J_{H7\text{-}H3}$ = 6.2 Hz, 2H, H_7), 1.85 (t, $^5J_{Me\text{-}H6}$ = 2.3 Hz, 1H, Me) ppm. ^{13}C {^1H} NMR (101 MHz, $CDCl_3$) δ 136.3 (CH=, C_a), 133.7 (CH=, C_b), 129.4 (CH=, C_c), 117.7 (CH=, C_d), 82.5 (C≡, C_e), 75.1 (C≡, C_f), 69.6 (CH_2, C_g), 57.7 (CH_2, C_h), 3.6 (CH_3, Me) ppm. Spectroscopic data were in agreement with those previously reported in the literature.[46]

(44) Lee, S. I.; Park, S. Y.; Park, J. H.; Jung, I. G.; Choi, S. Y.; Chung, Y. K.; Lee, B. Y. *J. Org. Chem.* **2006**, *71*, 91-96.
(45) For the synthesis of (*E*)-penta-2,4-dien-1-ol, see the experimental section in Chapter 1.
(46) Kimura, M.; Ezoe, A.; Mori, M.; Tamaru, Y. *J. Am. Chem. Soc.* **2005**, *127*, 201-209.

- Synthesis of (*E*)-(3-(penta-2,4-dien-1-yloxy)prop-1-yn-1-yl)benzene (**26h**)

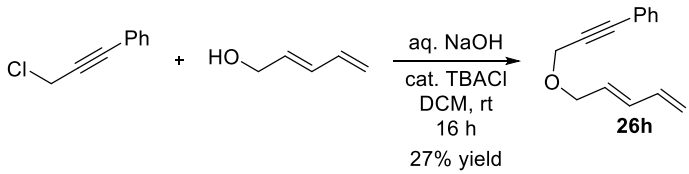

A mixture of product (*E*)-penta-2,4-dien-1-ol[45] (1 g, 11.9 mmol), (3-chloro-1-propyn-1-yl)-benzene (2.63 mL, 18.5 mmol), tetrabutylammonium chloride (0.175 g, 0.63 mmol), 50% aqueous NaOH (4.75 g, 119 mmol) and DCM (5.0 mL) was vigorously stirred at room temperature overnight. The reaction mixture was then poured into 16 mL of distilled water. The phases were separated and the aqueous phase was extracted with pentane (5 x 8 mL). The combined organic phases were washed with brine (2 x 8 mL), dried over magnesium sulfate and concentrated *in vacuo*. The desired product was purified by distillation (b.p. = 104 °C, p =0.038 mbar) to yield **26h** as pale yellow oil (643 mg, 28% yield).

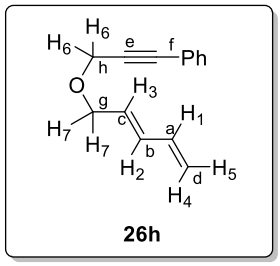

^{1}H NMR (400 MHz, $CDCl_3$) δ 7.53 - 7.41 (m, 2H, H_{Ph}), 7.38 - 7.23 (m, 3H, H_{Ph}), 6.42 - 6.26 (m, 2H, H_1 and H_2), 5.81 (dt, $^3J_{H3-H2}$ = 15.0 Hz, $^3J_{H3-H7}$ = 6.1 Hz, 1H, H_3), 5.24 (dd, $^3J_{H4-H1}$ = 16.7 Hz, $^2J_{H4-H5}$ = 1.0 Hz, 1H, H_4), 5.13 (dd, $^3J_{H5-H1}$ = 8.9 Hz, $^2J_{H5-H4}$ = 1.0 Hz, 1H, H_5), 4.38 (s, 2H, H_6), 4.18 (d, $^3J_{H7-H3}$ = 6.1 Hz, 2H, H_7) ppm. ^{13}C {^{1}H} NMR (101 MHz, $CDCl_3$) δ 136.2 (CH=, C_a), 134.1 (CH=,C_b), 131.8 (2C, CH_{arom}, C_{Ph}), 129.3 (CH=, C_c), 128.4 (C_{arom}, C_{Ph}), 128.3 (2C, C_{arom}, C_{Ph}), 122.7 (C_{arom}, C_{Ph}), 117.9 (CH=, C_d), 86.3 (C≡, C_e), 85.1 (C≡, C_f), 69.8 (s, CH_2, C_g), 57.9 (CH_2, C_h) ppm. Spectroscopic data were in agreement with those previously reported in the literature.[47]

1.1.1. Synthesis of (*E*)-5-(but-2-yn-1-yloxy)penta-1,3-diene (**26i**)

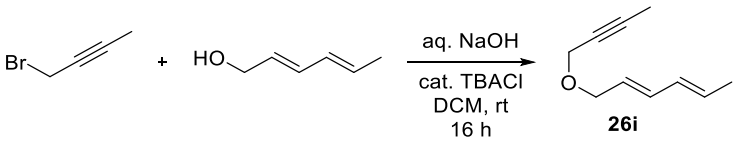

A mixture of (*E*,*E*)-hexa-2,4-dien-1-ol (1.1 mL, 9.46 mmol), 1-bromo-2-butyne (1.3 mL, 14.8 mmol), tetrabutylammonium chloride (0.13 g, 0.501

mmol), 50% aqueous NaOH (3.78 g, 94.6 mmol) and DCM (5.0 mL) was vigorously stirred at room temperature overnight. The reaction mixture was then poured into 14 mL of distilled water. The phases were separated, and the aqueous phase was extracted with pentane (5 x 7 mL). The combined organic phases were washed with brine (2 x 7 mL), dried over magnesium sulfate and concentrated *in vacuo*. The desired product was purified by distillation (b.p. = 75 °C, p = 5 mbar) to afford the target product **26i** pure as a colorless oil (984 mg, 69% yield).

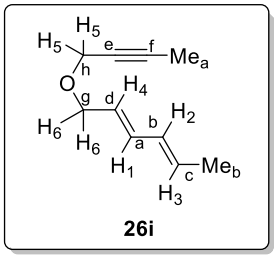

26i

^{1}H NMR (300 MHz, $CDCl_3$) δ 6.19 (dd, , $^{3}J_{H1\text{-}H4}$ = 15.3 Hz, $^{3}J_{H1\text{-}H2}$ = 10.5 Hz, 1H, H_1), 6.03 (dd, $^{3}J_{H2\text{-}H3}$ = 15.0 Hz, $^{3}J_{H2\text{-}H1}$ = 10.5 Hz, 1H, H_2), 5.77 - 5.50 (m, 2H, H_3 and H_4), 4.05 (q, $^{5}J_{H5\text{-}Mea}$ = 2.3 Hz, 2H, H_5), 4.01 (d, $^{3}J_{H6\text{-}H4}$ = 6.8 Hz, 2H, H_6), 1.82 (t, $^{5}J_{H5\text{-}Mea}$ = 2.3 Hz, 3H, Me_a), 1.73 (d, $^{3}J_{H3\text{-}Meb}$ = 6.4 Hz, 3H, Me_b) ppm. ^{13}C {^{1}H} NMR (75 MHz, $CDCl_3$) δ 133.8 (CH=, C_a), 130.8 (CH=, C_b), 130.2 (CH=, C_c), 126.0 (CH=, C_d), 82.4 (C≡, C_e), 75.2 (C≡, C_f), 69.9 (CH_2, C_g), 57.5 (CH_2, C_h), 18.1 (CH_3, Me_b), 3.6 (CH_3, Me_a) ppm. Spectroscopic data were in agreement with those previously reported in the literature.[47]

- Synthesis of (*E*)-5-(pent-3-yn-1-yloxy)penta-1,3-diene (**26j**)

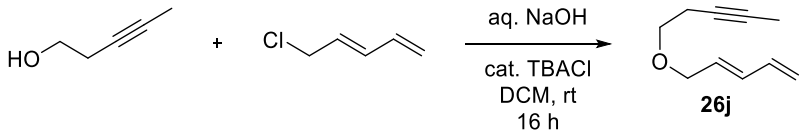

A mixture of *E*-pentyn-1-ol (0.5 mL, 5.25 mmol), 5-chloropenta-1,3-diene (0.988 mg, 8.18 mmol), tetrabutylammonium chloride (77.3 mg, 0.278 mmol), 50% aqueous NaOH (2.1 g, 52.5 mmol) and DCM (2.0 mL) was vigorously stirred at room temperature overnight. The reaction mixture was then poured over 7 mL of distilled water. The phases were separated and the aqueous phase was extracted with pentane (5 x 5 mL). The combined organic phases were washed with brine (2 x 5 mL), dried over magnesium sulfate and concentrated *in vacuo*. The resulting residue was purified by distillation (b.p. = 49 °C, p = 7.1 mbar) to afford the target pure product **26j** as a colorless oil (584 mg, 74% yield).

(47) Ni, Y.; Montgomery, J. *J. Am. Chem. Soc.* **2004**, *126*, 11162-11163.

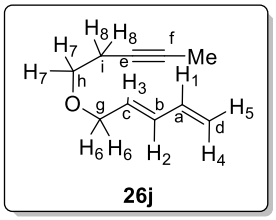

26j

^{1}H NMR (400 MHz, $CDCl_3$) δ 6.35 (ddd, $^3J_{H1-H4}$ = 16.5 Hz, $^3J_{H1-H5}$ = 9.8 Hz, 1H, H_1), 6.30 - 6.19 (m, 1H,H_2), 5.77 (dt, $^3J_{H3-H2}$ = 15.0 Hz, $^3J_{H3-H6}$ = 6.0 Hz, 1H, H_3), 5.22 (dd, $^3J_{H4-H1}$ = 16.5 Hz, $^2J_{H4-H5}$ = 0.9 Hz, 1H, H_4), 5.10 (dd, $^3J_{H5-H1}$ = 9.8 Hz, $^2J_{H5-H4}$ = 0.9 Hz, 1H, H_5), 4.05 (d, $^3J_{H6-H3}$ = 6.1 Hz, 2H, H_6), 3.52 (t, $^3J_{H7-H8}$ = 7.1 Hz, 2H, H_7), 2.42 (tq, $^3J_{H8-H7}$ = 7.1 Hz, $^5J_{H8-Me}$ = 2.5 Hz, 2H, H_8), 1.78 (t, $^5J_{Me-H8}$ = 2.5 Hz, 3H, Me) ppm. ^{13}C {^{1}H} NMR (101 MHz, $CDCl_3$) δ 136.4 (CH=, C_a), 133.4 (CH=, C_b), 130.1 (CH=, C_d), 117.7 (CH_2=, C_e), 76.8 (C≡, C_f), 76.0 (C≡, C_g), 71.1 (CH_2, C_h), 69.0 (CH_2, C_i), 20.3 (CH_2, C_j), 3.7 (Me) ppm. Spectroscopic data were in agreement with those previously reported in the literature.[47]

4.4.3 Synthesis of Phosphaamidine Ligand

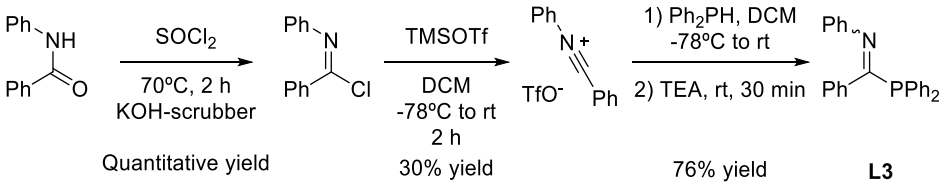

N-phenyl benzamide (6.04 g, 30 mmol) was dissolved in thionyl chloride (9.36 mL, 15.4 g, 129 mmol) and the resulting reaction mixture was heated at 70 °C for 2 h, which resulted in the evolution of HCl and SO_2 that were neutralized using an aqueous KOH-scrubber. The reaction mixture was cooled down to room temperature, after which the remaining thionyl chloride was removed *in vacuo* to afford the product as a pale brown solid in quantitative yield (6.4 g). ^{1}H NMR (500 MHz, $CDCl_3$) δ 8.25 - 8.19 (m, 2H), 7.62 - 7.55 (m, 1H), 7.55 - 7.48 (m, 2H), 7.48 - 7.42 (m, 2H), 7.30 - 7.21 (m, 1H), 7.09 - 7.04 (m, 2H) ppm. ^{13}C {^{1}H} NMR (126 MHz, $CDCl_3$) δ 147.8 (C=N), 143.4 (C_{arom}), 135.6 (C_{arom}), 132.2 (CH_{arom}), 129.6 (CH_{arom}), 129.0 (CH_{arom}), 128.6 (CH_{arom}), 125.2 (CH_{arom}), 120.6 (CH_{arom}) ppm. Spectroscopic data were in agreement with those previously reported in the literature.[48]

Trimethylsilyl trifluoromethanesulfonate (TMSOTf, 7.1 mL, 8.7 g, 39.0 mmol) was added in 5 minutes to a solution of *N*-phenylbenzimidoyl chloride (6.47 g, 30.0 mmol) in DCM (25 mL) at -78 °C. The mixture was warmed to room temperature and stirred for 2 h, which resulted in a darkening of the

(48) van Dijk, T.; Burck, S.; Rong, M. K.; Rosenthal, A. J.; Nieger, M.; Slootweg, J. C.; Lammertsma, K. *Angew. Chem., Int. Ed.* **2014**, *53*, 9068-9071.

solution to a reddish-brown color. All volatiles were removed *in vacuo* to give a pale brown solid, which was re-dissolved in the minimum amount of DCM and layered with an equal amount of pentane. The mixture was allowed to stand at 7 °C, which resulted in the formation of pale brown crystals that were isolated by filtration and dried *in vacuo* to afford *N*-benzylidynebenzenaminium trifluoromethanesulfonate as a pale brown solid (3 g, 76% yield). ^{1}H NMR (400 MHz, $CDCl_3$) δ 8.48 (d, J = 8.5 Hz, 2H), 8.07 (d, J = 7.9 Hz, 2H), 7.91 (t, J = 7.6 Hz, 1H), 7.65 (t, J = 7.4 Hz, 1H), 7.63 (dd, J = 8.5, 7.6 Hz, 2H), 7.52 (dd, J = 7.9, 7.4 Hz, 2H) ppm. ^{13}C{^{1}H} NMR (100.1 MHz, $CDCl_3$) δ 139.0 (CH_{arom}), 136.8 (CH_{arom}), 134.1 (CH_{arom}), 130.4 (CH_{arom}), 130.2 (CH_{arom}), 129.2 (C_{arom}), 128.6 (CH_{arom}), 123.3 (C_{arom}), 102.9 (C=N) ppm. Spectroscopic data were in agreement with those previously reported in the literature.[48]

Diphenylphosphine (1.47 mL, 8.28 mmol) was slowly added to a solution of (*N*-phenyl)(phenyl)carbonitrilium triflate (3 g, 9.11 mmol) in DCM (25 mL) at -78 °C. The reaction mixture was stirred for 15 minutes at the same temperature, after which it was warmed to room temperature generating an orange suspension, which turned into an orange solution after 5 minutes. The reaction mixture then was stirred for 30 minutes. Triethylamine (2.8 mL, 2.03 g, 20.1 mmol) was added, which turned the color of the reaction mixture to red/brown. After stirring for 30 minutes, all volatiles were removed *in vacuo* and the product was extracted into MTBE (3 x 20 mL). The combined fractions were filtered over Celite® eluting with MTBE. Evaporating all volatiles *in vacuo* resulted in a yellow oil, which solidified after washing thoroughly with pentane. The product was obtained as a yellow solid and as a mixture of *E*-**L3** and *Z*-**L3** in a 1.0:0.5 ratio, respectively, according to ^{31}P{^{1}H} NMR spectroscopy. Spectroscopic data were in agreement with those previously reported in the literature.[49] ^{1}H NMR (400 MHz, $CDCl_3$) δ 7.65 - 6.58 (m, 20H, H_{Ph}) ppm. ^{13}C {^{1}H} NMR (101 MHz, $CDCl_3$) δ 151.7 (C_{Ph}), 151.4 (C_{Ph}),137.7 (C_{Ph}), 134.9 (d, $^{1}J_{C-P}$ = 19.1 Hz; C_{Ph}), 134.3 (C_{Ph}), 134.1 (C_{Ph}), 129.2 (C_{Ph}), 128.8 (C_{Ph}), 128.5 (C_{Ph}), 128.4 (C_{Ph}), 128.3 (C_{Ph}), 127.8 (C_{Ph}), 123.8 (C_{Ph}), 123.4 (C_{Ph}), 120.8 (C_{Ph}), 119.4 (C_{Ph}) ppm. ^{31}P {^{1}H} NMR (162 MHz, $CDCl_3$) δ 8.0 (s, *E*-**L3**), -1.5 (s, *Z*-**L3**) ppm.

(49) van Dijk, T.; Burck, S.; Rosenthal, A. J.; Nieger, M.; Ehlers, A. W.; Slootweg, J. C.; Lammertsma, K. *Chem.--Eur. J.* **2015**, *21*, 9328-9331.

4.4.4 Synthesis of Rhodium Complexes

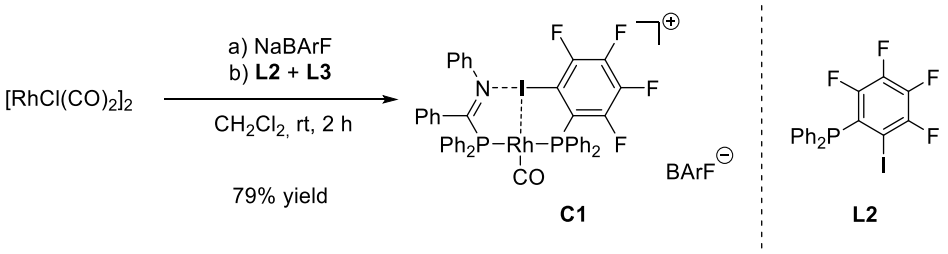

In a glove box filled with N_2, $[RhCl(CO)_2]_2$ (60.1 mg, 0.15 mmol) were dissolved in CH_2Cl_2 (1 mL) in an amberized glass vial provided with a magnetic stirrer. Then, NaBArF (269 mg, 0.30 mmol) was added to the previous solution together with CH_2Cl_2 (1 mL). The mixture was stirred for 1 h at room temperature. In parallel, a solution of 2-iodo-3,4,5,6-tetrafluorophenyl-diphenylphosphine **L2**[8a] (142 mg, 0.30 mmol) and phosphaamidine **L3**, (113 mg, 0.30 mmol) in CH_2Cl_2 (2 mL) was prepared in a vial provided with a magnetic stirrer. The mixture was stirred at room temperature for 1 h. The solution containing **L3** and **L2** was added dropwise to the solution containing the Rh precursor with observation of some bubbling. This mixture was stirred for 1 h at room temperature and then filtered with a nylon filter to remove the NaCl precipitate. The resulting solution was partially evaporated (to *ca.* 1 mL volume) and then mixed with *n*-pentane (5 mL), with which a precipitate was formed. This precipitate was washed with cold diethyl ether (3 x 1 mL) and *n*-pentane (3 x 2 mL) and dried *in vacuo* to afford metal complex **C1** (432 mg, 79% yield).

^{1}H NMR (500 MHz, CD_2Cl_2) δ 7.76 – 7.70 (m, 9H, H_{Ph}), 7.67 – 7.44 (m, 23H, H_{Ph}), 7.31 (s, 2H, H_{Ph}), 7.17 (dt, J = 17.2, 7.5 Hz, 2H, H_{Ph}), 6.99 (t, J = 7.9 Hz, 2H, H_{Ph}), 6.92 (d, J = 8.0 Hz, 2H, H_{Ph}), 6.48 (d, J = 6.9 Hz, 2H, H_{Ph}) ppm. ^{19}F{^{1}H} NMR (471 MHz, CD_2Cl_2) δ -62.97 (s, 24F), -116.79 – -116.89 (m, 1F), -117.52 – -118.71 (m, 1F), -141.20 – -143.19 (m, 1F) -146.15 – -147.88 (m, 1F) ppm. ^{31}P{^{1}H} NMR (202 MHz, CD_2Cl_2) δ 81.7 (ddd, J_{P-P} = 275.8 Hz, J_{P-Rh} = 110.9 Hz, J_{P-F} = 13.8 Hz), 67.4 (dd, J_{P-P} = 275.8 Hz, J_{P-Rh} = 117.0 Hz). ^{11}B{^{1}H} NMR (160 MHz, CD_2Cl_2) δ -6.7 ppm. ^{13}C {^{1}H} NMR (126 MHz, CD_2Cl_2) δ 162.1 (q, J_{C-B}= 49.9 Hz, C_{BArF}), 146.7 (d, J_{C-P} = 24.0 Hz), 135.1 (C_{BArF}), 133.7 (d, J_{C-P} = 12.3 Hz, C_{Ph}), 133.0 (dt, J_{C-P} = 11.8 Hz, J_{C-Rh} = 2.7 Hz, C_{Ph}), 132.9 (d, J_{C-P} = 12.4 Hz, C_{Ph}), 130.3 (C_{Ph}), 130.1 (C_{Ph}), 130.0 (C_{Ph}), 130.0 (C_{Ph}), 129.9 (C_{Ph}), 129.7 (C_{Ph}), 129.2 (qm, J_{C-P} = 32.4 Hz, C_{Ph}), 128.7 (C_{Ph}), 128.5 (C_{Ph}), 128.1 (C_{Ph}), 127.6 (C_{Ph}), 127.5 (C_{Ph}), 127.1 (C_{Ph}), 125.0 (q, J_{C-F} = 271.9 Hz, C_{BArF}), 121.6 (C_{Ph}), 118.0 – 117.7

(m, C_{BArF}) ppm. HRMS (ESI$^+$): *m/z* calcd for $C_{44}H_{30}F_4INOP_2Rh^+$ [M-BArF]$^+$ 955.9791, found 955.9833.

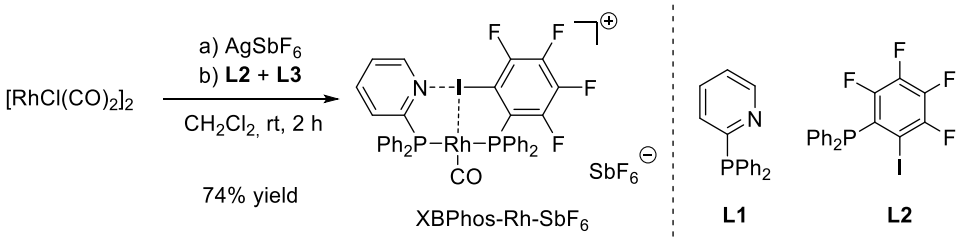

In a glove box filled with N_2, $[RhCl(CO)_2]_2$ (34.3 mg, 0.08 mmol) were dissolved in CH_2Cl_2 (0.5 mL) in an amberized glass vial provided with a magnetic stirrer. Then, $AgSbF_6$ (60.6 mg, 0.17 mmol) was added to the previous solution together with CH_2Cl_2 (0.5 mL). The mixture was stirred for 1 h at room temperature. In parallel, a solution of 2-iodo-3,4,5,6-tetrafluorophenyl-diphenylphosphine **L2**[8a] (79.6 mg, 0.17 mmol) and 2-(diphenylphosphaneyl)pyridine **L3**, (46.5 mg, 0.17 mmol) in CH_2Cl_2 (1 mL) was prepared in a vial provided with a magnetic stirrer. The mixture was stirred at room temperature for 1 h. The solution containing **L2** and **L3** was added dropwise to the solution containing the Rh precursor with observation of some bubbling. This mixture was stirred for 2 h at room temperature and then filtered with a nylon filter to remove the AgCl precipitate. The resulting solution was partially evaporated (to *ca.* 1 mL volume) and then mixed with *n*-pentane (3 mL), with which a precipitate was formed. This precipitate was washed with cold diethyl ether (3 x 1 mL) and *n*-pentane (3 x 2 mL) and dried *in vacuo* to afford metal complex XBPhos-Rh-SbF_6 (136 mg, 74% yield).

^{1}H NMR (500 MHz, CD_2Cl_2) δ 8.91 (dm, J = 5.0 Hz, 1H, H_{Pyr}), 7.95 (tm, J = 7.8, Hz, 1H, H_{Pyr}), 7.76 – 7.42 (m, 21H, H_{Ph}), 7.36 (ddm, J = 7.8, 3.0 Hz, 1H, H_{Py}) ppm. ^{19}F{^{1}H} NMR (471 MHz, CD_2Cl_2) δ -116.46 – -116.64 (m, 1F), - 17.74 – -117.96 (m, 1F), -142.54 – -142.74 (m, 1F), -147.60 – -147.78 (m, 1F) ppm. ^{31}P{^{1}H} (162 MHz, CD_2Cl_2) δ 79.20 (ddd, J_{P-P} = 275.5 Hz, J_{P-Rh} = 110.6 Hz, J_{P-F} = 13.8 Hz), 50.38 (dd, J_{P-P} = 275.5 Hz, J_{P-Rh} = 116.5 Hz) ppm. ^{13}C NMR (126 MHz, CD_2Cl_2) δ 152.1 (dd, J_{C-P} = 67.3 Hz, J_{C-Rh} = 5.3 Hz, C_{Py}) 149.6 (d, J_{C-P} = 19.4 Hz, C_{Py}), 139.1 (d, J_{C-Ph} = 4,5 Hz, C_{Py}), 134.0 (d, J_{C-Ph} = 12.5 Hz), 133.0 (d, J = 13.7 Hz, C_{Ph}) 132.9 (dd, J = 20.2, 2.6 Hz, C_{Ph}), 130.1 (dd, J_{C-P} = 11.0 Hz, J_{C-Rh} = 1.8 Hz, C_{Ph}), 129.6 (C_{Py}), 127.4 (d, J_{C-P} = 1.5 Hz, C_{Py}) ppm.

4.4.5 General Methodology for the Cycloaddition Reactions

AgBArF (0.024 mmol) was added to a solution of the rhodium precursor (6.1 μmol) in dry DCM (0.1 M) under inert atmosphere at room temperature. After stirring the mixture for 1 min, the dienyne substrate (0.12 mmol) was added and the mixture was stirred at room temperature for 5 h. The mixture was filtered through a short pad of silica, which was further eluted with DCM (2 mL). The filtrate was concentrated *in vacuo* and the resulting crude mixture was analyzed by NMR spectroscopy. The cycloadducts were isolated after purification by silica gel column chromatography.

4.4.6 Characterization of the [4+2] Cycloaddition Products

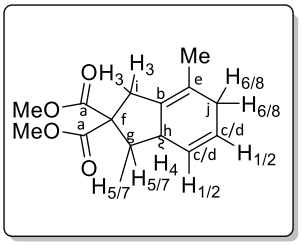

Product **27a** was prepared following the general procedure starting from substrate **26a** (0.138 g, 0.55 mmol), XBPhos-Rh-BArF (48.8 mg, 0.027 mmol) and AgBArF (38.6 mg, 0.11 mmol). It was obtained as a colorless oil (123.8 mg, 90% yield, see Figure 4.32 and Figure 4.33).^{1}H NMR (400 MHz, $CDCl_3$) δ 5.80 – 5.68 (m, 2H, H_1 and H_2), 3.73 (s, 3H, OMe), 3.70 (s, 3H, OMe), 3.06 – 2.89 (m, 2H, H_3), 2.89 – 2.79 (m, 1H, H_4), 2.68 – 2.64 (m, 1H, H_5), 2.61 (dd, $^2J_{H6\text{-}H8}$ = 12.5 Hz, $^3J_{H6\text{-}H1/2}$ = 6.9 Hz, 1H, H_6), 2.53 – 2.38 (m, 1H, H_7), 1.74 (t, $^2J_{H6\text{-}H8}$ = 12.5 Hz, 1H, H_8), 1.63 (s, 3H, Me) ppm. ^{13}C{^{1}H} NMR (101 MHz, $CDCl_3$) δ 173.0 (C=O, C_a), 172.6 (C=O, C_a), 131.2 (C=, C_b), 126.8 (CH=, C_c), 125.7 (CH=, C_d), 122.7 (C=, C_e), 57.8 (C_{quat}, C_f), 52.9 (CH_3, OMe), 52.8 (CH_3, OMe), 40.1 (CH_2, C_g) 39.7 (CH, C_h), 36.1 (CH_2, C_i), 32.7 (CH_2, C_j), 18.9 (CH_3, Me) ppm. HRMS (ESI$^+$): *m/z* calcd for $C_{14}H_{18}O_4$ $[M+Na]^+$ 273.1097, found 273.1109.

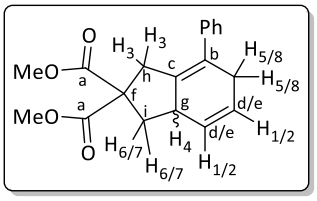

Product **27d** was prepared following the general procedure starting from substrate **26d** (0.094 g, 0.301 mmol), XBPhos-Rh-BArF (26.4 mg, 0.015 mmol) and AgBArF (59.6 mg, 0.06 mmol). It was obtained as a white solid (82.6 mg, 88% yield, see Figure 4.36 and Figure 4.37). ^{1}H NMR (400 MHz, $CDCl_3$) δ 7.43 – 7.22 (m, 6H, H_{Ph}), 5.95 – 5.83 (m, 2H, H_1 and H_2), 3.78 (s, 3H, OMe), 3.67 (s, 3H, OMe), 3.22 – 3.02 (m, 3H, H_3, H_4 and H_5), 3.00 – 2.86

(m, H_6 and H_7), 2.70 (dd, $^2J_{H8\text{-}H9}$ = 12.5 Hz, $^4J_{H8\text{-}H4}$ = 6.9 Hz, 1H, H_8), 1.91 (t, $^2J_{H9\text{-}H8}$ = 12.5 Hz, 1H, H_9) ppm. $^{13}C\{^1H\}$ NMR (101 MHz, $CDCl_3$) δ 172.9 (C=O, C_a), 172.2 (C=O, C_a), 141.5 (C=, C_b), 134.3 (CH=, C_c), 128.2 (C_{arom}, C_{Ph}), 127.9 (C_{arom}, C_{Ph}), 126.7 (C_{arom}, C_{Ph}), 126.3 (CH=, C_d), 125.6 (CH=, C_e), 57.6 (C_{quat}, C_f), 52.9 (CH_3, OMe), 52.7 (CH_3, OMe), 40.2 (CH_2, C_g), 39.6 (CH, C_h), 37.3 (CH_2, C_i), 32.2 (CH_2, C_j) ppm. HRMS (ESI^+): *m/z* calcd for $C_{19}H_{20}O_4$ $[M+Na]^+$ 335.1254, found 335.1255. m.p.: 92-97 °C

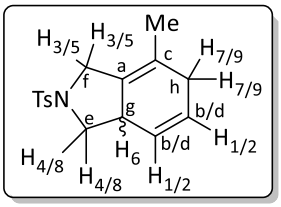

Product **27e** was prepared following the general procedure starting from substrate **26e** (0.101 g, 0.35 mmol), XBPhos-Rh-BArF (30.8 mg, 0.017 mmol) and AgBArF (68 mg, 0.07 mmol). It was obtained as a white solid (61.3 mg, 60% yield, see Figure 4.38 and Figure 4.39). ^1H NMR (400 MHz, $CDCl_3$) δ 7.72 (d, $^3J_{H11\text{-}H10}$ = 8.1 Hz, 2H, H_{Ts}), 7.32 (d, $^3J_{H10\text{-}H11}$ = 8.1 Hz, 1H, H_{Ts}), 5.77 (ddt, $^3J_{H1\text{-}H2}$ = 9.6 Hz, $^3J_{H1\text{-}H6}$ = 4.8 Hz, $^4J_{H1\text{-}H7/9}$ = 2.5 Hz, 1H, H_1), 5.66 (dt, $^3J_{H2\text{-}H1}$ =.9.7 Hz, $^3J_{H2\text{-}H7/9}$ = 3.0 Hz, 1H, H_2), 3.96 (dq, $^2J_{H3\text{-}H5}$ = 13.4 Hz, 1.9 Hz, 1H, H_3), 3.83 (dd, $^2J_{H4\text{-}H8}$ = 8.7 Hz, $^3J_{H4\text{-}H6}$ = 7.9 Hz, 1H, H_4), 3.79 (d, $^2J_{H5\text{-}H3}$ = 13.4 Hz, 1H, H_5), 3.13 - 2.89 (m, 1H, H_6), 2.70 - 2.58 (m, 1H, H_7), 2.58 (d, $^3J_{H8\text{-}H6}$ = 11.5 Hz, $^2J_{H8\text{-}H4}$ = 8.7 Hz, 1H, H_8), 2.49 - 2.34 (m, 1H, H_9), 2.42 (s, 3H, H_{Ts}), 1.58 (bs, 3H, Me) ppm. $^{13}C\{^1H\}$ NMR (101 MHz, $CDCl_3$) δ 143.4 (C_{arom}, C_{Ts}), 133.8 (C_{arom}, C_{Ts}), 129.7 (C_{arom}, C_{Ts}), 127.8 (C=, C_a), 127.6 (C_{arom}, C_{Ts}), 126.9 (CH=, C_b), 124.2 (CH=, C_c), 123.5 (C=, C_d), 52.7(CH_2, C_e), 49.0 (CH_2, C_f), 38.9 (CH, C_g), 32.3 (CH_2, C_h), 21.5 (CH_3, C_{Ts}), 18.9 (CH_3, Me) ppm. HRMS (ESI^+): *m/z* calcd for $C_{16}H_{20}NO_2S$ $[M+H]^+$ 290.1209, found 290.1217. m.p.: 104-110 °C.[50]

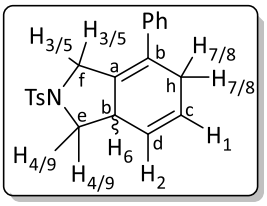

Product **27f** was prepared following the general procedure starting from substrate **26f** (0.101 g, 0.29 mmol), XBPhos-Rh-BArF (25.3 mg, 0.014 mmol) and AgBArF (56 mg, 0.06 mmol). It was obtained as a white solid (71.8 mg, 71% yield, see Figure 4.40 and Figure 4.41). ^1H NMR (500 MHz, $CDCl_3$) δ 7.60 (d, $^3J_{H11\text{-}H10}$ = 8.3 Hz, 2H), 7.35 - 7.18 (m, 5H, H_{Ts} and H_{Ph}), 7.11 - 7.05 (m, 2H, H_{Ph}), 5.86 (ddt, $^3J_{H1\text{-}H2}$ = 10.0 Hz, $^3J_{H1\text{-}H6}$ = 4.8 Hz, $^3J_{H1\text{-}H7/9}$ = 2.5 Hz, 1H, H_1), 5.69 (d, $^3J_{H2\text{-}H1}$ = 10.0 Hz, 1H, H_2), 4.13 (dd, $^2J_{H3\text{-}H5}$ = 13.9 Hz, $^4J_{H3\text{-}H6}$ = 3.4 Hz, 1H, H_3), 3.83 (dd, $^2J_{H4\text{-}H9}$ = 8.9 Hz, $^3J_{H4\text{-}H6}$ = 7.9 Hz, 1H, H_4), 3.65 (d,

(50) Full characterization of compound **2g** has not been previously reported in the literature. However, ^1H and $^{13}C\{^1H\}$ NMR data are in agreement with those previously reported in ref 44.

$^{2}J_{H5-H3}$ = 13.9 Hz, 1H, H_5), 3.20 – 3.15 (m, 1H, H_6), 3.08 – 2.98 (m, 1H, H_7), 2.90 – 2.79 (m, 1H, H_8), 2.65 (dd, $^{3}J_{H9-H6}$ = 11.4 Hz, $^{2}J_{H9-H4}$ = 8.9 Hz, 1H, H_9), 2.37 (s, 3H, H_{Ts}) ppm. $^{13}C\{^{1}H\}$ NMR (126 MHz, $CDCl_3$) δ 143.5 (C_{arom}, C_{Ts}), 140.2 (C_{arom}, C_{Ph}), 134.2 (C_{arom}, C_{Ts}), 130.7 (C=, C_a), 129.8 (C=, C_b), 129.8 (C_{arom}, C_{Ts}), 128.6 (C_{arom}, C_{Ph}), 127.7 (C_{arom}, C_{Ph}), 127.6 (C_{arom}, C_{Ts}), 127.5 (C_{arom}, C_{Ph}), 126.9 (CH=, C_c), 123.3 (CH=, C_d), 52.4 (CH_2, C_e), 50.2 (CH_2, C_f), 39.7 (CH, C_g), 31.7 (CH_2, C_h), 21.7 (CH_3, C_{Ts}). m.p.: 168–170 °C. Spectroscopic data were in agreement with those previously reported in the literature.[51]

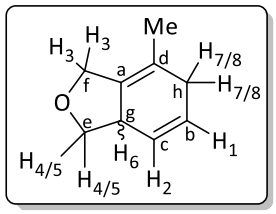

Product **27g** was prepared following the general procedure starting from substrate **26g** (0.10 g, 0.29 mmol), XBPhos-Rh-BArF (25.3 mg, 0.014 mmol) and AgBArF (56 mg, 0.06 mmol). It was obtained as a colorless oil (71.8 mg, 71% yield, see Figure 4.42 and Figure 4.43). ^{1}H NMR (500 MHz, $CDCl_3$) δ 5.87 – 5.80 (m, 1H, H_1), 5.79 – 5.72 (m, 1H, H_2), 4.42 – 4.31 (m, 2H, H_3), 4.16 (t, $^{2}J_{H4-H5}$ = 7.4 Hz, 1H, H_4), 3.22 (dd, $^{3}J_{H5-H6}$ = 11.3 Hz, $^{2}J_{H5-H4}$ = 7.4 Hz, 1H, H_5), 3.13 – 3.01 (m, 1H), 2.72 (dd, $^{2}J_{H7-H8}$ = 21.5 Hz, $^{3}J_{H7-H1}$ = 11.5 Hz, 1H, H_7), 2.51 (dt, $^{2}J_{H7-H8}$ = 21.4 Hz, $^{3}J_{H8-H1}$ = 5.5 Hz, 1H, H_8), 1.64 (s, 3H, Me) ppm. $^{13}C\{^{1}H\}$ NMR (126 MHz, $CDCl_3$) δ 131.3 (C=, C_a), 127.1 (CH=, C_b), 123.4 (CH=, C_c), 121.9 (C=, C_d), 72.1 (CH_2, C_e), 68.1 (CH_2, C_f), 40.3 (CH, C_g), 32.7 (CH_2, C_h), 19.2 (CH_3, Me) ppm. Compound **27e** did not provide a good high-resolution mass spectrum using APCI as the ionization source.

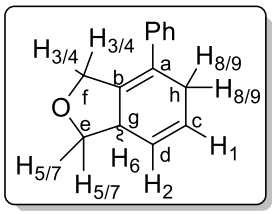

Product **27h** was prepared following the general procedure starting from substrate **26h** (0.10 g, 0.29 mmol), XBPhos-Rh-BArF (44.3 mg, 0.025 mmol) and AgBArF (100 mg, 0.1 mmol). It was obtained as a colorless oil (22.8 mg, 23% yield, see Figure 4.44 and Figure 4.45). ^{1}H NMR (400 MHz, $CDCl_3$) δ 7.38 – 7.11 (m, 5H, H_{Ph}), 5.96 – 5.87 (m, 1H, H_1), 5.81 – 5.73 (m, 1H, H_2), 4.59 – 4.51 (m, 1H, H_3), 4.20 – 4.11 (m, 2H, H_4 and H_5), 3.26 – 3.09 (m, 3H, H_6, H_7 and H_8), 2.98 – 2.84 (m, 1H, H_9) ppm. $^{13}C\{^{1}H\}$ NMR (101 MHz, $CDCl_3$) δ 140.9 (C=, C_a), 134.9 (C=, C_b), 129.7 (C_{arom}, C_{Ph}), 128.6 (C_{arom}, C_{Ph}), 127.6 (C_{arom}, C_{Ph}), 127.5 (C_{arom}, C_{Ph}), 127.2 (CH=, C_c), 123.4 (CH=, C_d), 71.8 (CH_2, C_e), 69.2 (CH_2, C_f), 41.3 (CH, C_g), 31.7 (CH_2, C_h) ppm. Compound **27f** did not provide a good high-resolution mass spectrum using APCI as the ionization source.

(51) Park, K. H.; Choi, S. Y.; Kim, S. Y.; Chung, Y. K. *Synlett* **2006**, 527–532.

4.4.7 Single Crystal X-Ray Structure Determinations

Crystal preparation: Crystals of **27d**, **27e** and **27f** were grown by slow diffusion in pentane/diethyl ether (90:10, v/v). The measured crystals were prepared under inert conditions immersed in perfluoropolyether as protecting oil for manipulation.

Data collection: Crystal structure determination of **27d**, **27g** and **27h** were carried out using a Apex DUO Kappa 4-axis goniometer equipped with an APPEX 2 4K CCD area detector, a Microfocus Source E025 IuS using MoK_α radiation (0.71073 Å), Quazar MX multilayer Optics as monochromator and an Oxford Cryosystems low temperature device Cryostream 700 plus (T = -173 °C). Full-sphere data collection was used with ω and φ scans. *Programs used:* Data collection APEX-2[52], data reduction Bruker Saint[53] V/.60A and absorption correction SADABS[54].

Structure Solution and Refinement: Crystal structure solution was achieved using the computer program SHELXT.[55] Visualization was performed with the program SHELXle.[56] Missing atoms were subsequently located from difference Fourier synthesis and added to the atom list. Least-squares refinement on F^2 using all measured intensities was carried out using the program SHELXL 2015.[57] All non-hydrogen atoms were refined including anisotropic displacement parameters.

Comments to the structures: Compound **27d** crystallized as the racemate in the centro-symmetrical space group *P*-1. Compound **27g** crystallized as the racemate in the centro-symmetrical space group $P2_1/c$. The asymmetric unit of compound **27h** contained one molecule of the organic compound in the chiral space group $P2_1$. The absolute structure could be determined reliably with a Flack

(52) Data collection with APEX II v2014.9-0. Bruker (2014). Bruker AXS Inc., Madison, Wisconsin, USA.
(53) Data reduction with Bruker SAINT+ version V8.35A. Bruker (2013). Bruker AXS Inc., Madison, Wisconsin, USA.
(54) SADABS: V2014/5 Bruker (2001). Bruker AXS Inc., Madison, Wisconsin, USA. For this software, see the following reference: Blessing, R. H. *Acta Cryst.* **1995**, *A51*, 33-38.
(55) For SHELXT; V2014/4 (Sheldrick 2014), see the following reference: Sheldrick, G. M. *Acta Cryst.* **2015**, *A71*, 3-8.
(56) For SHELXle, see the following reference: SHELXle; Hübschle, C. B.; Sheldrick, G. M.; Dittrich, B. *J. Appl. Cryst.* **2011**, *44*, 1281-1284.
(57) For SHELXL and SHELXL-2014/7 (Sheldrick 2014), see the following reference: SHELXL; Sheldrick, G. M. *Acta Cryst.* **2015**, *C71*, 3-8.

value of 0.05(9) and a Flack value based on Parsons' quotients of 0.08(4)[58]. The Flack (Parsons or Hooft) parameter value for the correct absolute structure determination should be 0; the inverted structure would give 1; always taking in account the standard deviation. The absolute configuration based on the absolute structure of the measured crystal was determined with *R*(C2).

- Crystal data and structure refinement for **27d**.

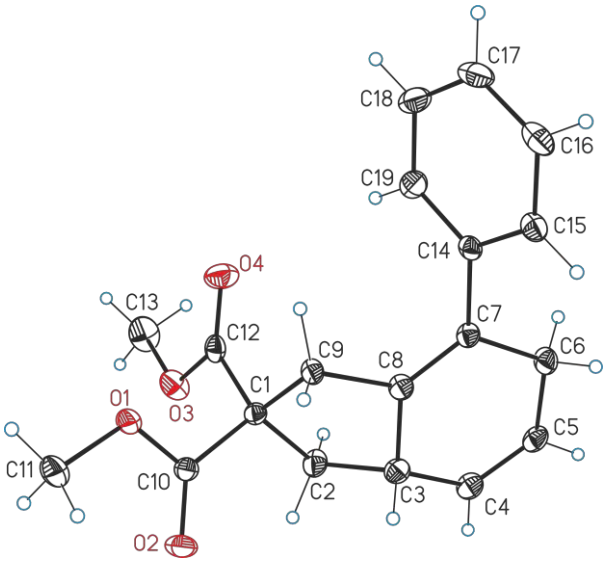

Figure 4.3. ORTEP drawing (thermal ellipsoids drawn at a 50 % probability level) showing the structure of product **27d**.

Empirical formula	$C_{19}H_{20}O_4$	
Formula weight	312.35	
Temperature	100(2)K	
Wavelength	0.71073 Å	
Crystal system	triclinic	
Space group	*P* -1	
Unit cell dimensions	a = 7.3448(4) Å	α = 77.3161(18)°
	b = 10.2147(6) Å	β = 88.990(3)°
	c = 11.2849(6) Å	γ = 84.549(3)°
Volume	796.89(8) Å^3	
Z	2	
Density (calculated)	1.302 Mg/m^3	
Absorption coefficient	0.091 mm^{-1}	

(58) (a) Flack, H. D. *Acta Cryst.* **1983**, *A39*, 876-881. (b) Parsons, S.; Flack, H. *Acta Cryst.* **2004**, *A60*, s61. (c) Parsons, S.; Flack, H. D.; Wagner, T. *Acta Cryst.* **2013**, *B69*, 249-259. Flack X determined using 1698 quotients [(I+)-(I-)]/[(I+)+(I-)]

F(000)	332
Crystal size	0.400 x 0.300 x 0.020 mm^3
Theta range for data collection	1.916 to 32.107°
Index ranges	-8<=h<=10,-14<=k<=14,-11<=l<=16
Reflections collected	11327
Independent reflections	5139[R(int) = 0.0250]
Completeness to theta =32.107°	92.3%
Absorption correction	Multi-scan
Max. and min. transmission	0.74 and 0.70
Refinement method	Full-matrix least-squares on F^2
Data / restraints / parameters	5139/ 0/ 210
Goodness-of-fit on F^2	1.035
Final R indices [I>2sigma(I)]	R1 = 0.0541, wR2 = 0.1311
R indices (all data)	R1 = 0.0764, wR2 = 0.1435
Largest diff. peak and hole	0.747 and -0.317 e.$Å^{-3}$

Bond lengths [Å]	
C1-C10	1.516(2)
C1-C12	1.527(2)
C1-C2	1.5597(19)
C1-C9	1.5602(18)
C2-C3	1.535(2)
C3-C4	1.496(2)
C3-C8	1.5111(19)
C4-C5	1.330(2)
C5-C6	1.4995(19)
C6-C7	1.5137(19)
C7-C8	1.3362(19)
C7-C14	1.4915(18)
C8-C9	1.5064(19)
C10-O2	1.2078(17)
C10-O1	1.3396(17)
C11-O1	1.4514(19)
C12-O4	1.1994(18)
C12-O3	1.3405(17)
C13-O3	1.4470(19)
C14-C15	1.3984(19)
C14-C19	1.399(2)
C15-C16	1.394(2)
C16-C17	1.386(2)
C18-C19	120.46(14)

Angles [°]	
C10-C1-C12	108.77(11)
C10-C1-C2	112.63(11)
C12-C1-C2	108.52(11)
C10-C1-C9	110.11(11)
C12-C1-C9	110.92(11)
C2-C1-C9	105.88(10)
C3-C2-C1	104.89(11)
C4-C3C8	113.12(12)
C4-C3C2	116.37(12)
C8-C3C2	101.44(11)
C5-C4-C3	122.36(13)
C4-C5-C6	124.16(13)
C5-C6-C7	114.01(12)
C8-C7-C14	122.74(12)
C8-C7-C6	120.81(12)
C14-C7-C6	116.45(12)
C7-C8-C9	128.94(12)
C7-C8-C3	124.76(12)
C9-C8-C3	106.12(11)
C8-C9-C1	103.52(10)
O2-C10-O1	123.60(14)
O2-C10-C1	125.78(13)
O1-C10-C1	110.59(11)
O4-C12-O3	123.91(14)
O4-C12-C1	126.47(13)
O3-C12-C1	109.61(12)
C15-C14-C19	118.96(12)
C15-C14-C7	119.58(12)
C19-C14-C7	121.47(12)
C16-C15-C14	120.30(14)
C17-C16-C15	120.23(14)

C16-C17-C18	119.97(14)
C17-C18-C19	120.08(15)
C18-C19-C14	120.46(14)
C10-O1-C11	115.32(12)
C12-O3-C13	115.17(13)

- Crystal data and structure refinement for **27e**.

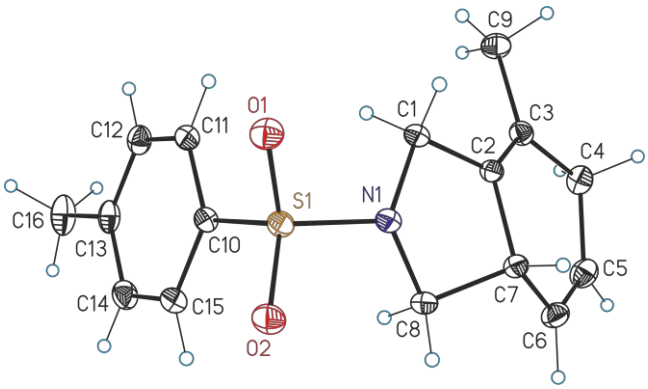

Figure 4.4. ORTEP drawing (thermal ellipsoids drawn at a 50 % probability level) showing the structure of product **27e**.

Empirical formula	$C_{16}H_{19}NO_2S$	
Formula weight	289.38	
Temperature	100(2)K	
Wavelength	0.71073 Å	
Crystal system	monoclinic	
Space group	$P\,2_1/c$	
Unit cell dimensions	a = 13.8211(5) Å	α = 90°
	b = 7.9161(3) Å	β = 102.8982(9)°
	c = 13.5898(5) Å	γ = 90°
Volume	1449.33(9) $Å^3$	
Z	4	
Density (calculated)	1.326 Mg/m^3	
Absorption coefficient	0.224 mm^{-1}	
F(000)	616	
Crystal size	0.500 x 0.400 x 0.100 mm^3	
Theta range for data collection	2.985 to 32.639°.	
Index ranges	-17<=h<=20,-11<=k<=11,-20<=l<=15	
Reflections collected	23328	
Independent reflections	5174[R(int) = 0.0245]	
Completeness to theta =32.107°	97.5%	
Absorption correction	Multi-scan	

Max. and min. transmission	0.74 and 0.66
Refinement method	Full-matrix least-squares on F^2
Data / restraints / parameters	5174/ 0/ 183
Goodness-of-fit on F^2	1.085
Final R indices [I>2sigma(I)]	R1 = 0.0330, wR2 = 0.0901
R indices (all data)	R1 = 0.0375, wR2 = 0.0936
Largest diff. peak and hole	0.494 and -0.357 e.Å^{-3}

Bond lengths [Å]	
S1-O2	1.4347(7)
S1-O1	1.4371(7)
S1-N1	1.6291(8)
S1-C10	1.7638(9)
N1-C8	1.4836(12)
N1-C1	1.4895(11)
C1-C2	1.5105(13)
C2-C3	1.3345(12)
C2-C7	1.5069(12)
C3-C9	1.5014(13)
C3-C4	1.5079(14)
C4-C5	1.5022(15)
C5-C6	1.3316(14)
C7-C6	1.4969(13)
C7-C8	1.5347(13)
C10-C15	1.3955(12)
C10-C11	1.3978(12)
C11-C12	1.3925(13)
C12-C13	1.4006(14)
C13-C14	1.3933(15)
C13-C16	1.5065(14)
C14-C15	1.3943(13)

Angles [°]	
O2-S1-O1	119.95(4)
O2-S1-N1	106.61(4)
O1-S1-N1	106.33(4)
O2-S1-C10	108.27(4)
O1-S1-C10	107.82(4)
N1-S1-C10	107.24(4)
C8-N1-C1	109.73(7)
C8-N1-S1	119.41(6)
C1-N1-S1	118.42(6)
N1-C1-C2	102.55(7)
C3-C2-C7	124.09(8)
C3-C2-C1	126.86(8)
C7-C2-C1	108.53(7)
C2-C3-C9	123.30(9)
C2-C3-C4	120.41(8)
C9-C3-C4	116.28(8)
C5-C4-C3	113.66(8)
C6-C5-C4	123.55(9)
C6-C7-C2	113.01(8)
C6-C7-C8	116.71(8)
C2-C7-C8	101.94(7)
C5-C6-C7	121.43(9)
N1-C8-C7	100.65(7)
C15-C10-C11	120.50(8)
C15-C10-S1	118.98(7)
C11-C10-S1	120.46(7)
C12-C11-C10	119.40(8)
C11-C12-C13	120.83(9)
C14-C13-C12	118.89(9)
C14-C13-C16	120.78(9)
C12-C13-C16	120.32(10)
C13-C14-C15	121.06(9)
C14-C15-C10	119.30(9)

- Crystal data and structure refinement for **27f**.

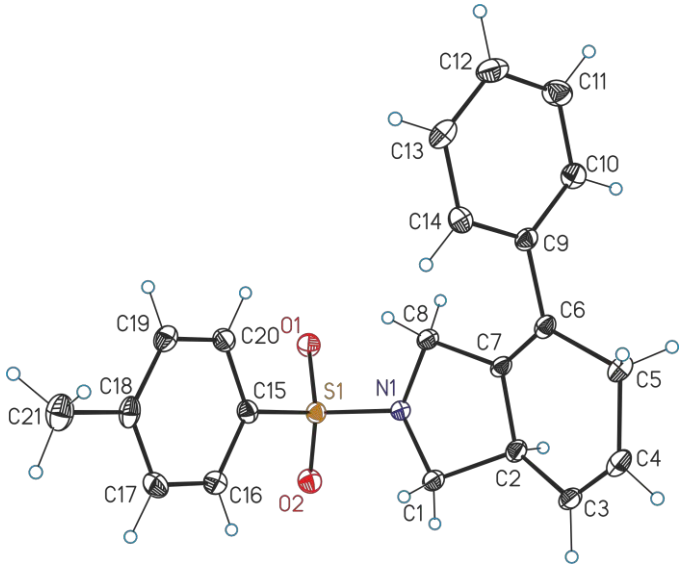

Figure 4.5. ORTEP drawing (thermal ellipsoids drawn at a 50 % probability level) showing the structure of product **27f**.

Empirical formula	$C_{21}H_{21}NO_2S$	
Formula weight	351.45	
Temperature	100(2)K	
Wavelength	0.71073 Å	
Crystal system	monoclinic	
Space group	$P\,2_1$	
Unit cell dimensions	a = 9.751(2) Å	α = 90°
	b = 7.4965(17) Å	β = 106.943(5)°
	c = 12.502(3)) Å	γ = 90°
Volume	874.2(3) $Å^3$	
Z	4	
Density (calculated)	1.335 Mg/m^3	
Absorption coefficient	0.199 mm^{-1}	
F(000)	312	
Crystal size	0.300 x 0.040 x 0.010 mm^3	
Theta range for data collection	1.703 to 31.635°	
Index ranges	-14<=h<=14,-10<=k<=11,-18<=l<=17	
Reflections collected	19323	
Independent reflections	5749[R(int) = 0.0620]	
Completeness to theta =31.635°	99.5%	
Absorption correction	Multi-scan	
Max. and min. transmission	0.74 and 0.61	

Refinement method	Full-matrix least-squares on F^2
Data / restraints / parameters	5749/ 1/ 227
Goodness-of-fit on F^2	1.029
Final R indices [I>2sigma(I)]	R1 = 0.0463, wR2 = 0.0950
R indices (all data)	R1 = 0.0685, wR2 = 0.1028
Largest diff. peak and hole	0.392 and -0.372 e.Å^{-3}

Bond lengths [Å]	
S1-O2	1.4314(19)
S1-O1	1.446(2)
S1-N1	1.633(2)
S1-C15	1.764(3)
N1-C1	1.485(4)
N1-C8	1.487(3)
C1-C2	1.530(4)
C2-C3	1.503(4)
C2-C7	1.509(4)
C3-C4	1.318(4)
C4-C5	1.505(4)
C5-C6	1.520(4)
C6-C7	1.332(4)
C6-C9	1.495(4)
C7-C8	1.507(4)
C9-C10	1.393(4)
C9-C14	1.397(4)
C10-C11	1.394(4)
C11-C12	1.389(4)
C12-C13	1.382(4)
C13-C14	1.391(4)
C15-C16	1.388(4)
C15-C20	1.399(4)
C16-C17	1.397(4)
C17-C18	1.390(4)
C18-C19	1.396(4)
C18-C21	1.509(4)
C19-C20	1.389(4)

Angles [°]	
O2-S1-O1	120.01(12)
O2-S1-N1	106.89(12)
O1-S1-N1	105.96(12)
O2-S1-C15	108.23(12)
O1-S1-C15	107.58(13)
N1-S1-C15	107.59(12)
C1-N1-C8	109.6(2)
C1-N1-S1	120.00(17)
C8-N1-S1	119.22(18)
N1-C1-C2	100.1(2)
C3-C2-C7	112.5(2)
C3-C2-C1	118.3(2)
C7-C2-C1	102.4(2)
C4-C3-C2	121.9(3)
C3-C4-C5	123.8(3)
C4-C5-C6	113.0(2)
C7-C6-C9	123.0(2)
C7-C6-C5	120.5(2)
C9-C6-C5	116.5(2)
C6-C7-C8	127.4(2)
C6-C7-C2	124.1(2)
C8-C7-C2	108.2(2)
N1-C8-C7	102.7(2)
C10-C9-C14	118.9(2)
C10-C9-C6	120.8(2)
C14-C9-C6	120.3(2)
C9-C10-C11	120.7(3)
C12-C11-C10	119.9(3)
C13-C12-C11	119.8(3)
C12-C13-C14	120.5(3)
C13-C14-C9	120.3(2)
C16-C15-C20	120.6(2)
C16-C15-S1	119.1(2)
C20-C15-S1	120.3(2)
C15-C16-C17	119.5(3)
C18-C17-C16	120.9(3)
C17-C18-C19	118.7(2)
C17-C18-C21	120.7(3)
C19-C18-C21	120.5(3)
C20-C19-C18	121.3(3)
C19-C20-C15	119.0(2)

4.4.8 Copies of NMR Spectra

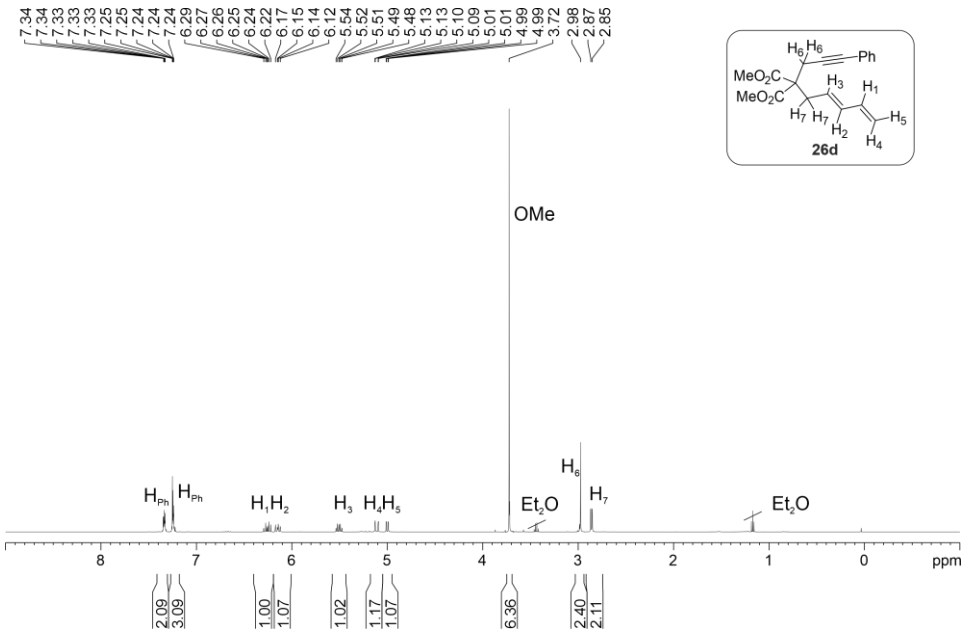

Figure 4.6. ^{1}H NMR spectrum of substrate **26d**.

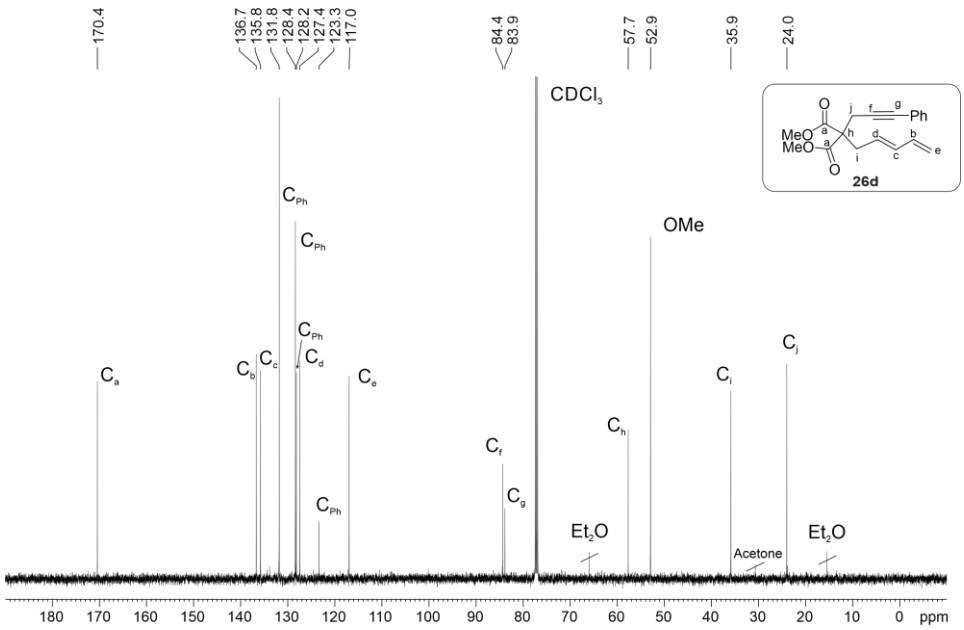

Figure 4.7. ^{13}C{^{1}H} NMR spectrum of product **26d**.

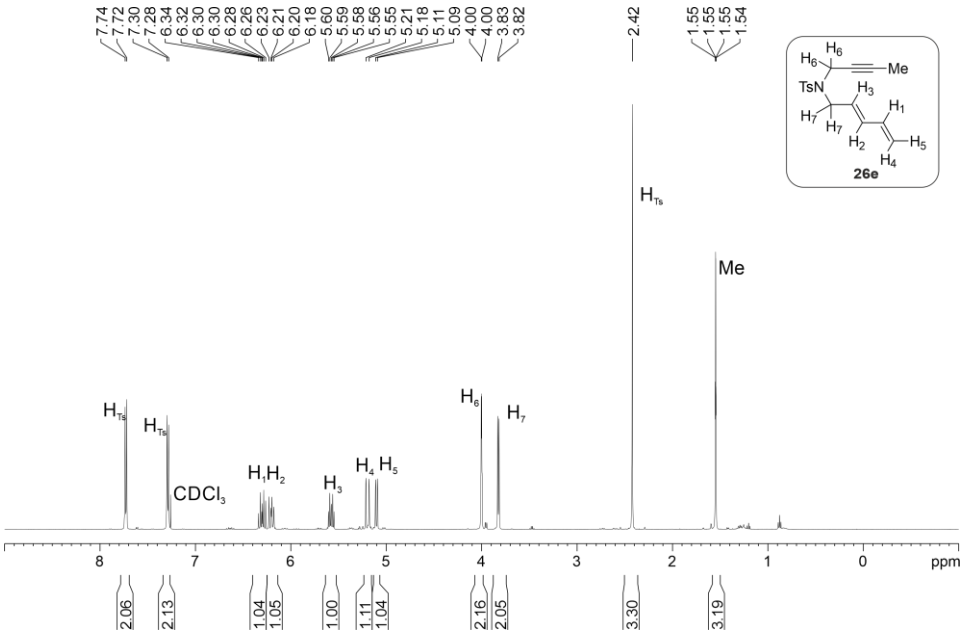

Figure 4.8. ^{1}H NMR spectrum of substrate **26e**.

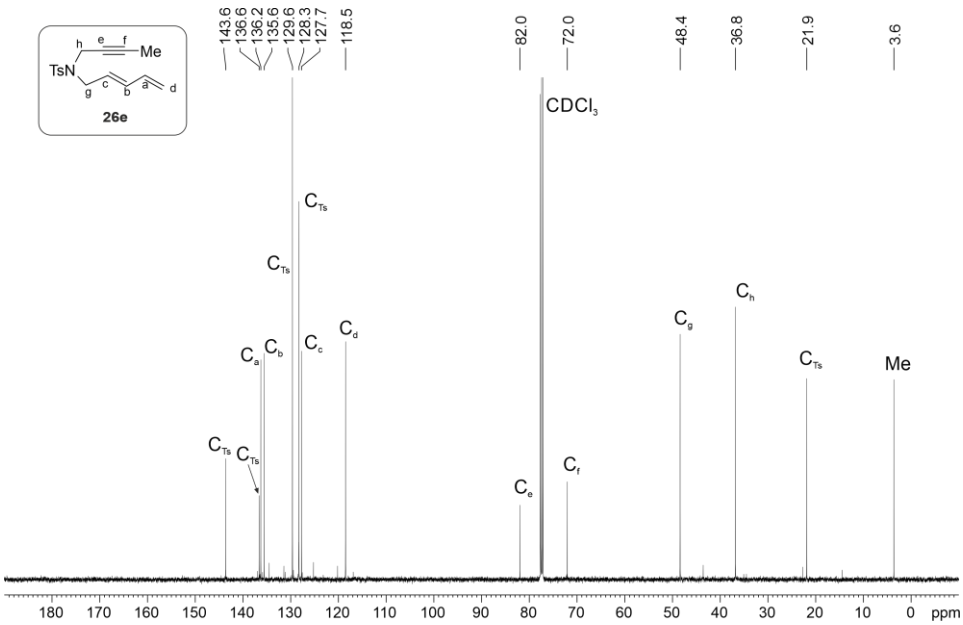

Figure 4.9. ^{13}C{^{1}H} NMR spectrum of product **26e**.

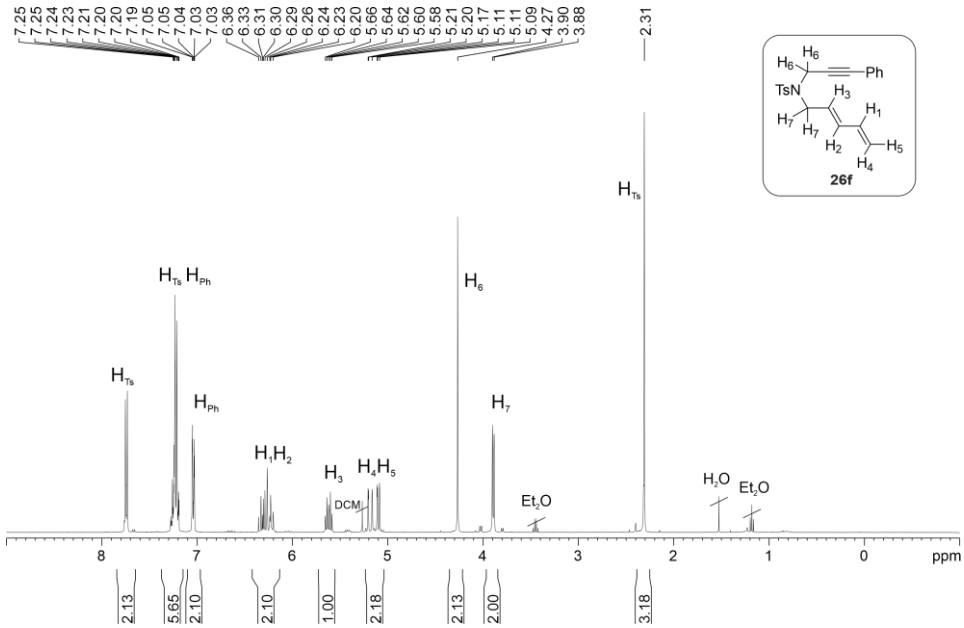

Figure 4.10. ^{1}H NMR spectrum of substrate **26f**.

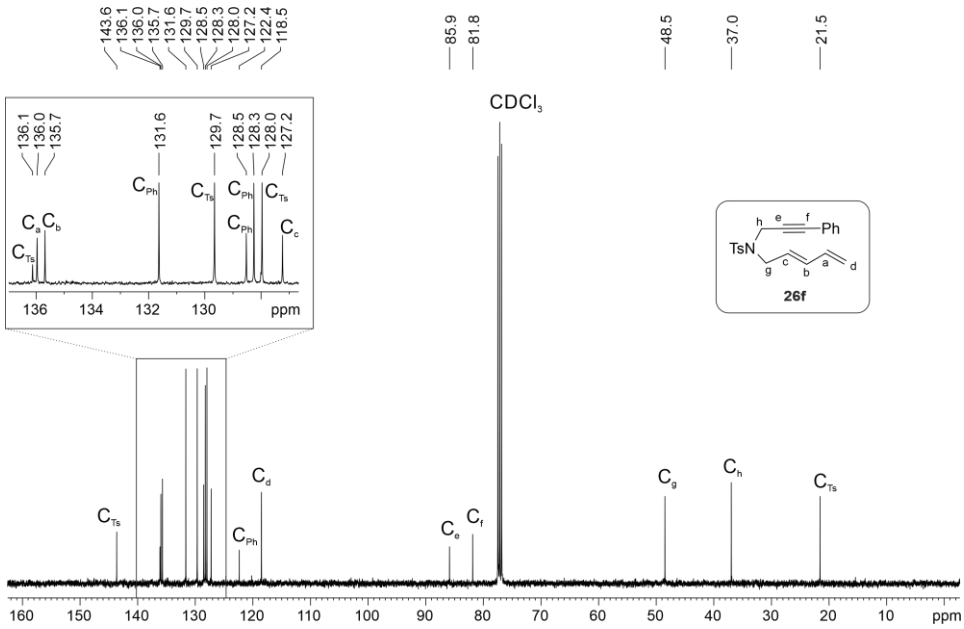

Figure 4.11. $^{13}C\{^{1}H\}$ NMR spectrum of product **26f**.

UNIVERSITAT ROVIRA I VIRGILI
TRANSITION METAL-CATALYZED CYCLOADDITION REACTIONS FOR THE FORMATION
OF EIGHT- AND SIX-MEMBERED RINGS
Nuria Llorente González

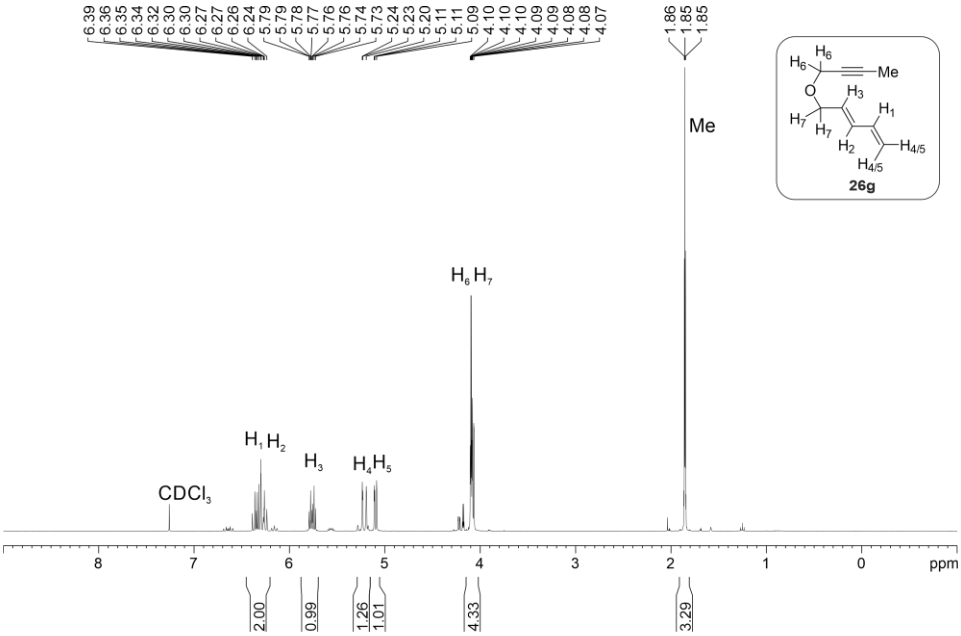

Figure 4.12. ^{1}H NMR spectrum of substrate **26g**.

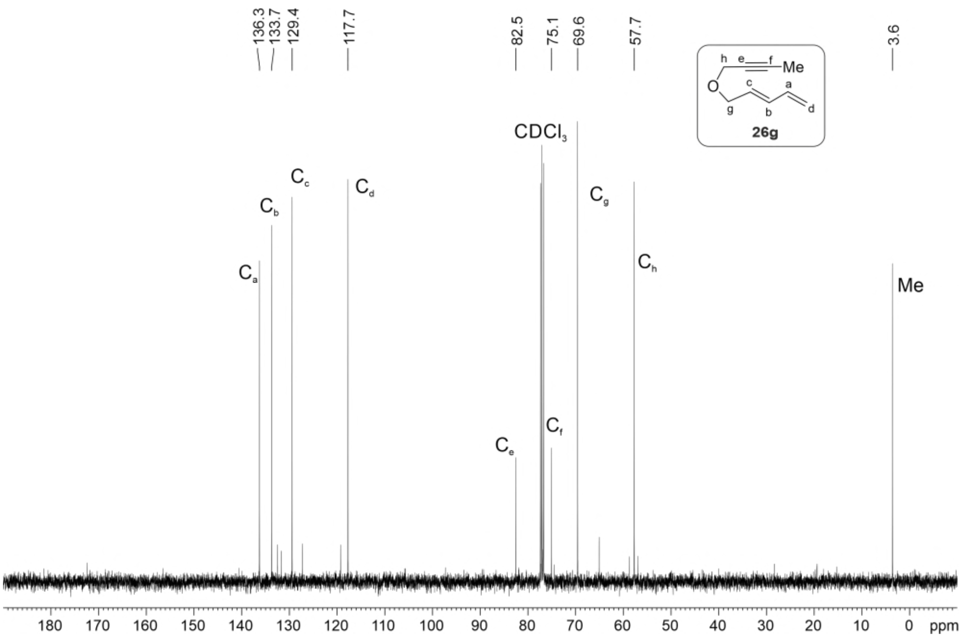

Figure 4.13. ^{13}C{^{1}H} NMR spectrum of product **26g**.

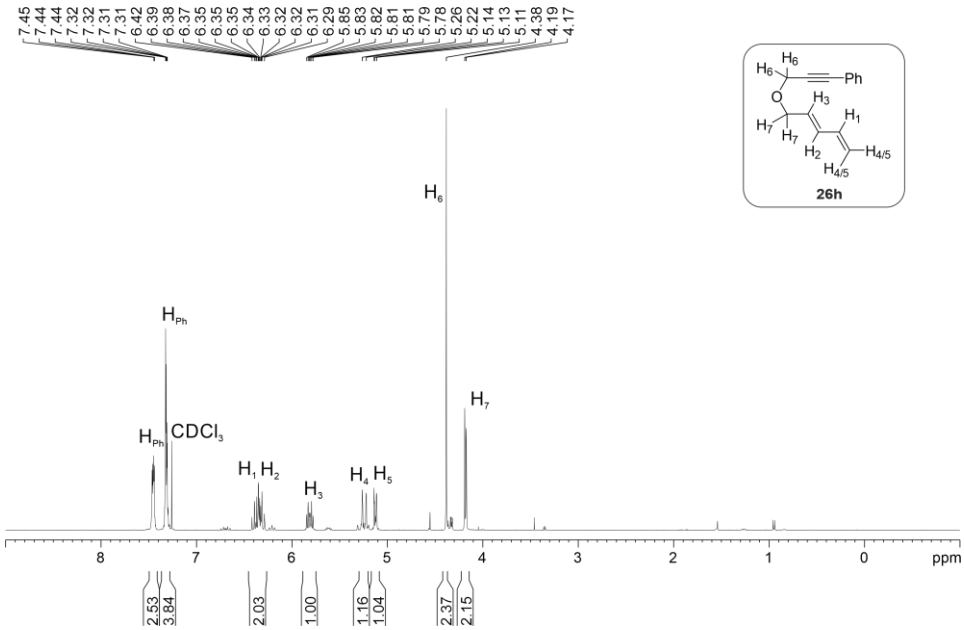

Figure 4.14. ^{1}H NMR spectrum of substrate **26h**.

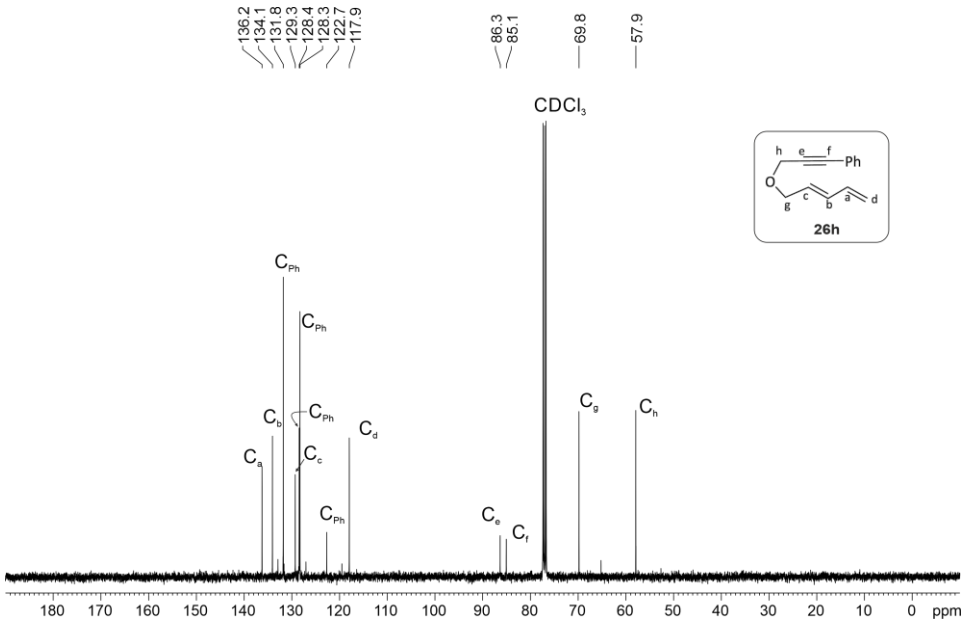

Figure 4.15. $^{13}C\{^{1}H\}$ NMR spectrum of product **26h**.

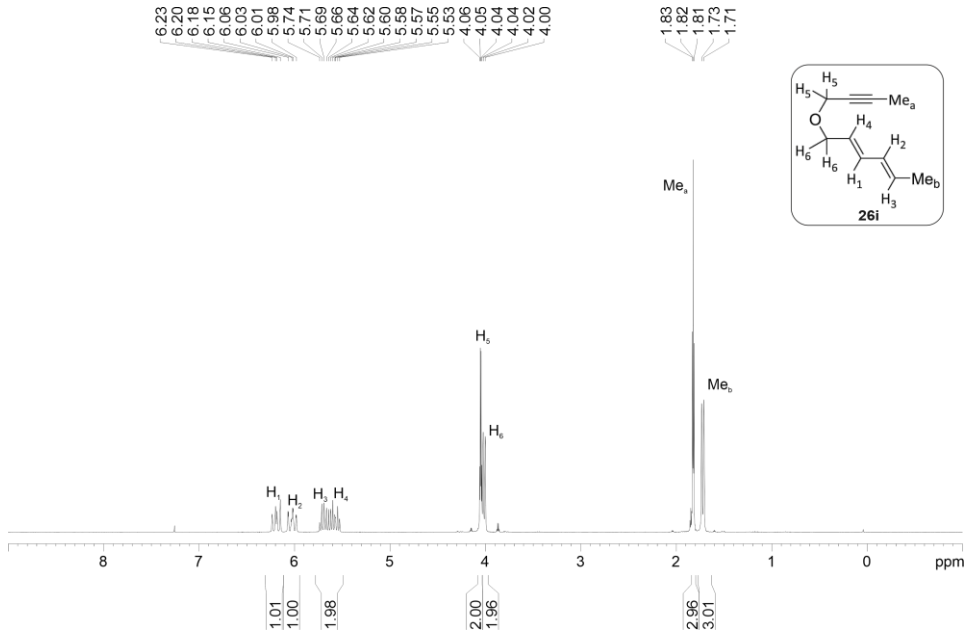

Figure 4.16. ^{1}H NMR spectrum of substrate **26i**.

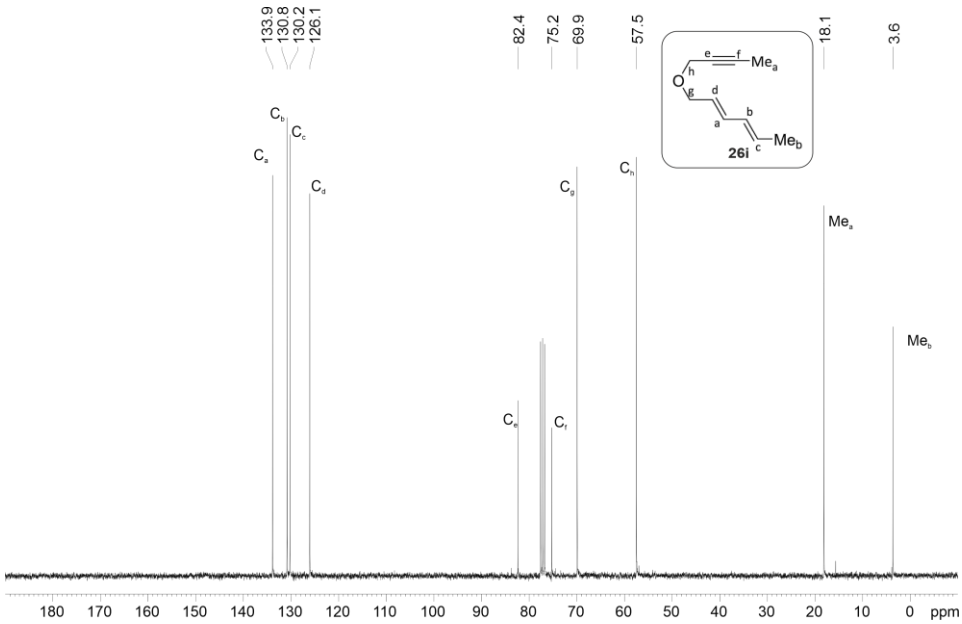

Figure 4.17. $^{13}C\{^{1}H\}$ NMR spectrum of product **26i**.

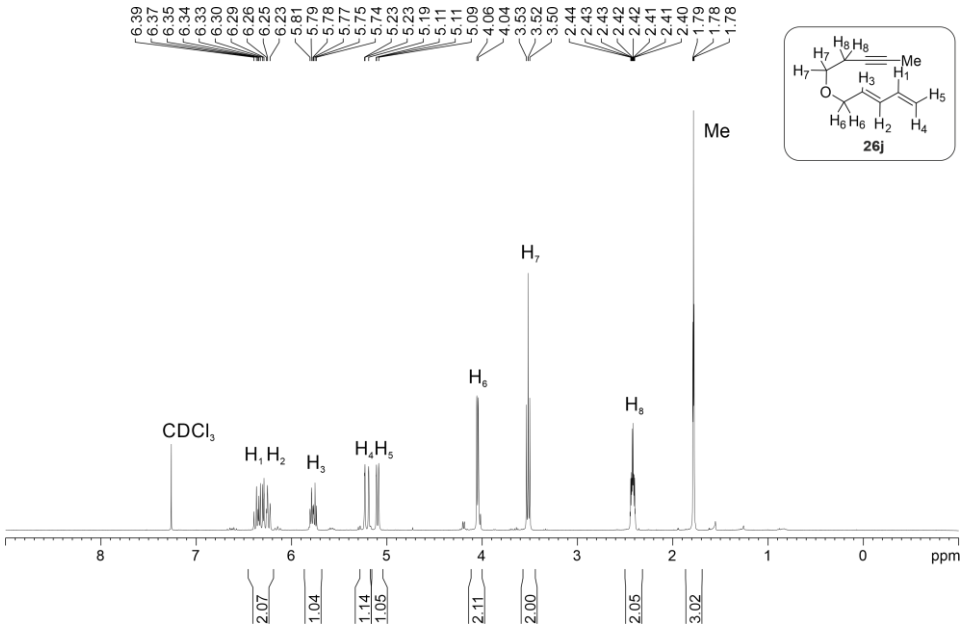

Figure 4.18. ^{1}H NMR spectrum of substrate **26j**.

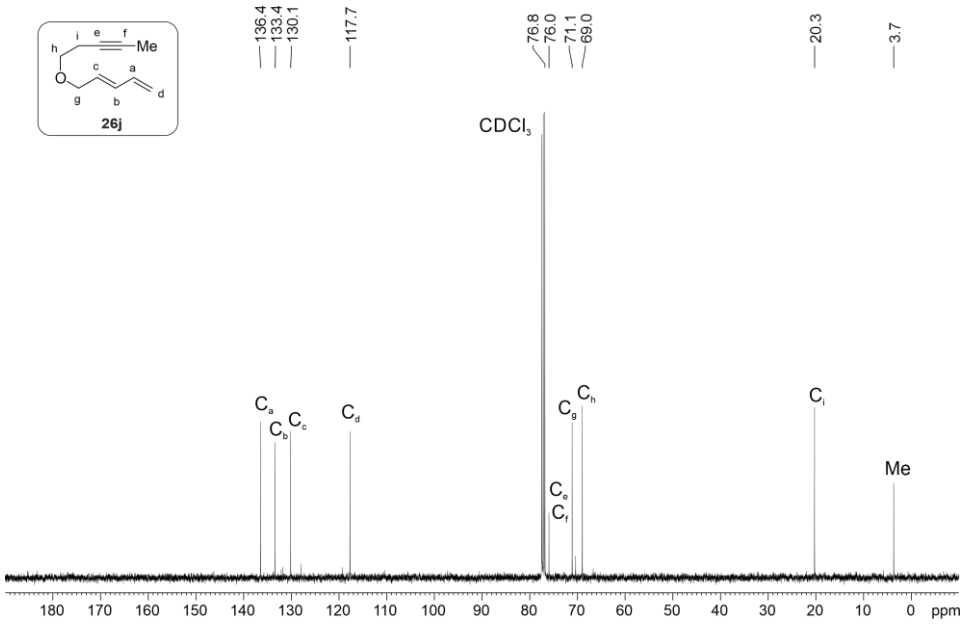

Figure 4.19. $^{13}C\{^{1}H\}$ NMR spectrum of product **26j**.

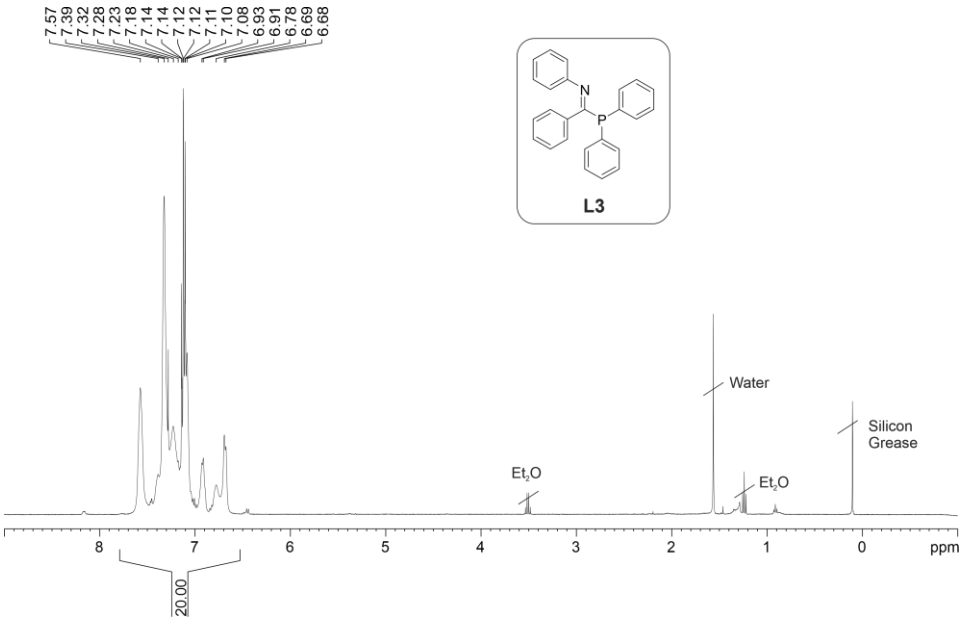

Figure 4.20. ^{1}H NMR spectrum of ligand **L3**

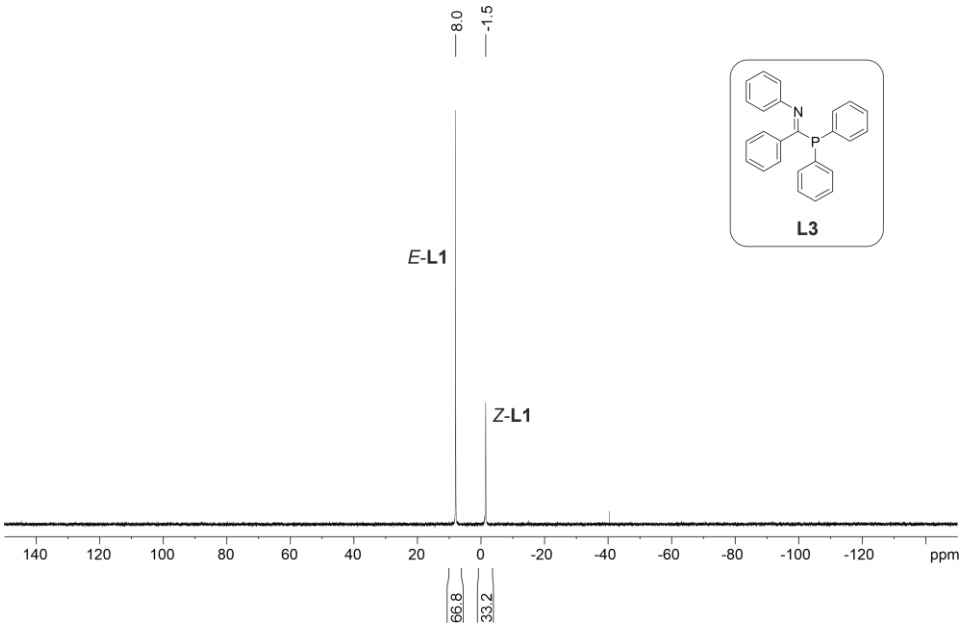

Figure 4.21. $^{31}P\{^{1}H\}$ NMR spectrum of ligand **L3**.

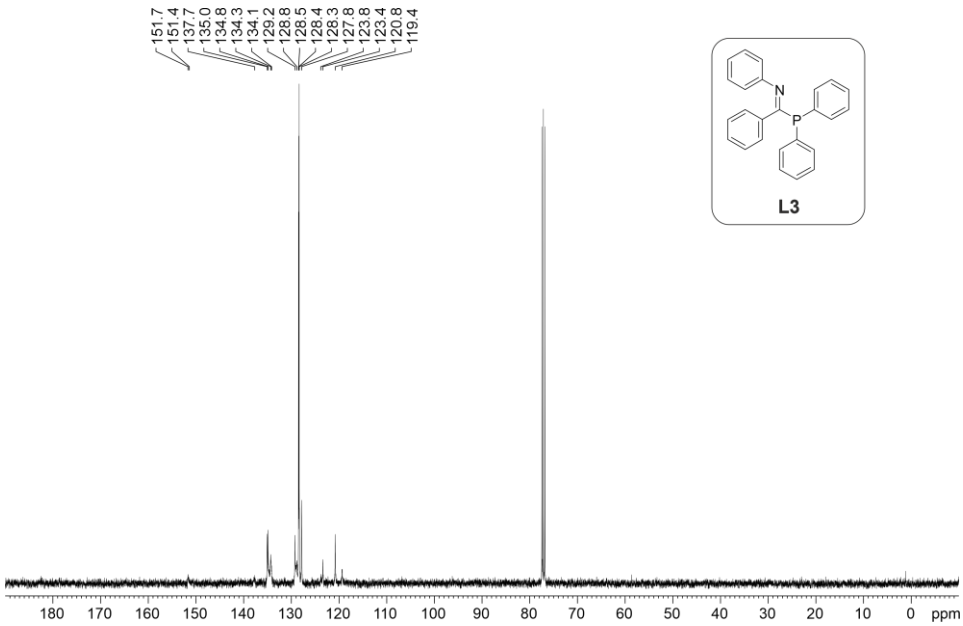

Figure 4.22. $^{13}C\{^{1}H\}$ NMR spectrum of ligand **L3**.

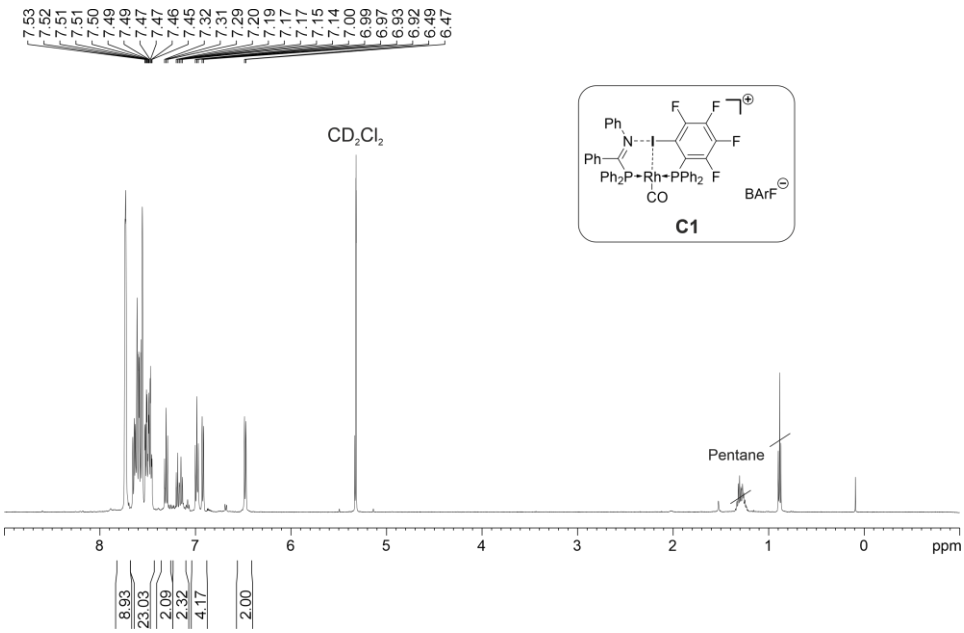

Figure 4.23. ^{1}H NMR spectrum of complex **C1**

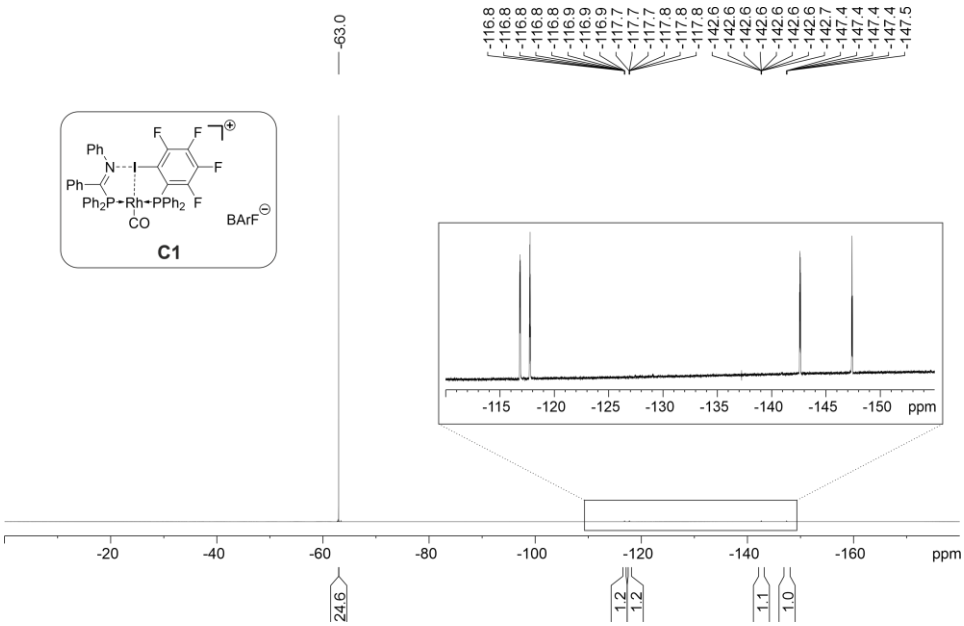

Figure 4.24. $^{19}F\{^{1}H\}$ NMR spectrum of complex **C1**

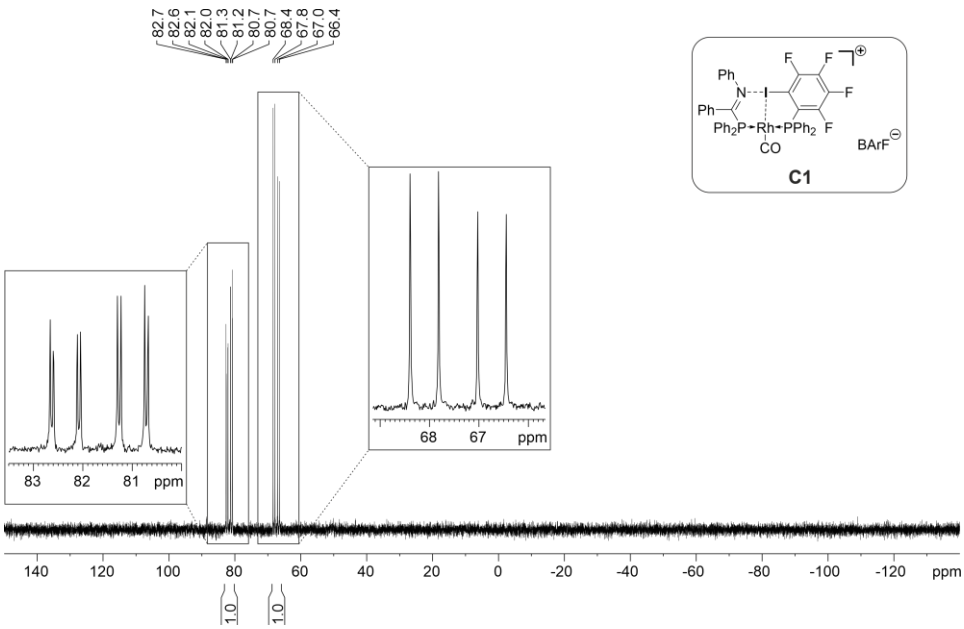

Figure 4.25. $^{31}P\{^{1}H\}$ NMR spectrum of complex **C1**.

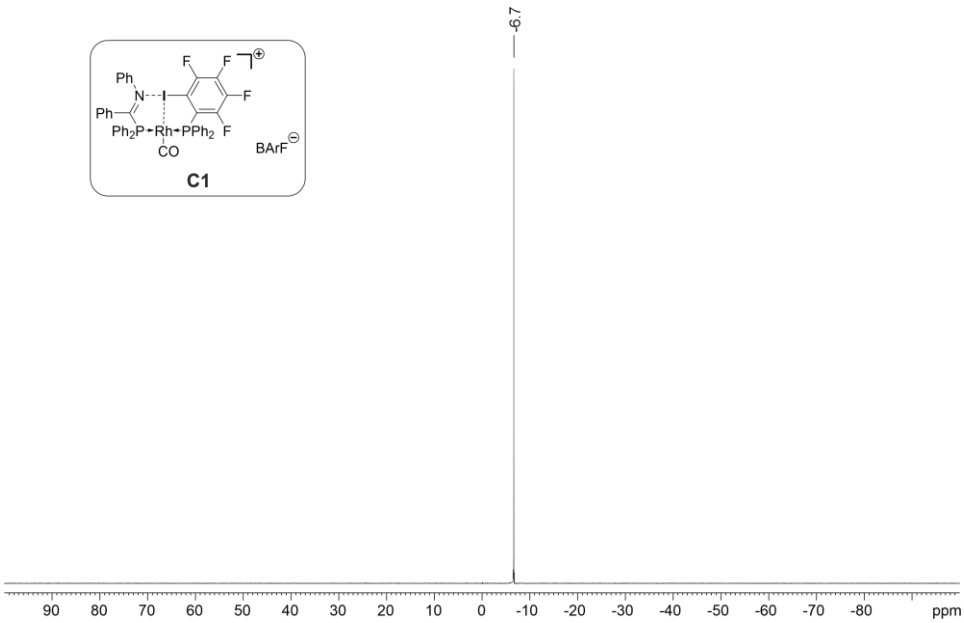

Figure 4.26. $^{11}B\{^{1}H\}$ NMR spectrum of complex **C1**.

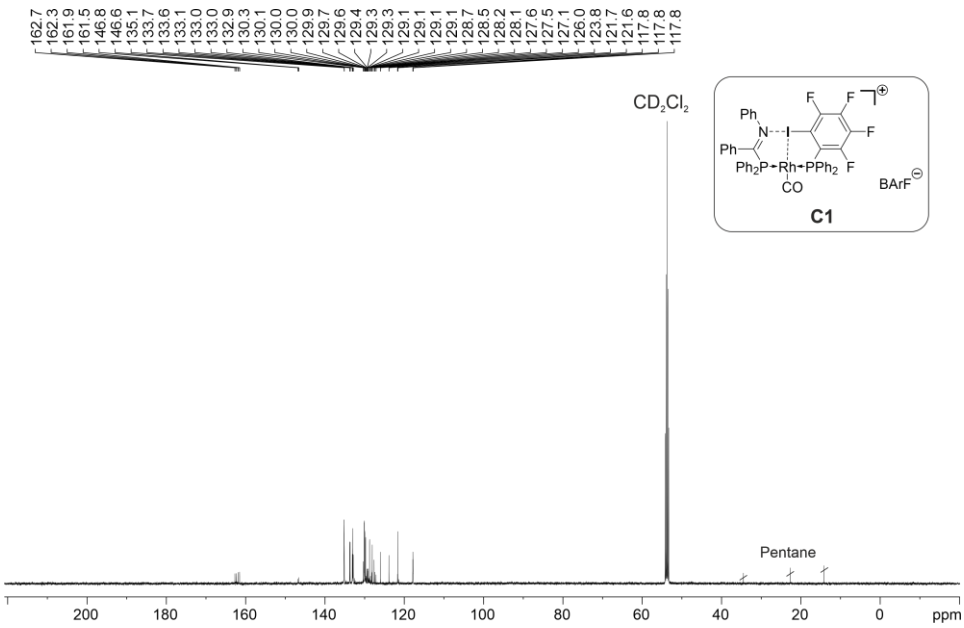

Figure 4.27. $^{13}C\{^{1}H\}$ NMR spectrum of complex **C1**.

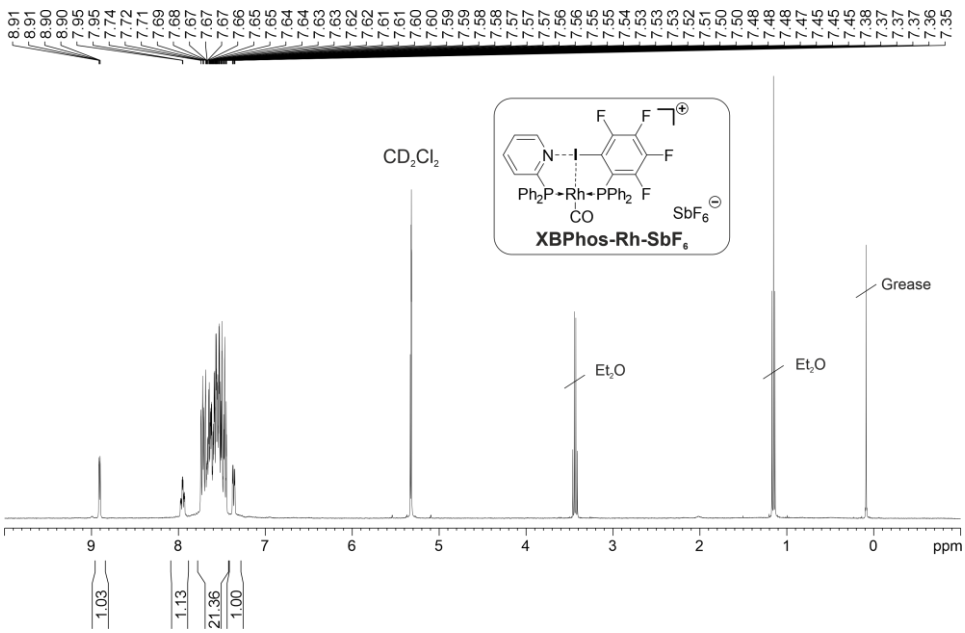

Figure 4.28. ^{1}H NMR spectrum of complex XBPhos-Rh-SbF_6.

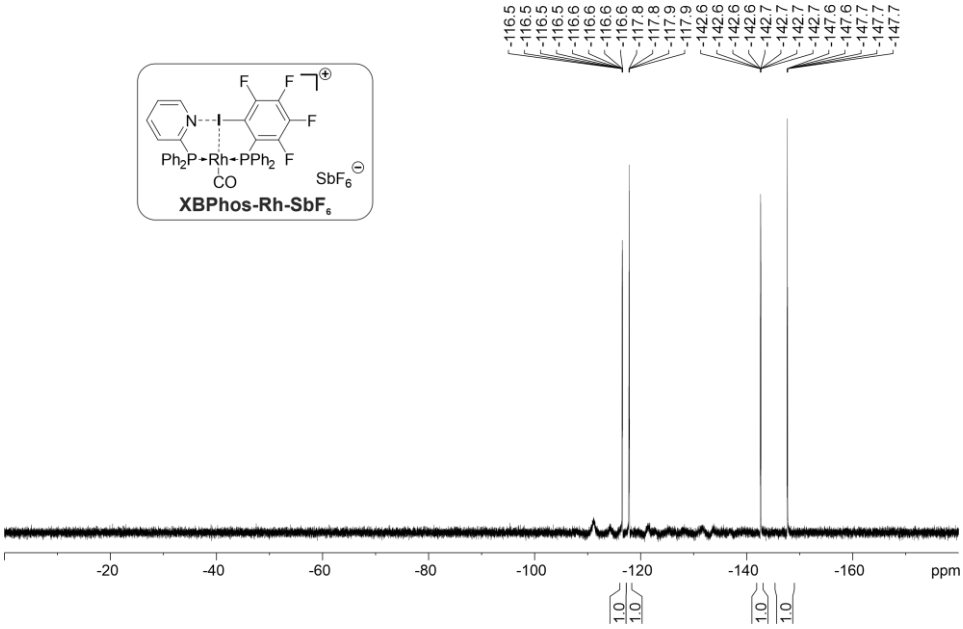

Figure 4.29. $^{19}F\{^{1}H\}$ NMR spectrum of complex XBPhos-Rh-SbF_6.

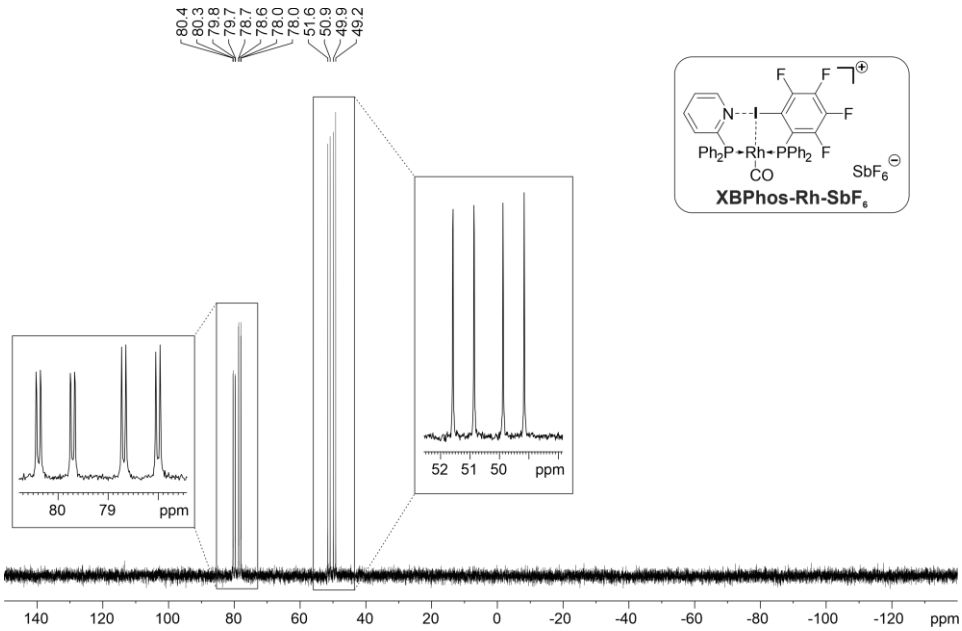

Figure 4.30. $^{31}P\{^{1}H\}$ NMR spectrum of complex XBPhos-Rh-SbF_6.

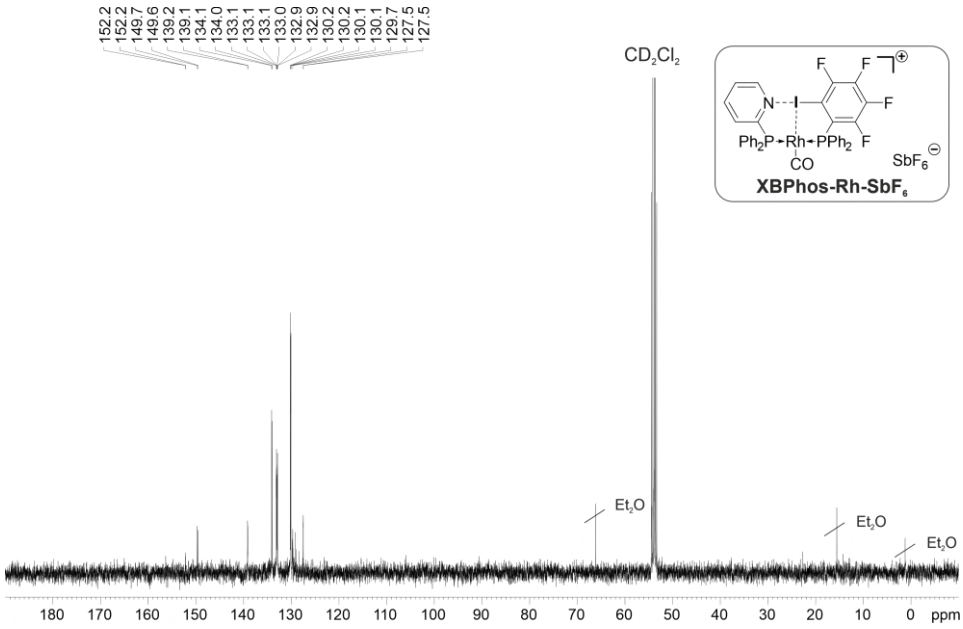

Figure 4.31. $^{13}C\{^{1}H\}$ NMR spectrum of complex XBPhos-Rh-SbF_6.

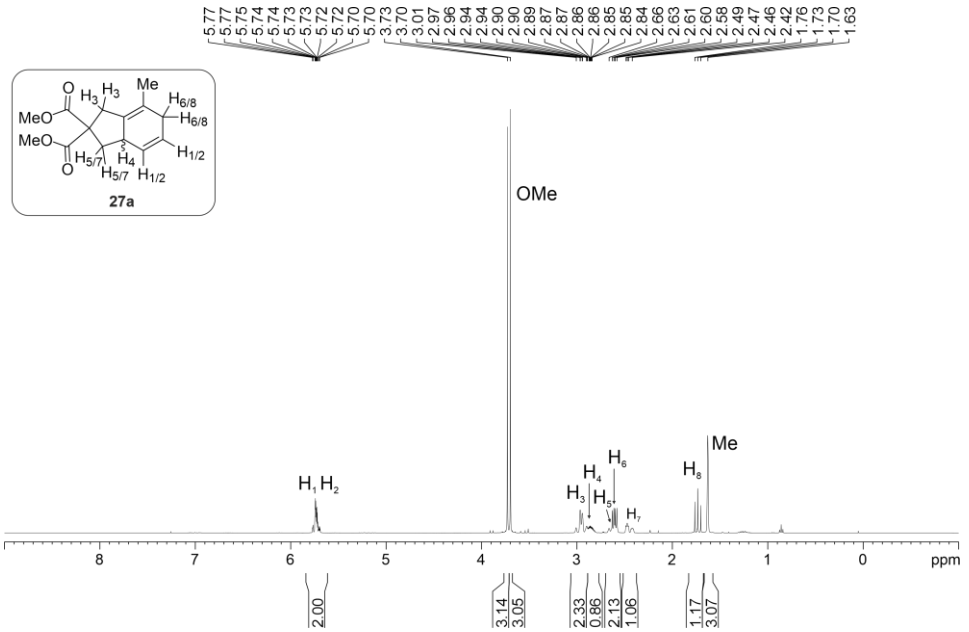

Figure 4.32. ^{1}H NMR spectrum of product **27a**.

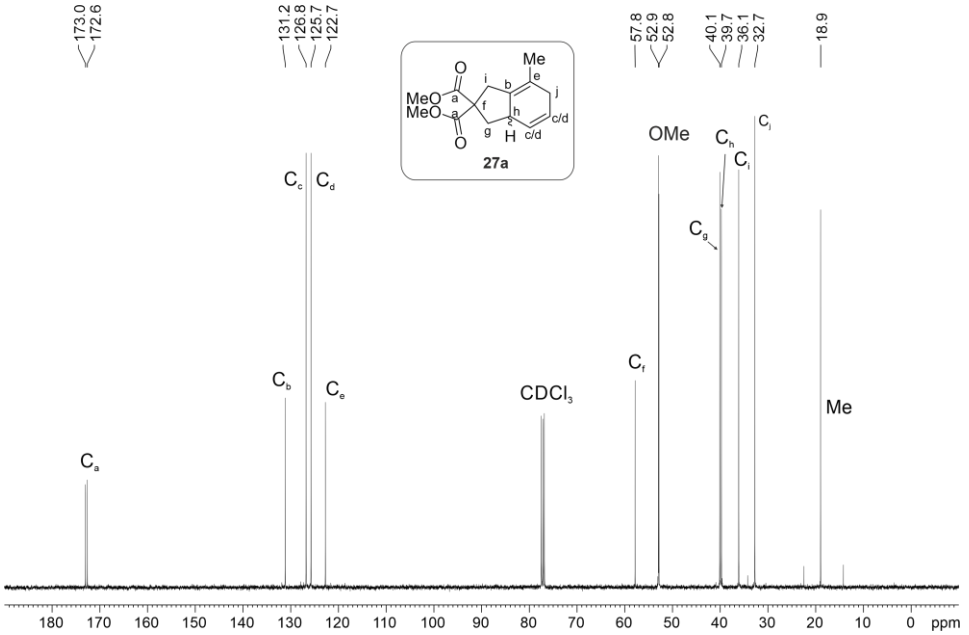

Figure 4.33. $^{13}C\{^{1}H\}$ NMR spectrum of product **27a**.

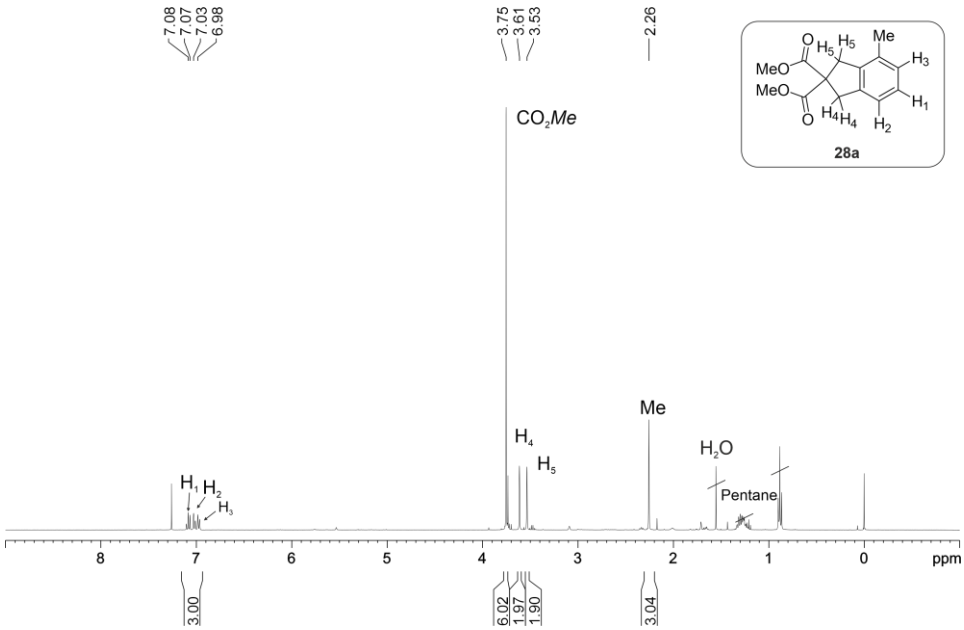

Figure 4.34. ^{1}H NMR spectrum of product **28a**.

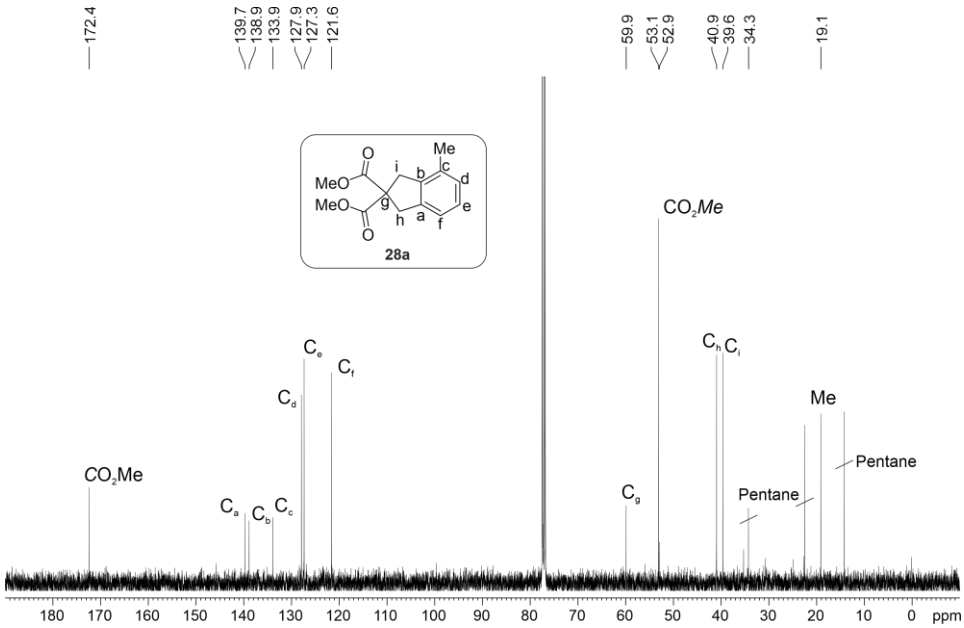

Figure 4.35. $^{13}C\{^{1}H\}$ NMR spectrum of product **28a**.

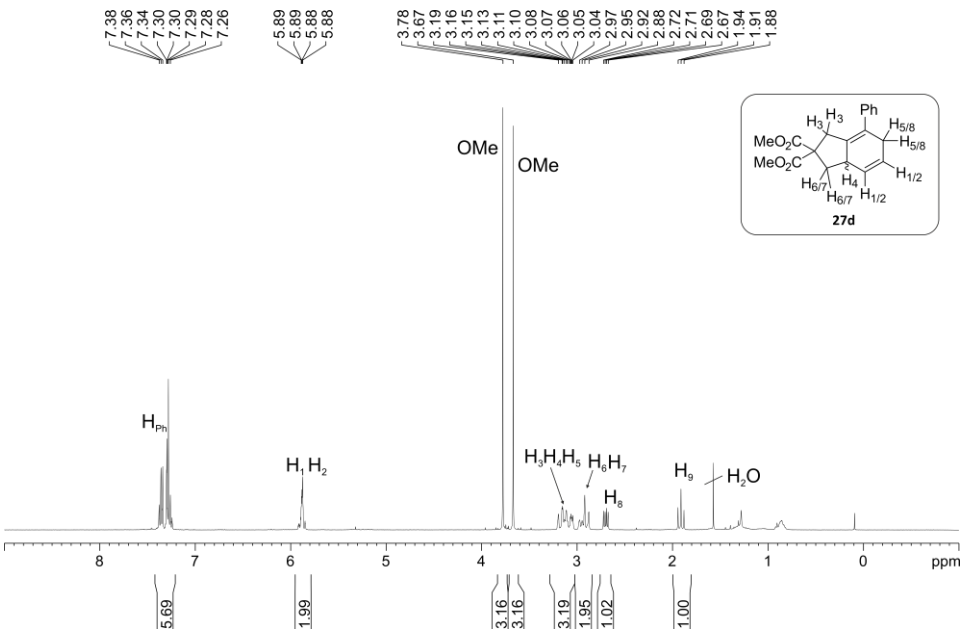

Figure 4.36. ^{1}H NMR spectrum of product **27d**.

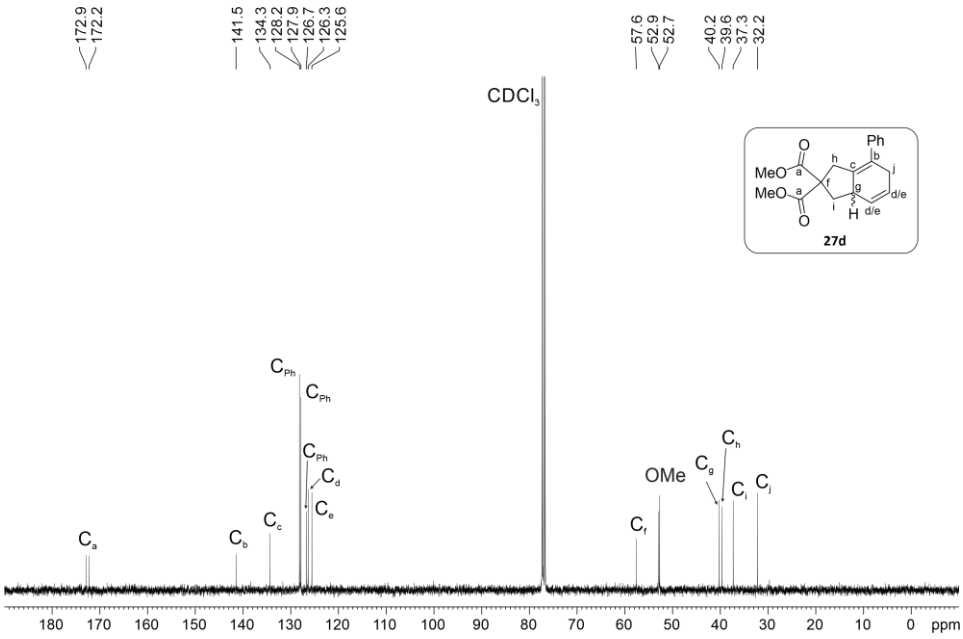

Figure 4.37. $^{13}C\{^{1}H\}$ NMR spectrum of product **27d**.

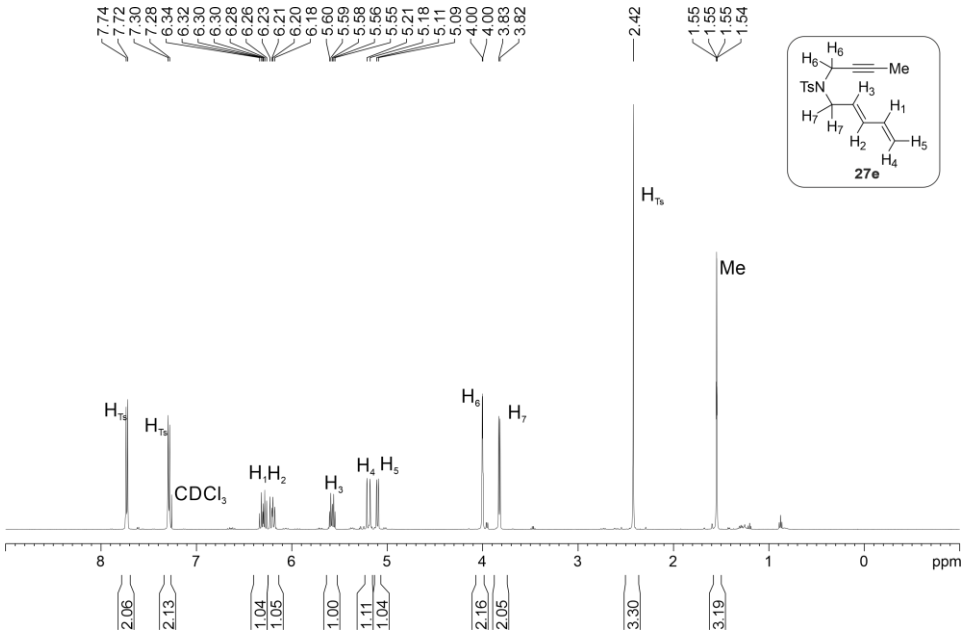

Figure 4.38. ^{1}H NMR spectrum of product **27e**.

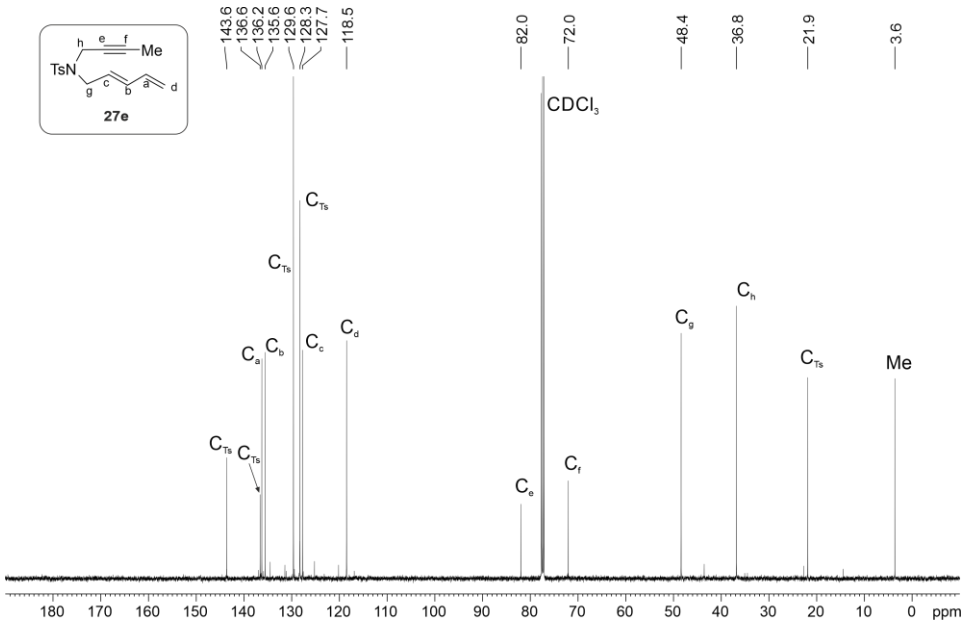

Figure 4.39. $^{13}C\{^{1}H\}$ NMR spectrum of product **27e**.

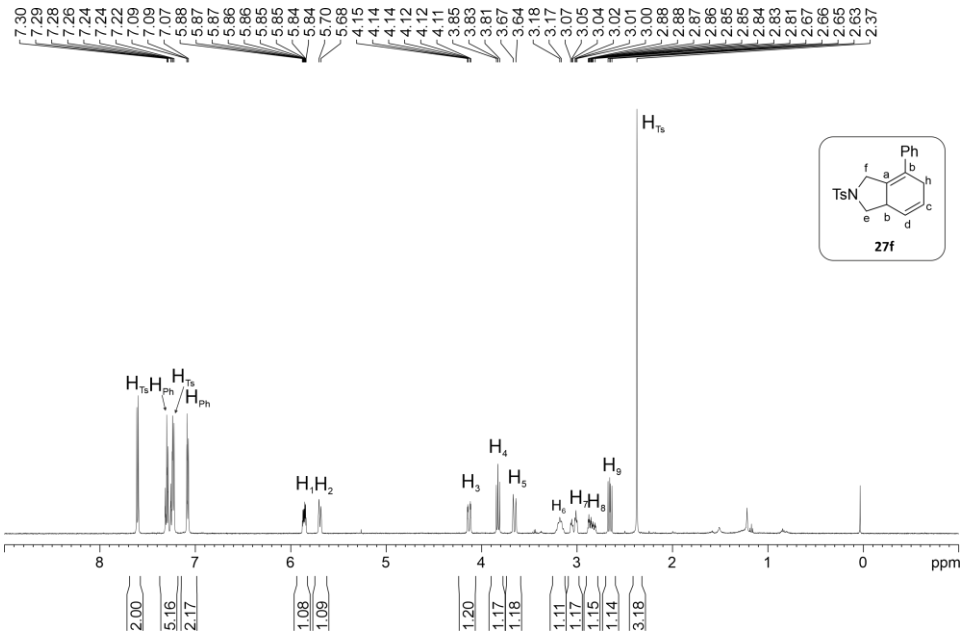

Figure 4.40. ^{1}H NMR spectrum of product **27f**.

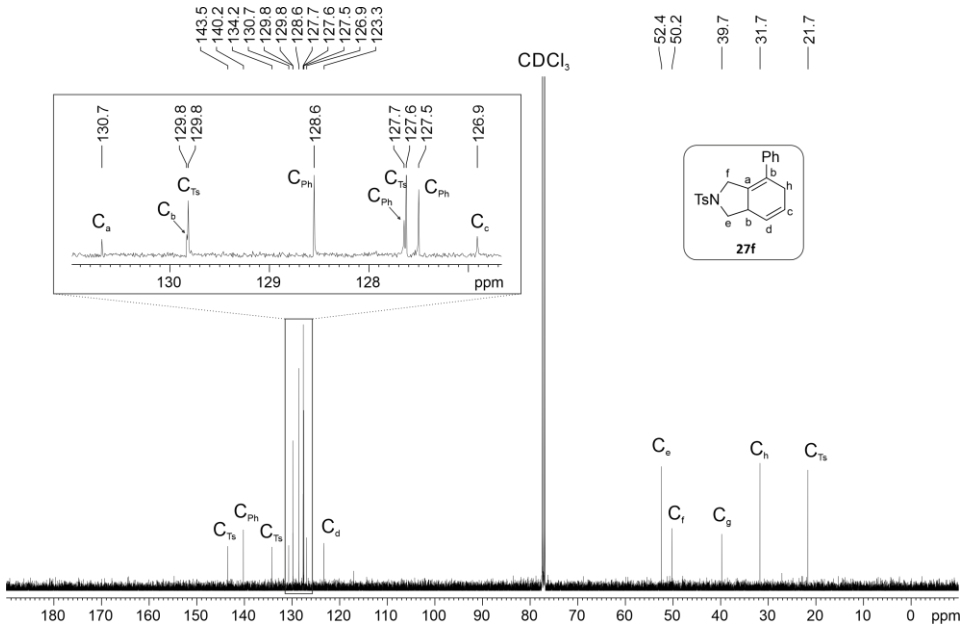

Figure 4.41. ^{13}C{^{1}H} NMR spectrum of product **27f**.

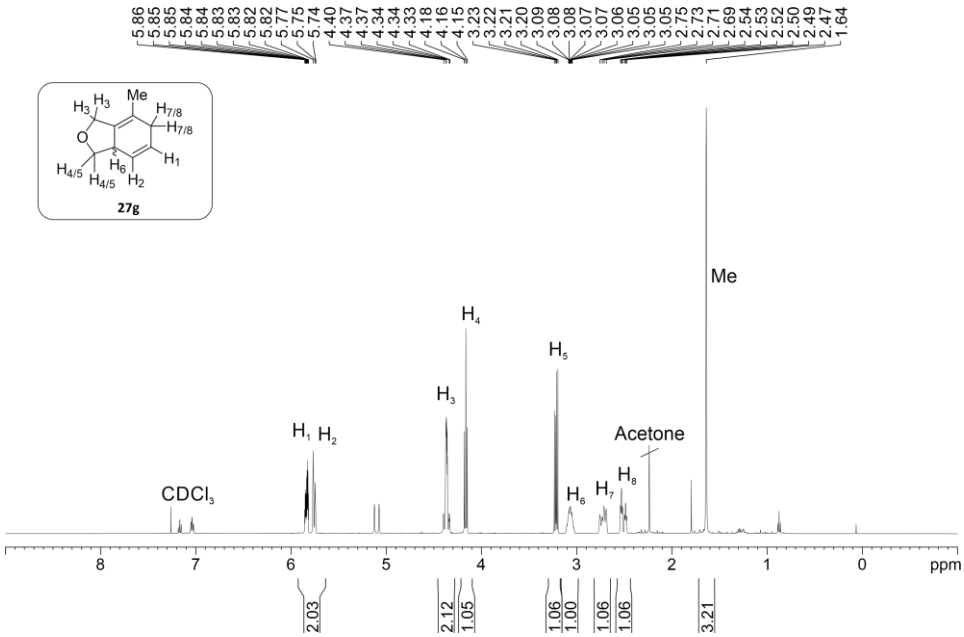

Figure 4.42. ^{1}H NMR spectrum of product **27g**.

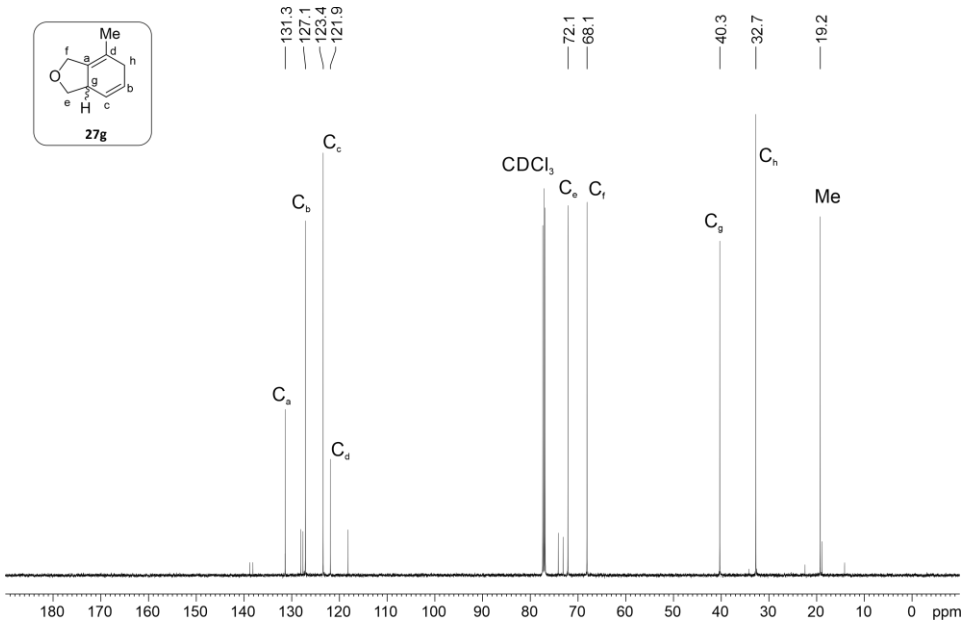

Figure 4.43. $^{13}C\{^{1}H\}$ NMR spectrum of product **27g**.

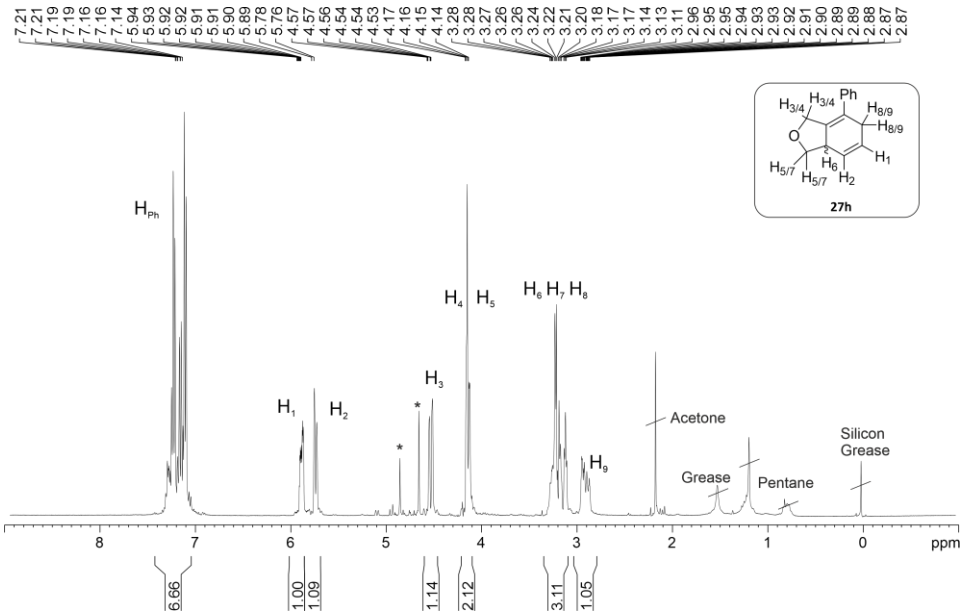

Figure 4.44. ^{1}H NMR spectrum of product **27h**.

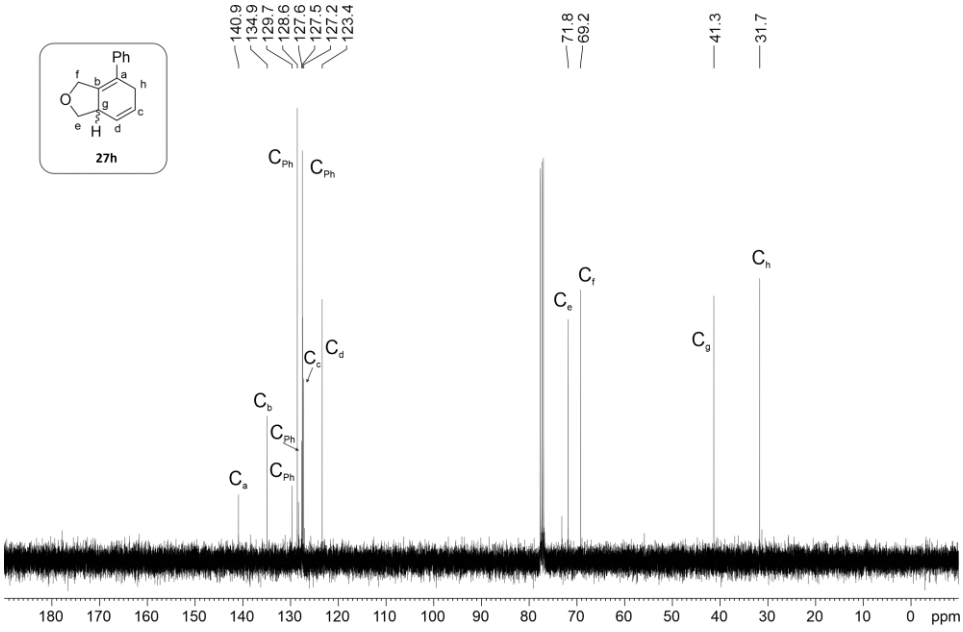

Figure 4.45. ^{13}C{^{1}H} NMR spectrum of product **27h**.

UNIVERSITAT ROVIRA I VIRGILI
TRANSITION METAL-CATALYZED CYCLOADDITION REACTIONS FOR THE FORMATION OF EIGHT- AND SIX-MEMBERED RINGS
Nuria Llorente González

CONCLUSIONS

- Nickel-catalyzed intramolecular [4+4] cycloadditions for the preparation of *cis*-eight-membered fused [6.3.0] bicyclic compounds and *trans*- or *cis*-eight-membered fused [6.4.0] bicyclic systems from structurally diverse bisdienes are reported. The catalytic intramolecular [4+4] cycloaddition reaction proceeds efficiently on a set of bisdienes linked by a three-atom chain to afford *cis*-configured eight-membered carbocycles fused to a five-membered ring. Analogously, the reported chemistry for bisdienes linked by a four-atom chain gives access to *trans*- or *cis*-configured eight-membered carbocycles fused to a six-membered ring. Computational studies on the stereo-determining step of the reaction have demonstrated that the stereochemical outcome of the reaction is dictated by the length of the chain linking the two diene units, and the geometry of the C=C double bonds in the diene units of the substrates.

- An enantioselective version of the nickel-catalyzed intramolecular [4+4] cycloaddition of bisdiene substrates for the preparation of *cis*-eight-membered fused [6.4.0] bicyclic systems from (*E*,*Z*)-configured bisdiene **1** (*i.e.*, (*E*)-6-(((*Z*)-penta-2,4-dien-1-yl)oxy)hexa-1,3-diene) was developed. An initial evaluation of enantiopure ligands, followed by a thorough HTE screening study led to the discovery of phosphoramidite ligand **L27**, which was capable of catalyzing the intramolecular [4+4] cycloaddition reaction of substrate **1** in good yield (57% yield) and moderate levels of enantioselectivity (30% ee). Further ligand design, and incorporation of the required structural variations in **L27** for achieving higher levels of stereoinduction, led to the discovery of ligand **L37**, which provided a slightly higher enantioselectivity (38% ee) with the cycloaddition yields remaining similar to those with ligand **L27**. This is, to the best of our knowledge, the first example of a catalytic enantioselective intramolecular [4+4] cycloaddition reaction. As potential research activities for the future, it would be highly interesting to expand the research perspectives developed within this PhD thesis for this challenging chemistry.

- We have explored nickel-catalyzed [(4+2)+2] cycloaddition reactions between a diene unit tethered to an alkene/alkyne group (4+2 carbon component in the cycloaddition process) in the presence of alkynes to yield eight-membered rings. Unfortunately, none of the nickel catalysts derived from the studied ligands mediated the formation of the corresponding [4+4]

cycloadducts. Under the assayed experimental conditions, substrates have been mainly transformed into unidentifiable products (probably oligomers/polymers of the starting materials). It is interesting to note that nickel catalysts derived from triphenylphosphine or ligands containing cyclohexyl-substituted phosphino groups led to the corresponding [4+2] cycloadducts and/or other cyclic byproducts.

- A new Fe(II) dimeric complex derived from a pyridine-oxazoline ligand has been efficiently synthesized. The structure of this complex has been unequivocally determined by single crystal X-Ray crystallography. All attempts to isolate low-valent analogous complexes have failed. Attempts to generate *in situ* the low-valent analogous iron complexes as suitable catalysts for [4+4] cycloaddition reactions have also failed.

- We have demonstrated the versatility and efficacy of XBPhos-Rh-BArF combined with silver BArF as catalyst for intramolecular [4+2] cycloadditions of dienynes. This cycloaddition reaction proceeded efficiently on a set of structurally diverse dienynes to afford six-membered carbocycles fused to a five-membered ring. The products were isolated as 1,4-unconjugated cyclohexenes, without aromatization taking place. The halogen-bonded complex C1 has been prepared and used in this chemistry, albeit with less efficiency compared to that of XBPhos Rh BArF. A tentative rationalization of the reaction pathway involving a Rh/Ag cooperative process has also been provided. Coordination of the dienyne to silver has been demonstrated, which led us to preliminary hypothesize that the intramolecular [4+2] cyclizations may be proceeding via a silver complexation, transmetallation, oxidative cyclization, 1,3-allyl migration and reductive elimination sequence as a probable reaction pathway towards the final cycloadducts.

UNIVERSITAT ROVIRA I VIRGILI
TRANSITION METAL-CATALYZED CYCLOADDITION REACTIONS FOR THE FORMATION OF EIGHT- AND SIX-MEMBERED RINGS
Nuria Llorente González

UNIVERSITAT ROVIRA I VIRGILI
TRANSITION METAL-CATALYZED CYCLOADDITION REACTIONS FOR THE FORMATION OF EIGHT- AND SIX-MEMBERED RINGS
Nuria Llorente González

SUMMARY

Cycloaddition reactions entail the formation of cyclic systems from unsaturated molecules (or parts of the same molecule) with a net reduction of the bond multiplicity. By facilitating the formation of several bonds in a single process, these transformations enable the formation of complex molecules in organic synthesis. Most cycloadditions require the presence of functional groups in the substrate in order to activate the multiple bonds and make the transformation possible. One way to overcome this limitation is the use of transition metal complexes as catalysts. Transition-metal-catalyzed cycloaddition reactions involve the complexation of olefin, diene, or acetylene units to the metal center with modification of the reactivity of such moieties. Not only an enhancement on the reaction rate is observed in the presence of the metal catalyst, but also the modification of the stereochemical outcome of the reaction can be achieved. An impressive variety of structurally diverse eight-membered rings can be synthesized by metal-catalyzed [4+4]-cycloaddition reactions, which provide one of the most direct and efficient procedures for synthesizing said rings. These [4+4] cycloadditions leading to the formation of eight-membered rings are forbidden by the Woodward-Hoffman rules, with the use of metal catalysts being a key strategy for promoting these reactions.

The present doctoral thesis has focused on the design of new catalytic systems for achiral or enantioselective [4+4] cycloaddition reactions lacking an efficient and (stereo)selective solution. Detailed investigations on the use of nickel(0)-based catalysts for intramolecular [4+4]-cycloadditions were investigated (Scheme 4.10). Nickel(0) complexes derived from electron-rich triarylphosphines proved to be efficient catalysts for intramolecular [4+4]-cycloadditions of an array of structurally diverse bis-dienes (10 examples, up to 78% isolated yield). The reported synthetic methodology led to *cis*-eight-membered fused [6.3.0] bicyclic compounds as well as *trans*- or *cis*- eight-membered fused [6.4.0] bicyclic systems. Computational studies on the stereo-determining step of the reaction, in combination with experimental results, demonstrated that the stereochemical outcome of these [4+4] cycloadditions is dictated by the length of the chain linking the two diene units and the geometry of the C=C double bonds of the substrates.

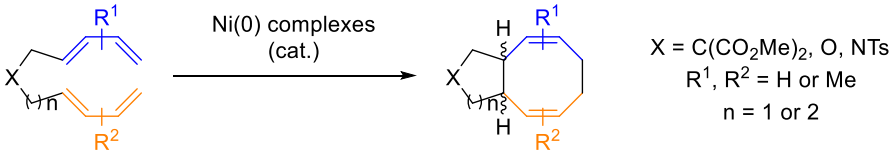

Scheme 4.10. Nickel-catalyzed intramolecular [4+4]-cycloadditions studied.

Following the results obtained for the achiral nickel-catalyzed [4+4] cycloaddition reactions, an attractive approach for biasing the enantioselectivity in this transformation was envisioned. The fact that the stereochemical outcome of the reaction was dependent on the geometry of the C-C double bonds in the diene units of the substrates led us to develop an enantioselective version of this transformation. Our strategy relied on the vacancy present in the coordination sphere of the metal for *E,Z*-bisdiene substrates, which allowed for the participation of one molecule of the phosphine ligand in the stereo-determining step of the transformation (Scheme 4.11). A set of structurally diverse enantiopure phosphorus ligands was explored and optimization studies were carried out for these systems in various types of intramolecular [4 + 4] cycloaddition reactions. The moderate enantioselectivities obtained with the optimal phosphoramidite ligand (up to 38% ee; see structure in Scheme 2) are, to the best of our knowledge, the highest reported to date for an intramolecular [4+4]-cycloaddition reaction.

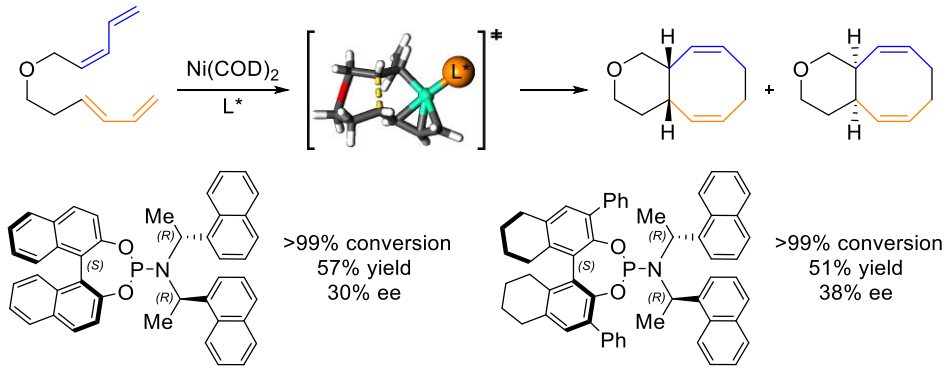

Scheme 4.11. Enantioselective nickel-catalyzed intramolecular [4+4]-cycloadditions.

Our research has also been directed towards the development of alternative approaches for the synthesis of eight-membered rings. With our expertise in [4+4] cycloaddition reactions, we met the challenge of developing nickel-catalyzed [(4+2)+2] cycloaddition reactions between a substrate with embedded diene and alkene/alkyne units and a separate alkyne molecule. The catalytic activity of nickel(0) complexes was studied with an array of phosphorus and nitrogen-based ligands for an array of substrates (see Scheme 4.12a). Unfortunately, no efficient catalytic system was discovered. Another pursued

approach consisted of developing intramolecular Fe-Catalyzed [4+4] cycloadditions. To this end, an Fe(II) complex derived from a pyridine-oxazoline ligand was synthesized and its structure univocally determined by single crystal X-Ray crystallography (Complex **C1** in Scheme 4.12b). It is reported in the literature that low oxidation-state Fe-complexes are needed for [4+4] cycloadditions to proceed. However, all the attempts to isolate such complexes were unsuccessful, as well as our attempts to generate said complexes *in situ* and use them subsequently in catalysis.

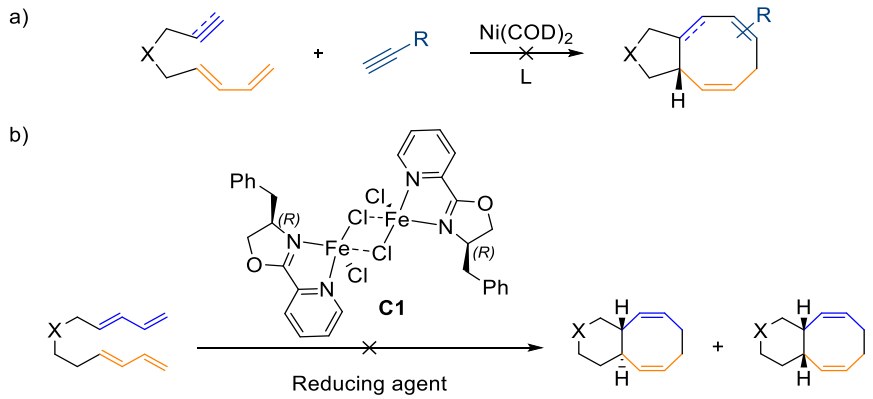

Scheme 4.12. Different Approaches Towards the Synthesis of Eight-Membered Rings

Research efforts have also been directed to the application of supramolecular catalysts based on rhodium complexes derived from halogen-bonded diphosphines in [4+2]-cycloaddition reactions. A general representation of the [4+2] cycloadditions studied is depicted in Scheme 4.13. The cycloadditions proceeded efficiently and led to an array of structurally diverse six-membered carbocycles fused to a five-membered ring. The products were isolated as 1,4-unconjugated cyclohexenes, without the undesired aromatized products being formed. A tentative rationalization of the reaction pathway involving a Rh/Ag cooperative process has also been suggested.

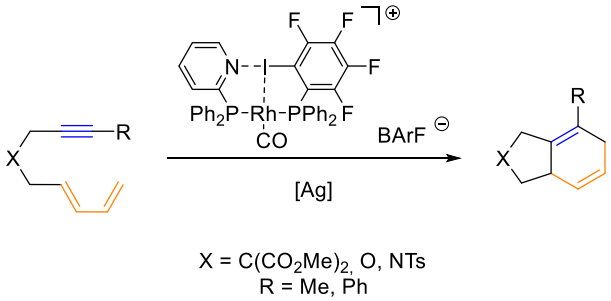

Scheme 4.13. XBPhosRh-Catalyzed Intramolecular [4+2]-Cycloadditions of Dienynes.

In summary, the versatility of metal-catalyzed cycloadditions has been demonstrated throughout this doctoral thesis. Our studies regarding intramolecular Ni-catalyzed [4+4]-cycloadditions of an array of bisdienes enabled the efficient preparation of *cis*- or *trans*- eight-membered rings fused to five- or six membered rings. Our studies allowed gaining a deep mechanistic understanding of the transformation. This knowledge has allowed the development of enantioselective versions of this transformation with moderate enantioselective excesses. In addition, the reactivity of XBPhosRh complexes and silver BArF in intramolecular [4+2] cycloadditions of dienynes has been explored. An array of structurally diverse [4+2] cycloadducts was prepared and isolated as 1,4-unconjugated cyclohexenes in good yields.

RESUMEN

Las reacciones de cicloadición conllevan la formación de sistemas cíclicos a partir de moléculas insaturadas (o partes de la misma molécula) con una reducción neta de la multiplicidad de enlaces. Al facilitar la formación de varios enlaces en un solo proceso, estas reacciones posibilitan la formación de moléculas complejas en síntesis orgánica. La mayoría de las cicloadiciones requieren la presencia de grupos funcionales en el sustrato para activar los enlaces múltiples y hacer posible la transformación. Una forma de superar esta limitación es el uso de complejos de metales de transición como catalizadores. Las reacciones de cicloadición catalizadas por metales de transición implican la complejación de unidades de alqueno, dieno o alquino al centro metálico con la modificación de la reactividad de dichos grupos funcionales hidrocarbonados. No sólo se observa una mejora en la velocidad de reacción en presencia del catalizador metálico, sino que también se puede lograr modificar el resultado estereoquímico de la reacción. Se puede sintetizar una impresionante variedad de anillos de ocho miembros estructuralmente diversos mediante reacciones de cicloadición [4+4] catalizadas por metales, las cuales proporcionan uno de los procedimientos más directos y eficientes para sintetizar dichos anillos. Estas cicloadiciones [4+4] que conducen a la formación de anillos de ocho miembros están prohibidas por las reglas de Woodward–Hoffman, siendo el uso de catalizadores metálicos una estrategia clave para promover dichas reacciones.

La presente tesis doctoral se ha centrado en el diseño de nuevos sistemas catalíticos para reacciones de cicloadición [4+4] de tipo aquiral o enantioselectiva que carecen de una solución eficiente y (estereo)selectiva. Se ha investigado en detalle el uso de catalizadores basados en níquel(0) para las cicloadiciones [4+4] intramoleculares (

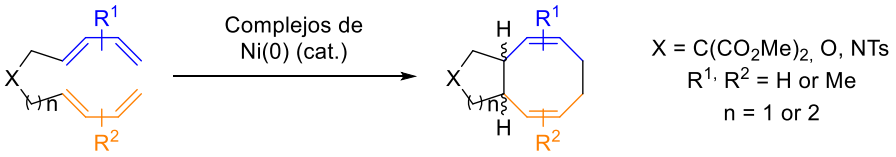

Esquema 1). Los complejos de níquel(0) derivados de triarilfosfinas ricas en electrones han demostrado ser catalizadores eficientes para las cicloadiciones [4+4] intramoleculares de una serie de bisdienos estructuralmente diversos (10 ejemplos, hasta un 78% de rendimiento aislado). La metodología sintética descrita dio lugar a compuestos bicíclicos fusionados [6.3.0] de ocho miembros *cis*, así como a sistemas bicíclicos fusionados de ocho miembros [6.4.0] *trans* o *cis*. Los estudios

computacionales sobre el paso estereodeterminante de la reacción, en combinación con los resultados experimentales, demostraron que la estereoquímica de estas cicloadiciones [4+4] viene dictada por la longitud de la cadena que une las dos unidades de dieno y la geometría de los dobles enlaces C=C de los sustratos.

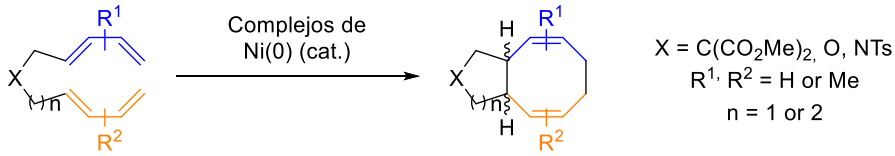

Esquema 1. Estudio de las cicloadiciones intramoleculares [4+4] catalizadas por níquel.

A raíz de los resultados obtenidos para las reacciones de cicloadición [4+4] aquirales catalizadas por níquel, se planteó un enfoque para favorecer la enantioselectividad en esta transformación. El hecho de que el resultado estereoquímico de la reacción dependiera de la geometría de los dobles enlaces C-C en las unidades de dieno de los sustratos nos llevó a desarrollar una versión enantioselectiva basada en la vacante presente en la esfera de coordinación del metal para los sustratos de *E,Z*-bisdieno. Este efecto permitía la participación de una molécula del ligando de fosfina en el paso estereodeterminante de la transformación (Esquema 2). Se exploraron un conjunto de ligandos de fósforo estructuralmente diversos y se llevaron a cabo estudios de optimización para estos sistemas en varios tipos de reacciones de cicloadición intramolecular [4 + 4]. Las enantioselectividades moderadas obtenidas con el ligando fosforamidito óptimo (hasta un 38% de ee; véase la estructura en el Esquema 2) son, según nuestro mejor conocimiento, las más altas descritas hasta la fecha para una reacción de cicloadición [4+4] intramolecular.

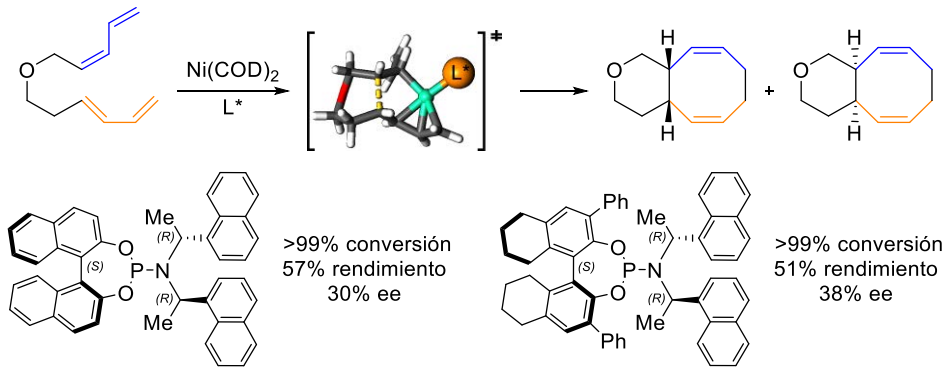

Esquema 2. Reacciones intramoleculares de [4+4]-cicloadición enantioselectivas catalizadas por níquel.

Por otro lado, se han abordado enfoques alternativos para la síntesis de anillos de ocho miembros. Gracias a nuestra experiencia en reacciones de cicloadición [4+4], se abordó el reto de desarrollar reacciones de cicloadición [(4+2)+2] catalizadas por níquel entre un sustrato con unidades de dieno y alqueno/alquino y una molécula de alquino independiente. La actividad catalítica de los complejos de níquel(0) se estudió con una serie de ligandos basados en fósforo y nitrógeno para una serie de sustratos (véase el Esquema 3a). Lamentablemente, no se descubrió ningún sistema catalítico eficiente. Otro enfoque perseguido ha consistido en desarrollar cicloadiciones [4+4] intramoleculares catalizadas por complejos de hierro. Para ello, se sintetizó un complejo de Fe(II) derivado de un ligando de piridina-oxazolina y su estructura se determinó inequívocamente mediante cristalografía de rayos X de monocristal (Complejo **C1** en el Esquema 3b). En la literatura se indica que los complejos de hierro de bajo estado de oxidación son necesarios para que se produzcan las cicloadiciones [4+4]. Sin embargo, todos nuestros intentos de aislar dichos complejos fueron infructuosos, así como los de generar dichos complejos *in situ* y utilizarlos posteriormente en catálisis.

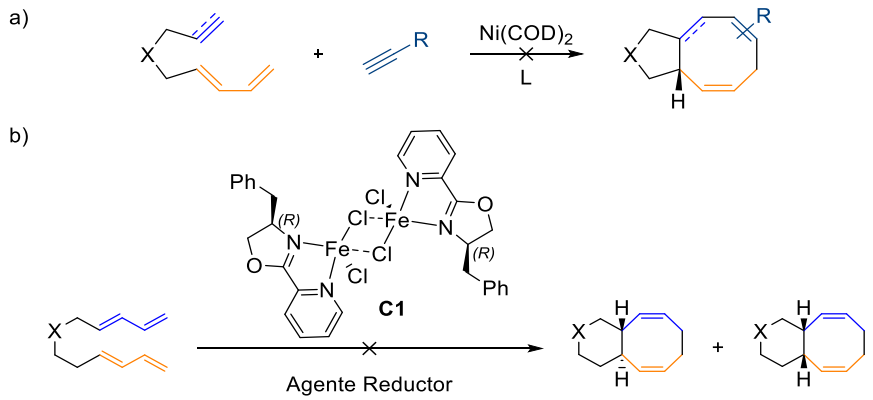

Esquema 3. Diferentes enfoques para la síntesis de anillos de ocho miembros.

Nuestra investigación también se ha dirigido a la aplicación de catalizadores supramoleculares basados en complejos de rodio derivados de difosfinas con enlaces halógenos en reacciones de cicloadición [4+2]. El **Esquema 4** muestra una representación general de las cicloadiciones [4+2] estudiadas. Las reacciones fueron eficientes y dieron lugar a una serie de carbociclos de seis miembros estructuralmente diversos fusionados a un anillo de cinco miembros. Los productos se aislaron como 1,4-ciclohexenos no conjugados, sin que se formaran los productos aromatizados no deseados. También se ha sugerido una racionalización tentativa de la vía de reacción que implica un proceso cooperativo Rh/Ag.

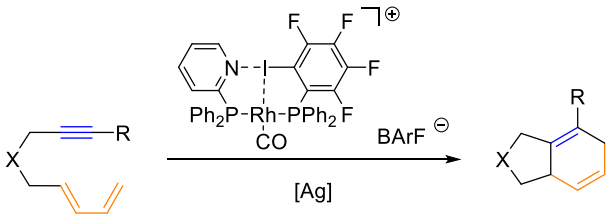

X = $C(CO_2Me)_2$, O, NTs
R = Me, Ph

Esquema 4. Cicloadiciones [4+2] intramoleculares de dieninos catalizadas por XBPhos-Rh.

En resumen, a lo largo de esta tesis doctoral, se ha demostrado la versatilidad de las cicloadiciones catalizadas por metales. Nuestros estudios sobre las cicloadiciones [4+4] intramoleculares catalizadas por Ni de una serie de bisdienos permitieron la preparación eficiente de anillos de ocho miembros *cis* o *trans* fusionados a anillos de cinco o seis miembros. Gracias a estos estudios, se ha podido obtener un profundo conocimiento mecanístico de la transformación. Este conocimiento ha permitido el desarrollo de versiones enantioselectivas de esta transformación con excesos enantioméricos moderados. Además, se ha explorado la reactividad de los complejos XBPhos-Rh-BArF y AgBArF en las cicloadiciones [4+2] intramoleculares de dieninos. Se prepararon una serie de cicloaductos [4+2] estructuralmente diversos y se aislaron como ciclohexenos 1,4-no conjugados con buenos rendimientos.

RESUM

Les reaccions de cicloaddició comporten la formació de sistemes cíclics a partir de molècules insaturades (o parts de la mateixa molècula) amb una reducció neta de la multiplicitat d'enllaços. Al facilitar la formació de diversos enllaços en un únic procés, aquestes reaccions fan possible la formació de molècules complexes en síntesi orgànica. La majoria de les cicloaddicions requereixen la presència de grups funcionals en el substrat per activar els enllaços múltiples i fer possible la transformació. Una manera de superar aquesta limitació és l'ús de complexos de metalls de transició com a catalitzadors. Les reaccions de cicloaddició catalitzades per metalls de transició impliquen la complexació d'unitats d'alquens, diens o alquins al centre metàl·lic amb la modificació de la reactivitat d'aquestes subunitats. No només s'observa una millora en la velocitat de reacció en presència del catalitzador metàl·lic, sinó que també es pot aconseguir la manipulació del resultat estereoquímic de la reacció. Es pot sintetitzar una varietat d'anells de vuit membres estructuralment diversos mitjançant reaccions de cicloaddició [4 + 4] catalitzades per metalls, les quals proporcionen un dels procediments més directes i eficients per sintetitzar aquests anells. Aquestes cicloaddicions [4 + 4] que condueixen a la formació d'anells de vuit membres estan prohibides per les regles de Woodward-Hoffman, essent l'ús de catalitzadors metàl·lics una estratègia clau per promoure aquestes reaccions.

La present tesi doctoral s'ha centrat en el disseny de nous sistemes catalítics per a reaccions de cicloaddició [4 + 4] aquirals o enantioselectives que no tenen una solució eficient i (estereo)selectiva. S'ha investigat en detall l'ús de catalitzadors basats en níquel(0) per a les cicloaddicions [4 + 4] intramoleculars (Esquema 5). Els complexos de níquel(0) derivats de triarilfosfines riques en electrons han demostrat ser catalitzadors eficients per a les cicloaddicions [4 + 4] intramoleculars d'una sèrie de bisdiens estructuralment diversos (10 exemples, fins a un 78% de rendiment aïllat). La metodologia sintètica descrita va conduir a compostos bicíclics fusionats [6.3.0] de vuit membres *cis*, així com sistemes bicíclics fusionats de vuit membres [6.4.0] *trans* o *cis*. Els estudis computacionals sobre el pas estereodeterminant de la reacció, en combinació amb els resultats experimentals, van demostrar que el resultat estereoquímic d'aquestes cicloaddicions [4 + 4] ve dictat per la longitud de la cadena que uneix les dues unitats de diè i la geometria dels dobles enllaços (C = C) dels substrats.

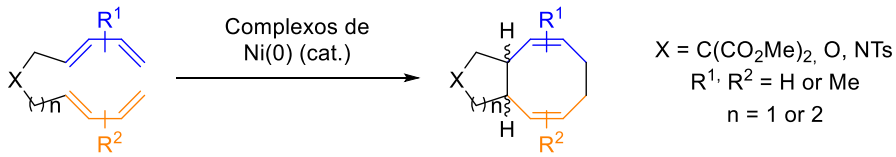

Esquema 5. Estudi de las cicloaddicions intramoleculars [4+4] catalitzades per níquel.

Arran dels resultats obtinguts per les reaccions de cicloaddició [4 + 4] aquirals catalitzades per níquel, es va plantejar un enfoc per afavorir la enantioselectivitat d'aquesta transformació. El fet de què el resultat estereoquímic de la reacció depengués de la geometria dels dobles enllaços C-C present a les unitats de diè dels substrats, ens va portar a desenvolupar una versió enantioselectiva. L'estratègia es basava en la vacant present a l'esfera de coordinació del metall per als substrats d'*E*, *Z*-bisdiè, la qual cosa permetia la participació d'una molècula del lligand de fosfina en el pas estereodeterminant de la transformació (Esquema 6). Es va explorar un conjunt de lligands de fòsfor estructuralment diversos i es van dur a terme estudis d'optimització per a aquests sistemes en diversos tipus de reaccions de cicloaddició intramolecular [4 + 4]. Les enantioselectivitats moderades obtingudes amb el lligand òptim de tipus fosforamidito (fins a un 38% ee; vegeu l'estructura en l'Esquema 6) són, segons el nostre millor coneixement, les més altes descrites fins a la data per a una reacció de cicloaddició intramolecular [4+ 4].

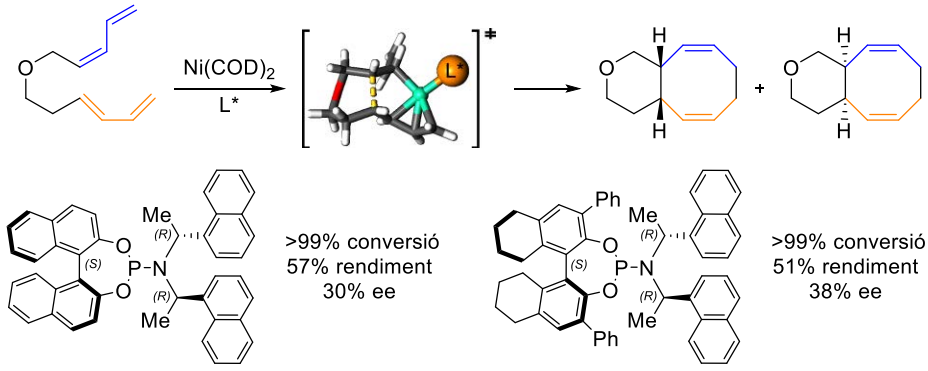

Esquema 6. Reaccions intramoleculars de cicloaddició [4+4] enantioselectives catalizades per níquel

Altres activitats d'investigació també es van dirigir al desenvolupament d'alternatives per a la síntesi d'anells de vuit membres. Gràcies a la nostra experiència en reaccions de cicloaddició [4 + 4], ens vàrem enfrontar al repte de desenvolupar reaccions de cicloaddició [(4 + 2) +2] catalitzades per níquel entre un substrat amb unitats de diè i alquè / alquí contingudes al substrat i una molècula d'alquí independent. L'activitat catalítica dels complexos de níquel(0) es

va estudiar amb una sèrie de lligands de tipus fòsfor i nitrogen per a una sèrie de substrats (vegeu l'Esquema 7a). Lamentablement, no es va descobrir cap sistema catalític eficient. Una altra alternativa perseguida va consistir en desenvolupar cicloaddicions [4+4] intramoleculars catalitzades per complexes de ferro. Amb aquesta finalitat, es va sintetitzar un complex de Fe(II) derivat d'un lligand de piridina-oxazolina i la seva estructura es va determinar inequívocament mitjançant cristal·lografia de raigs X de monocristall (complex **C1** en l'Esquema 7b). A la literatura s'indica que els complexos de Fe de baix estat d'oxidació són necessaris per a què es produeixin les cicloaddicions [4+4]. No obstant això, tots els nostres intents d'aïllar aquests complexos van ser infructuosos, així com els de generar aquests complexos *in situ* i utilitzar-los posteriorment en catàlisi.

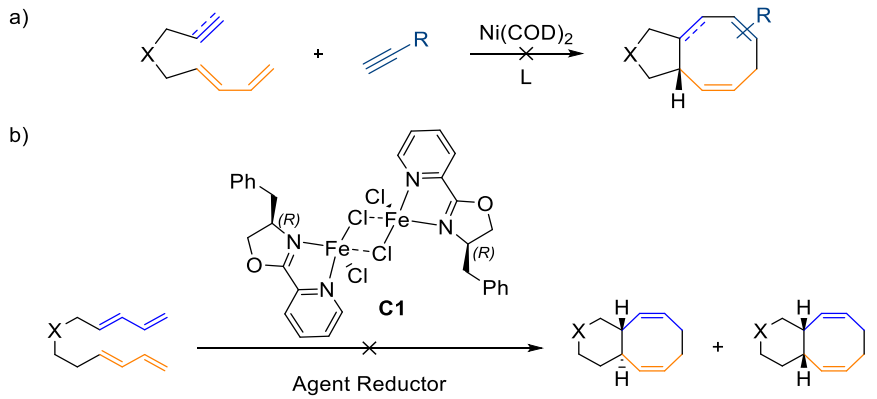

Esquema 7. Diferents alternatives per a la síntesi d'anells de vuit baules.

Els esforços de recerca també s'han dirigit a l'aplicació de catalitzadors supramoleculars basats en complexos de rodi derivats de difosfines amb enllaços d'halogen en reaccions de cicloaddició [4 + 2]. L'Esquema 8 mostra una representació de les cicloaddicions [4 + 2] estudiades. Les reaccions van ser eficients i van donar lloc a una sèrie de carbocicles de sis membres estructuralment diversos fusionats a un anell de cinc membres. Els productes es van aïllar com 1,4-ciclohexadiens no conjugats, sense que es formessin els productes aromatitzats no desitjats. També s'ha suggerit una racionalització temptativa del camí reacció que implica un procés cooperatiu de rodi i plata.

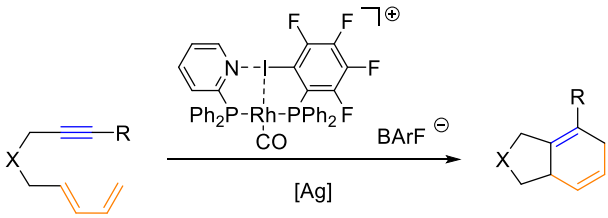

X = $C(CO_2Me)_2$, O, NTs
R = Me, Ph

Esquema 8. Cicloaddicions intramoleculars [4+2] de dienins catalitzades per XBPhosRh.

En resum, al llarg d'aquesta tesi doctoral s'ha demostrat la versatilitat de les cicloaddicions catalitzades per metalls. Els nostres estudis sobre les cicloaddicions [4 + 4] intramoleculars catalitzades per Ni d'una sèrie de bisdiens van permetre la preparació eficient d'anells de vuit membres *cis* o *trans* fusionats a anells de cinc o sis membres. Gràcies a aquests estudis, s'ha pogut obtenir un profund coneixement mecanístic de la transformació. Aquest coneixement ha permès el desenvolupament de versions enantioselectives d'aquesta transformació amb excessos enantiomèrics moderats. A més, s'ha explorat la reactivitat dels complexos XBPhosRh i BArF de plata en les cicloaddicions [4 + 2] intramoleculars de dienins. Es van preparar una sèrie de cicloaductes [4 + 2] estructuralment diversos i es van aïllar com 1,4-ciclohexadiens no conjugats amb bons rendiments.

UNIVERSITAT ROVIRA I VIRGILI
TRANSITION METAL-CATALYZED CYCLOADDITION REACTIONS FOR THE FORMATION OF EIGHT- AND SIX-MEMBERED RINGS
Nuria Llorente González

UNIVERSITAT ROVIRA I VIRGILI
TRANSITION METAL-CATALYZED CYCLOADDITION REACTIONS FOR THE FORMATION OF EIGHT- AND SIX-MEMBERED RINGS
Nuria Llorente González

UNIVERSITAT
ROVIRA i VIRGILI